Targeted dendrimeric prodrugs for 5-Aminolaevulinic acid photodynamic therapy

Tewari, Kunal Mahesh

Award date:
2016

Awarding institution:
University of Bath

Targeted dendrimeric prodrugs for 5-aminolaevulinic acid photodynamic therapy

By Kunal Mahesh Tewari

A thesis submitted for the degree of Doctor of Philosophy

University of Bath

Department of Pharmacy and Pharmacology

July 2016

Signed ..... Date .....

ॐ भूः भुवः स्वः ।
तत्सवितुर्वरेण्यं
भर्गो देवस्य धीमहि ।
धियो यो नः प्रचोदयात् ॥

Oh Creator of the Universe!

We meditate upon thy supreme splendour.

May thy radiant power illuminate our intellects,

Destroy our sins, and guide us

In the right direction!

To my Family and Friends

Table of Contents

Abstract ix

Acknowledgements xi

Abbreviations xiii

List of Figures xvii

List of Schemes xxv

CHAPTER 1: INTRODUCTION 1

1.1 Brief history of Photodynamic therapy (PDT) 1

1.2 Photochemical and photophysical basis of PDT 5

1.3 Photosensitisers in PDT 7

1.3.1 First-generation photosensitisers 8

1.3.2 Second-generation photosensitisers 10

1.3.2.1 Porphyrins 12

1.3.2.2 Chlorins and bacteriochlorins 14

1.3.2.3 Phthalocyanines and naphthalocyanines 17

1.3.2.4 Non-porphyrin based photosensitisers 18

1.3.3 Third-generation photosensitisers 21

1.4 Novel PDT techniques 24

1.4.1 Nanotechnology 24

1.4.2 Two-photon PDT (TP-PDT) 25

1.4.3 Metronomic PDT 27

1.4.4 Theranostics 27

1.5 Light sources in PDT 30

1.6 Singlet Oxygen 32

1.7 PHOTODYNAMIC ACTION 34

1.8 APPLICATIONS OF PDT 37

1.8.1 Anticancer PDT 37

1.8.2 Antimicrobial PDT 39

1.9 AMINOLEVULINIC ACID-PDT (ALA-PDT) 42

1.9.1 Haem biosynthesis 43

1.9.2 Advantages of ALA-PDT 44

1.9.3 Clinical applications of ALA-PDT 44

1.9.4 Drawbacks of ALA-PDT and strategies to improve its effectiveness 45

1.10 OBJECTIVES OF THE PROJECT 65

CHAPTER 2: RESULTS AND DISCUSSION (PREPARATION OF EFFECTOR UNITS) 67

2.1 INTRODUCTION TO DENDRIMERS 67

2.1.3 Dendrimers in Photodynamic therapy 69

2.2 SYNTHESIS OF ALA DENDRONS 70

2.2.1 Synthesis of first-generation ALA dendrons 70

2.2.2 Synthesis of second-generation ALA dendrons 78

2.3 SUMMARY 84

CHAPTER 3: RESULTS AND DISCUSSION (PREPARATION OF CORE MOLECULES) 85

3.1 CHOICE OF CORE UNIT 85

3.1.1 Synthesis of core unit 86

3.2 BIOORTHOGONAL LIGATIONS AND CLICK CHEMISTRY 88

3.2.1 Basic concept 88

3.2.2 Cu (I) catalysed azide-alkyne cycloaddition/click chemistry 89

3.2.3 Synthesis of non-targeted ALA dendrons 90
3.3 BIOMOLECULES IN PDT 101
3.3.1 Synthesis of vitamin E-ALA dendrons 101
3.3.2 Synthesis of thymidine-ALA dendrimers 106
3.3.4 Synthesis of glycoside-ALA dendrimers 109
3.4 SUMMARY 111
CHAPTER 4: RESULTS AND DISCUSSION (TARGETED ALA DENDRONS) 113
4.1 INTRODUCTION TO TARGETED PHOTODYNAMIC THERAPY 113
4.1.1 EGFR-targeted photodynamic therapy 114
4.2 SYNTHESIS OF TARGETING UNIT 116
4.2.1 Amide coupling of dendrimer to partially protected peptide in solution (A) 119
4.2.2 Amide coupling of dendrimer to resin-bound peptide (B) 120
4.2.3 On-resin click coupling (C) 120
4.2.4 Click coupling in solution (D) 128
4.2.5 Click coupling via microwave irradiation (E) 131
4.3 BIOLOGICAL EXPERIMENTS 135
4.3.1 Background 135
4.3.2 Time-course fluorescence studies 136
4.3.3 Cytotoxicity and MTT assay 140
4.4 SUMMARY 144
CHAPTER 5: RESULTS AND DISCUSSION (PEPTIDE-PORPHYRIN CONJUGATES) 145
5.1 BACKGROUND 145
5.2 Strain promoted azide-alkyne cycloaddition (SPAAC) 146

5.3 SYNTHESIS OF PEPTIDE PORPHYRIN CONJUGATES 147
5.4 BIOLOGICAL EVALUATION 156
5.4.1 PDT activity and MTT assay for **(195)** 156
5.4.2 Cellular uptake of porphyrin conjugates 159
5.4.3 Preliminary studies 160
5.4.4 PDT activity and MTT assay for **(196)** and **(197)** 164
5.5 SUMMARY 166

CHAPTER 6: RESULTS AND DISCUSSION (CPP-PORPHYRIN AND CPP-ALA CONJUGATES) 167

6.1 INTRODUCTION TO CELL PENETRATING PEPTIDES 167
6.2 APPLICATIONS OF CPPS IN PHOTODYNAMIC THERAPY 167
6.2 SYNTHESIS OF CPPS 172
6.4 SYNTHESIS OF CPP-PORPHYRIN DERIVATIVE 181
6.5 BIOLOGICAL EVALUATION 183
6.5.1 PDT activity and MTT assay 183
6.6 SUMMARY 185

CHAPTER 7: EXPERIMENTAL 187

7.1 GENERAL 187
7.2 SYNTHESIS OF COMPOUNDS 189
7.3 BIOLOGICAL ASSAYS 266
7.3.1 Materials and Methods 266
7.3.2 Stock solutions 267
7.3.3 Cell lines 267
7.3.4 Trypsination 268
7.3.5 Statistical Analysis 268

7.3.6 Time-course fluorescence studies 269

7.3.7 Photodynamic treatment 269

7.3.8 MTT assay 270

7.3.9 Fluorescence Microscopy 271

OVERALL SUMMARY AND FUTURE WORK 273

REFERENCES 277

Abstract

Photodynamic therapy (PDT) is an emerging therapy for the treatment of cancer and various other human disorders. 5-Aminolaevulinic acid (ALA) is a simple natural product that is of great interest for PDT because it can be converted within cells via the haem biosynthetic pathway to the photosensitiser, protoporphyrin IX (PpIX). ALA-PDT has become a first line clinical approach for the treatment of cancerous and precancerous skin lesions (e.g Bowen's disease, basal skin carcinomas, and actinic keratosis) that would otherwise require significant conventional surgery. However, ALA being a zwitterion suffers from poor lipid solubility and at the same time has stability issues at physiological or alkaline pH.

The work herein describes some novel strategies to enhance the delivery of ALA to specific cell types using targeted ALA dendrimeric prodrugs. Specifically, it describes the synthesis of molecules consisting of branched units with 3 or more copies of ALA attached to a central core structure (e.g. gallic acid) using copper-catalysed azide-alkyne click chemistry (CuAAC). Selective delivery of the dendrimeric ALA cargo was achieved by attachment of a homing peptide to an independently addressable functional group on the prodrug core. As proof of concept of this approach, systems were prepared containing a peptide that allows selective targeting of the epidermal growth factor receptor (EGFR) which is overexpressed in a variety of tumours. Targeted ALA delivery and PpIX production was studied with these prodrugs in EGFR-expressing breast adenocarcinoma cells (MDA-MB-231 cells) and a peptide-targeted derivative with 9 ALA units was found to have enhanced PDT efficacy compared to an equimolar dose of ALA. Other targeting units that have been attached to these dendrimeric ALA prodrugs include biomolecules such as vitamin E, thymidine (a nucleoside) and a glucose derivative. Additionally, strain-promoted azide-alkyne cycloadditions (SPAAC) of the same EGFR-targeting peptide with some classical photosensitisers were also investigated and biological studies in EGFR-overexpressing cell lines were carried out. Lastly, a group of cell penetrating peptide-ALA conjugates have been synthesised via CuAAC as a novel approach for targeted ALA delivery.

Acknowledgements

First and foremost I would like to thank my supervisor Dr. Ian Eggleston for giving me this amazing opportunity of coming 4000 miles away from my home and allowing me to shine some light on a very interesting field of photodynamic therapy. I am very grateful to him for his guidance and constantly backing me through many ups and downs I might have faced during these four years. A special thanks to him also for taking up the gladiator's challenge by proof-reading my thesis.

I would also like to thank my co-supervisor Dr Charareh Pourzand for allowing me to work in her laboratory and introducing me to the amazing world of cellbiology. It was also a pleasure working with you both in the lab and during the workshops. A huge thanks also to Dr Tina Radka and Dr Olivier Reelfs from Dr Pourzand's laboratory for helping me learn some basic and crucial biological techniques coupled with some useful advice which allowed smooth completion of all the biological experiments in a limited time frame.

I would also like to thank Faculty of Science (University of Bath) for providing me a Fee Waiver Scholarship which helped me undertake a PhD degree here at Bath.

Thanks also to Prof. A. J. MacRobert, Z. Mazhari and Dr E. Yaghini from University College London, London for carrying out the preliminary biological studies on some of my compounds and advice on experimental design.

I would also like to thank Dr. Tim Woodman for his guidance and assistance with NMR data (some times at very short notice), Dr Anneke Lubben for advice on mass spectrometry, and Dr. Sofia Pascu and Fernando Cortezon for assistance with microwave synthesis. A huge thanks also to Dr Ben Groombridge (for keeping track on my thesis) and all the technical staff from my department and Faculty of Science for the smooth running of my project.

When I first started working in the lab, I found a very special friend and colleague in Dr Ruggero Dondi whom I can't thank enough for helping me around in the laboratory and teaching me some new and interesting branches

of chemistry and for having an infinite number of 4 pm coffees. A huge thanks also to other members from the IME group, Dr Benjamin Young and Annabel Hampshire and all the project students over the years for your friendship and support through these years.

A PhD life can be very demanding, time limiting and stressful and countering the same could be an uphill task. Thankfully I managed to make some amazing and hopefully lifelong friends who kept me sane and helped me pass through the probationary period of CHEERS. This included Dr. Natalie Griffiths (saved my soft drinks a number of times from getting admixed with –OH groups), Dr Amit Nathubhai (for trying to admix them with –OH groups and for being a big brother), Dr Helen McGuire (my first friend in Bath), Dr Joanna Swarbrick (for teaching me the true meaning of perfection and for being an amazing friend), Dr Kimberley Luetchford (thanks for the secret cookies), Dr Terrence Kantner (positivity), Dr Nour Alhusein (for stealing my tea bags), Dr Maksims Jevglevskis (for getting me addicted to Monster), Dr Christopher Roche (fight for your right), Dr Ondrej Baszczynski and Dr Wolfgang Dohle (for giving me company in the office during the weekends and Friday Parade trips), Dr Elvis Twum, Dr Alex Ciupa, Dr Ricardo Resende, Dr Marco Mottinelli, Laura Newton, Majdah Raji Alotaibi, Mike Kenny, Tiago Fortunato, Dr Alexander Disney, Dr Gerta Cami-Kobeci and Dr Mehrnoosh Ostovar for all your friendship and support.

I am also very grateful to my friends from 3.22, Dr Sarah Cordery, Hilda Phan, Molly Li, Khaled Almansour, John Nikolettos, Fotios Baxevanis, Alice Maciel Tabosa, Joana Martir, Ricardo Diaz De Leon Ortega, James Clarke, Dr Magdalena Hoppel, Dr Andrea Pensado-Lopez, Panagiota Zarmpi, Dr Giovanna Mencarelli, Alistair Taverner, Dr Magdalena Perez Ortiz for all the good social times we had and apologies for breaking into your labs and offices countless number of times.

A decision as big as doing a PhD far away from home wouldn’t have been possible without the support and motivation from my parents and my cute little sister whom I love the most in this universe and can’t thank them enough for allowing me to follow my dreams.

Abbreviations

μM	Micromolar
AcOH	AcOH
ACPH	Acylpeptide hydrolase
ALA	5-Aminolevulinic acid
APA	Aminopeptidase A
APB	Aminopeptidase B
APN/M	Aminopeptidase N or M
Ar	Aryl
ARMD	Age-related macular degeneration
BCC	Basal cell carcinoma
Boc	*t*-butoxycarbonyl
BPD	Benzoporphyrin derivative
$CaCO_3$	Calcium carbonate
CPP	Cell-penetrating peptide
CuAAC	Copper catalysed azide-alkyne cycloaddition
DBCO	Dibenzocyclooctyne
DBU	1,8-diazabicycloundec-7-ene
DCM	Dichloromethane (methylene chloride)
DFO	Desferrioxamine
DHPY	2, 5-dicarboxyethyl-3,6-dihydropyrazine
DIEA	*N,N*-Diisopropylethylamine
DMAP	4-Dimethylaminopyridine
DMEM	Dulbecco's modified Eagle's Medium
DMF	*N,N*-dimethylformamide
DMSO	Dimethylsulfoxide
DNA	Deoxyribonucleic acid
EDC	1-Ethyl-3-(3'-dimethylaminopropyl)carbodiimide
EDTA	Ethylenediaminetetraacetic acid
EEDQ	N-Ethoxycarbonyl-2-ethoxy-1,2-dihydroquinoline
EGFR	Epidermal growth factor receptor
EPR	Enhanced permeability and retention effect
ER	Endoplasmic reticulum
ESI	Electrospray ionisation

Et	Ethyl
Et_2O	Diethyl ether
Et_3N	Triethylamine
EtOAc	Ethyl acetate
EtOH	Ethanol
FCS	Foetal calf serum
Fe	Iron (elemental)
Fe^{2+}	Iron (ferrous)
Fe^{3+}	Iron (ferric)
FMK	N-formylkynurenine
Fmoc	9-Fluorenylmethyloxycarbonyl
g	Gram
GATG	Gallic acid-triethylene glycol
h	Hour(s)
H_2O	Water
HATU	1-[Bis(dimethylamino)methylene]-1*H*-1,2,3-triazolo[4,5-*b*]pyridinium 3-oxide hexafluorophosphate
HCl	Hydrochloride (salt) or hydrochloric acid
HpD	Haematoporphyrin derivative
HOBt	1-Hydroxybenzotriazole
HPLC	High pressure liquid chromatography
HPV	Human papilloma virus
Hz	Hertz
IC	Iron chelator
IR	Infrared (spectroscopy)
J	Coupling constant (Hz)
KTP	Potassium titanyl phosphate
M	Molar
MAL	Methyl ester of 5-aminolevulinic acid
Me	Methyl
MeCN	Acetonitrile
MeOH	Methanol
$MgSO_4$	Magnesium sulfate
Min	Minute(s)

mM	Millimolar
mmol	millimole
Mp	Melting point
MS	Mass spectrometry
MTT	3-(4,5-dimethyl-2-thiazolyl)-2,5-diphenyl-2*H*-tetrazolium bromide
$NaHCO_3$	Sodium hydrogencarbonate
nM	Nanomolar
NMR	Nuclear magnetic resonance (spectroscopy)
NSCLC	Non-small cell lung cancer
PBS	Phosphate-buffered saline
Pd/C	Palladium on carbon
PDT	Photodynamic therapy
PEG	Polyethylene glycol
Ph	Phenyl
PpIX	Protoporphyrin IX
PS	Photosensitiser
PUVA	Psoralen Ultraviolet A (phototherapy)
PyBOP	Benzotriazol-1-yl-oxytripyrrolidinophosphonium hexafluorophosphate
PY	2,5-dicarboxyethylpyrazine
Pyr	Pyridine
R_f	Retention factor (thin layer chromatography)
ROS	Reactive oxygen species
R_t	Retention time (HPLC chromatogram)
RT	Room temperature
SPAAC	Strain-promoted azide-alkyne cycloaddition
SPPS	Solid-phase peptide synthesis
t Bu	*tert*-butyl
t BuOK	Potassium *tert*-butoxide
TBAF	Tetrabutylammonium fluoride
Tf	Transferrin
TFA	Trifluoroacetic acid
THF	Tetrahydrofuran

TIPS-Cl	Triisopropylsilyl chloride
TIS	Triisopropylsilane
TLC	Thin layer chromatography
UV	Ultraviolet (radiation)
UVA	Ultraviolet A (radiation)
Z-Cl	Benzyl chloroformate
Z-OSu	Nα-(Benzyloxycarbonyloxy) succinimide

List of Figures

Figure 1. Structures of psolaren, acridine orange and eosin. 2

Figure 2. Structure of haematoporphyrin. 3

Figure 3. Modified Jablonski diagram showing type 1 and type 2 photooxygenation processes. 5

Figure 4. Overview of type 1 reactions during PDT..... 6

Figure 5. Overview of type 2 reactions during PDT..... 7

Figure 6. Structure of Photofrin **(5)**..... 10

Figure 7. Basic structures of porphyrin-based second-generation photosensitisers. 11

Figure 8. Core structure of porphyrin derivatives (porphin). 12

Figure 9. Chemical structures of 5,10,15,20-tetraphenylporphyrin **(6)** (TPP) and 4,4',4''-(20-(4-aminophenyl)porphyrin-5,10,15-triyl)tris(1-methylpyridin-1-ium) **(7)**. 12

Figure 10. UV-Vis spectrum of a typical synthetic porphyrin showing the Soret band and Q bands. 13

Figure 11. Molecular structures of m-THPP **(8)** and Protoporphyrin IX **(9)**..... 13

Figure 12. Basic structure of chlorins and bacteriochlorins. 14

Figure 13. Structure of chlorophyll a **(10)**, chlorophyll b **(11)** and bacteriochlorophyll a **(12)**..... 15

Figure 14. Structure of verteporfin **(13)**. 15

Figure 15. Structure of m-THPC **(14)**. 16

Figure 16. Structures of SnET2 **(15)** and NPe6 **(16)**. 17

Figure 17. Basic structures of phthalocyanines and naphthalocyanines. 17

Figure 18. Structures of some clinically used phthalocyanine photosensitisers **(17)**-**(19)**. 18

Figure 19. Structures of some non-porphyrin photosensitisers **(20)**-**(29)**. 20

Figure 20. Structures of pheophorbide-a **(30)** and different targeting units **(31)**-**(34)**. 21

Figure 21. Chemical structures of Ce6 **(35)** and its [Tyr3]-octrotate conjugates **(36)** and **(37)**..... 23

Figure 22. Representation of a two-photon excitation process. 25

Figure 23. Structure of conjugated porphyrin dimers used in a two photon PDT study. 26

Figure 24. Representation of concept for theranostics. 28

Figure 25. Schematic representation of a theranostic system containing photosensitiser, MRI agent, targeting peptide and PEG group. 29

Figure 26. Molecular orbital diagram for molecular oxygen 32

Figure 27. Overview of the PDT effect. Targeted generation of $^1O_2$ in tumour tissue leads to a selective photodynamic effect. 35

Figure 28. Clinical applications of PDT on a range of human infections 40

Figure 29. Structures of simple N-acylated ALA derivative **(52)** and **(53)**..... 46

Figure 30. Linear and non-linear aliphatic esters of ALA. 47

Figure 31. Cyclic, aromatic and halogen-substituted benzyl esters of ALA. 49

Figure 32. Ethylene glcol esters of ALA..... 50

Figure 33. Structure of EDTA **(60)**. 51

Figure 34. Structure of DFO **(61)**. 52

Figure 35. Structure of CP94 **(62)**..... 52

Figure 36. Chemical structures of thiosemicarbazone derivatives **(63)**-**(66)**. 53

Figure 37. Pseudopeptide derivatives of ALA **(67)** and **(68)**. 54

Figure 38. ALA peptide-prodrugs **(69)** and **(70)** based on phenylalanine..... 55

Figure 39. Dipeptide derivatives of ALA. 55

Figure 40. Structure of a cell penetrating peptide conjugate with ALA **(71)**. 56

Figure 41. Structure of ALA-poly(L-histidine) prodrugs **(72)**..... 56

Figure 42. Structure of cathepsin E-activatable ALA prodrug **(73)**. 56

Figure 43. Folic acid-conjugated with MAL via a peptide spacer **(74)**..... 57

Figure 44. Structures of vitamin-ALA conjugates **(75)**-**(77)**. 58

Figure 45. Structures of nucleoside-ALA conjugates **(78)**-**(81)**. 58

Figure 46. Structures of glycoside-ALA conjugates **(82)**-**(84)**. 59

Figure 47. Illustration of a ALA pseudopolyrotaxane prodrug micelles for PDT 59

Figure 48. Structures of dendritic derivatives with 6-18 copies of ALA **(85)**-**(89)**. 60

Figure 49. Structures of ALA dendrimers **(90)**-**(92)**. 61

Figure 50. Reported dendrimeric prodrugs of ALA **(93)**. 62

Figure 51. Structures of ALA dendrimers **(94)** and **(95)**. 63

Figure 52. Model for peptide-targeted ALA dendrimers. 66

Figure 53. Representation of an EPR effect 68

Figure 54. Chemical structure of 32(+)DPZn dendrimer **(96)**. 69

Figure 55. Application of ligatable ALA dendrons. 70

Figure 56. Structures of the building blocks Tris and Ext. Tris **(97)** and **(98)**. 71

Figure 57. Structure of 2nd generation ALA dendron (initial approach). 78

Figure 58. Proposed structure of a 2nd generation ALA dendron **(125)** synthesized from isophthalic acid. 81

Figure 59. Structures of first- and second-generation ALA dendrons **(105)**, **(107)** and **(125)**. 84

Figure 60. Model for targeted-ALA dendron showing the core unit and its conjugation to effector units via copper-catalysed azide-alkyne cycloaddition. 85

Figure 61. Multifunctional GATG core **(132)** and simplified model core **(133)**. 86

Figure 62. Overview of recently developed biorthogonal ligation chemistries. 89

Figure 63. HPLC for click coupling reaction of **(138)** and **(105)** after 16 h. 92

Figure 64. HPLC chromatogram for click coupling reaction of **(143)** and **(144)** after 1h. 94

Figure 65. Overlay of HPLC chromatograms for clicked ALA dendrons **(145)** and **(146)**. 96

Figure 66. HPLC chromatograms for click coupling reaction of **(148)** and **(149)** after 72 h. 98

Figure 67. Overlay of HPLC chromatograms for clicked ALA dendrons **(150)** and **(151)**. 100

Figure 68. HPLC chromatograms for click coupling reaction of **(154)** and **(155)** after 72 h. 103

Figure 69. Overlay of HPLC chromatograms for clicked ALA dendrons **(156)** and **(157)**. 105

Figure 70. HPLC chromatogram for crude reaction mixture for **(162)**. 108

Figure 71. Overlay of HPLC chromatogram for thymidine conjugate **(163)** showing **(162)** (Boc-protected derivative) and **(161)** (azide). 109

Figure 72. Representation of singlet oxygen production by biodegradable and non-biodegradable nanostructures inside tumour cells 114

Figure 73. Chemical structure of EGFR-targeting phthalocyanine-peptide conjugates **(168a-b)**. 115

Figure 74. Model for peptide-targeted ALA dendron system. 116

Figure 75. HPLC chromatograms for peptide-azido core unit **(177)** and **(179)**. 122

Figure 76. HPLC chromatograms for peptide-ALA dendron **(181)** and **(182)**. 126

Figure 77. HPLC chromatograms for peptide-ALA dendron **(175)** and **(180)**. 128

Figure 78. HPLC chromatograms for peptide-ALA dendron **(181)**. 130

Figure 79. HPLC chromatograms for **(183)** post-microwave irradiation at two different temperature conditions (70 °C and 80 °C). 133

Figure 80. Chemical structure of the targeted ALA dendrimer **(181)**. 134

Figure 81. ALA-induced PpIX fluorescence in phenol red and phenol red-free DMEM. 136

Figure 82. ALA-induced PpIX generation from **(145)**, **(150)** and **(181)** in MDA-MB-231 cells. 138

Figure 83. PDT effect of ALA on MDA-MB-231 cells at different time intervals. 140

Figure 84. PDT effect of **(145)**, **(150)** and **(181)** on MDA-MB-231 cells after incubation for 4 h. 142

Figure 85. Different strategies explored for developing peptide-porphyrin conjugates 145

Figure 86. Structures of cyclooctyne **(184)** and its modified derivatives **(185)**-**(189)**. 147

Figure 87. Structure of an EGFR-targeted porphyrin photosensitiser synthesized via SPAAC. 148

Figure 88. Structures of **(190)**, **(191)** and **(13)**. 148

Figure 89. Structures of the two regioisomers of verteporfin (I and II) **(13)**. 149

Figure 90. Chemical structure of verteporfin-DBCO conjugate **(194)**. 151

Figure 91. HPLC chromatograms for peptide-photosensitiser conjugates **(195)**-**(197)**. 155

Figure 92. Phototoxicity of EGFR-targeted porphyrin **(195)**. 157

Figure 93. Cellular uptake of EGFR-targeted porphyrin **(195)**. 159

Figure 94. PDT effect of **(196)** on MDA-MB-231 cells at various concentrations. 160

Figure 95. The PDT effect of EGFR-targeted photosensitiser **(196)** on MDA-MB-231 cells in different types of 96 well plates. 163

Figure 96. The PDT effect of EGFR-targeted photosensitisers **(196)** and **(197)** on MDA-MB-231 cells. 165

Figure 97. Structure of some reported CPP-porphyrin conjugates. 169

Figure 98. HPLC chromatograms for the crude isolated azido CPPs **(200)**-**(203)**. 176

Figure 99. Chemical structures for CPP-ALA conjugates **(211)**-**(214)** and isolated yields after HPLC purification. 178

Figure 100. HPLC chromatograms for crude CPP-ALA derivatives **(210)**-**(214)**. 180

Figure 101. HPLC chromatograms for the CPP-porphyrin conjugate **(215)**. 182

Figure 102. The PDT effect of CPP-porphyrin conjugate **(215)** on MDA-MB-231 and MCF-7 cells. 184

Figure 103. Spectrum of the Sellas 4kW UVA lamp as measured by spectroradiometer 266

Figure 104. PDT activity on a protected 96-well plate been carried under UVA lamp..... 270

List of Schemes

Scheme 1. Isolation procedure for the production of HpD and its commercial variants from impure haematoporphyrin dihydrochloride. 9

Scheme 2. Proposed reaction pathways for singlet oxygen-mediated oxidation of tryptophan. 34

Scheme 3. Bioconversion of ALA **(40)**. 42

Scheme 4. Bioconversion of ALA to haem. 43

Scheme 5. Degradation pathway of ALA under alkaline conditions 46

Scheme 6. Synthesis of urethane and acetyl-protected ALA-dipeptide ester derivatives. 54

Scheme 7. Convergent and divergent routes of synthesis for dendrimers. 67

Scheme 8. Synthesis of Boc-ALA **(99)**. 71

Scheme 9. Synthetic route adopted for preparation of first generation ALA dendrons (Initial approach). 72

Scheme 10. Initial attempts for hydrogenolysis of **(90)**. 73

Scheme 11. Mechanism of intramolecular rearrangement of amino Tris esters. 73

Scheme 12. Hydrogenolysis of **(90)** and **(102)** under acidic conditions. 74

Scheme 13. Acylation of **(92)** with 4-pentynoic acid **(104)**. 74

Scheme 14. Acylation of **(92)** and **(103)** with 4-pentynoic acid succinimido ester **(106)**. 75

Scheme 15. Strategies adopted for the effective N-acylation of Tris **(97)**. 75

Scheme 16. Silylation strategy for acylation of Tris compounds. 76

Scheme 17. Work-up strategy to remove excess TBAF post-desilylation.....77

Scheme 18. Coupling of Boc-ALA **(99)** with **(108)** and **(114)**.. 78

Scheme 19. Synthesis of a triacid **(119)** from Tris **(97)**.....79

Scheme 20. Synthesis of ALA dendron **(124)**.....80

Scheme 21. Attempted coupling of triacid **(119)** with ALA dendron **(124)**.. 81

Scheme 22. Initial attempt to conjugate **(126)** with 4-pentynoic acid.. 82

Scheme 23. Synthesis of ligatable 5-aminoisophthalic acid derivative **(127)**.....82

Scheme 24. Synthesis of 2nd generation ALA dendron **(125)**.. 83

Scheme 25. Synthesis of azido-PEG-chloro derivative **(135)**. 86

Scheme 26. Synthesis of core molecules **(138)** and **(140)**.. 87

Scheme 27. Proposed mechanism of CuAAC. 90

Scheme 28. Preparation of **(141)** via Cu(I)-catalysed click coupling of azide **(138)** and alkyne **(105)**.....91

Scheme 29. Modified click strategy for the preparation of model compound **(143)**.....92

Scheme 30. Click strategy for the preparation of model compound **(144)**.. 93

Scheme 31. Deprotection of model ALA dendrons **(143)** and **(144)**.. 95

Scheme 32. Click couplings between **(147)** and ALA dendrons **(105)** and **(107)**.....97

Scheme 33. Boc cleavage for model ALA dendrons **(148)** and **(149)**.. 99

Scheme 34. Conjugation of vitamin-E with azido spacer **(153)**.. 102

Scheme 35. Synthesis of vitamin E-ALA dendrons **(154)** and **(155)** (Boc-protected)..... 102

Scheme 36. Synthesis of vitamin E-ALA dendrons **(156)** and **(157)** (TFA salts).. 104

Scheme 37. Bioconjugation of 2-thymidine with **(142)**. 106

Scheme 38. Bioconjugation of 2-thymidine **(158)** with 11-azido undecanoic acid **(160)**.. 107

Scheme 39. Synthesis of thymidine ALA dendrimer **(162)** (Boc-protected derivative).. 107

Scheme 40. Synthesis of thymidine ALA dendrimer **(162)** (TFA salt). 108

Scheme 41. Bioconjugation of **(142)** with 2,3,4,6-tetra-O-benzyl-D-gluco-pyranose **(164)**.. 110

Scheme 42. Click coupling of ALA dendron **(105)** with **(165)**.. 110

Scheme 43. Attempt to cleave Z group from **(166)**.. 111

Scheme 44. Synthesis of the targeting peptide **(172)**.. 117

Scheme 45. Different strategies adopted to synthesize peptide-targeted ALA dendrimers. 118

Scheme 46. Synthesis of targeted dendrimer **(174)**..... 119

Scheme 47. Coupling of the peptide **(171)** with Boc-protected ALA dendrimer **(148)** on resin..... 120

Scheme 48. Coupling of the azido units **(142)** and **(147)** to the resin-bound peptide **(171)**.. 121

Scheme 49. On-resin click coupling of **(176)** and **(105)**. 124

Scheme 50. On-resin click coupling of peptide derivative **(178)** with alkyne derivatives **(105)** and **(107)**.. 124

Scheme 51. On-resin click coupling of peptide derivative **(176)** with alkyne derivatives **(105)** and **(107)**.. 126

Scheme 52. Solution click coupling of peptide conjugate **(179)** with alkyne derivative **(105)**. 129

Scheme 53. Click coupling of peptide conjugate **(179)** with alkyne derivative **(105)** via microwave irradiation.. 131

Scheme 54. Cellular conversion of MTT to its insoluble purple formazan product..... 135

Scheme 55. Reaction mechanism for strain-promoted azide-alkyne cycloaddition (SPAAC). 146

Scheme 56. Scheme of synthesis for the preparation of DBCO conjugate of **(190)**..... 150

Scheme 57. Scheme of synthesis for the preparation of Ce6-DBCO conjugate **(193)**.. 151

Scheme 58. Synthesis of peptide-targeted porphyrins **(195)**-**(197)**.. 152

Scheme 59. Proposed route of synthesis for CPP-ALA conjugates. 170

Scheme 60. Design of ligatable cell penetrating peptide **(200)** derived from penetratin. 170

Scheme 61. Design of ligatable cell penetrating peptide Tat-(48-57)-GYKG, **(201)**..... 171

Scheme 62. Design of ligatable cell penetrating peptide **(202)**..... 171

Scheme 63. Design of ligatable cell penetrating peptide **(203)** (pVEC-N_3)..... 172

Scheme 64. Synthesis of azidolysine **(205)** using imidazole-1-sulfonyl azide hydrochloride.. 172

Scheme 65. Preparation of azido penetratin **(200)**.. 173

Scheme 66. Preparation of azido CPPs **(201)**-**(203)**.. 174

Scheme 67. Synthesis of CPP-ALA conjugate **(210)** based on penetratin.. 177

Scheme 68. Synthesis of cell-penetrating peptide-porphyrin conjugate **(215)** via SPAAC. 181

List of Tables

Table 1. Clinically used light sources in PDT 31

Table 2. Different coupling conditions for on-resin click coupling of the targeted dendrimer **(181)**. 123

Table 3. Microwave irradiation conditions for targeted ALA dendron **(181)**. 132

Table 4. Summary of different synthetic strategies adopted to synthesize EGFR-targeted ALA dendrimers. 134

Table 5. Sequences of common CPP 167

CHAPTER 1: INTRODUCTION

1.1 Brief history of Photodynamic therapy (PDT)

Therapeutic approaches involving light (visible and non-visible) have long been applied in ancient Egypt, India and China to treat various diseases such as psoriasis, rickets, vitiligo, cancer and psychosis.[1] The Greek physician Herodotus in 600 BC reported the benefits of sunlight (heliotherapy) on the restoration of health, which was further supported by Hippocrates (460-375 BC) who also reported the use of heliotherapy to treat human illness.[2] In the eighteenth and nineteenth centuries, the use of sunlight was applied to treat a range of disorders, including tuberculosis, rickets, scurvy, rheumatism, paralysis, edema and muscle weakness, but it was the Danish physician Niels Rydberg Finsen who provided the first scientific evidence for the potential use of other forms of light in therapy. Finsen used red light for the amelioration of suppuration and scarring from smallpox, however his most important findings were for the treatment and cure of *lupus vulgaris* (a tubercular condition of skin causing reddish brown plaques) by using ultraviolet light from a carbon arc.[3] Finsen was later awarded a Nobel Prize for Physiology-Medicine in 1903[2] in recognition of this work.

Photochemotherapy combines the use of both a chemical agent (or photosensitizing agent) and light. In such an approach, light of an appropriate wavelength is focussed on the target tissues where the chemical is localized in order to generate a therapeutic effect.[1] The principle of photochemotherapy has been known for over 3000 years and it was applied in ancient India for the treatment of the skin disease vitiligo using extracts from the plant *Psoralea corylifolia* followed by exposure to sunlight. In the 1970s, the combination of UVA light and psoralen **(1)** (Figure 1), which is derived from the seeds of *P. corylifolia*, began to be used clinically to treat psoriasis, which became known as PUVA therapy. More recently, PUVA has also been used for the treatment of other dermatological conditions such as mycosis fungoides and atopic eczema.[2, 4]

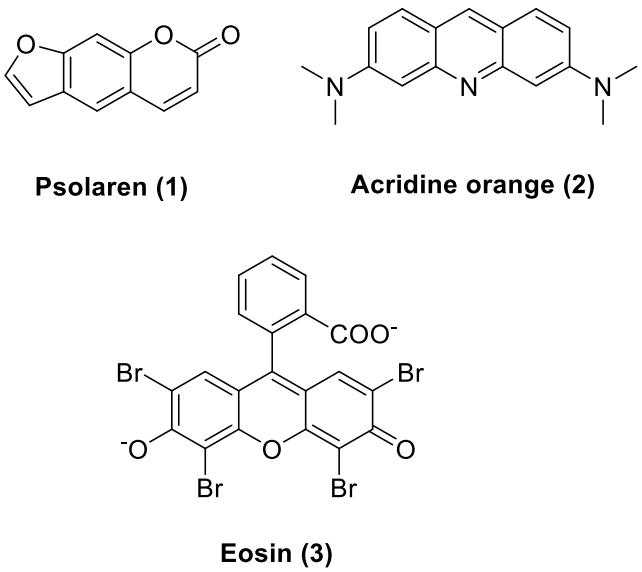

Figure 1. Structures of psolaren, acridine orange and eosin.

The concept of photodynamic action started taking shape in the late 1800s when one of Prof. Herman von Tappeiner's medical students, Oscar Raab, at Ludwig-Maximillian University, Munich, observed some inconsistencies in his data while working on the antimalarial properties of acridine orange **(2)** (Figure 1).[5] He noticed that a specific concentration of acridine orange was able to kill paramecia within 60-100 min compared to 800-1000 min from previous experiments. This made Raab and von Tappeiner thoroughly analyse their experimental protocols and led to the discovery that the tenfold decrease in time was due to differences in the lighting conditions between the two sets of experiments. They subsequently went on to prove that a combination of light and acridine orange is required to kill paramecia, however the role of oxygen in such photodynamic processes was still unknown at this stage.[6]

Following the publication of these results in 1900, further research was initiated by von Tappeiner in collaboration with Albert Jesionek from the University of Munich. They investigated topical application of the dye eosin **(3)** (Figure 1) together with sunlight or arc-lamp light for the treatment of facial basal cell carcinoma and observed total tumor resolution and a 12 month relapse-free period in two-thirds of the patients.[7]

In 1904, von Tappeiner and Jodlbauer investigated the application of aniline-based dyes and light in protozoa and reported for the first time that oxygen

was required for photosensitization.[8] The results from the above experiments were collated into a book in which the word 'photodynamic therapy' was coined to describe this oxygen-dependent photosensitization process.[9]

Herman von Tappeiner is thus considered to be one of the pioneers of photobiology. However, another important phase in the field of photodynamic therapy came with the discovery and subsequent investigation of haematoporphyrin **(4)** (Figure 2).[10]

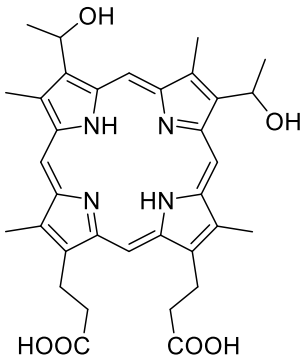

Haematoporphyrin (4)

Figure 2. Structure of haematoporphyrin.

Haematoporphyrin was isolated in 1841 by Scherer in an impure form by treating dried blood with concentrated sulfuric acid and washing the resulting precipitate free of iron.[11] Further treatment with ethanol gave a residue with a blood-red colour, indicating that iron was not essential for the colour of the blood. Later in 1867, Thudichum described the absorption spectrum and fluorescence of this purple-red substance, while Hoppe-Seyler (1871) was the first to describe the same purple-red substance by its original name 'Haematoporphyrin'.[9, 12, 13] The first report on the biological properties of haematoporhyrin came in 1908 when Walter Hausmann investigated the effect of this photosensitiser on paramecia and red blood cells.[14] This was followed by Pfeiffer's work in 1911 and Hausmann (1911) who reported sensitisation on guinea-pigs and white mice with haematoporphyrin **(4)**, describing fairly acute, sub-acute, and chronic photosensitivity changes and some phototoxicity with intense light.[15] The first study on the photosensitizing effects of haematoporhyrin in humans was attempted by a German doctor, Friedrich Meyer-Betz, who in 1913 decided to self-administer 200 mg of

haematoporhyrin, followed by exposing himself to sunlight.[16] Following the injection, Meyer-Betz suffered from erythema and oedema on the areas of his body which were exposed to sunlight, and remained photosensitive for more than two months.

The next important stage in the study of haematoporphyrin as a photosensitizing agent was the observation of its tumour-localizing properties.[9] Policard in 1924 investigated the selective localization of haematoporphyrin in experimental rat sarcomas, which were exposed to light from a Wood lamp following administration of the sensitizer (a Wood lamp is a low-output mercury arc covered by a Wood filter (barium silicate and 9% nickel oxide) that emits wavelengths 320–450 nm (peak 365 nm). The resulting red fluorescence which was observed from the tumours was attributed to the accumulation of sensitizer.[17] Another major finding was reported by Auler and Banzer in 1942 who were the first to observe photodynamic action involving the selective uptake of haematoporphyrin **(4)** in primary and metastatic tumours as well as in lymph nodes in comparison to the normal surrounding tissue.[18] However, in all the above experiments, consistent uptake of sensitizer was not possible without administering large doses of haematoporhyrin. Further investigations into the chemical nature of haematoporhyrin studied previously revealed that it was not in fact a pure compound but a variable mixture of a number of porphyrins.[9] Subsequent attempts to isolate the active component gave rise to the discovery of haematoporphyrin derivative (HpD) which is discussed in further detail in Section 1. All these studies helped to lay the foundations for the development of the technique of photodynamic therapy (PDT) into the clinical technique that is used today. Photodynamic therapy (PDT) in general can be described as a non-thermal therapeutic technique in which targeted destruction of diseased tissue is achieved by exposure to light after selective administration of a light-activated photosensitising drug (photosensitiser).[19] The major advantage of PDT is that the therapeutic effect is highly controlled as it is limited to the illuminated area, and takes place only during illumination, which significantly reduces side-effects.

The three key components of PDT are:

1. Photosensitiser (PS)
2. Light source (preferably red light)
3. Molecular oxygen

Each of the three key components above are harmless (inert) on their own but, in combination, they may give rise to lethal cytotoxic agents causing cell death.

1.2 Photochemical and photophysical basis of PDT

The photochemical and photophysical basis of PDT can be explained by a modified Jablonski diagram as illustrated in Figure 3.[2]

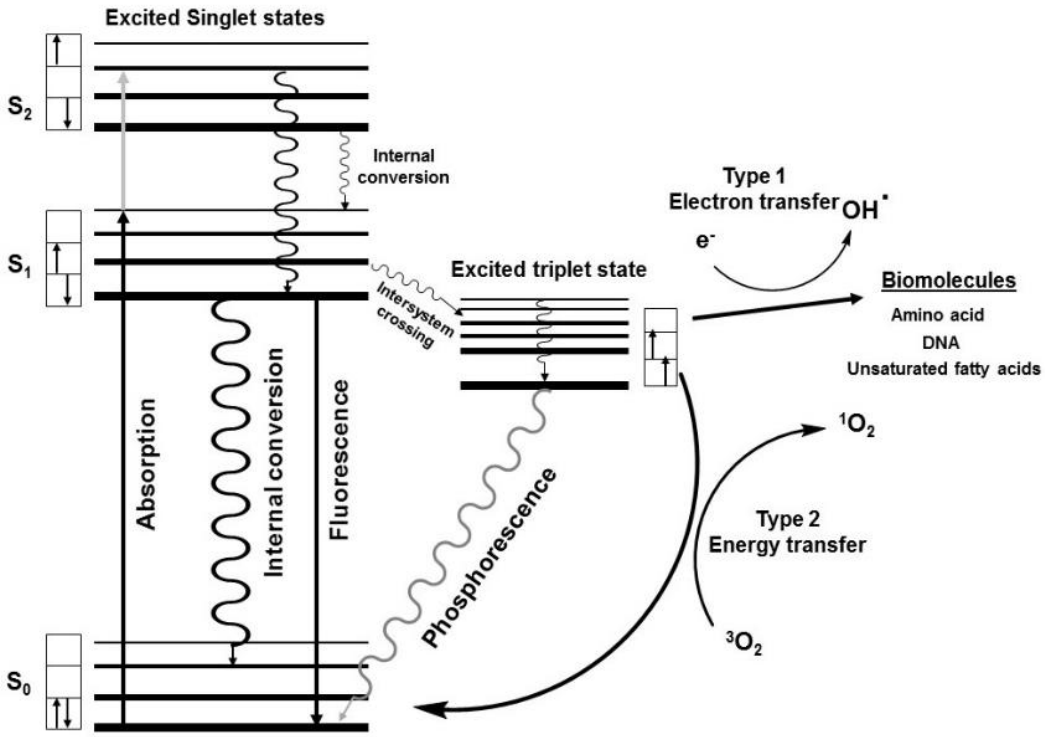

Figure 3. Modified Jablonski diagram showing type 1 and type 2 photooxygenation processes (adapted from *Bonnett et al.*[2]).

A photosensitiser molecule upon absorption of light of the appropriate energy is excited from the ground state (S_o, electrons with opposite spins) to an excited single state (S_1). This state is unstable and loses its energy either through fluorescence (by emission of light) or by producing heat

(internal conversion). However through a process of intersystem crossing, the excited singlet state photosensitiser may also form a stable excited triplet state (electrons with parallel spins). The excited triplet state is much more stable in comparison to the excited singlet state and has a lifetime of microseconds. It has been noted that the slower the decay of this triplet state, the longer is the PDT effect.[19]

The excited state of a photosensitiser may initiate a chemical reaction in a substrate causing damage to the living tissue by two different mechanisms.[2]

Type 1 mechanism: This is based on electron transfer and generates free radicals by either electron transfer to (or from) substrates or by hydrogen atom abstraction from the substrate (Figure 4). The resulting radicals or radical ions then react with ground state oxygen to produce oxygenated products such as superoxide ion (O_2^-), hydrogen peroxide (H_2O_2) and hydroxyl radical ($OH^{\cdot}$). These may then go on to react with biomolecules in targeted tissue.

Type 1 mechanism-electron transfer

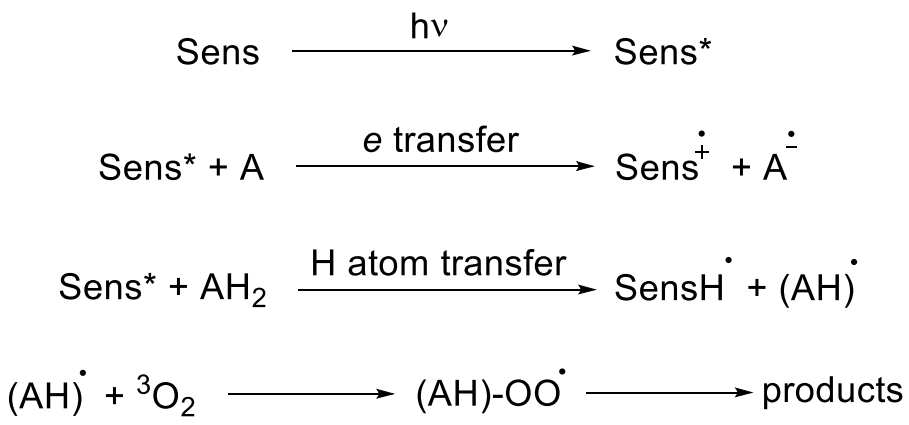

Figure 4. Overview of type 1 reactions during PDT (derived from Bonnett *et al.*).[2]

Type 2 mechanism: This involves transfer of electronic excitation energy from the excited triplet state of a sensitizer (T_1) to ground state molecular oxygen ($^3O_2$) to give the sensitizer in its ground state, S_0, and singlet oxygen ($^1O_2$) (Figure 5).

Type 2 mechanism-energy transfer

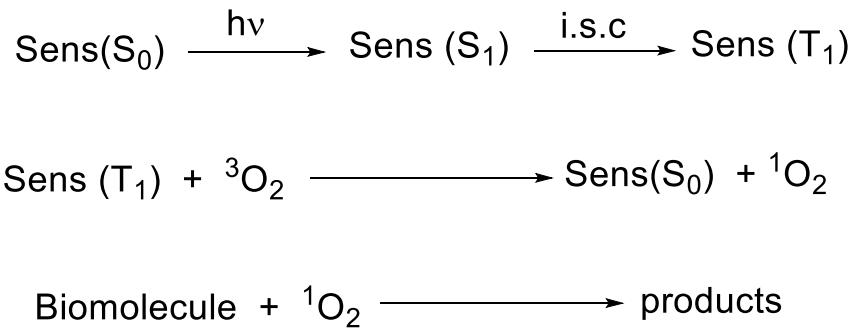

Figure 5. Overview of type 2 reactions during PDT (derived from Bonnett *et al.*).[2]

1.3 Photosensitisers in PDT

A photosensitiser in PDT is a chemical agent which absorbs light of a specific wavelength and generates lethal cytotoxic agents such as singlet oxygen.[19] A photosensitiser for clinical use should ideally possess the following properties:[19, 20]

1. Chemical stability.
2. Selectivity towards the target tissue.
3. Rapid clearance from a patient's body.
4. Efficient production of singlet oxygen.
5. No dark or systemic toxicity.
6. Easily synthesised and no toxic by-products upon light activation.
7. Strong absorption and high extinction coefficient in the red/near infrared region of the electromagnetic spectrum (600–850 nm) to allow activation at deeper levels of tissue.

Many photosensitiser molecules have been identified or developed and are mainly classified as first and second generation photosensitisers. A detailed description of some of these follow below.

1.3.1 First-generation photosensitisers

Photosensitisers such as acridine orange, eosin, psoralen, haematoporphyrin and haematoporphyrin derivative (HpD) were the first group of compounds that were tested for their PDT activities, and are hence termed first-generation photosensitisers. These molecules are either natural products, or early synthetic dye molecules that were not developed specifically for phototherapies. This section focuses mainly on haematoporphyrin and its derivatives as these molecules have been investigated in some detail for PDT and have shown clinical real clinical potential.[21] As noted earlier, the fluorescent properties of haematoporphyrin were first reported as early as 1867, and it was only later shown to be a potent photosensitiser by Hausmann.[1, 9] However, Schwartz *et al.* in 1955 while investigating the nature of haematoporphyrin found the sensitizer to be a crude mixture of various other porphyrins, most of which had different biological properties.[22] Partial purification gave pure haematoporphyrin with the structure shown in Figure 4, which itself was found to have poor tumour-localizing properties, and it was as also shown to be only a weakly phototoxic agent. Schwartz later developed a general purification system (Scheme 1) in which haematoporphyrin dihydrochloride was subjected to a series of acid and base treatments before obtaining a purified fraction, which was later identified by the name haematoporhyrin derivative (HpD).[2] HpD was found to be a powerful photosensitiser and had better affinity for tumour cells than the parent compound, haematoporphyrin **(4)**.[9, 22]

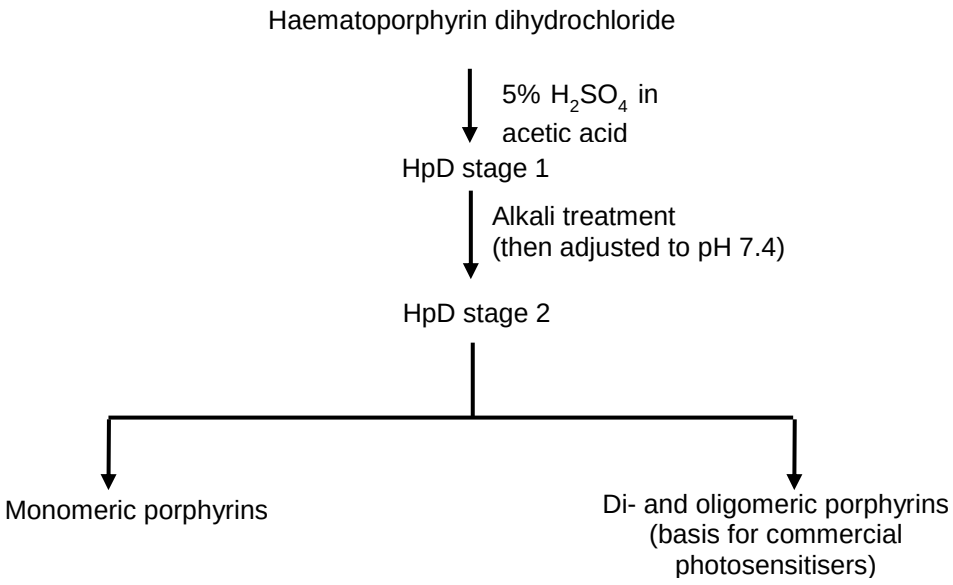

Scheme 1. Isolation procedure for the production of HpD and its commercial variants from impure haematoporphyrin dihydrochloride.

Following up on Schwartz's work on HpD, Lipson from the Mayo Clinic along with Baldes investigated the effect of HpD on malignant tissue and found that HpD had enhanced localization in malignant tissue with improved PDT properties.[23-26] Lipson *et al.* later in 1966 conducted the first human PDT studies using HpD in a female patient with extended recurrent ulcerated cancer of the mammary gland.[27] The results showed recurrence of cancerous lesions after several weeks, however the study gave substantial evidence of neoplastic tissue death by HpD-mediated PDT.

Another early *in vivo* PDT study with HpD was carried out by Diamond *et al.* in 1972 using glioma cells that had been implanted subcutaneously in rats.[28] It was found that cells that were treated with HpD and light suffered a growth arrest for up to 20 days post-photosensitization along with a reduction in tumour volumes. A few years later, Kelly and Snell also demonstrated that light activation of HpD eliminated bladder carcinoma in mice.[29] At around the same time, Thomas J. Dougherty and co-workers at the Roswell Park Cancer Institute, New York also began a pioneering set of investigations into HpD-mediated PDT. They initially purified HpD by removing the monomers to form a product which was later called Photofrin®. This then led to an extensive clinical survey by Dougherty and his colleagues in 1978, which involved

25 patients with cutaneous and sub-cutaneous malignancies.[30] The results were promising and the majority of the patients showed complete or partial response in cutaneous or sub-cutaneous malignant lesions. HpD received its first regulatory approval (marketed as Photofrin **(5)** by QLT Phototherapeutics Inc, Vancouver) (Figure 6) in 1995. The initial approval in Canada was limited only to papilloma of the bladder, but subsequent approvals worldwide were obtained for other indications in France (oesophagus, bladder), Germany (lung), Japan (lung, oesophagus, stomach, and cervix), Netherlands (lungs, oesophagus) and for palliative use (bronchus, oesophagus) in the UK in 1999. Other commercial variants of HpD were also developed e.g Hematodrex (Bulgaria), Photocarcinorin (China), Photosan (Germany) and Photogem (Russia). After its original FDA approval, HpD has since received regulatory approval in more than 40 countries.[2]

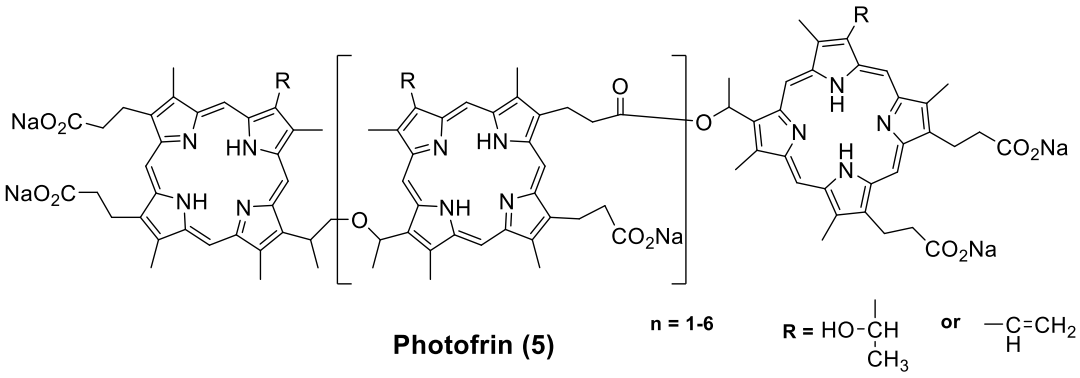

Figure 6. Structure of Photofrin **(5)**.

1.3.2 Second-generation photosensitisers

Although HpD showed some promising clinical activity and subsequently received a number of regulatory approvals, it suffers from various drawbacks such as:

1. Difficulty in reproducing the complex mixture of dimers and oligomers of HpD.
2. Modest PDT effect vs cancer cells.
3. Limited selectivity between tumour and normal tissue.
4. Long clearance time leading to prolonged skin photosensitivity in

patients for several weeks.

To overcome the shortfalls of first generation photosensitisers like HpD, a new generation of photosensitising agents have therefore been developed, based on porphyrin or porphyrin-like macrocyclic structures such as chlorins, bacteriochlorins, pheophorbides, bacteriopheophorbides, texaphyrins, porphycene and phthalocyanins (Figure 7).

These photosensitisers are all single substances with a fixed composition that are typically available by straightforward and high-yielding syntheses. Second-generation photosensitisers have also been designed specifically to have significant absorption at wavelengths in the far red (660-700 nm) or near infrared regions (700-850 nm) of the electromagnetic spectrum. Such wavelengths allow deeper penetration of the light up to 20 mm into tissue, compared to 5-10 mm at 630 nm.[31, 32]

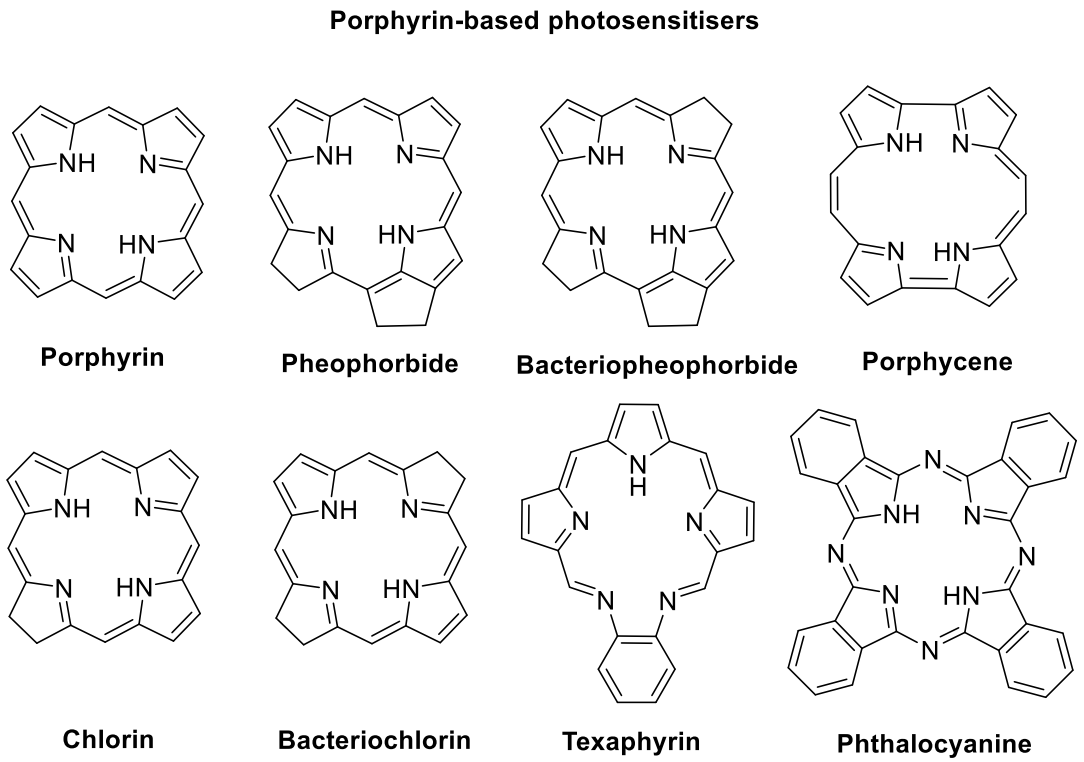

Figure 7. Basic structures of porphyrin-based second-generation photosensitisers.

A brief overview of some of these second generation photosensitisers is given below, grouped according to the core structure of the parent macrocycle.

1.3.2.1 Porphyrins

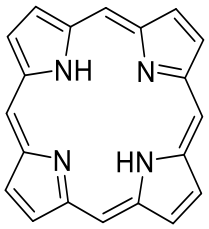

Porphyrin

Figure 8. Core structure of porphyrin derivatives (porphin).

Porphyrins are a group of heterocyclic and macrocyclic organic compounds consisting of four modified pyrrole sub-units joined by methine bridges (=C-) in a cyclic arrangement (Figure 8). The simplest unsubstituted tetrapyrrole ring arrangement is known as porphin, while substituted compounds are known as porphyrins.[33, 34] The porphyrin system is aromatic with 18π electrons and are generally planar with low solubility in organic solvents and water. However substitution at the periphery increases their solubility in organic solvents. For example 5, 10, 15, 20-tetraphenylporphyrin **(6)** (TPP) is insoluble in water whereas modification with polar groups on the phenyl rings **(7)** increases the solubility in water (Figure 9).

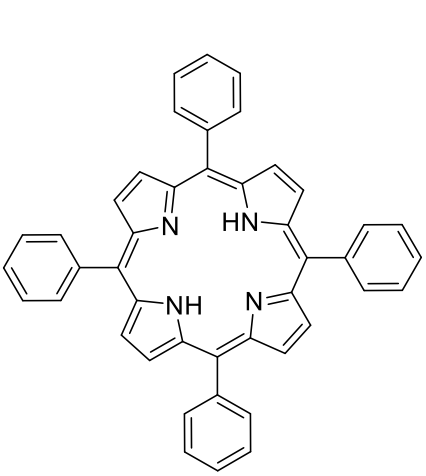

(6)

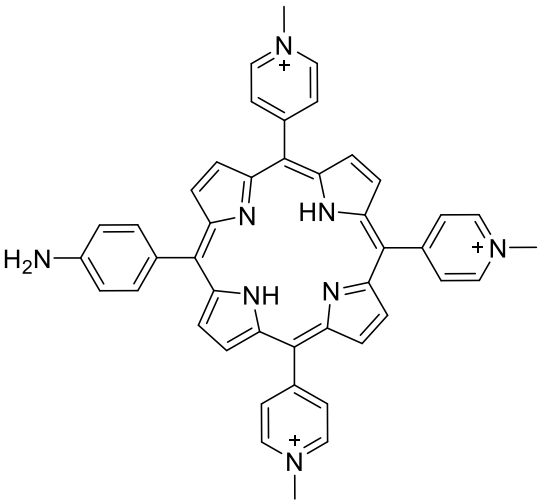

(7)

Figure 9. Chemical structures of 5,10,15,20-tetraphenylporphyrin **(6)** (TPP) and 4,4',4''-(20-(4-aminophenyl)porphyrin-5,10,15-triyl)tris(1-methylpyridin-1-ium) **(7)**.

Porphyrins readily form complexes with metal ions which modifies their fluorescent and photodynamic properties. For example, the Al, Zn and Si complexes of phthalocyanines have been used in clinical studies and have shown enhanced PDT activities.[35] Porphyrins also have characteristic UV spectra with an intense band at around 400 nm called the Soret or B band, and four distinct bands in the region 500-600 nm called the Q bands (Figure 10).[2]

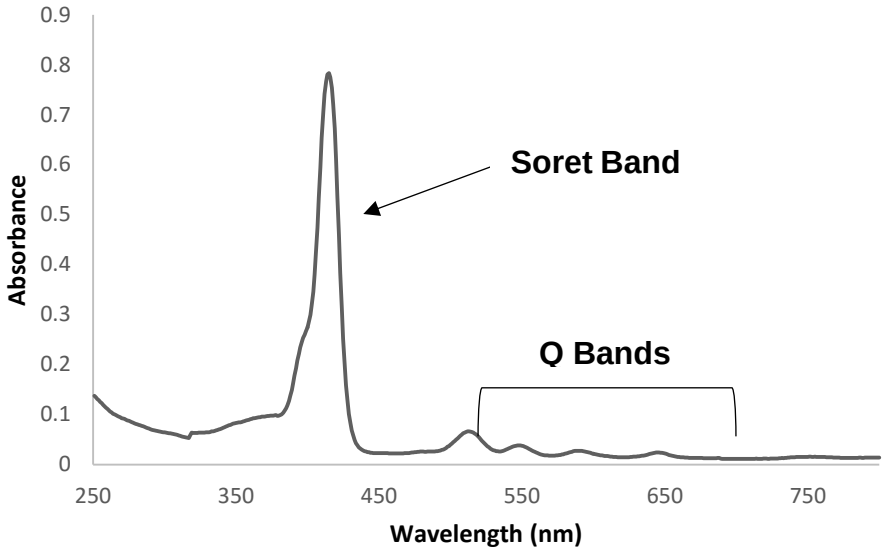

Figure 10. UV-Vis spectrum of a typical synthetic porphyrin showing the Soret band and Q bands.

Over the years, many second-generation porphyrin-type photosensitisers have been synthesized and developed. Two important examples are *meta*-tetra(hydroxyphenyl)porphyrin **(8)** (*m*-THPP) and protoporphyrin IX **(9)** (Figure 11).

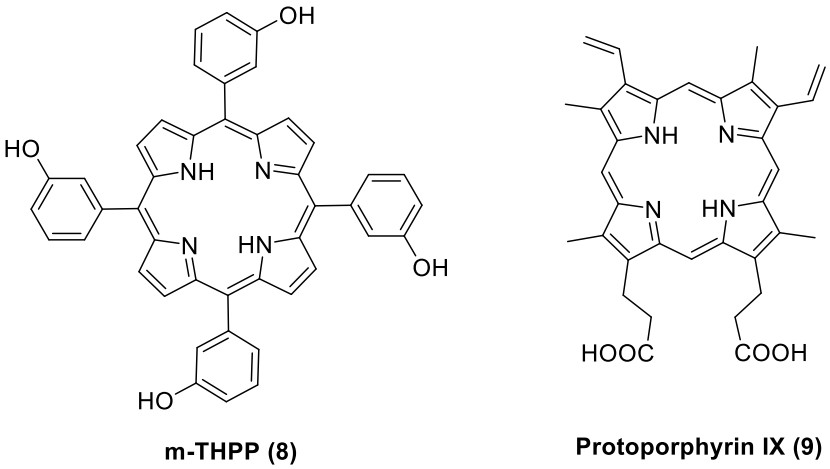

Figure 11. Molecular structures of m-THPP **(8)** and Protoporphyrin IX **(9)**.

m-THPP **(8)** is one member of a large possible family of tetrahydroxyphenyl porphyrins. The hydroxyl functional group makes this group of molecules amphiphilic and causes small hyperchromic and bathochromic effects on Q Band 1. *m*-THPP **(8)** has been shown to be 25-30 times more potent compared to HpD in tumour photonecrosis upon irradiation at 648 nm.[36] Amongst the other different isomers studied, the all-*ortho* derivative was found to cause severe skin photosensitivity and clinical trials were subsequently discontinued.[2, 36]

Protoporphyrin IX **(9)** is actually a natural product and is an important precursor in haem biosynthesis. Its use in PDT and diagnosis is via its biosynthetic precursor, 5-aminolevulinic acid (5-ALA or ALA), or prodrugs thereof. ALA-induced protoporphyrin IX **(9)** was approved by the US FDA (Levulan) in 1999 for the treatment of actinic keratosis. The methyl ester of ALA (Metvixia) received FDA approval in 2004 for treatment of actinic keratosis, whereas its hexyl ester (Hexvix) received approval in 2010 for bladder cancer diagnosis and was shown to produce PpIX 50-100 times more efficiently than ALA at an equivalent dosage.[19, 37] The methyl ester of ALA is also an active component of Visonac, which is currently in phase 2 clinical trials (NCT01347879) in the USA for the treatment of acne vulgaris.[38]

1.3.2.2 Chlorins and bacteriochlorins

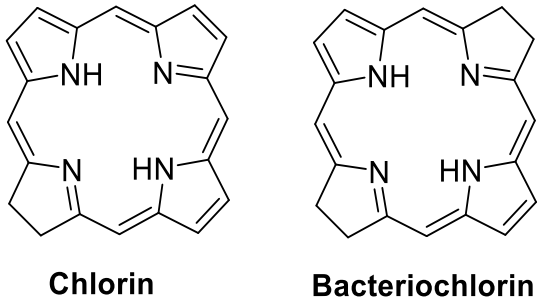

Figure 12. Basic structure of chlorins and bacteriochlorins.

Chlorins and bacteriochlorins are β-dihydroporphyrins and β-tetrahydroporphyrins respectively that are formed by reduction of one or two peripheral double bonds in the porphyrin skeleton (Figure 12).[31] These macrocycles play an important role in nature. Chlorin is the chromophore of

chlorophyll *a* and *b* **(10, 11)**, while bacteriochlorin is the chromophore of the bacterial photosynthetic pigment, bacteriochlorophyll *a* **(12)** (Figure 13). Compared to a porphyrin, a chlorin has a much more intense Q Band I and it is shifted to a longer wavelength. The intensity of this band is further increased in the case of bacteriochlorins.[2]

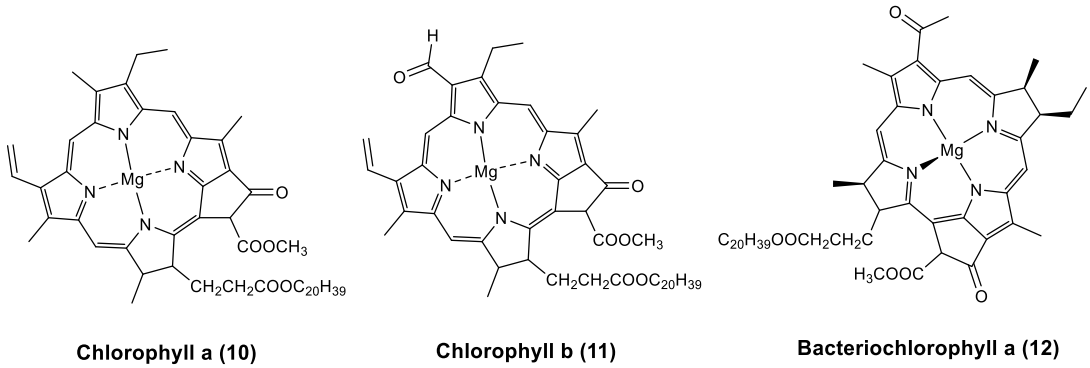

Figure 13. Structure of chlorophyll a **(10)**, chlorophyll b **(11)** and bacteriochlorophyll a **(12)**.

Several photosensitisers from the chlorin group have been evaluated for their PDT efficacy. This includes the benzoporphyrin derivative monoacid ring A **(13)** (BPD-MA, verteporfin, Visudyne®), *meta*-tetra(hydroxyphenyl)chlorin **(14)** (*m*-THPC, Foscan®), tin ethyl etiopurpurin **(15)** (SnET2, Rostaporfin, Purlytin™) and *N*-aspartyl chlorin e6 **(16)** (NPe6, Talaporfin, Ls11).[35] Verteporfin **(13)** is activated by light at 689 nm and was approved by the FDA in 1999 for the treatment of age-related macular degeneration (Figure 14). Verteporfin also causes less skin photosensitivity than Photofrin® due to the rapid clearance of the drug from the body.[39, 40]

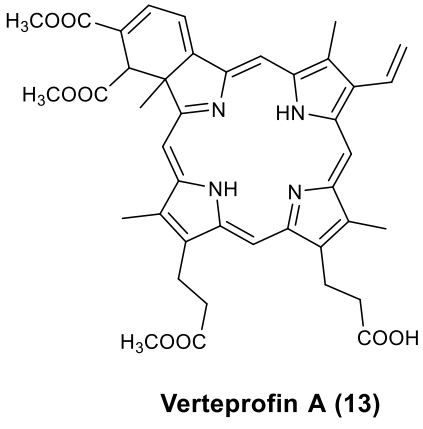

Figure 14. Structure of verteporfin **(13)**.

m-THPC **(14)** (Temoporfin, Foscan®), which is formed by reduction of one of the pyrrole rings in *m*-THPP **(8)**, has a red-shifted Q band absorption compared to photofrin **(5)** λ_{max} (652 nm vs 630 nm) and a significantly higher molar absorption coefficient (15 fold) (Figure 15).

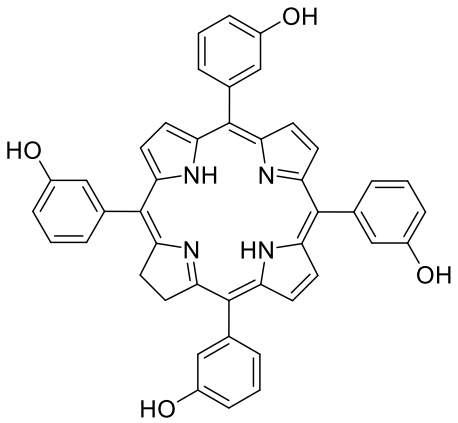

Figure 15. Structure of m-THPC **(14)**.

It was the first sensitizer that was used in a clinical study for PDT of prostate cancer in 2002.[41] It has received regulatory approval in Europe for the treatment of neck and scalp cancer and is also used successfully in the treatment of breast and pancreatic cancer.[35, 42, 43] A water-soluble formulation of *m*-THPC has also been developed under the name of Fospeg® and showed lower dark toxicity when tested in the epidermoid carcinoma cell line, A431, over a wide range of fluences. The only drawback that has been reported for *m*-THPC is high skin photosensitivity, which was similar to that of Photofrin.[19, 44, 45]

Other chlorin derivatives such as SnET2 **(15)** (Rostaporfin, Purlytin™) have completed phase 2 clinical studies for cutaneous AIDS-related Kaposi's sarcoma (Figure 16).[46] Rostaporfin may be activated at a much greater depth in tissue compared to Photofrin® by irradiation at 664 nm, but has problems of possible dark toxicity and skin photosensitivity.[47] *N*-Aspartyl chlorin e6 **(16)** (NPe6, Talaporfin, Ls11) was approved in Japan in 2003 for the treatment of lung cancer and has also shown potential for the treatment of fibrosarcoma, liver, brain and oral cancer. Unlike Photofrin®, NPe6 causes minimal skin photosensitivity (Figure 16).[48, 49]

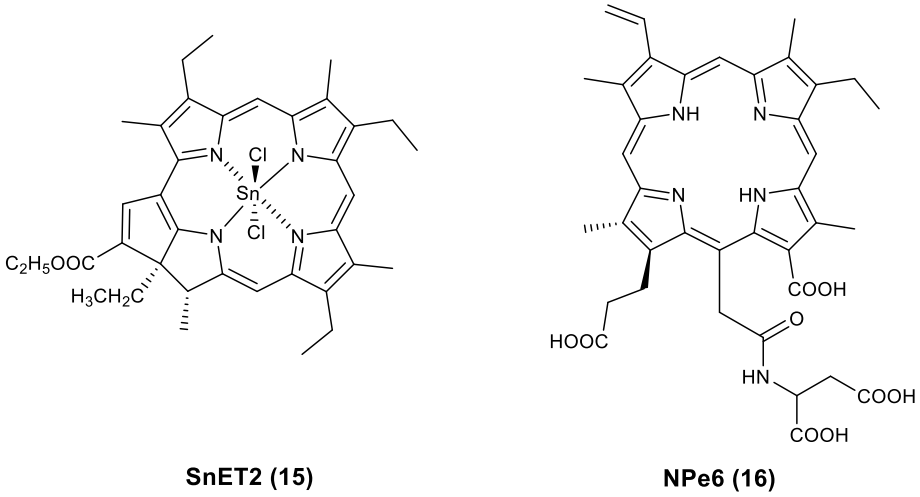

SnET2 (15) **NPe6 (16)**

Figure 16. Structures of SnET2 **(15)** and NPe6 **(16)**.

Several clinically important photosensitisers from the bacteriochlorin group like TOOKAD and its water-soluble derivative TOOKAD Soluble have been tested against prostate cancer.[50, 51] LUZ11 is another derivative which recently completed phase 2 clinical trials for head and neck cancer.[52] The key features for photosensitisers of the bacteriochlorin group are that near IR light between 700-800 nm may be used for activation, and this has been found to be effective against pigmented tumours which are coloured and can absorb longer wavelengths.[53]

1.3.2.3 Phthalocyanines and naphthalocyanines

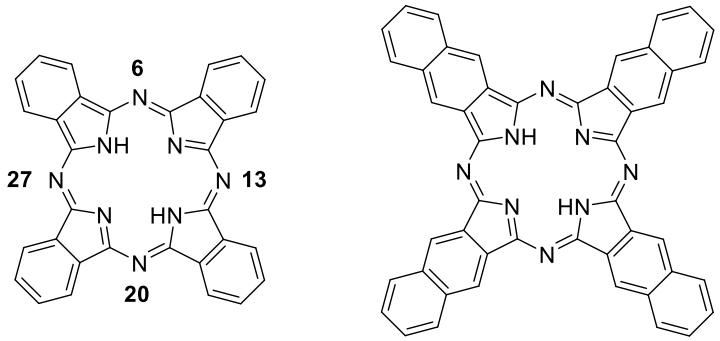

Phthalocyanine **Naphthalocyanine**

Figure 17. Basic structures of phthalocyanines and naphthalocyanines.

Phthalocyanines (Pc) also fall into the tetrapyrrole group of photosensitisers, but have the carbon atoms at the meso positions (6, 13, 20 and 27) replaced by N. The presence of multiple meso-nitrogens and fused benzene rings

results in the formation of stable metal complexes from these photosensitisers. Unlike porphyrins, the Q bands (650-750 nm) of phthalocyanines are much more intense than the Soret bands, a property which is ideal for PDT.[2, 41]

The complexes of phthalocyanines with Zn, Al, and Si **(17)**-**(19)** have been used in clinical studies, however due to the hydrophobic nature of these compounds, a formulation modification (e.g liposomes) was required (Figure 18).[35] The aluminium complex of phthalocyanine **(18)** (Photosens) was approved in Russia in 2001 for the treatment of stomach, skin, lip, oral and breast cancer, however it showed prolonged photosensitivity for several weeks.[54] Silicon phthalocyanine **(19)** (Pc4) has undergone *in vivo* and clinical studies along with completion of phase 1 trials for actinic keratosis, Bowen's disease, skin cancer and mycosis fungoides (NCT00103246).[55]

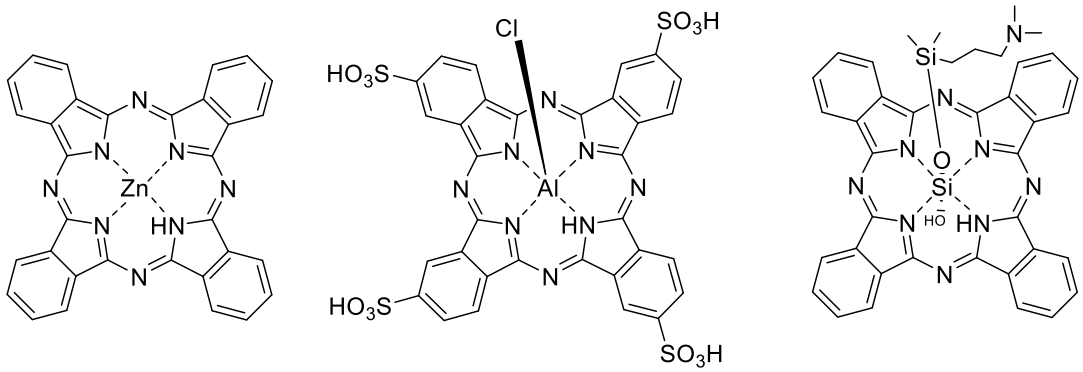

Figure 18. Structures of some clinically used phthalocyanine photosensitisers **(17)-(19)**.

1.3.2.4 Non-porphyrin based photosensitisers

Over the years many non-porphyrin photosensitisers have been developed and include among others anthraquinones, phenothiazines, xanthenes, cyanines and curcuminoids (Figure 19). Hypericin **(20)** is an anthraquinone derivative extracted from St. John's Wort and has a peak absorption at 600 nm. It has been shown to release ROS to target cancer cells, however clinical trials against squamous cell carcinoma and basal cell carcinoma have yielded unsatisfactory results.[56, 57] Phenothiazinium dyes such as methylene blue **(21)** (absorbs at 660 nm) and toluidine blue **(22)** (absorbs at 630 nm) have been studied for their antimicrobial applications as well as for anti-cancer

properties.[58, 59] Methylene blue **(21)** has been included in clinical PDT treatments for basal cell carcinoma and Kaposi's sarcoma as well as completed clinical trials for chronic periodontitis (NCT01535690).[60, 61] Toluidine blue **(22)** is currently undergoing Phase 3 clinical trials for chronic periodontitis (NCT01330082).[35, 58, 60, 62] Rose Bengal **(23)** comes from the xanthene class of photosensitiser and absorbs at 549 nm. The presence of a heavy atom such as iodine has been shown to increase the triplet yield of the molecule by intersystem crossing leading to an enhanced singlet oxygen yield. Rose Bengal **(23)** has entered clinical trials for allogeneic stem cell transplantation.[63] Curcumin **(24)** is a well-known component of the spice turmeric and is a new entry in the PDT field. It absorbs at 420 nm and is a hydrophobic molecule requiring a formulation vehicle in order to be used as a photosensitiser. Curcumin **(24)** has found most applications so far in antimicrobial PDT for the destruction of oral pathogens.[64, 65]

Apart from the photosensitisers discussed above, which have been studied in some detail and in some cases have undergone clinical trials, there are some further miscellaneous photosensitisers that have been investigated for *in vitro* anti-microbial applications. These include cationic riboflavin **(25)** (flavin-based, natural product-derived)), ASQI **(26)** (squaraines, synthetic dye), DIMPy-BODIPY **(27)** (BODIPY, synthetic dye), hypocrellin **(28)** (natural product) and cationic phenalenones **(29)** (synthetic dyes)-see Figure 19.

Non-porphyrin based photosensitisers

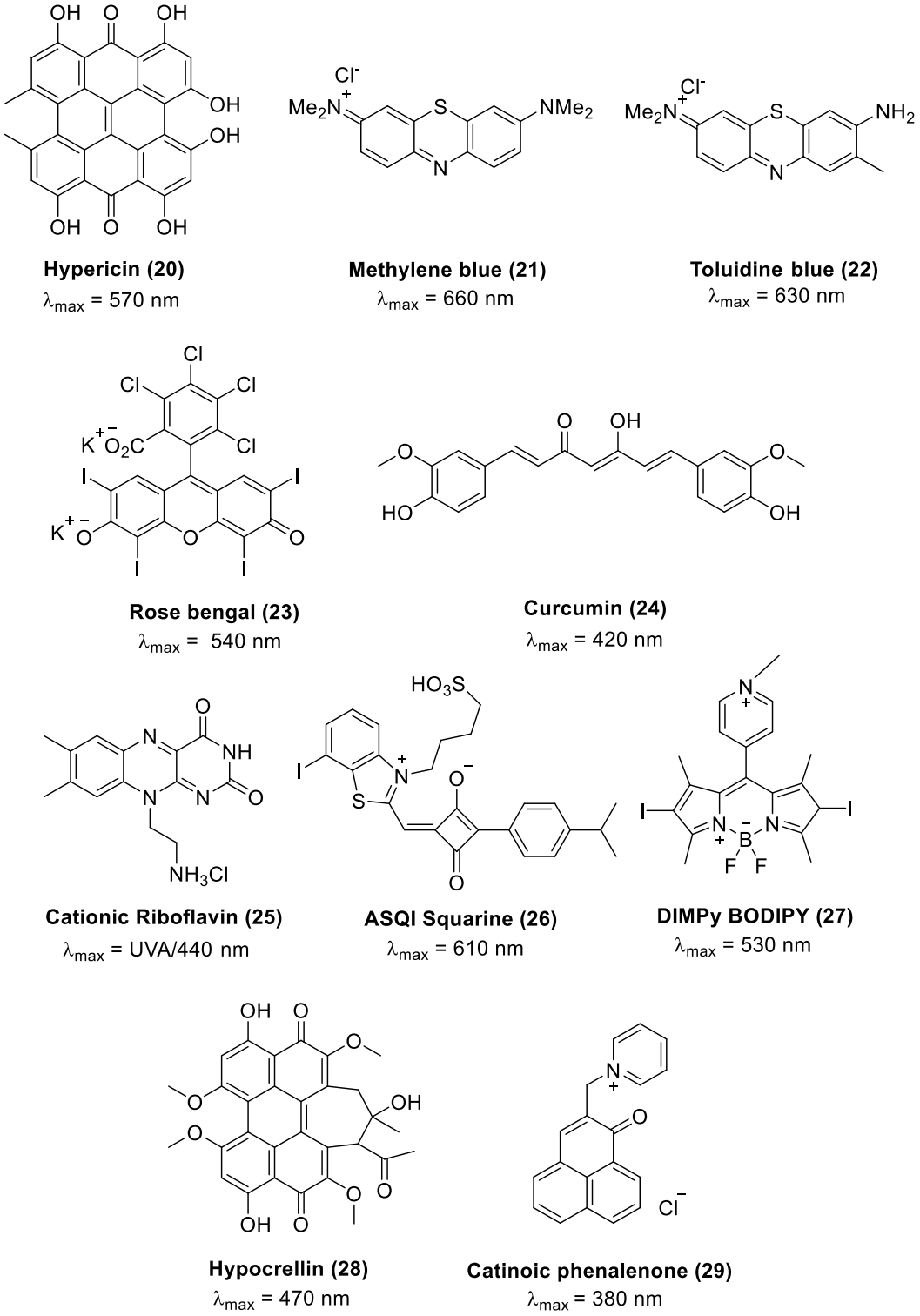

Figure 19. Structures of some non-porphyrin photosensitisers **(20)**-**(29)**.

1.3.3 Third-generation photosensitisers

Recently, much work in the PDT field has been focused on the so-called 3rd generation of photosensitising agents, with the aim of increasing the selective accumulation of photosensitisers in targeted tissue, usually tumours. Some of the strategies adopted towards this approach are the conjugation of photosensitisers with biologically active elements such as peptides, anti-tumour monoclonal antibodies, proteins such as transferrin or epidermal growth factor, folic acid and carbohydrate derivatives.[53, 66]

For example, You *et al.* in 2015 investigated the synthesis and evaluation of derivatives of the non-selective photosensitiser, pheophorbide-a **(30)**, conjugated to folic acid **(31)** and three specific targeting peptides, CRGDLASLC **(32)**, *cyclo*(RGDfK) **(33)** and leuprorelin **(34)** (Figure 20).[67]

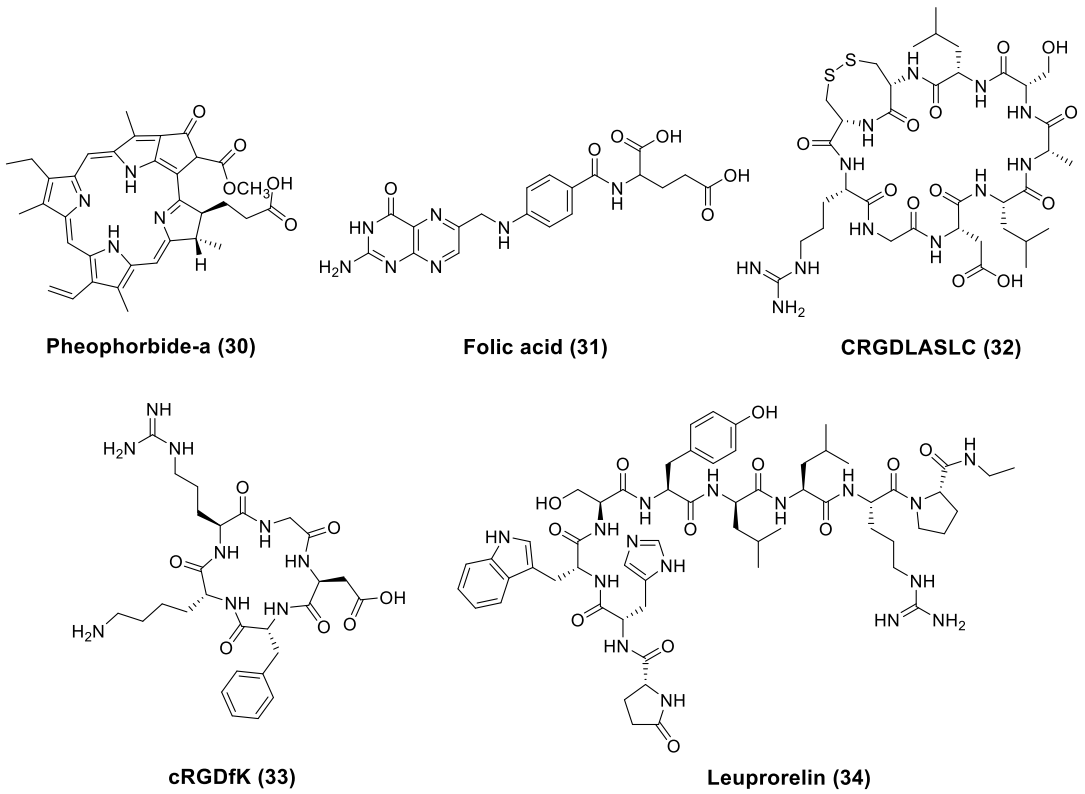

Figure 20. Structures of pheophorbide-a **(30)** and different targeting units **(31)**-**(34)**.

Folic acid **(31)** is a ligand which targets the folate receptor which is overexpressed on the surface of many malignant cells. On the other hand, the CRGDLASLC **(32)** peptide binds to the $\alpha_v\beta_6$ integrin receptor, which is

overexpressed in head and neck cancer cells, whereas *cyclo*(RGDfK) **(33)** recognises the $\alpha_v\beta_3$ integrin receptor which plays an important role in tumour angiogenesis, progression and metastasis of various cancer cells. Leuprorelin **(34)** has been approved for the treatment of advanced stage prostate cancer and can be used as a targeting unit for the luteinizing hormone-releasing hormone (LHRH) receptor that is overexpressed in ovarian, breast and prostate cancer cells. Biological evaluation showed enhanced cellular uptake followed by PDT activity for all the pheophorbide-a **(30)** conjugates in cells expressing the receptors of corresponding targeting units.

Stuchinskaya *et al.* have reported antibody-phthalocyanine gold nanoparticle conjugates in which anti-HER2 antibodies were attached to the nanoparticles to enhance the drug targeting.[68] The 4-component system (anti-HER2 antibody–phthalocyanine photosensitiser–PEG–gold nanoparticle) was tested in SK-BR-3, MDA-MB-231 and MCF-10A cell lines and the *in vitro* studies revealed enhanced selectivity towards breast cancer cells overexpressing the HER2 epidermal growth factor receptor, with enhanced PDT activity in these cell lines also.

Ligand-targeted PDT with verteporfin **(13)** has been attempted by conjugation with the factor VII (fVII) protein.[69] fVII has a high affinity and specificity for tissue factor (TF), which has been shown to be overexpressed in many types of cancer cells including solid cancers and leukaemia, and has also has selective expression in pathological neovascular endothelial cells in cancer. Results with a fVII-verteporfin conjugate showed it to have better selectivity and a stronger PDT activity in the MDA-MB-231 breast cancer cell line compared to verteporfin itself.

Finally, Kascakova *et al.* have investigated the cell line-specific uptake and photodynamic activity of two conjugates **(36)** and **(37)** containing chlorin e6 **(35)** and the somatostatin analogue [Tyr3]-octreotate (Figure 22). [70] Biological evaluation in human erythroleukemic K562 cells showed enhanced uptake for conjugate **(36)** in cell lines overexpressing the neuropeptide somatostatin receptor compared to wild-type cells. Compared to non-conjugated Ce6 **(35)**, PDT activity for **(36)** was lower, however it had higher photostability than Ce6

(35) which could compensate for its lower phototoxicity. Conjugate **(37)** did not show any receptor-mediated activity, possibly due to its high hydrophobicity.

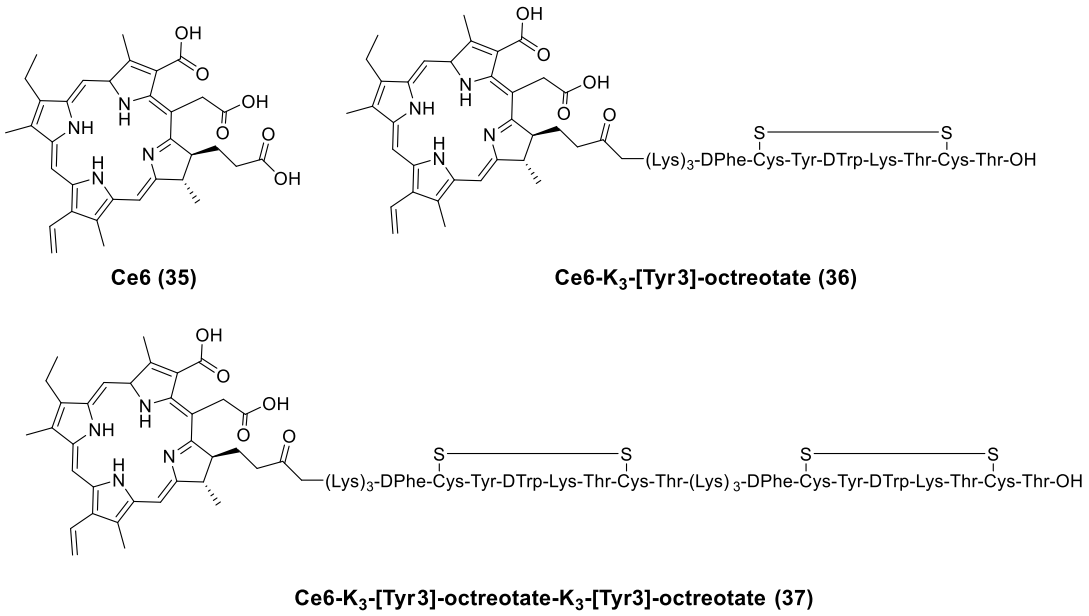

Figure 21. Chemical structures of Ce6 **(35)** and its [Tyr3]-octrotate conjugates **(36)** and **(37)**.

1.4 Novel PDT techniques

1.4.1 Nanotechnology

There have been many applications of nanotechnology in the development of photosensitising agents for PDT. Nanoparticles are in general sub-microscopic particles made from naturally occurring or synthetic materials and can carry multiple copies of theranostic agents (Section 1.4.4) in a targeted manner.[20] The development of nanoparticles for PDT has the following advantages:

1. Nanoparticles have a large surface to volume ratio. A large number of photosensitiser molecules can thus be delivered to the target cells.[71]

2. Diffusion of photosensitiser molecules into tumour tissue is facilitated, as is their retention, due to the enhanced permeability and retention effect (EPR).[72]

3. Premature release of photosensitisers and their inactivation by plasma components is prevented, thus reducing their overall photosensitivity.[73]

4. Nanoparticle encapsulation can give photosensitisers amphiphilic properties which thus allows them to travel unhindered through the blood stream.[74]

5. Nanoparticles allow surface modification with functional groups or targeting groups which further improves the biodistribution, pharmacokinetics, cell uptake and targeting potential.[75]

Nanoparticles for PDT applictions can be classified into active and passive carriers based on the functional roles they play in enhancing PDT activity. The active carriers can be further sub-classified based mechanism of activation into photosensitiser nanoparticles, upconversion nanoparticles and self-lighting nanoparticles. The passive carriers can be further sub-classified into biodegradable and nonbiodegradable nanoparticles based on the material composition.[76] For example, Khdair *et al.* investigated dioctyl sodium sulfosuccinate (Aerosol-OT) and sodium alginate for the encapsulation of the photosensitiser methylene blue and evaluated these nanoparticles in two

breast cancer cell lines: MCF-7 and 4T1.[77] Following PDT, the level of intracellular reactive oxygen species was significantly increased and a higher incidence of necrosis was observed in both cell lines. Nuclear localization of methylene blue from the nanoparticles was also observed in the tumour cells, whereas free drug treatment resulted in accumulation of the drug in endolysosomal vesicles.

1.4.2 Two-photon PDT (TP-PDT)

In a single-photon PDT experiment, the photosensitiser absorbs a photon of light and moves to an excited singlet state which on intersystem crossing leads to a triplet state. The duration of this triplet state allows its interaction with molecular oxygen and the formation of singlet oxygen which is highly reactive and causes almost instantaneous cell damage (Type 2 reaction). The minimum energy required in this process makes only visible light of wavelengths below 850 nm suitable. Two-photon PDT (TP-PDT) involves absorption of two low energy photons simultaneously by the photosensitiser and leads to a total energy absorption which is twice that of each absorbed photon (Figure 22).[78]

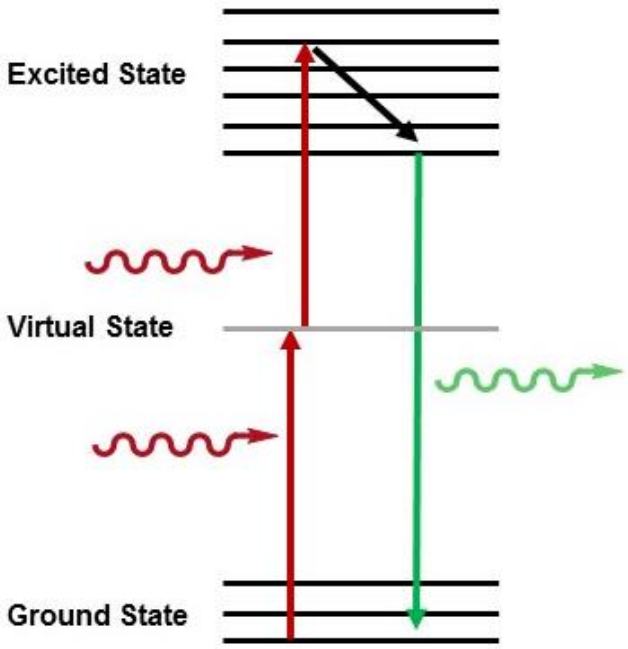

Figure 22. Representation of a two-photon excitation process.

TP-PDT is thus advantageous compared to single photon PDT, in that wavelengths longer than 850 nm can provide enough energy to produce singlet oxygen. This in turn means that longer wavelengths (IR) could be used which will penetrate deeper into the targeted tissue.[79] Also, since this process is highly dependent on the intensity of light, parameters can be altered in such a way that the event of TP-PDT occurs only in the focal plane of light delivered from a pulsed laser, thus achieving a precise spatial targeting. For example Collins *et al.* in 2008 reported the synthesis and evaluation of a series of photosensitisers derived from porphyrin-based molecular wires **(38a-e)** which had high two-photon cross-sections (Figure 23).[79]

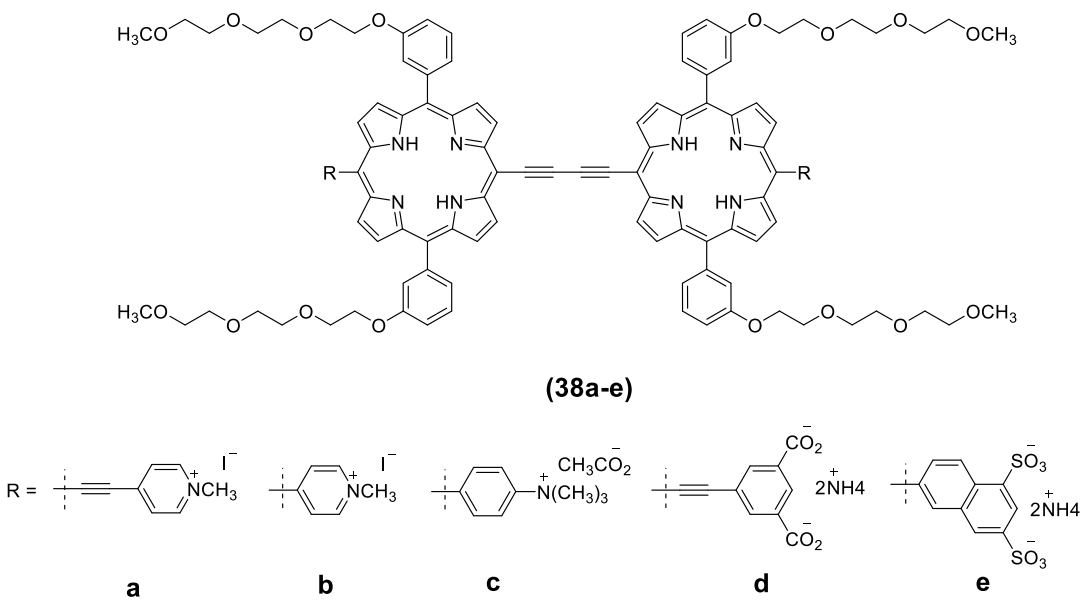

Figure 23. Structure of conjugated porphyrin dimers used in a two photon PDT study.[79]

These compounds were evaluated *in vitro* in human ovarian adenocarcinoma cells (SK-OV-3) and the results were compared with a commercial photosensitiser, verteporfin. **(38a)** was found to be the most promising candidate amongst other derivatives (Figure 23) based on its PDT activity, cell uptake and high two-photon cross-section, and was taken further for *in vivo* studies to test selective closure of blood vessels using the dorsal skinfold window chamber model for non-invasive visualization of blood vessels. The results were encouraging and the authors were able to demonstrate the feasibility of two-photon photodynamic therapy as a new strategy for targeted occlusion of blood vessels.

1.4.3 Metronomic PDT

The term metronomic was introduced to describe continuous low-dose administration of chemotherapeutic agents after it was found that low-dose chemotherapy is more anti-angiogenic than the conventional high-dose therapy.[80, 81] Metronomic PDT (mPDT) involves delivering both the light and the photosensitiser over an extended period of time at a very low dose, thus improving the tumour-specific response via cell-specific apoptosis.[82] However mPDT presents two technical challenges:[82]

1. Continuous delivery of photosensitiser over an extended period of time (days or weeks) to ensure a high concentration of drug within the tumour and avoiding systemic toxicity.
2. Continuous delivery of light to the tumour in a minimally invasive way.

Davies *et al.* in 2007 reported a study which involved the delivery of ALA via mPDT for up to 4 days to CNS-1 tumour-bearing female Lewis rats. Results from bioluminescence imaging showed that there was no sign of any tumour regrowth at 26 days post-tumor implantation.[83]

1.4.4 Theranostics

Theranostics refers to the combination of therapeutics and diagnostics and is a term introduced by Funkhouser in 2002.[84] Such systems can deliver both imaging and therapeutic agents within the same dose, the functionality of which could be switched between either thus leading to improved detection and treatment of disease (Figure 24). Theranostics can thus help in understanding the phenotype and heterogeneity of a tumour before the treatment is initiated.

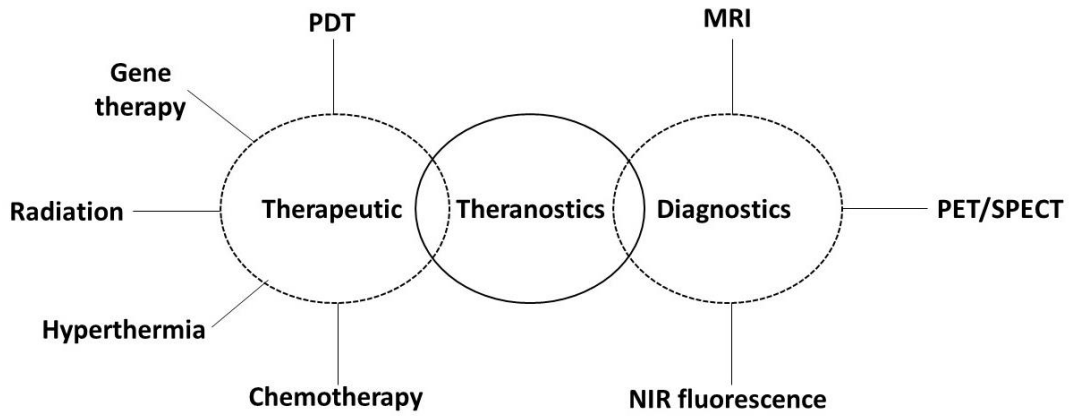

Figure 24. Representation of concept for theranostics.[85]

Kopelman *et al.* (2005) reported a theranostic system which consisted of a photosensitiser (Photofrin) and MRI contrast agents encapsulated into a polyacrylamide core.[86] The surface of the nanoparticle was further functionalized with PEG groups an integrin receptor- targeting peptide (Figure 25). Encapsulation of Photofrin within the nanoparticle was advantageous as it prevented the direct exposure of the sensitiser to the physiological environment and also allowed a significant reduction in the time interval between administration of Photofrin and light illumination (from 24 h to 1 h). Biological evaluation indicated selective accumulation of the nanoparticles in an $\alpha_v\beta_3$-overexpressing cell line (MDA-435) compared to MCF-7 cells ($\alpha_v\beta_3$ negative). The *in vivo* therapeutic activity of the Photofrin-containing nanoparticles was evaluated in rats bearing intracerebral 9L tumours, and gliomas treated with the nanoparticles produced massive regional necrosis which resulted in shrinkage of tumour mass. Tumour kill was also established by increased mobility of water molecules, which was monitored by spatially resolved magnetic resonance around the tumour cells, through the MRI component of the theranostic agent.

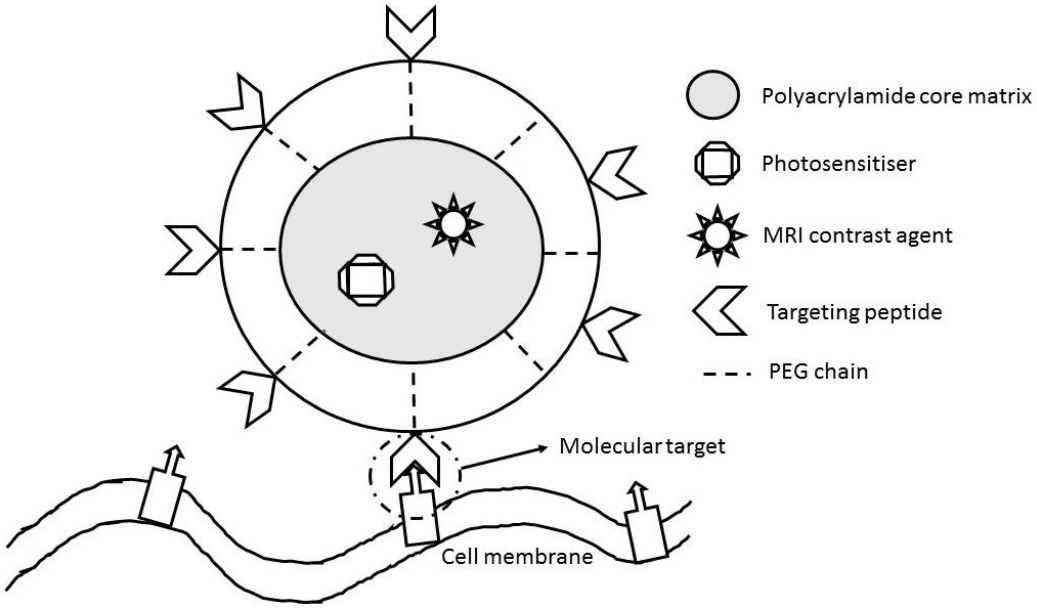

Figure 25. Schematic representation of a theranostic system containing photosensitiser, MRI agent, targeting peptide and PEG group.[86]

Other novel strategies have also been adopted to bring imaging and therapeutic agents together such as nanoagents (carbon nanotubes), quantum dots (QDs) and liposome-like porphysomes.[87]

1.5 Light sources in PDT

To achieve a required PDT effect, the target tissue needs to be irradiated with light of an appropriate dose and wavelength which in turn generates enough singlet oxygen.[88] Many light sources have been used clinically in PDT (Table 1) with further types currently under investigation.[89] Lamps and lasers are the two most commonly used types of light source for PDT, and the choice of one over the other depends on the location of the tumour, dose of light required and the type of photosensitiser used.

Lasers (light amplification by stimulated emission of radiation) provide light which is easily focussed and give a single colour (monochromatic).[90] A major advantage of using lasers is that they produce monochromatic light which can be injected directly into fibres and delivered to the target site using specially designed fibre optics.[89] Lamps on the other hand, provide a broad range of wavelengths and can be combined with different photosensitisers having different absorption maxima. Hence a common type of lamp could be used for PDT treatment with Foscan, Photofrin or ALA (eg. Dye laser).[89]

Different light sources have been approved clinically for ALA-PDT. Blu-U® light has been approved for Levulan® emitting at 400 nm, whereas Aktilite® has been approved for Metvixia® emitting at 630 nm.[91]

In recent years light emitting diodes (LED) have shown potential in PDT. LEDs offer some advantages over their counterparts; they are more affordable, stable, require low maintenance and can be arranged in a number of combinations to effectively illuminate difficult anatomic areas.

Table 1. Clinically used light sources in PDT (adapted from Brancaleon *et al.*).[89]

Light Source		Wavelength	Bandwidth	Light delivery
Lasers	Argon laser	488 and 514.5 nm	Monochromatic	Direct or optical fibre
	Dye laser pumped by Argon laser	500-750 (based on type of dye)	5-10 nm	Direct or optical fibre
	Metal vapour laser	UV or visible (based on type of metal)	Monochromatic	Direct or optical fibre
	Dye laser pumped by metal vapour	500-750 (based on type of dye)	5-10 nm	Direct or optical fibre
	Solid state optical parametric oscillator	250-2000 nm	Monochromatic	Direct or optical fibre
	Semiconductor diode lasers	600-950 nm	Monochromatic	Optical fibre
Lamps	Tungsten filament	400-1100 nm	10-100 nm	Direct or via
	Xenon arc	300-1200 nm	10-100 nm	Liquid light guide
	Sodium (phosphor coated)	590-670 nm	10-80 nm	Direct illumination
	Fluorescent	400-450 nm	Approx. 30 nm	Direct illumination
	Metal Halide	250-730 nm (depending on metal)		Direct or Liquid light guide

1.6 Singlet Oxygen

Molecular oxygen has a triplet electronic configuration in its ground state with two unpaired electrons occupying two degenerate antibonding π -orbitals (Figure 26). The excited singlet state however, which exists in two forms ($^1\sum_g O_2$ and $^1\Delta_g O_2$), has electrons with opposite spins.[92] The $^1\Delta_g O_2$ form (also known as $^1O_2$) is involved in the process of photosensitization, while $^1\sum_g O_2$ is too short-lived (10^{-11}–10^{-9} s in solution) to show any biologically activity.[93]

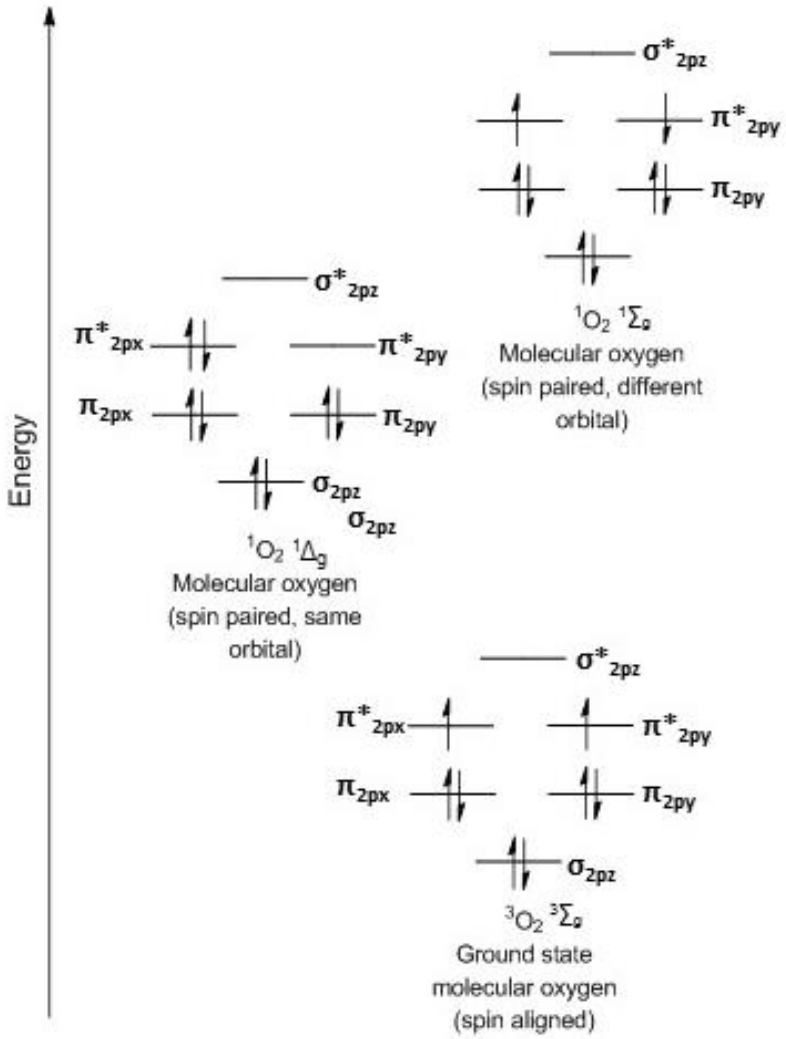

Figure 26. Molecular orbital diagram for molecular oxygen (adapted from Josefsen *et al.*).[92]

Unlike other reactive oxygen species, singlet oxygen is generally produced only when exogenous or endogenous photosensitisers absorb light energy. However, reactive oxygen species such as H_2O_2 and O_2^- are produced under normal physiological conditions inside cells and can readily interconvert to

other ROS species. This can make it difficult to identify which ROS is responsible for a particular cellular response.

The reaction between $^1O_2$ and proteins has multiple effects and includes oxidation of side-chains, backbone fragmentation, dimerization/aggregation, unfolding or other conformational changes, enzymatic inactivation, and alterations in cellular handling and turnover. The most common targets for $^1O_2$-mediated oxidations are lipids (cholesterol and phospholipids), aromatic and heteroaromatic amino acids (Trp, Tyr, His), sulfur-containing amino acids (Cys, Met), and nucleic acid bases (guanine and guanosine).

Tryptophan **(39)** is a highly sensitive towards various oxidizing agents including singlet oxygen. In general, tryptophan undergoes photooxidation to give an unstable primary intermediate, 3-hydroperoxyindolenine **(39a)**, which then further rearranges to form N-formylkynurenine **(39c)** (FMK).[94] At least three different pathways have been proposed for this transformation to FMK **(39c)** (Scheme 2). The first pathway involves heterolysis of the O-O hydroperoxide bond, followed by ring expansion to yield **(39h)** which then breaks down into FMK **(39c)**.[95, 96] Another pathway involves homolysis- or heterolysis-induced decomposition of O-O bond of the tricyclic hydroperoxide (**39e**). This gives an 8-membered hydroxyketone intermediate **(39f)** followed by decomposition to FMK **(39c)**.[97] Finally, a dioxetane **(39b)** that is derived from a ring-chain tautomerism between **(39)** and **(39e)** is also a likely intermediate.[98, 99]

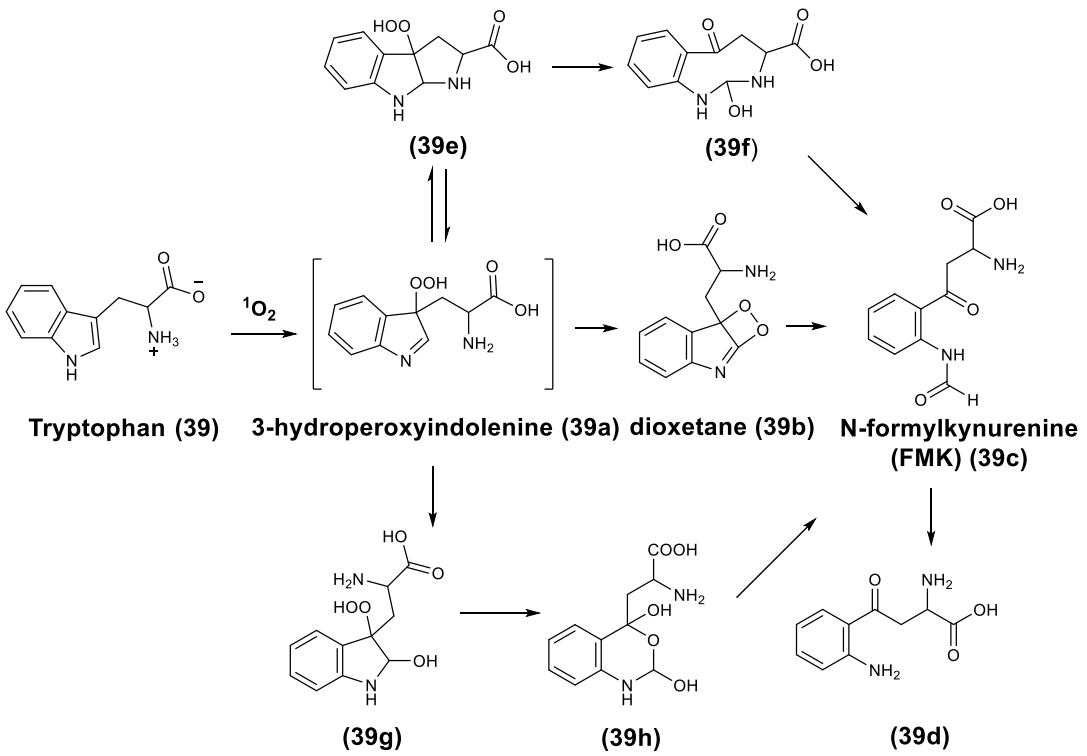

Scheme 2. Proposed reaction pathways for singlet oxygen-mediated oxidation of tryptophan.[94]

1.7 Photodynamic action

A photosensitiser on exposure to light of a specific wavelength can deliver a PDT effect mainly through the following mechanisms:

1. Direct cytotoxic effects
2. Vascular damage
3. Immunological responses

The biological substrates typically involved are mitochondria, lysosomes, plasma membranes and nuclei, and their oxidative damage ultimately leads to cell death (Figure 27). A number of factors may govern the importance of one mechanism over another, such as the type of photosensitiser, its extracellular and intracellular localization, dose of photosensitiser or light, type of tumour and its level of oxygenation.[33, 100, 101]

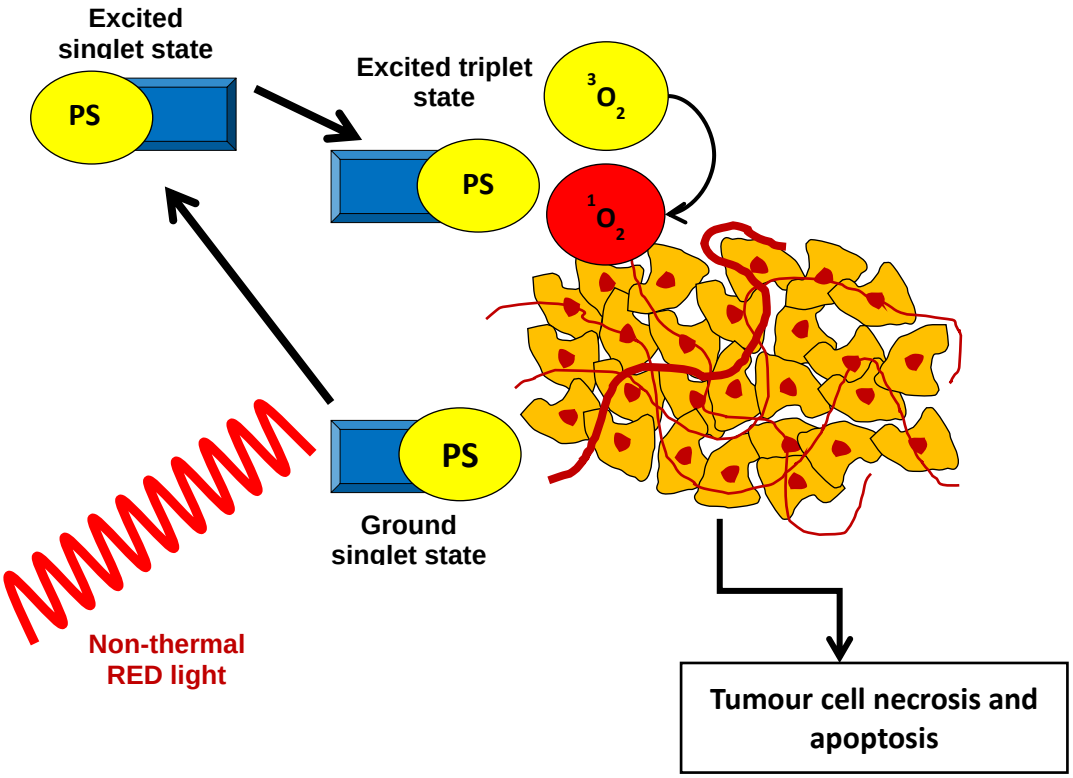

Figure 27. Overview of the PDT effect. Targeted generation of $^1O_2$ in tumour tissue leads to a selective photodynamic effect.

A detailed description for each of the biological mechanisms of PDT is given below.

Direct Cytotoxic effects

$^1O_2$ has a very short lifetime and hence the site of photodamage is generally considered to coincide with the location of accumulation of the photosensitiser in tumour cells. Once activated, $^1O_2$ oxidises amino acid residues (Trp, His, Cys, and Met),[102] lipids and proteins thus causing irreversible damage to the sub-cellular targets such as lysosomes, Golgi apparatus, mitochondria and endoplasmic reticulum (ER). The extent of photodamage however depends upon the type of photosensitiser used, dose of light or photosensitiser, and time interval between the photosensitiser being administered and light exposure. Hydrophobic photosensitisers easily diffuse across plasma membranes, while ones which are less hydrophobic, due to their polar nature, are taken up by endocytosis.[103] In general, cell death induced by PDT can occur by apoptosis, necrosis or autophagy. Necrosis is the result of

administration of high doses of photosensitiser or light, thus causing swelling of the cytoplasm and disruption of the plasma membrane, leading to release of the intracellular contents, and triggering an inflammatory response. Apoptosis, also known as programmed cell death, is the most common pathway for PDT. It involves shrinkage of cells, membrane blebbing, nuclear fragmentation and formation of apoptotic bodies which are scavenged by phagocytes.[104]

Vascular damage

Through the process of angiogenesis, solid tumours inside a body grow by inducing growth of blood vessels. This enables them to have a constant supply of oxygen and nutrients.[105] However, due to leaky blood vessels and the incomplete cell borders of the tumour cells, this may allow accumulation of a photosensitiser in the tumour. When photosensitisers are activated with light localized either in the endothelial cells or bound to blood vessel walls, a series of events are triggered which ultimately leads to complete or partial vascular shutdown, severe hypoxia, absolute blood stasis and ultimately haemorrhage.[106]

Immunological responses

The third type of mechanism for biological damage by PDT involves the presence of immune mediators such as leukocytes and macrophage invasion which lead to tumour destruction (immunogenic cell death, ICD).[107] The inflammatory process releases inflammatory mediators such as proteinases, peroxidases, cytokines, growth factors, and other immune-regulators which in turns stimulate various white blood cell components (neutrophils and macrophages).[108] These macrophages remove damaged cancer cells through phagocytosis, which presents the proteins from the tumour cells to CD4 helper T lymphocytes. This is followed by activation of CD8 cytotoxic T lymphocytes which induces both necrosis and apoptosis wherever a new tumour cell is located, thus leading to long term effect.[108] PDT thus tends to be immune-stimulatory whereas chemotherapy and surgery are immunosuppressive.[20]

1.8 Applications of PDT

1.8.1 Anticancer PDT

Clinical applications of PDT in cancer date back to the 1970s when Dougherty and co-workers used HpD against bladder cancer.[29] Since then PDT has found widespread application to treat various types of cancer, some of which are described below:

Skin Cancer

PDT has been extensively applied clinically for the treatment of both malignant and non-malignant skin tumours.[109, 110] Actinic keratoses are dry scaly patches of skin formed as a result of damage due to years of exposure to solar radiation.[111] ALA hydrochloride as a solution (Levulan, DUSA, USA) has been approved for the treatment of actinic keratoses along with blue light (Blu-U lamp, DUSA, USA). The methyl ester of ALA (Metvix in Europe and Metvixia in USA; Photocure ASA in Norway and Galderma S.A in France) has also received regulatory approval in Europe and Australia for the treatment of basal cell carcinoma (BCC), actinic keratoses and Bowen's disease, in combination with red light.[112]

Head and Neck cancer

Photofrin, ALA and Foscan have been evaluated against head and neck tumours.[112] Biel *et al.* conducted clinical studies using Photofrin against squamous cell carcinomas of the oral cavity, pharynx or larynx and Kaposi's sarcoma, along with melanoma and squamous cell carcinoma in the head and neck area. Complete clinical response in patients with early stage oral cavity, larynx, pharynx and nasopharynx lesions monitored over 15 years was observed.[113] Second-generation photosensitisers, such as Foscan, have also been clinically tested against advanced stages of head and neck cancer. In one study with 128 patients, the results showed that there was a complete tumour mass reduction in approximately 40% of lesions, whereas the remaining lesions showed at least 50% reduction.[114] Foscan (Biolitech Pharma Ltd, Dublin, Ireland) was approved by the EU in 2001 for the treatment of head

and neck cancer.[115]

Digestive system cancers

Applications of PDT in the gastrointestinal tract include treatment of Barrett's oesophagus and various grades of dysplasia and oesophageal cancer. Corti *et al.* conducted clinical studies using HpD against oesophageal cancer and concluded that PDT is an effective therapy for early stage cancer, however due to limitations of tissue depth penetration, it was not successful with T2 tumours.[116] Further investigations comparing Photofrin to omeprazole showed that PDT treatment was favoured for the elimination of high grade dysplasia (77% vs 39% with omeprazole).[117] This led to FDA approval in 2003 for Photofrin-mediated PDT in patients who do not undergo surgery.[112] Other applications of PDT in the GI tract include studies against cholangiocarcinoma[118] non-resectable pancreatic cancer[119] and hepatocellular carcinoma.[120]

Urinary system cancers

Porphyrin derivatives have been used both as therapeutic and diagnostic tools for tumours of the urinary system which include prostate cancer and bladder cancers. PDT has been used in the treatment of bladder cancer and the first reported study was with HpD for the treatment of 50 superficial bladder transitional cell carcinomas (TCC) which achieved a 74% complete response rate from a group of 37 patients.[121] The study was also repeated for treatment of refractory carcinoma in situ (CIS) of the bladder, but in spite of the 74% of complete response observed, a significant percentage of patients showed disease recurrence after 2 years.[121, 122] A better response to PDT was observed in bladder CIS and superficial TCC by working on dosimetry and changing the photosensitiser to Photofrin.[123, 124] Studies were also performed with ALA-induced PpIX and similar results were observed, but without the prolonged photosensitivity which was seen with Photofrin.[125] The hexyl ester of ALA has also been shown to accumulate preferentially in neoplastic bladder tissue and produce fluorescence when illuminated. It has been approved for fluorescence diagnosis of bladder cancer (Hexvix, Photocure ASA in Norway

and Cysview, Photocure Inc in USA).[126]

Non-small cell lung cancer (NSCLC)

Hayata *et al.* in 1982 were the first to report the use of PDT for NSCLC using HpD to effect tumour necrosis and reopening of the airway. This has since been found to be more specific and lesion-oriented compared to other available treatments.[127] Studies using Photofrin-mediated PDT were conducted in 54 patients with 64 lung carcinoma lesions and an 85% complete response rate was observed.[128] These results were confirmed by similar studies done by other groups.[128, 129]

Brain tumours

PDT has been utilized as a supporting treatment in various clinical investigations for brain tumours. The photosensitisers that have been used are HpD, ALA and Foscan along with light sources such as lamps, dye lasers, gold vapour potassium titanyl phosphate (KTP) dye lasers, and diode lasers. Stylli *et al.* in 2005 reported a study with HpD on patients diagnosed with glioblastoma multiforme and anaplastic astrocytomas.[130] The results showed that more than 30% of the glioblastoma patients survived for more than two years, whereas in the case of anaplastic astrocytomas, around 60% of the patients treated survived for more than 3 years. Studies were also reported by Muller *et al.*[131] in 2006 and Stummer *et al.*[132] in 2006 using HpD (for supratentorial gliomas) and ALA (for malignant gliomas) respectively, however the results obtained were not statistically significant in comparison to control groups.

1.8.2 Antimicrobial PDT

Antimicrobial PDT also known by the term photodynamic inactivation (PDI), lethal photosensitization, photo-activated disinfection (PAD) or photodynamic antimicrobial chemotherapy (PACT) is seen as a promising alternative treatment for infections associated with multi-drug resistant pathogens. In the past few years, it has been found that by altering the physicochemical properties of certain photosensitisers (e.g. imparting positive charge), they can

be used to inactivate almost all classes of micro-organisms including gram positive and negative bacteria, fungi, viruses and other parasites.[133] Figure 28 below shows a range of human infections that have been clinically treated by PDT.

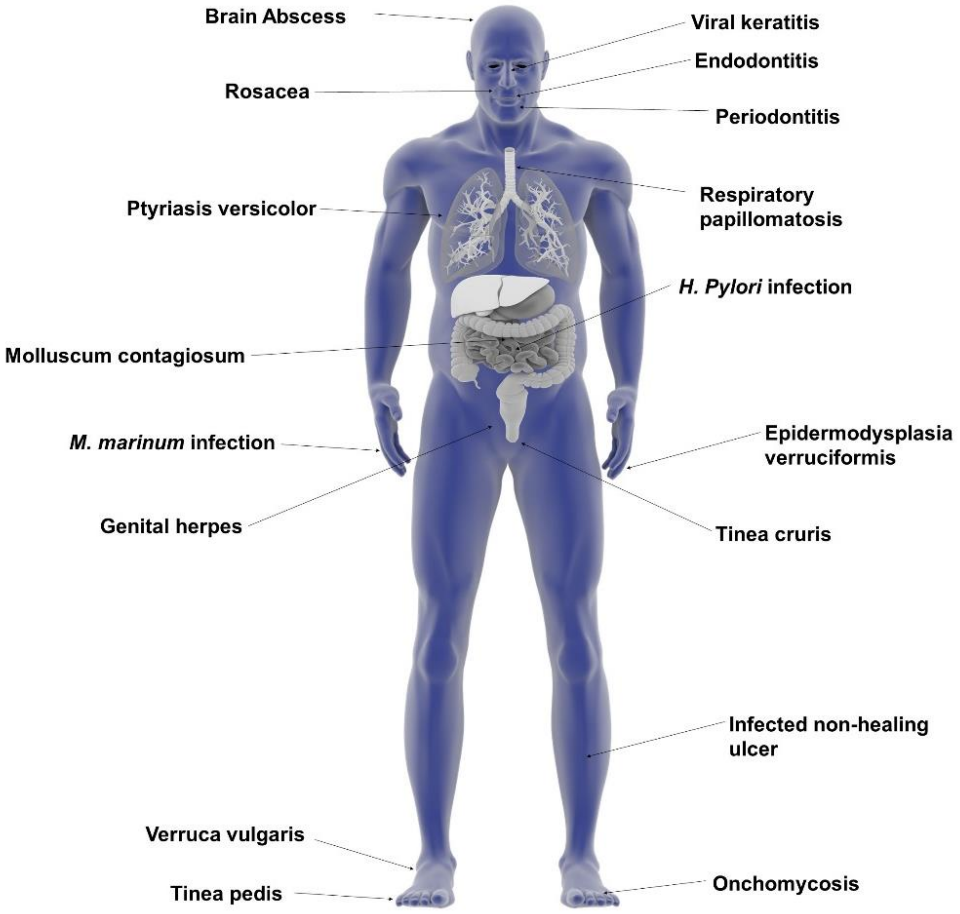

Figure 28. Clinical applications of PDT on a range of human infections (adapted from Kharkwal *et al.*).[133]

Viral Lesions

Clinical studies in the area of viral lesions were initially directed towards the human papilloma virus (HPV). Abramson *et al.* in 1992 reported a study of the use of dihematoporphyrin ether against respiratory papillomatosis caused by HPV, and found that the growth of papilloma decreased significantly in comparison to control patients.[134, 135] Another application of PDT against cutaneous warts caused by the virus was reported by Schroeter *et al*, wherein ALA was administered to patients and complete response with minimum side

effects was observed after PDT.[136]

Dermatological infections

Acne vulgaris is one of the most common non-viral dermatological disorders, and is caused by *Propionibacterium acnes*.[133] Over the years, many PDT studies have been conducted against acne with encouraging results being obtained with either ALA or MAL. Hongcharu *et al.* in 2000 was the first to report a clinical study involving ALA and since then many other clinical studies have been reported involving different light sources or regimens in order to improve the specificity of treatment, as well as to reduce the incubation time of the drug.[137-139]

Dental Infections

PDT has found wide application in the field of dentistry for treatment of common bacterial diseases such as dental caries and periodontal diseases. Periodontitis is an inflammatory disease involving progressive loss of alveolar bone and can cause loosening and loss of teeth. Oliveira *et al.* in 2007 conducted a study involving toluidine blue O and 660 nm laser illumination in patients with aggressive periodontitis, and reported encouraging clinical effects.[140] Ge *et al.* repeated the same study by replacing toluidine blue with methylene blue, and observed less bleeding in the PDT group compared to control group.[141] Other applications of PDT in dentistry include treatment for necrotic pulp and periapical lesions.[133]

Other applications of PDT to treat infections include treatments for leishmaniasis and peptic ulcer disease. Leishmaniasis is a disease caused by protozoan parasites and is usually spread by the bite of certain types of sandflies. There are three main types of this disease: cutaneous (most common), mucocutaneous and visceral leishmaniasis.[133] Asilian *et al.* reported a placebo-controlled randomized clinical trial comparing the efficacy of ALA-mediated photodynamic therapy with topical paronomycin for treatment of old world cutaneous leishmaniasis in a total of 57 patients with 95 lesions.[142] Results showed approximately 94% complete improvement in patients treated with ALA as compared to 41% with paranomycin. Peptic ulcer disease is a

common gastric infection and is found to be commonly associated with *Helicobacter pylori* (*H. pylori*). Wilder-Smith *et al.* conducted the first ever clinical trial involving humans using ALA and blue light (410 nm) and found a marked reduction in *H. pylori* numbers in comparison to the control.[143]

1.9 Aminolevulinic acid-PDT (ALA-PDT)

5- Aminolevulinic acid **(40)** (ALA) is an intermediate in the haem biosynthetic pathway and has been a point of interest for many researchers in the field of PDT (Scheme 3).

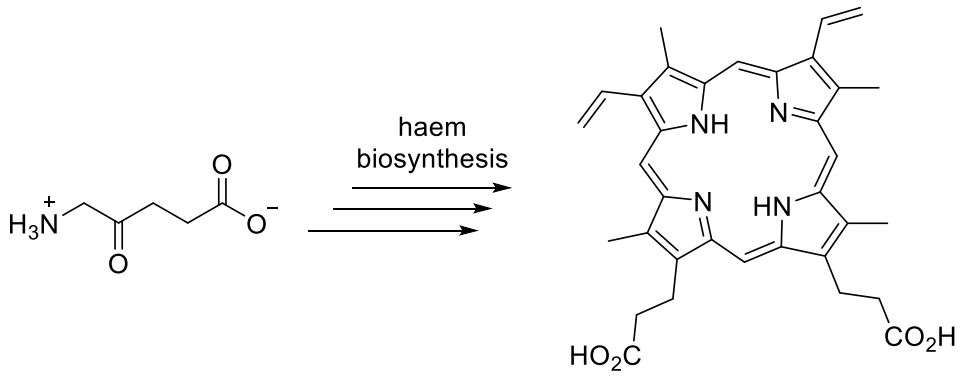

ALA (40) **Protoporphyrin IX (PpIX) (9)**

Scheme 3. Bioconversion of ALA **(40)**.

ALA **(40)** is not a photosensitiser as such, but can induce the intracellular synthesis of a photosensitiser, protoporphyrin IX **(9)** (PpIX) by entering into the biochemical pathway for the synthesis of haem (Scheme 4).[66, 144]

1.9.1 Haem biosynthesis

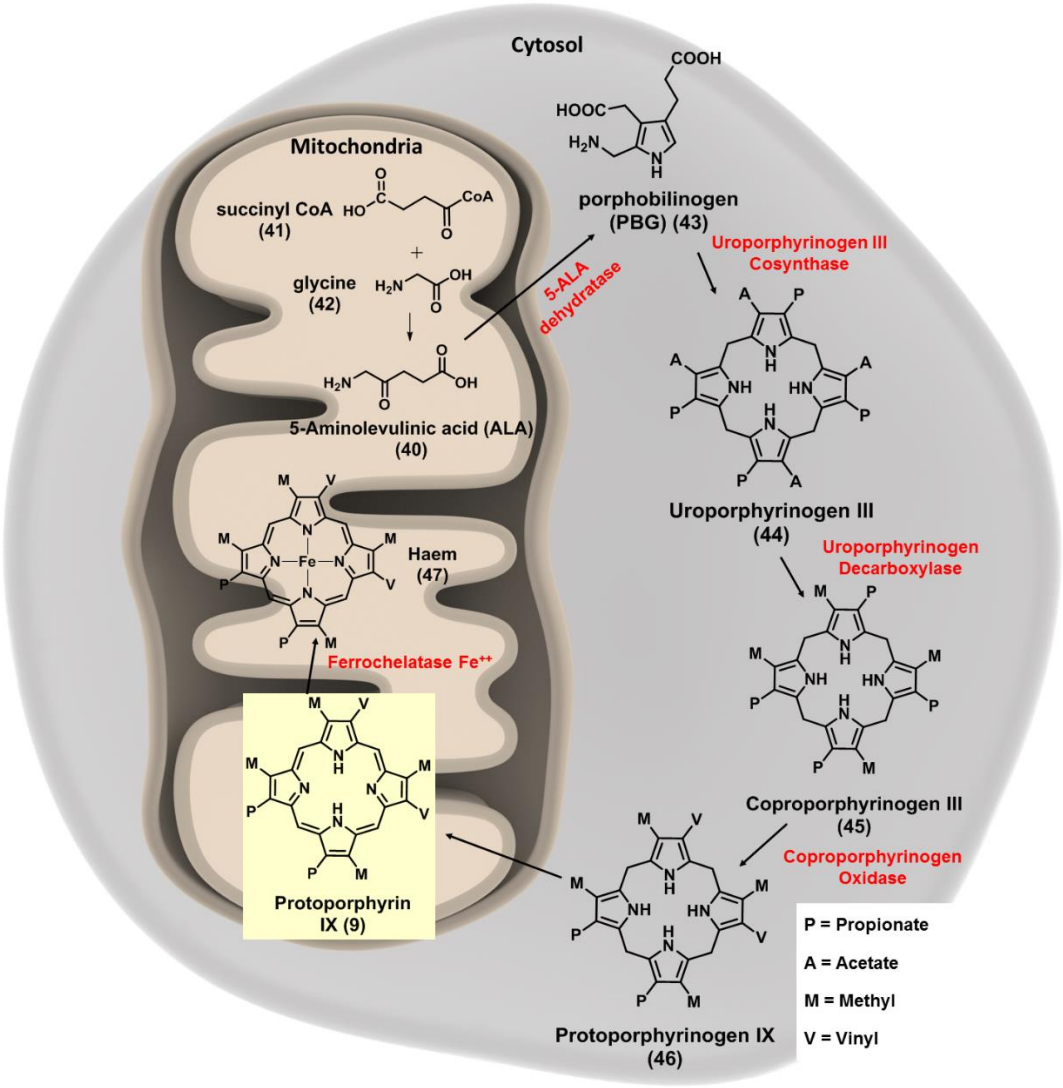

Scheme 4. Bioconversion of ALA to haem (adapted from Pottier *et al.)* [126].

Scheme 4 shows the pathway of haem biosynthesis. The haem biosynthetic pathway begins with a condensation reaction between glycine **(41)** and succinyl-CoA **(42)** in the mitochondrion to form ALA **(40)** which becomes the source of C and N atoms for the construction of the haem macrocycle. This reaction is catalysed by ALA synthase and involves pyridoxal-5-phosphate as the cofactor. The synthesized ALA then enters the cytosol and a condensation reaction between two units of ALA mediated by the enzyme ALA dehydratase (ALAD) forms monopyrrole porphobilinogen **(43)** (PBG). Four units of PBG **(43)** oligomerize to a linear tetrapyrrole intermediate, followed by cyclisation by the enzyme uroporphyrinogen III co synthase to give the cyclic tetrapyrrole

intermediate, uroporphyrinogen III **(44)**. The tetrapyrrole intermediate now undergoes a decarboxylation of the four acetate side chains to methyl groups (catalysed by uroporphyrinogen decarboxylase) to form coproporphyrinogen III **(45)**, which is then carried to the intermembrane space of the mitochondrion. Subsequent steps in the mitochondrion lead to formation of protoporphyrin IX **(9)** and later haem **(47)**, by insertion of iron by the enzyme ferrochelatase.

1.9.2 Advantages of ALA-PDT

Administration of exogenous ALA **(40)** bypasses the rate-limiting step in the biosynthesis of haem, and thus can produce photosensitising amounts of PpIX **(9)** in malignant, premalignant, and certain other abnormal tissues. The metabolic conversion of exogenous ALA into a photosensitising concentration of PpIX is relatively fast, requiring only 1-3 h. Furthermore, since PpIX is part of a biosynthetic pathway, it has a built-in clearance mechanism that restricts possible systemic patient photosensitivity to less than 2 days. In comparison to other photosensitisers, ALA can be administered both topically and systemically and when applied topically, the photosensitized area is restricted to the site of application with no systemic effects. An additional and an important advantage of ALA-PDT is its rapid photobleaching. PpIX molecules react with singlet oxygen and are converted to products which are no longer photosensitive.[126]

1.9.3 Clinical applications of ALA-PDT

ALA and simple ester derivatives have received clinical approval both for PDT and diagnostic applications. The methyl ester of ALA (Metvix) has been approved in Europe and Australia for treatment of various skin disorders such as actinic keratosis and basal cell carcinoma (see Section 1.3.2.1). The hexyl ester of ALA, also known as Hexvix, was approved in Europe for endoscopic fluorescence diagnosis of bladder cancer, whereas the US-FDA approved ALA with a Blu-U light source for treatment of actinic keratosis (Section 1.3.2.1).

1.9.4 Drawbacks of ALA-PDT and strategies to improve its effectiveness

ALA is a zwitterion at physiological pH, which results in poor lipid solubility and limits its passage through biological barriers such as cellular membranes.[145] As a result, ALA has a poor penetration through the stratum corneum.[146] One of the most common approaches to influence the drug penetration into the skin is to alter the composition and structure of the stratum corneum by employing formulation-based chemical permeation enhancers.[146-148] In the case of ALA, many permeation enhancers have been investigated such as dimethyl sulfoxide (DMSO),[148] 1-[2-(decylthio)-ethyl]azacycpentan-2-one (HPE-101),[149] glycerol monooleate,[150] 6-ketocholestanol (2% w/w)[151] and oleic acid[152]. Experimentally, penetration enhancers, such as DMSO, have shown relatively higher concentrations of ALA up to a certain depth in skin, however ALA delivery was not significant when compared to control.[146]

At physiological or alkaline pH, ALA is also unstable with respect to self-condensation through formation of Schiff bases. Buffered solutions of ALA at physiological pH discolour even at low temperature due to decomposition of ALA, thus stock solutions for clinical use need to be freshly prepared.[153] The instability of ALA under neutral and alkaline conditions has been investigated in some detail. Under alkaline conditions, ALA **(40)** has been shown to undergo dimerization and forms 2, 5-dicarboxyethyl-3,6-dihydropyrazine **(50)** (DHPY), which oxidises spontaneously to 2,5-dicarboxyethylpyrazine **(51)** (PY, Scheme 5).[154, 155] Other degradation pathways of the ALA dimer **(48)** to form porphobilinogen **(43)** and pseudo-porphobilinogen **(49)** have also been proposed.[155-157]

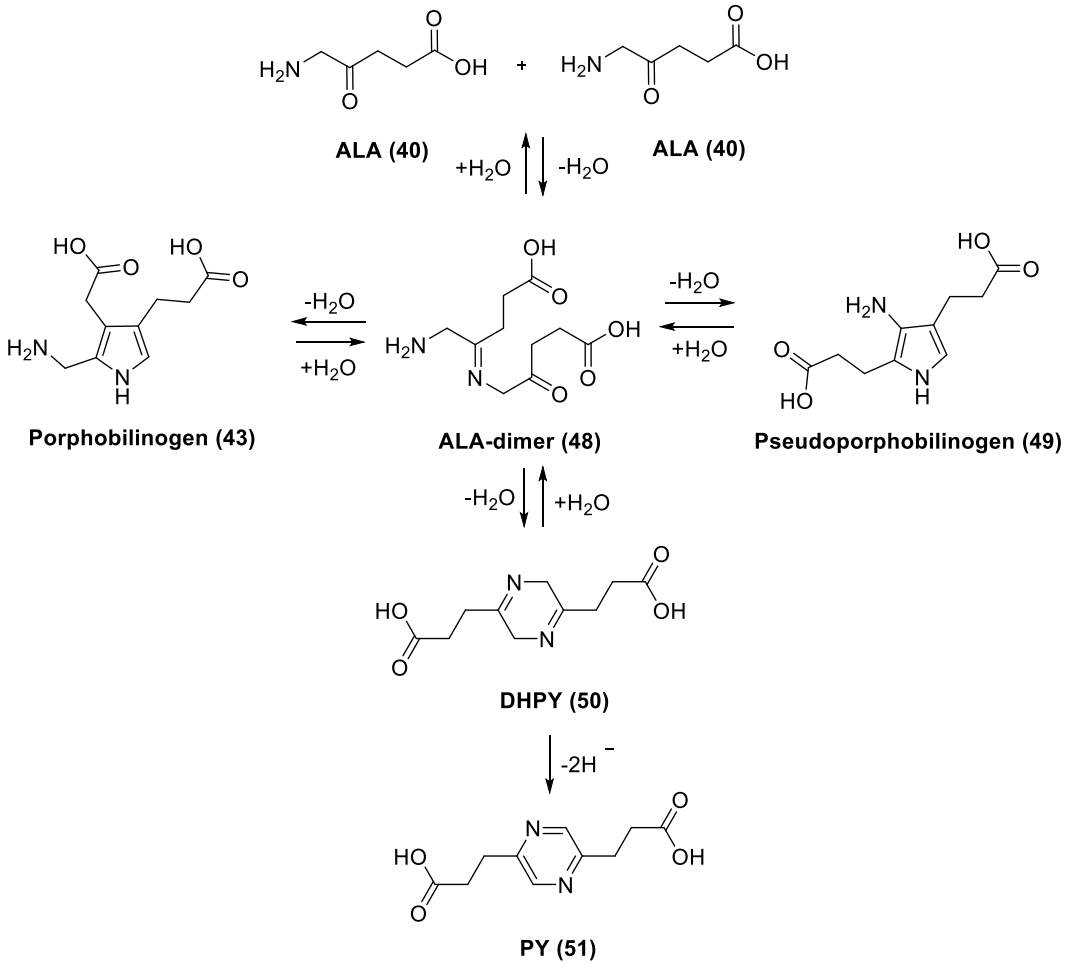

Scheme 5. Degradation pathway of ALA under alkaline conditions (adapted from Bunke *et al.*).[155]

Significantly, simple N-acylated ALA derivatives such as **(52)** and **(53)** have been shown to be completely stable at physiological pH, but they do not generate PpIX in cells, presumably due to the lack of suitable enzymes activities required to release ALA (Figure 29).[158, 159]

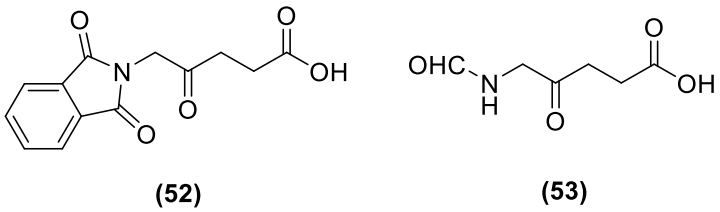

Figure 29. Structures of simple N-acylated ALA derivative **(52)** and **(53)**.

Over the years, many prodrugs of ALA have been suggested to overcome issues of stability, as well as enhancing lipid solubility and improving targeting.[160-162]

Esters

The synthesis of ALA esters has been the most exploited prodrug strategy, and several of these have been shown to give a quicker, more homogeneous, and more effective PpIX production than ALA itself. Many ALA ester-based prodrugs have been synthesized with linear, branched, or cyclic alkyl ester groups, as well as examples with aromatic, heteroaromatic, perfluorinated hydrocarbon, or ethylene glycol-type moieties (Figure 30).[161, 163-166] At pH 5, ALA and simple esters have comparable stability.[167]

A number of *n*-alkyl esters **(54a-h)** and **(55a-i)** of ALA have been synthesized to improve the lipophilicity as well as to increase diffusion across cell membranes.[158, 163-165] Some of these are shown in Figure 30.

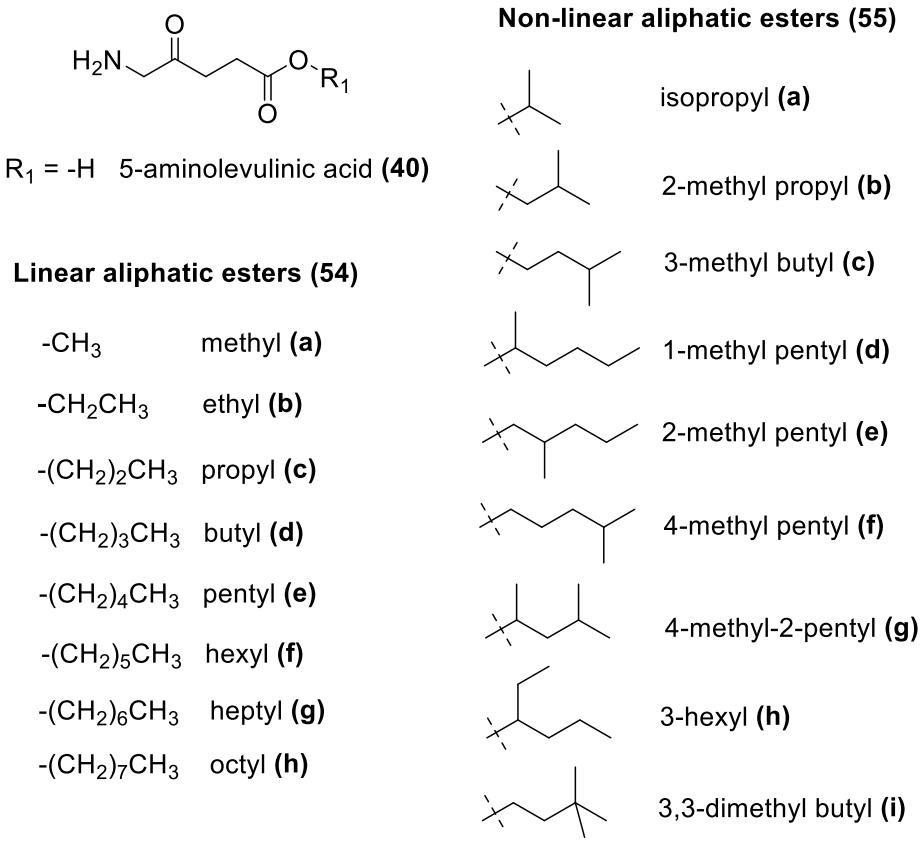

Figure 30. Linear and non-linear aliphatic esters of ALA.

Peng *et al.* (1996) were the first to report a comparative study on the effectiveness of ALA esters vs ALA. This showed that ALA-methyl, ethyl and propyl esters **(54a-c)** produced more PpIX fluorescence in both murine and

human tissues as compared to free ALA.[165] Similar results were also obtained by Kloek *et al.* (1996) and Gaullier *et al.* (1997) while evaluating ALA esters **(54a-f) (**Figure 30).[163, 164, 168] Gaullier also observed that enzymatic hydrolysis was faster for the case of long chain ALA esters **(54f-h)** in comparison to short chain ester prodrugs. In some cases, PpIX production was 30-150 times more efficient than for free ALA, thus indicating faster cellular uptake of the prodrugs and ALA-induced PpIX formation.[163] However some variations in terms of PpIX production have been observed from ALA esters having similar lipophilicity. For example, Uehlinger *et al.* (2000) noted that the hexyl ester of ALA **(54f)** showed PpIX fluorescence which was an order of magnitude higher than cyclo-hexyl ester **(56e)** even though both the conjugates had similar log P values.[166] These results were further confirmed by Whitaker *et al.* (2000) in a report on the synthesis and *in vitro* biological evaluation of a series of linear, non-linear aliphatic and cyclic-ALA esters in pancreatic tumour cells (Figure 30 and 31).[169] Lower PpIX production was found for conjugates **(55a,d,g-h)** which shared the common feature of having a branch point next to the site of ester cleavage. This presumably inhibits the interaction of the prodrug ester unit with the active site of cellular esterases.[169, 170]

A range of ALA prodrugs have also been synthesized based on cyclic, aromatic or halogen-substituted benzyl esters and the production of PpIX compared to that obtained with equimolar doses of ALA (Figure 31).[162, 164, 169, 171]

Kloek *et al.* (1996) reported the synthesis and biological evaluation of tetrahydrofuranyl **(56c)** and tetrahydropyranyl **(56d)** esters of ALA and found enhanced PpIX fluorescence for both the conjugates *in vitro* (Figure 31). Godal *et al.* reported the synthesis of cyclic **(56e)** aromatic **(57a-i)** and halogen substituted benzyl esters **(58a-f)** of ALA, and biological evaluation *in vitro/ in vivo* showed significantly enhanced PpIX fluorescence compared to ALA **(40)** for aromatic esters, especially the benzyl and ring-alkylated benzyl esters **(57a-b,g-i)**. In contrast, the cyclohexyl ester **(56e)** produced the least PpIX fluorescence amongst all the prodrugs tested and was only as effective as ALA itself. Halogen-substituted benzyl esters **(58a-f)** showed intermediate PpIX

fluorescence, and amongst them the mono-halogenated esters showed higher PpIX fluorescence than the di- or penta-substituted esters.[171]

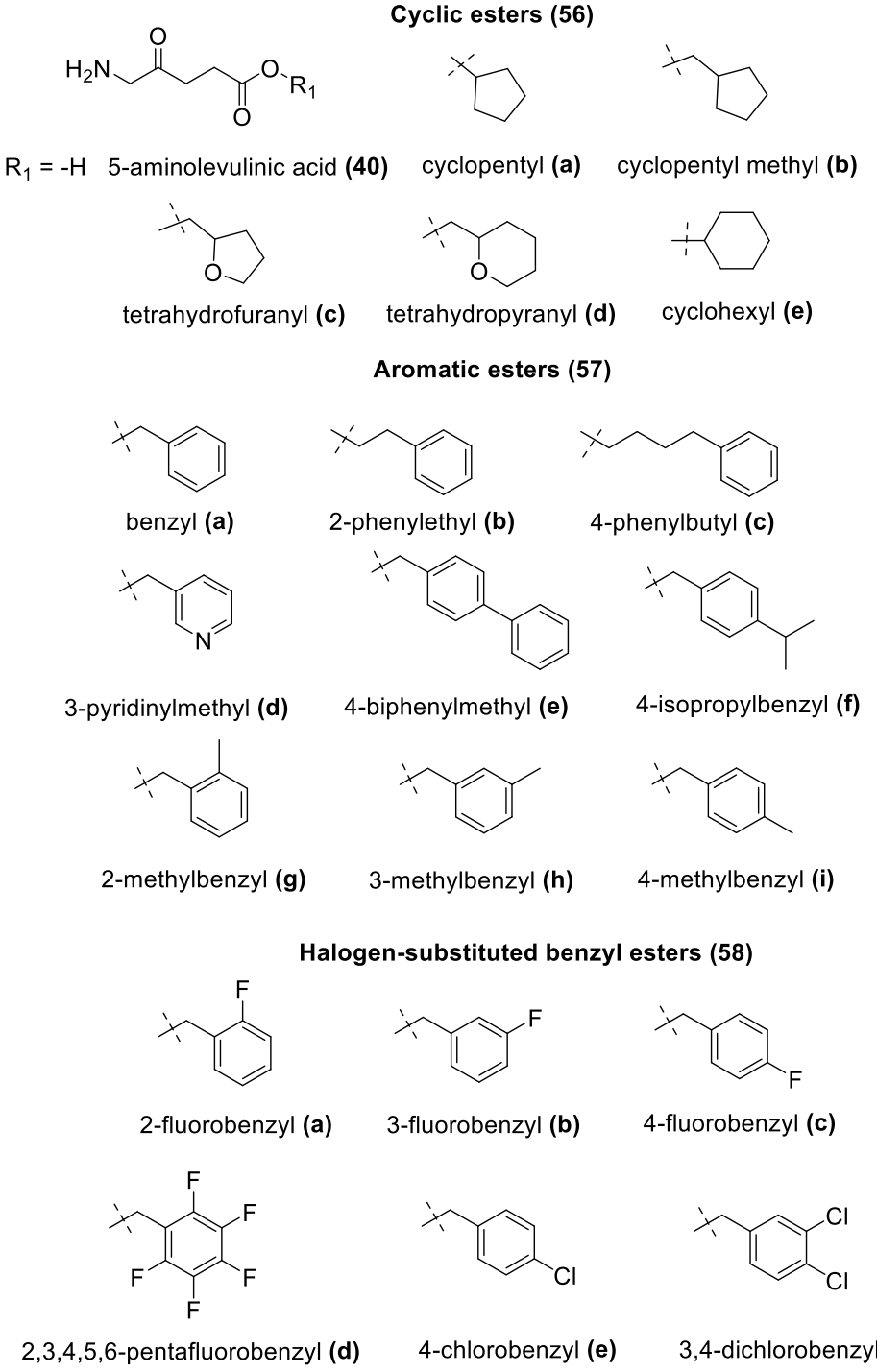

Figure 31. Cyclic, aromatic and halogen-substituted benzyl esters of ALA.

Although aliphatic ALA esters have been shown to induce higher PpIX production with an increase in carbon chain length, increasing ALA prodrug lipophilicity in this way brings the limitation of reduced water solubility for esters

which are derived from long-chain alcohols.[164, 172] In contrast, poly(ethylene glycol) derivatives, which have been used for a large number of pharmaceutical applications, potentially offer the advantage of both improved water and lipid solubility.[162]

Berger *et al.* (2009) reported the synthesis of ethylene glycol esters of ALA **(59a-c)** and tested their biological efficacy in human and rat cell lines of carcinoma and endothelial origin (Figure 32). It was found that a high PpIX fluorescence compared to free ALA was observed in endothelial cells in comparision to tumour cells, especially for long-chain ethers.[172] Godal *et al.* also reported the synthesis of ethylene glycol esters **(59d-e)**, but biological evaluation *in vivo* showed that a lower PpIX fluorescence was produced compared to the simple hexyl ester (Figure 32).[171]

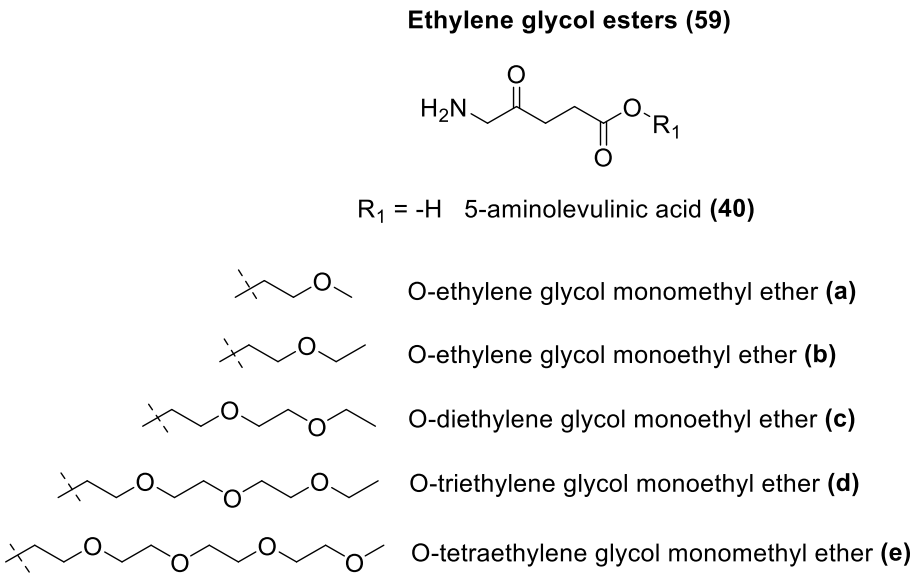

Figure 32. Ethylene glcol esters of ALA.

As already noted, the use of ALA esters can result in increase PpIX production in various cell types, but with a greater enhancement in tumour cells. Brunner *et al.* (2001) also proposed that a reduction in the concentration for ALA esters **(54f)** and **(57a)** followed by shorter incubation time would be favourable for PpIX generation in cancerous cells compared to free ALA.[173]

Iron chelators

It has been observed that differences in the accumulation of PpIX in healthy cells and malignant cells are due to differences in the activity of enzymes in the haem biosynthetic pathway such as porphobilinogen deaminase and ferrochelatase. This forms the basis of a therapy combining iron chelators with ALA PDT where cells are deprived of Fe^{2+} in the last step of haem synthesis, thus leading to higher levels of PpIX.[174] Iron chelators such as EDTA, desferrioxamine (DFO), 2-allyl-2-isopropylacetamide and 1,10-phenanthroline have indeed shown potential in preclinical studies for increasing PpIX levels upon ALA administration.[175-181]

Berg *et al.* demonstrated that administration of EDTA **(60)** (Figure 33) in combination with ALA in epithelial skin tumours moderately increases intracellular PpIX levels.[175]

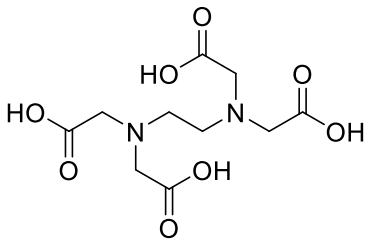

EDTA (60)

Figure 33. Structure of EDTA **(60)**.

However, EDTA is a non-specific chelator which chelates other metal ions. It also has a lower affinity for iron compared to that of CP94 and DFO (see below).[175]

Desferrioxamine **(61)** DFO is a hexadentate siderophore which has been shown to have anti-proliferative activities against various tumour cell lines (Figure 34).[176] It has also been shown to have medical applications by acting as chelating agent and removing excess iron from the body.[177] However, due to its hydrophilic nature it is unsuitable for topical application. It has also been shown that long exposure to DFO **(61)** leads to iron starvation from healthy tissue leading to cell death, which also limits the use of DFO **(61)** for topical ALA-PDT.[178]

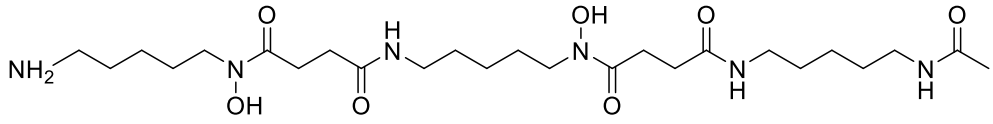

DFO (61)

Figure 34. Structure of DFO **(61)**.

1,2-Diethyl-3-hydroxypyridin-4-one **(62)** (CP94) is a low molecular weight lipophilic chelator which has high specificity for iron (Fe^{2+}) and has perhaps shown the most promise in ALA-PDT (Figure 35).[179] Blake *et al.* investigated the combination of CP94 **(62)** with ALA and MAL in human glioma cells,[180] and observed that CP94 **(62)** significantly enhanced PpIX accumulation and subsequent PDT cytotoxicity. This combination may therefore be useful both in photodiagnosis and /or PpIX-induced PDT treatment of glioma.

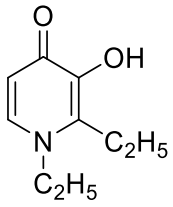

CP94 (62)

Figure 35. Structure of CP94 **(62)**.

Most recently, Mrozek-Wilczkiewicz *et al.* reported the synthesis of some novel thiosemicarbazone iron chelators and evaluated them for their PDT activity in combination with ALA (Figure 36).[181] Biological evaluation in HCT 116 colorectal carcinoma cells with a wild-type (+/+) or deleted (−/−) tumour suppressor TP53 gene showed significant photocytotoxicity for compounds **(63)** and **(64)** when combined with ALA **(40)**, whereas a much weaker activity was seen with compounds **(65)** and **(66)**.

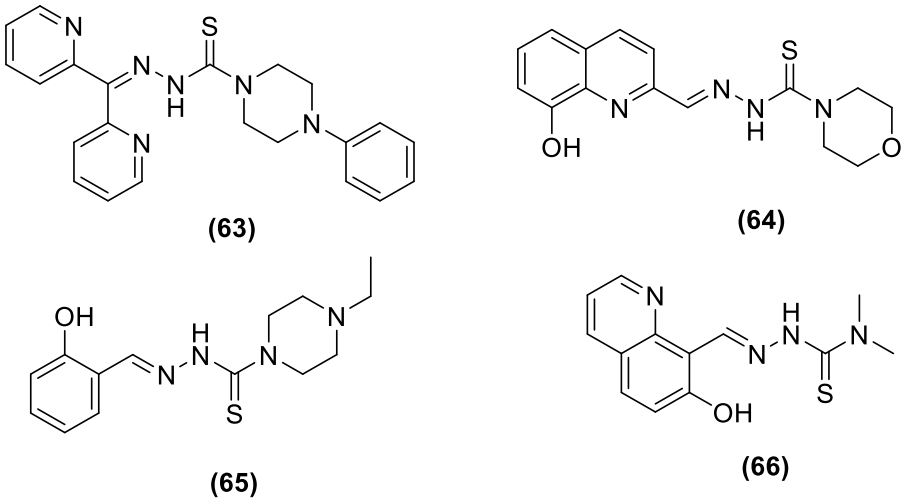

Figure 36. Chemical structures of thiosemicarbazone derivatives **(63)**-**(66)**.

Peptide prodrug derivatives

Peptide derivatives of ALA have also been synthesized to provide prodrugs with improved physicochemical properties relative to ALA itself.[182-192] This approach also provides the possibility of achieving selective ALA release in particular cell lines.[182] Berger *et al.* investigated the synthesis of ALA peptide prodrugs by two different approaches and evaluated them for their PpIX production (Figure 37).[172, 183] The first approach involved synthesizing acidic, basic and neutral amino acid ALA-derivatives **(67a**-**e)** as potential substrates for cellular peptidases APA, APB or APN/M (Figure 37).[172] Biological evaluation in endothelial and carcinoma cell lines A549, HCEC and EC219 showed that prodrugs containing a neutral amino acid sidechain **(67c)** induced the highest PpIX production, however basic amino acid derivative (**67d)** or acidic derivative (**67e)** did not show any favourable results (minimal PpIX production). The second approach involved the synthesis and evaluation of pseudo di- and tripeptide derivatives (Gly-Gly and Gly-Pro) of ALA **(68a**-**f)** as potential substrates for cellular di/tripeptidases or peptide transporters at the cell surface, to target human endothelial cells or carcinoma cells in cancer (Figure 37).[183] Biological evaluation in human endothelial (HCEC) and human lung carcinoma cells (A549) showed the peptide derivatives of ALA to be substrates for Gly/Pro-specific cellular transport systems and enzymatic activities. The dipeptide derivatives were also less cytotoxic in the absence of light as compared to the amino acid derivative **(67a**-**e)**.

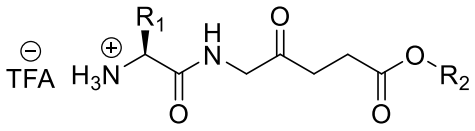

(67a-e)

R_1 = Me; R_2 = Me **(a)**
R_1 = Me; R_2 = hexyl **(b)**
R_1 = Bn; R_2 = Me **(c)**
R_1 = -$(CH_2)_4$-NH_3TFA;R_2 = Me **(d)**
R_1 = -CH_2-COOH; R_2 = Me **(e)**

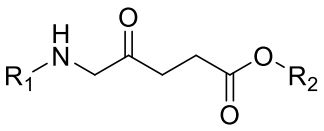

(68a-f)

R_1 = Gly-Gly; R_2 = Et **(a)**
R_1 = Gly-Pro; R_2 = Et **(b)**
R_1 = Gly-Gly; R_2 = $O(CH_2CH_2O)_2CH_2CH_3$ **(c)**
R_1 = Gly-Gly; R_2 = $O(CH_2CH_2O)_3CH_2CH_3$ **(d)**
R_1 = Gly-Gly-Gly; R_2 = Me **(e)**
R_1 = Gly-Gly; R_2 = Me **(f)**

Figure 37. Pseudopeptide derivatives of ALA **(67)** and **(68)**.

A significant feature in the synthetic approaches used by Berger *et al.* was that an excess of the activated amino acid components or ALA derivative was used for the formation of the critical amino acid-ALA peptide bond, presumably to compensate for the instability of ALA under the basic coupling conditions. Rogers *et al.* developed an alternative approach by employing only one equivalent each of an acylated amino acid active ester and ALA.HCl.[184] The instability of ALA under basic conditions was avoided by slow neutralisation of ALA.HCl in the presence of the active esters (Scheme 6).

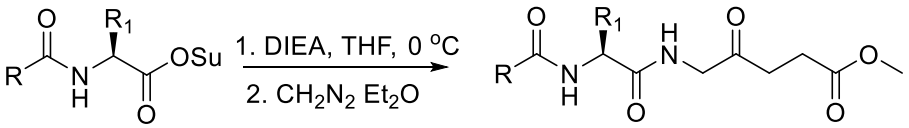

Amino acid
+
5-ALA.HCl

ALA-dipeptide

R = CH_3, OBn

Scheme 6. Synthesis of urethane and acetyl-protected ALA-dipeptide ester derivatives.

Bourré *et al.* in 2008 reported the synthesis of some N-acetyl prodrugs based on phenylalanine and tested their biological efficacy in transformed PAM212 keratinocyte cells and pig skin explants (Figure 38).[186] The synthesized prodrugs were uncharged, more lipophilic than ALA, but at the same time remained water soluble. These were also stable in solution, unlike the corresponding ALA peptides with a free N-terminus.[183] Fluorescence spectroscopy revealed both **(69)** and **(70)** to be efficiently taken up by cells and converted to PpIX, however better results were obtained with compound **(69)** (methyl ester) in comparison to **(70)** (free carboxy terminus). PDT studies with both **(69)** and **(70)** in cells were in agreement with the results obtained from

fluorescence pharmacokinetics, and the cell survival was significantly reduced in comparison to equimolar doses of ALA **(40)**.

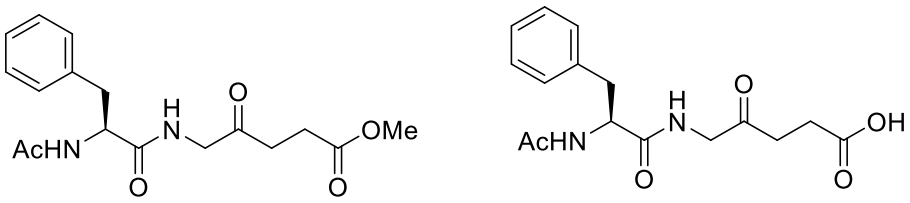

(69) **(70)**

Figure 38. ALA peptide-prodrugs **(69)** and **(70)** based on phenylalanine.

Giuntini *et al.* reported a series of 27 dipeptide prodrugs of ALA with the general structure Ac-Xaa-ALA-OR where Xaa was an α-amino acid providing appropriate lipophilicity and water solubility to the prodrug (Figure 39).[187] All the ALA prodrugs were taken up effectively in PAM212 keratinocytes as compared to ALA itself, however only the L-amino acid derivatives produced PpIX.[185] This clearly demonstrated the potential of desgning peptide prodrugs of ALA which are cleaved by a disease-specific/cell-line specific enzyme activity. In a subsequent study, Bourré *et al.* showed that compounds of the general structure in Figure 39 are substrates for the enzyme acylpeptide hydrolase (ACPH). D-amino acid derivatives are not substrates, and PpIX production is also limited in cell lines with a low expression of this enzyme.[185] Further *in vivo* studies with these compounds provided support for their potential use in topical treatment of basal cell carcinomas and for systemic administration.[188]

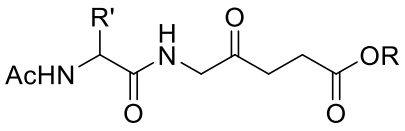

General structure of dipeptide ALA prodrug

Figure 39. Dipeptide derivatives of ALA.

Several studies have reported the synthesis and biological evaluation of more complex ALA peptide prodrugs, designed to provide improved and selective delivery. Dixon *et al.* (2007) reported the synthesis of a 9-residue ALA-containing cell-penetrating peptide conjugate **(71)** using Fmoc-solid phase

chemistry (Figure 40).[189] The synthesized peptide was based on a heptapeptide fragment of the cell penetrating peptide, penetratin. Biological results showed effective uptake and intracellular conversion of the peptide to protoporphyrin IX in PAM212 cells.

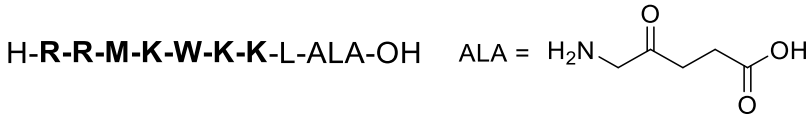

(71)

Figure 40. Structure of a cell penetrating peptide conjugate with ALA **(71)**.

Johnson *et al.* in 2012 reported a series of pH sensitive ALA-poly(L-histidine) prodrugs **(72)** and their activity in the human colon cancer HCT116 cell line (Figure 41).[190] The results showed that the phototoxicity and selectivity of the synthesized prodrugs were higher than ALA itself, especially for the conjugate having 15 L-histidine residues.

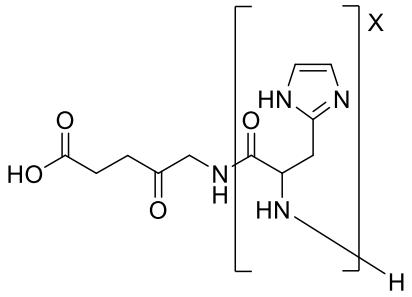

(72)

Figure 41. Structure of ALA-poly(L-histidine) prodrugs **(72)**.

Abd-Elgaliel *et al.* have also described the synthesis and selective activity of a cathepsin E-cleavable ALA peptide prodrug **(73)** (Figure 42).[191] Biological evaluation showed that ALA was liberated in cathepsin E-positive pancreatic tumour cells, but not in normal pancreatic tissue, thus allowing delivery of selective photodynamic therapy (PDT) to cancerous tissues.

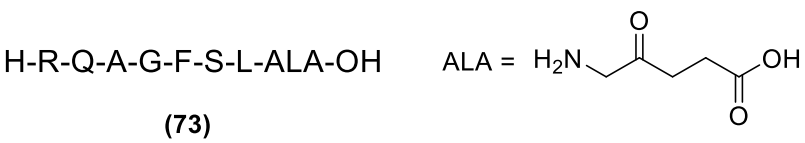

(73)

Figure 42. Structure of cathepsin E-activatable ALA prodrug **(73)**.

Guaragna *et al.* in 2015 reported the synthesis of a novel folic acid-based photosensitiser delivery system in which the prodrug 5-aminolevulinic acid methyl ester (MAL) was conjugated to folic acid via a polypeptide spacer **(74)** (Figure 43).[192] The peptide spacer consisted of four consecutive β-Ala units linked to an α-Asp residue, with the aim of improving the water solubility and cellular stability of the final conjugate. However the biological and stability studies are yet to be reported.

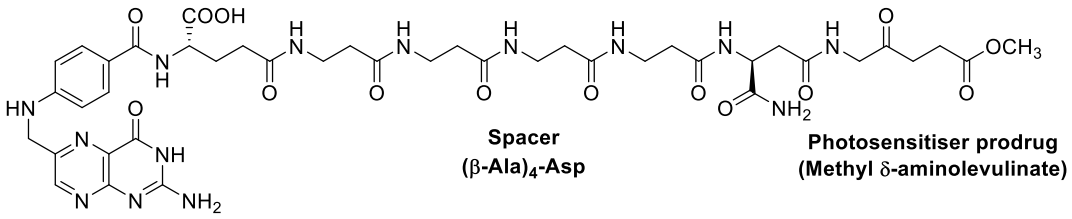

(74)

Figure 43. Folic acid-conjugated with MAL via a peptide spacer **(74)**.

Other targeting derivatives

Various groups have reported bioconjugates of ALA with vitamins, nucleosides and glycosides (Figure 44) with the rationale of overcoming the stability issues of ALA as well as improving its targeting potential. Vallinayagam *et al.* reported the attempted synthesis of novel bioconjugates of ALA with vitamin E **(75)**, vitamin D_3 **(76)** and biotin **(77)**.[193] Vitamin E (or α-tocopherol) is known to incorporate easily into natural membranes which might facilitate the transport of ALA into the interior of cancer cells, whereas it has been shown that pretreatment with vitamin D may improve the efficacy of ALA-PDT in a variety of tumour models.[193-195] All the conjugates were synthesized in moderate yield, except vitamin D_3-ALA **(76)**, where degradation was observed in the final acidic deprotection step.

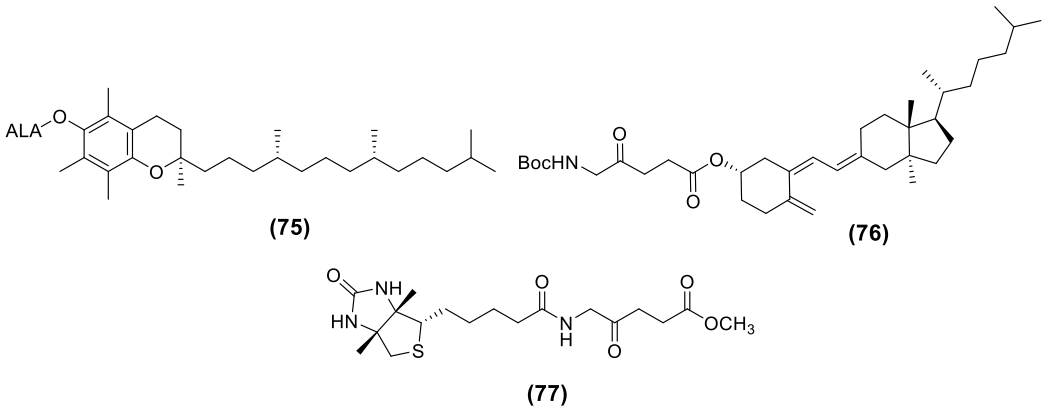

Figure 44. Structures of vitamin-ALA conjugates **(75)-(77)**.

Nucleoside analogues have long being studied for their tumour activity and they act by inhibiting cellular division.[196] Gurba *et al.* reported the synthesis of nucleoside-ALA bioconjugates (Figure 45) with adenosine (mono, bis and tris bioconjugate) and thymidine (bis-bioconjugate).[197] The conjugates were tested in various cell lines including human colon (SW480), breast (MCF7), lung (A549), ovarian (A2780) and cervix (HeLa). The thymidine conjugate of ALA **(81)** was found to show enhanced PpIX production (approx. 1.5 times) in all the cell lines except SW480 as compared to equimolar ALA **(40)**. However the adenosine conjugates **(78)**-**(80)** were found to show poor PpIX production as compared to ALA in all the cell lines, suggesting that they may not be substrates for adenosine receptors.

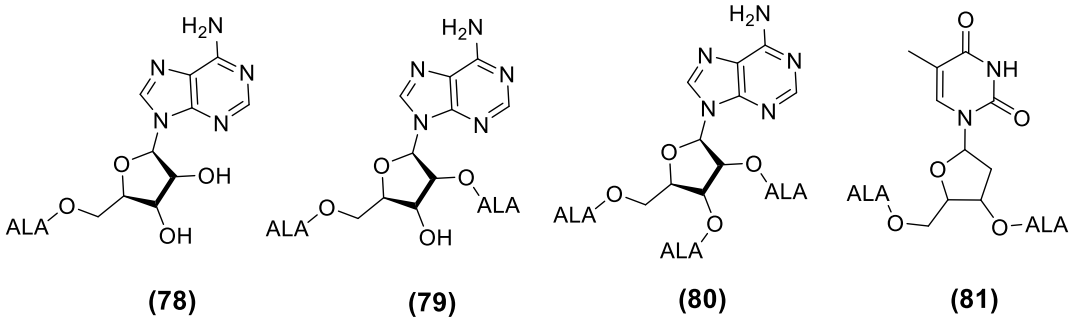

Figure 45. Structures of nucleoside-ALA conjugates **(78)**-**(81)**.

Glycosylated porphyrins and chlorins have been previously synthesized and shown the potential to improve the uptake of these photosensitisers into cells.[198-200] Vallinayagam *et al.* also reported the synthesis and biological evaluation of glycoside esters of ALA with α-glucose **(82)**, α-mannose **(83)**, or α-galactose **(84)** (Figure 46). The results confirmed that the glycoside esters

of ALA showed better selectivity in producing PpIX in human cancer and angiogenic endothelial cells as compared to free ALA.

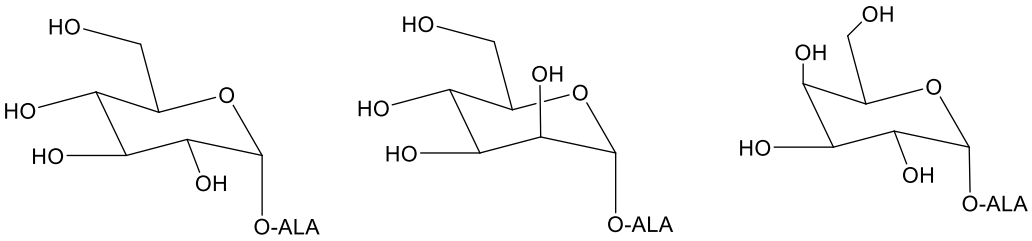

(82) **(83)** **(84)**

Figure 46. Structures of glycoside-ALA conjugates **(82)**-(**84)**.

Very recently, Tong *et al.* reported novel 5-aminolevulinic acid (ALA) pseudopolyrotaxane prodrug micelles that have dual pH-responsive properties (Figure 47).[201]

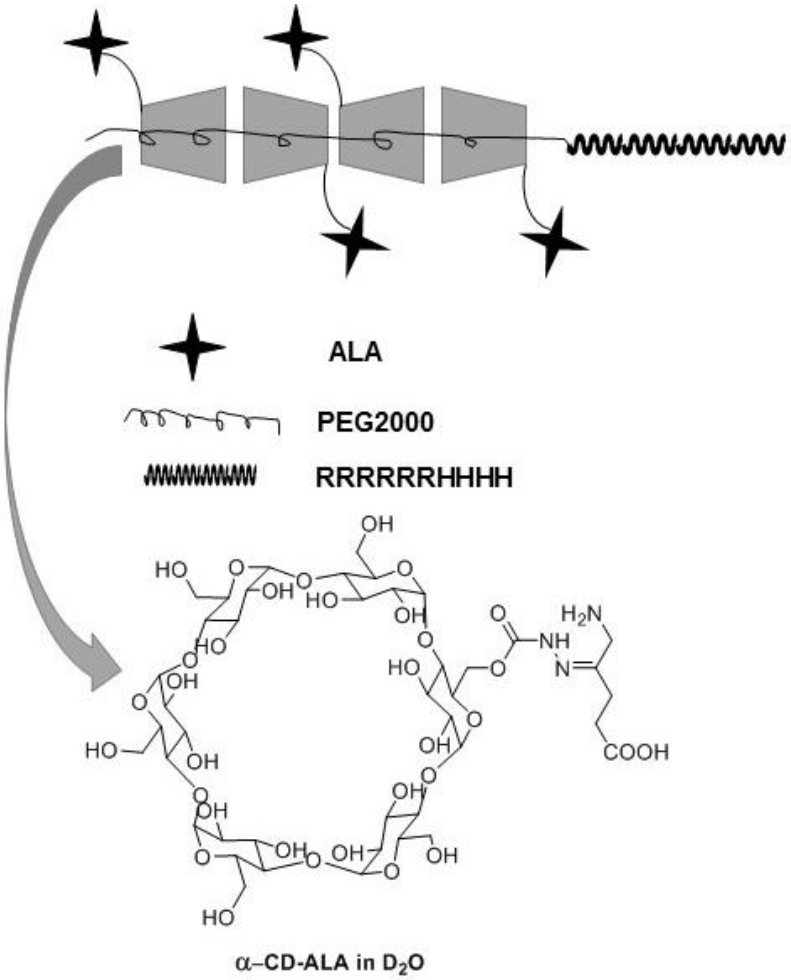

Figure 47. Illustration of a ALA pseudopolyrotaxane prodrug micelles for PDT (adapted from Tong *et al.*)[201]

As shown in the Figure 47, ALA was conjugated to α-cyclodextrin (CD) through an acid-labile hydrazone bond, while the pH-responsive CPP, R6H4 (RRRRRRHHHH) was conjugated to PEG to form PEG–R_6H_4. The two elements were combined to give a pseudopolyrotaxane prodrug via inclusion complexation between α-CD and PEG. Once internalised within tumour cells through endocytosis, ALA was released by cleavage of the hydrazone bond in response to the lowered endo-/lysosomal pH followed by conversion to protoporphyrin IX for PDT activity.

Dendrimers

Polyvalent drug carriers such as dendrimers are a promising new strategy for the delivery of high payloads of photosensitisers in PDT.[202] In ALA-PDT eight molecules of ALA are required to build the tetrapyrrole structure of PpIX (Scheme 3), hence delivering multiple units of ALA on a single core would boost the synthesis of PpIX. Battah *et al.* in 2001 reported the synthesis of a series of novel ALA-containing dendrimers bearing 6 to 18 ALA residues **(85)-(89)** and their biological evaluation in the keratinocyte cell line, PAM 212. Enhanced PpIX fluorescence was observed for **(88)** in comparison to ALA at an equimolar dose, along with higher phototoxicity upon irradiation of cells (Figure 48).[203]

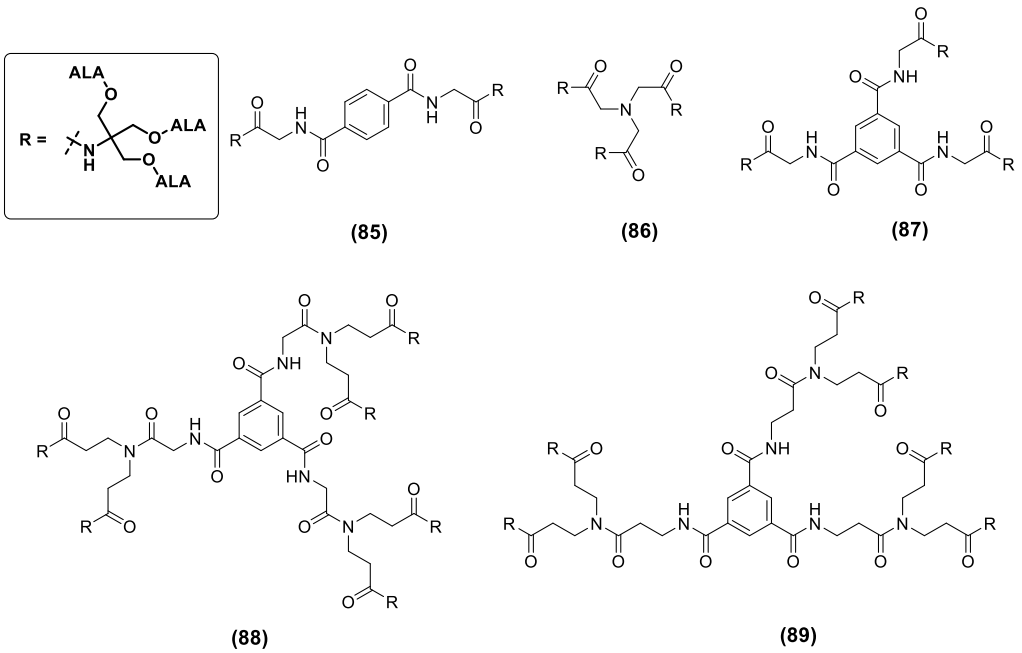

Figure 48. Structures of dendritic derivatives with 6-18 copies of ALA **(85)-(89)**.[203]

In order to identify improvements in the basic structure of ALA dendrons which would allow effective design of larger ALA dendrimers with 6, 9 or 18 ALA copies, low molecular weight dendritic derivatives were also investigated by Battah *et al.* (2006) with three copies of ALA conjugated as esters via methylene or propylene linkers to a quaternary carbon, functionalised with an aminobenzyloxycarbonyl **(90)**, nitro **(91)** or amino group **(92)** (Figure 49).[204] Biological evaluation in the PAM212 keratinocytic cell line showed enhanced PpIX fluorescence for all the three ALA dendrimers in comparison to equimolar free ALA, while **(91)** (with a propylene linker) was found to be the most active amongst the three dendrimers. The study concluded that lipophilicity and steric hindrance within the dendritic structure are key factors that can influence the efficacy of dendrimeric ALA conjugates which would potentially restrict the access of intracellular esterases for liberation of ALA. The conjugate **(92)** was also studied for *in vitro* efficacy in LM3 cells and was found to produce similar porphyrin levels compared to free ALA.[205] However *in vivo* studies in tumour-bearing mice showed lower porphyrin levels from the dendron **(92)** as compared to free ALA after topical administration, which may be due to the retention of the lipophilic conjugate within the stratum corneum at the application site.

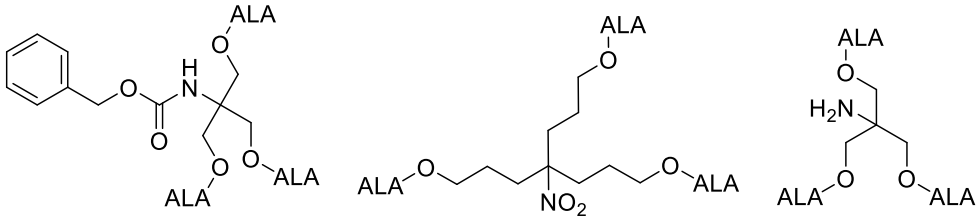

(90) **(91)** **(92)**

Figure 49. Structures of ALA dendrimers **(90)**-**(92)**.

Following the preliminary studies with low molecular weight ALA dendrons and some second generation dendrons having 18 copies of ALA, Battah *et al.* (2007) investigated another 18-ALA dendrimer **(93)** which was built on a tripodal aromatic core with oligoamidoamine branches. The ability of **(93)** to enter the tumorigenic cell lines PAM 212 and A431 and the resulting PpIX-induced phototoxicity was studied (Figure 50).[206] Fluorescence pharmacokinetics revealed significant PpIX production in both the cell lines by

(93) in comparison to free ALA, across a range of concentrations between 0.01 to 0.1 mM. These results were further supported by a higher phototoxicity post-irradiation of the cells. An important result highlighted in this study was that the internalisation of the high molecular weight ALA dendrimer **(93)** occurred through an endocytic route and mainly via the micropinocytosis pathway. This mechanism would be expected for a non-targeted macromolecular prodrug such as **(93).**

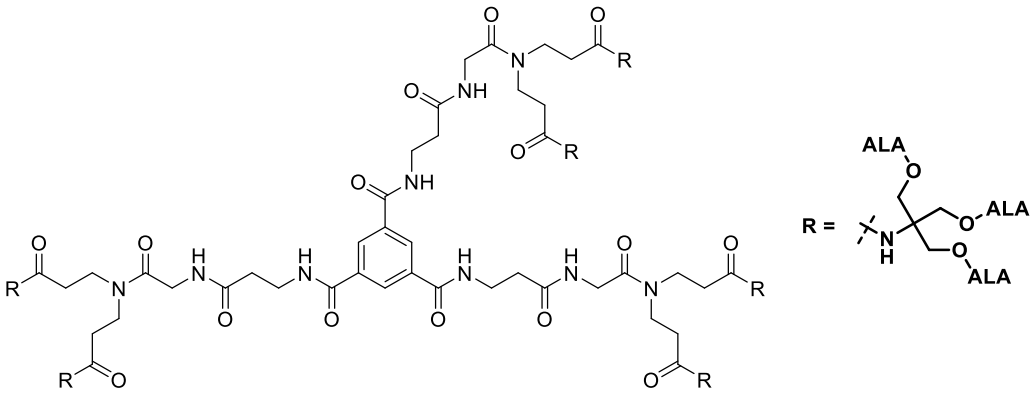

(93)

Figure 50. Reported dendrimeric prodrugs of ALA **(93)**.

The enhancement in PpIX production observed with the 18 ALA dendron **(93)** in *in vitro* studies was also confirmed by *in vivo* evaluation in a murine tumour model. Here, **(93)** showed a sustained release of PpIX for over 24 h, and the basal values were not reached until 48 h post-intraperitoneal administration of **(93)**.[207] In contrast, PpIX production for ALA was observed for only 3-4 h.

An additional application of the ALA dendron **(93)** was reported by François *et al.* (2012) for fluorescence diagnosis of bladder cancer, and where a sustained release of PpIX was observed even after 24 h post-administration of the prodrug intravesically.[208] A significantly lower dose of the prodrug was required to produce the same effect in comparision to free ALA (0.7 vs 180 mM) and the hexyl ester of ALA (0.7 vs 8 mM). Significant tumour specificity vs muscle and normal urothelium was also observed as compared to hexyl-ALA **(54f),** making it potentially a good alternative for fluorescence-guided cystoscopy.

Recently Rodriguez *et al.* (2015) investigated ALA dendrimers **(94)** (6-ALA units) and **(95)** (9-ALA units) for their PDT effect in mammary LM3 carcinoma cells. *In vitro* studies showed enhanced PpIX production (*ca.* 4 times) for ALA dendrimers **(94)** and **(95)** at a lower concentration as compared to free ALA (Figure 51).[209] Topical application of these dendrimers **(94)** and **(95)** on the skin overlying a subcutaneous LM3 implanted tumour showed lower amounts of PpIX in distant skin as compared to free ALA, which induced similar profiles of PpIX in distant skin and skin overlying tumour. This suggests a promising use of these dendrimers in superficial cancer models. A possible application in vascular PDT was also investigated for the dendrimers **(94)** and **(95)** by assessing their selectivity towards macrophages over endothelial cells. Biological evaluation in Raw 264.7 macrophages and HMEC-1 microvasculature cells showed enhanced porphyrin synthesis by the dendrimers **(95)** (6 fold) and **(94)** (4.6 fold) in macrophages as compared to endothelial cells. Free ALA in comparison to the ALA dendrimers **(94)** and **(95)** had only a slight selectivity towards macrophages (1.7 fold) thus showing a possible application of these dendrimers in vascular PDT.

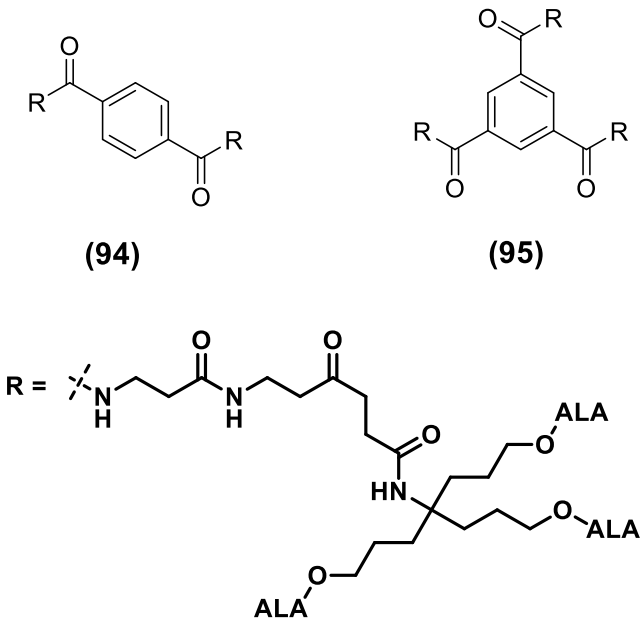

Figure 51. Structures of ALA dendrimers **(94)** and **(95)**.

1.10 Objectives of the project

5-Aminolevulinic acid photodynamic therapy has been successfully used clinically both as a therapeutic and diagnostic tool for treatment of cancer. However it suffers from various drawbacks such as stability, low lipid solubility and targeting effect. As discussed in section 1.10.3, various strategies have been explored to overcome these drawbacks. These includes ALA-esters to improve its lipophilicity, conjugation with a peptide sequence or a biomolecule (nucleoside, vitamin, glycoside and folic acid) to improve its targeting effect and synthesizing ALA-dendrimers to deliver multiple copies of ALA.

The overall aim of this project was to build upon some of these strategies to develop novel prodrug systems for the targeted delivery of multiple ALA units.

Our specific objectives were to:

- Develop an efficient synthetic route to ALA dendron derivatives, suitable for application in copper-catalysed azide-alkyne cycloaddition (CuAAC) chemistry.
- Apply these building blocks for the preparation of simple biomolecule-targeted ALA prodrugs.
- Apply these building blocks for the preparation of a novel peptide-targeted delivery system for ALA, in which multiple ALA dendrons (effectors) are attached to a peptide-targeted core unit via CuAAC chemistry. The general model structure of such a targeted dendrimeric ALA prodrug system is outlined in Figure 52.
- Evaluate the ability of peptide-targeted ALA dendrimers to generate PpIX in a cancer cell line, and assess the potential of these prodrugs for PDT.
- Explore other peptide-based strategies for the targeted delivery of ALA dendrons and other photosensitiser molecules.

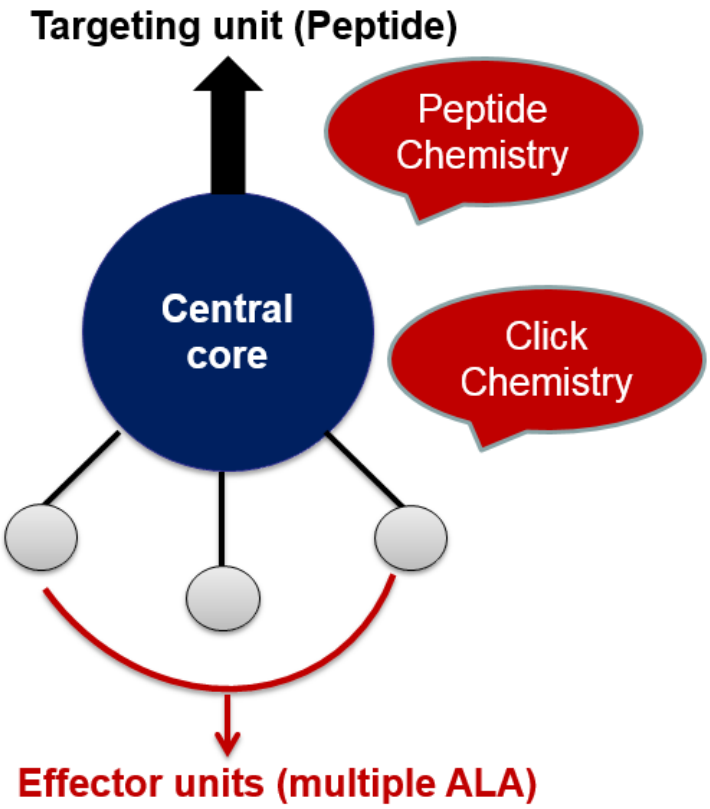

Figure 52. Model for peptide-targeted ALA dendrimers.

CHAPTER 2: RESULTS AND DISCUSSION (Preparation of effector units)

2.1 Introduction to dendrimers

Dendrimers in general are well-defined, highly branched, globular macromolecules with multiple arms arising from a central core.[210] Such architecture provides many advantages for drug delivery. Dendrimers are multivalent and allow attachment of several copies of drug molecules, targeting groups and solubilizing groups in a well-defined manner. They also give reproducible pharmacokinetic behaviour due to their low polydispersity.[211] Dendrimers can be chemically synthesized either by divergent or convergent approaches (Scheme 7).

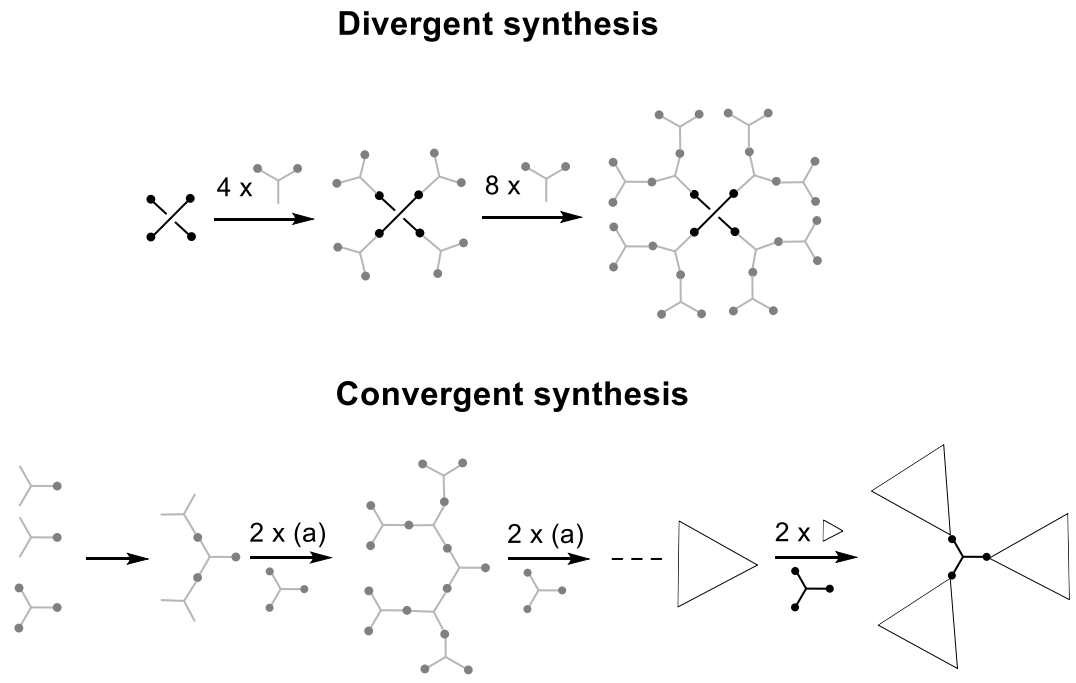

Scheme 7. Convergent and divergent routes of synthesis for dendrimers (adapted from Klajnert *et al.*)[212].

A divergent approach involves synthesis from the core and moves outwards through a series of reactions which must be driven to completion to avoid any defects in the dendrimers.[213] Convergent approaches, which were developed by Hawker and Frechet, involve assembling small synthesized molecules on the outer surface and through chemical reactions moving inwards towards the

core.[214, 215] Since the convergent approach involves functionalisation of a smaller number of reactive sites, the chances of any side reactions as compared to the divergent approach are minimal. In recent years, dendrimers have also been synthesized via click chemistry involving azide-alkyne cycloaddition.[216-218] The high efficiency and simplicity of such reactions are very suitable for both chemical strategies of dendrimer synthesis.

The terminal groups of dendrimers allow multiple drug molecules to be attached which can lead to an enhanced therapeutic effect, whereas dendrimers which allow localization of unstable drug molecules deeper within the dendrimer structure can shelter them from the environment. The size and structure of dendrimers may also be favourable for carrying a high payload of therapeutic agents to tumours, as it favours their entry into the highly permeable tumour vasculature, and the abnormal tumour lymphatic system retains the dendrimers due to the enhanced permeability and retention effect (EPR) (Figure 53).[219]

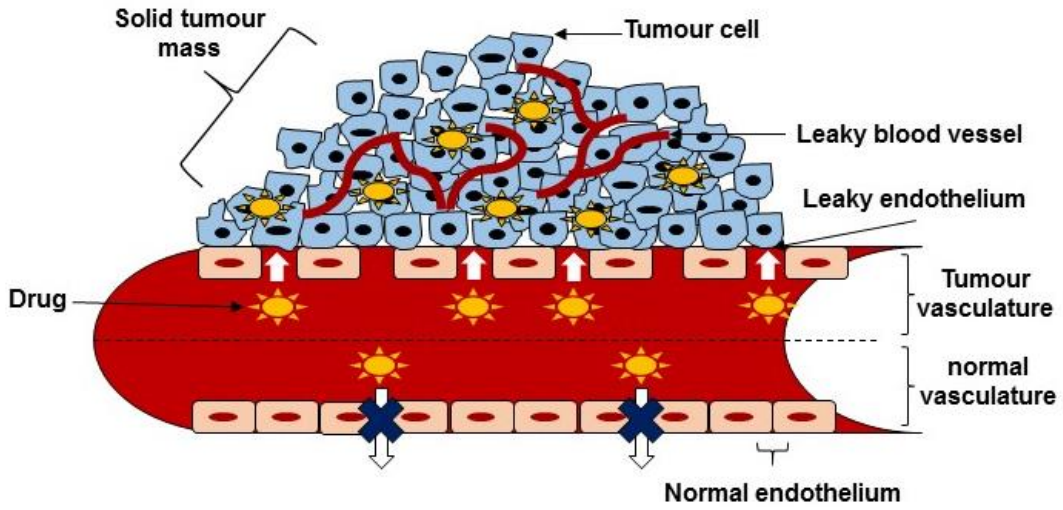

Figure 53. Representation of an EPR effect (adapted from Kumar *et al.*[220]). The figure shows that the normal endothelium has tightened cell-cell junctions resulting in less drug entry. In the case of tumours, the vascular endothelium has cell-cell junction with a wider gap opening, thus leading to an enhanced accumulation of macromolecuar drugs.[219]

2.1.3 Dendrimers in Photodynamic therapy

One of the recent developments in the field of dendrimers is their application to photodynamic therapy.[202] Dendrimers containing multiple copies of ALA (3 to 18) have been synthesized and evaluated *in vitro* and *in vivo* for their ALA-mediated PpIX release and for their PDT activity (Section 1.9.4). It was found that by attaching multiple copies of ALA, efficient and sustained release of PpIX from ALA was observed as compared to free ALA at equimolar doses.[207] Since the terminal amino group of each copy of ALA is protonated *in vivo,* this also led to increased water solubility for the ALA-dendrimer conjugate.[209] Attempts have also been made to synthesize dendrimer conjugates with porphyrins acting as a core unit. For instance, Nishiyama *et al.* in 2003 reported the synthesis and biological studies of third-generation aryl ether dendrimers having Zn-porphyrin as the core photosensitiser surrounded by either 32 positively charged groups ($C(O)N(H)(CH_2)_2NMe_3$) [32(+)DPZn] or negatively charged (COO^-) [32(-)DPZn] groups on its periphery (Figure 54).[221]

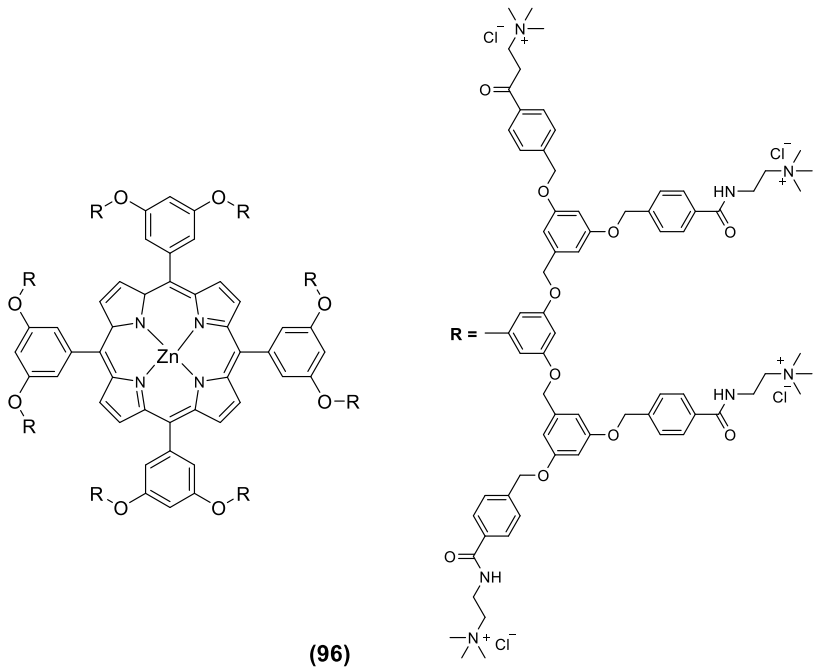

(96)

Figure 54. Chemical structure of 32(+)DPZn dendrimer **(96)**.

Biological studies revealed both type of dendrimers to be internalized into Lewis lung carcinoma cells, however the PDT effect of the positively charged dendrimers was found to be 230 times higher than its negative counterpart. This is possibly due to strong adsorption of the positively charged dendrimer to the negatively charged membrane components (glycoproteins) through electrostatic interactions.[221]

2.2 Synthesis of ALA dendrons

The objectives of this project required the preparation of a series of ALA dendron derivatives which could be attached to a core molecule or targeting unit via copper catalysed azide-alkyne cycloaddition (CuAAC) (Figure 55). The current section discusses the stepwise synthesis of such ALA dendrons (effector units) which involved attachment of multiple copies of ALA on to a multifunctional building block by controlled synthesis via ester linkages (Figure 55).

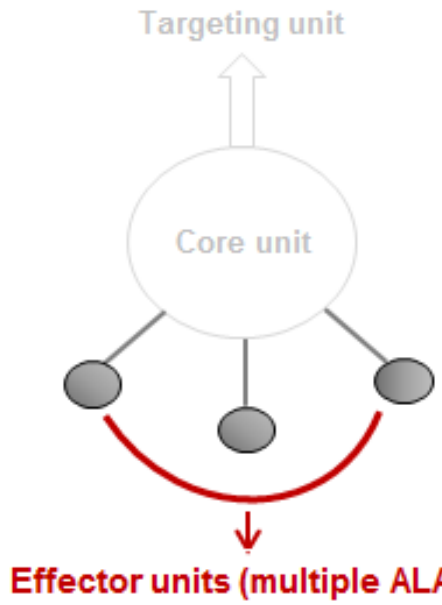

Figure 55. Application of ligatable ALA dendrons. The effector units are attached to the core by CuAAC chemistry .

2.2.1 Synthesis of first-generation ALA dendrons

Tris(hydroxymethyl)aminomethane, Tris **(97)** and 4-amino-4-(3-hydroxypropyl)-1,7-heptanediol, Ext-Tris **(98)** were chosen as the intitial building blocks (Figure 56).

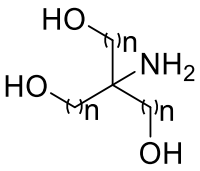

(97), n = 1;
(98), n = 3

Figure 56. Structures of the building blocks Tris and Ext. Tris **(97)** and **(98)**.

The choice of these building blocks was based on their simple structure, multiple hydroxyl groups for attachment of effector units (ALA) and the terminal amino group which could be acylated with an alkyne derivative (4-pentynoic acid, 4-PA) to generate ligatable building blocks. The effector units were synthesized by modification of the procedures reported by Battah *et al*.[203, 204] The first step was the Boc protection of ALA **(99)**. Here, a suspension of ALA.HCl **(40)** in THF was treated with di-*tert* butyl dicarbonate, followed by slow addition of base, DIEA. This released the ALA slowly into the solution so that it could be intercepted by the excess acylating agent in solution before competing self-condensation could intervene (Scheme 8).[222] The product **(99)** was obtained in a higher yield (80% vs 60%) than the originally reported procedure which uses aq NaOH/dioxane as the solvent, without slow neutralisation of ALA.[203]

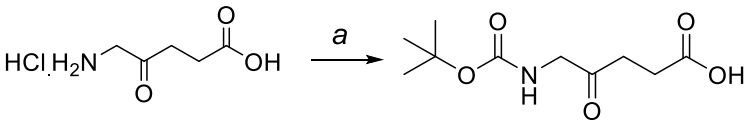

(40) **(99)**

Scheme 8. Synthesis of Boc-ALA **(99)**. *Reagents and conditions: a.* Di-*tert* butyl dicarbonate, THF, DIEA, 16 h, **78%.**

Boc-protection of ALA was followed by the stepwise assembly of the first generation ALA dendrons **(90)** and **(102)** (Scheme 9). The building blocks **(97)** and **(98),** as discussed earlier, have multiple attachment sites (for N and O acylation) and hence the next step in the scheme of synthesis involved selective Z-protection of the amino groups of the building blocks **(97)** and **(98)**. In the case of **(97)**, benzyl chloroformate (Z-Cl) was used for the protection of the amino group of **(97)**. The reaction was caried out in a biphasic mixture of

EtOAc/H_2O and sodium bicarbonate at RT to give **(100)** in 47% yield. The protection of the amino group of the extended dendron **(98)** was carried out using N-(benzyloxycarbonyloxy) succinimide (Z-OSu). Previous work in our laboratory has shown that both N and O acylation occurs when Z-Cl is used for the preparation of **(98)**, and hence the less reactive Z-OSu was used.[223] Purification of the crude product by silica gel chromatography gave **(101)** which, however showed, an additional peak in ^{1}H-NMR at δ 2.74 ppm, probably due to N-hydroxysuccinimide. Subsequent purification by precipitation of the crude product from the minimum quantity of cold water, followed by centrifugation gave the expected purified product **(101)** in 42% yield. The resulting Z-protected derivatives **(100)** and **(101)** were then esterified with Boc-protected ALA **(99)** via EDC.HCl/DMAP activation. EDC.HCl was used as a coupling agent over DCC as reported by Battah *et al.*[203] for better separation of the urea by-product (water soluble), and the reactions were carried out in dry DCM at 30 °C for 48 h to give the expected Z-protected conjugates **(90)** and **(102)** in good yields (Scheme 9).

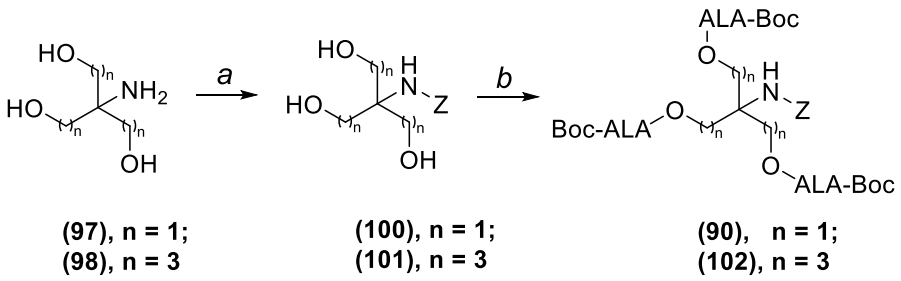

(97), n = 1;
(98), n = 3

(100), n = 1;
(101), n = 3

(90), n = 1;
(102), n = 3

Scheme 9. Synthetic route adopted for preparation of first generation ALA dendrons (Initial approach). *Reagents and conditions*: *a*. Z-Cl, EtOAc/H_2O, $NaHCO_3$, RT, 5 h, **47% (100)**; Z-OSu, THF, RT, 20 h, **42% (101)**; *b.* Boc-ALA, EDC.HCl, DMAP, DCM, 30 °C, 48 h, **43% (90), 40% (102)**;

In order to transform **(90)** and **(102)** into ligatable derivatives, the next step involved cleavage of the Z group. Deprotection of **(90)** was first attempted via transfer hydrogenolysis in order to avoid the inconvenience of using H_2 gas (Scheme 10). Treatment of **(90)** with ammonium formate (hydrogen donor) and Pd/C in MeOH according to the method of Baldoli *et al.*[224] showed the presence of a new ninhydrin-positive spot on the TLC baseline. However, work up of the reaction followed by TLC analysis showed multiple spots which were

also ninhydrin positive, but with higher R_f values compared to the original baseline spot. When conventional hydrogenolysis of **(90)** was attempted replacing ammonium formate with H_2 gas, similar results were obtained.

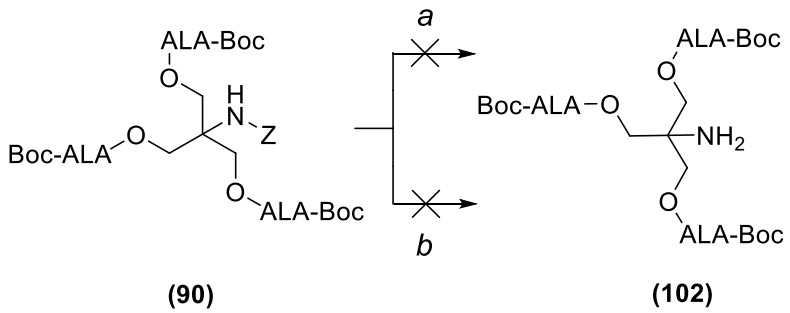

(90) **(102)**

Scheme 10. Initial attempts for hydrogenolysis of **(90)**. *Reagents and conditions*: *a.* Pd/C, ammonium formate, MeOH, RT, 1.5 h; *b.* Pd/C, H_2, MeOH, 1.5 h, RT.

Due to the conversion of the initial polar ninhydrin-positive product to less polar materials, it was suspected that the free amine initially formed on hydrogenolysis of **(90)** was undergoing acylation via intra or intermolecular reaction with the ALA ester units. This is consistent with a report by Newkome *et al.* who observed intramolecular rearrangement of the ester derivative **(97a)** via a five-membered cyclic intermediate to form the amide **(97b)** (Scheme 11).[222, 224] Such a side reaction was not reported by Battah *et al.* when carrying out the hydrogenolysis of **(90)** with Pd/C in EtOAc/MeOH.[203]

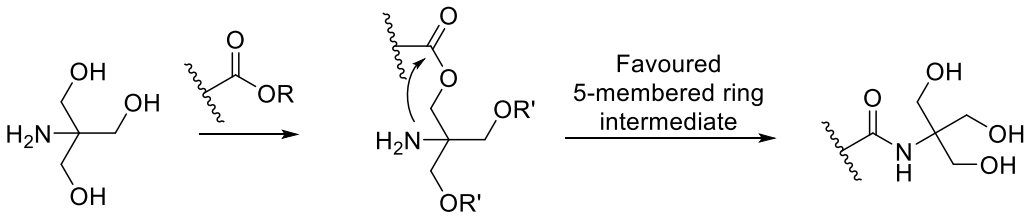

(97) **(97a)** **(97b)**

Scheme 11. Mechanism of intramolecular rearrangement of amino Tris esters.

In order to suppress such a rearrangement, the hydrogenolysis of **(90)** was repeated under acidic conditions (Scheme 12). In this way the final product thus obtained would be a salt and unreactive towards any possible O to N-acyl migration. Two conditions were attempted: either with AcOH/MeOH as solvent, or with precisely one equivalent of HCl in MeOH. The expected deprotected

product **(92)** was isolated as the salt in both the experiments (Scheme 12), however the procedure involving AcOH was favoured over methanolic HCl to avoid the risk of any additional Boc cleavage.

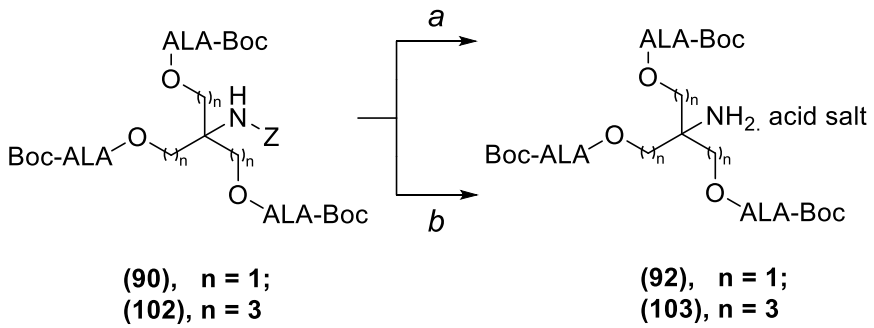

Scheme 12. Hydrogenolysis of **(90)** and **(102)** under acidic conditions. *Reagents and conditions*: *a.* **(90)**, Pd/C, H_2, MeOH, 2M HCl in dioxane; *b.* **(90)** or **(102),** 10% Pd/C, H_2, MeOH/AcOH (3:1, v/v), RT, 30 min, **90% (92)**, **96% (103)**.

The last step for the preparation of ligatable ALA dendrons (Scheme 13) involved attachment of an alkyne handle to the intermediates **(92)** and **(103)**. 4-Pentynoic acid **(104)** was chosen as the alkyne spacer due to its simple structure and ready availability. For the preparation of **(105)**, 4-pentynoic acid **(104)** was first activated with EDC.HCl/HOBt followed by addition of **(92)** and dropwise addition of DIEA (Scheme 13). The reaction proceeded to give the expected product **(105)**, but in low yields (11%).

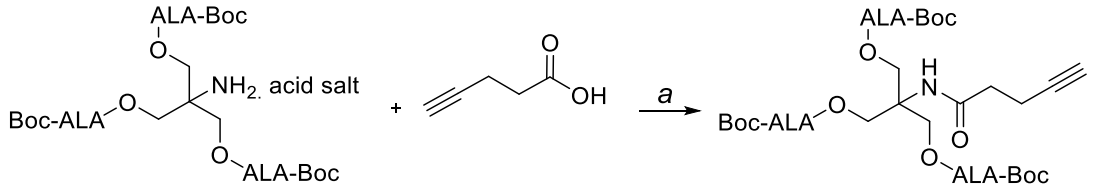

Scheme 13. Acylation of **(92)** with 4-pentynoic acid **(104)**. *Reagents and conditions: a*. EDC.HCl, HOBt.hydrate, DIEA, DMF, RT, 32 h, **11%**.

A similar outcome was obtained using the succinimido ester of 4-pentynoic acid **(106)** (prepared by treatment with N-hydroxysuccinimide and EDC.HCl), but for the extended dendron **(107)**, an acceptable yield (40%) of the expected product was obtained (Scheme 14).

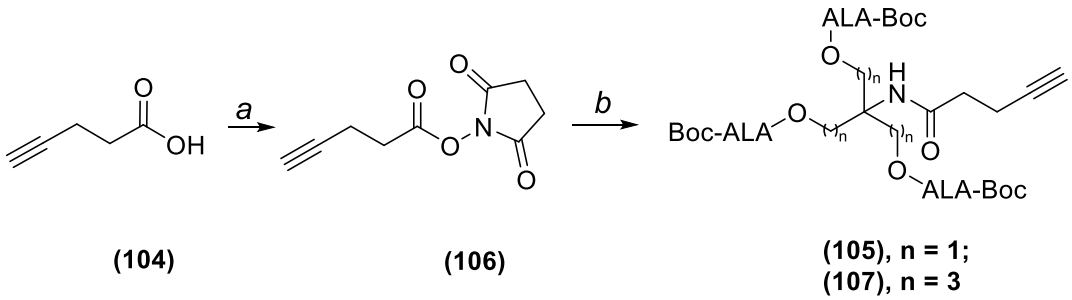

Scheme 14. Acylation of **(92)** and **(103)** with 4-pentynoic acid succinimido ester **(106)**. *Reagents and conditions: a.* N-hydroxysuccinimide, EDC.HCl, DMF, RT, 16 h, **71%** *b.* **(106)**, DIEA, DMF, RT, 48h, **7% (105)** and **40% (107)**.

The low yield for **(105)** showed that it is apparently difficult to neutralise the acetate derivative **(92)** with DIEA for acylation without competing intramolecular rearrangement or other side reactions observed previously.

To overcome the issues encountered during the synthesis of ALA dendrons **(105)** and **(107)**, an alternative route of synthesis was investigated which involved N-acylation of Tris **(97)** with 4-pentynoic acid **(104)** in the first step. This would provide a conjugate having only free hydroxyl groups available for acylation with Boc-ALA **(99)** and thus avoid any inter/intramolecular acyl group migrations later in the synthesis. Scheme 15 gives an overview of the different experimental conditions that were attempted with **(97)**.

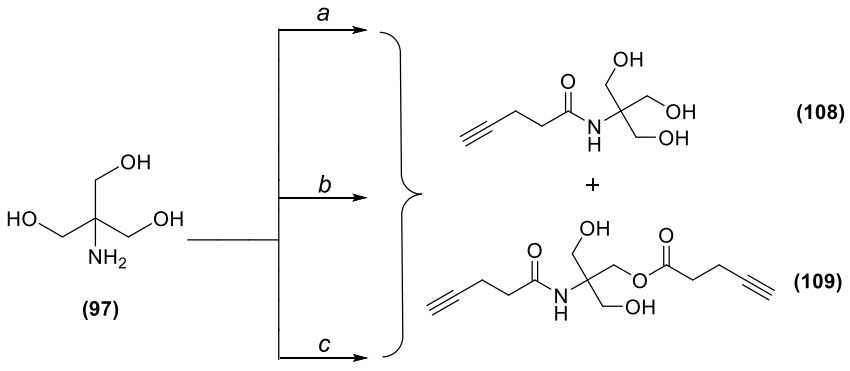

Scheme 15. Strategies adopted for the effective N-acylation of Tris **(97)**. *Reagents and conditions*: *a.* **(106)**, THF, DIEA, RT, 48 h; *b.* **(106)**, EtOAc, H_2O, DIEA, RT, 48 h; *c.* 4-pentynoic acid, DCC, HOBt.hydrate, DIEA, DMF, RT, 48 h.

Initial attempts to acylate the amino function of **(97)** with **(106)** gave a mixture of N- and O- acylated products as shown by ^{1}H NMR analysis. Changing the solvent to THF, or using 4-pentynoic acid **(104)** and DCC/HOBt activation gave

similar results. To avoid competitive N- and O-acylations, a modification in the synthetic route was therefore made (Scheme 16), and the three hydroxyl groups in **(97)** were initially silylated using TIPS-Cl and imidazole according to the procedure of Cunico *et al.*[225]

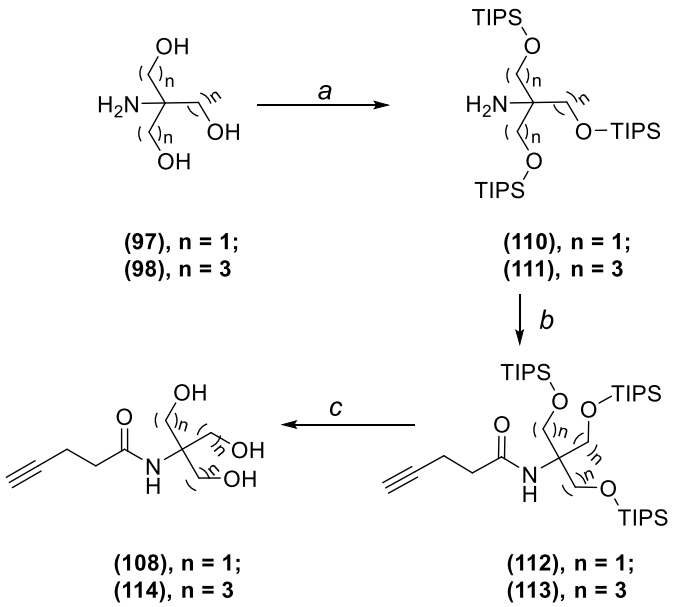

Scheme 16. Silylation strategy for acylation of Tris compounds. *Reagents and conditions: a.* TIPS-Cl, imidazole, DMF, 50 °C, 60 h, **quant (110)**; 48 h, **94% (111)**; *b.* 4-pentynoic acid, EDC.HCl, HOBt.hydrate, DIEA, 30 °C, 24 h, **82% (112)**, **81% (113)**; *c.* TBAF, THF, Dowex (50WX8, hydrogen form, 200-400 mesh), $CaCO_3$, MeOH, 3 h, **70% (108)**, 16 h, **65% (114)**.

TIPS-Cl was chosen for the protection due to its low cost and ready availability. The TIPS group can also be readily removed with fluoride ion under mild conditions. The reaction proceeded smoothly and the expected product **(110)** was obtained in quantitative yield. This was followed by acylation with 4-pentynoic acid **(104)** using EDC.HCl/HOBt activation, which gave the expected product **(112)** in excellent yield (82%). The next step involved removal of the silyl protecting groups using TBAF. The reaction was monitored by TLC and after 3 h, complete disappearance of the starting material was observed along with the appearance of a new spot. However the expected product **(108)** was highly water-soluble and hence a conventional work up procedure involving aqueous phase extraction could not be followed. Avoiding aqueous extraction did not permit removal of excess tetrabutylammonium fluoride, which otherwise is difficult to remove by column chromatography. As a solution, Kaburagi *et al.* (2007) reported a simple work up strategy for

TBAF-promoted desilylation which involves treatment with sulfonic acid ion exchange resin and calcium carbonate (Scheme 17).[226] The treatment results in a tetrabutylammonium-resin complex and calcium fluoride which are insoluble and can be removed by simple filtration of the reaction mixture.

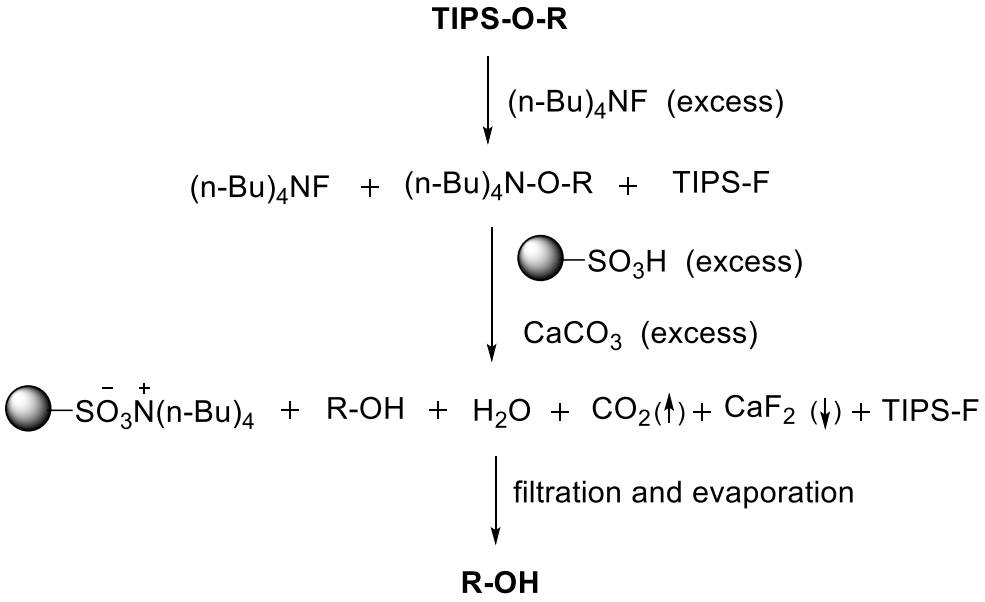

Scheme 17. Work-up strategy to remove excess TBAF post-desilylation (adapted from Kaburagi *et al.*).[226]

This strategy was applied for the isolation of **(108)**. The work-up was carried out by treating the residue from the desilylation reaction with DOWEX ion exchange resin (50WX8, hydrogen form, 200-400 mesh) and $CaCO_3$ in MeOH as solvent. The reaction was initially monitored for 16 h (to ensure complete desilylation) and showed appearance of a new spot at the end of 3 h along with disappearance of starting material. However, multiple spots were observed on TLC at the end of 16 h, and hence the reaction time was subsequently restricted to 3 h, which resulted in a very good yield of **(108)** (70%). The modified steps followed in Scheme 16 were also applied for the extended dendron **(98)** and similar results were obtained leading to formation of **(114)** in a yield of 65%.

The overall approach compares very favourably to a recently reported direct synthesis of **(108)** via EEDQ activation of 4-pentynoic acid.[227] Our approach is suitable for both **(108)** and **(114)** and a wide range of acylated Tris dendrimers

(discussed in section 2.2.2).

Finally, intermediates **(108), (114)** with free hydroxyl groups were esterified with Boc-ALA **(99)** via EDC.HCl/DMAP activation, as previously (Scheme 18). This gave **(105)** and **(107)** in excellent yields (89% and 77% respectively).

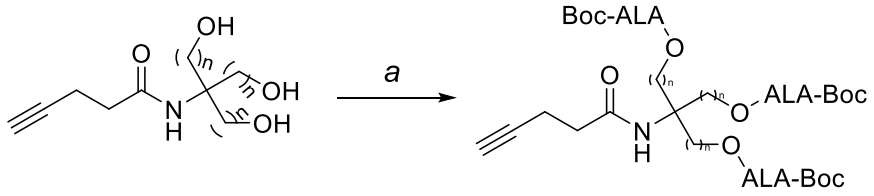

(108), n = 1;
(114), n = 3

(105), n = 1;
(107), n = 3

Scheme 18. Coupling of Boc-ALA **(99)** with **(108)** and **(114)**. *Reagents and conditions: a.* **(99)**, EDC.HCl, DMAP, dry DCM, 30 °C, 48 h, **89% (105)**; 32 h, **77% (107)**.

2.2.2 Synthesis of second-generation ALA dendrons

The successful synthesis of ligatable first-generation ALA dendrons was followed by the investigation of synthetic strategies for building a second-generation ALA dendron. Such an ALA dendron would have 9 copies of Boc-ALA within the same building block **(115)** as compared to 3-ALA units in the first generation ALA dendrons **(105)** and **(107)** (Figure 57).

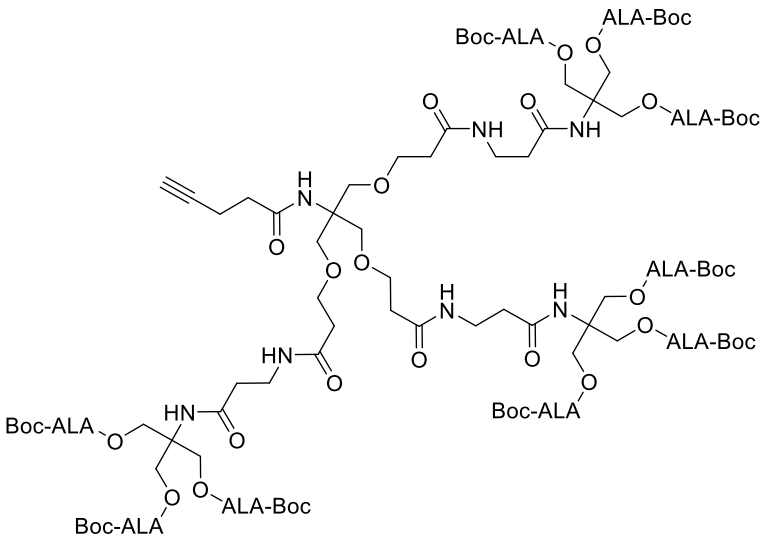

(115)

Figure 57. Structure of 2nd generation ALA dendron (initial approach).

An initial approach involved synthesizing a triacid component (Scheme 19) which would serve as a building block for the attachment of a first generation ALA intermediate **(92)**. The first step of this synthetic route was to generate a triester derivative based on a method described by Cardona *et al.*[228] 1,4- Addition of Tris **(97)** to *tert*-butyl acrylate **(116)** in a mixture of DMSO/H_2O (9:1) with NaOH as base gave **(117)** in 26% yield. The yield of the reaction was lower (26%) than that reported in the literature (54%), possibly due to some loss at the stage of evaporation of DMSO under vacuum. This reaction was followed by acylation of the amino group with 4-pentynoic acid using EDC.HCl/HOBt activation to obtain the expected alkyne derivative **(118)** in good yield (63%). The last step of this scheme involved cleavage of the *t*-butylester groups using TFA at 0 °C, to give the required triacid **(119)**, which was used for the next step without any further purification.

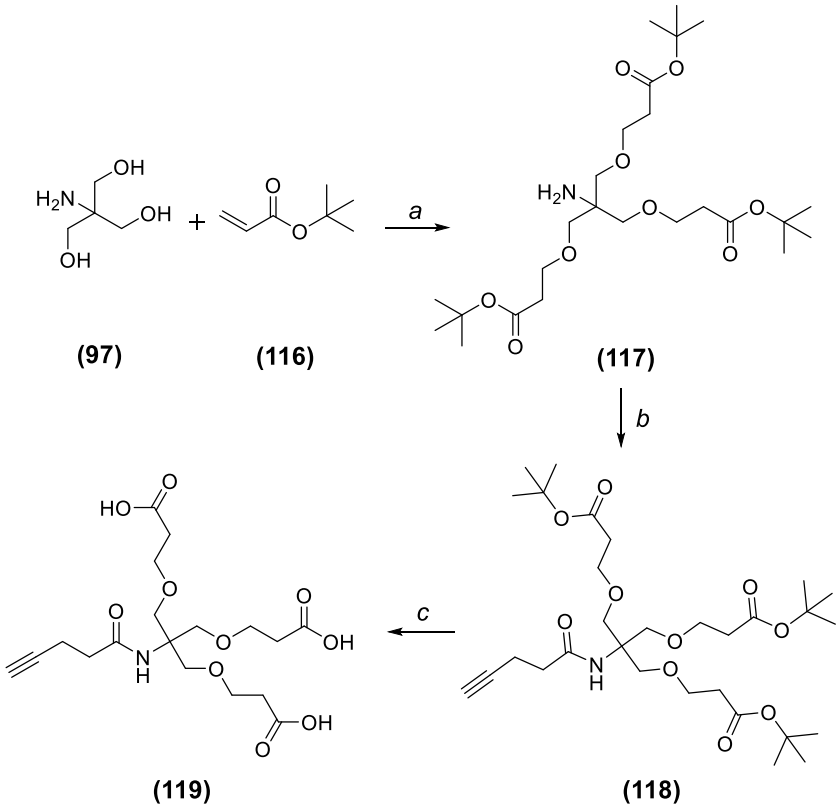

Scheme 19. Synthesis of a triacid **(119)** from Tris **(97)**. *Reagents and conditions: a.* NaOH, DMSO/H_2O, RT, 24 h, **26%**; *b.* 4-pentynoic acid, EDC.HCl, HOBt.hydrate, DIEA, DMF, RT, 36 h, **63%**; *c*. DCM, TFA, RT, 4 h, **88%**.

A modified first-generation ALA dendron intermediate for attachment to triacid **(119)** was synthesized as follows (Scheme 20):

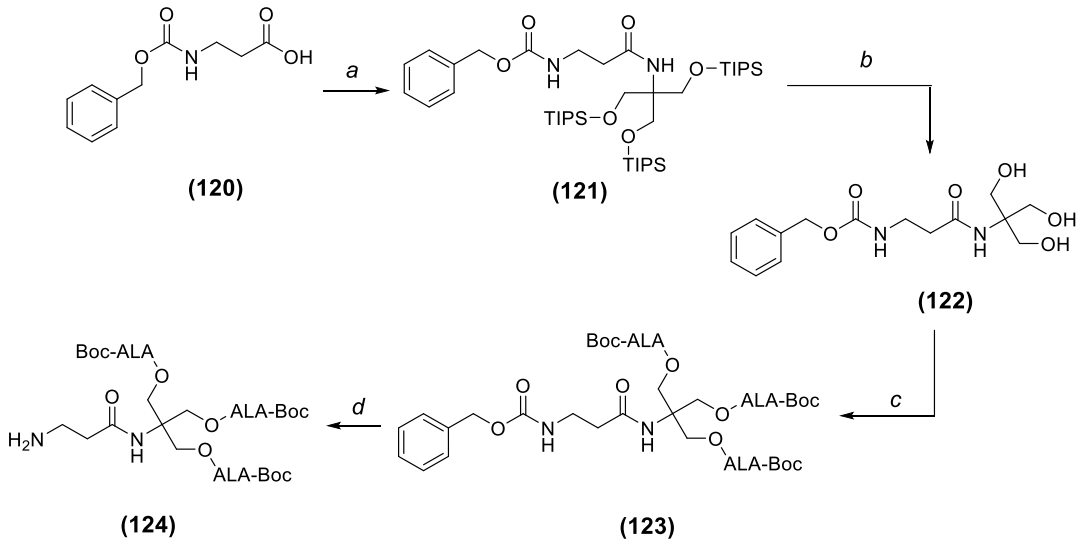

Scheme 20. Synthesis of ALA dendron **(124)**. *Reagents and conditions: a.* **(110)**, EDC.HCl, HOBt.hydrate, DIEA, RT, 36 h, **49%**; *b.* TBAF, THF, Dowex, $CaCO_3$, MeOH, 3 h, **74%**; *c.* **(99)**, EDC.HCl, DMAP, DCM, 32 ˚C, 36 h, **72%**; *d.* Pd/C, H_2, MeOH:AcOH (3:1), 20 min, **79%**.

Silylated Tris derivative **(110)** was first acylated with Z-β-ALA-OH **(120)** using EDC.HCl/HOBt activation to give **(121)** in 49% yield. The β-ALA spacer was expected to provide a more reactive amino function for acylation with the triacid **(119)**, as well as avoiding problems of *N*, *O*-migration on *N*-deprotection (Section). The next step was the removal of the silyl groups using a similar strategy as above which gave **(122)** in good yield.[229] Esterification of **(122)** with Boc-ALA using EDC.HCl and DMAP then gave **(123)** in 72% yield. Z-deprotection using PD/C and H_2 as previously yielded **(124)** as the acetate salt.

The acylation of triacid **(119)** with **(124)** was then explored. Initially the reaction was carried out using EDC.HCl/HOBt activation and the reaction was monitored by TLC (Scheme 21). However, TLC showed no trace of any new spots nor disappearance of the starting material **(124)**. The acylation was also attempted by changing the coupling agent to HATU, however it gave a similar result.

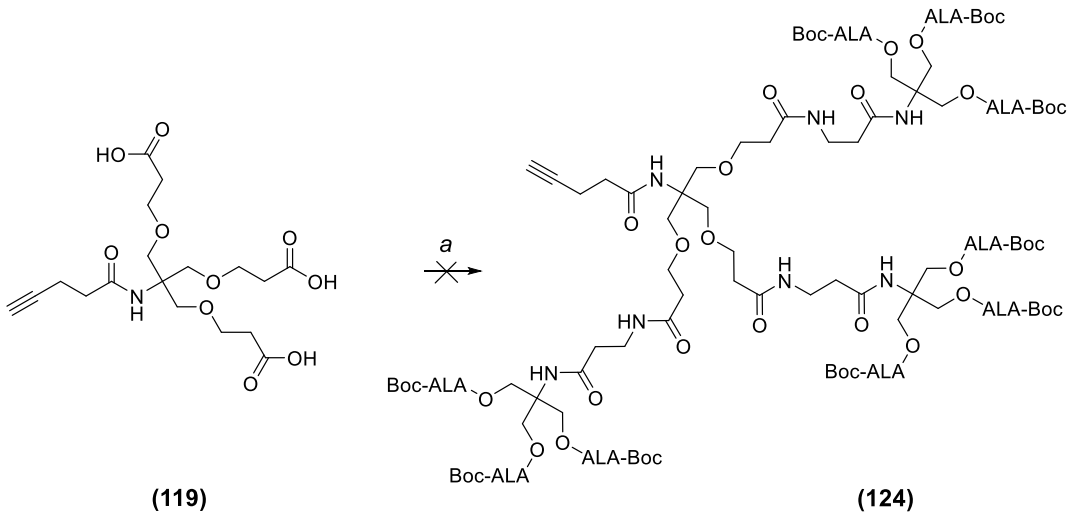

(119) **(124)**

Scheme 21. Attempted coupling of triacid **(119)** with ALA dendron **(124)**. *Reagents and conditions: a.* **(124)**, EDC.HCl, HOBt.hydrate, DIEA, RT, HATU, DMF, 32 h.

An alternative strategy was explored by using 5-aminoisophthalic acid as the dendron core. The choice of this core was based on the fact that the two carboxylic acid groups are held in a fixed spatial arrangement on the aromatic ring, which might thus favour attachment of bulky ALA dendrons. The attached amino group can also be acylated with an alkyne derivative to generate ligatable building blocks (Figure 58).

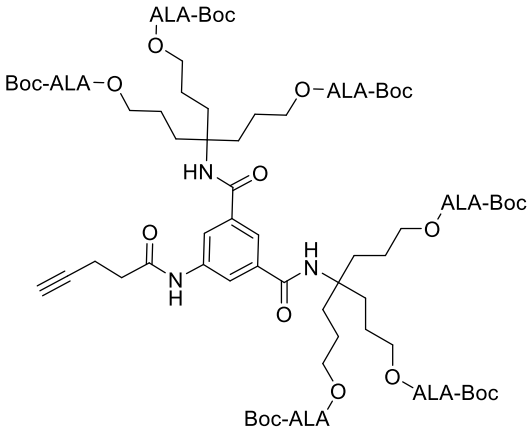

(125)

Figure 58. Proposed structure of a 2nd generation ALA dendron **(125)** synthesized from isophthalic acid.

The first step of the synthesis involved acylation of 5-aminoisophthalic acid **(126)** with 4-pentynoic acid **(104)** using EDC.HCl/HOBt activation (Scheme 22). The reaction was monitored by TLC, and after 32 h of reaction,

multiple spots were observed. This suggested the possible formation of coupled products derived from the desired conjugate **(127)** and isophthalic acid, which was supported by NMR of the crude product.

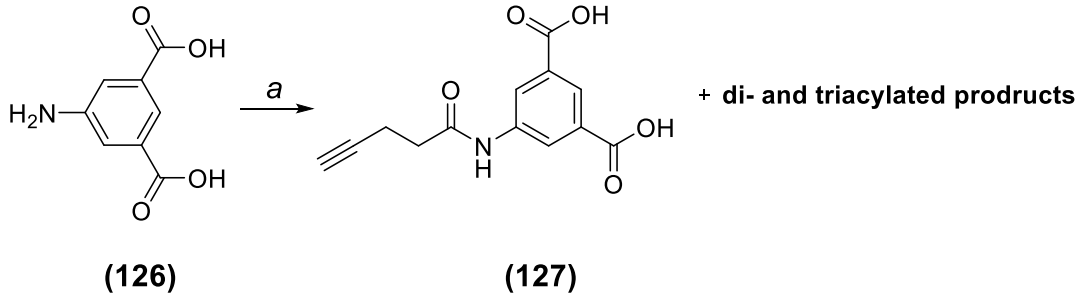

(126) **(127)**

Scheme 22. Initial attempt to conjugate **(126)** with 4-pentynoic acid. *Reagents and conditions: a.* 4-pentynoic acid, EDC.HCl, HOBt.hydrate, DIEA, RT, 36 h.

The synthetic strategy was modified and **(126)** was esterified by treatment with EtOH and in the presence of catalytic amount of H_2SO_4 to yield the bis-ethyl ester **(128)** in good yield (Scheme 23). This reaction was followed by the acylation of **(128)** with 4-pentynoic acid under EDC.HCl/HOBt activation forming the expected alkyne derivative **(129)** in excellent yield (97%). The ethyl ester groups were then hydrolysed with NaOH/MeOH to obtain **(127)** as a white solid.

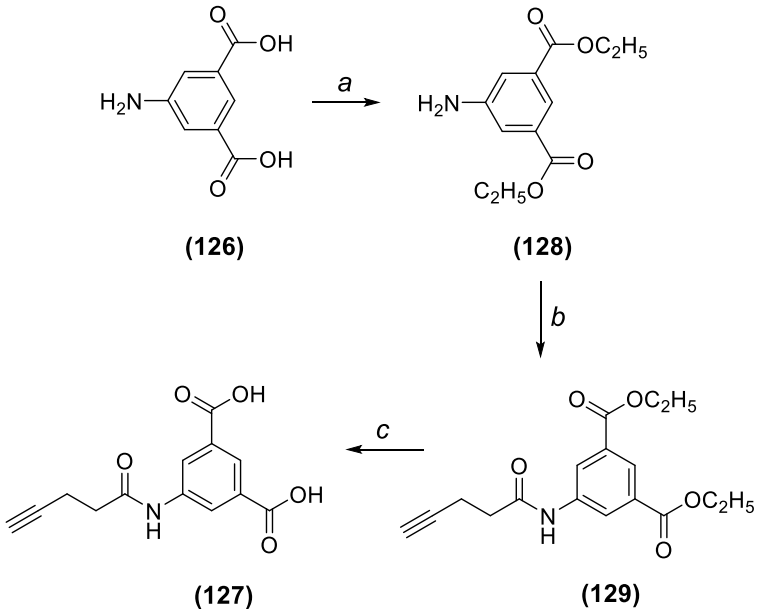

(126) **(128)** **(129)** **(127)**

Scheme 23. Synthesis of ligatable 5-aminoisophthalic acid derivative **(127)**. *Reagents and conditions: a.* EtOH, Conc. H_2SO_4, reflux, 20 h, **77%**; *b.* 4-pentynoic acid, EDC.HCl, HOBt.hydrate, DIEA, DMF, RT, 36 h, **97%**; *c.* NaOH, MeOH, 55 °C, 2 h, **96%**.

The intermediate **(127)** was then acylated with **(111)** using EDC/HOBt activation to give the expected silyl protected derivative **(130)** (Scheme 24).

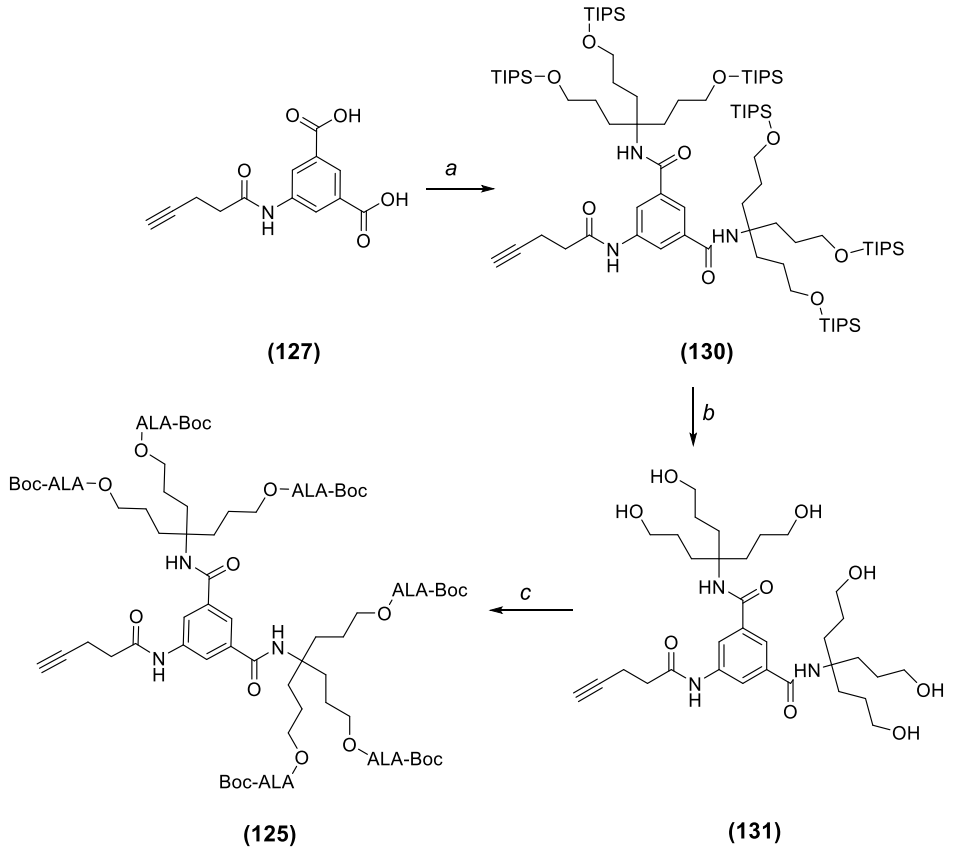

Scheme 24. Synthesis of 2nd generation ALA dendron **(125)**. *Reagents and conditions: a.* **(111)**, EDC.HCl, HOBt.hydrate, DIEA, DMF, RT, 36 h, **64%**; *b.* TBAF.H_2O, AcOH, THF, RT, 4 h; *c.* **(99)**, EDC.HCl, DMAP, DCM, RT, 36 h.

Following the successful preparation of **(130)**, the conversion to **(131)** was attempted on a trial scale. The silyl groups of **(130)** were removed using TBAF using the same conditions as previously to obtain **(114)**. Although ^{1}H-NMR of the product obtained after column chromatography showed traces of silyl groups, esterification with Boc-ALA using EDC.HCl and DMAP gave the desired product **(125)** which was confirmed by mass spectrometry.

2.3 Summary

In summary, two synthetic routes were investigated for the synthesis of first-generation ALA dendrons **(105)** and **(107)**, which involved either N- (*via* Z) or O- (*via* silyl) terminal protection of the building blocks **(97)** and **(98)** prior to attachment of multiple copies of Boc-ALA. In the second approach, initial protection of the three hydroxyl groups of **(97)** and **(98)** proved to be advantageous as it avoided completely the problem of O- and N- acyl group migration. This gave a high-yielding route to both **(105)** and **(107)**. In contrast, the initial approach involving the Z-protection gave problems of acyl group migration for the Tris derivative **(90)** which resulted in low overall yields. The dendrons **(105)** and **(107)** thus obtained bearing three Boc-protected ALA units then served as key intermediates for all the targeted and non-targeted ALA dendrimers discussed in the current work (Figure 59).

Synthesis of second-generation ALA dendrons involved initially an attempt to attach ALA dendrons **(124)** to triacid component **(119)**; however, no successful outcome was observed under different coupling conditions. An alternate strategy with 5-aminoisophthalic acid as the dendron core proved to be successful, and a second-generation ALA dendron with 6 copies of ALA **(125)** was successfully synthesized on a trial scale and confirmed by mass spectrometry.

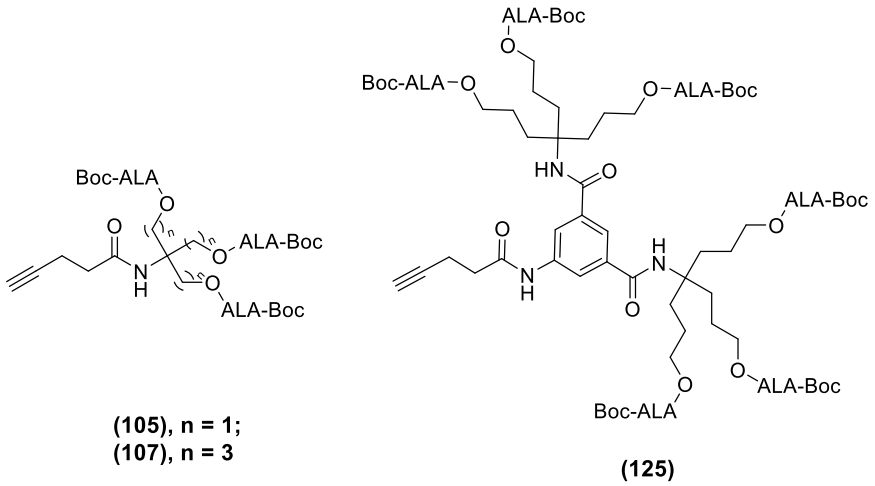

Figure 59. Structures of first- and second-generation ALA dendrons **(105)**, **(107)** and **(125).**

CHAPTER 3: RESULTS AND DISCUSSION (Preparation of core molecules)

Having developed a successful synthesis of alkyne-functionalised ALA dendrons, the next step was to investigate the synthesis of complementary azide-containing core molecules, suitable for attachment to various targeting units (Figure 60).

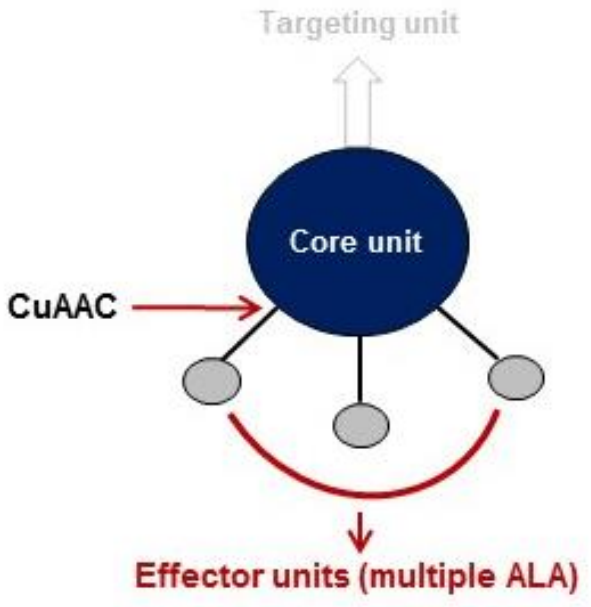

Figure 60. Model for targeted-ALA dendron showing the core unit and its conjugation to effector units via copper-catalysed azide-alkyne cycloaddition.

The following section discusses the different strategies that were explored for the preparation of core units followed by their conjugation to effector units.

3.1 Choice of core unit

Gallic acid and *p*-hydroxybenzoic acid were chosen as the central core units for the synthesis of 1st generation targeted ALA dendrimers. Gallic acid has three hydroxyl groups to load spacer arms with an azido function, which in turn may participate in coupling with the effector units through azide-alkyne cycloaddition. In the specific gallic acid derivative chosen for this study,[230] the spacer arms consist of triethylene glycol units that were designed to aid water solubility and to counteract the hydrophobic effect of the aromatic nucleus. The carboxylic acid function of the building block provides the means to attach a

targeting group such as a peptide (Figure 61). *p*-Hydroxybenzoic acid derivative **(133)** was chosen as a test model to explore different reaction conditions for attaching multiple ALA units.

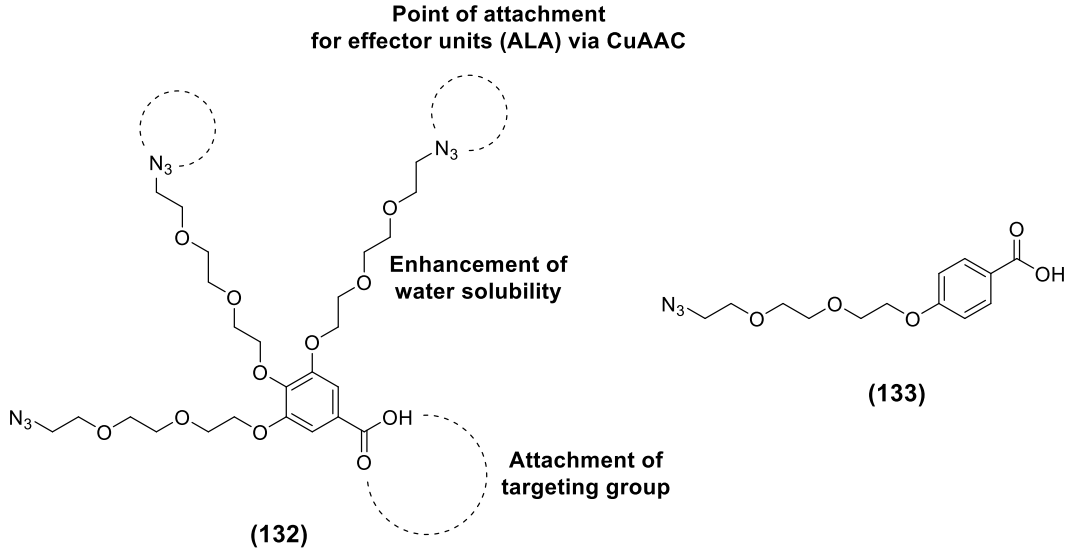

Figure 61. Multifunctional GATG core **(132)** and simplified model core **(133)**.

Roy and co-workers have reported the synthesis of gallic acid triethylene glycol (GATG)-based dendrimers derived from **(132)**, but faced a common issue of low yields in synthesising the repeating unit of GATG, via a four-step sequence from triethylene glycol.[231-233] The procedure was later modified by Amaral *et al.* using a commercially available chlorohydrin as one starting material, providing a high yielding and large-scale route to the GATG derivative **(132)**.[230]

3.1.1 Synthesis of core unit

The azido-chloro derivative required for the spacer arm in **(132)** and **(133)** was prepared according to the method of Amaral *et al.* as outlined in Scheme 25.[230]

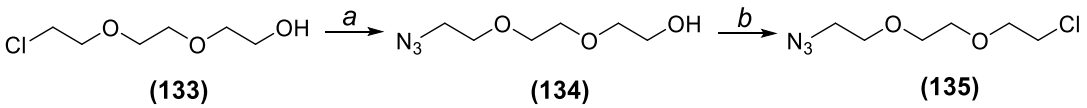

Scheme 25. Synthesis of azido-PEG-chloro derivative **(135)**. *Reagents and conditions*: *a.* NaN_3, H_2O, 75 °C, 48 h, **99%** *b.* $SOCl_2$, BTEAC, 65 °C, 3 h, **74%**.

Herein the chlorohydrin derivative **(133)** was treated with sodium azide in water to give azido-alcohol, **(134)** (99%) which was then further treated with thionyl

chloride and benzyltriethylammonium chloride (BTEAC) to give the required azido-chloro derivative **(135)** in 74% yield.

The basic building block for the initial model prodrug structure was *p*-hydroxybenzoic acid **(136)** which was first esterified with MeOH in the presence of sulfuric acid to give **(137)** in moderate yield (33%) (Scheme 26). **(137)** was then alkylated according to the procedure of Amaral *et al.*[30] with **(135)** in the presence of 18-crown-6 to give the expected model structure **(138)** in 75% yield. 18-Crown-6 was used as it is able to complex potassium ions effectively, thus increasing the nucleophilicity of the phenoxide from **(137)**. Amaral's procedure[230] was also applied for the gallic acid core structure, and the expected derivative **(140)** was also obtained in very good yield (72%).

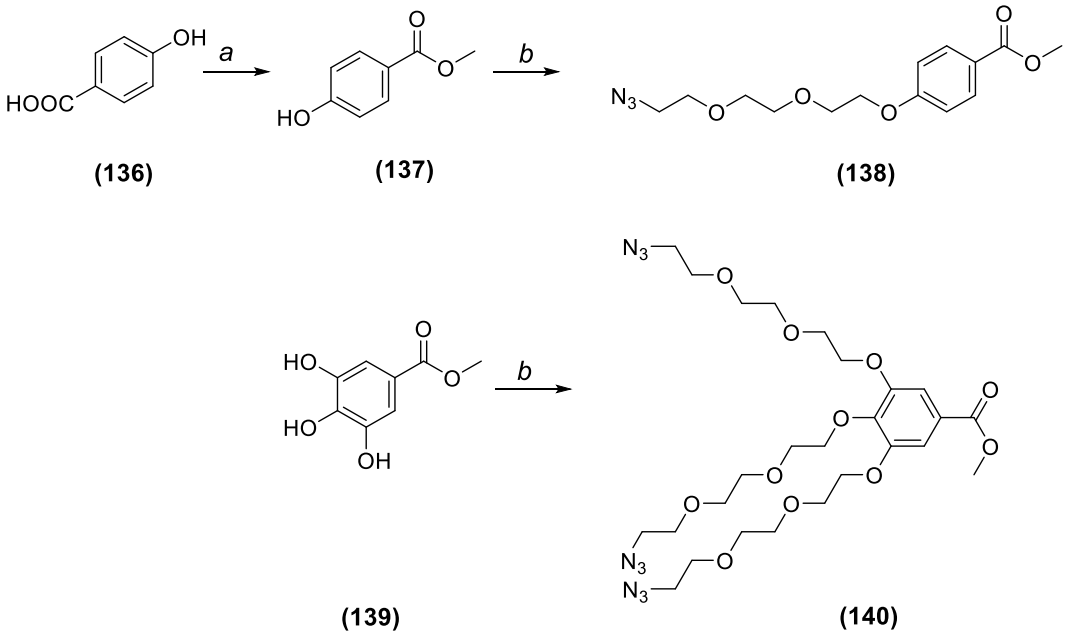

Scheme 26. Synthesis of core molecules **(138)** and **(140)**. *Reagents and conditions*: *a.* MeOH, Conc. H_2SO_4, 20 h, **40%** *b.* **(137)** or **(139)**, K_2CO_3, 18-Crown-6. DMF, DMF, 80 °C, 36 h, **75% (138)**, **72% (140)**.

3.2 Bioorthogonal ligations and click chemistry

3.2.1 Basic concept

Bioorthogonal ligations are a type of chemical reaction involving two mutually reactive functional groups or handles which react with each other under physiological conditions without interfering or interacting with any biomolecules present.[234] The term bioorthogonal chemistry was first introduced in 2003 by C. Bertozzi[235] and since then many such chemical reactions which meet the specific requirements of bioorthogonal ligations have been developed. These requirements include:[236]

1. Both the functional groups should be bioinert and non-toxic.

2. The rate of the reaction should be high, even at low concentrations of the starting material.

Various types of bioorthogonal ligations have been reported including copper (I) catalysed azide-alkyne cycloadditions (CuAAC), strain-promoted azide-alkyne cycloadditions (SPAAC), tetrazine ligations and photoclick reactions (between a tetrazine and alkene component).[236-238] An overview of chemical reactions of these types are shown in Figure 62.

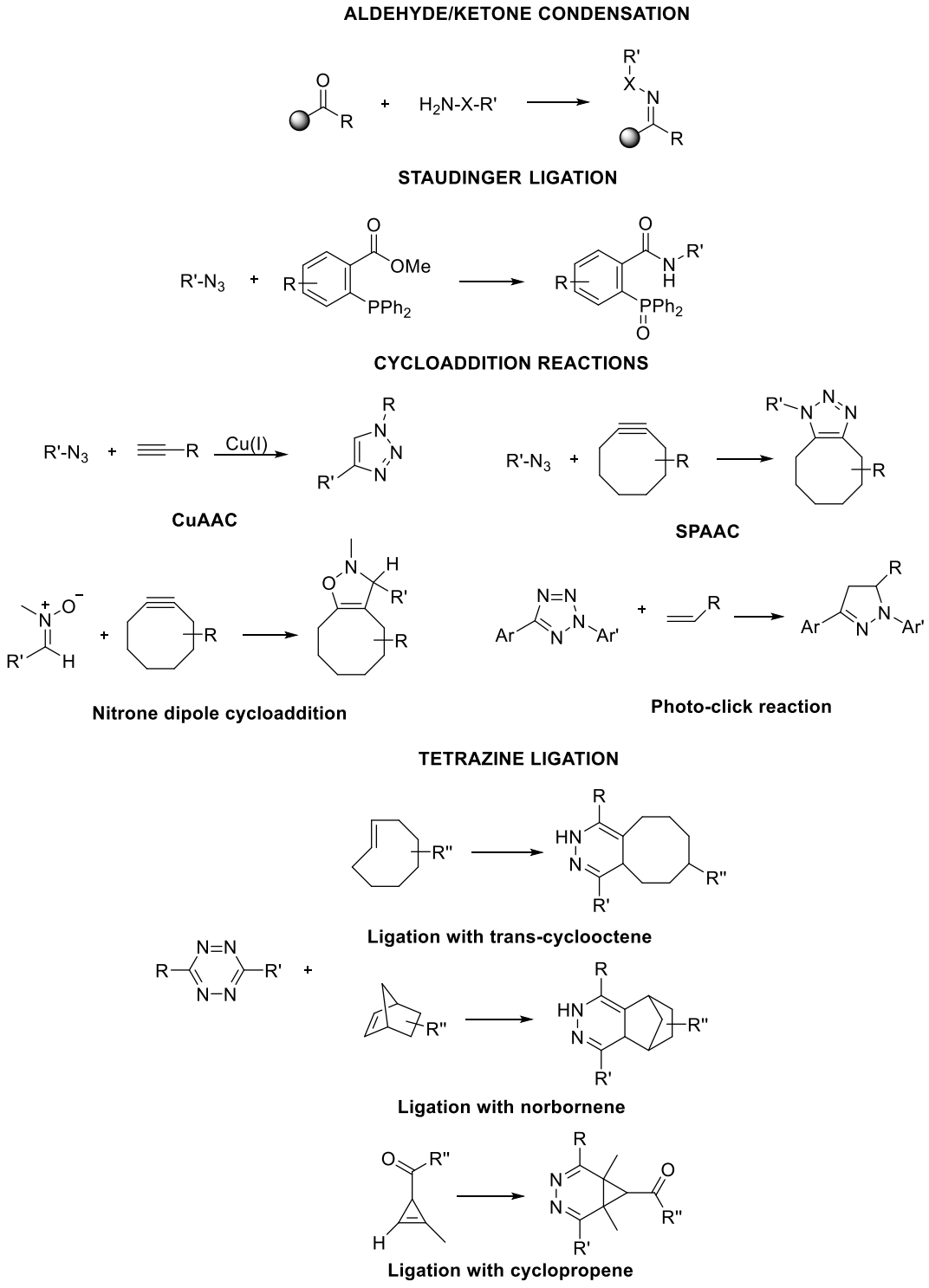

Figure 62. Overview of recently developed biorthogonal ligation chemistries.[236-238]

3.2.2 Cu (I) catalysed azide-alkyne cycloaddition/click chemistry

Copper-catalysed azide alkyne cycloaddition (CuAAC) is a widely used synthetic technique for the assembly of multifunctional molecules through the formation of 1,4-disubstituted 1,2,3-triazoles.[239] As originally described, the

Huisgen cycloaddition reaction between an organic azide and alkyne occurs at elevated temperature for several hours resulting in a mixture of 1,4- and 1,5-triazoles.[240, 241] However, it was found by Sharpless *et al.* that the involvement of a catalytic amount of Cu(I) accelerates the reaction at low temperature to form 1,4-triazole products only (Scheme 27).[239] The advantages of CuAAC are that it is stereospecific, robust, and product isolation is usually simple. CuAAC typically involves inexpensive reagents and catalysts, and proceeds with high efficiency and minimal by-products, under mild reaction conditions. Polar solvents such as water may also be used.[216]

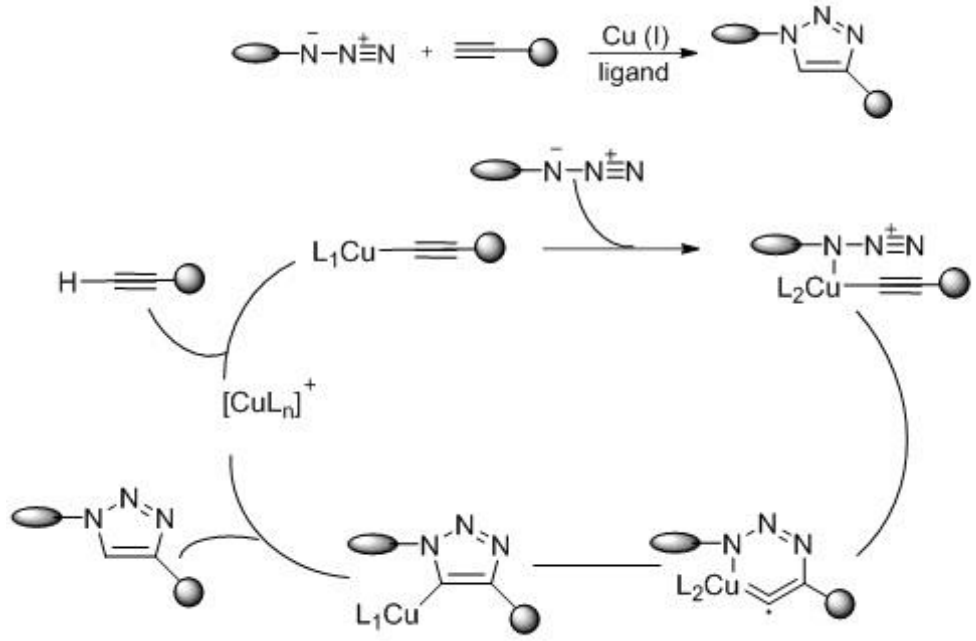

Scheme 27. Proposed mechanism of CuAAC.[216]

The reaction begins with the formation of a complex between an alkyne and copper, followed by the coordination of an organic azide with the copper centre. The mechanism then proceeds via a six-membered metallocycle transition state to the copper triazolide species, which undergoes reductive elimination to give the 1,4-disubstituted triazole.

In recent years, CuAAC has been applied to PDT in order to generate a variety of novel photosensitiser structures.[242-244]

3.2.3 Synthesis of non-targeted ALA dendrons

For the synthesis of the simplified model ALA dendron derivative **(141)**, a CuAAC click coupling was first attempted between azide **(138)** (1 eq) and alkyne derivative **(105)** (1 eq). The reaction was carried out in the presence of

$CuSO_4$ and sodium ascorbate (reducing agent) with DMSO/H_2O (9:1) as the solvent (Scheme 28). The use of $CuSO_4$ as a source of Cu(I) and a reducing agent (in this case sodium ascorbate) is one of the most commonly applied conditions in CuAAC.[216] Both the starting materials **(138)** (azide) and **(105)** (alkyne) had good solubility in DMSO, whereas stock solutions of $CuSO_4$ and sodium ascorbate were prepared in water.

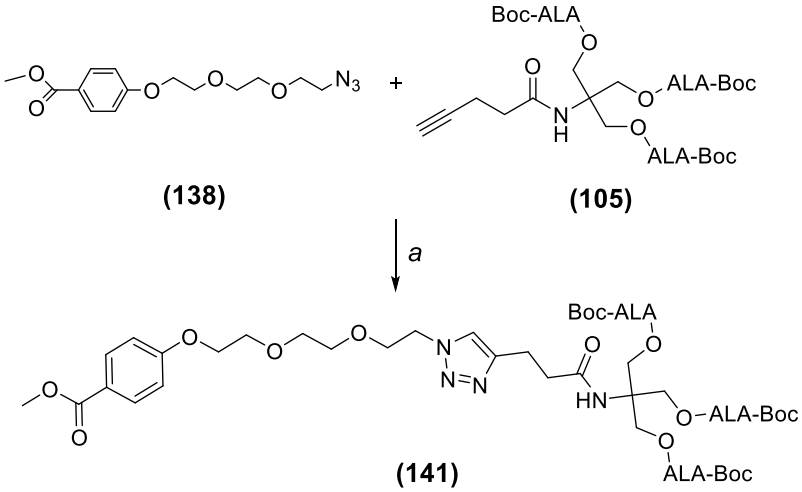

Scheme 28. Preparation of **(141)** via Cu(I)-catalysed click coupling of azide **(138)** and alkyne **(105)**. *Reagents and conditions*: *a.* $CuSO_4$, sodium ascorbate, DMSO/H_2O (9:1), 16 h.

The reaction was monitored by analytical HPLC, and after 16 h although there was a significant amount of unreacted azide **(138)** (R_t = 9.4 min) remaining, a new peak at 10.1 min was observed (Figure 63). The reaction was subsequently repeated changing the stoichiometry of alkyne:azide (2:1)[245] which resulted in complete disappearance of the starting material (azide) and the appearance of a distinct product peak on HPLC. Mass spectrometry confirmed the formation of the expected triazole **(141)**.

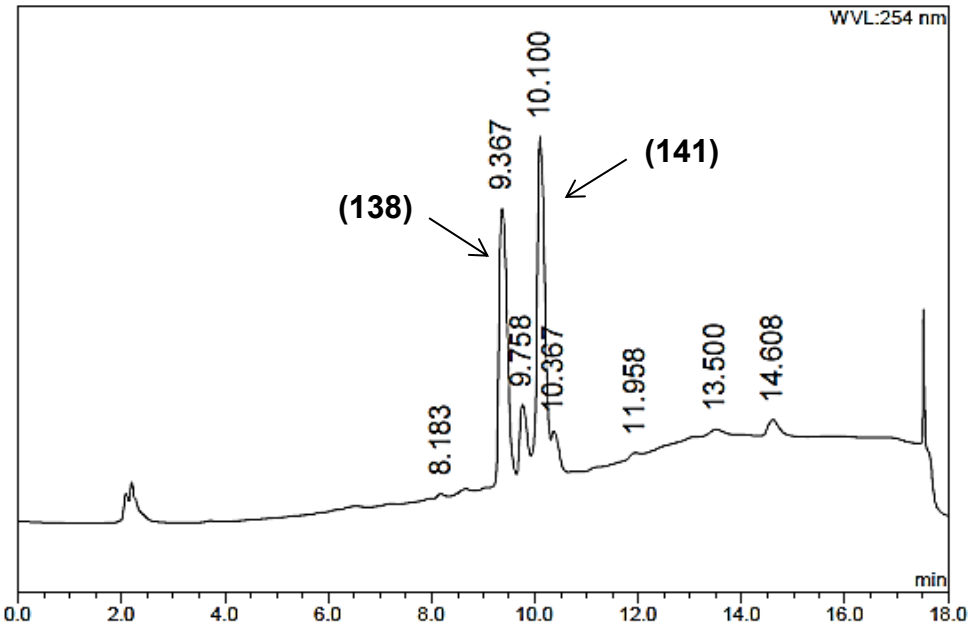

Figure 63. HPLC for click coupling reaction of **(138)** and **(105)** after 16 h.

Having established the general feasibility of preparing clicked dendrons such as **(141)**, the synthetic scheme was modified. Firstly the methyl ester of the **(138)** was hydrolysed to give the free acid (**142)** using aq. KOH/THF (Scheme 29). This would allow the attachment of a targeting unit, either after or before the click coupling. Secondly, the reaction solvent for the click reaction was changed to DMSO/H_2O/tBuOH (90:5:5 v/v/v), as this has been shown to limit potential side reactions in various CuAAC.[246]

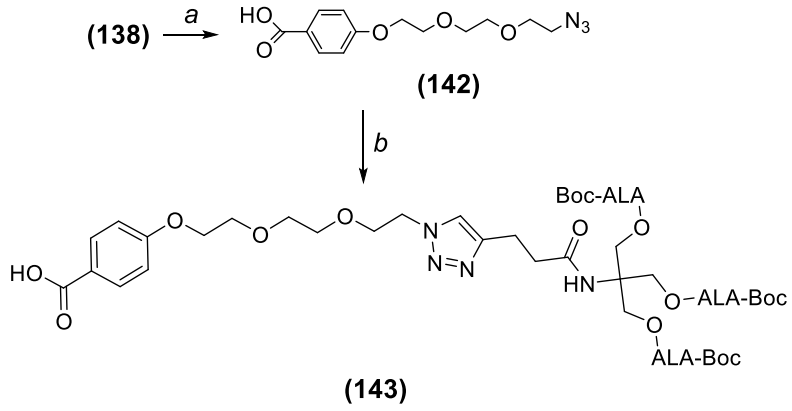

Scheme 29. Modified click strategy for the preparation of model compound **(143)**. *Reagents and conditions*: *a.* aq. KOH, THF, 50 °C, 24 h, **87%** *b.* **(105)**, $CuSO_4$, sodium ascorbate, DMSO/H_2O/*t*-BuOH (90:5:5 v/v/v), RT, 12 h, **53%**.

When azide **(142)** was coupled with alkyne derivative **(105)**, using the modified solvent mixture (Scheme 30), after 1 h reaction a single peak was observed on HPLC (R_t = 9.43 min), together with a very small amount of unreacted **(142)** (R_t = 7.89 min) (Figure 64). No further change was observed on prolonged reaction (12 h). The product was isolated by semi-preparative HPLC and was confirmed to be the expected triazole **(143)** by NMR and mass spectrometry. The final yield of **(143)** was 46%. A similar strategy was adopted for Ext Tris dendron **(107)** and the Boc protected clicked product **(144)** was isolated by semi-preparative HPLC with a yield of 44%.

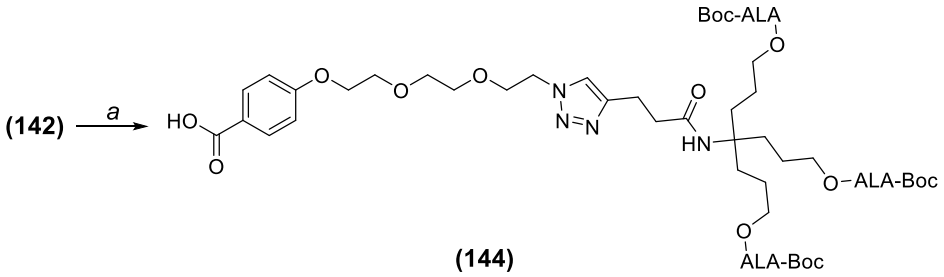

Scheme 30. Click strategy for the preparation of model compound **(144)**. *Reagents and conditions*: *a.* $CuSO_4$, sodium ascorbate, DMSO/H_2O/*t*-BuOH (9/0.5/0.5 v/v/v), RT, 12 h, **44%**.

Figure 64 shows the HPLC chromatograms for crude reaction mixtures for **(143)** and **(144)** showing the presence of new species at 9.43 min **(143)** and 9.62 min **(144)**, with disappearance of azide starting material at 7.89 min.

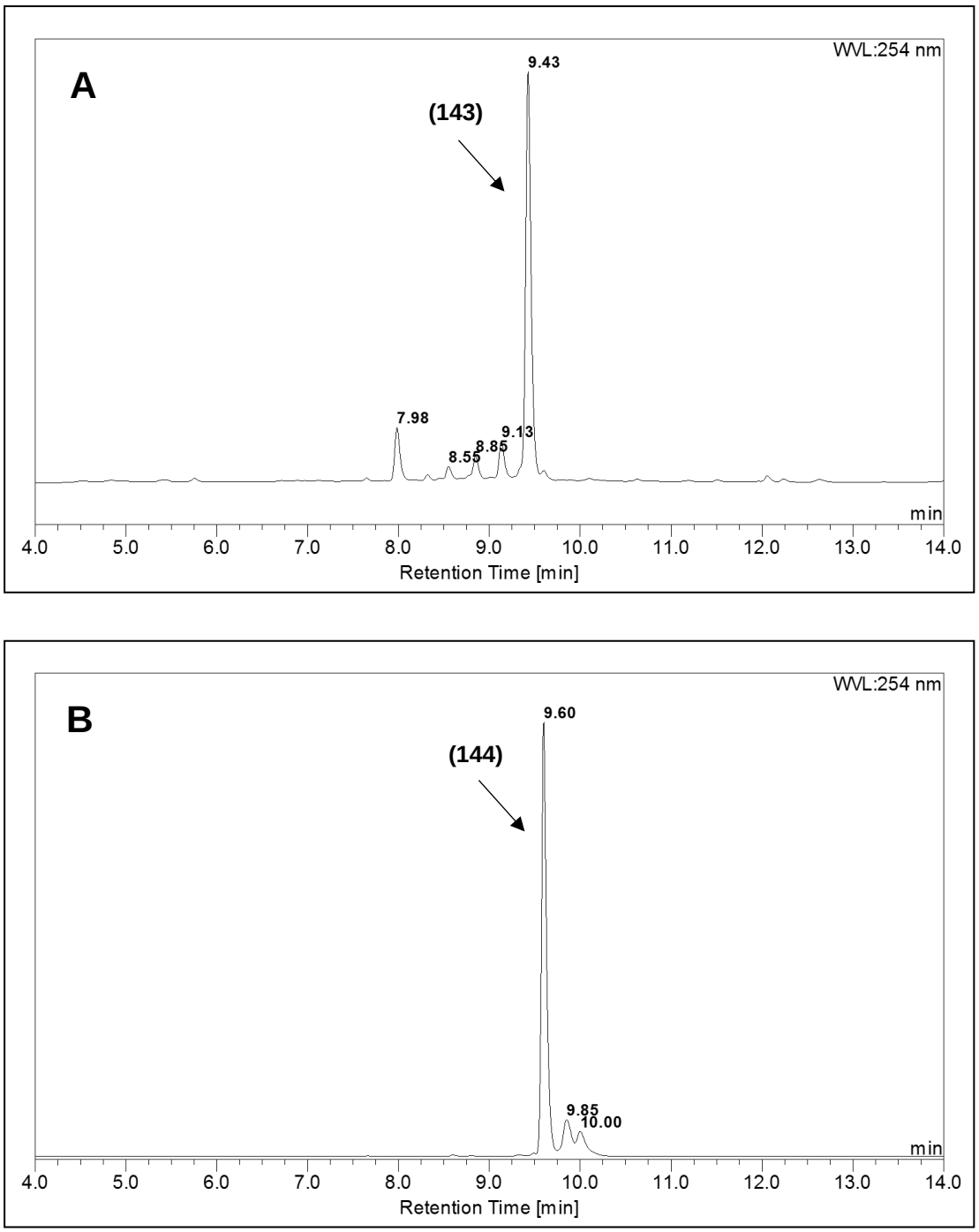

Figure 64. HPLC chromatogram for click coupling reaction of **(143)** and **(144)** after 1h.

A. Crude reaction mixture showing Boc-protected clicked product **(143)**.

B. Crude reaction mixture showing Boc-protected clicked product **(144)**.

The Boc protecting groups from dendrimers **(143)** and **(144)** were removed by treatment with 50% TFA in DCM (Scheme 31). The deprotection reactions were monitored by analytical HPLC with complete disappearance of starting materials and formation of a single new species being observed at the end of

30 min. The final conjugates **(145)** and **(146)** were freeze-dried from H_2O and obtained as TFA salts. The trifluoroacetic acid (TFA) salts of the resulting ALA dendrimers were prepared in preference to the hydrochloride salts as the former has an intrinsic buffering capacity,[247] and so would mitigate possible acidification of cell culture media and a consequent reduction in porphyrin yield, which is optimal between pH 7.0 (for the enzyme uroporphyrinogen decarboxylase) and 7.5 (for the enzyme coproporphyrinogen oxidase).[204] The final structures of the conjugates were confirmed by ^{1}H NMR, ^{13}C NMR and mass spectrometry.

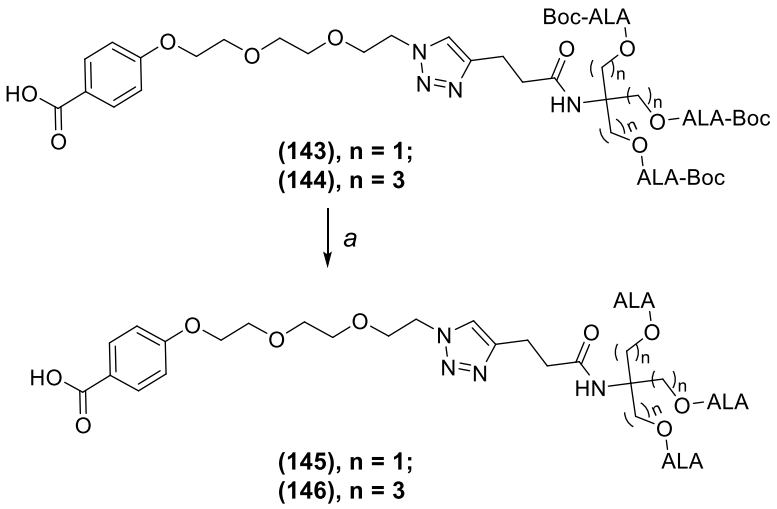

Scheme 31. Deprotection of model ALA dendrons **(143)** and **(144)**. *Reagents and conditions*: *a.* TFA: DCM (1:1, v/v), 30 min, 0 °C then RT**, 92% (145)**, **94% (146)**.

Figure 65 (A and B) shows an overlay of HPLC chromatograms for the two dendrimer systems. In each case the final clicked-ALA dendron **(145)** and **(146)** is shown along with the peaks for the Boc-protected clicked prodrugs and the starting azide **(142)**. The respective retention times for **(145)** and **(146)** were 4.80 and 4.98 min, i.e the extended Tris derivative **(146)** as expected was slightly more lipophilic than the Tris based compound **(145)**.

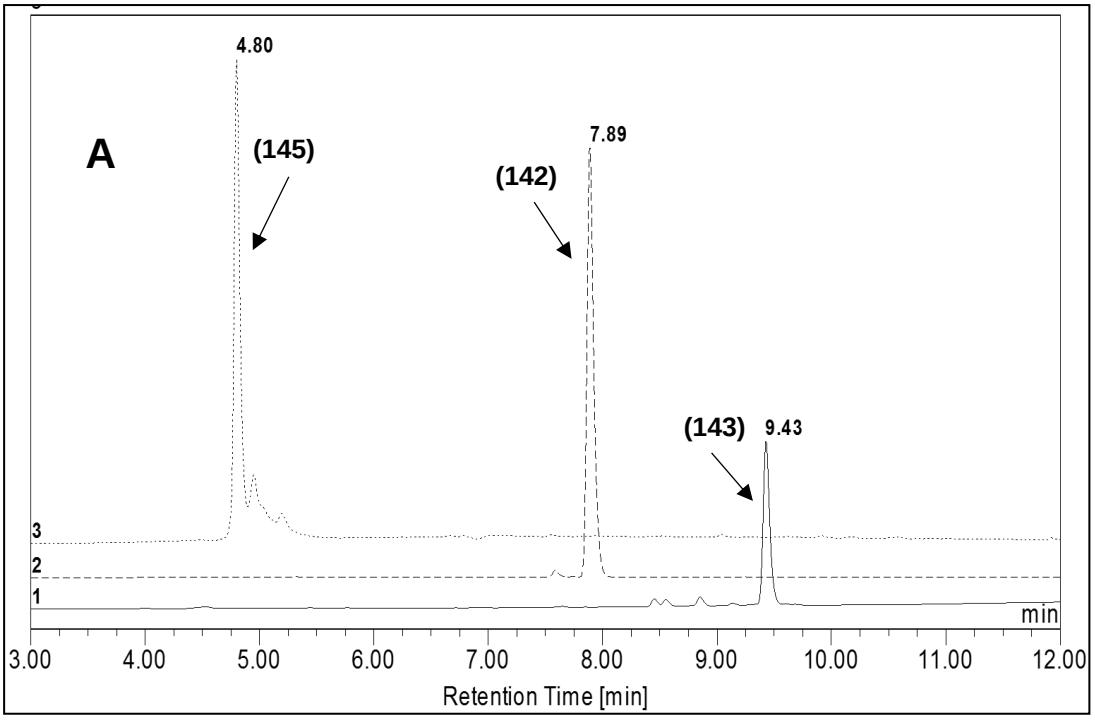

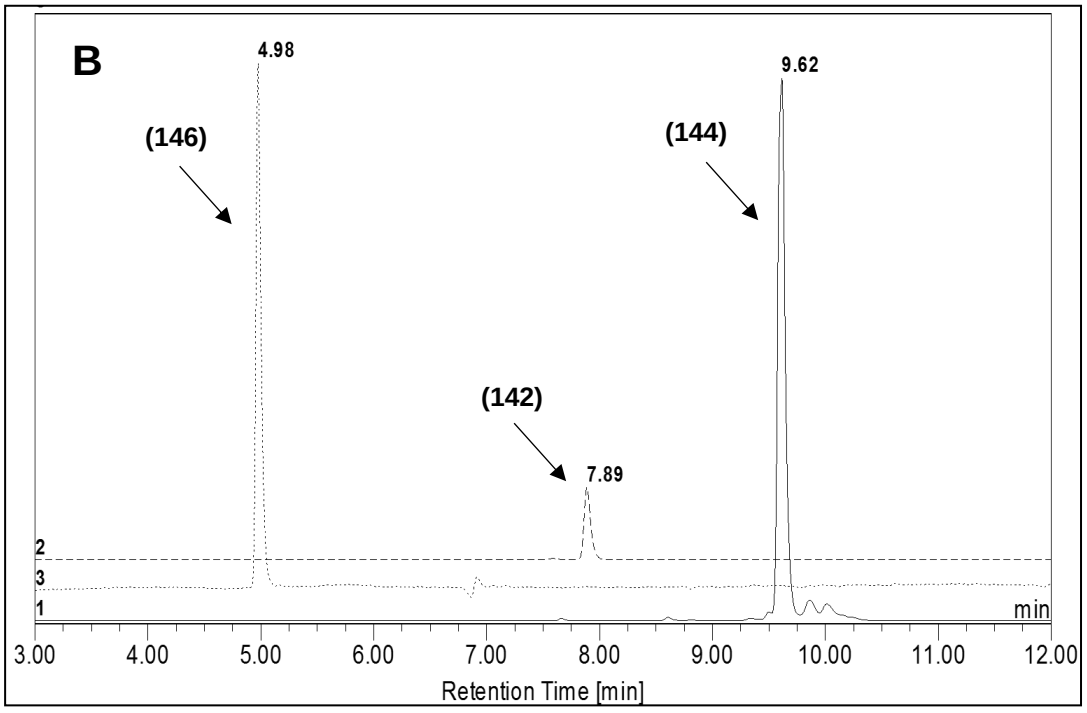

Figure 65. Overlay of HPLC chromatograms for clicked ALA dendrons **(145)** and **(146)**.

A. Overlay showing the product **(145)** and the starting azide **(142)** and Boc protected clicked prodrug **(143)**.

B. Overlay showing the product **(146)** and the starting azide **(142)** and Boc protected clicked prodrug **(144)**.

Click couplings were then attempted on the trivalent azide **(147)** using the optimised reaction conditions above with both alkyne derivatives **(105)** and **(107)** (Scheme 32).

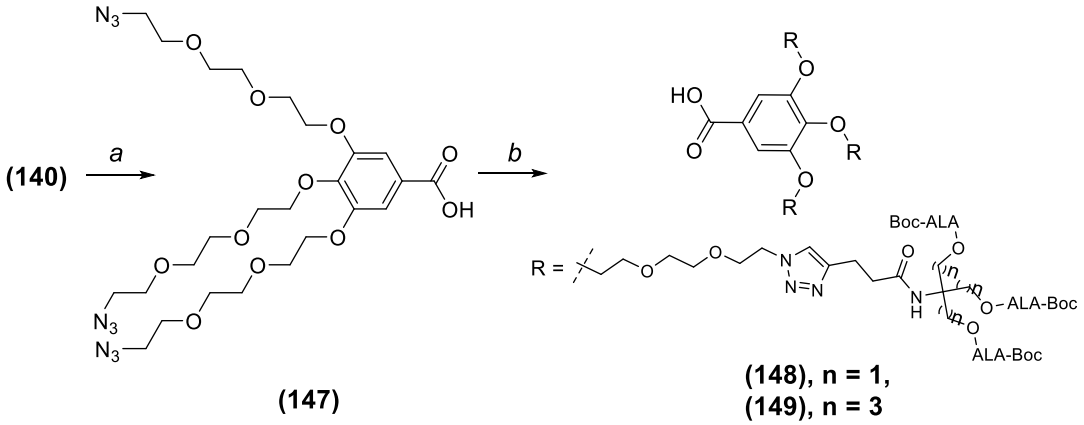

Scheme 32. Click couplings between **(147)** and ALA dendrons **(105)** and **(107).** *Reagents and conditions*: *a.* aq. KOH, THF, 50 °C, 24 h, **94%** *b.* **(105) or (107)**, $CuSO_4$, sodium ascorbate, DMSO/H_2O/*t*-BuOH (9/0.5/0.5 v/v/v), RT, 72 h, **50% (148), 52% (149)**.

The reactions were carried out for 72 h and monitored by HPLC (Figure 66). In both cases a major product peak was observed with disappearance of the starting material **(147)** (azide). The product peaks eluted at 10.5 min for **(148)** and 11 min for **(149)**.

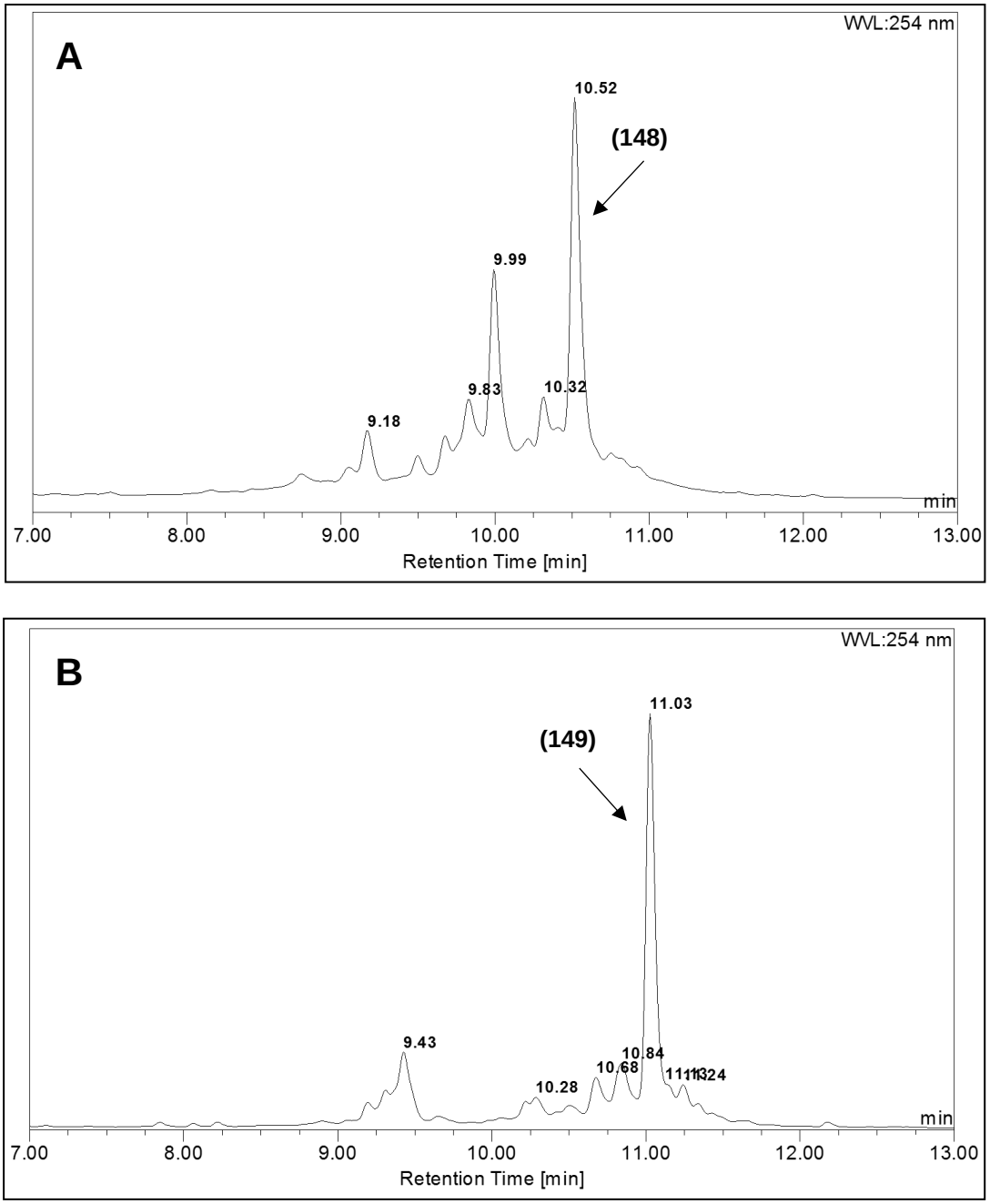

Figure 66. HPLC chromatograms for click coupling reaction of **(148)** and **(149)** after 72 h.

A. Crude reaction mixture showing Boc-protected clicked prodrug **(148)**.

B. Crude reaction mixture showing Boc-protected clicked prodrug **(149)**.

The final products were isolated by semi-preparative HPLC in yields of 50% and 52% for **(148)** and **(149),** respectively, and their structures were confirmed by ^{1}H NMR (which showed the expected integration of 3 x CH signals for the triazole units), ^{13}C NMR and mass spectrometry.The Boc protecting groups from dendrimers **(148)** and **(149)** were removed by treatment with 50% TFA in DCM for 30 min to give **(150)** and **(151)** as TFA salts in good yields

(Scheme 33). The conjugates obtained were once again characterized by ^{1}H NMR, ^{13}C NMR and mass spectrometry.

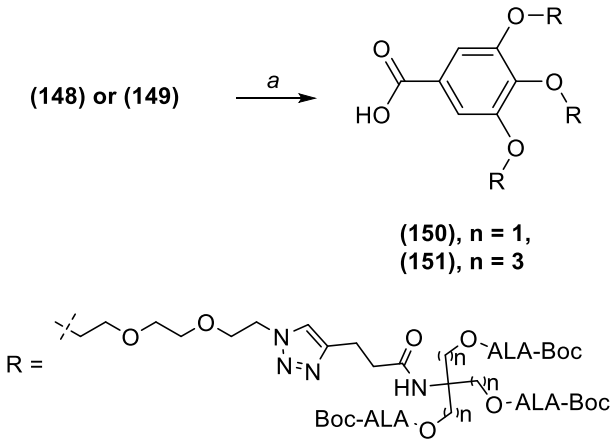

Scheme 33. Boc cleavage for model ALA dendrons **(148)** and **(149)**. *Reagents and conditions*: *a.* TFA: DCM (1:1, v/v), 30 min, ice-cold then RT**, 88% (150)**, **90% (151)**.

Figure 67 shows an overlay of the HPLC chromatograms for the two gallic acid-derived dendrimer systems. Once again, as expected, the final deprotected conjugates **(150)** and **(151)** are relatively hydrophilic due to the multiple protonated amino functions of the ALA units.

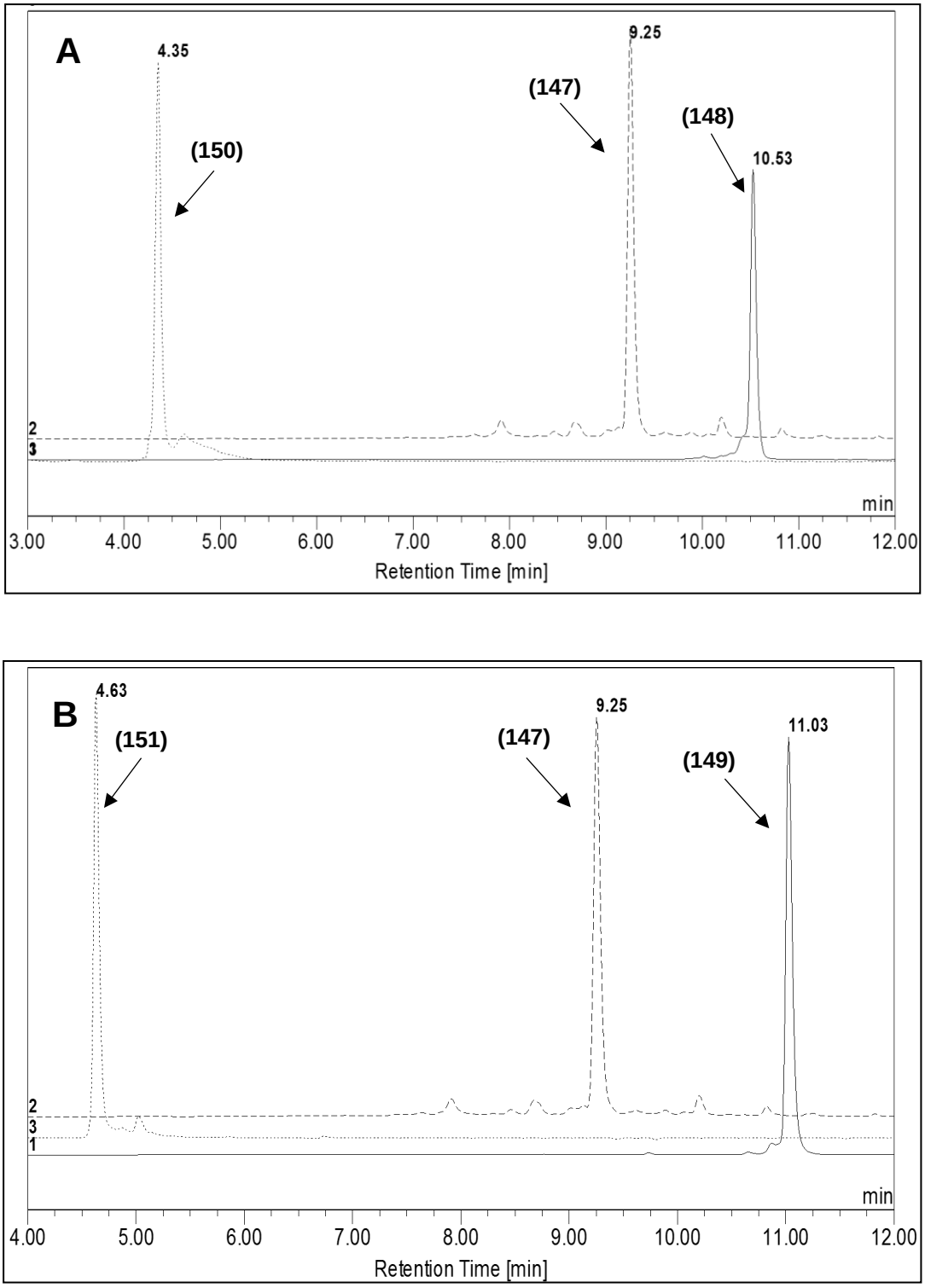

Figure 67. Overlay of HPLC chromatograms for clicked ALA dendrons **(150)** and **(151).**

A. Overlay showing the product **(150)** and the starting azide **(147)** and the Boc-protected clicked prodrug **(148)**.

B. Overlay showing the product **(151)** and the starting azide **(147)** and the Boc-protected clicked prodrug **(149)**.

Attempts were also made to couple trivalent azide **(147)** with alkyne derivative **(105)** by changing the copper source from $CuSO_4$ to Cu(I) iodide and Cu(I) trifluoromethanesulfonate benzene complex. The use of a Cu(I) salt in CuAAC avoids the use of a reducing agent[248] and, for the current work, the reactions could be carried out in DMSO only, thus avoiding a mixture of solvents. However on monitoring the reaction, the Cu(I) iodide-mediated click reaction did not show any new peaks on HPLC, while reactions with Cu(I) triflate benzene complex gave the Boc-protected dendrimer **(148)**, but with lower yield.

3.3 Biomolecules in PDT

As discussed previously attachment of biomolecules to photosensitisers has become an area of interest for various researchers in recent years. In PDT, selectivity between a healthy cell and a tumour cell has always been a concern and attempts to deal with this include the attachment of targeting peptides, biomolecules and antibodies to the photosensitisers. An effective ALA prodrug-mediated PDT treatment requires that the drug should be effectively internalized inside the target cell through appropriate receptor and transport systems.[249] Also, once inside the cell, ALA should be released from the prodrug and subsequently converted into protoporphyrin IX through an enzymatic pathway. Biomolecules which have been investigated to date with ALA include nucleosides such as adenosine and thymidine that target nucleoside receptors, sugars such as glucose, galactose and mannose, and vitamins such as vitamin E, vitamin D3 and biotin (discussed in chapter 1).

3.3.1 Synthesis of vitamin E-ALA dendrons

The synthesis of first-generation ALA dendrons targeted with vitamin E was attempted as shown in Schemes 34 and 35. In this work, racemic α-tocopherol (hereafter referred to as vitamin E) was used, as in the study by Vallinayagam *et al.*[193] on ALA-vitamin conjugates. The p-hydroxybenzoic acid derivative azide core **(142)** was first esterified with vitamin E **(152)** using standard coupling conditions of EDC.HCl and DMAP (Scheme 34). After 36 h HPLC showed efficient conversion of **(152)** to the desired ester, which was isolated

in good yield. The conjugate **(153)** was characterized by IR, ^{1}H NMR, ^{13}C NMR and mass spectrometry.

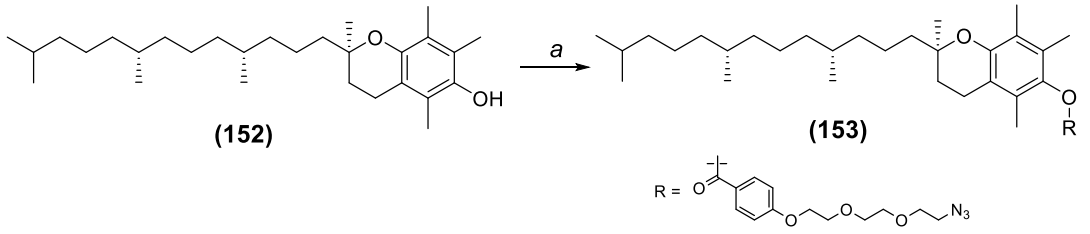

Scheme 34. Conjugation of vitamin-E with azido spacer **(153)**. *Reagents and conditions*: **(142)**, vitamin E, EDC.HCl, DMAP, DCM, 32 °C, 36 h, **75%**.

The azido conjugate **(153)** was then coupled with both the alkyne derivatives **(105)** and **(107)** using Cu(I) trifluoromethanesulfonate benzene complex in DMSO. For these reactions, the previously established CuAAC conditions of $CuSO_4$ and sodium ascorbate were not used, as the starting material **(153)** is highly lipophilic and insoluble in water. Both reactions were carried out for 72 h and monitored by analytical HPLC (Figure 68). Disappearance of starting material **(153)** and formation of a new species as a broad single peak was seen at 14.6 min for **(154)** and 11.8 min for **(155)** respectively. The crude products were purified by semi-preparative HPLC and the conjugates **(154)** and **(155)** were both obtained as colourless oils in good yields (Scheme 35).

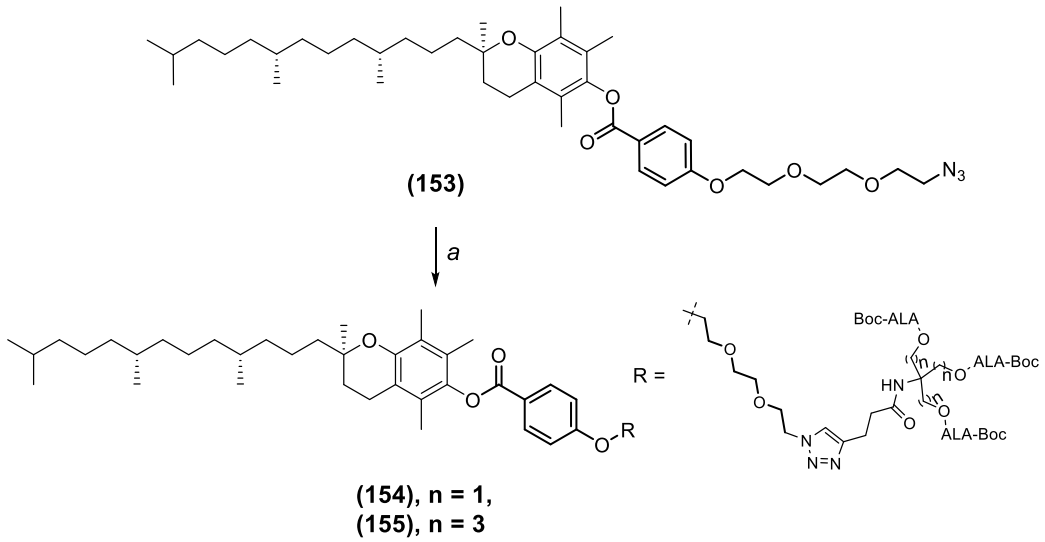

Scheme 35. Synthesis of vitamin E-ALA dendrons **(154)** and **(155)** (Boc-protected). *Reagents and conditions*: **(105)** or **(107)**, copper(I) trifluoromethanesulfonate benzene complex, DMSO, 72 h, RT, **54% (154)**, **59% (155)**.

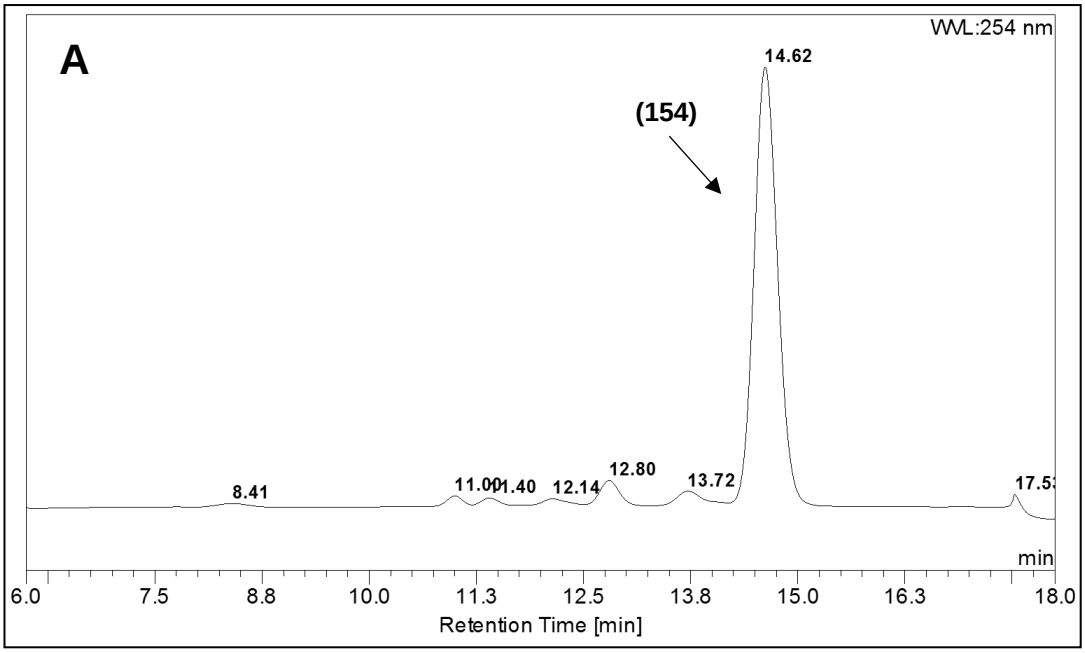

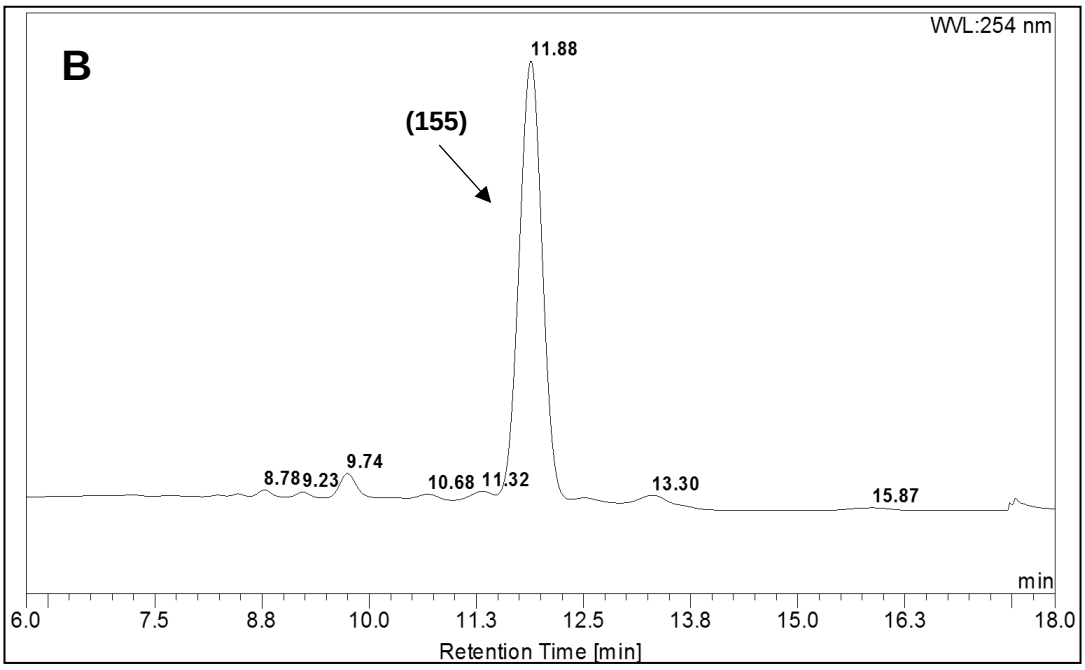

Figure 68. HPLC chromatograms for click coupling reaction of **(154)** and **(155)** after 72 h.

A. Crude reaction mixture showing Boc-protected vitamin E ALA clicked prodrug **(154)**.

B. Crude reaction mixture showing Boc-protected vitamin E ALA clicked prodrug **(155)**.

Surprisingly, the Ext. Tris derivative **(155)** shows a somewhat shorter retention time than **(154)**, despite the presence of longer alkyl chains within the dendrimer unit.

The Boc protecting groups of the protected dendrimers **(154)** and **(155)** were removed by treating the conjugates with 50% TFA in DCM for 30 min (Scheme 36). The reactions were monitored by analytical HPLC which showed disappearance of starting materials **(154)** and **(155)**, and formation of new species at 4.6 min **(156)** and 4.5 min **(157)** respectively (Figure 69). The final conjugates were freeze-dried from H_2O to obtain the bio-conjugates of ALA-vitamin E **(156)** and **(157)** as TFA salts.

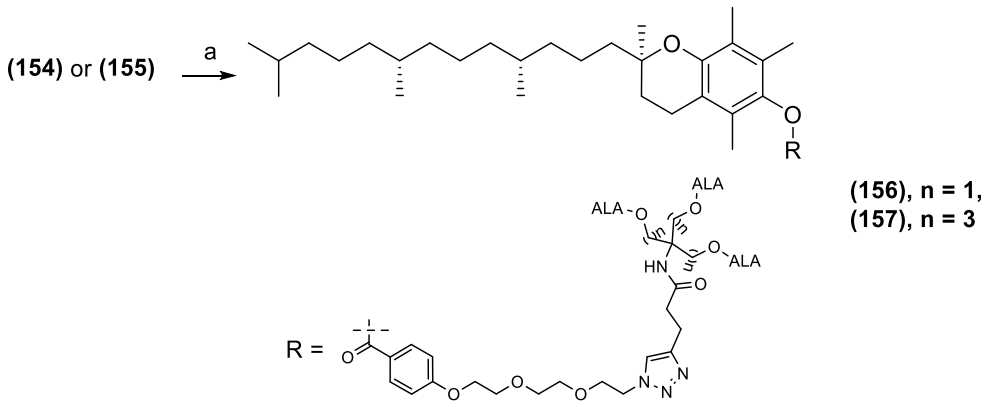

Scheme 36. Synthesis of vitamin E-ALA dendrons **(156)** and **(157)** (TFA salts). *Reagents and conditions*: *a.* TFA: DCM (1:1, v/v), 30 min, ice-cold then RT**, 97% (156)**, **96% (157)**.

Figure 69 shows the overlay for HPLC chromatograms, each showing the ALA-vitamin E bioconjugates **(156)** and **(157)** with the peaks for the starting materials **(154)** and **(155)** (Boc-protected derivative). Significantly, despite conjugation with the highly lipophilic vitamin E unit, both **(156)** and **(157)** were water-soluble and apparently have similar lipophilicities, based on HPLC retention times to the non-targeted conjugates **(150)** and **(151)** with 9 ALA units.

Vallinayagam *et al.* have proposed that conjugation of ALA to vitamin E should lead to enhanced uptake due to increased lipophilicity of the resulting bioconjugate relative to ALA.[193] Although this effect may not be relevant to **(156)** and **(157)**, it has been reported by other authors that co-administration of vitamin E may lead to enhancement of PDT effects with ALA and other photosensitisers.[250, 251] Therefore **(156)** and **(157)** may nonetheless offer an effective way of delivering both ALA and vitamin E for PDT.

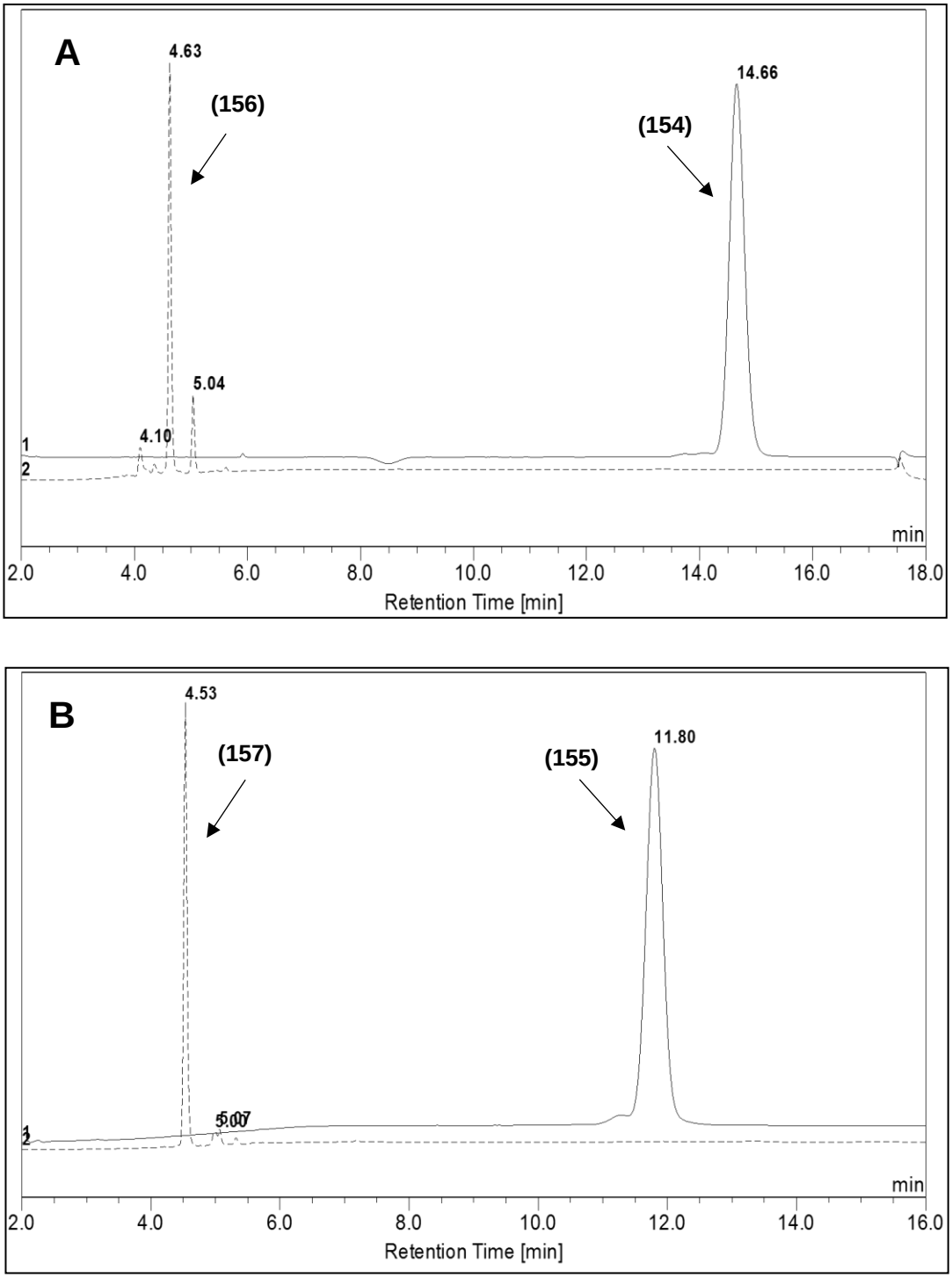

Figure 69. Overlay of HPLC chromatograms for clicked ALA dendrons **(156)** and **(157).**

A. Overlay showing the product **(156)** and Boc-protected vitamin E ALA clicked prodrug **(154)**.

B. Overlay showing the product **(157)** and Boc-protected vitamin E ALA clicked prodrug **(155)**.

3.3.2 Synthesis of thymidine-ALA dendrimers

Nucleoside derivatives have been in use clinically for the treatment of cancer and other disorders for over 50 years. They inhibit cellular division by incorporation into DNA and RNA and thus interfering with cellular metabolism.[196] A thymidine-ALA bioconjugate has previously been reported and been shown to provide enhanced PpIX synthesis,[197] therefore thymidine was chosen as the targeting unit for an ALA dendrimer in the current project.

The synthesis of a dendrimeric ALA-thymidine conjugate was first attempted by the same strategy as for the vitamin E derivatives **(156)** and **(157)**. Esterification of the 3' and 5' hydroxyl groups of thymidine with **(142)** was attempted using EDC.HCl and DMAP activation (Scheme 37). However, after monitoring the reaction for 36 h at RT, no new species was observed.

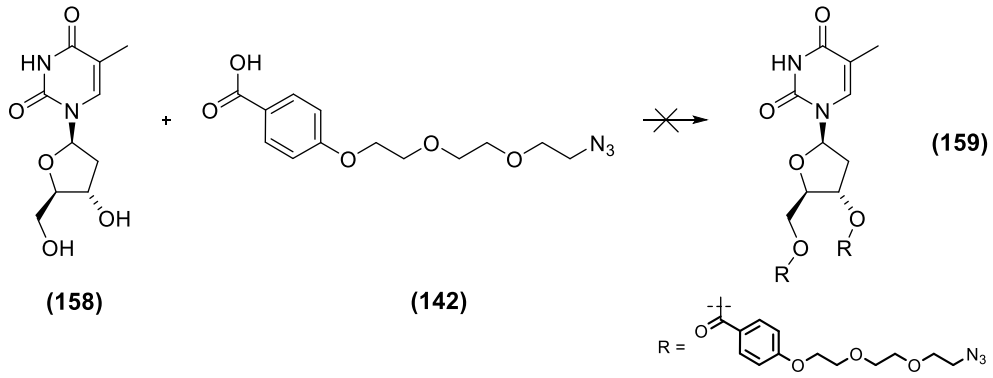

Scheme 37. Bioconjugation of 2-thymidine with **(142)**. *Reagents and conditions: a.* EDC.HCl, DMAP, dioxane, RT, 36 h.

In view of this result, **(142)** was replaced with a simple aliphatic azido acid of comparable length, which it was reasoned would be more reactive towards the hydroxyls of the somewhat hindered thymidine core.

When thymidine **(158)** was treated with 11-azidoundecanoic acid **(160)** using the same activation conditions, analytical HPLC after 48 h showed the formation of a single new species at 11.3 min (Scheme 38). Purification by semi-preparative HPLC gave **(161)** as a yellowish oil in very good yield.

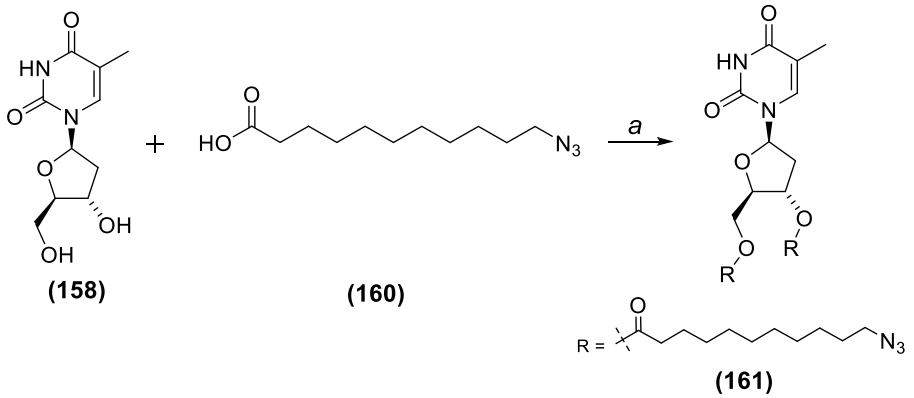

Scheme 38. Bioconjugation of 2-thymidine **(158)** with 11-azido undecanoic acid **(160)**. *Reagents and conditions: a.* EDC.HCl, DMAP, Dioxane, RT, 48 h, **73%**.

The thymidine-azido conjugate **(161)** was coupled with alkyne derivative **(105)** in DMSO using copper(I) trifluoromethanesulfonate benzene complex and the reaction was monitored by analytical HPLC for 24 h (Scheme 39). Formation of a new species **(162)** at 12.87 min was observed in addition to the unchanged starting material **(161)** (Figure 70). The crude material was purified by semi-preparative HPLC to give **(162)** as white solid in 54% yield. This demonstrates the feasibility of attaching more than one copy of an ALA dendron to a core targeting unit by CuAAC.

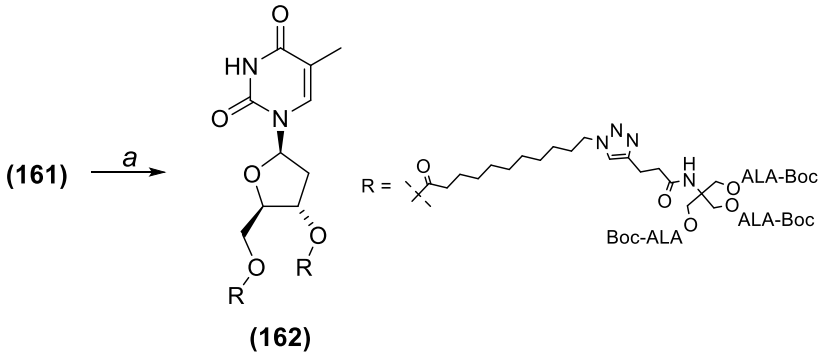

Scheme 39. Synthesis of thymidine ALA dendrimer **(162)** (Boc-protected derivative). *Reagents and conditions: a.* **(105)**, copper(I) trifluoromethanesulfonate benzene complex, DMSO, RT, 24 h, **54%**.

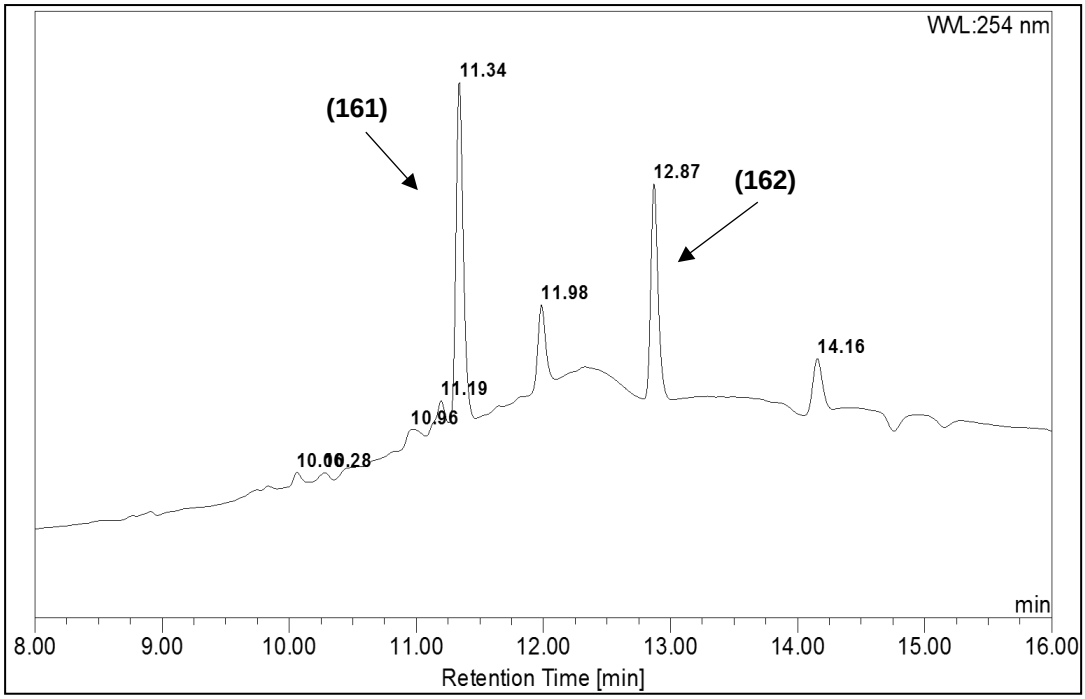

Figure 70. HPLC chromatogram for crude reaction mixture for **(162)**.

The Boc protecting groups of the dendrimer **(162)** were removed by treating the conjugate with 50% TFA in DCM for 30 min. The reaction was monitored by analytical HPLC (Scheme 40), which again showed the disappearance of the starting material **(162)** and formation of a single new species at 5.97 min **(163)** (Figure 71).

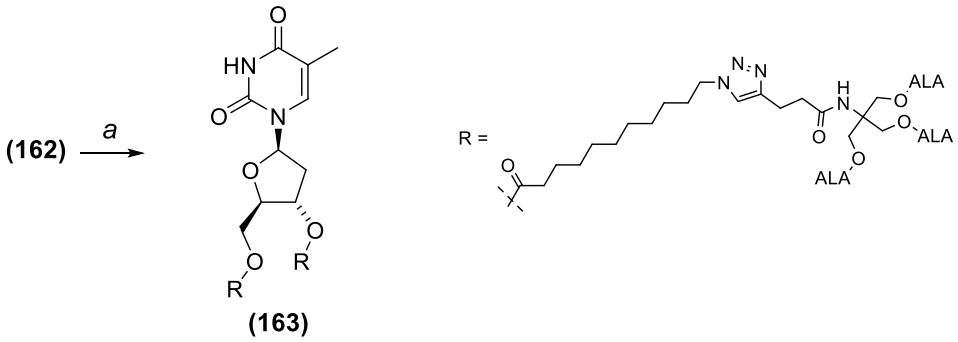

Scheme 40. Synthesis of thymidine ALA dendrimer **(162)** (TFA salt). *Reagents and conditions: a.* TFA: DCM (1:1), ice-cold then RT, 30 min, **93%**.

The product was freeze-dried from H_2O to give the novel thymidine-ALA dendrimer **(163)** as the TFA salt. The structure was confirmed by mass spectrometry and ^1H NMR which showed the expected integration of 2 x CH signals for the triazole units.

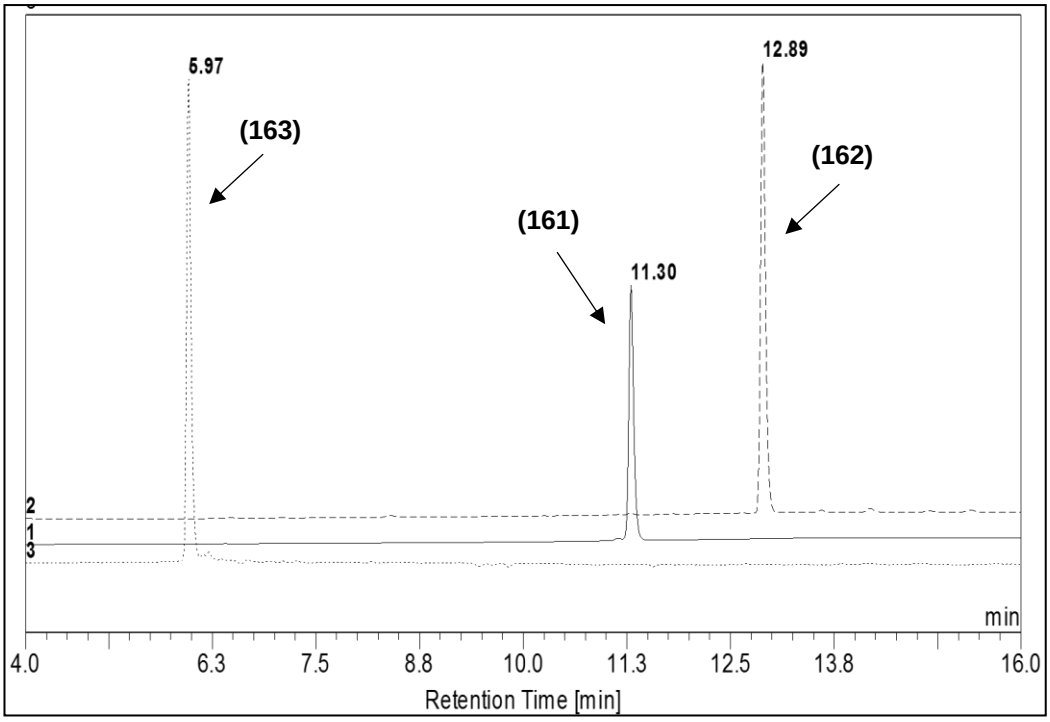

Figure 71. Overlay of HPLC chromatogram for thymidine conjugate **(163)** showing **(162)** (Boc-protected derivative) and **(161)** (azide).

3.3.4 Synthesis of glycoside-ALA dendrimers

The conjugation of carbohydrates with tetrapyrrolic structures has been studied by various researchers.[249, 252] It is known that due to the increased metabolism and energy demand of cancer and proliferating endothelial cells, glycosylation pathways may undergo deregulation. This glycosylation also provides a possibility for interaction of specific conjugates with lectin-type receptors in certain cancer cell types and hence makes targeting such cells with the help of carbohydrates an attractive choice.[249]

For the current study, 2,3,4,6-tetra-O-benzyl-D-gluco-pyranose **(164,** mixture of α and β anomers**)** was chosen as a precursor targeting unit. O-Benzyl groups served as protecting groups for the hydroxyl functional groups on **(164)**, with the exception of the anomeric hydroxyl function which was required for attachment of the azido handle. The first step of the synthesis involved coupling of **(142)** with the anomeric hydroxyl group of **(164)** using EDC.HCl and DMAP (Scheme 41). Formation of a new species was observed by analytical HPLC, which was isolated by semi-preparative HPLC to give the expected monosaccharide **(165)** in 70% yield. ^{1}H NMR showed **(165)** to be a

mixture of predominantly the β anomer (20:1, β:α). The presence of the major β-product was confirmed by the large coupling constant (8.0 Hz) observed for the anomeric proton at δ 5.86, compared to that of α-anomer (δ 6.58, J = 4.0). The preferential formation of the β-anomer of **(165)** upon acylation of **(164)** with EDC.HCl is consistent with the report of Vallinayagam *et al.* who observed a distinct change in the proportion of α vs β-linked products when **(164)** was acylated using DCC compared to EDC.HCl as coupling agent.[249]

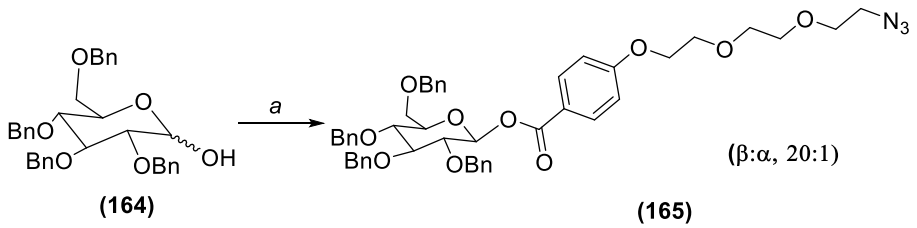

(164) (165)

Scheme 41. Bioconjugation of **(142)** with 2,3,4,6-tetra-O-benzyl-D-gluco-pyranose **(164)**. *Reagents and conditions: a*. **(142)**, EDC.HCl, DMAP, DCM, ice-cold then RT, 36 h, **70%**.

The azido conjugate **(165)** thus obtained was coupled with the alkyne derivative **(105)** using the previous CuAAC conditions, and after 36 h analytical HPLC indicated complete disappearance of starting material **(165)**, and appearance of a new peak was observed at 12.53 min (Scheme 42). The crude material was purified by semi-preparative HPLC and freeze-dried from H_2O to give the expected bioconjugate **(166)** in 54% yield. ^1H NMR once again confirmed **(166)** to be predominantly the β anomer (7:1, β:α).

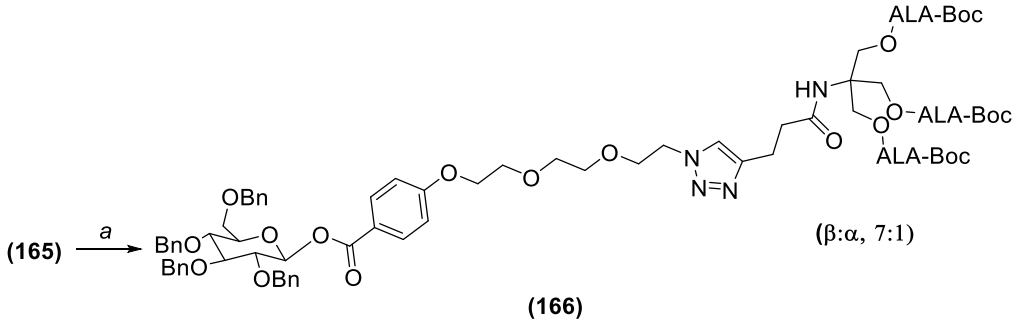

(166)

Scheme 42. Click coupling of ALA dendron **(105)** with **(165)**. *Reagents and conditions: a.* **(105)**, copper(I) trifluoromethanesulfonate benzene complex, DMSO, RT, 36 h, **54%**.

The next step of the synthesis required removal of the *O*-benzyl protecting groups from sugar **(166)**. This was first attempted according to the method of Vallinayagam *et al.*[249] using catalytic hydrogenolysis with 10% Pd/C and H_2

gas (Scheme 43). The triazole unit was expected to resist reduction, as Castro *et al.* have described the successful O-debenzylation of a similar carbohydrate-triazole derivative under such conditions.[253]

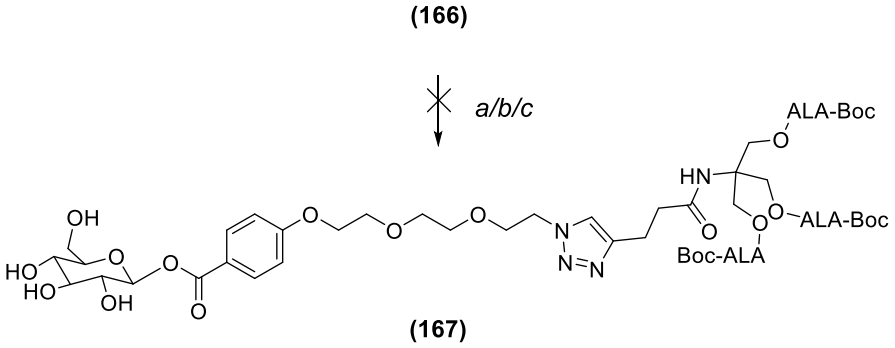

Scheme 43. Attempt to cleave Z group from **(166)**. *Reagents and conditions: a.* Pd/C, H_2, DCM/EtOH (2:1), 16 h; *b.* Pd/C, H_2, MeOH, 16 h; *c*. $Pd(OH)_2$, H_2, MeOH, 16 h.

The reaction was monitored by analytical HPLC, however after stirring for 16 h, no change was observed. This procedure (Scheme 43) has been reported to be effective for the complete debenzylation of ALA conjugates of **(82)**-**(84)** where ALA is attached to the anomeric hydroxyl group.[245] Neither changing the solvent to MeOH nor replacing the catalyst with the more active $Pd(OH)_2$ was effective. Presumably in this case the presence of the bulky dendrimeric group in **(166)** significantly hinders the deprotection compared to simpler related ALA conjugates.[249]

3.4 Summary

A successful synthetic route was developed to conjugate first-generation ALA dendrons (Chapter 2) to azido core units **(142)** and **(147)** via CuAAC. The clicked dendrons thus synthesised had 3 or 9 copies of ALA attached to the dendron and were obtained in good yields.

The building blocks **(142)** and **(147)** were also used for the preparation of biomolecule-targeted ALA prodrugs. Vitamin E was conjugated with azido core unit **(142)** followed by coupling with ALA dendrons **(105)** and **(107)** via CuAAC to yield **(156)** and **(157)** in moderate yields. A similar strategy was also attempted for conjugation of thymidine with **(142)**, however no successful outcome was observed. The synthetic route was thus changed to replace an

aromatic core-azide **(142)** with an aliphatic-azido spacer unit **(160),** which gave the expected azido-thymidine conjugate **(161)**. Click coupling with ALA dendron **(105)** gave the final thymidine-ALA dendrimer **(163)** having 6 copies of ALA. Lastly, the conjugation of ALA dendron **(105)** to 2,3,4,6-tetra-O-benzyl-D-gluco-pyranose **(164)** was also studied. However, attempts to remove the Bn protecting groups from conjugate **(166)** using catalytic hydrogenolysis in the presence of 10% Pd/C or $Pd(OH)_2$ were not successful.

CHAPTER 4: RESULTS AND DISCUSSION (Targeted ALA dendrons)

4.1 Introduction to targeted photodynamic therapy

Photodynamic therapy, in comparison to other conventional forms of cancer treatments, is a minimally invasive technique (Chapter 1). However PDT faces a challenge of tumour selectivity and, at times, it becomes difficult to irradiate only the tumour cells due to their close proximity to normal cells.[254, 255] In the past few years, much work has been carried out on targeted photodynamic therapy with the aim of enhancing the accumulation of photosensitisers inside tumour cells by active or passive targeting.[256] Passive targeting relies on the morphological and physiological differences between normal and tumour cells to deliver and accumulate nanostructures containing photosensitisers selectively within the cells.[257] These nanostructures can be either biodegradable (made of natural or synthetic compounds) or non-biodegradable (polyacrylamide, silica-based or metallic particles). Photosensitisers encapsulated within the biodegradable nanostructures are released for the production of singlet oxygen, whereas non-biodegradable nanostructures relies on the diffusion of singlet oxygen through these structures to biological targets (Figure 72). An example of a biodegradable nanostructure was reported by Pierre *et al.* in 2001 which involved encapsulation of ALA into liposomes made from ceramide, palmitic acid, cholesterol and cholesterol sulfate, which therefore resembled the lipid composition of the stratum corneum.[258] The liposome formulation was found to successfully deliver ALA to the target skin layer. Non-biodegradable nanostructures are stable to pH and temperature fluctuations, which also allows control over the size, shape and porosity of these nanostructures during their preparation. Tang *et al.* in 2008 reported the preparation of polyacrylamide-based nanostructures encapsulating methylene blue, which undergoes rapid enzymatic inactivation when used clinically.[259] The encapsulated methylene blue was stable to reduction by diaphorase enzymes and was also found to have a good PDT effect against C6 glioma cells.

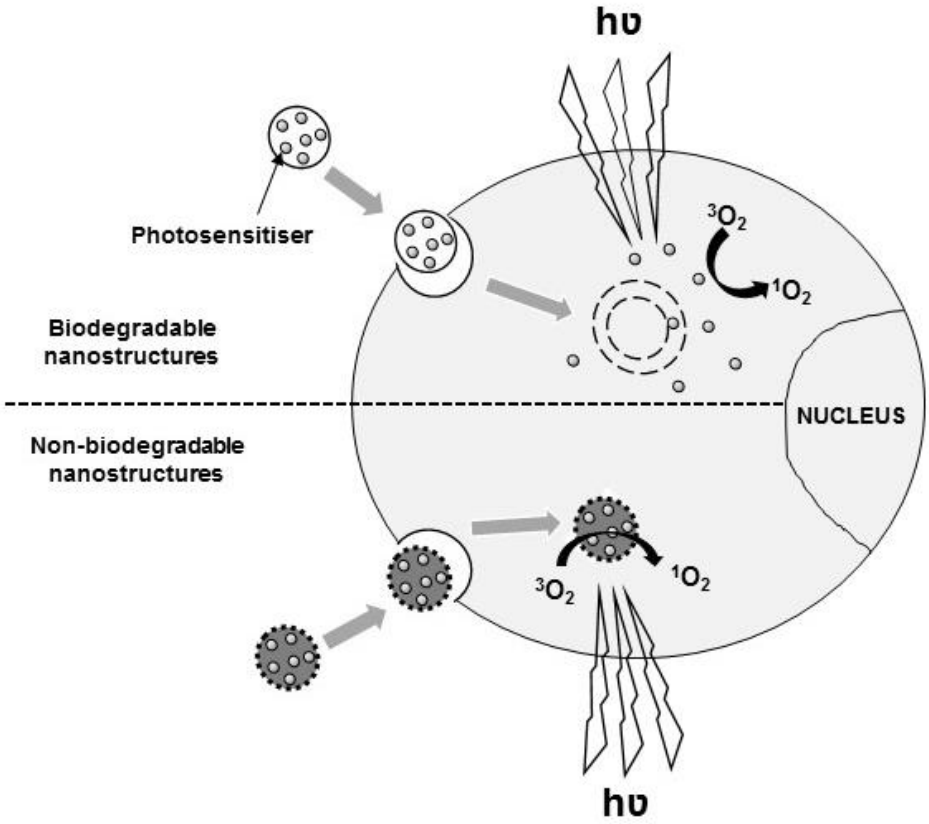

Figure 72. Representation of singlet oxygen production by biodegradable and non-biodegradable nanostructures inside tumour cells (adapted from Shirasu *et al.*).[256]

4.1.1 EGFR-targeted photodynamic therapy

The epidermal growth factor receptor (EGFR) is a cell-surface receptor and belongs to the ErbB family of tyrosine kinases. Overexpression of this receptor has been identified in various types of cancer including ovarian, breast, prostate, bladder, pancreatic and colorectal cancers.[260] This has led to the development of various therapeutic agents such as monoclonal antibodies (mAbs), tyrosine kinase inhibitors (TKIs), antisense oligonucleotides, antibody-based immunoconjugates and other agents like FR-18, peptides, affibodies and nanobodies.[261] Photodynamic therapy targeted towards the EGFR receptor is a promising new therapeutic strategy for cancer treatment. Kadish *et al.* in 2010 reported experiments on benzoporphyrin derivative (BPD) conjugates in the EGFR overexpressing cell line A431 and EGFR-negative NR6 cells, and found the conjugates to be highly selective towards A431 cells with a 90% decrease in cell viability.[262] Selective targeting of prodrug structures or photosensitisers for PDT may also be achieved by conjugation to

specific peptides that recognise the overexpression of the EGFR receptor in certain cancer cell lines. Master *et al.* in 2012 reported a study on A431 cells using the phthalocyanine PC4 photosensitiser conjugated with peptide ligands, which was found to have better tumour-selective accumulation and PDT effects as compared to that seen in MCF-7 cells.[263] Ongarora *et al.* in 2012 reported the synthesis of phthalocyanine-peptide conjugates **(168a-b)** which were designed to target the epidermal growth factor receptor and evaluated them in human carcinoma A431 and Hep2, human colorectal HT-29, and kidney vero (negative control) cells (Figure 73).[264] The two peptide sequences (LARLLT and YHWYGYTPQNVI) were selected based on their reported EGFR targeting properties and ease of conjugation to various molecules. The phthalocyanine conjugate linked to the LARLLT peptide via a PEG spacer was found to be efficiently internalized by EGFR-positive cell lines and was found to be non-toxic to the cells.

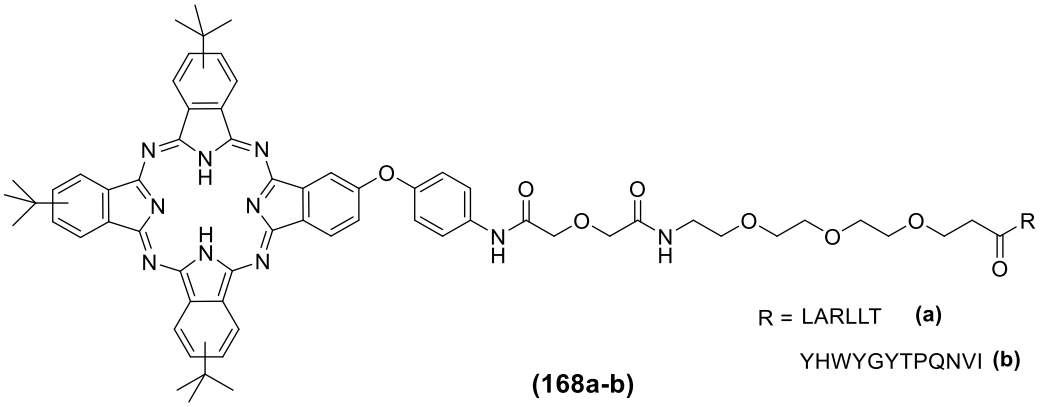

Figure 73. Chemical structure of EGFR-targeting phthalocyanine-peptide conjugates **(168a-b)**.[264]

Building on the tools developed in the previous chapters for the synthesis of ALA dendrons (Chapter 2) and their ligation to biomolecules (Chapter 3), the aim of this part of the project was to generate a structure in which ALA dendron units were attached to a core unit displaying a specific targeting peptide. (Figure 74).

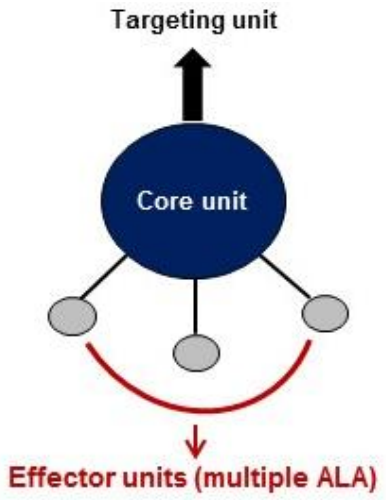

Figure 74. Model for peptide-targeted ALA dendron system. Multiple ALA units are attached to a peptide-targeted core unit via CuAAC chemistry.

4.2 Synthesis of targeting unit

For this work, the targeting peptide LARLLT described by Ongaro was selected. The advantages of using short peptide ligands are their easy synthesis and their low immunogenicity. LARLLT was identified from computational screening of a virtual peptide library and had been shown to target EGFR both *in vitro* and *in vivo*.[265] The peptide was synthesized on 2-chlorotrityl resin on a 0.65 mmol scale by Fmoc SPPS. 2-Chlorotrityl resin is a commonly used resin in solid-phase peptide synthesis for the synthesis of C-terminal peptide acids, particularly for the generation of protected peptide fragments.[266] Coupling of the first amino acid (Fmoc-Thr(tBu)-OH) **(169)** was carried out manually using DIEA as base. The resin was then transferred to an Activotec automated peptide synthesiser for the coupling of the remaining amino acids using PyBOP activation. The success of the final step of the synthesis, the removal of the Fmoc group from the terminal amino acid, was confirmed by the Kaiser test to yield the resin-bound peptide **(171)** (Scheme 44).

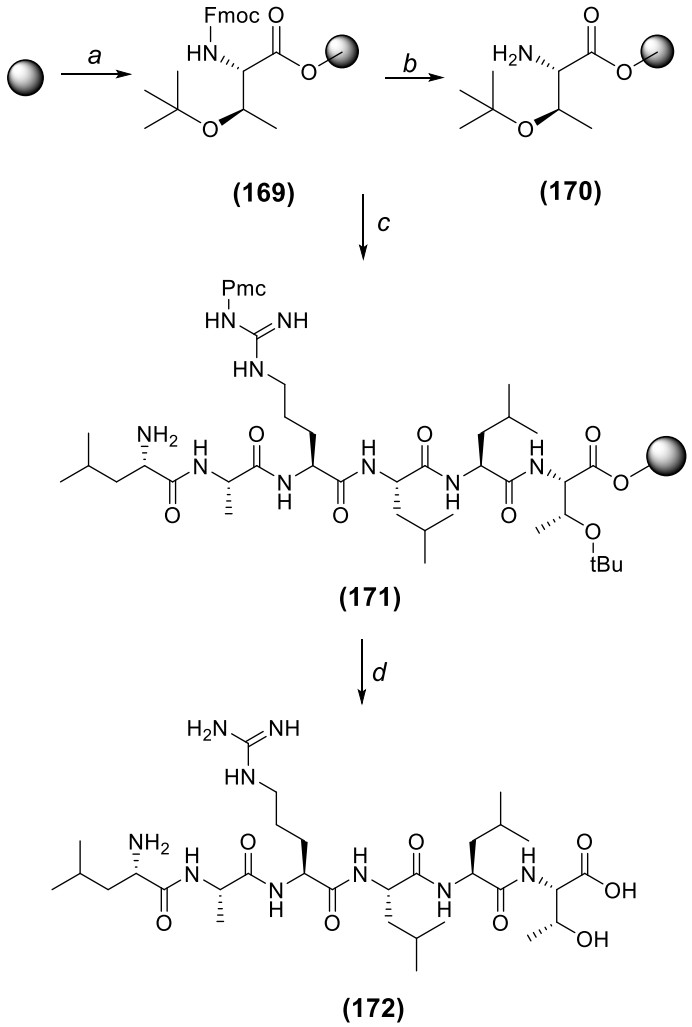

Scheme 44. Synthesis of the targeting peptide **(172)**. *Reagents and conditions: a*. Fmoc-Thr(tBu)-OH, DIEA, DMF, RT, 1 h; *b*. Piperidine/DMF (1:4 v/v), 5 + 10 min; *c*. PyBOP, DIEA, DMF; *d*. TFA/TIS/H_2O (95:2.5:2.5, v/v/v), 3 h, **85%**.

Cleavage from the resin and full side-chain deprotection was achieved using TFA/TIS/H_2O (95:2.5:2.5, v/v/v) to give **(172)** in 85% yield. **(172)** was characterised by mass spectrometry and the purity was confirmed by analytical HPLC which showed a single peak (R_t = 5.5 min). Having confirmed the success of the solid-phase synthesis of the targeting peptide, the resin-bound material was used to explore the attachment of ALA dendron units.

4.3 Coupling of ALA dendrons to the targeting unit

The next step of the synthesis involved coupling of the EGFR targeting peptide **(172)** with ALA dendrons **(105)** and **(107)**. Scheme 45 summarises the different strategies that were explored to prepare these targeted ALA conjugates.

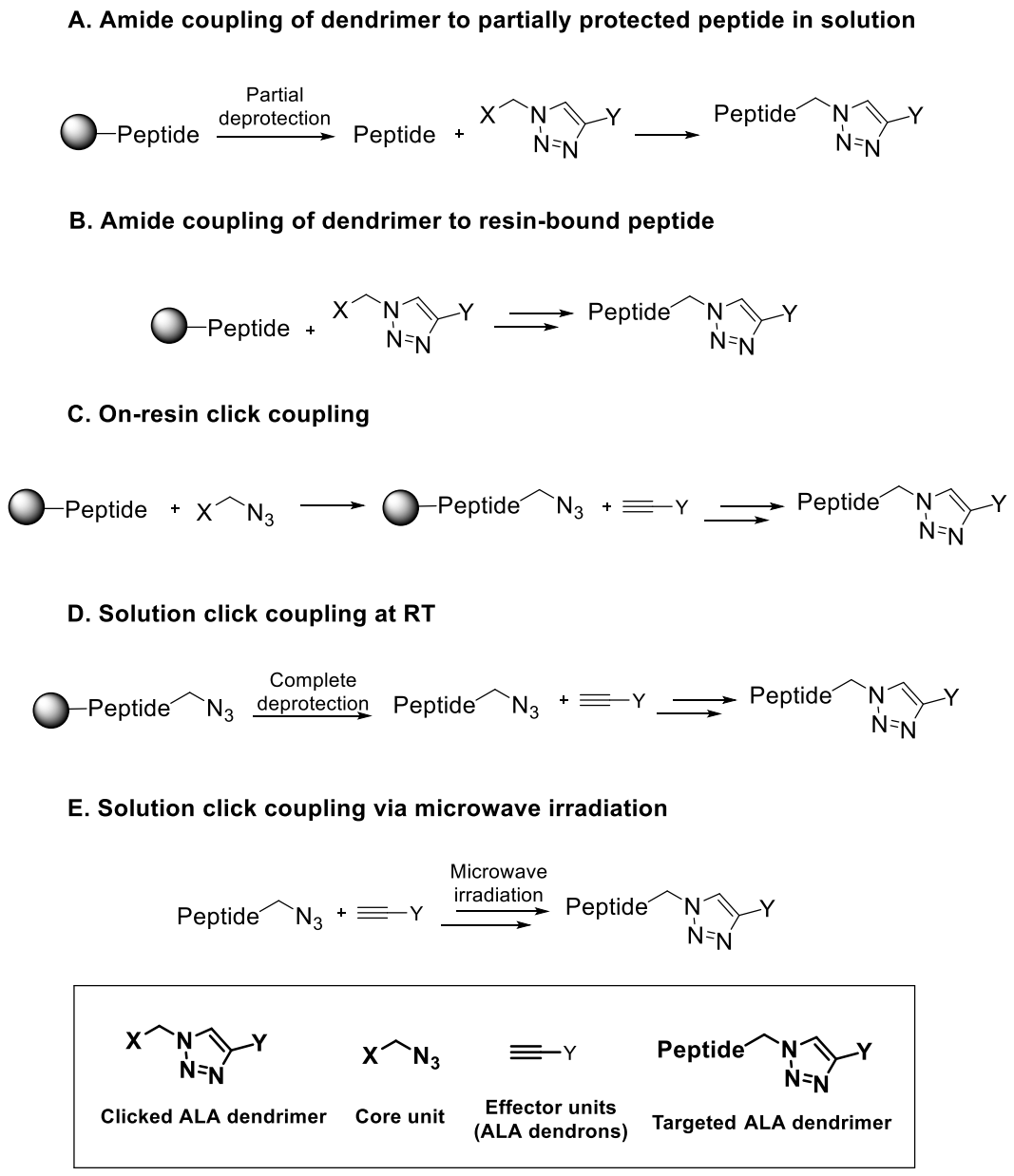

Scheme 45. Different strategies adopted to synthesize peptide-targeted ALA dendrimers.

4.2.1 Amide coupling of dendrimer to partially protected peptide in solution (A)

In order to investigate the coupling of the targeting peptide to the click products **(148)** and **(149)**, a partially protected peptide derivative **(173)** was required. This was obtained by treatment of **(171)** with 1% TFA in DCM (Scheme 46). This cleavage solution is mild enough to cleave the peptide from the resin leaving the Arg and Thr side-chain protecting groups still intact. The coupling of the partially deprotected peptide **(173)** to the clicked dendron was then first attempted using standard conditions of EDC.HCl/HOBt activation and DIEA as a base (Scheme 46). The reaction was monitored by analytical HPLC for 36 h. However the HPLC profile did not show any change in the peaks for the starting materials, nor appearance of new product peaks. Repeating the reaction using 1-[bis(dimethylamino)methylene]-1H-1,2,3-triazolo[4,5-b] pyridinium 3-oxid hexafluorophosphate (HATU) as coupling agent also did not change the outcome.

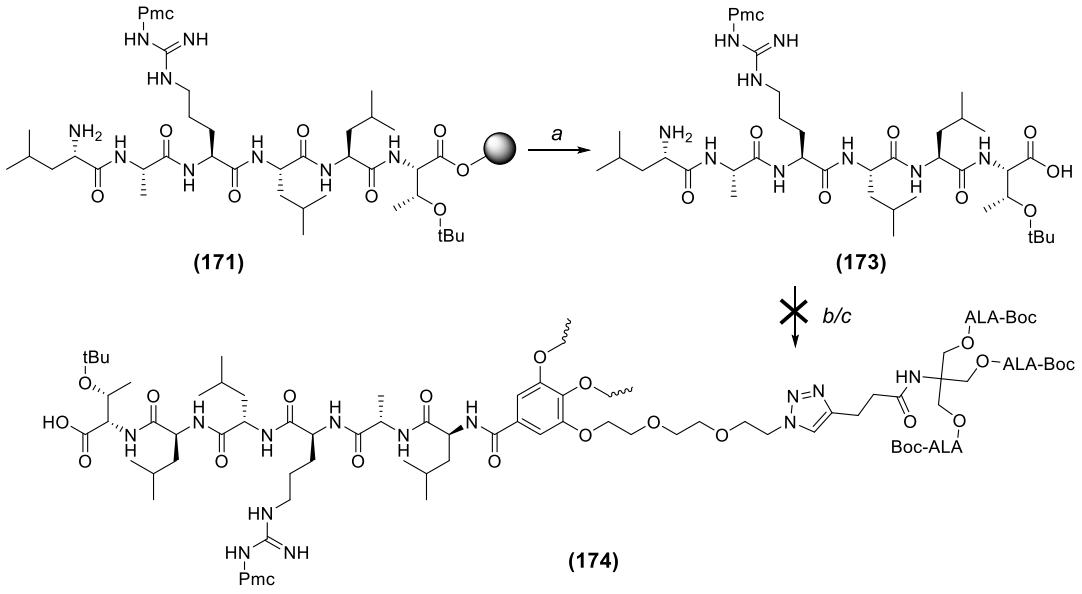

Scheme 46. Synthesis of targeted dendrimer **(174)**. *Reagents and conditions: a*. 1% TFA in DCM, 10% pyridine in MeOH, **69%**; *b*. **(148)**, EDC.HCl, HOBt.hydrate, DIEA, DCM, 36 h, RT or *c*. HATU, DIEA, DCM, 36 h, RT.

4.2.2 Amide coupling of dendrimer to resin-bound peptide (B)

As the initial attempt to conjugate the partially protected targeting peptide with the clicked ALA dendrimer **(148)** in solution did not give the desired results, an alternative strategy was attempted by conjugating the clicked dendrimer **(148)** directly to the peptide on resin **(171)** (Scheme 47). The coupling reaction was carried out in DMF at RT for 16 h with HATU and DIEA. This was then followed by the cleavage of the peptide and the side-chain protecting groups from the resin with TFA/TIS/H_2O (95:2.5:2.5 v/v/v). Analytical HPLC showed the absence of non-acylated LARLLT **(172)** and the appearance of a new peak at 6.09 min. Mass spectrometry confirmed the successful coupling of the targeting peptide and ALA dendrimer **(148)**, although the final recovery of **(181)** was very low due to problems during HPLC purification (overloading column).

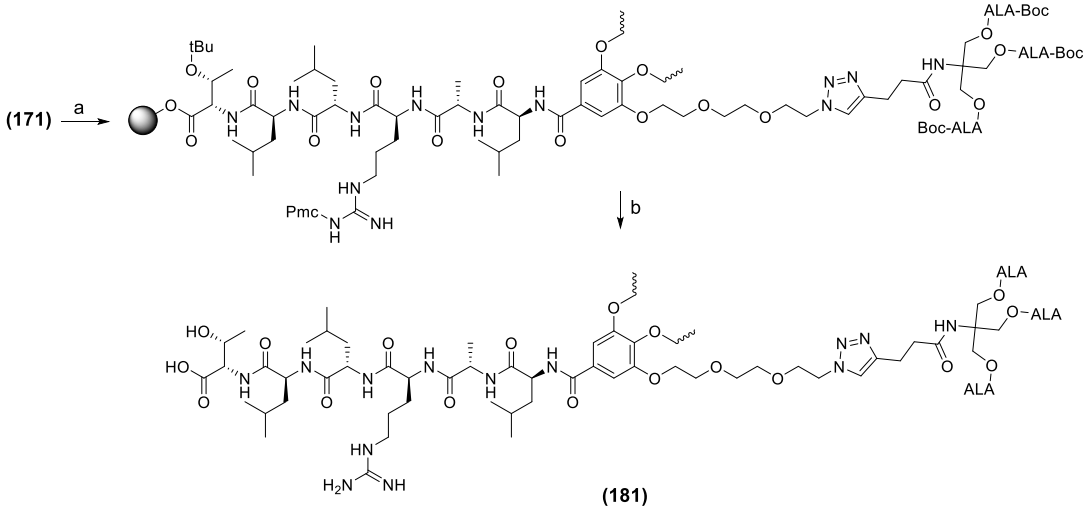

Scheme 47. Coupling of the peptide **(171)** with Boc-protected ALA dendrimer **(148)** on resin. *Reagents and conditions* a. **(148)**, HATU, DIEA, 16 h, RT b. TFA/TIS/H_2O (95:2.5:2.5 v/v/v), 3 h, **5%**.

4.2.3 On-resin click coupling (C)

Although the previous approach was successful, there are number of limitations for the above strategy (section 4.2.2) which includes the need for a large scale synthesis and HPLC purification of a purified sample of ALA dendrimer **(148)** or **(149)** for each experiment. The synthetic strategy was therefore modified, so as to carry out the click coupling of the effector units to the core azido unit already attached to the peptide. As shown in Scheme 48,

the azido spacer units **(142)** and **(147)** (readily available) were coupled with the EGFR peptide **(171)** on resin. The acylated intermediates **(176)** and **(178)** could then be subjected to on-resin coupling with an alkyne derivative **(105)**. A sample of each resin-bound peptide **(176)** and **(178)** was treated with TFA/TIS/H_2O (95:2.5:2.5 v/v/v) to generate the fully deprotected azido peptides **(177)** and **(179)**. The purity was confirmed by analytical HPLC (Figure 75) and the intermediates were subsequently used in approaches D and E.

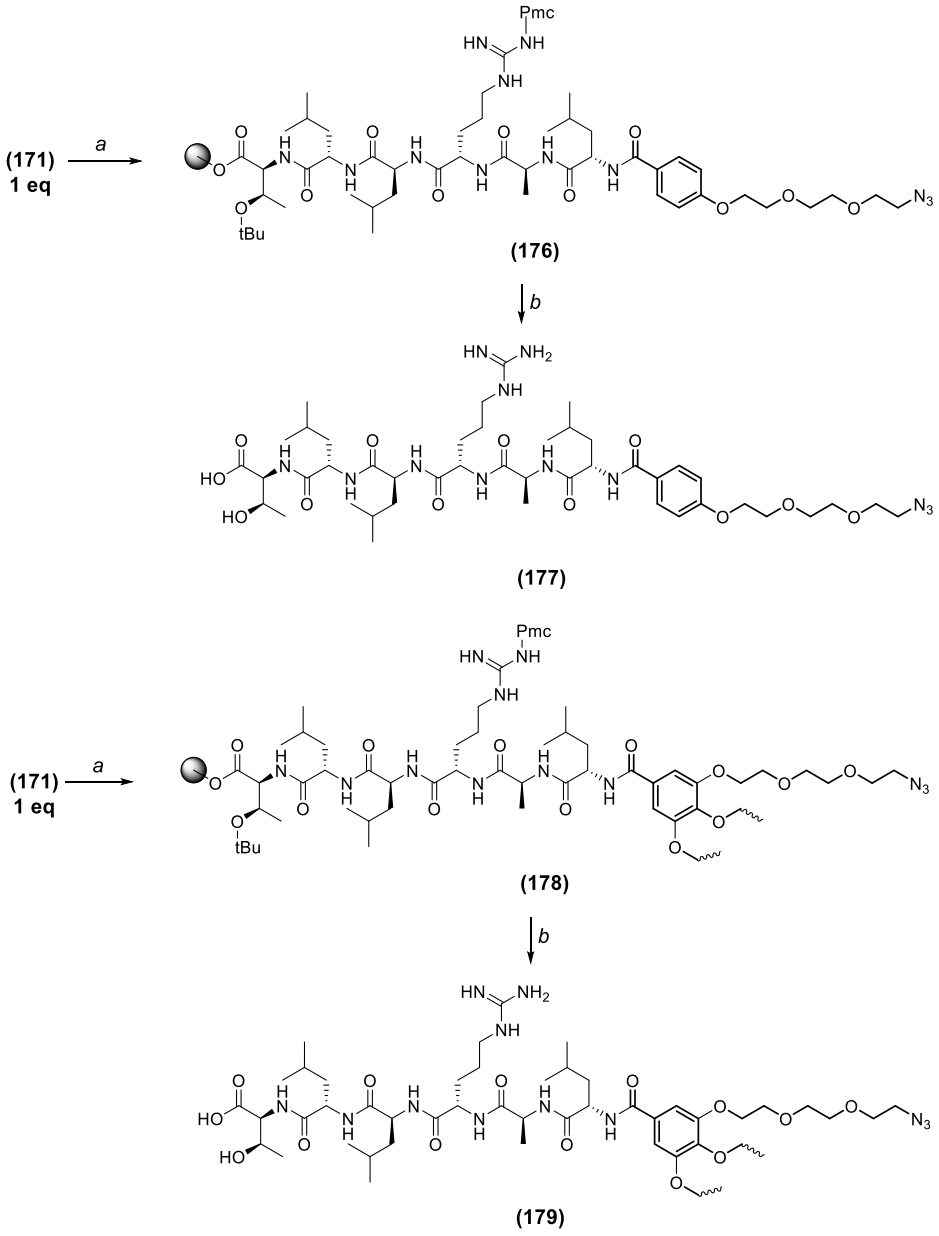

Scheme 48. Coupling of the azido units **(142)** and **(147)** to the resin-bound peptide **(171)**. *Reagents and conditions: a.* **(142)** (2 eq) or **(147)** (2 eq), HATU (2 eq), DIEA, DMF, RT, 24 h; *b.* TFA/TIS/H_2O (95:2.5:2.5 v/v/v), 3 h, **57% (177)**, **54% (179)**.

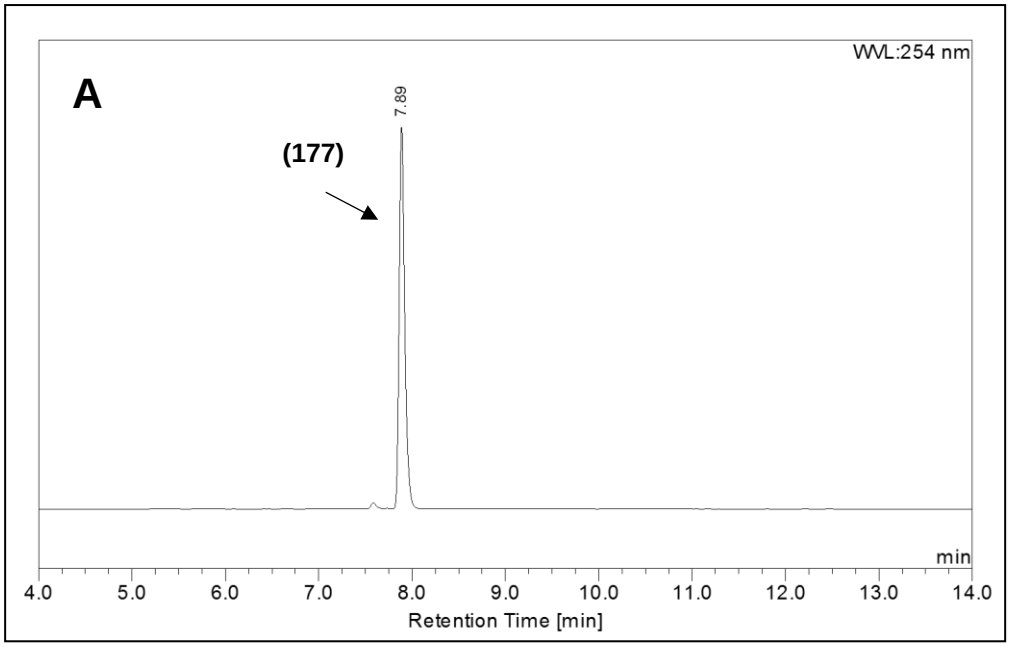

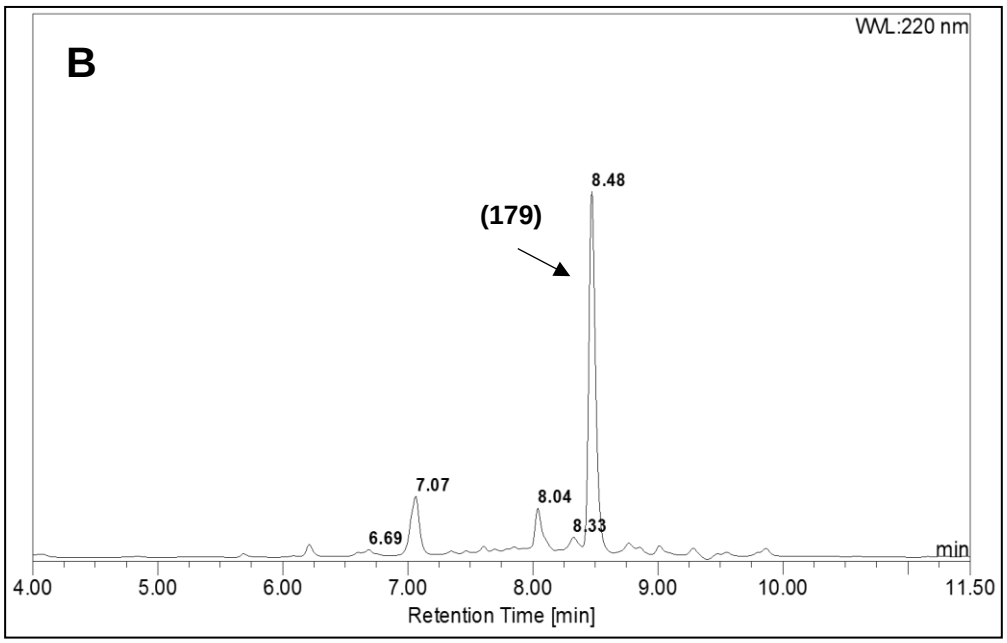

Figure 75. HPLC chromatograms for peptide-azido core unit **(177)** and **(179)**.

A. Crude reaction mixture showing peptide-azido core unit **(177)**.

B. Crude reaction mixture showing peptide-azido core unit **(179).**

A CuAAC click coupling was then attempted between the azide-containing resin-bound peptide **(178)** and alkyne unit **(105).** The different reaction conditions that were attempted are summarised in Table 2.

Table 2. Different coupling conditions for on-resin click coupling of the targeted dendrimer **(181)**.

-N3	≡	Coupling conditions	Solvent	Outcome
(179)	**(105)**	$CuSO_4$, sodium ascorbate	DMSO/H_2O/*t*-BuOH	×
(179)	**(105)**	CuI	DMSO	×
(179)	**(105)**	CuI, DIEA	20% piperidine in DMF	✓
(179)	**(105)**	CuI, DIEA	DMF/2,6-lutidine (7:3)	×
(179)	**(105)**	$(CF_3SO_3Cu)_2.C_6H_6$	DMSO	✓
(179)	**(107)**	$(CF_3SO_3Cu)_2.C_6H_6$	DMSO	✓

In each experiment, a solution of 6 eq **(105)** and 6 eq $(CF_3SO_3Cu)_2.C_6H_6$ in DMSO was agitated with 1 eq resin-bound azido-peptide **(179)** in a SPPS vessel for 5 days. The resin was then treated with TFA/TIS/H_2O for 3 h and the product was analysed by HPLC.

×: No reaction observed by analytical HPLC

✓: Presence of new species observed by analytical HPLC and confirmed by mass spectrometry

Initially standard conditions of CuAAC were applied as discussed in the previous chapter ($CuSO_4$, sodium ascorbate, DMSO/H_2O/*t*-BuOH). However after 3 days, HPLC did not show any progress. This could be attributed to the shrinking of the polystyrene resin in H_2O which was the part of the solvent mixture (DMSO/H_2O/*t*-BuOH). Alternative Cu sources were then investigated that have been previously used for on-resin peptide coupling. Zhang *et al.* (2006) reported a range of coupling conditions using different Cu species to carry out the solid phase synthesis of peptidotriazoles.[248] This included Cu(I) iodide and 20% piperidine in DMF. It has been shown that Cu species which get deposited on the resin are dissolved by 20% piperidine in DMF and thus can be washed away at the end of the reaction.[248] Using Cu(I) salts in click coupling avoids the use of reducing agents, although its recommended to add a catalytic amount of ascorbic acid to protect Cu(I) from oxidation. The peptide derivative with the azido spacer **(176)** was coupled with **(105)** in the presence of Cu(I) iodide and 20% piperidine in DMF and the reaction was carried out for

48 h (Scheme 49). The final conjugate was cleaved from the resin along with removal of side-chain protecting groups using TFA:TIS:H_2O (95:2.5:2.5 v/v/v). Analytical HPLC showed several peaks, however mass spectrometry did show the presence of the expected final conjugate **(180)**.

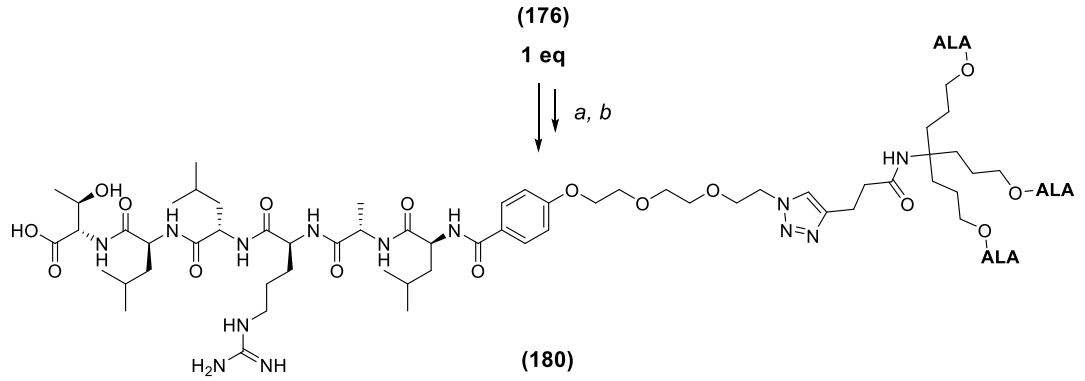

Scheme 49. On-resin click coupling of **(176)** and **(105).** *Reagents and conditions: a.* 2 eq **(105),** Cu(I)I, ascorbic acid, DIEA, 20% piperidine in DMF, 48 h *b*. TFA/TIS/H_2O (95:2.5:2.5 v/v/v), 3 h, multiple peaks.

Optimum reaction conditions were achieved when **(178)** was coupled with alkyne derivatives **(105)** and **(107)** in the presence of copper(I) trifluoromethanesulfonate benzene complex in DMSO for 5 days. The final product was obtained by cleavage from the resin along with side chain deprotection by treating the resin with TFA/TIS/H_2O (95:2.5:2.5 v/v/v) (Figure 76). Purification by semi-preparative HPLC gave the expected products **(181)** and **(182)** in 30% and 25% yields respectively (Scheme 50).

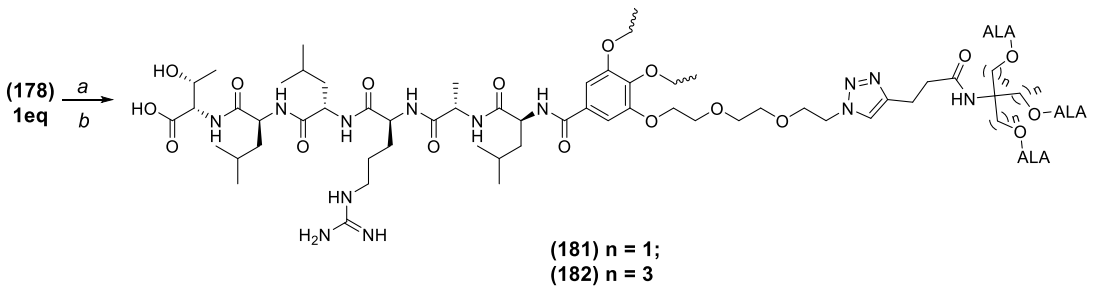

Scheme 50. On-resin click coupling of peptide derivative **(178)** with alkyne derivatives **(105)** and **(107)**. *Reagents and conditions: a.* Copper(I) trifluoromethanesulfonate benzene complex, DMSO, 5 d, RT; *b.* TFA/TIS/H_2O (95:2.5:2.5 v/v/v), 3 h, **30% (181)**, **25% (182)**.

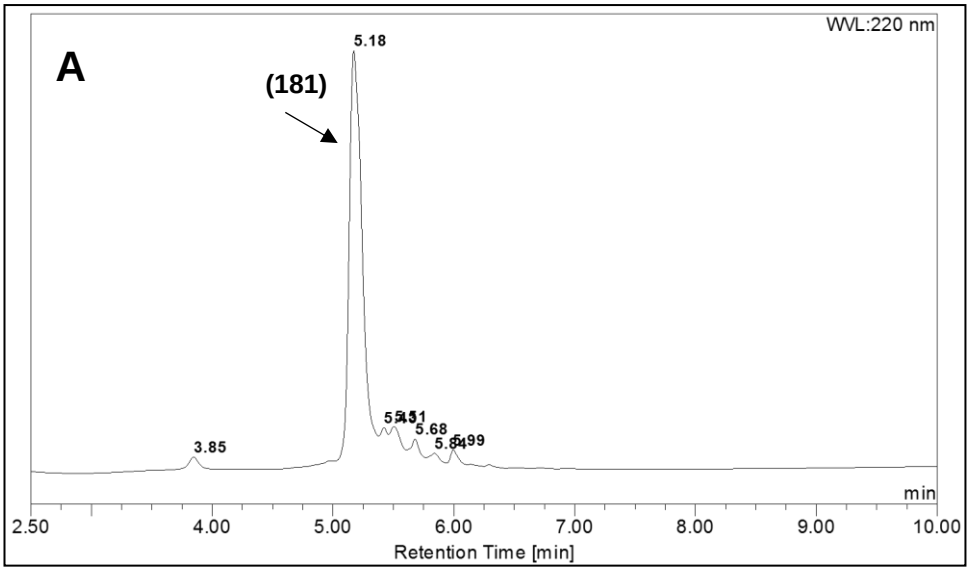
A
WVL:220 nm
5.18
(181)
3.85
5.68
min
2.50
4.00
5.00
6.00
7.00
8.00
9.00
10.00
Retention Time [min]

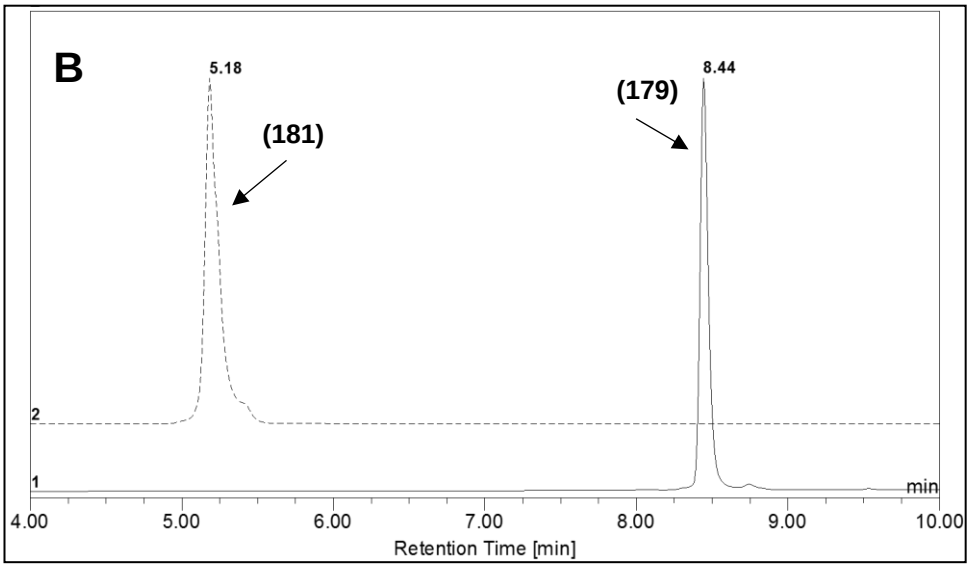
B
5.18
(181)
8.44
(179)
2
1
min
4.00
5.00
6.00
7.00
8.00
9.00
10.00
Retention Time [min]

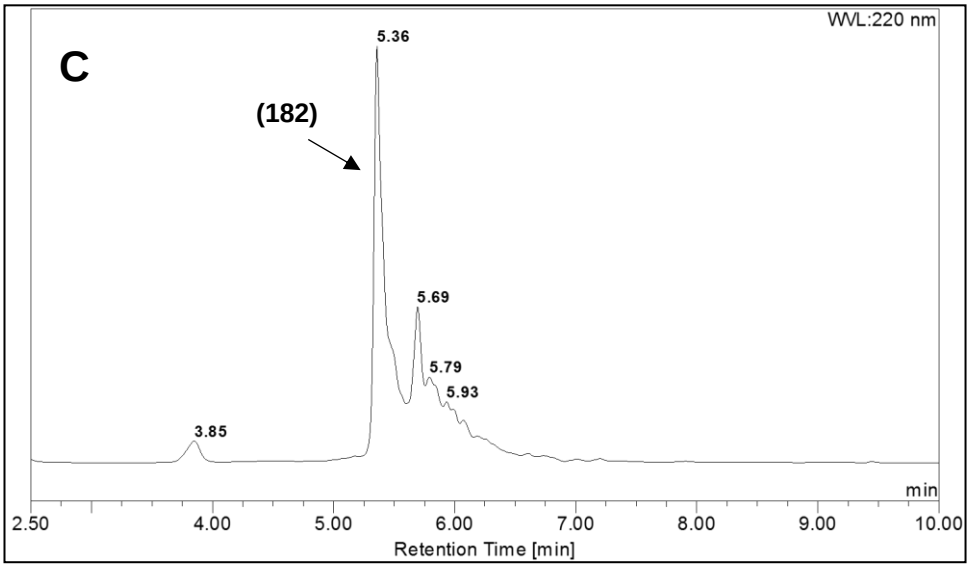
C
WVL:220 nm
5.36
(182)
5.69
5.79
5.93
3.85
min
2.50
4.00
5.00
6.00
7.00
8.00
9.00
10.00
Retention Time [min]

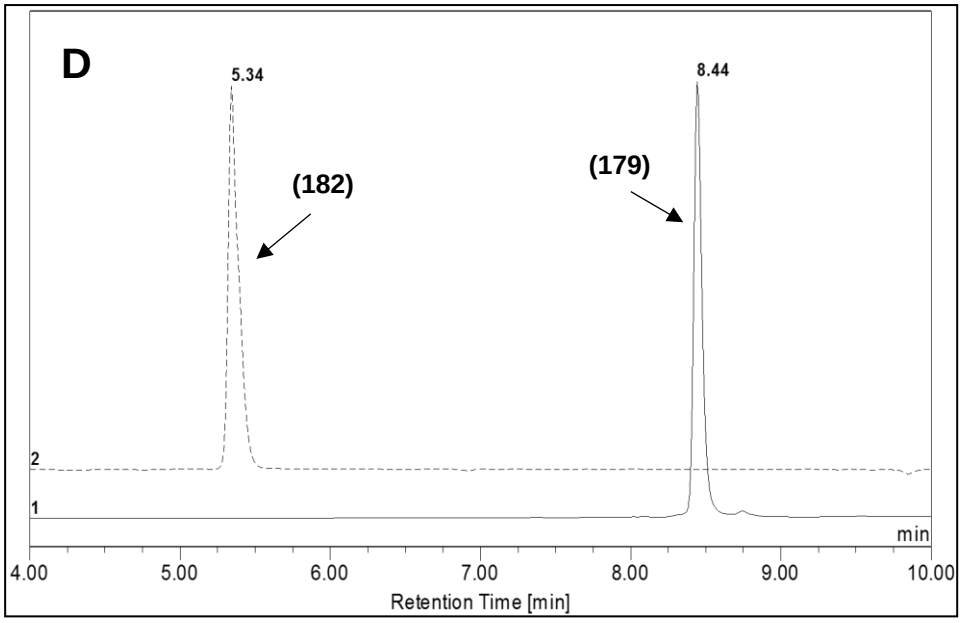

Figure 76. HPLC chromatograms for peptide-ALA dendron **(181)** and **(182)**.

A. Crude reaction mixture showing **(181)**.

B. Overlay for the final product **(181)** and starting azido-peptide **(179)**.

C. Crude reaction mixture showing **(182)**.

D. Overlay for the final product **(182)** and starting azido-peptide **(179)**.

The optimised conditions from above were also applied to the resin-bound peptide derivative functionalised with the hydroxybenzoic core **(176)**. **(176)** was coupled with alkyne derivatives **(105)** and **(107)** (Scheme 51). The expected products **(175)** and **(180)** were isolated by semi-preparative HPLC and obtained in moderate yields.

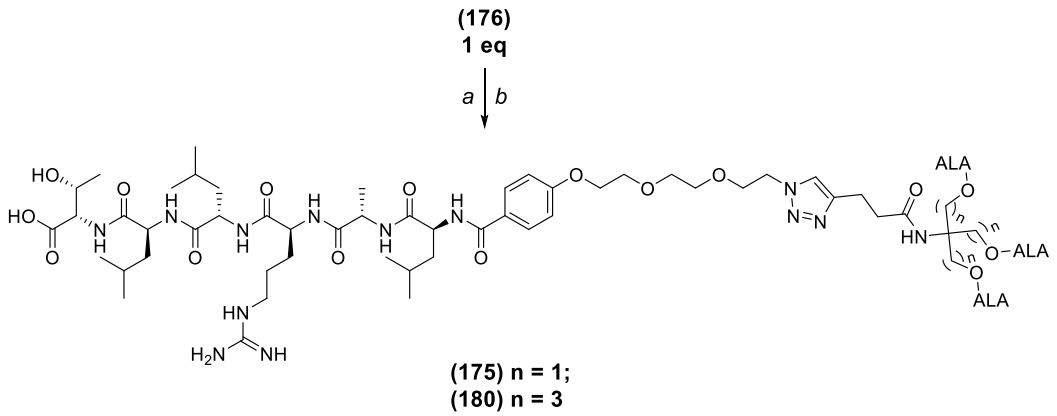

Scheme 51. On-resin click coupling of peptide derivative **(176)** with alkyne derivatives **(105)** and **(107)**. *Reagents and conditions: a.* 2 eq **(105)** or **(107),** copper(I) trifluoromethanesulfonate benzene complex, DMSO, 5 d, RT; *b.* TFA/TIS/H_2O (95:2.5:2.5 v/v/v), 3 h, **53% (175)**, **38% (180)**.

Figure 77 shows the HPLC chromatograms of the crude reaction mixtures for **(175)** and **(180)**.

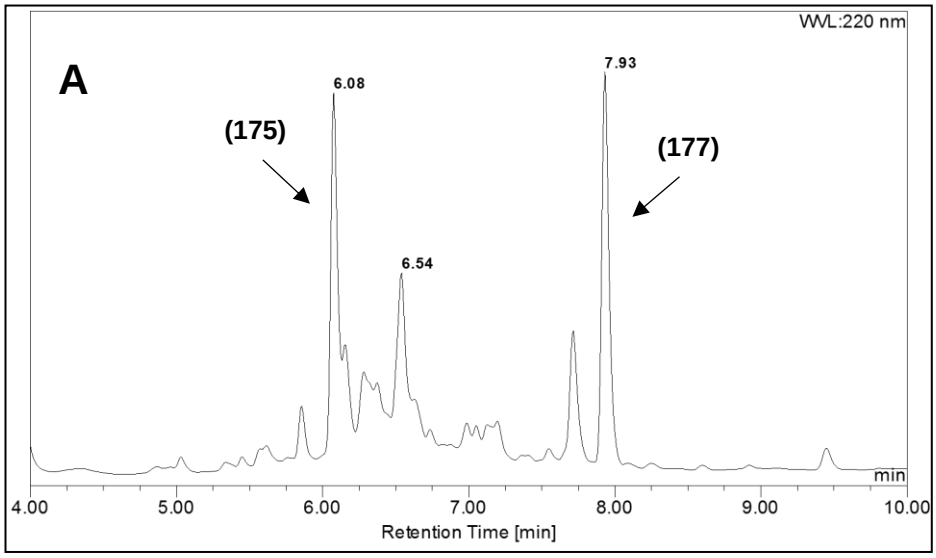

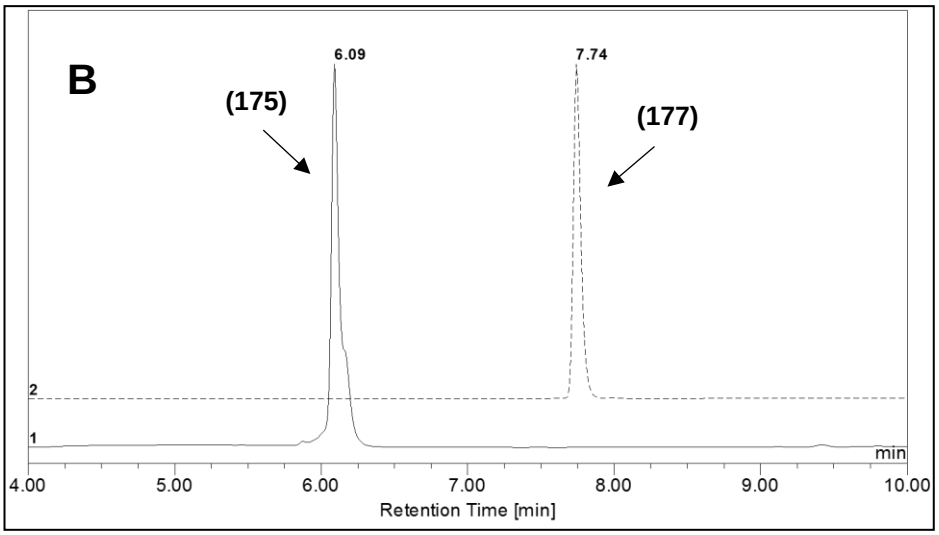

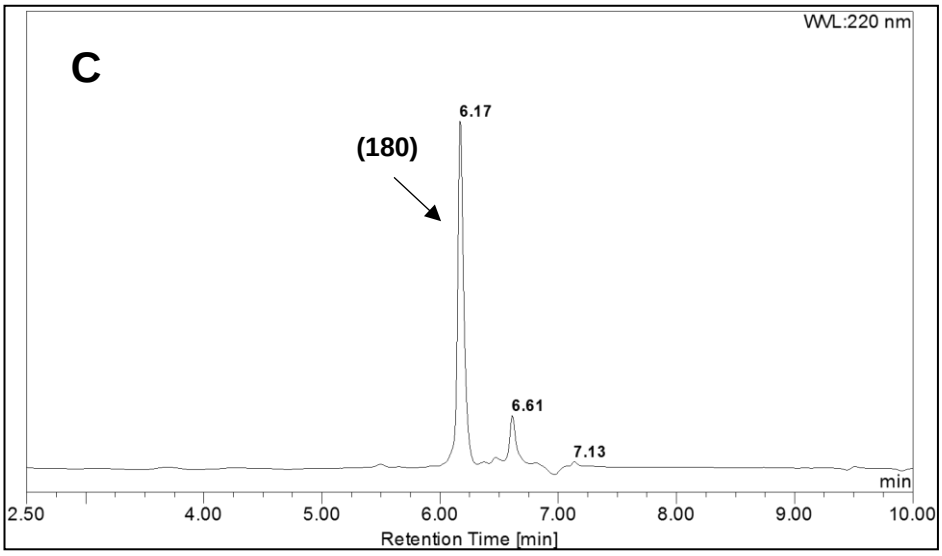

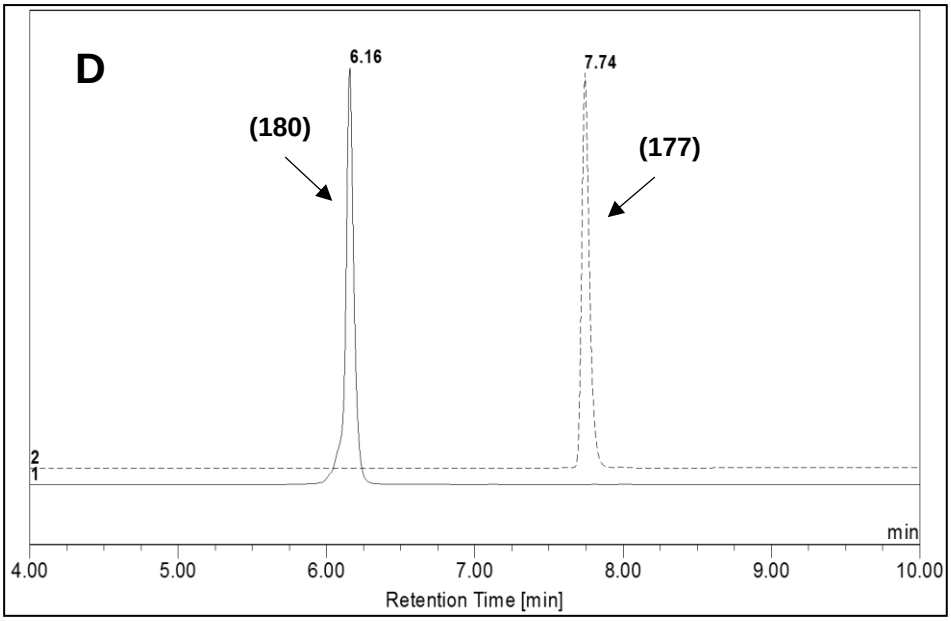

Figure 77. HPLC chromatograms for peptide-ALA dendron **(175)** and **(180)**.

A. Crude reaction mixture showing **(175)**.

B. Overlay for the final product **(175)** and starting material **(177)**.

C. Crude reaction mixture showing **(180)**.

D. Overlay for the final product **(180)** and starting material **(177)**.

4.2.4 Click coupling in solution (D)

Loading of the core units **(142)** and **(147)** on the peptide-resin followed by on-resin click coupling proved to be a successful strategy for synthesizing targeted ALA dendrons. However the yields of the reactions were modest and the reaction could not be monitored (on-resin coupling). A modification was therefore made to the above strategy and the peptide-gallic acid core derivative **(178)** was first cleaved from the resin to obtain **(179)** (see section 4.2.3) so that click coupling with the alkyne derivative **(105)** could be carried out in solution (Scheme 52).

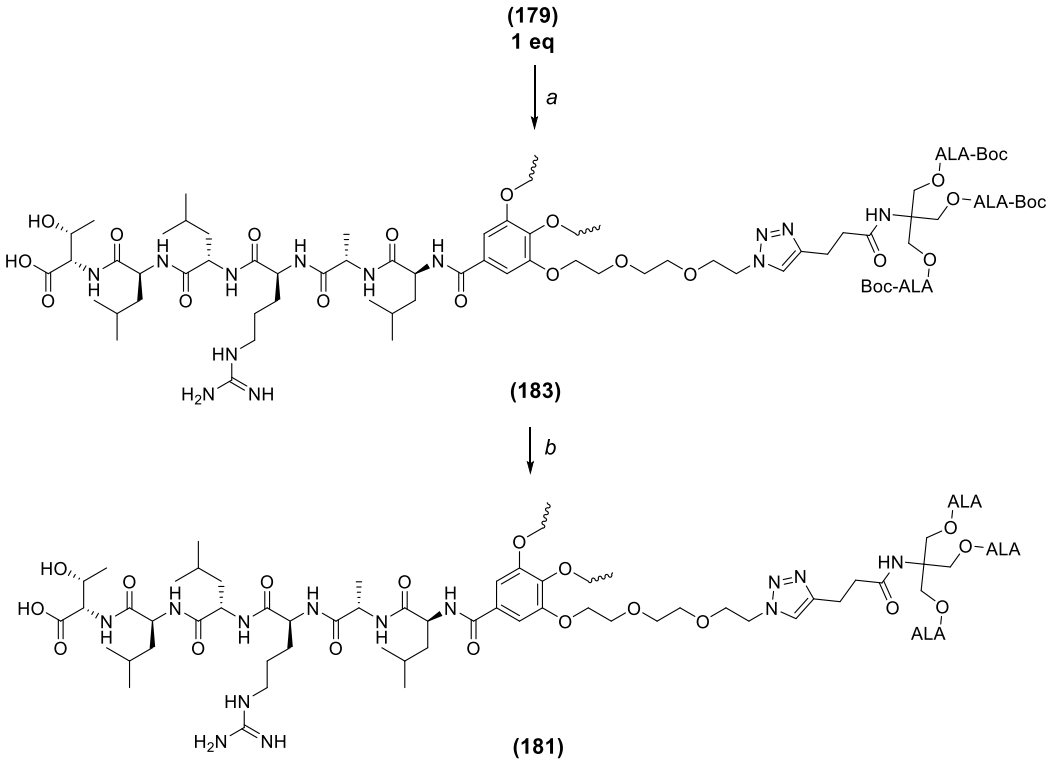

Scheme 52. Solution click coupling of peptide conjugate **(179)** with alkyne derivative **(105)**. *Reagents and conditions* a. 6 eq **(105)**, copper(I) trifluoromethanesulfonate benzene complex, DMSO, 36 h, RT, **69%** b. TFA:DCM (1:1 v/v), 30 min, **94%**.

This allowed the progress of the CuAAC to be easily followed by analytical HPLC, and complete disappearance of the starting material **(179)** and formation of a new peak at 9.94 min **(183)** was observed at the end of 36 h (Figure 78). The product was obtained as the Boc protected derivative, which was then treated with TFA to obtain **(181)** as the TFA salt in 69% yield.

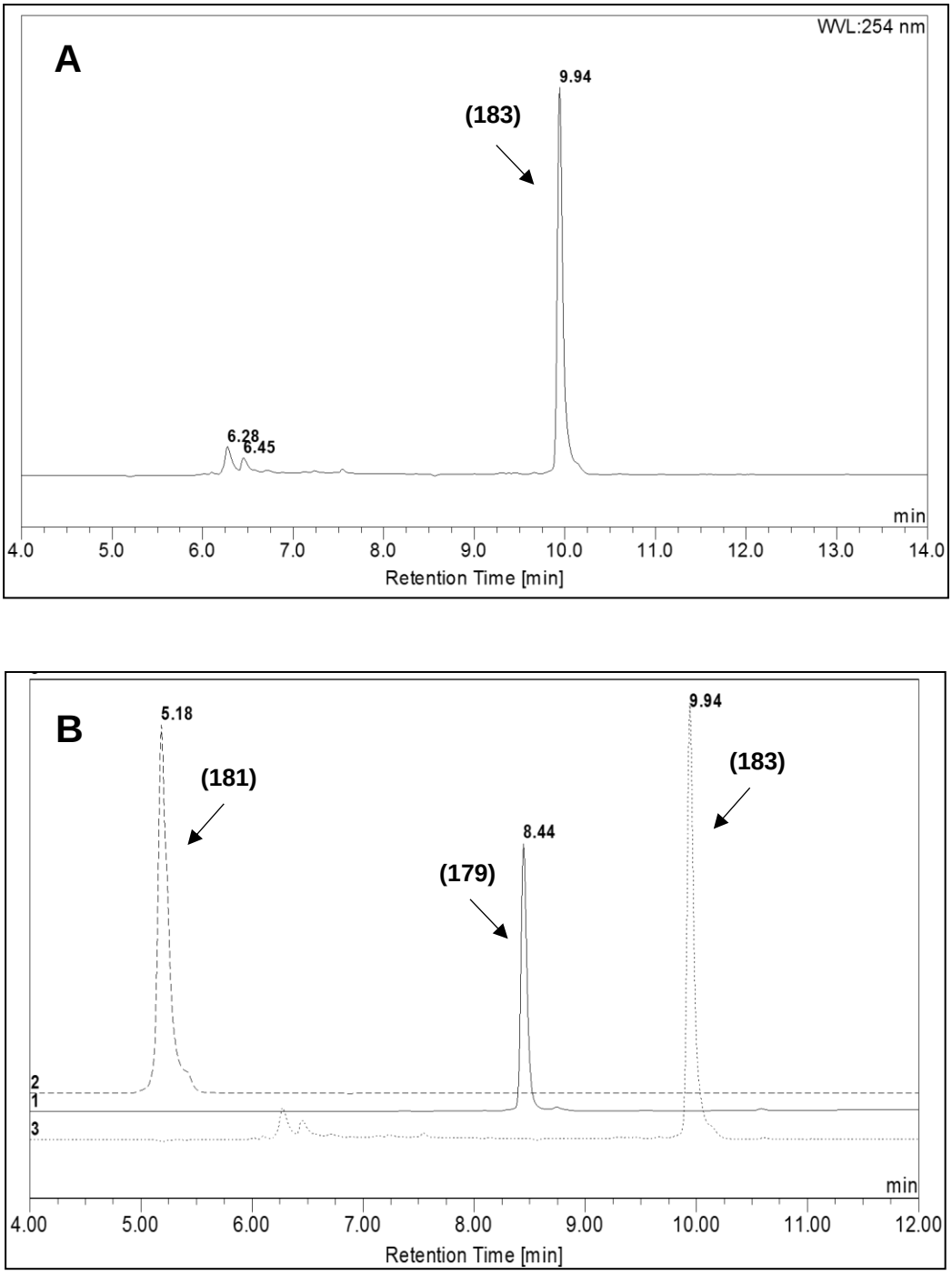

Figure 78. HPLC chromatograms for peptide-ALA dendron **(181)**.

A. Crude reaction mixture showing **(181)**.

B. Overlay for the final product **(181)** and starting materials **(179)** and **(183)**.

4.2.5 Click coupling via microwave irradiation (E)

The above strategies helped to identify the right Cu source and optimum conditions that allowed the progress of the reaction to be monitored. A final attempt to further reduce the duration of reaction was made by following the strategy in 4.2.4, but carrying out the reaction under microwave irradiation. Various successful examples of solid-phase peptide synthesis and the preparation of peptidomimetics via CuAAC under microwave irradiations have been reported with high yields.[267, 268]

A reaction vial containing the alkyne derivative **(105),** targeting core **(179)** and copper(I) trifluoromethanesulfonate benzene complex in DMSO was irradiated at 10-15 W at a predetermined temperature and for a fixed time (Scheme 53).

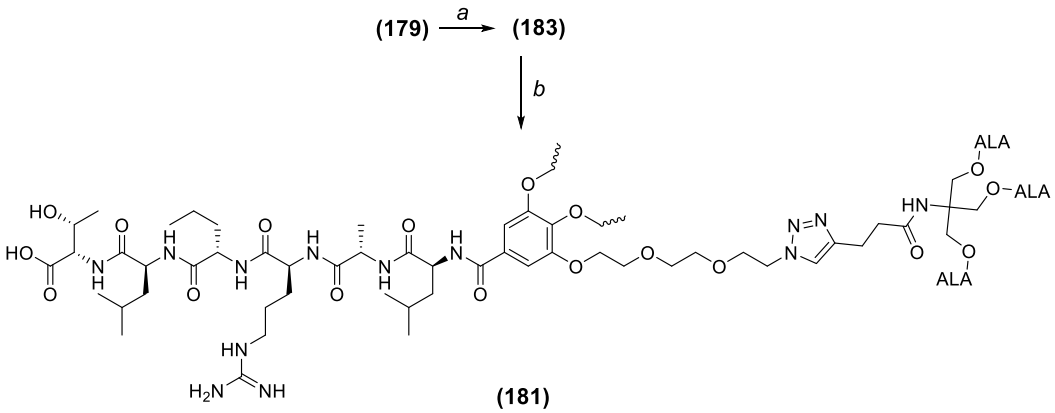

Scheme 53. Click coupling of peptide conjugate **(179)** with alkyne derivative **(105)** via microwave irradiation. *Reagents and conditions: a.* 6 eq **(105)**, copper(I) trifluoromethanesulfonate benzene complex, DMSO, 10 min, 70 °C, microwave irradiation (10-15 W), **75%**; *b.* TFA:DCM (1:1 v/v), 30 min, **95%**.

The results from these experiments are summarised in Table 4. When the reaction was carried out at 70 °C for 5 min, no disappearance of starting material or appearance of new species was observed by HPLC. However repeating the same reaction for 10 and 15 min showed a single product peak with complete disappearance of starting material, azido-peptide **(179)**.

Table 3. Microwave irradiation conditions for targeted ALA dendron **(181)**.

Temp (°C)	Time (min)	Solvent	Outcome
70	5	DMSO	No reaction
70	10	DMSO	Clean conversion to product
70	15	DMSO	Clean conversion to product
80	5	DMSO	Additional peaks observed
80	10	DMSO	Additional peaks observed
80	15	DMSO	Additional peaks observed
100	5	DMSO	Additional peaks observed
100	10	DMSO	Additional peaks observed
100	15	DMSO	Additional peaks observed

In each experiment, a solution of 6 eq **(105)** and 6 eq $(CF_3SO_3Cu)_2.C_6H_6$ in DMSO was treated with 1 eq azido peptide **(179)** in a MW vessel followed by microwave irradiation (10-15 W) at different temperature and time conditions. The reaction mixture was then analysed by HPLC

Reactions carried out at 80 °C and 100 °C showed additional peaks at a higher retention time in addition to the product peak, suggesting a possible dimerization of alkyne **(105)** (Figure 79).[269]

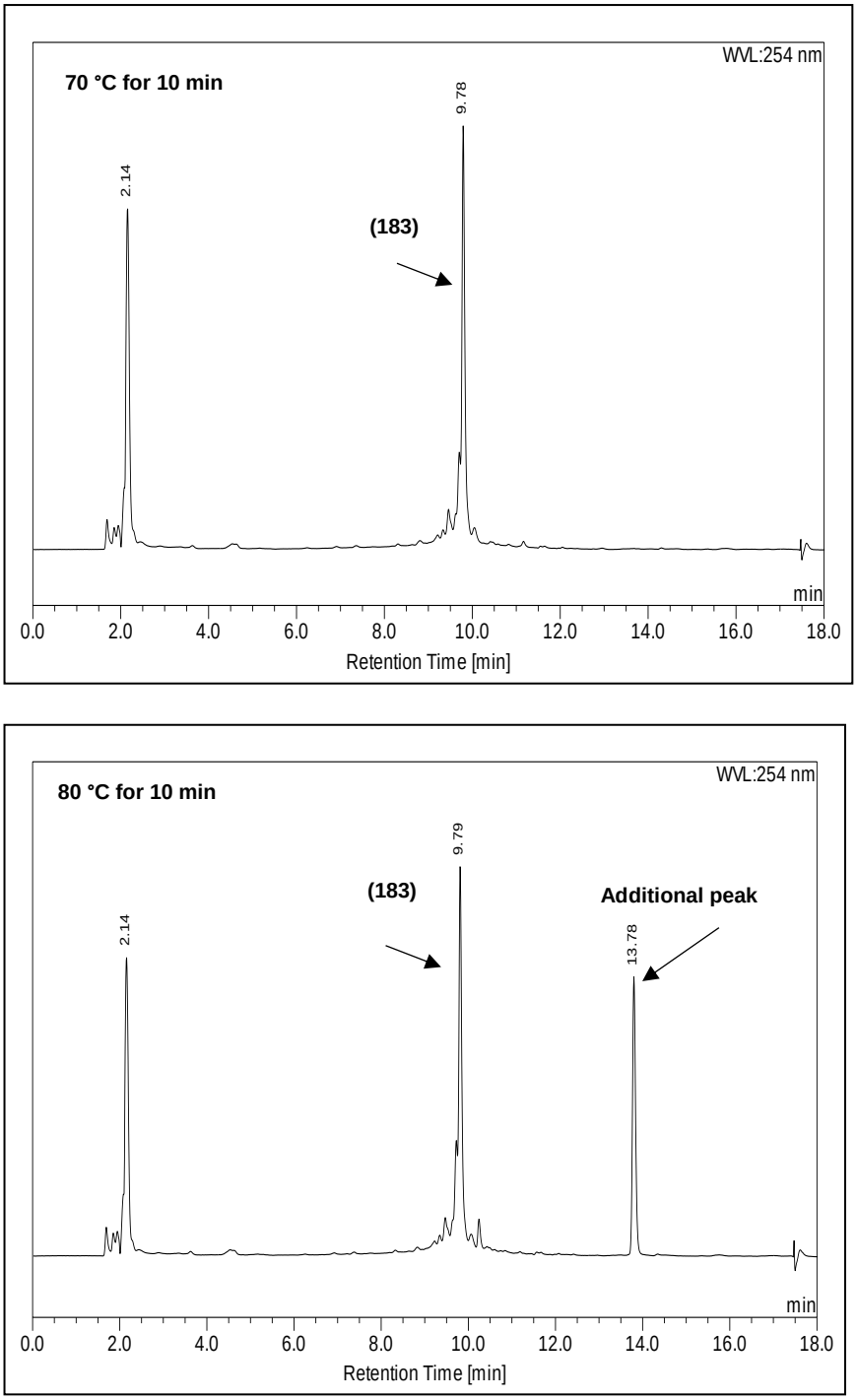

Figure 79. HPLC chromatograms for **(183)** post-microwave irradiation at two different temperature conditions (70 °C and 80 °C).

Following the reaction at 70 °C for 10 min (Scheme 52), the product was isolated by semi-preparative HPLC and Boc protecting groups were removed with TFA to obtain **(181)** in 95% yield asin Scheme 53.

Table 4 summarises the outcome of different synthetic strategies adopted for synthesizing the targeted ALA dendrimer **(181)** (Figure 80)

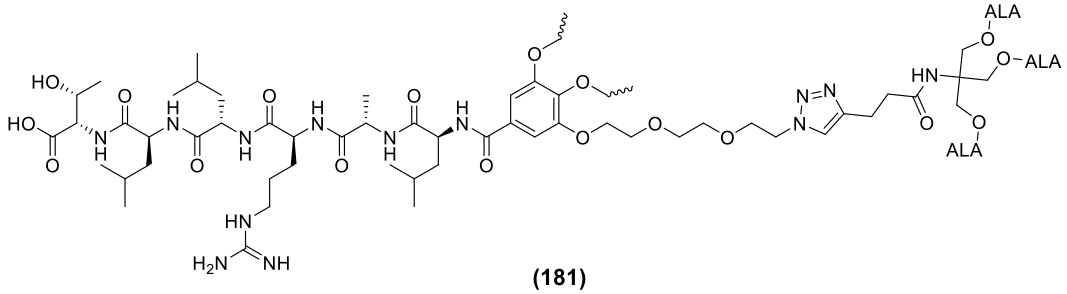

(181)

Figure 80. Chemical structure of the targeted ALA dendrimer **(181)**.

Table 4. Summary of different synthetic strategies adopted to synthesize EGFR-targeted ALA dendrimers.

Mode of synthesis	Reaction time	Yield (%)[a]
Solution coupling	×	NA
On resin coupling	16 h	5[b]
On resin click coupling	5 d	30[b]
Solution click coupling	36 h	69[c]
Microwave irradiation (in solution)	10 min	75[c]

×: No reaction observed by analytical HPLC

[a]Isolated yields after semi-preparative HPLC.

[b]Fully deprotected derivative **(181)**.

[c]Boc-protected derivative **(183)**.

4.3 Biological experiments

4.3.1 Background

Time-course fluorescence studies

The purpose of these studies was to measure the evolution of PpIX fluorescence from the prodrugs over time. In this case, the cells were incubated with ALA for a fixed period of time and PpIX fluorescence was measured using a CLARIOstar high performance microplate reader (410 nm excitation and 635 nm emission).

Photocytotoxicity/PDT activity

In order to investigate the PDT effect of the synthesized conjugates, phototoxicity studies were carried out by irradiating the cells incubated with prodrugs for a fixed time period corresponding to a specific light dose for short duration of time. The cytotoxicity was then assessed by MTT assay.

MTT assay

In order to determine the cytotoxicity of the synthesized prodrugs with or without irradiation an MTT assay was carried out.[270] The principle of this assay is based on the fact that mitochondrial activity is linearly correlated with the number of viable cells. The assay uses 3-[4,5-dimethylthiazol-2-yl]-2,5 diphenyl tetrazolium bromide (MTT) which is reduced by cellular dehydrogenases to form the water-insoluble purple-blue formazan dye (Scheme 54).

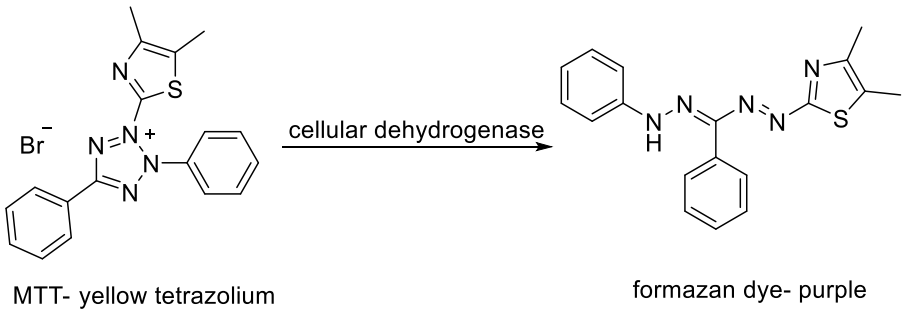

Scheme 54. Cellular conversion of MTT to its insoluble purple formazan product

The formazan is dissolved in DMSO and the absorbance is determined colorimetrically, which gives a measure of metabolic activity and hence the number of viable cells.

4.3.2 Time-course fluorescence studies

The build-up of PpIX fluorescence induced by the ALA dendrimers **(145)** (3-ALA units), **(150)** (9-ALA units), and **(181)** (EGFR targeting with 9 ALA units) was investigated in MDA-MB-231 cells (EGFR-overexpressing breast cancer cell line). The cells were incubated with freshly prepared solutions of ALA and ALA containing dendrimers **(145), (150) and (181)** for 24 h. Serum-free medium was used in order to avoid loss of PpIX from cells, thus leading to loss of fluorescence signal.[168, 206] Phenol red-free DMEM was also used during those fluorescence measurements. Phenol red was found to produce significant autofluorescence during the initial experiments which interfered with the PpIX detection (Figure 81).

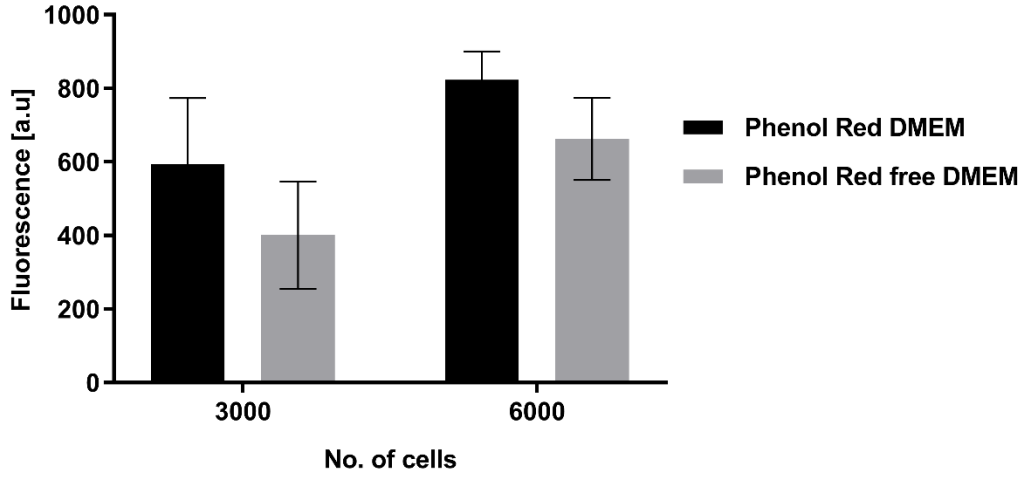

Figure 81. ALA-induced PpIX fluorescence in phenol red and phenol red-free DMEM.

MDA-MB-231 cells were seeded in a 96 well plate at two different densities (3000 and 6000). ALA at a concentration of 1 mM was incubated with the cells for 4 h and fluorescence measurements were performed with CLARIOstar high performance microplate reader (CLARIOstar® BMG LABTECH, United Kingdom). The results were expressed as mean ± SD (n = 3).

It was observed that wells containing phenol red DMEM showed higher apparent ALA-induced PpIX fluorescence at both cell densities as compared

with ones in phenol red-free medium at the same concentration. Hence it was concluded that phenol red-free DMEM was the right medium for all the fluorescence measurements. The concentration selected for ALA was 1.0 mM which was below the limit at which any toxic effects should be observed.[206] Equimolar concentrations of ALA dendrimers (adjusted for number of ALA units) were used along with two or three higher doses to investigate any possible dark toxicity. The PpIX fluorescence was measured at the end of 4, 8 and 24 h and the results are shown in Figure 82 (A-C).

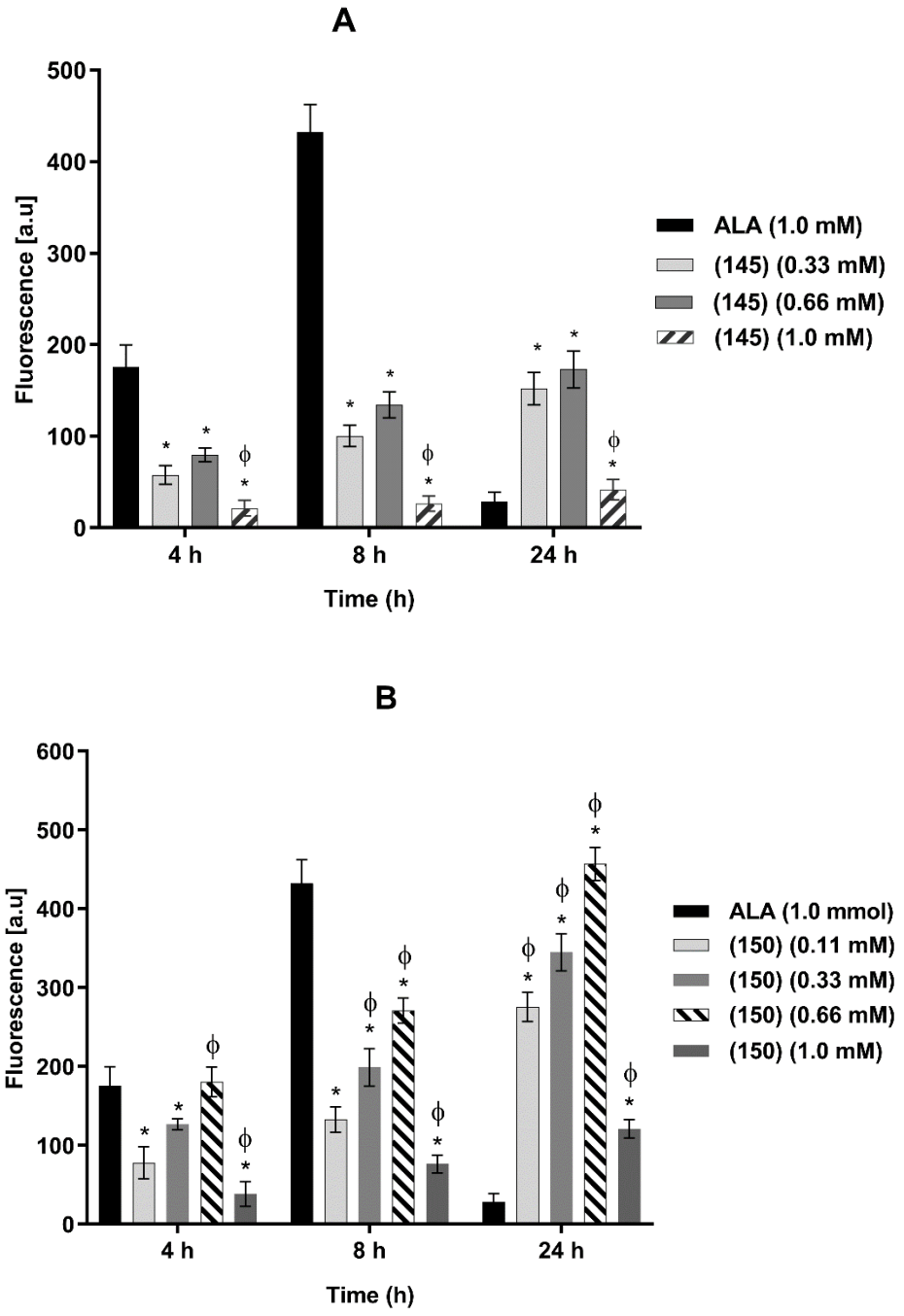

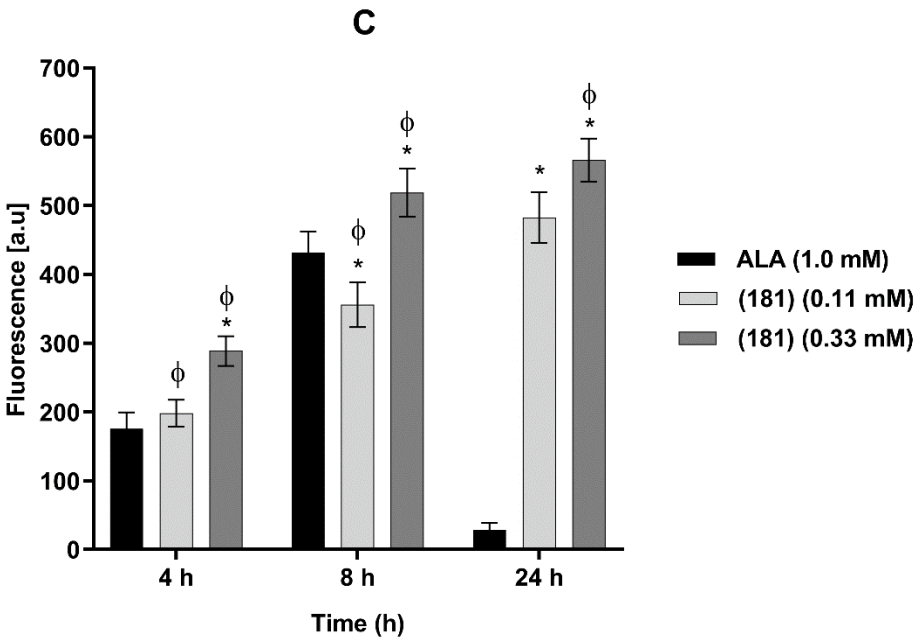

Figure 82 (**A-C).** ALA-induced PpIX generation from **(145)**, **(150)** and **(181)** in MDA-MB-231 cells.

A. MDA-MB-231 cells were treated with **(145)** (0.11 mM) and were incubated at 37 °C in the dark. Fluorescence readings taken at 4, 8 and 24 h intervals and the results were compared with an equimolar concentration of ALA (1.0 mM). Additional experiments with a higher concentration of ALA prodrug **(145)** (0.33 mM) were also included in this current study (n = 3).

B. MDA-MB-231 cells were treated with ALA dendrimer **(150)** (0.11 mM) and the same protocol was followed as for **A.** above. Higher concentrations of **(150)** (0.33, 0.66 and 1.0 mM) were also included in this study.

C. MDA-MB-231 cells were treated with EGFR targeted ALA-dendrimer **(181)** (0.33 mM) and the same protocol was followed as for **A.** above. A higher concentration of **(181)** (0.66 mM) was also included in this study.

Results are expressed as mean ± SD (n = 3)

* : $p<0.05$ significantly different from the ALA treated cells.

Φ: $p<0.05$ significantly different from ALA prodrug treated cells **(145)**, **(150)** and **(181)** at different doses.

From the results, it can be deduced that the synthesized ALA dendrimers show a sustained release of PpIX in comparison to equimolar concentrations of ALA, which shows a sharp decline at the end of 24 h. A similar release pattern was also observed with higher concentrations of the ALA dendrimers. These results are in agreement with previous work by Casas *et al.* where they had observed

sustained release of ALA-induced PpIX from an 18-ALA dendron over 24 h, and where basal values were not reached until 48 h.[207] ALA-induced PpIX fluorescence was initially investigated with **(145)** and **(150)** (Figure 82 A-B). The cells incubated with these two conjugates showed a lower release of PpIX (0.33 and 0.66 mM for **(145)** and 0.11, 0.33 and 0.66 mM for **(150)**) at the end of 4 and 8 h in comparison to free ALA (1.0 mM). **(145)** showed almost 50% of PpIX fluorescence compared to ALA at the end of 4 h, while it showed only 25% at the end of 8 h. However **(150)** produced a similar PpIX fluorescence to ALA at the end of 4 h, while it was 60% at the end of 8 h. When **(145)** and **(150)** at a concentration of 1.0 mM (3 times or 9 times the concentration of ALA) were incubated with cells, a decrease in porphyrin levels was observed at all time points (4, 8 and 24 h) indicating possible dark toxicity.

PpIX fluorescence was then investigated with the EGFR-targeted dendrimer **(181)** at two different concentrations (0.11 and 0.33 mM) (Figure 82 C). The level of ALA-induced PpIX fluorescence from the dendrimers was higher in comparison to equimolar doses of ALA. The release of PpIX was also higher in comparison to **(145)** and **(150)** consistent with the desired enhanced and selective delivery of the targeted ALA dendrimer.

4.3.3 Cytotoxicity and MTT assay

Having established that non-toxic concentrations of the synthesized ALA dendrimers produced PpIX in MDA-MB-231 cells, the effectiveness of **(145), (150)** and **(181)** for PDT was investigated. In order to establish appropriate experimental conditions, ALA was initially incubated with the cells and irradiated with light for different time intervals. Irradiation was performed from above the plates (see section 7.3.7) using a broad spectrum UVA lamp whose emission overlapped with the Soret band absorption of PpIX (405 nm). Cell viability was assessed by MTT assay as previously and the results are shown in Figure 83.

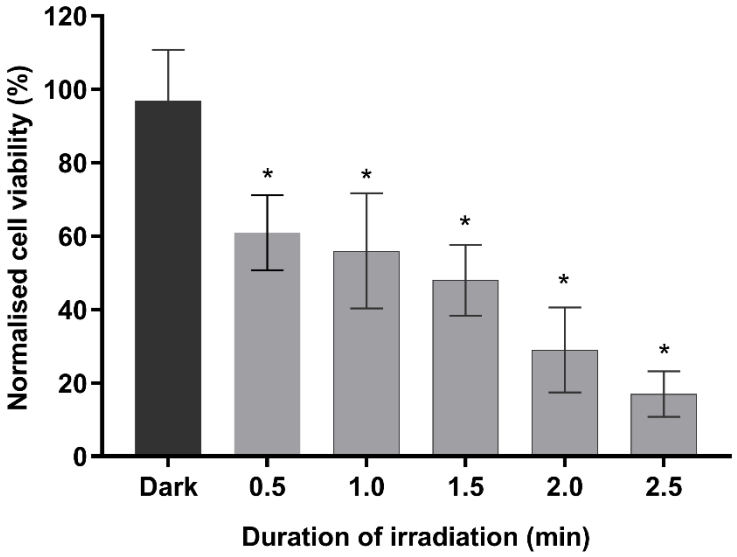

Figure 83. PDT effect of ALA on MDA-MB-231 cells at different time intervals.

MDA-MB-231 cells were treated with ALA (1.0 mM) and were incubated for 4 h at 37 °C in the dark. Cells were illuminated with UVA lamp for 0.5, 1.0, 1.5, 2.0 and 2.5 min. MTT analysis was carried out 24 h after light illumination, and the results were expressed as mean ± SD (n = 3) and plotted as percentage normalised cell viability.

*: $p<0.05$ significantly different from non-irradiated cells (dark)

It could be deduced from the results that light doses of 0.5, 1.0 and 1.5 min should be suitable for the study.

Phototoxicity studies were now carried out in MDA-MB-231 cells by incubating ALA and dendrimers **(145)** or **(150)** and EGFR-targeted ALA dendrimer **(181)**

at a range of concentrations for 4 h at 37 °C, and irradiating them with UVA light for different time intervals up to 1.5 min. Control cells were treated identically except that they were either not treated with ALA dendrimers (**145)**, (**150)** and (**181)** (or free ALA), or not irradiated. Statistical analysis was done at the end of study by plotting the percentage of enzymatic activity of the investigated compounds with respected to control cells (without any compounds). These results are shown below (Figure 84 A-C).

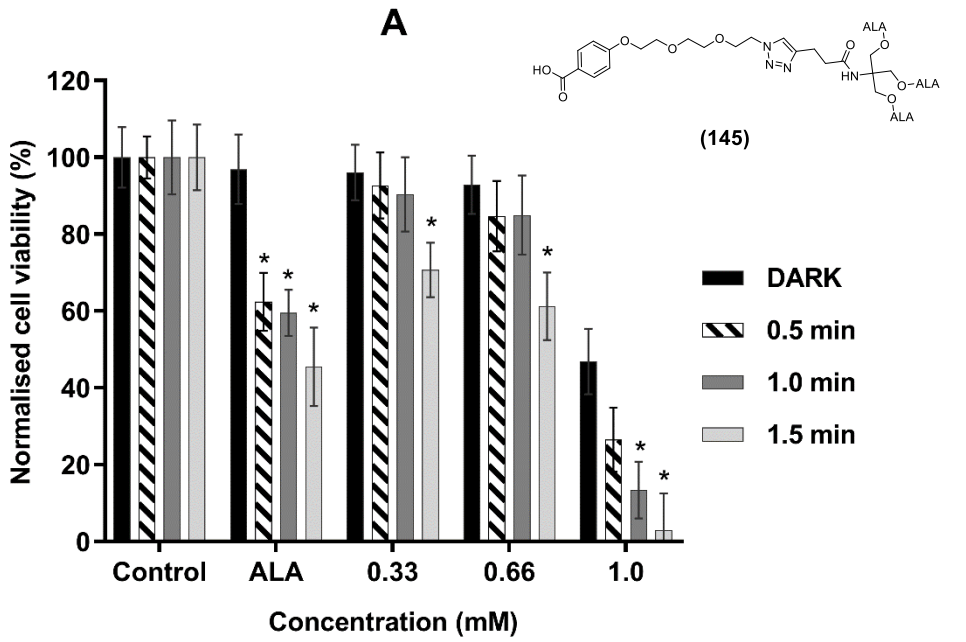

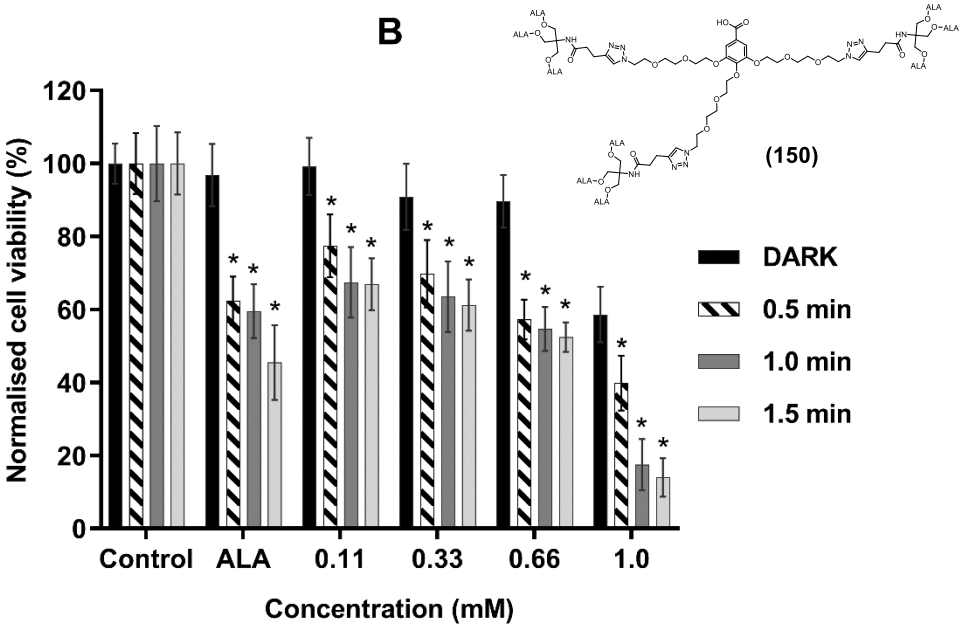

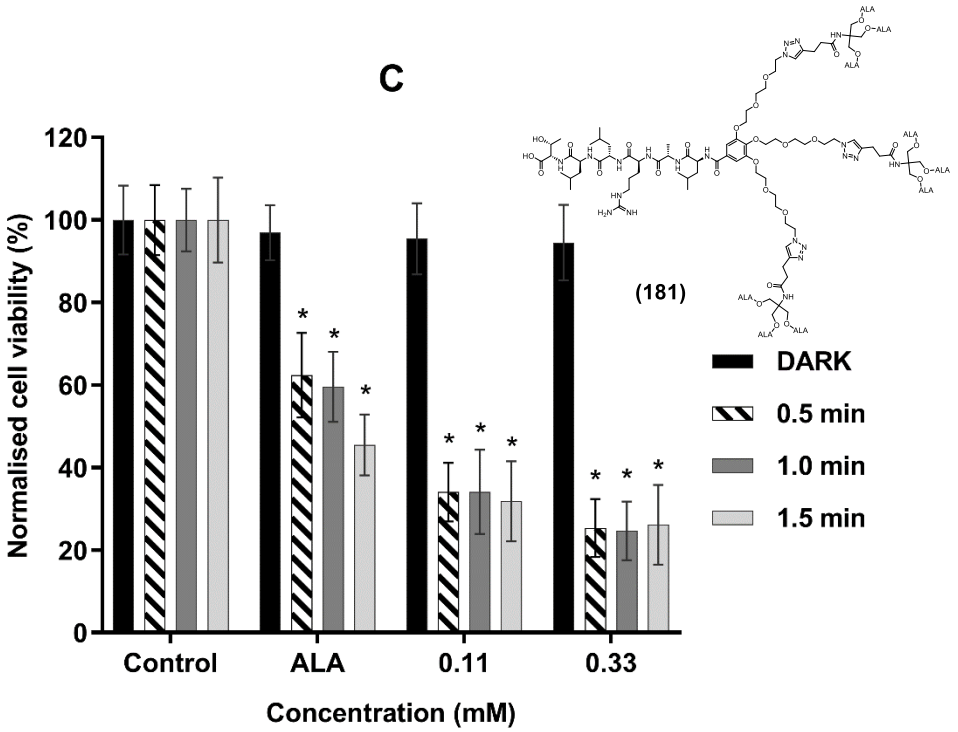

Figure 84 (A-C). PDT effect of **(145)**, **(150)** and **(181)** on MDA-MB-231 cells after incubation for 4 h.

A. MDA-MB-231 cells were treated with ALA dendrimer **(145)** (0.33 mM) and were incubated for 4 h at 37 °C in the dark. Cells were illuminated with UVA lamp for 0.5, 1.0 and 1.5 min. MTT analysis was carried out 24 h after light illumination and the results were compared with equimolar doses of ALA (1.0 mM). Higher concentrations of **(145)** (0.66 and 1.0 mM) were also included in this study.

B. MDA-MB-231 cells were treated with ALA dendrimer **(150)** (0.11 mM) and the same protocol was followed as for **A.** above. Higher concentrations of **(150)** (0.33, 0.66 and 1.0 mM) were also included in this study.

C. MDA-MB-231 cells were treated with EGFR targeted ALA-dendrimer **(181)** (0.11 mM) and the same protocol was followed as for **A.** above. Higher dose of **(181)** (0.33 mM) was also included in this study.

Results were expressed as mean ± SD (n = 3) and plotted as percentage normalised cell viability.

*: $p<0.05$ significantly different from non-irradiated cells (dark).

The results (Figure 84 A-C) show a difference in percentage of cell viability for ALA prodrugs **(145)** (3-ALA units), **(150)** (9-ALA units) and **(181)** (targeted 9-ALA units) in comparison to free ALA. **(145)** (with 3-ALA units attached) was found to be the least active conjugate of all the three ALA derivatives investigated in comparison to free ALA. At a dose of 0.33 and 0.66 mM and irradiation times of 0.5 and 1.0 min, the prodrug **(145)** showed almost the same cell viability in comparison to cells which were treated with the same concentration but not irradiated (dark). These results were slightly improved when the exposure time for the above two doses were increased to 1.5 min (cell viability was 66% for 0.33 mM and 62% for 0.66 mM), however it was still lower than that observed with free ALA (48% at 1.0 mM concentration).

The 9-ALA conjugate **(150)** showed better results in comparison to **(145)**. The cell viability at a concentration of 0.33 mM and 0.66 mM, showed a decrease across all three exposure times. With 0.5 min light exposure, cell viability was 69% (0.33 mM) and 57% (0.66 mM). These results are consistent with an improvement in PDT activity with increasing dendrimer (more ALA units leading to increased PpIX production).

(181) which is an EGFR targeting dendrimer with 9-ALA units showed cell viability of 35% at 0.11 mM and around 25% at 0.33 mM thus indicating better uptake and release of ALA inside the cell from the dendrimer. The dark toxicity (cytotoxicity without irradiation) for the ALA and its dendrimers were also assessed. It can be noted from the data above that the dendrimers did not show any dark toxicity at equimolar doses. However **(145)** and **(150)** showed dark toxicity at dose of 1 mM which was three or nine times the concentration of free ALA employed in these experiments.

4.4 Summary

In summary, different synthetic strategies were attempted to conjugate EGFR targeting peptide to ALA dendrons. Amide coupling of peptide to an ALA dendron in solution gave no result, whereas attachment of the dendron to the peptide on resin gave the desired product, although isolated in low yield. Changing the synthetic strategy by attaching initially the core azido unit to the peptide on resin, followed by coupling of ALA dendrons **(105)** and **(107)** *via* copper catalysed azide-alkyne cycloaddition gave the expected products **(181)** and **(182)** with moderate yields (30% and 25% respectively). The reaction time could be significantly reduced and the recovery of the clicked product was significantly improved when the CuAAC reaction was carried out in solution with a fully deprotected azido-peptide. Tthe reaction time could be further decreased significantly when coupling in solution was carried out under microwave conditions.

Biological evaluation in the EGFR-overexpressing cell line MDA-MB-231 showed sustained release of PpIX from the synthesized ALA dendrimers **(145)**, **(150)** and **(181)** in comparison to equimolar doses of ALA. ALA dendrimer **(145)** was found to show the least PpIX production in comparision to free ALA and similar results were also found in PDT experiments where it was the least active of all the conjugates tested at different doses. ALA dendrimer **(150)** with 9 copies of ALA attached showed a PpIX release which was better than **(145)** but still less than free ALA at all time points. The peptide targeted ALA dendrimer **(181)** was found to be the most efficient of all the conjugates in terms of having higher PpIX production as well as enhanced PDT activity in comparision to free ALA.

CHAPTER 5: RESULTS AND DISCUSSION (Peptide-porphyrin conjugates)

5.1 Background

Porphyrins and their analogues as discussed previously constitute a major group of photosensitisers in PDT (Chapter 1). Considerable effort in recent years has been given to the development of peptide-targeted photosensitisers to improve the pharmacokinetic properties and tissue-specificity of otherwise hydrophobic derivatives and Chapter 1 discusses some examples of this approach. In general, peptide-porphyrin conjugates can be synthesized by either covalently linking a peptide to the photosensitisers, or alternatively multiple units of peptide and photosensitiser units can be attached to a core structure.[271] Another approach that has been explored is to modify the surface of liposomes encapsulating porphyrin photosensitisers by peptide units (Figure 85).

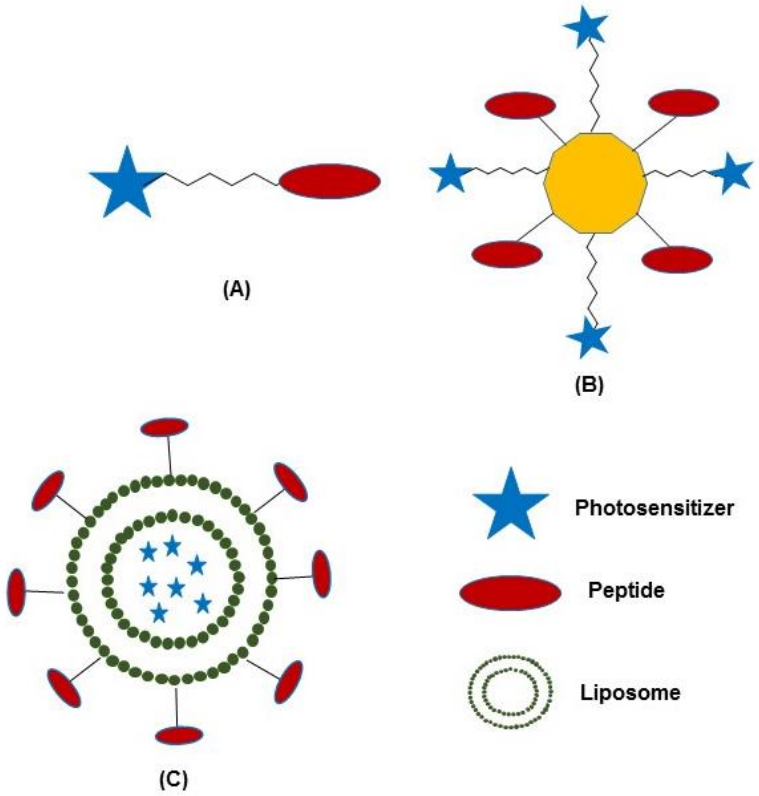

Figure 85. Different strategies explored for developing peptide-porphyrin conjugates **a.** direct conjugation **b.** dendrimer **c.** liposome (adapted from Olivo *et al.*).[271]

5.2 Strain promoted azide-alkyne cycloaddition (SPAAC)

Copper-catalysed azide-alkyne cycloaddition, as discussed previously, leads to the formation of a triazole and has been used for the assembly of various multifunctional molecules (Chapter 3). However, it has been reported that the presence of copper as a catalyst in CuAAC may lead to toxicity in bacterial as well as mammalian cells and thus limits its applications for the preparation of therapeutic agents.[272, 273] Recently bioorthogonal ligation chemistry has yielded a range of novel reactions related to the original triazole approach in which the use of a strained alkyne component replaces the need for copper catalysis.[237, 274] Wittig *et al.* (1961) were the first to report a reaction between cyclooctyne and phenyl azide which proceeded rapidly to give a triazole product. Forty years later Bertozzi *et al.*[236] repeated the same reaction under physiological conditions and noted that a strained cyclooctyne requires much less activation energy for triazole formation compared to a simple terminal alkyne (Scheme 55). The requirement for an exogenous catalyst is thus avoided, although a mixture of triazole regioisomers may be formed, depending on the cyclooctyne structure.[275]

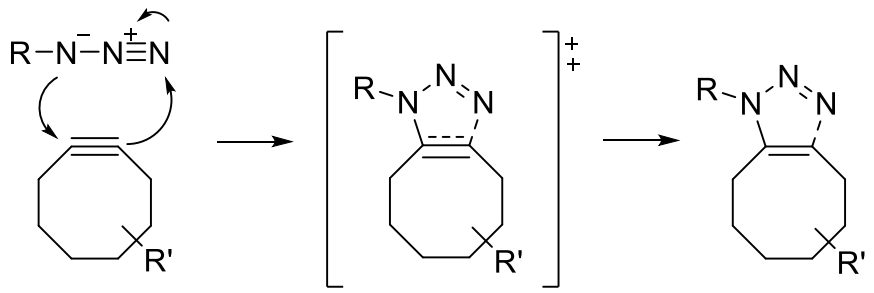

Scheme 55. Reaction mechanism for strain-promoted azide-alkyne cycloaddition (SPAAC).

However, cyclooctynes typically suffer from poor water solubility, which limits their applications in biological environment and, over the years, chemical modifications on the cyclooctyne ring have been carried out to overcome the solubility issue as well as improve the second-order rate constant of the click reaction (Figure 86). Bertozzi *et al.* investigated some of the modifications on the cyclooctyne ring and found **(185)** and **(186)** to be highly reactive, whereas Boons *et al.*[276] fused two benzene rings to the cyclooctyne which provided additional ring strain and found the second order rate constant of the modified

cyclooctyne **(188)** to be approximately three times higher than the simple cyclooctyne **(184)**. van Delft *et al.* reported a further increase in the reactivity of (**188)** by synthesizing aza-dibenzocyclooctyne **(189)** which had the favourable kinetics of **(188)** as well as the increased hydrophilicity of **(186).**[277] Symmetrical cyclooctynes such as **(187)** have the advantage that they can only generate a single triazole product.[278]

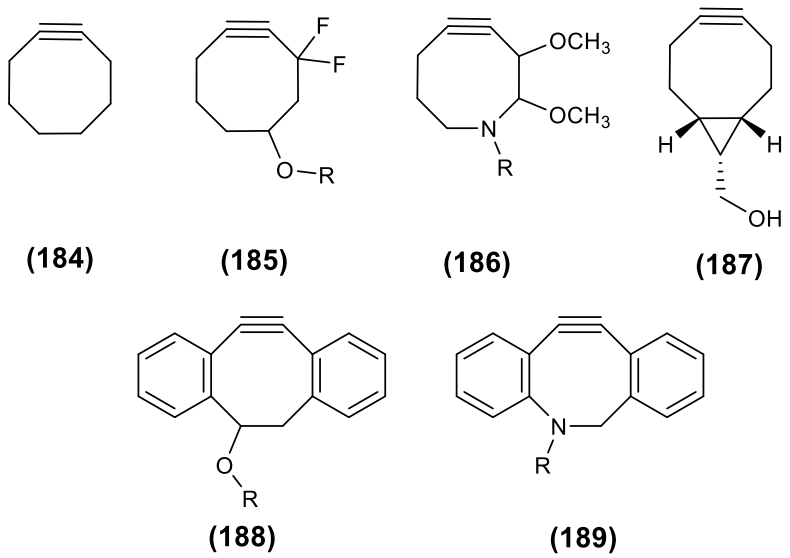

(184) **(185)** **(186)** **(187)** **(188)** **(189)**

Figure 86. Structures of cyclooctyne **(184)** and its modified derivatives **(185)-(189)**.

5.3 Synthesis of peptide porphyrin conjugates

Applying the tools developed previously (chapter 4) for the synthesis of EGFR-targeted ALA derivatives, the aim of this chapter was to prepare alternative EGFR-targeted photosensitisers using strain-promoted azide-alkyne cycloaddition (SPAAC) and assess their biological efficacy in selected cell lines (Figure 87). Strain promoted azide-alkyne cycloaddition was favoured over CuAAC for the current work as previous studies on porphyrin-related compounds have shown incorporation of copper into the macrocycle under CuAAC, hence necessitating the protection of the macrocycle by making a Zn complex.[272]

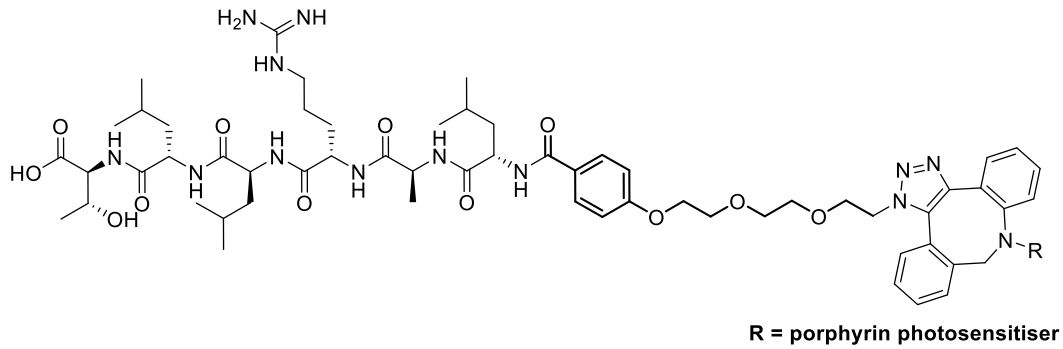

Figure 87. Structure of an EGFR-targeted porphyrin photosensitiser synthesized via SPAAC.

For the current work, a dibenzocyclooctyne (DBCO) derivative was chosen as the strained alkyne as these are widely available and have been used in a variety of applications.[277] Three different tetrapyrrole derivatives were selected for the synthesis of targeted peptide-porphyrin conjugates: 5-(4-aminophenyl)-10,15,20-triphenylporphyrin **(190)**, chlorin e6 derivative **(191)** and verteporfin **(13)** (Figure 88).

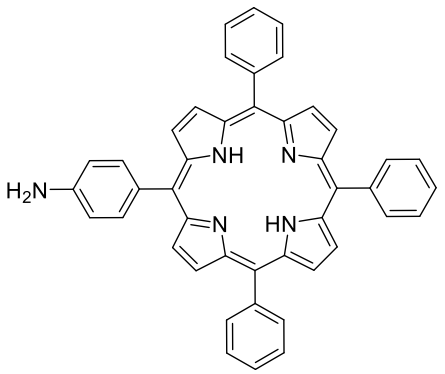

(190)

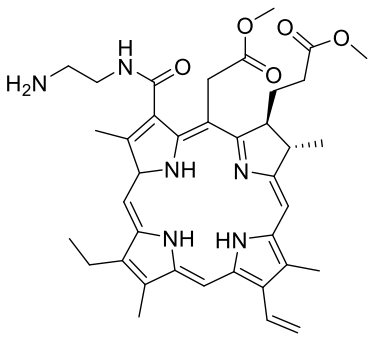

(191)

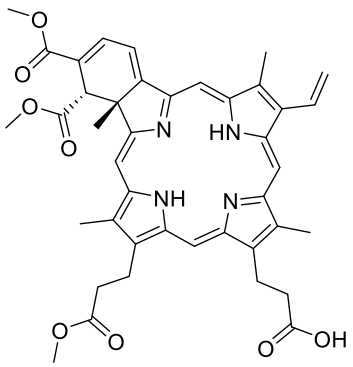

(13)

Figure 88. Structures of **(190)**, **(191)** and **(13)**.

5-(4-Aminophenyl)-10,15,20-triphenylporphyrin **(190)** is a porphyrin-type macrocycle and is largely water insoluble and highly hydrophobic. The clinically used chlorin e6 is a derivative of chlorophyll a and it possesses three chemically distinct carboxylic acid functions that have been previously functionalized with biomolecules such as peptides, sugars, lipoproteins, polyethylene glycols, and polyamines.[279-286] Chlorin e6 also has a superior absorption in the red region of the visible spectrum along with one order of magnitude higher extinction coefficient than the corresponding porphyrin.[287] VISUDYNE® (verteporfin), a benzoporphyrin derivative is a 1:1 mixture of two equally active regioisomeric esters (Verteporfin I and II, Figure 89) and is used as a photosensitiser in photodynamic therapy for the treatment of the wet form of macular degeneration.[288]

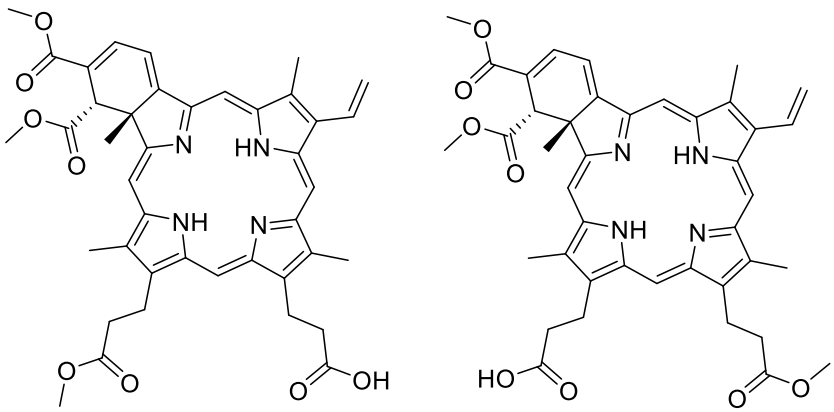

Figure 89. Structures of the two regioisomers of verteporfin (I and II) **(13)**.

Preparing specific peptide-targeted conjugates of the above three photosensitisers **(190)**, **(191)** and **(13)** would potentially enhance their uptake in EGFR-overexpressing cancer cell line. In the case of 5-(4-aminophenyl)-10,15,20-triphenylporphyrin **(190)**, it should also increase its water solubility as well as balance the hydrophobicity of the photosensitiser with a hydrophilic peptide. A DBCO-functionalised derivative of **(192)** was synthesised as shown in Scheme 56. TPP **(6)** was nitrated and reduced to **(190)** by a modification of the method of Luguya *et al*.[289] The amino group of porphyrin **(190)** was then acylated with DBCO-acid (small excess) using EDC.HCl/HOBt activation and DIEA as base (Scheme 56). The reaction was monitored by TLC and analytical

HPLC (Figure 91). The product **(192)** was isolated in good yield and was characterized by NMR and mass spectrometry.

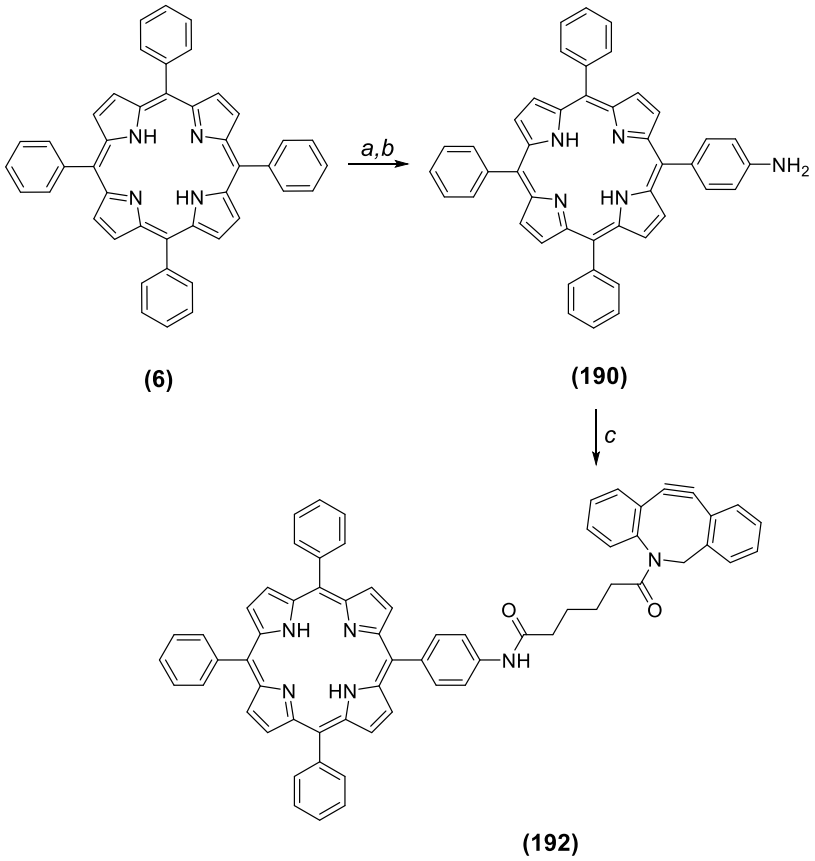

Scheme 56. Scheme of synthesis for the preparation of DBCO conjugate of **(190)**. *Reagents and conditions: a.* $NaNO_2$, TFA, 3 min; *b.* 5% Pd/C, $NaBH_4$, MeOH/DCM (1:4 v/v), 30 min, **31%**; *c.* DBCO-acid, EDC.HCl, HOBt. Hydrate, DIEA, DCM, RT, overnight, **76%**.

A selectively derivatised chlorin e6 derivative **(191)** was prepared starting from pheophorbide a (prepared by Dr R. Dondi from Pheophytin-a from Spirulina spp).[290] Pheophorbide a **(30)** was treated with 1,2-diaminoethane according to the method of Smith *et al.*[290] and the product **(191)** was acylated with DBCO-acid as for **(192)** (Scheme 57). Purification by column chromatography gave **(193)** in 57% yield.

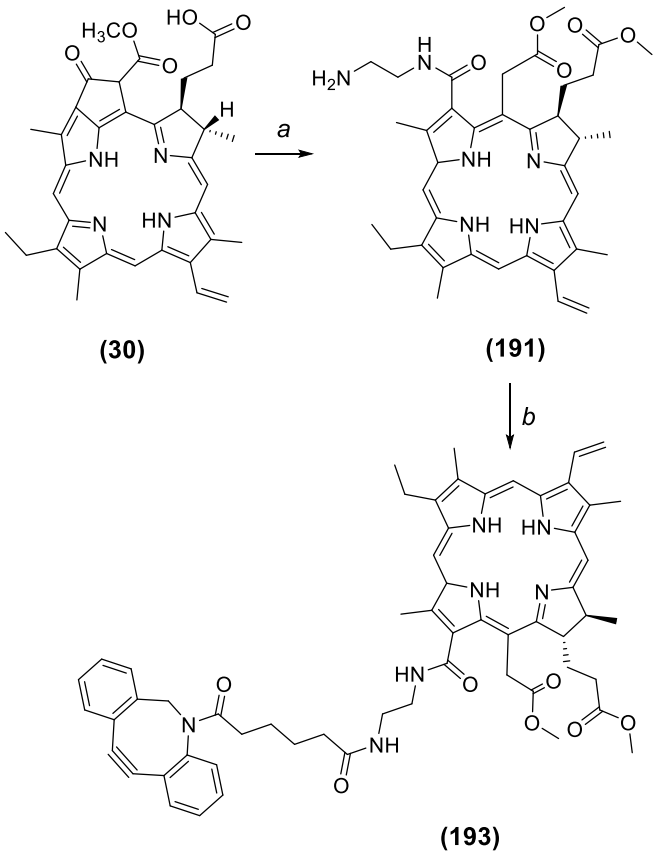

Scheme 57. Scheme of synthesis for the preparation of Ce6-DBCO conjugate (**193).** *Reagents and conditions: a.* 1,2-diaminoethane, anhydrous THF, overnight, **quant**; *b.* DBCO, EDC.HCl, HOBt. hydrate, DIEA, DCM, RT, overnight, **57%**.

The required verteporfin-DBCO derivative **(194)** was synthesised by Dr R. Dondi from commercial verteporfin (mixture of esters) and the corresponding DBCO-NH_2 derivative (Figure 90).

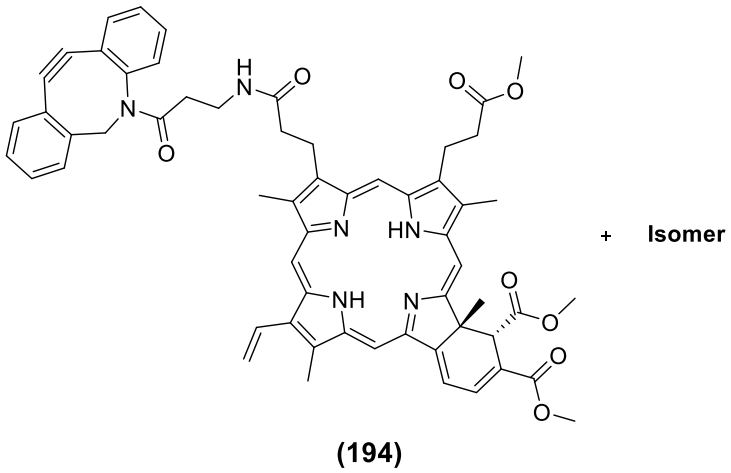

Figure 90. Chemical structure of verteporfin-DBCO conjugate **(194)**.

With the three DBCO derivatives **(192)**-**(194)** in hand, SPAAC to produce EGFR-targeted conjugates (See Figure 87) could be investigated. Reaction of 2 eq of the DBCO-photosensitiser conjugates **(192)**-**(194)** with the azido-functionalised EGFR peptide **(177)** proceeded smoothly in DMSO to give the expected conjugates **(195)**-**(197)** in good yields. The final conjugates were obtained as an inseparable mixture of triazole regioisomers as expected due to the unsymmetrical structure of the DBCO unit (Scheme 58).

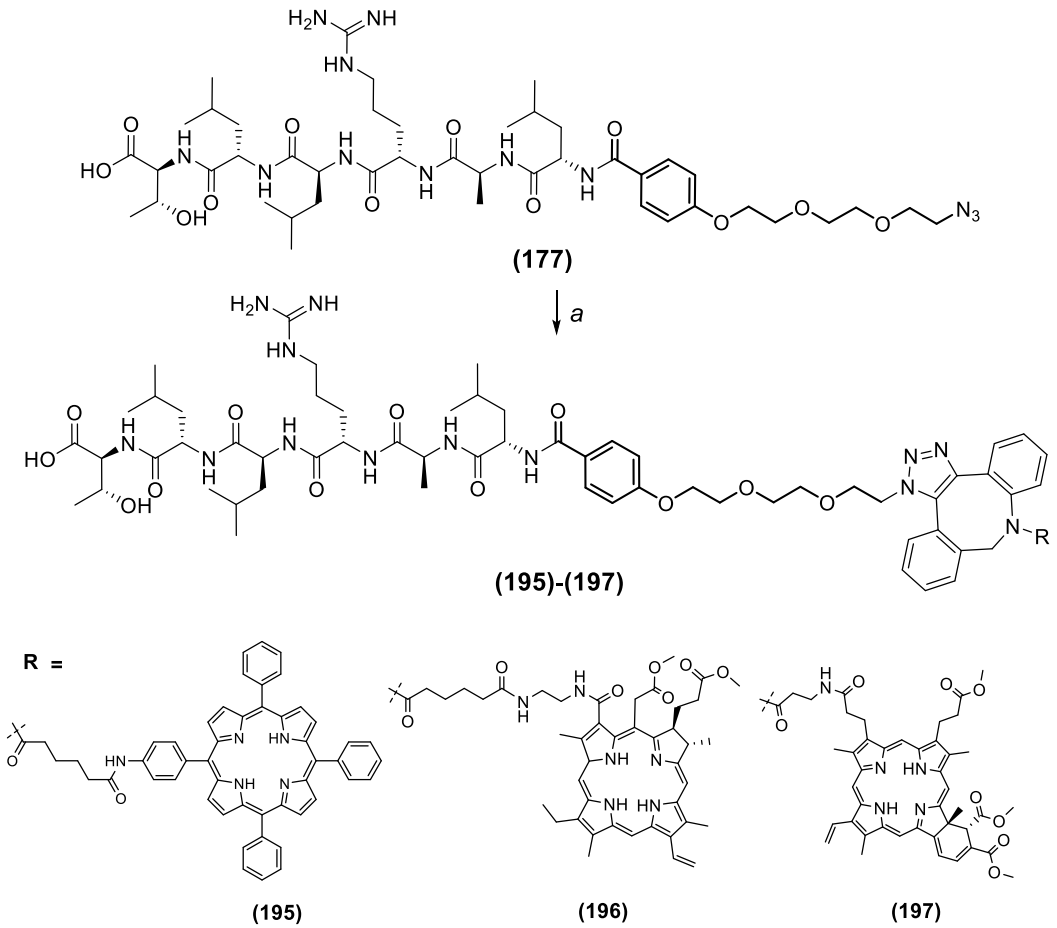

Scheme 58. Synthesis of peptide-targeted porphyrins **(195)**-**(197)**. Reagents and conditions: *a.* **(192)**-**(194)**, DMSO, RT, 8 h, **68% (195)**, **66% (196)**, **73% (197)**.

It should be noted that conjugates **(195)** and **(196)** were mixture of two regioisomers while **(197)** was a mixture of four regioisomers, since verteporfin itself is a mixture of two isomeric ester derivatives.

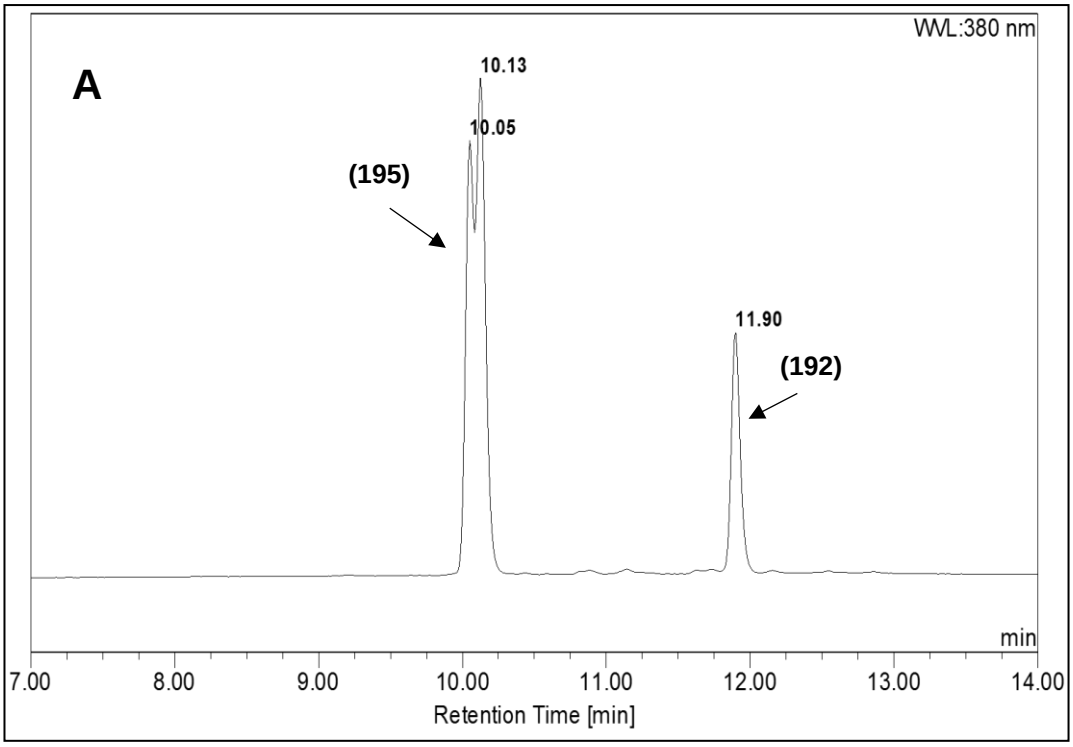
A
WVL:380 nm
10.13
10.05
(195)
11.90
(192)
min
7.00
8.00
9.00
10.00
11.00
12.00
13.00
14.00
Retention Time [min]

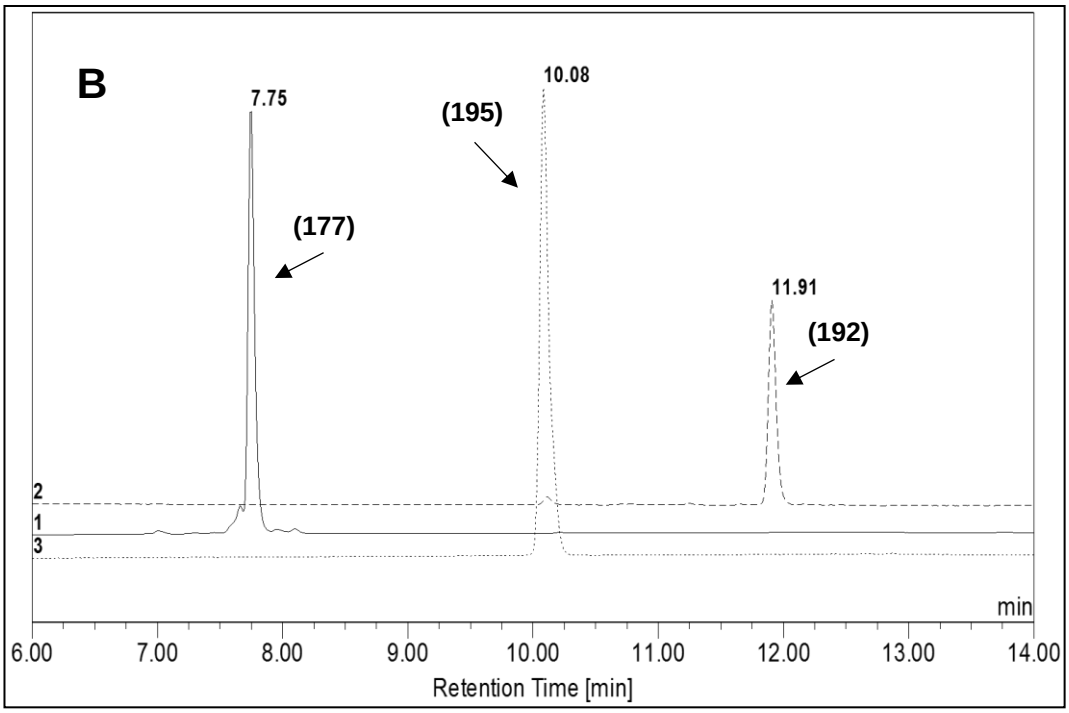
B
7.75
10.08
(195)
(177)
11.91
(192)
2
1
3
min
6.00
7.00
8.00
9.00
10.00
11.00
12.00
13.00
14.00
Retention Time [min]

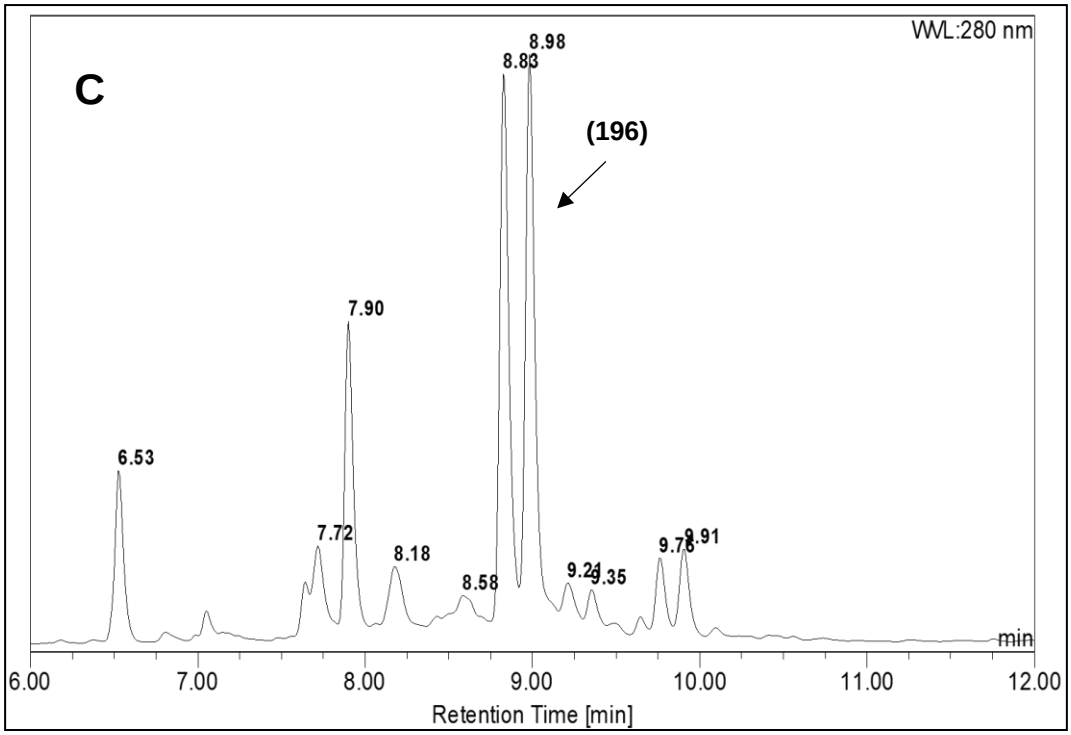
C
WL:280 nm
(196)
8.98
8.83
7.90
6.53
7.72
8.18
8.58
9.21
9.35
9.78
9.91
min
6.00
7.00
8.00
9.00
10.00
11.00
12.00
Retention Time [min]

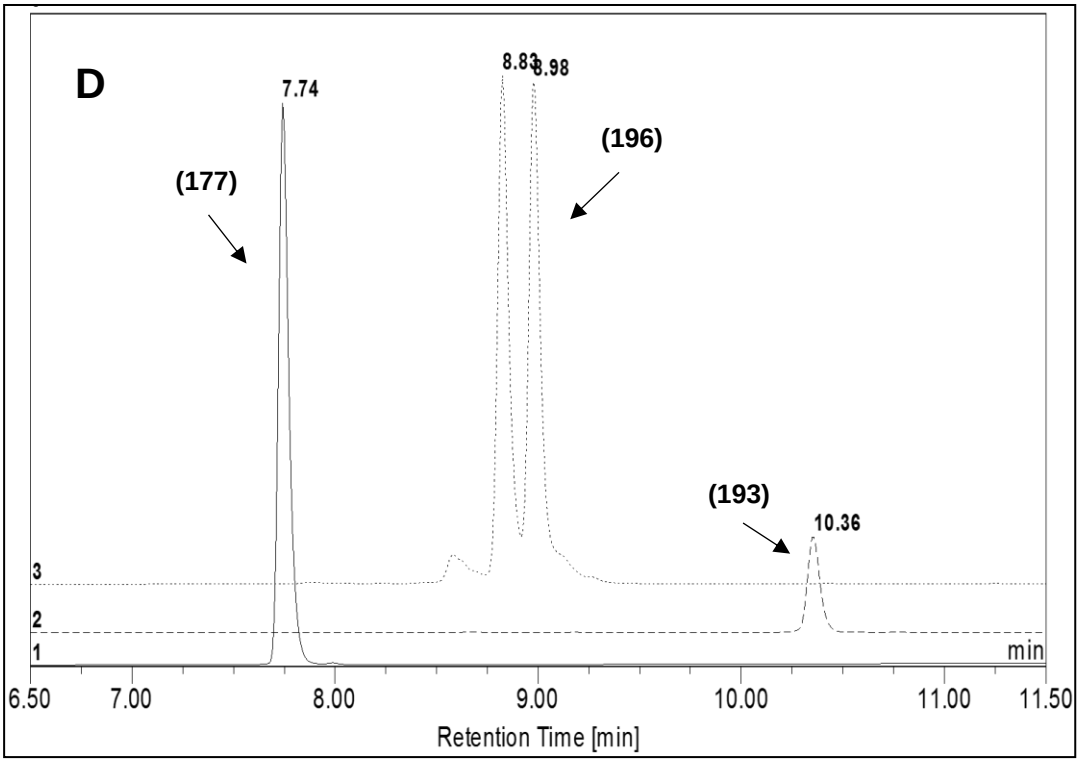
D
7.74
8.83
8.98
(196)
(177)
(193)
10.36
3
2
1
min
6.50
7.00
8.00
9.00
10.00
11.00
11.50
Retention Time [min]

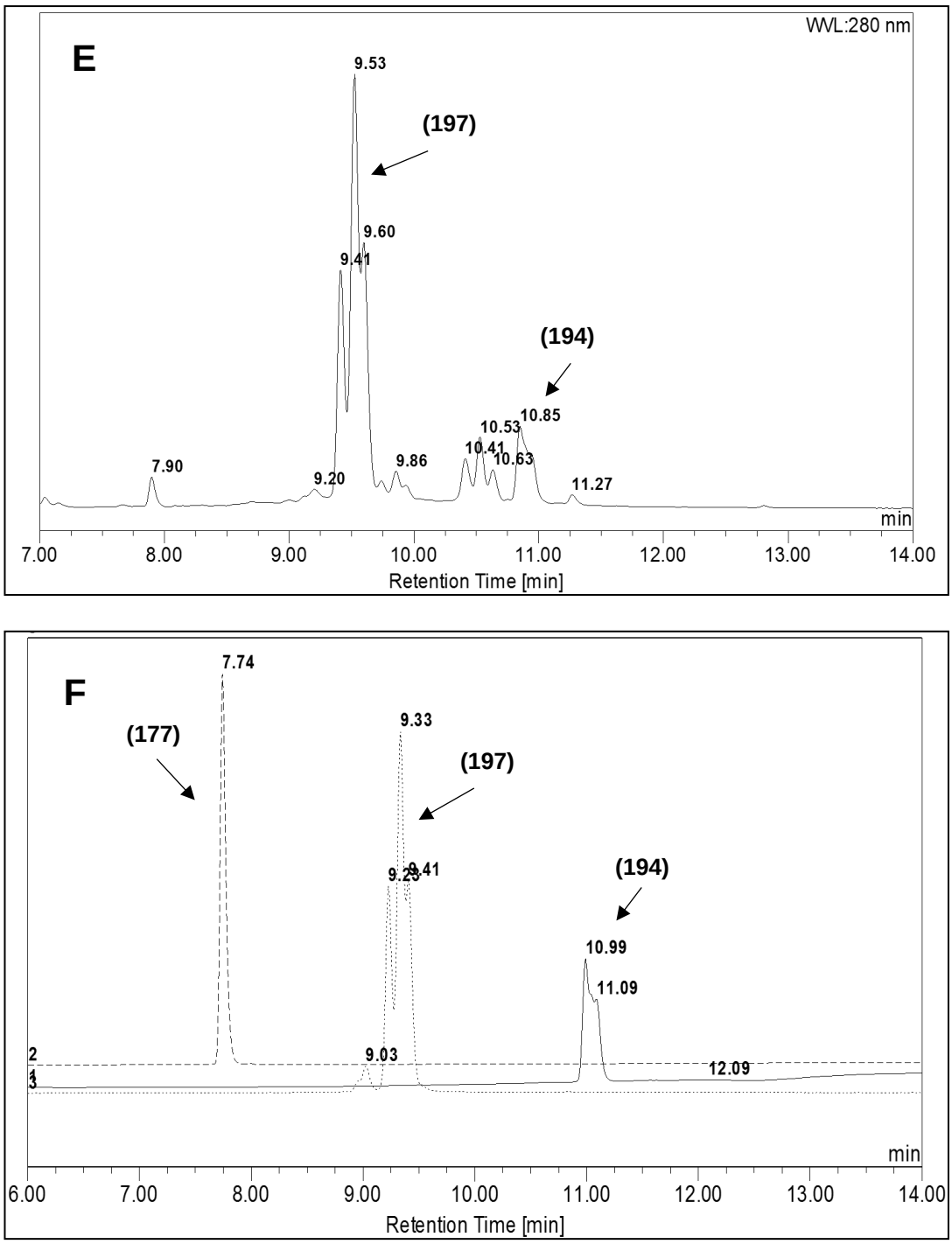

Figure 91. HPLC chromatograms for peptide-photosensitiser conjugates **(195)**-**(197)**.

A. Crude reaction mixture showing **(195)** and **(192)**.

B. Overlay for the final product **(195)** and starting materials **(177)** and **(192)**.

C. Crude reaction mixture showing **(196)**.

D. Overlay for the final product **(196)** and starting materials **(177)** and **(193)**.

E. Crude reaction mixture showing **(197)** and **(194)**.

F. Overlay for the final product **(197)** and starting materials **(177)** and **(194)**.

5.4 Biological evaluation

PART 1: Biological studies involving **(195)** including the cell viability by MTT and cellular uptake studies by fluorescence microscopy were performed in Prof A. J. MacRobert's laboratory by Z. Mazhari and Dr E. Yaghini at University College London, London.

5.4.1 PDT activity and MTT assay for (195)

Two different cell lines were used to assess the phototoxic effects of the synthesized targeted porphyrin **(195)**: MDA-MB-231 (EGFR-overexpressing breast cancer cell line) and MCF-7 (non-EGFR-overexpressing breast cancer cell line). The cells were incubated with a range of concentrations of drug in 96 well plate format for 24 h, before illumination (blue light) from the bottom of the plate at two different time intervals (7 and 10 min). This incubation period is required for internalisation of the porphyrin within the cells before the light treatments are conducted on the plates. The blue light source used for the above experiments has an emission at 420 nm which overlaps with the absorption of the porphyrin Soret band. MTT assays were conducted 48 h after light treatment and the results are shown in Figure 92 (A and B).

From the results (Figure 92 A-B), it can be can deduced that, while similar concentrations and illumination periods were used for both cell lines, significant cytotoxic effects were only observed in MDA-MB-231 cells. Figure 91 A shows that as the concentration and light illumination time increases, the corresponding cytotoxicity also increases in MDA-MB-231 cells. When the MTT was conducted 48 h post light illumination, a concentration and time-dependent cell killing was observed with approximately 32% cell viability in MDA-MB cells as compared to 91% in MCF-7 cells at a similar concentration of 1.4 µM.

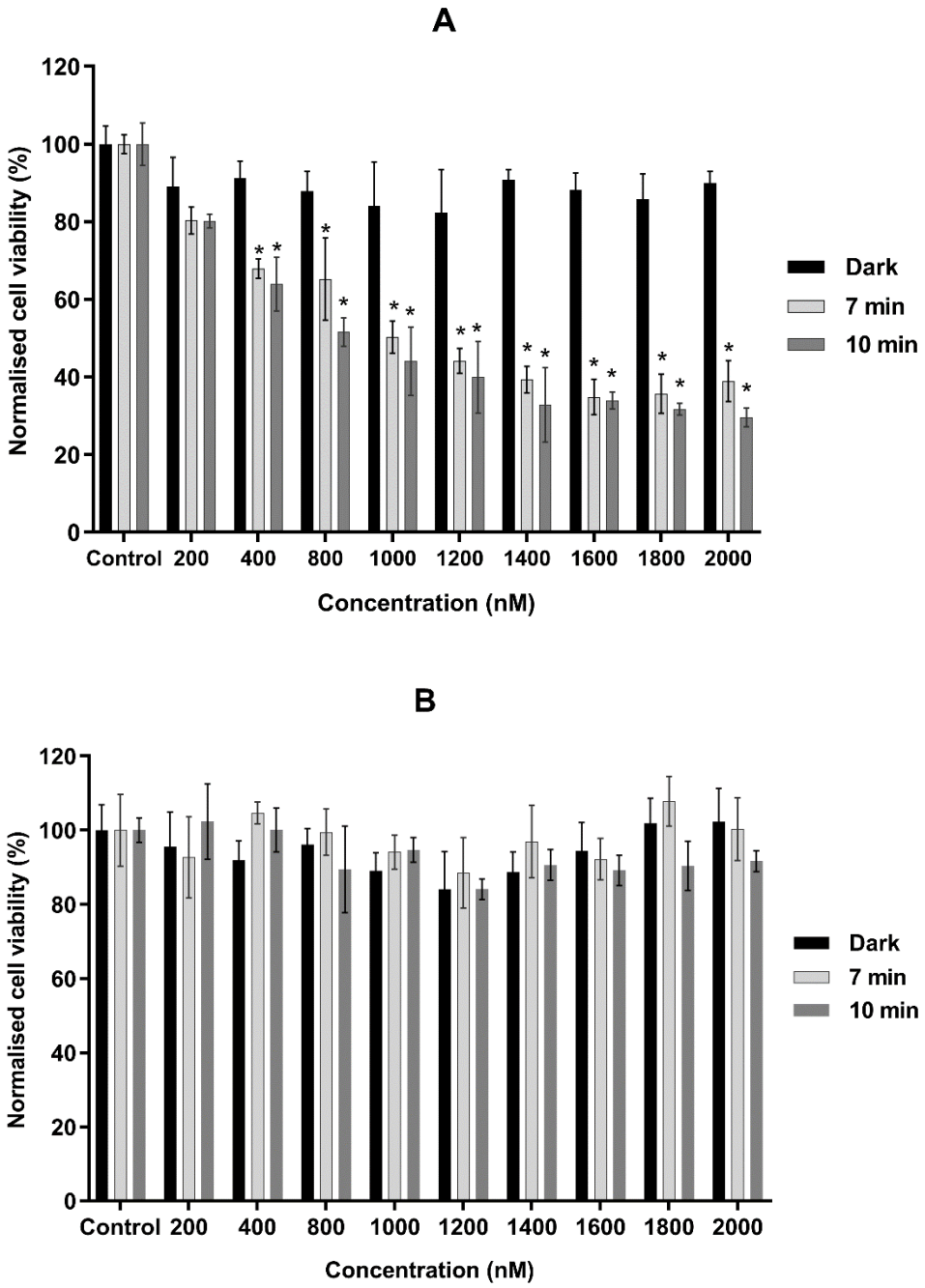

Figure 92 (A-B). Phototoxicity of EGFR-targeted porphyrin **(195)**.

A. MDA-MB-231 cells (EGFR overexpressing cell line) were incubated with various concentrations of **(195)** for 24 h. Cells were illuminated with a blue lamp for 7 or 10 min. MTT analysis was performed 48 h after light illumination.

B. Similar treatments were done for MCF-7 cells (non-EGFR overexpressing cell line).

The control samples were treated identically except that they were either not irradiated but incubated with various concentration of **(195)** (dark) or not treated with **(195)** (control). The results were expressed as mean ± standard deviation (n = 6).

*: $p<0.05$ significantly different from non-irradiated cells (dark).

These results clearly show that the targeted porphyrin derivative **(195)** destroys the cancer cells which are overexpressing the EGFR receptor but, in the case of MCF-7 cells which show lower EGFR expression, a lower PDT effect was seen throughout the range of concentrations. These results are in agreement with the previous work reported on EGFR-targeted PDT with other photosensitisers which has shown higher degrees of selective toxicity towards EGFR-positive cells.[264]

5.4.2 Cellular uptake of porphyrin conjugates

In order to confirm the selective cellular uptake of the targeted porphyrin **(195)**, MDA-MB-231 cells were incubated with 10 μM **(195)** for 24 h and the fluorescence of the samples was detected with an Olympus IMT-2 microscope (Figure 93).

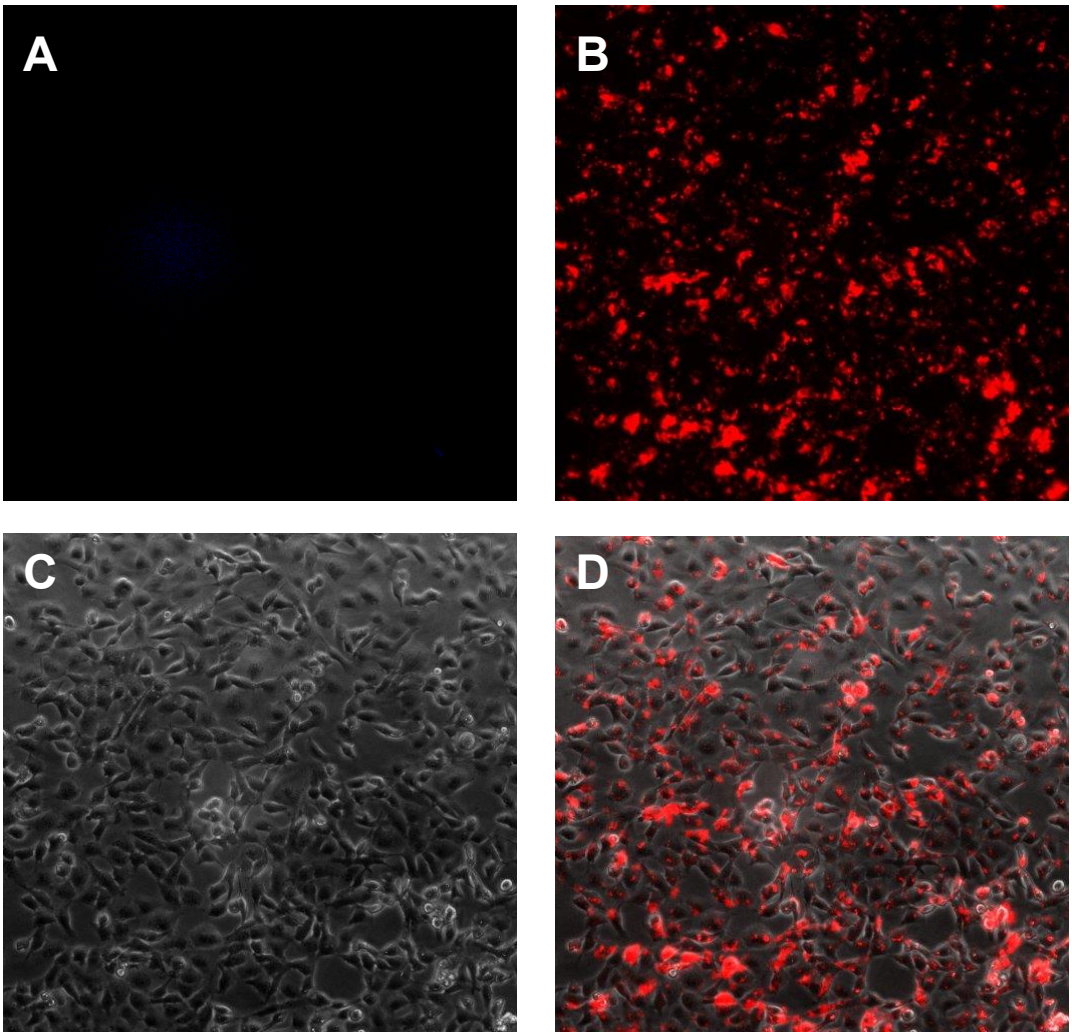

Figure 93. Cellular uptake of EGFR-targeted porphyrin **(195)** A. Control B. Fluorescence image of **(195)** C. Phase contrast D. Merged (B & C).

The results showed that there was a clear uptake of the peptide-porphyrin conjugate **(195)** after 24 h in the cells as compared to the control sample which did not show any fluorescence signal. These findings were therefore consistent with the MTT cell viability results obtained above.

PART 2: Biological studies involving **(196)** and **(197)** were performed at University of Bath.

5.4.3 Preliminary studies

Phototoxic effects of the targeted photosensitisers **(196)** (Ce6 conjugate) and **(197)** (Verteporfin conjugate) were assessed in MDA-MB-231 cells. The cells were incubated with a range of concentrations of **(196)** for 24 h before light illumination for 1.0 min. As in section 5.4.1, this incubation period was required for internalisation of the photosensitisers within the cells before the light treatment was conducted on the plates. Illumination here was from above with a broad-spectrum UVA lamp whose emission overlapped with the Soret bands of **(196)** and **(197)**. MTT assay was conducted 48 h after the light treatment and initial results for **(196)** are shown in Figure 94.

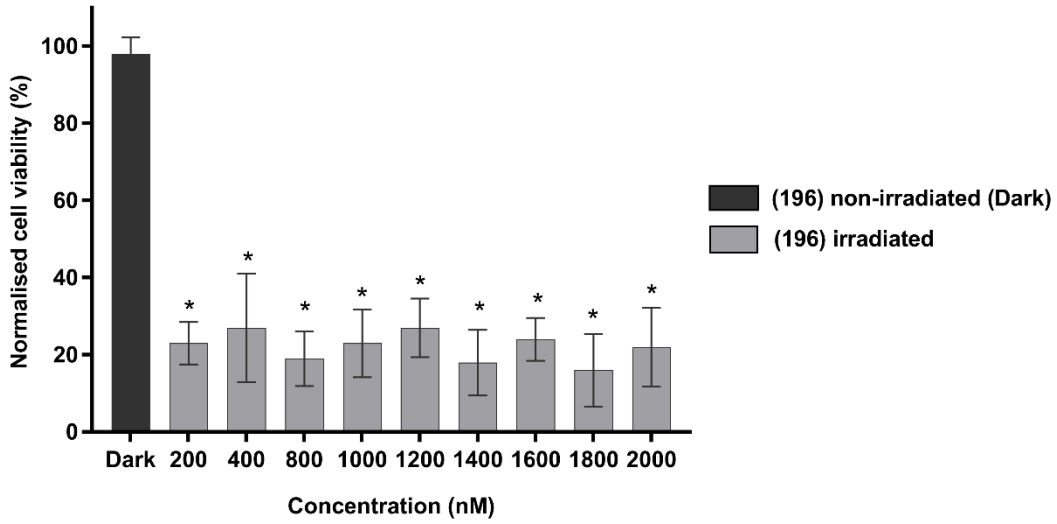

Figure 94. PDT effect of **(196)** on MDA-MB-231 cells at various concentrations.

MDA-MB-231 cells were treated with **(196)** at different concentrations (200-2000 nM) and were incubated for 24 h at 37 °C in the dark. Cells were irradiated with UVA lamp for 1.0 min. MTT analysis was carried out 48 h after light illumination and the results were expressed as mean ± SD (n = 3) and plotted as percentage normalised cell viability.

* : $p<0.05$ significantly different from the control (dark).

These initial results showed that a similar PDT effect was occuring across different concentrations of **(196)** and at the same light dose. This suggested

that leakage of light (cross-talk) was occurring between different wells containing cells incubated with different concentrations of **(196)**. Different types of 96 well plates were therefore investigated with the aim of reducing this possible cross talk effect.

Three types of 96 well plates were chosen for this study: clear, black wall with clear base, and complete black plate. Cells were grown in each of these plates followed by incubation of **(196)** with the cells at three different concentrations (200, 1000 and 2000 nM). The plates were then illuminated with light at different time intervals (0.5, 1.0, 1.5 and 2.0 min) and MTT assays were performed 48 h after the light illumination. The results are summarised in Figure 95 (A-C).

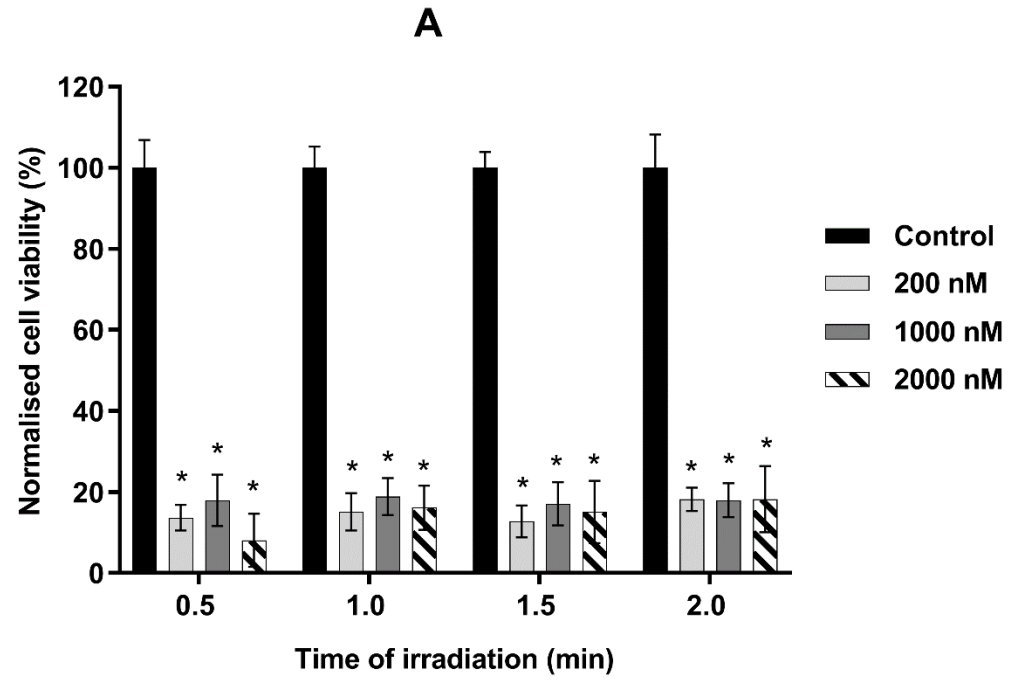
A
Normalised cell viability (%)
120
100
80
60
40
20
0
0.5
1.0
1.5
2.0
Time of irradiation (min)
Control
200 nM
1000 nM
2000 nM

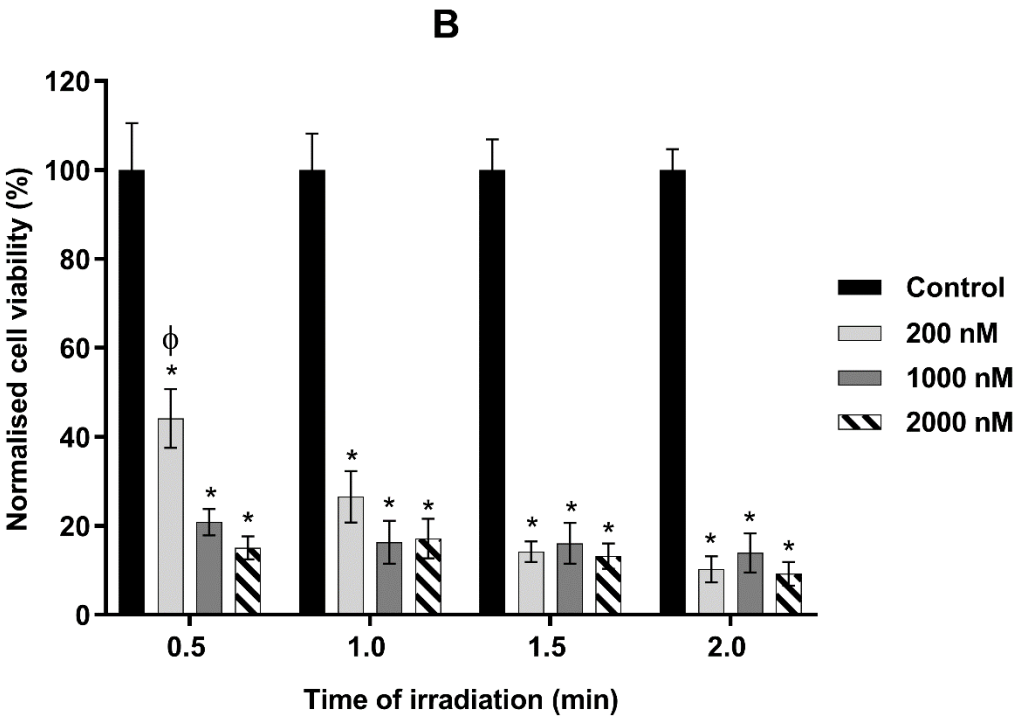
B
Normalised cell viability (%)
120
100
80
60
40
20
0
0.5
1.0
1.5
2.0
Time of irradiation (min)
Control
200 nM
1000 nM
2000 nM

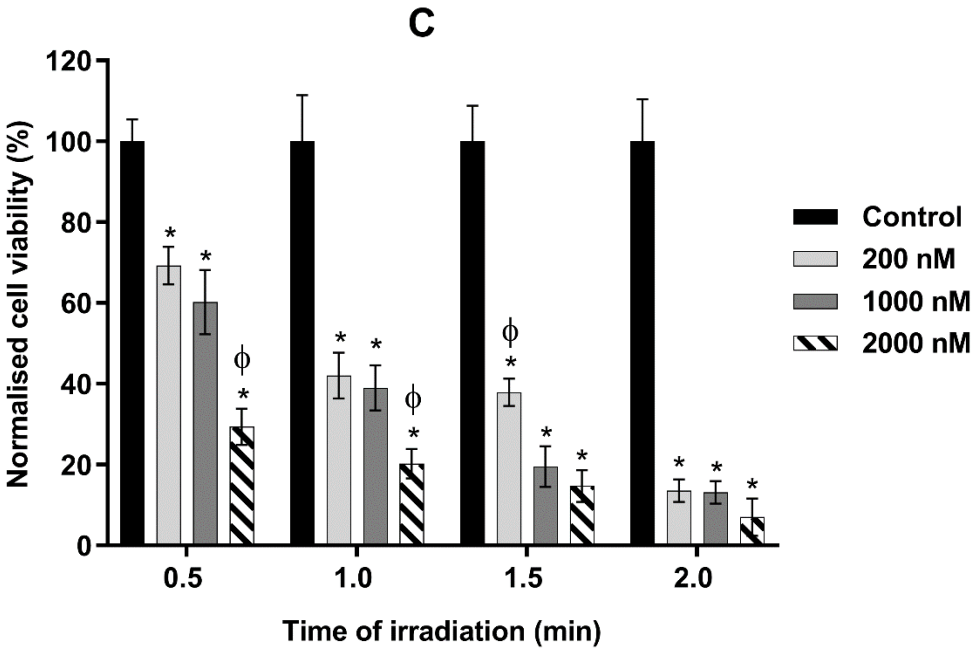

Figure 95 (A-C). The PDT effect of EGFR-targeted photosensitiser **(196)** on MDA-MB-231 cells in different types of 96 well plates.

A: MDA-MB-231 cells were treated with different doses of EGFR-targeted photosensitiser **(196)** in a **clear 96 well plate** and were incubated for 24 h at 37 °C in the dark. Cells were illuminated with UVA lamp for 0.5, 1.0 and 1.5 min and MTT analysis was carried out 48 h after light illumination. The results were expressed as mean ± SD (n = 3) and plotted as percentage normalised cell viability.

B: Same treatment was followed as for **A.** above in a **96 well plate with black walls and clear base**.

C: Same treatment was followed as for **A.** above in a **completely black 96 well plate**.

* : $p<0.05$ significantly different from the control.

Φ: $p<0.05$ significantly different EGFR-targeted porphyrin **(196)** illuminated with UVA light for 0.5 1.0 or 1.5 min.

The results above demonstrate the effect of the properties of different types of 96 well plates on the cell viability when illuminated from above. In the case of clear plates, a similar cell death was seen across the three concentrations chosen, indicating cross talk between wells as observed above. However, in the case of black plates and plates having black walls with a clear base, concentration and time-dependent cell death was observed, indicating effective blocking of cross talk between different wells. The data also suggested the completely black plates to be the optimum choice for further

studies. This is because in the case of plates having a black wall with clear base, the normalised cell viabilities were consistently lower than the ones observed in completely black plates. This again suggests some possible cross talk between the wells from the clear bottom side. Another important observation made from the above study was the choice of different time intervals for light illumination. It was noted that light intervals of 0.5, 1.0 and 1.5 min produced concentration and light dependent cell death. Exposure of cells for 2.0 min caused significant cytotoxicity irrespective of the concentration, and so this condition was omitted from further studies.

5.4.4 PDT activity and MTT assay for (196) and (197)

PDT studies for **(196)** (LARLLT-Ce6) and **(197)** (LARLLT-verteporfin) were carried out on MDA-MB-231 cells using the optimized conditions from above (Section 5.4.3). It had previously been observed that the peptide-porphyrin conjugate **(196)** showed enhanced cell killing in EGFR-overexpressing cells (MDA-MB-231) as compared to MCF-7 cells (breast cancer cell line which does not overexpress EGFR). MDA-MB-231 cells were incubated with a range of concentrations of drug for 18 h before light illumination (UVA lamp) at different time intervals (0.5, 1.0 and 1.5 min). MTT assay was conducted 48 h after light treatment and the results are shown in Figure 96 (A and B).

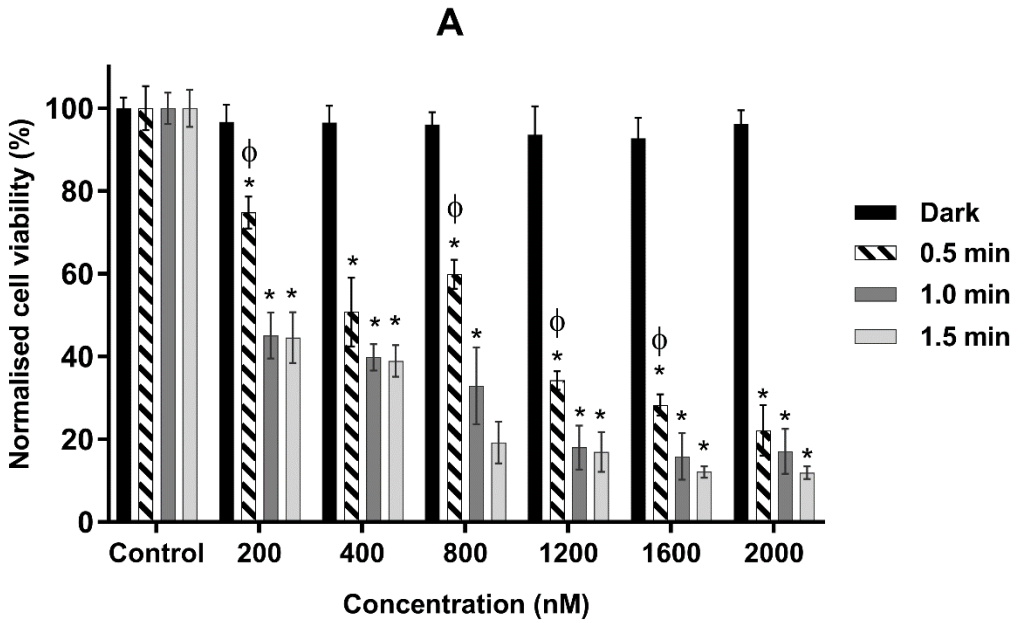

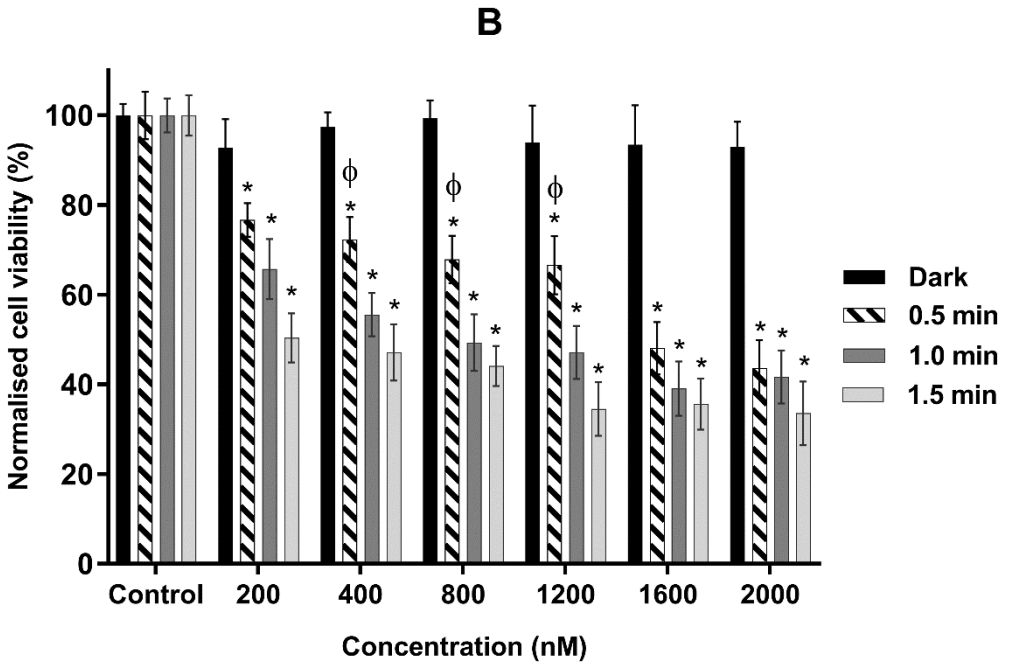

Figure 96 (A-B). The PDT effect of EGFR-targeted photosensitisers **(196)** and **(197)** on MDA-MB-231 cells.

A: MDA-MB-231 cells were treated with different doses of EGFR-targeted photosensitiser **(196)** in a **completely black 96 well plate** and were incubated for 24 h at 37 °C in the dark. Cells were illuminated with a UVA lamp for 0.5, 1.0 and 1.5 min and MTT analysis was carried out 48 h after light illumination. The results were expressed as mean ± SD (n = 4) and plotted as percentage normalised cell viability.

B: Same treatment was followed as for **A.** above with EGFR-targeted photosensitiser **(197)**.

* : $p<0.05$ significantly different from the dark conditions.

Φ: $p<0.05$ significantly different from EGFR-targeted photosensitiser **(196)** or **(197)** illuminated with UVA light for 0.5, 1.0 or 1.5 min.

The same concentration and illumination periods were used for both the compounds **(196)** (LARLLT-Ce6) and **(197)** (LARLLT-verteporfin). MTT results for cells treated with **(196)** showed concentration and time-dependent cell killing across all the concentrations (Figure 96 A). A 33% cell viability was observed at 800 nM and irradiation for 1.0 min, while only 17% cell viability was observed at 2000 nM for the same light exposure. The results also showed that control cells (without drug treatment) and dark conditions (cells treated with **(196)** but without light illumination) did not show any reduction in cell viability, indicating no cytotoxicity of the peptide-photosensitiser conjugate in

the absence of light.

MTT assay on cells treated with **(197)** (Verteporfin conjugate) also showed time-dependent cell killing across all concentrations (Figure 96 B). A 50% cell viability was observed at a concentration of 800 nM and irradiation for 1.0 min, whereas approximately 42% cell viability was observed at a concentration of 2000 nM for the same light exposure.

Comparison of the data obtained for both the conjugates **(196)** and **(197)** showed enhanced cell killing for the chlorin e6-peptide conjugate as compared to verteporfin-peptide conjugate at a given dose of light and drug concentration. For example, a 16% cell viability was observed for **(196)** at a concentration of 1600 nM and 1.0 min light exposure as compared to 39% cell viability observed for **(197)** at the sames dose of light and drug.

Overall, the results are consistent with the findings obtained with **(195)** (LARLLT-TPP). **(196)** and **(197)** both show concentration and time-dependent phototoxicity consistent with enhanced uptake in the EGFR-overexpressing cell line. Although a few anti-EGFR immunoconjugates with chlorin e6 have been described,[291, 292] these appear to be the first examples of the targeting of these photosensitisers with a short EGFR-selective peptide.

5.5 Summary

New EGFR-targeted photosensitisers based on 5-(4-aminophenyl)-10,15,20-triphenylporphyrin **(190)**, chlorin e6 derivative **(191)** and verteporfin **(13)** were synthesized via SPAAC with an unprotected targeting azido-peptide **(177)**. The syntheses were straightforward and the expected products **(195)**-**(197)** were obtained in good yields.

Biological studies involving conjugate **(195)** were done at University College London and showed selective phototoxicity in the EGFR-overexpressing cell line MDA-MB-231, compared to MCF-7 (non-EGFR-overexpressing cell line).

Biological studies involving targeted conjugates **(196)** and **(197)** were done at University of Bath and showed effective PDT activity for Ce6 conjugate **(196)** and verteporfin conjugate **(197)** in MDA-MB-231 cells.

CHAPTER 6: RESULTS AND DISCUSSION (CPP-porphyrin and CPP-ALA conjugates)

6.1 Introduction to cell penetrating peptides

Cell-penetrating peptides (CPPs) in general are short sequences, typically 8-30 amino acids, that are able to cross cell membranes and also deliver a range of bioactive cargo either covalently or non-covalently attached, which otherwise would be poorly internalised.[293, 294] Some of the main characteristics of CPPs are low toxicity, ability to carry cargo of varying size, and their ability to cross the membranes of various cell types. They thus having a great potential for targeted drug delivery.[295-297] Some of the most commonly studied CPPs are summarised in Table 5.

Table 5. Sequences of common CPP[293, 294]

Peptide	Sequence	Origin
Tat (48-60)	GRKKRRQRRRPPQ	Protein-derived
Penetratin	RQIKIWFQNRRMKWKK	Protein-derived
pVEC	LLIILRRRIRKQAHAHSK	Protein-derived
Pep-1	KETWWETWWTEWSQPKKKRKV	Chimeric
MAP	KLALKLALKALKAALKLA	Synthetic
Transportan	GWTLNSAGYLLGKINLKALAALAKKIL	Chimeric
VP22	NAKTRRHERRRKLAIER	Protein-derived
Oligoarginine	R_n (n = 6-12)	Designed

6.2 Applications of CPPs in photodynamic therapy

CPPs have been intensely explored as biocompatible carriers and found to have great potential for targeted drug delivery.[293, 294] In recent years, there have been several investigations into the conjugation of CPP with various photosensitisers to improve their pharmacokinetic properties, solubility and tissue-specificity for both PDT of cancer[298-301] and anti-microbial

applications[302, 303]. Some of the reported CPP-porphyrin conjugates that have been synthesized and evaluated are shown in Figure 97. Sibrian-Vazquez *et al.* (2006) reported the synthesis and *in vitro* evaluation of porphyrin-peptide conjugates bearing the nuclear-localizing sequence SV40 or a fusogenic peptide (HIV-1 Tat 40-60 or octaarginine) connected to the photosensitiser by a low molecular weight poly(ethylene glycol) spacer (Figure 97).[298] Conjugates **(198a-c)** were based on a hydrophobic porphyrin, whereas **(198d-e)** were based on carboxylic acid-functionalized porphyrin. *In vitro* studies in human HEp2 cell line revealed enhanced cellular uptake for conjugates bearing the fusogenic peptide sequences **(198b)**, **(198c)** and **(198e)** in comparison to **(198a)** and **(198d)** bearing the nuclear-localizing sequence, SV40. However, the subcellular localization of these conjugates was dependent on the nature of substituents on the porphyrin. The hydrophobic porphyrin conjugates **(198a-c)** localized preferentially in the endoplasmic reticulum whereas carboxylic acid functionalized porphyrin **(198d)** and **(198e)** localized in the lysosomes. Dixon *et al.* (2007) reported the conjugation of ALA with a penetratin analogue **(71)** and biological studies confirmed the effective uptake of the conjugate by PAM212 cells and successful conversion to the PpIX.[189] Bourrè *et al.* (2010) reported the photoinactivation properties of a HIV-1Tat peptide-porphyrin conjugate **(199)** against gram-positive and gram-negative bacterial strains.[302] Wang *et al.* (2012) also reported further photophysical and photobiological studies on the same peptide. It was found that the conjugation of the hydrophobic tetraphenyl porphyrin unit to the C-terminus of the cationic Tat peptide gave a water soluble bioconjugate.[304] Cellular uptake studies were carried out in HN5 human head and neck squamous cell carcinoma and the conjugate **(199)** was found to localise in endo/lysosomal membranes, a property which is useful for photochemical internalisation.

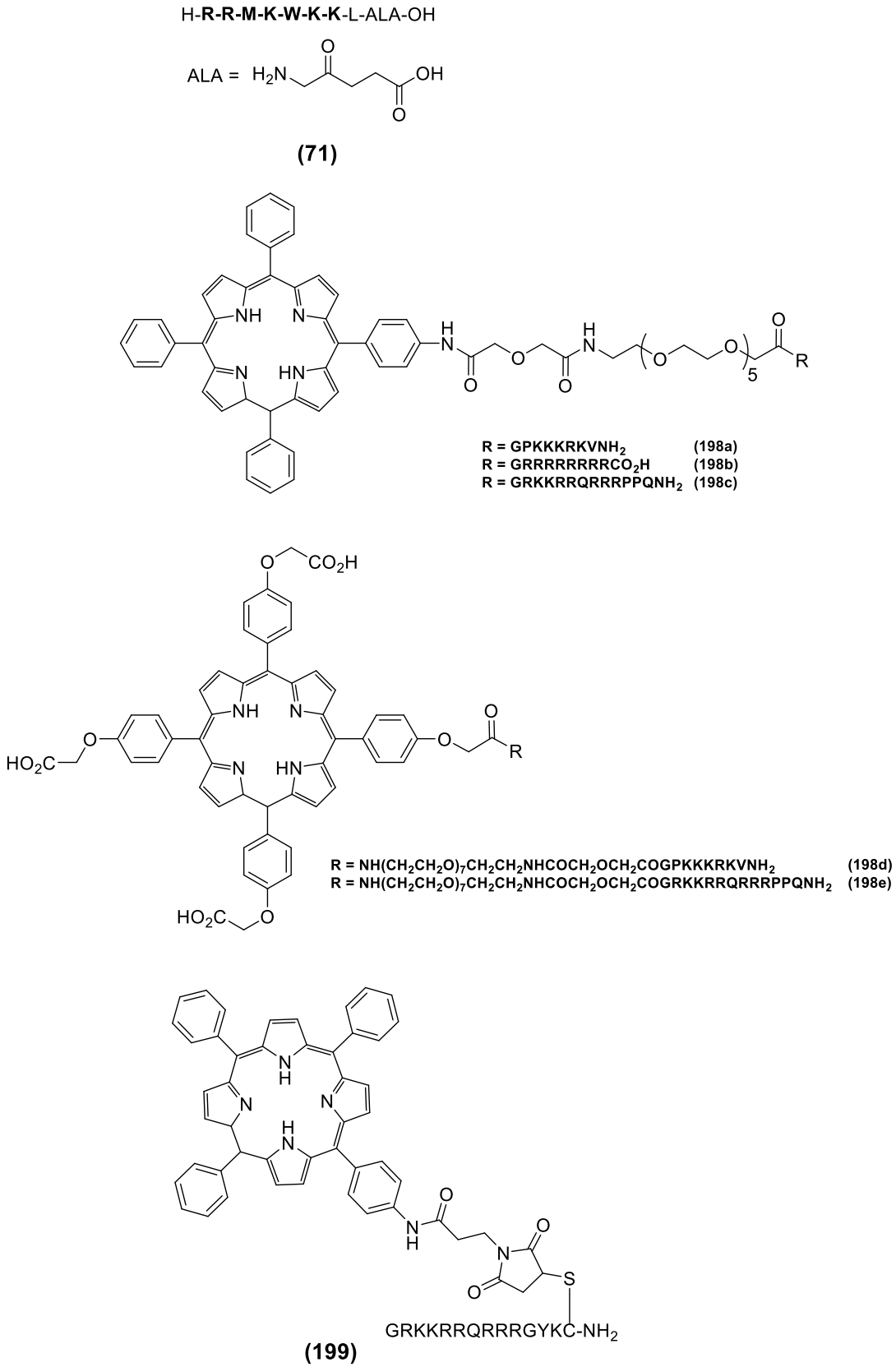

Figure 97. Structure of some reported CPP-porphyrin conjugates.

The main aim of this chapter was to build upon the chemistry developed in chapter 3 to attach ALA dendrons to selected cell-penetrating peptides via copper-catalyzed azide-alkyne cycloaddition (Scheme 59).

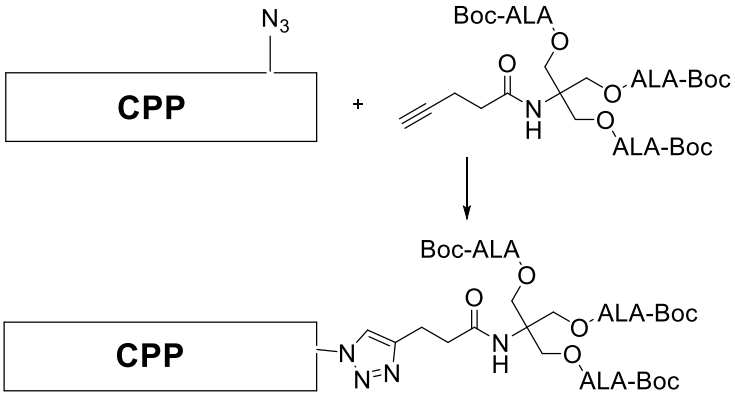

Scheme 59. Proposed route of synthesis for CPP-ALA conjugates.

Four cell-penetrating peptide sequences were chosen **(200)**-**(203)** and modified to include an amino acid side chain suitable for CuAAC. Peptide **(200)** is a C-terminal heptapeptide (RRMKWKK) derived from the third helix of the *Antennapedia* transcription factor,[293, 305] wherein the peptide was extended at the C-terminus by glycine and the amino acid lysine next to the C-terminal glycine was replaced by azidolysine (Scheme 60).

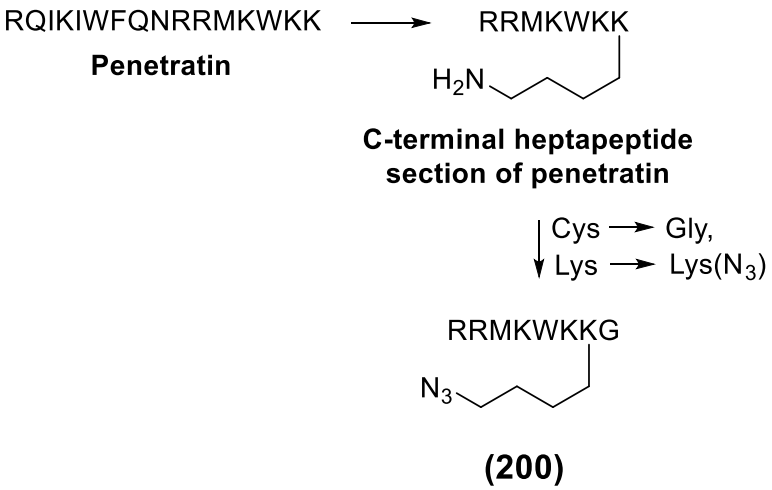

Scheme 60. Design of ligatable cell penetrating peptide **(200)** derived from penetratin.

Peptide **(201)** is derived from a HIV-1 Tat (48–57) analogue, wherein the peptide was extended at the C-terminus by the tetrapeptide amide GYKC-NH_2.[304] Here, the amino acid lysine from the C-terminal extension

(GYKC) was replaced by azidolysine for ligation with effector units (ALA dendron) *via* CuAAC, and cysteine was replaced by glycine to facilitate loading of the Rink amide resin (Scheme 61).

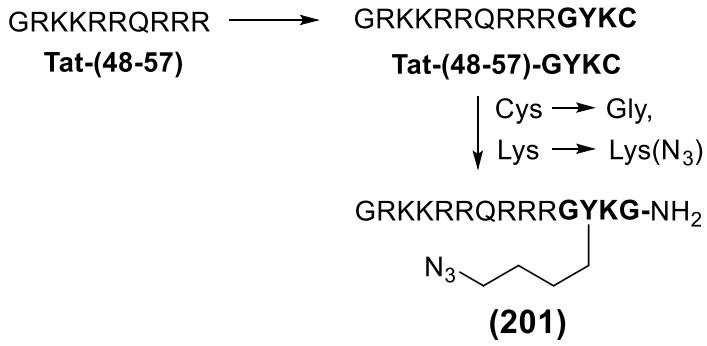

Scheme 61. Design of ligatable cell penetrating peptide Tat-(48-57)-GYKG, **(201)**.

Peptide **(202)** is an extension of cell penetrating peptide **(201)** at the N-terminus by LGASWHRPDKG, which is derived from residues 1-21 of the N-terminus of human herpes virus 8-encoded protein, vMIP-II (**LGASWHRPDKC**CLGYQKRPLP). This peptide has previously displayed a significant binding affinity for the chemokine coreceptor CXCR4.[306] The CXCR4 receptor is overexpressed in many forms of cancer (prostate, breast, cervical, brain, ovarian etc), so peptide **(202)**, would be expected to provide enhanced delivery to tumour cells compared to Tat peptide **(201)** (Scheme 62)

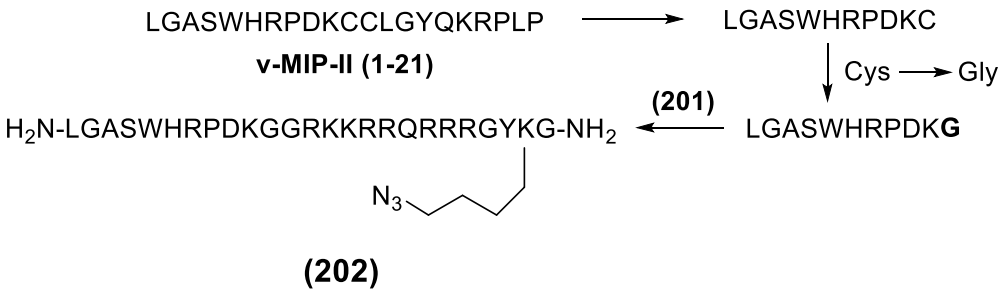

Scheme 62. Design of ligatable cell penetrating peptide **(202)**.

Finally, pVEC **(203)** is a CPP derived from murine vascular endothelial-cadherin protein and for the current work, the C-terminal lysine was again replaced by azidolysine (Scheme 63).[307]

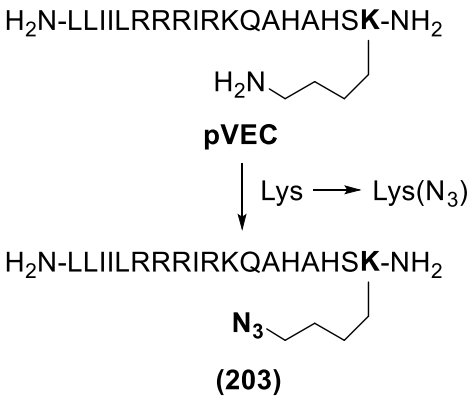

Scheme 63. Design of ligatable cell penetrating peptide **(203)** (pVEC-N_3)

6.2 Synthesis of CPPs

An azidolysine derivative suitable for Fmoc SPPS was prepared according to the method of Chapman *et al.* (2010), using the Stick diazo transfer reagent (imidazole-1-sulfonyl azide hydrochloride) (Scheme 64).[308] The final product **(205)** was obtained as a solid in good yield, and the structure was confirmed by IR which showed the disappearance of amino group peaks and the presence of the expected band at 2100 cm^{-1} due to the azido function.

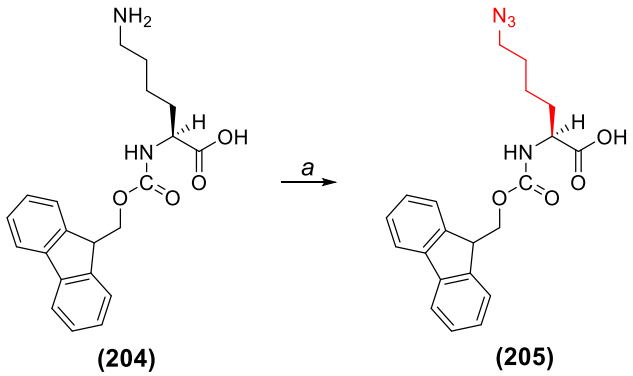

Scheme 64. Synthesis of azidolysine **(205)** using imidazole-1-sulfonyl azide hydrochloride. *Reagents and conditions: a.* Imidazole-1-sulfonyl azide hydrochloride, $NaHCO_3$, $CuSO_4.5H_2O$, H_2O, 16 h, RT, **68%**.

Peptides **(200)**-**(203)** were synthesised by Fmoc peptide synthesis on Rink amide MBHA resin, using PyBOP activation. Scheme 65 shows the preparation of the C-terminally ligatable azido-cell penetrating peptide **(200)**. The first step of the synthesis was to remove the Fmoc protection from the Rink amide MBHA resin using piperidine in DMF (1:4, v/v) which was confirmed by a positive Kaiser test. This was followed by attachment of the first

amino acid, Fmoc-Gly-OH using DIC/DIEA pre-activation (Scheme 65). Capping of the resin was performed using acetylation (Ac_2O/DIEA/DMF, 1:1:8 v/v/v) to block any unreacted amino groups on the resin. The peptide chain was then assembled using PyBOP/DIEA activation followed by cleavage from the resin including side-chain deprotection with TFA/TIS/H_2O (95:2.5:2.5 v/v/v). This gave the final azido-containing CPP **(200)** in 65% yield. The peptide was analysed by analytical HPLC (Figure 98) and the identity was confirmed by mass spectrometry.

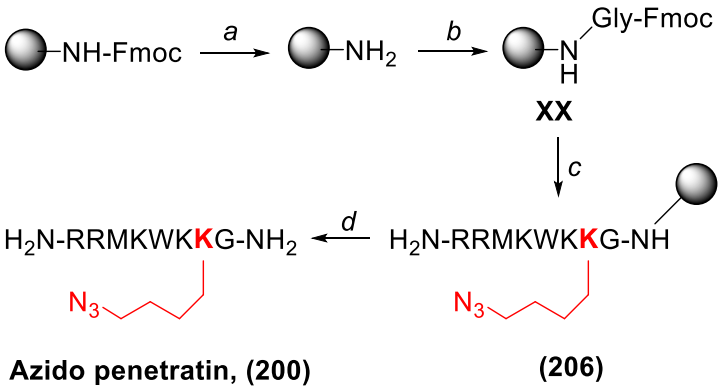

Scheme 65. Preparation of azido penetratin **(200)**. *Reagents and conditions: a.* Piperidine/DMF (1:4, v/v), 20 min; *b.* Fmoc-Gly-OH, DIC, DIEA, DMF, RT, 30 min; *c.* Fmoc SPPS, PyBOP, DIEA, DMF, 60 °C; *d.* TFA/TIS/H_2O (95:2.5:2.5 v/v/v), 3 h, RT, **65%**.

The remaining peptides **(201)**-**(203)** were synthesized on a similar scale as **(200)** and cleavage of a sample of the resin in each case gave the peptides **(201)**-**(203)** in good yields of 45-65% and reasonable purity (Scheme 66).

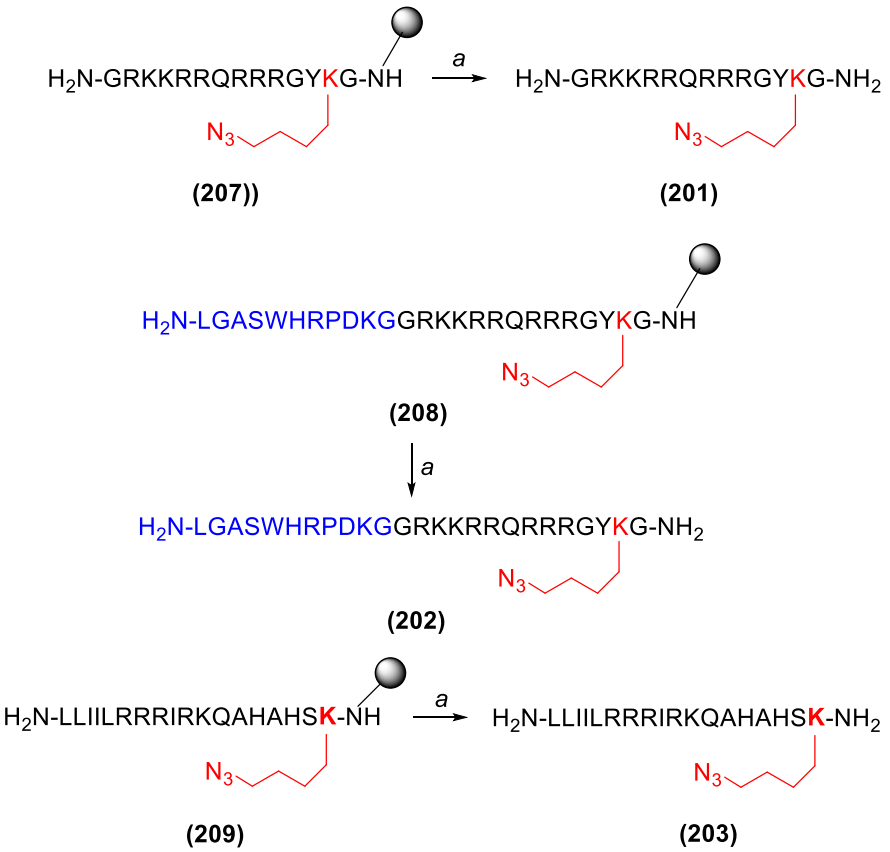

Scheme 66. Preparation of azido CPPs **(201)-(203)**. *Reagents and conditions: a.* TFA/TIS/H_2O (95/2/5/2/5,v/v/v), 3 h, RT, **67% (201), 47% (202), 59% (203).**

Figure 98 A-D shows the chromatograms of the crude peptides **(200)-(203)**.

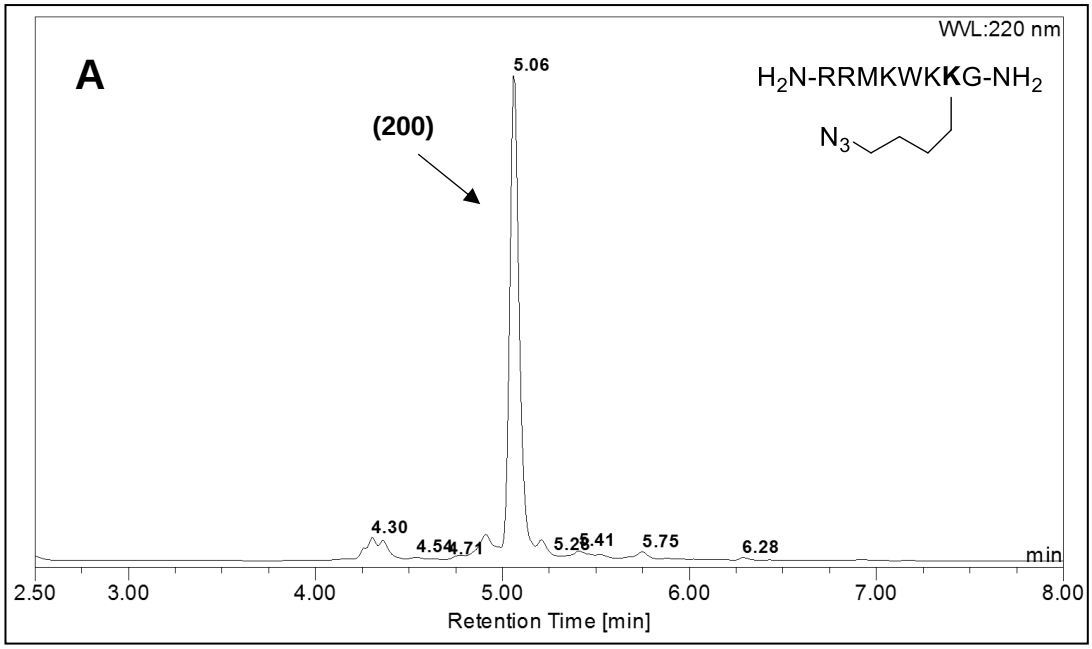
A
WVL:220 nm
5.06
(200)
H2N-RRMKWKKG-NH2
N3
4.30
4.54
4.71
5.28
5.41
5.75
6.28
min
2.50
3.00
4.00
5.00
6.00
7.00
8.00
Retention Time [min]

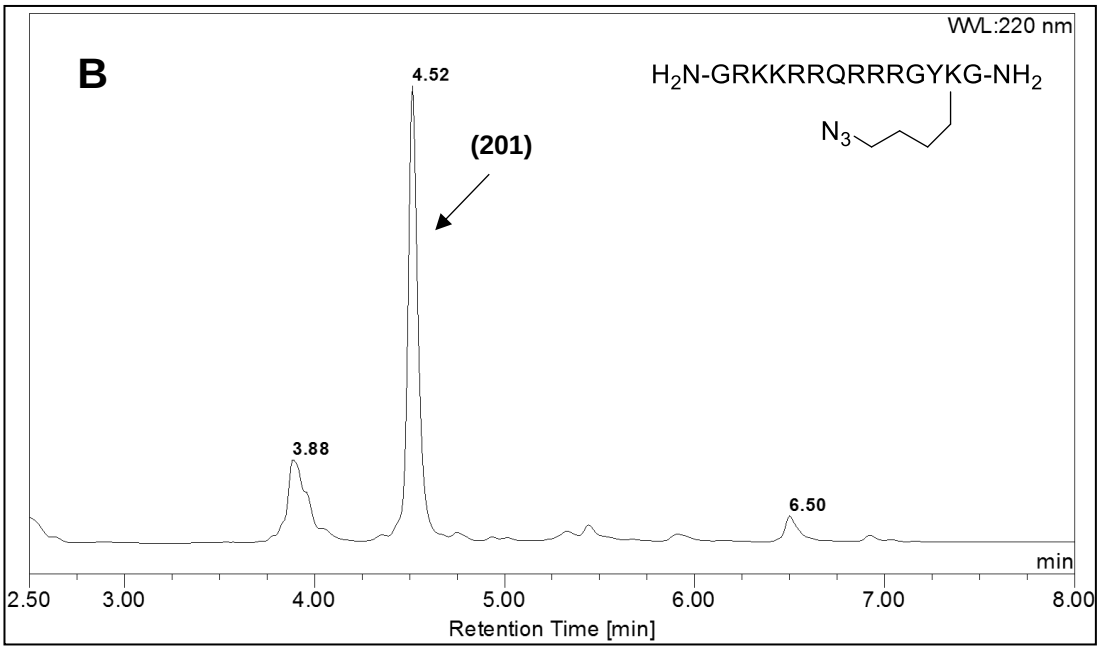
B
WVL:220 nm
4.52
(201)
H2N-GRKKRRQRRRGYKG-NH2
N3
3.88
6.50
min
2.50
3.00
4.00
5.00
6.00
7.00
8.00
Retention Time [min]

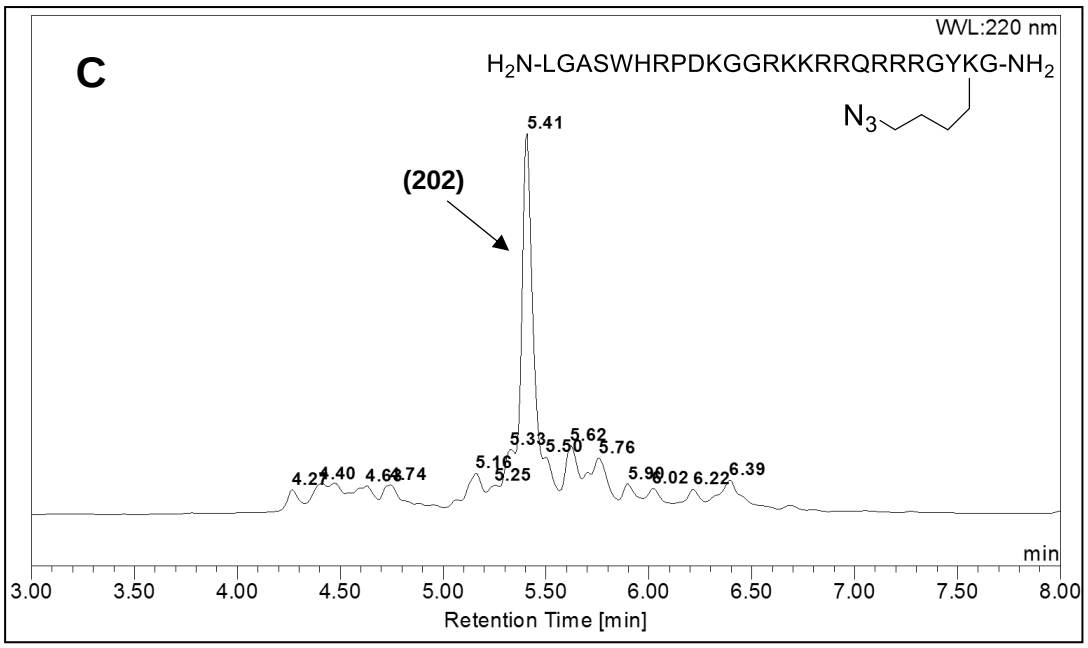

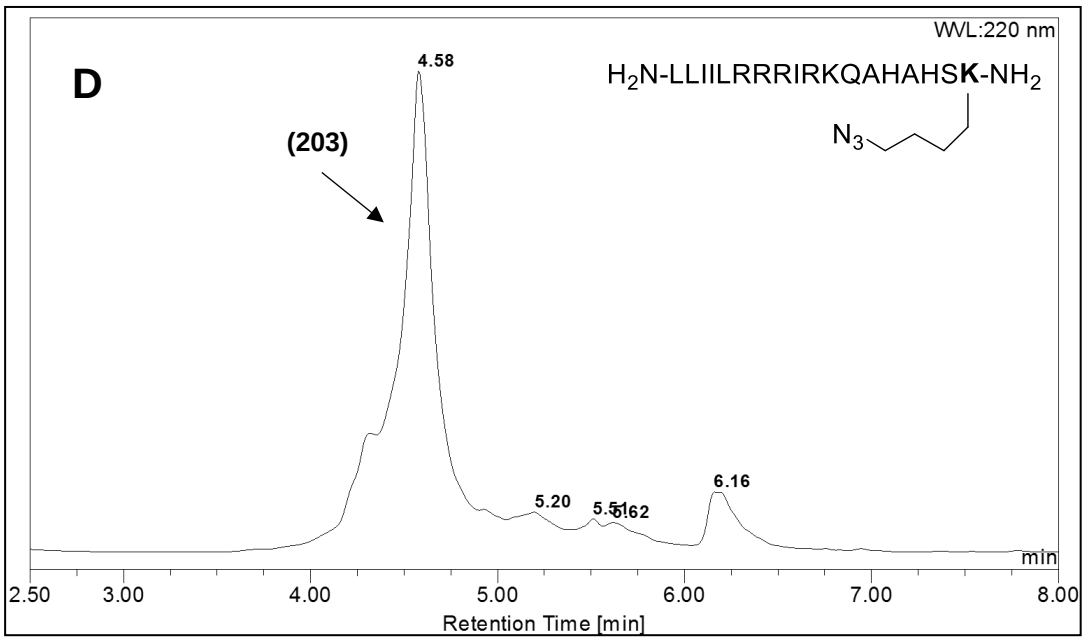

Figure 98. HPLC chromatograms for the crude isolated azido CPPs **(200)-(203)**.

A. (200), penetratin derived CPP.

B. (201), Tat-(48-57) derived CPP.

C. (202), v-MIP-II derived CPP.

D. (203), pVEC derived CPP.

6.3 Synthesis of CPP-ALA derivatives

Having verified the successful synthesis of the cell-penetrating peptides **(200)**-**(203)**, the next step involved the conjugation of ALA dendrons to the CPPs on resin via CuAAC.

The resin-bound azido CPP **(206)** was reacted with the ALA dendron **(206)** by CuAAC using copper(I) trifluoromethanesulfonate benzene complex (Scheme 67). The reaction was carried out for 5 days on-resin, followed by cleavage from the resin and side chain deprotection using TFA/TIS/H_2O (95:2.5:2.5 v/v/v). Analysis of the crude product by HPLC showed the absence of **(200)** at 5.06 min and formation of a new species at 4.36 min. The product was purified by semi-preparative HPLC to give the final CPP-ALA conjugate **(210)** in 43% yield, whose identity was confirmed by mass spectrometry.

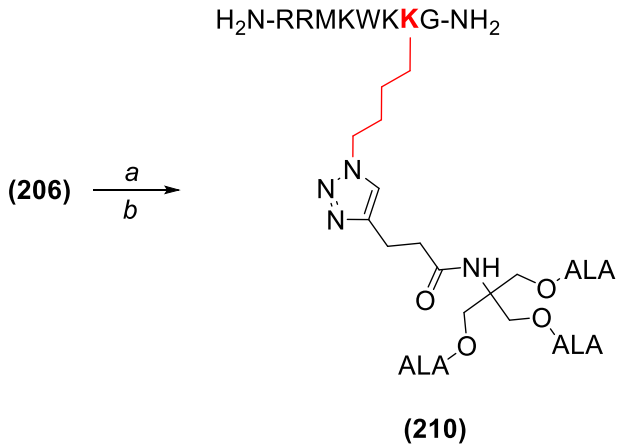

(210)

Scheme 67. Synthesis of CPP-ALA conjugate **(210)** based on penetratin. *Reagents and conditions: a.* **(105)**, copper (I) trifluoromethanesulfonate benzene complex, DMSO, RT, 5 d; *b.* TFA/TIS/H_2O (95/2/5/2/5,v/v/v), 3 h, RT, **43%**.

The other resin-bound azido CPPs (**207)** and **(208)** were subjected to CuAAC with alkyne **(105)** under the same conditions as for **(210)** (Figure 99). The conjugation with ALA effector units proceeded efficiently to give the respective CPP-ALA derivatives in 31-46% yield. pVEC peptide on resin **(209)** was conjugated with the alkyne **(105)** and **(107)** under the same conditions, giving the expected products **(213)** and **(214)** in 31% and 39% yield respectively (Figure 99). The yields of the pVEC-ALA conjugates **(213)** and **(214)** were slightly lower than the other CPP-ALA conjugates synthesised earlier

(210)-**(212)**. This could be due to the postion of azidolysine which is attached directly to the resin therefore making it slightly less accessible to the alkyne unit for CuAAC in comparision to other CPP-ALA conjugates **(210)**-**(212)** where the azidolysine residue is separated from the resin by a glycine residue. In the case of pVEC-ALA conjugate **(213)**, the reaction was also carried out for 3 days. However, cleavage from the resin showed the presence of azido-CPP **(203)** in addition to final CPP-ALA conjugate **(213)** on HPLC indicating incomplete coupling. An attempt was also made to conjugate azido-CPP **(203)** to alkyne **(105)** in solution, however monitoring the reaction by HPLC showed no change in the chromatogram. This could be possibly due to folding of the peptide on deprotection and hence making the azido function inaccessible for the effector units, although further studies are required to verify this issue. Figure 100 shows the HPLC chromatograms of the crude isolated CPP-ALA conjugates **(210)**-**(214)**. In all cases, the desired conjugate is present as the major component upon cleavage from the resin following 120 h reaction.

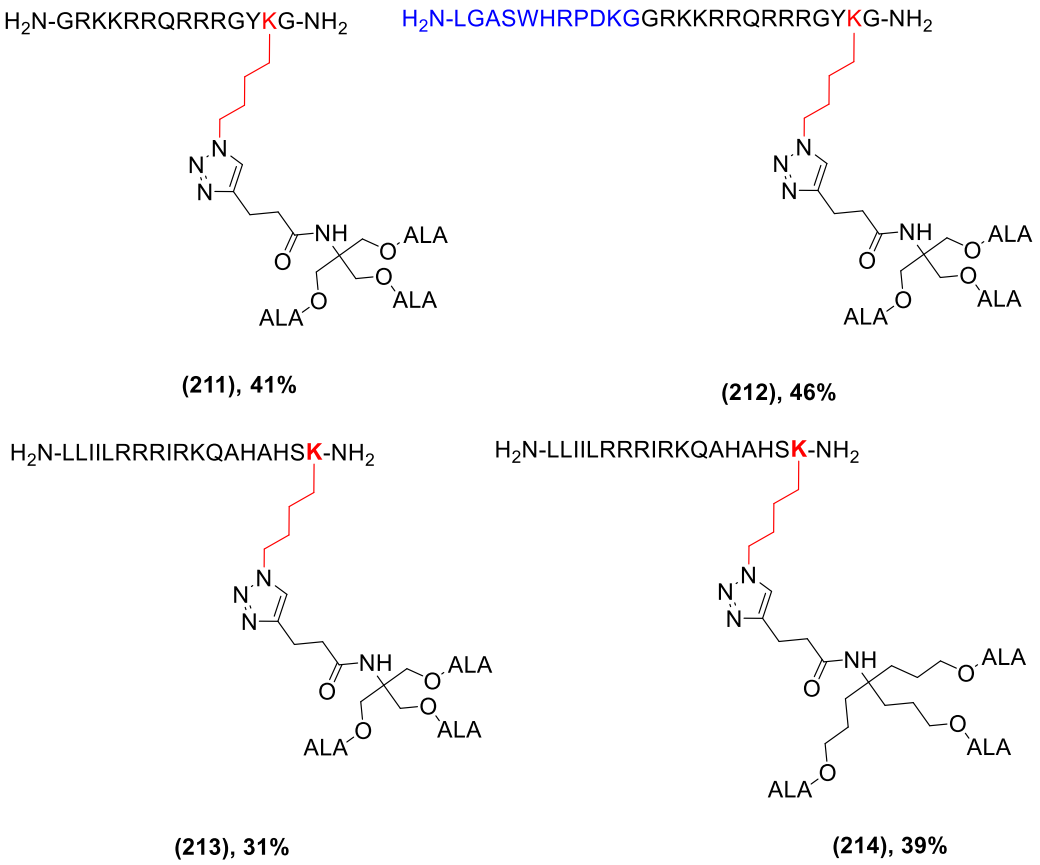

Figure 99. Chemical structures for CPP-ALA conjugates **(211)**-**(214)** and isolated yields after HPLC purification.

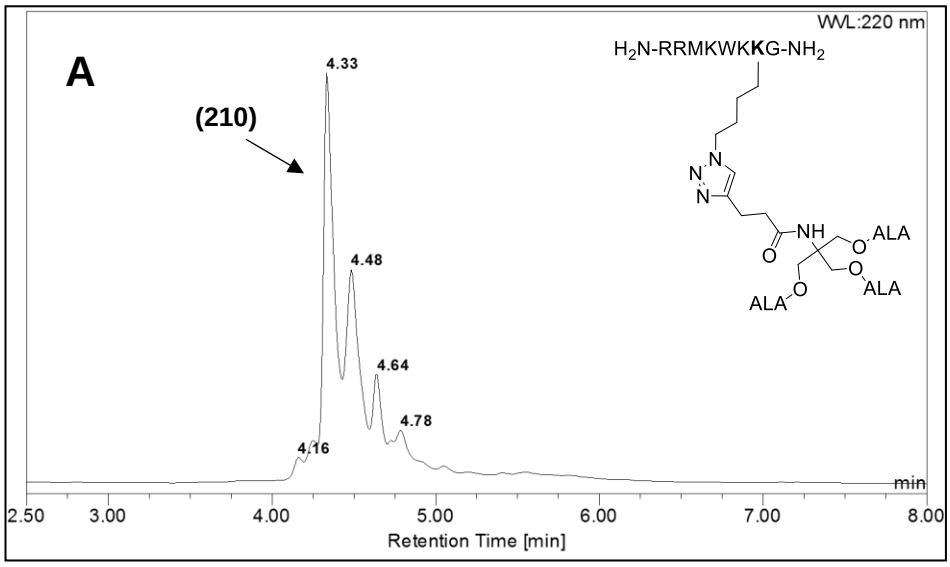
A
WVL:220 nm
H2N-RRMKWKKG-NH2
(210)
4.33
4.48
4.64
4.78
4.16
NH
O
ALA
ALA
ALA
min
2.50
3.00
4.00
5.00
6.00
7.00
8.00
Retention Time [min]

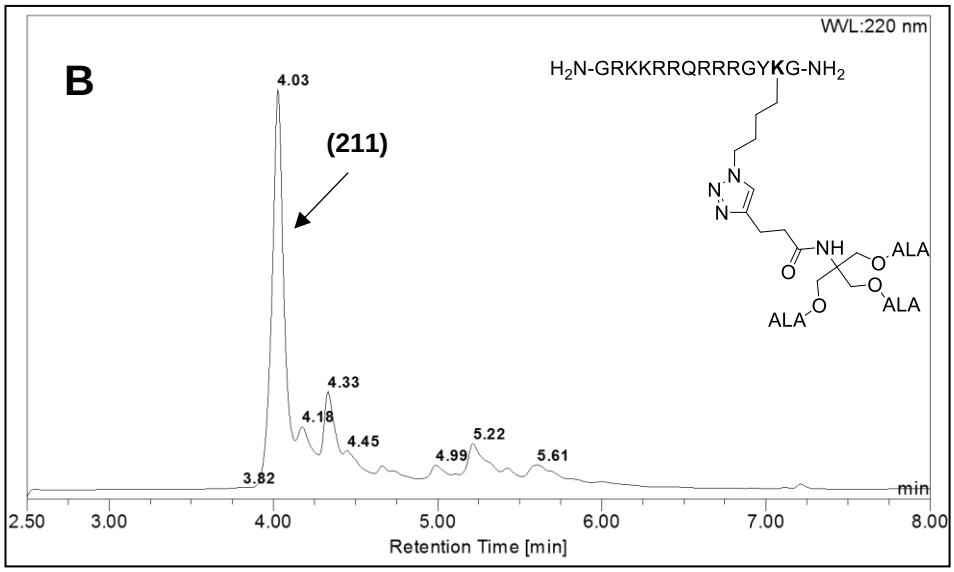
B
WVL:220 nm
H2N-GRKKRRQRRRGYKG-NH2
(211)
4.03
4.33
4.18
4.45
5.22
4.99
5.61
3.82
NH
O
ALA
ALA
ALA
min
2.50
3.00
4.00
5.00
6.00
7.00
8.00
Retention Time [min]

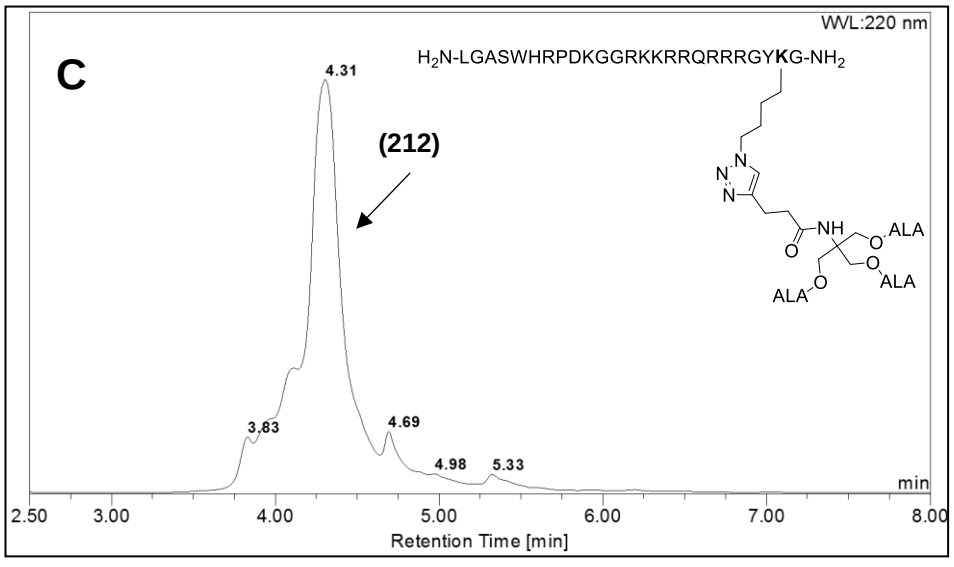
C
WVL:220 nm
H2N-LGASWHRPDKGGRKKRRQRRRGYKG-NH2
(212)
4.31
3.83
4.69
4.98
5.33
NH
O
ALA
ALA
ALA
min
2.50
3.00
4.00
5.00
6.00
7.00
8.00
Retention Time [min]

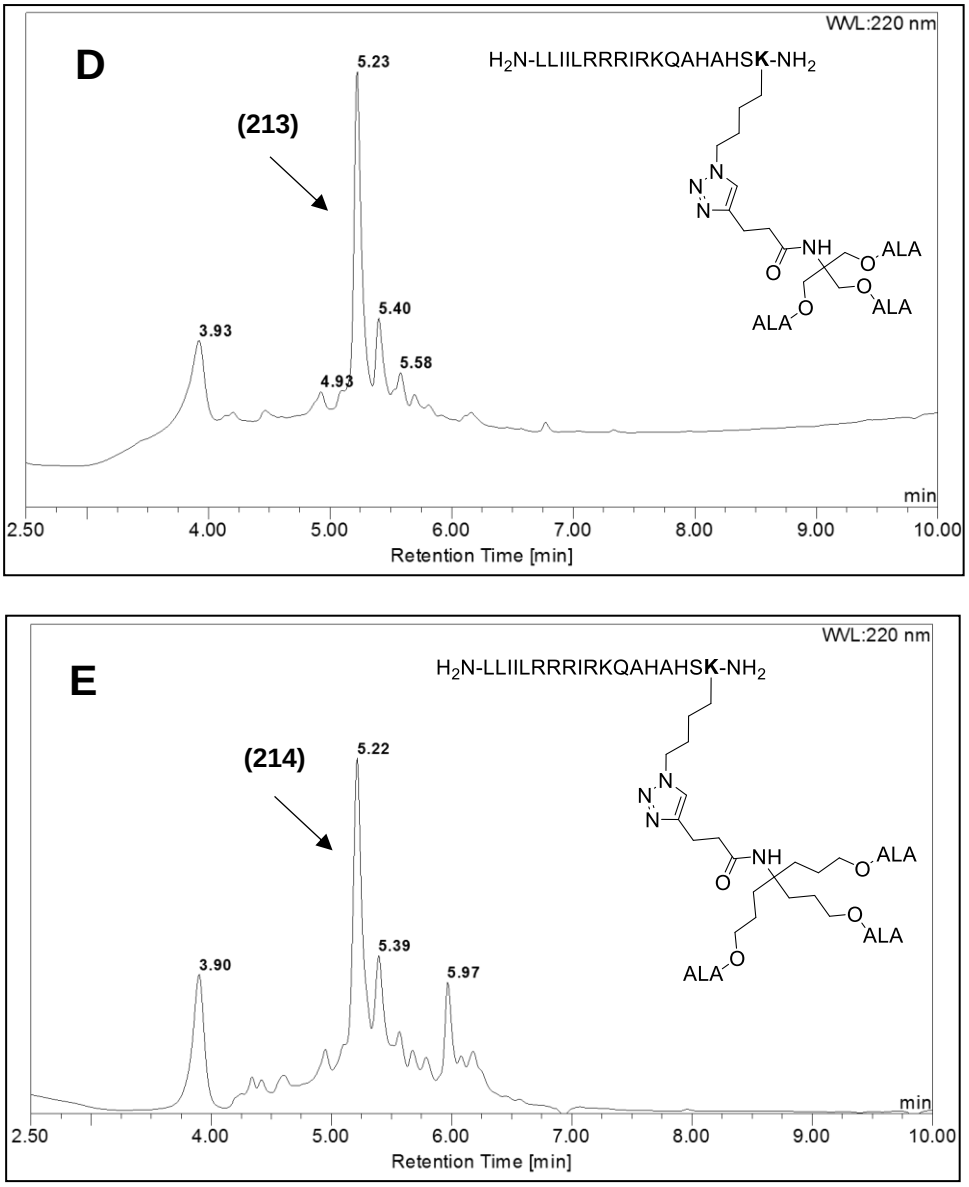

Figure 100. HPLC chromatograms for crude CPP-ALA derivatives **(210)**-**(214)**.

A. (210), penetratin derived CPP-ALA conjugate.

B. (211), Tat-(48-57) derived CPP-ALA conjugate.

C. (212), v-MIP-II derived CPP-ALA conjugate.

D. (213), pVEC derived CPP-ALA conjugate.

E. (214), pVEC derived CPP-ALA conjugate.

6.4 Synthesis of CPP-porphyrin derivative

The functionalised cell-penetrating peptide **(203)** synthesised previously was also conjugated in solution with a two-fold excess of dibenzocyclooctyne derivative of 5-(4-Aminophenyl)-10,15,20-triphenylporphyrin **(192)** via strain promoted azide-alkyne cycloaddition (Scheme 68). The reaction was carried out in DMSO at room temperature and monitored by analytical HPLC (Figure 101). Unlike the previously attempted CuAAC reaction, the reaction proceeded smoothly to give the expected product **(215)** in 69% yield as an inseparable mixture of triazole regioisomers. The final conjugate was purified by semi-preparative HPLC and confirmed by analytical HPLC and mass spectrometry.

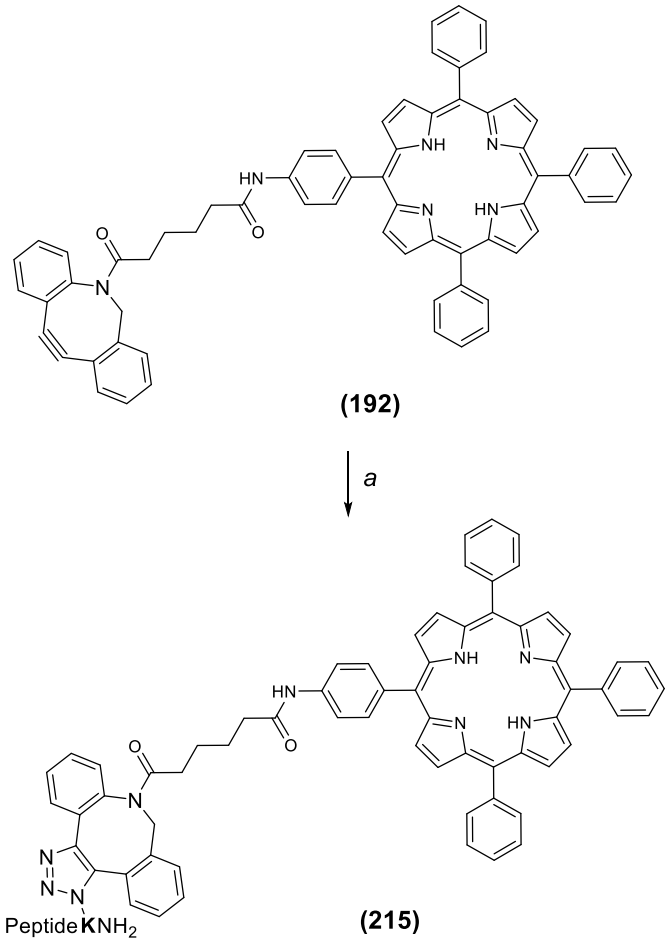

Peptide = LLIILRRRIRKQAHAHS-

Scheme 68. Synthesis of cell-penetrating peptide-porphyrin conjugate **(215)** via SPAAC. *Reagents and conditions a.* **(203)**, DMSO, RT, overnight, **69%**.

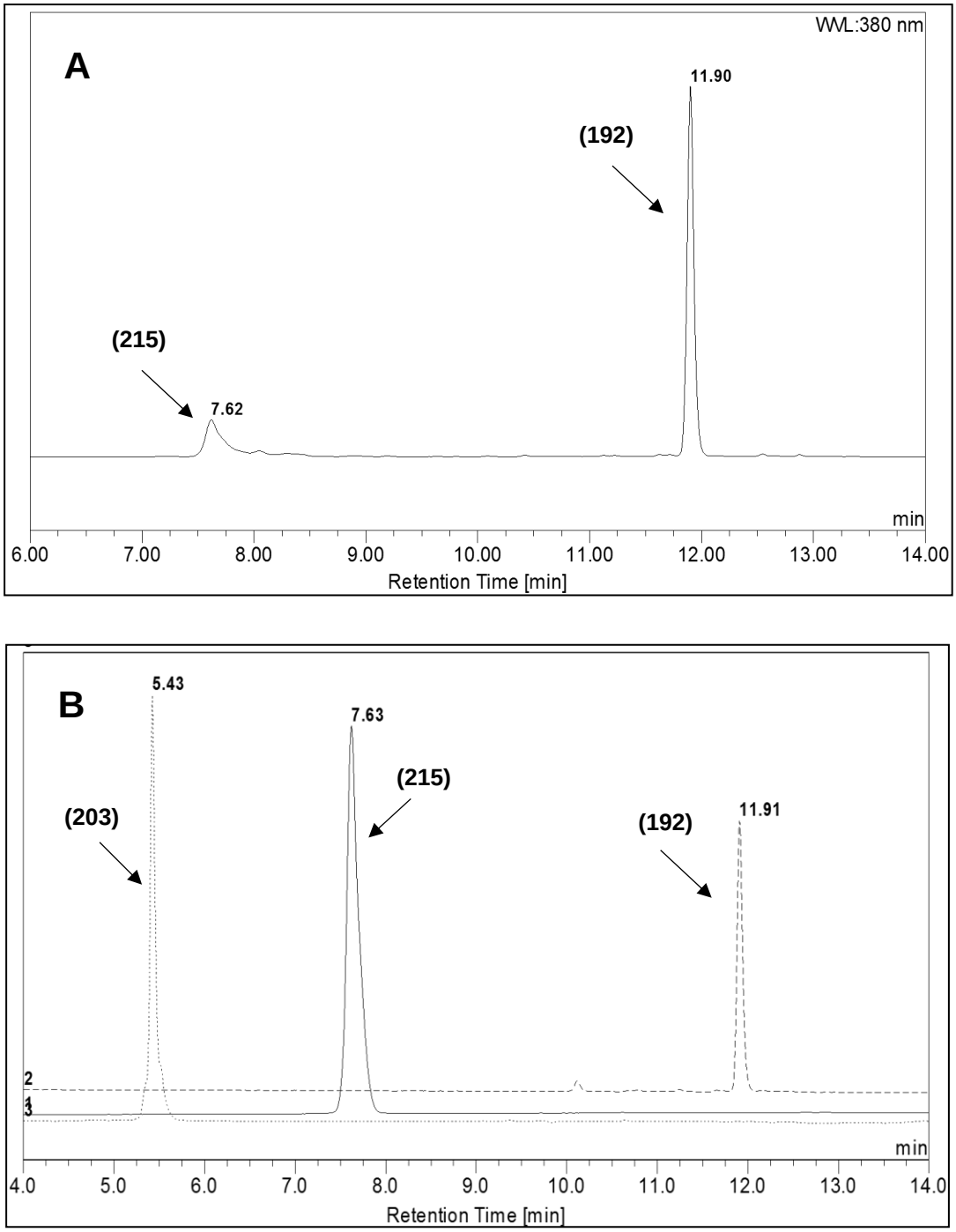

Figure 101. HPLC chromatograms for the CPP-porphyrin conjugate **(215)**.

A. Crude reaction mixture showing **(215)** and excess unchanged starting material **(192)**.

B. Overlay showing CPP-porphyrin conjugate **(215)** and starting materials (**192)** and **(203)**.

6.5 Biological evaluation

Biological studies involving **(215)** including the cell viability by MTT were carried out in Prof A. J. MacRobert's laboratory by Z. Mazhari and Dr E. Yaghini at UCL, London.

6.5.1 PDT activity and MTT assay

The phototoxicity of the CPP-porphyrin conjugate **(215)** was assessed on both MDA-MB-231 and MCF-7 breast cancer cell lines as for **(195)** (EGFR-targeted porphyrin) by incubating **(215)** at various concentrations for 24 h followed by illumination with a blue lamp at three time intervals (3, 5 and 7 min). MTT assay was carried out 48 h after light illumination and the results are summarised in Figure 102 (A and B).

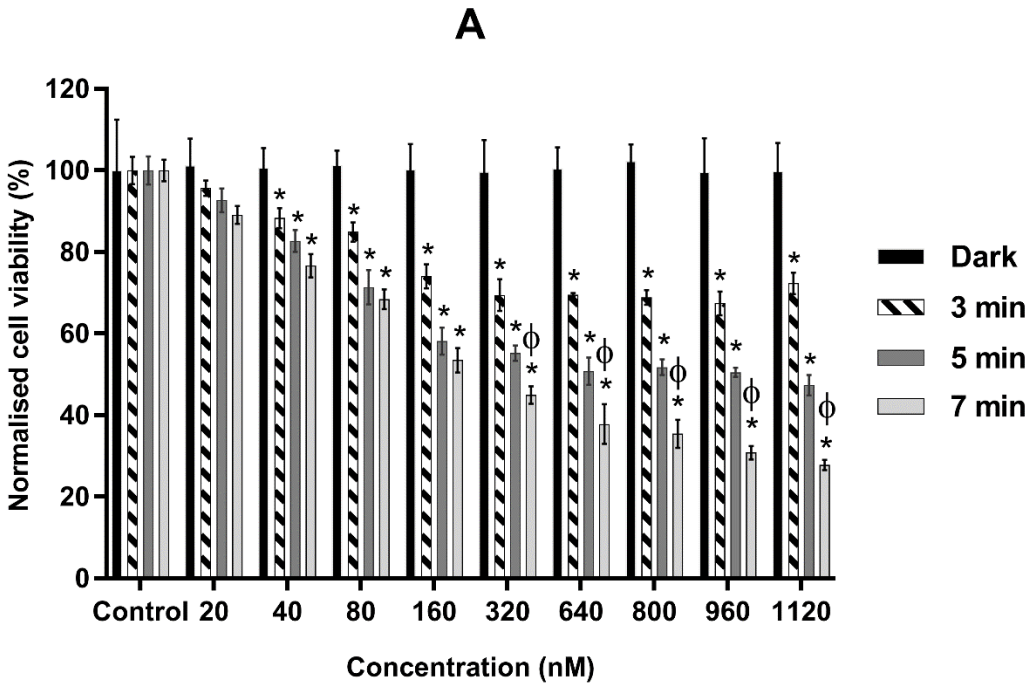

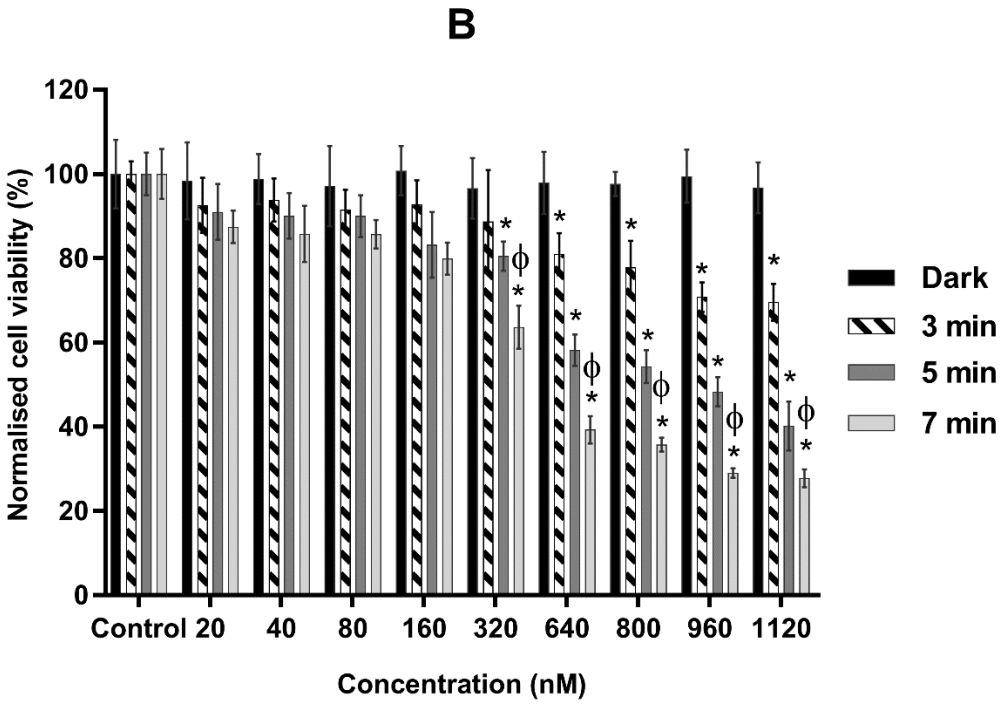

Figure 102 (A-B). The PDT effect of CPP-porphyrin conjugate **(215)** on MDA-MB-231 and MCF-7 cells.

A: MDA-MB-231 cells were treated with different concentrations of CPP-porphyrin conjugate **(215)** and were incubated for 24 h at 37 °C in the dark. Cells were illuminated with a blue lamp for 3.0, 5.0 and 7.0 min and MTT analysis was carried out 48 h after light illumination. The results were expressed as mean ± SD (n = 6) and plotted as percentage normalised cell viability.

B: Same treatment was followed as for **A.** above in MCF-7 cells.

* : $p<0.05$ significantly different from the dark conditions.

Φ: $p<0.05$ significantly different from CPP-porphyrin conjugate **(215)** illuminated for 3.0, 5.0 and 7.0 min.

The results above show significant PDT effects for both the cell lines incubated with the CPP- porphyrin conjugate **(215)**. At a concentration of 1120 nM and illumination for 7 min, both MDA-MB-231 cells and MCF-7 cells showed only 23% cell viability. These results were in agreement with the enhanced photosensitiser delivery and phototoxicity that has been previously observed with such CPP conjugates,[298] regardless of the receptor selectivity in both cell lines. Control experiments in the dark for CPP-porphyrin conjugate **(215)** showed no toxicity across all concentrations confirming that the decrease in

the cell viability was due to light and not due to any membrane-disrupting effects due to the CPP moiety.

6.6 Summary

Four cell-penetrating peptides **(200)**-**(203)** were synthesised, each containing a functionalised amino acid with a reactive group (azido), which could later take part in CuAAC with the ALA dendrons **(105)** or **(107)**. The azido-CPPs were coupled on resin with **(105)** or **(107)** via CuAAC to give the expected CPP-ALA conjugates **(210)**-**(214)** in good yields.

Conjugation of functionalised CPP **(203)** with dibenzocyclooctyne derivative **(192)** via SPAAC was also attempted. This gave the expected product **(215)** in 69% yield. Biological evaluation in EGFR-positive and -negative cell lines (MDA-MB-231 and MCF-7) showed significant PDT effects across a range of concentrations and light doses for this CPP-targeted porphyrin.

CHAPTER 7: EXPERIMENTAL

7.1 General

Chemical reagents were purchased from Sigma, Aldrich, Fluka, Acros and Novabiochem. Anhydrous DCM was obtained by distillation over calcium hydride. Peptide grade DMF was purchased from Rathburn Chemicals. All other solvents were purchased from Fisher Scientific. Analytical TLC was performed using silica gel 60 F_{254} pre-coated on aluminium sheets (0.25 mm thickness) and reverse-phase analytical TLC was performed with RP-18 F_{254s} pre-coated on aluminium sheets (0.27 mm thickness). Column chromatography was performed on silica gel 60 (35-70 micron) from Fisher Scientific. Melting points were recorded on an Electrothermal IA9200 melting point apparatus in open capillaries, and are quoted uncorrected. UV spectra were recorded on a Perkin-Elmer Lambda 19 uv/vis spectrophotometer. Fluorescence spectra were recorded on a Cary Eclipse fluorimeter. IR spectra were recorded on a Perkin-Elmer 782 infra-red spectrometer and values are given in cm^{-1}. ^{1}H and ^{13}C NMR spectra were recorded using a Bruker Advance DPX 500MHz FT and Varian Mercury VX 400MHz spectrometers. *J* values are given in Hz. Mass spectrometry was performed using a microTOF instrument from Bruker Daltonics (Bremen, Germany). Microwave irradiations were carried out using a Biotage® Initiator microwave synthesiser. Time-course fluorescence studies were carried out on a CLARIOstar high performance multimode microplate reader (CLARIOstar®, BMG LABTECH, United Kingdom). Analytical RP-HPLC was performed on a Dionex Ultimate 3000 system (Dionex, UK), with a VWD-3400 variable wavelength detector. Analyses were performed at 35 ± 0.1 °C on a Gemini 5 µm C18 110A column, (150 x 4.6 mm - Phenomenex, UK), equipped with a SecurityGuard C18 (ODS) 4 x 3.0 mm ID guard column (Phenomenex, UK), at a flow rate of 1 mL/min. Semi-preparative RP-HPLC was performed on a Dionex HPLC system equipped with a Phenomenex Gemini 5 µm C-18 (250 x 10 mm) column with a flow rate of 2.5 mL min^{-1}. Mobile phase A was 0.1% TFA in water and mobile phase B was 0.1% TFA in MeCN.

Gradient 1 was *T* = 0 min, *B* = 5%; *T* = 10 min, *B* = 95%; *T* = 15 min, *B* = 95%; *T* = 15.1 min, B = 5%; *T* = 18.1 min, *B* = 5%.

Gradient 2 was *T* = 0 min, *B* = 5%; *T* = 25 min, *B* = 95%; *T* = 35 min, *B* = 95%; *T* = 35.1min, *B* = 5%.

Gradient 3 was *T* = 0 min, *B* = 50%; *T* = 10 min, *B* = 95%; *T* = 15 min, *B* = 95%; *T* = 15.1 min, B = 5%; *T* = 18.1 min, *B* = 5%.

Gradient 4 was *T* = 0 min, *B* = 50%; *T* = 25 min, *B* = 95%; *T* = 35 min, *B* = 95%; *T* = 35.1min, *B* = 5%.

The completeness of solid phase acylations or deprotection reactions was confirmed by the Kaiser test.[309] A few beads of the resin were placed in an Eppendorf tube and 2-3 drops of the following solutions were added: 100 mM ninhydrin in EtOH, 2.1 M phenol in EtOH and 0.02 mM KCN in pyridine. The tube was heated and the presence of free/unacylated amino function was indicated by a dark blue colouration of the beads.

For estimating the loading of resin derivatised with Fmoc groups, an Fmoc loading test was performed at the end of the synthesis.[310] Fmoc-protected-resin (10 mg) in a graduated flask (10 mL) was treated with 2% DBU in DMF (2 mL) and agitated gently for 30 min. The solution was then diluted to 10 mL with MeCN and 2 mL of this solution was further diluted to 25 mL with MeCN (test sample). A similar treatment was performed for the reference sample but without the resin. Measurement of the test sample against the reference sample was done using a Unicam Helios UV/Vis spectrophotometer, and the absorbance was recorded at 304 nm. An estimate of the loading of the resin was then calculated using the equation:

$$\textbf{Fmoc (mmol/g)} = (\textbf{Abs}_{\textbf{sample}} - \textbf{Abs}_{\textbf{ref}}) \times \textbf{16.4/ mg of resin}$$

7.2 Synthesis of compounds

5-(*tert*-Butoxycarbonylamino)-4-oxopentanoic acid (99)[203]

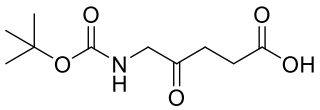

A stirred solution of ALA.HCl (1.68 g, 10.0 mmol) in dry THF (120 mL) was treated with di-*tert* butyl dicarbonate (4.66 g, 21.4 mmol). The mixture was cooled in an ice bath under N_2 and was then treated with a solution of DIEA (1.7 mL, 10.0 mmol) in dry THF (30 mL) added dropwise over 3 h. The mixture was then stirred overnight at RT, then the solvent was evaporated and the residue obtained was taken up in DCM (40 mL) and washed with aq. citric acid (2 x 40 mL). The organic phase was dried over $MgSO_4$, filtered, and the solvent evaporated to give the crude product which was purified by column chromatography on silica gel eluting with 10% MeOH in DCM + 0.05% AcOH. Removal of solvent gave **(99)** as a yellow oil (1.70 g, 78%); R_f = 0.59 (10% MeOH in DCM); IR (film) 3373 (NH), 2976 (CH), 1713 (CO), 1685 (CO); ^{1}H NMR (CD_3OD, 400MHz) δ 1.46 (9H, s, $(CH_3)_3C$), 2.59 (2H, t, J = 6.6, $COCH_2C\underline{H}_2$), 2.74 (3H, t, J = 6.4, $COC\underline{H}_2CH_2$), 3.93 (2H, s, $NHC\underline{H}_2CO$), 4.88 (1H, br, NH); ^{13}C NMR (CD_3OD, 100 MHz) δ 28.50 ($COCH_2\underline{C}H_2$), 28.68 ($(\underline{C}H_3)_3C$), 35.03 ($CO\underline{C}H_2CH_2$), 50.79 ($NH\underline{C}H_2CO$), 80.58 ($(CH_3)_3\underline{C}$), 158.40 (CO), 176.17 (CO), 207.49 (CO).

N-*Z*-*tris*(hydroxymethyl)aminomethane (100)[224]

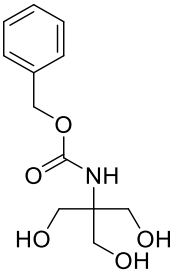

A stirred biphasic suspension of $NaHCO_3$ (4.4 g, 53 mmol) and *tris*-(hydroxymethyl) aminomethane, Tris **(97)** (5.0 g, 42 mmol) in H_2O and EtOAc (40 mL, 1:1) was treated with benzyl chloroformate (5.3 mL, 35 mmol), added

dropwise keeping the temperature around 20 °C. The mixture was stirred at RT for 5 h, then the suspended solid was filtered off and the two phases were left to separate. The aqueous phase was extracted with EtOAc (3 x 20 mL) and the combined organic extracts were then washed with H_2O (80 mL). The organic extracts were dried over $MgSO_4$, filtered, and the solvent evaporated to give the crude product as a white solid. Recrystallization from EtOAc/petroleum ether gave **(100)** as white solid (4.96 g, 47%); Mp = 100-102 °C (lit. 101-103 °C)[224]; ^{1}H NMR ($(CD_3)_2SO$, 400 MHz) δ 3.56 (6H, d, J = 5.6, 3 x C<u>H</u>$_2$OH), 4.47 (3H, t, J = 6.0, 3 x OH), 4.97 (2H, s, OC<u>H</u>$_2$Ph), 6.27 (1H, s, NH), 7.31-7.36 (5H, m, Ph).

N-(Benzyloxycarbonyl)aminomethane[tris-(methyl N-t-butyloxycarbonyl 5-aminolaevulinate)] (90)

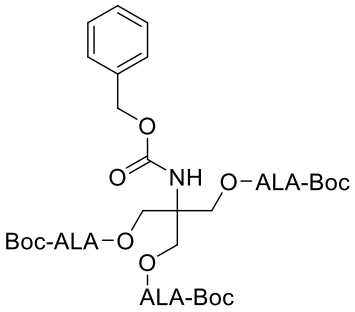

A solution of **(99)** (0.2 g, 0.9 mmol) in DCM (5 mL) was treated with dendron **(100)** (0.06 g, 0.23 mmol) in DCM (20 mL) and DMAP (0.01 g, 0.09 mmol). The reaction mixture was cooled in an ice-bath for 10 min and EDC.HCl (0.19 g, 1.01 mmol) was added. The reaction mixture was stirred under N_2 for 96 h at 30 °C, then it was partitioned with H_2O (30 mL) and the organic phase was washed with 10% aq. $NaHCO_3$ (2 x 30 mL), brine (2 x 30 mL) and dried over $MgSO_4$. The organic extract was filtered and solvent was evaporated to give the crude product as a yellow oil. Purification by column chromatography on silica gel eluting with 1-3% MeOH in DCM gave **(90)** as a yellow oil (0.08 g, 43%); ^{1}H NMR ($CDCl_3$, 400 MHz) δ 1.41 (27H, s, 3 x (C<u>H</u>$_3$)$_3$C), 2.57-2.63 (6H, m, 3 x C<u>H</u>$_2$CH$_2$CO), 2.66-2.72 (6H, m, 3 x CH$_2$C<u>H</u>$_2$CO), 3.95-4.02 (3 x COC<u>H</u>$_2$NH), 4.32 (3 x CC<u>H</u>$_2$O), 5.06 (3H, br, 3 x NH), 5.28 (1H, br, NH), 7.28-7.37 (5H, m, Ar).

2-Amino-2-(5-(*tert*-butoxycarbonyl) amino)-4-oxopentanoyl) oxy) methyl) propane-1,3-diyl bis(5-((*tert*-butoxycarbonyl) amino)-4-oxopentanoate) acetate salt (92)

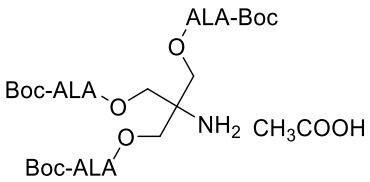

Method A

A solution of **(90)** (0.2 g, 0.8 mmol) in MeOH (25 mL) was treated with ammonium formate (0.2 g, 3.7 mmol) and the reaction flask was degassed with N_2. 10% Pd/C (40 mg) was added to the reaction mixture which was stirred for 1.5 h at RT, and the reaction was monitored by TLC (10% MeOH in DCM). No change was observed.

Method B

Method A was repeated omitting ammonium formate and stirring under an atmosphere of H_2.

Method C

Method B was repeated with the addition of 2M HCl in dioxane (60 µL) to the reaction mixture.

Method D

A solution of Z-protected amine **(90)** (0.1 g, 0.1 mmol) in MeOH: AcOH (8 mL, 3:1) was treated with 10% Pd/C (80 mg) and the pH of the solution was checked (acidic, pH 2.0). The mixture was stirred under an atmosphere of H_2 for 20 min at RT. The reaction mixture was filtered through celite, which was washed with MeOH. The solvents were evaporated and the residue was dried under vacuum to give **(92)** as a white solid (98 mg, 90%) which was used without further purification. ^{1}H NMR (CD_3OD, 400 MHz) δ 1.51 (27H, s, 3 x $(C\underline{H}_3)_3C$), 2.70 (6H, t, J = 6.4, 3 x $COCH_2C\underline{H}_2$), 2.82- 2.91 (6H, m, 3 x $COC\underline{H}_2CH_2$), 3.96-4.02 (6H, m, 3 x $COC\underline{H}_2NH$), 4.16 (6H, s, 3 x $CC\underline{H}_2O$).

2,5-Dioxopyrrolidin-1-yl pent-4-ynoate (106)[311, 312]

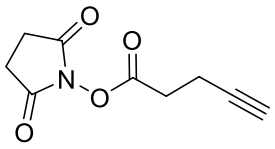

A solution of **(104)** (0.5 g, 5.1 mmol) and N-hydroxysuccinimide (0.59 g, 5.1 mmol) in DMF (12 mL) was stirred in an ice-bath and was treated with EDC.HCl (0.97 g, 5.1 mmol). The resulting mixture was stirred at RT for 16 h and the solvent was evaporated under vacuum. The residue was dissolved in EtOAc (10 mL) and was extracted with 5% aq. $NaHCO_3$ (2 x 10 mL), H_2O (10 mL) and brine (2 x 10 mL). The organic extracts were dried over $MgSO_4$, filtered, and the solvent evaporated to give the crude product (0.75 g). Recrystallization from CH_2Cl_2/petroleum ether gave **(106)** as white solid (0.53 g, 71%); Mp = 79.0-79.5 °C (lit. 79.9-80.5 °C)[312]; ^{1}H NMR ($CDCl_3$, 400 MHz) δ 2.02 (1H, t, J = 2.6, $\underline{H}C{\equiv}CCH_2CH_2$), 2.55-2.60 (2H, m, $HC{\equiv}CC\underline{H}_2CH_2$), 2.77-2.86 (6H, m, $HC{\equiv}CCH_2C\underline{H}_2$, $C\underline{H}_2C\underline{H}_2CO\text{-}N$).

Benzyl (1,7-dihydroxy-4-(3-hydroxypropyl)heptan-4-yl) carbamate (101)

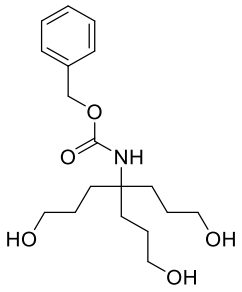

A solution of Z-OSu (0.55 g, 2.20 mmol) in THF (15 mL) was cooled to 0°C and the mixture was stirred under N_2. 4-Amino-4-(3-hydroxypropyl) heptane-1,7-diol (0.5 g, 2.4 mmol) and TEA (0.46 mL, 3.30 mmol) were added to the reaction mixture and it was allowed to stir at RT for 16 h, then the solvent was evaporated to give the crude product as a colourless oil. Purification by column chromatography on silica gel eluting with 0-20% MeOH in EtOAc gave **(101)** as a colourless oil (0.62 g). The product on dissolving in the minimum volume of cold water precipitated out as a white solid (0.3 g, 42%); Mp = 85-87 °C (uncorrected); R_f = 0.42 (10% MeOH in EtOAc); ^{1}H NMR (CD_3OD, 400 MHz)

δ 1.47-1.62 (6H, m, 3 x C$\underline{H}_2$CH$_2$CH$_2$OH), 1.66-1.82 (6H, m, 3 x CH$_2$C$\underline{H}_2$CH$_2$OH), 3.59 (6H, t, J = 8.0, 3 x CH$_2$CH$_2$CH$_2$OH), 5.07 (2H, s, OC$\underline{H}_2$Ph), 6.6 (1H, s, NH), 7.34-7.40 (5H, m, Ph); ^{13}C NMR (CD$_3$OD, 100 MHz) δ 27.49 (CCH$_2$C$\underline{H}_2$CH$_2$OH), 32.47 (C$\underline{C}$H$_2$CH$_2$CH$_2$OH), 58.31 ($\underline{C}$CH$_2$CH$_2$CH$_2$OH), 63.37 (CCH$_2$CH$_2$C$\underline{H}_2$OH), 66.71 (O$\underline{C}$H$_2$Ph), 128.65 (Ph), 128.90 (Ph), 129.50 (Ph), 138.73 (Ph), 156.73 (CO); [Found (ESI+) 340.2118 [M+H]$^+$, $C_{18}H_{30}N_1O_5$ requires 340.2123].

4-(((Benzyloxy) carbonyl) amino)-4-(3-((5-((tert-butoxycarbonyl) amino)-4-oxopentanoyl) oxy) propyl) heptane-1,7-diyl bis(5-((tert-butoxycarbonyl) amino)-4-oxopentanoate) (102)

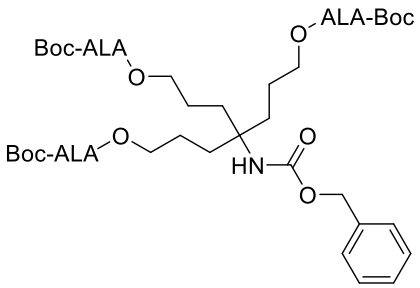

A solution of **(99)** (0.77 g, 3.54 mmol) in DCM (5 mL) was treated with dendron **(101)** (0.3 g, 0.88 mmol) in DCM (20 mL) and DMAP (0.04 g, 0.35 mmol). The reaction mixture was cooled in an ice-bath for 10 min and EDC.HCl (1.13 g, 3.89 mmol) was added. The reaction mixture was stirred under N_2 for 96 h at 30 °C, then it was partitioned with H_2O (30 mL) and the organic phase was washed with 10% aq. $NaHCO_3$ (2 x 30 mL), brine (2 x 30 mL) and dried over $MgSO_4$. The organic extract was filtered and solvent was evaporated to give the crude product as a yellow oil. Purification by column chromatography on silica gel eluting with 1-3% MeOH in DCM gave **(102)** as a yellow oil (0.3 g, 40%); R_f = 0.42 (5% MeOH in DCM); ^{1}H NMR ($CDCl_3$, 400 MHz) δ 1.41 (27H, s, 3 x (C$\underline{H}_3$)$_3$C), 1.48-1.58 (6H, m, 3 x C$\underline{H}_2$CH$_2$CH$_2$O), 1.60-1.70 (6H, m, 3 x CH$_2$C$\underline{H}_2$CH$_2$O) 2.57-2.63 (6H, m, 3 x C$\underline{H}_2$CH$_2$CO), 2.68-2.74 (6H, m, 3 x CH$_2$C$\underline{H}_2$CO), 4.01-4.04 (12H, 3 x CH$_2$CH$_2$C$\underline{H}_2$O, 3 x COC$\underline{H}_2$NH) 4.67 (1H, s, OCON$\underline{H}$C), 5.01 (2H, s, CH$_2$Ph), 5.32 (3H, s, COCH$_2$N$\underline{H}$) 7.28-7.33 (5H, m, Ph); ^{13}C NMR ($CDCl_3$, 100 MHz) δ 22.45 (CCH$_2$$\underline{C}H_2CH_2$O), 27.65 (CO$\underline{C}H_2CH_2$), 28.25 (($\underline{C}H_3$)$_3$C), 31.32 (COCH$_2$$\underline{C}H_2$), 34.24 (C$\underline{C}H_2CH_2CH_2$O),

50.17 (CO<u>C</u>H_2NH), 56.87 (<u>C</u>$CH_2CH_2CH_2O$), 64.59 (CCH_2CH_2<u>C</u>H_2O), 66.09 (O<u>C</u>H_2Ph), 79.76 ((CH_3)$_3$<u>C</u>), 127.87 (Ph), 128.05 (Ph), 128.47 (Ph), 154.12 (CO), 155.62 (CO), 172.35 (CO), 204.50 (CO); [Found (ESI+) 979.5135 $[M+H]^+$, $C_{48}H_{75}N_4O_{17}$ requires 979.5127].

4-Amino-4-(3-((5-((tert-butoxycarbonyl) amino)-4-oxopentanoyl) oxy) propyl) heptane-1,7-diyl bis(5-((tert-butoxycarbonyl) amino)-4-oxopentanoate) acetate salt (103)[203]

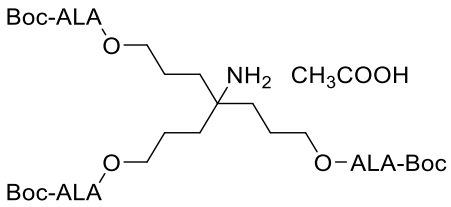

A solution of **(102)** (0.27 g, 0.28 mmol) in MeOH: AcOH (8 mL, 3:1) was treated with Pd/C (50 mg) and the pH of the solution was checked (acidic, pH 2.0). The mixture was stirred under an atmosphere of H_2 for 20 min at RT. The reaction mixture was filtered through celite, which was washed with MeOH. The solvents were evaporated and the residue was dried under vacuum to give **(103)** as a white solid (0.25 g, 96%) which was used without further purification. ^{1}H NMR ($CDCl_3$, 400 MHz) δ 1.40 (27H, s, 3 x (C<u>H</u>$_3$)$_3$C), 1.50-1.80 (12H, m, 3 x C<u>H</u>$_2CH_2CH_2O$, 3 x CH_2C<u>H</u>$_2CH_2O$), 2.60-2.62 (6H, m, 3 x C<u>H</u>$_2CH_2CO$), 2.72-2.80 (6H, m, 3 x CH_2C<u>H</u>$_2CO$), 4.02-4.07 (12H, m, 3 x CH_2CH_2C<u>H</u>$_2O$, 3 x COC<u>H</u>$_2$NH) 5.46 (2H, s, OCH_2Ph); ^{13}C NMR ($CDCl_3$, 100 MHz) δ 22.34 (CH_2<u>C</u>H_2CH_2O), 27.67 (<u>C</u>H_2CH_2CO), 28.25 (<u>C</u>H_3)$_3$C), 33.80 (CH_2<u>C</u>H_2CO), 34.25 (<u>C</u>$H_2CH_2CH_2O$), 50.15 (CO<u>C</u>H_2NH), 64.64 (CH_2CH_2<u>C</u>H_2O), 79.78 ((CH_3)$_3$<u>C</u>), 155.74 (CO), 172.40 (CO), 204.76 (CO); [Found (ESI+) 845.4857 $[M+H]^+$, $C_{40}H_{69}N_4O_{15}$ requires 845.4759].

3,3,9,9-Tetraisopropyl-2,10-dimethyl-6-(((triisopropylsilyl)oxy)methyl)-4,8-dioxa-3,9-disilaundecan-6-amine (110)

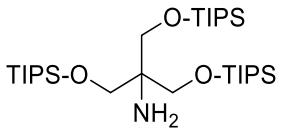

A solution of Trishydroxylmethylaminomethane **(97)** (0.5 g, 4.1 mmol) in DMF (40 mL) was treated with imidazole (1.40 g, 20.6 mmol) and triisopropylsilyl chloride, TIPS-Cl (4.0 mL, 21 mmol). The reaction mixture was then heated at 50 °C while stirring under N_2 for 60 h. The mixture was cooled down to RT and DMF was removed under reduced pressure, then the resulting crude mixture was dissolved in a mixture of EtOAc and H_2O (60 mL, 1:1). The organic phase was washed with 10% aq. $NaHCO_3$ (30 mL), brine (3 x 30 mL), dried over $MgSO_4$, filtered and the solvent was evaporated to give **(110)** as a colourless oil (2.4 g, quant) which was used without further purification. IR (film) 3380 (NH), 2943 (CH), 2867 (CH); ^{1}H NMR ($CDCl_3$, 400 MHz) δ 1.02-1.05 (63H, m, 9 x (OSiC<u>H</u>$(CH_3)_2$, OSiCH($C\underline{H}_3)_2$), 3.65 (6H, s, 3 x $C\underline{H}_2O$); ^{13}C NMR ($CDCl_3$, 100 MHz) δ 12.04 (OSi<u>C</u>H$(CH_3)_2$), 18.16 (OSiCH(<u>C</u>$H_3)_2$), 58.23 (<u>C</u>$(CH_2)_3$), 65.29 (C(<u>C</u>$H_2)_3$); [Found (ESI+) 612.4634 $[M+Na]^+$, $C_{31}H_{71}N_4NaO_3Si_3$ requires 612.4628].

***N*-(3,3,9,9-Tetraisopropyl-2,10-dimethyl-6-(((triisopropylsilyl)oxy)methyl)-4,8-dioxa-3,9-disilaundecan-6-yl)pent-4-ynamide (112)**

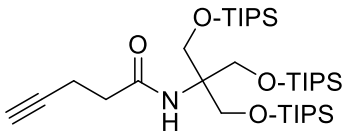

A solution of 4-pentynoic acid **(104)** (0.26 g, 2.70 mmol) in DMF (35 mL) was treated with EDC.HCl (0.6 g, 3.2 mmol) and HOBt. hydrate (0.7 g, 4.6 mmol) and the mixture was cooled to 0 °C for 40 min. DIEA (0.6 mL, 3.2 mmol) was then added to the reaction mixture and the pH checked (basic). The mixture was then treated with **(110)** (1.6 g, 2.7 mmol) and was stirred at RT under N_2 for 25 h. DMF was then removed under reduced pressure and the residue was dissolved in a mixture of EtOAc/H_2O (80 mL, 1:1). The organic layer was

washed with 5% aq. citric acid (40 mL), 10% aq. $NaHCO_3$ (40 mL), brine (40 mL), dried over $MgSO_4$, filtered and the solvent was evaporated to give the crude product as a colourless oil (1.57 g). Purification by column chromatography on silica gel eluting with 0-5% EtOAc in petroleum ether gave **(112)** as a colourless oil (1.47 g, 82%); R_f = 0.42 (5% EtOAc in petroleum ether); IR (film) 3423 (NH), 3315 (≡-H), 2943 (CH), 2867 (CH), 2100 (C≡C), 1669 (CO); ^{1}H NMR ($CDCl_3$, 400 MHz) δ 1.02-1.06 (63H, m, 9 x ($OSiCH(CH_3)_2$, $OSiCH(CH_3)_2$), 1.92-1.93 (1H, t, J = 2.6, $HC{\equiv}CCH_2CH_2$), 2.30-2.34 (2H, m, $HC{\equiv}CCH_2CH_2$), 2.43-2.46 (2H, m, $HC{\equiv}CCH_2CH_2$), 4.03 (6H, s, 3 x CCH_2O), 5.79 (1H, s, CH_2CONH); ^{13}C NMR ($CDCl_3$, 100 MHz) δ 12.06 ($OSiCH(CH_3)_2$), 14.87 ($HC{\equiv}CCH_2CH_2$), 18.12 ($OSiCH(CH_3)_2$), 36.27 ($HC{\equiv}CCH_2CH_2$), 61.31 (CCH_2O), 62.47 (CCH_2O), 68.92 ($HC{\equiv}CCH_2CH_2$), 83.39 ($CHCCH_2CH_2$), 170.16 (CH_2CONH); [Found (ESI+) 670.5137 $[M+H]^+$, $C_{36}H_{76}NNaO_4$ requires 670.5077].

***N*-[1,3-Dihydroxy-2-(hydroxymethyl)propan-2-yl]pent-4-ynamide (108)**

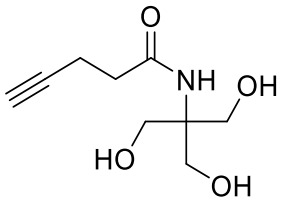

A solution of **(112)** (0.5 g, 0.8 mmol) in THF (20 mL) was treated with $TBAF.H_2O$ (1.1 g, 3.4 mmol) and AcOH (0.13 mL) was added to the reaction mixture (pH- neutral). The reaction mixture was stirred under N_2 for 3 h at RT and the solvent was removed under reduced pressure. The residue was then dissolved in MeOH (10 mL) and Dowex (50WX8, hydrogen form, 200-400 mesh) (2.35 g) and $CaCO_3$ (0.78 g) were added to the above solution. The mixture was stirred for 3 h, and then it was filtered through celite, which was washed with MeOH. The solvents were evaporated to give the crude product. Purification by column chromatography on silica gel eluting with 0-50% EtOAc in petroleum ether and then with 0-20% MeOH in EtOAc gave **(108)** as a white solid (0.11 g, 70%); Mp = 182-184 °C (Uncorrected); R_f = 0.48 (10% MeOH in EtOAc); IR (KBr disc) 3420-3230 (OH), 2931 (CH), 2118 (C≡C), 1627 (CO); ^{1}H NMR (CD_3OD, 400 MHz) δ 2.34-2.36 (1H, m, 1 x $HC{\equiv}CCH_2CH_2$), 2.52-2.56

(4H, m, C$\underline{H}_2$C$\underline{H}_2$CONH), 3.79 (6H, s, 3 x CC$\underline{H}_2$OH); ^{13}C NMR (CD_3OD, 100 MHz) δ 15.62 (HC≡C$\underline{C}H_2CH_2$), 36.4 (HC≡CCH$_2\underline{C}H_2$), 62.49 (C$\underline{C}H_2$OH, 63.68 ($\underline{C}CH_2$OH), 70.28 (H$\underline{C}$≡CCH$_2$CH$_2$), 83.56 (HC≡$\underline{C}$CH$_2$CH$_2$), 175.01 (CH$_2$CH$_2\underline{C}$ONH); [Found (ESI+) 224.0893 $[M+Na]^+$, $C_9H_{15}NNaO_4$ requires 224.0872].

3-({5-[(tert-Butoxycarbonyl) amino]-4-oxopentanoyl} oxy)-2-[({5-[(*tert*-butoxycarbonyl) amino]-4-oxopentanoyl} oxy) methyl]-2-(pent-4-ynoylamino) propyl 5-[(*tert*-butoxycarbonyl) amino]-4-oxopentanoate (105)

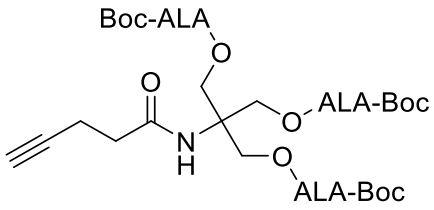

Method A

A solution of 4-pentynoic acid **(104)** (0.03 g, 0.23 mmol) in DMF (2 mL) was treated with EDC.HCl (0.06 g, 0.23 mmol) and HOBt hydrate (0.05 g, 0.38 mmol). The reaction mixture was cooled in an ice bath for 40 min and **(92)** (0.11 g, 0.13 mmol) was added. The reaction mixture was treated with DIEA (22 µL, 0.16 mmol) added over 1 h and stirred under N_2 for 48 h. The solvent was evaporated and the residue was dissolved in a mixture of EtOAc/H_2O (20 mL, 1:1). The organic layer was washed with 5% aq. citric acid (10 mL), 10% aq. $NaHCO_3$ (10 mL), brine (10 mL) and dried over $MgSO_4$. The organic extract was filtered, and the solvent was evaporated to give the crude product as a yellowish oil (0.03 g). Purification by column chromatography on silica gel eluting with 0-20% EtOAc in petroleum ether gave **(105)** as a yellowish oil (0.01 g, 11%); R_f = 0.32 (20% EtOAc in petroleum ether).

Method B

A solution of **(92)** (0.10 g, 0.12 mmol) in DMF (2 mL) was treated with **(106)** (0.05 g, 0.24mmol). The reaction mixture was treated with DIEA (18 µL, 0.15 mmol) added over 1 h and stirred under N_2 for 48 h. The solvent was

evaporated and the residue was dissolved in a mixture of EtOAc/H_2O (20 mL, 1:1) and the organic layer was washed with 5% aq. citric acid (10 mL), 10% aq. $NaHCO_3$ (10 mL), brine (10 mL) and dried over $MgSO_4$. The organic extract was filtered, and the solvent was evaporated to give the crude product as a yellowish oil (0.05 g). Purification by column chromatography on silica gel eluting with 0-20% EtOAc in petroleum ether gave **(105)** as a yellowish oil (7 mg, 7%); R_f = 0.36 (20% EtOAc in petroleum ether).

Method C

A solution of **(108)** (0.05 g, 0.23 mmol) in DCM (15 mL) was treated with **(99)** (0.20 g, 0.93 mmol) and DMAP (0.01 g, 0.09 mmol). The reaction mixture was cooled in an ice bath for 10 min and EDC.HCl (0.20 g, 1.03 mmol) was added. The reaction mixture was stirred under N_2 for 48 h at 30 °C, then the solvent was evaporated and the residue was dissolved in a mixture of EtOAc/H_2O (80 mL, 1:1). The organic layer was washed with 5% aq. citric acid (1 x 40 mL), 10% aq. $NaHCO_3$ (40 mL), brine (40 mL) and dried over $MgSO_4$. The organic extract was filtered, and the solvent was evaporated to give the crude product as a yellowish oil (0.20 g). Purification by column chromatography on silica gel eluting with 70-100% acetone in DCM gave **(105)** as a yellowish oil (0.18 g, 89%); R_f = 0.70 (30% acetone in DCM); IR (film) 3373 (NH), 2979 (CH), 2931 (CH) 2129 (C≡C); ^{1}H NMR ($CDCl_3$, 400 MHz) δ 1.40 (27H, s, 3 x $(C\underline{H}_3)_3C$), 2.01 (1H, t, J = 2.6, $\underline{H}C{\equiv}CCH_2CH_2$), 2.36-2.39 (2H, m, $HC{\equiv}CCH_2C\underline{H}_2$), 2.42-2.46 (2H, m, $HC{\equiv}CC\underline{H}_2CH_2$), 2.58-2.61 (6H, m, 3 x $COCH_2C\underline{H}_2$) 2.68-2.72 (6H, m, 3 x $COC\underline{H}_2CH_2$), 3.98-4.00 (6H, m, 3 x $COC\underline{H}_2NH$), 4.36 (6H, s, 3 x $CC\underline{H}_2O$), 5.33 (3H, s, $COCH_2N\underline{H}$), 6.33 (1H, s, $CON\underline{H}C$); ^{13}C NMR ($CDCl_3$, 100 MHz) δ 14.66 ($NHCOCH_2\underline{C}H_2$), 27.63 ($CO\underline{C}H_2CH_2$), 28.30 $(\underline{C}H_3)_3C$), 33.80 ($COCH_2\underline{C}H_2$), 34.23 ($HC{\equiv}CCH_2\underline{C}H_2$), 35.52 ($C\underline{C}H_2O$), 50.16 ($NH\underline{C}H_2CO$), 58.26 $(CH_2)_3\underline{C}$), 62.46 $(\underline{C}H_2)_3C$), 69.32 ($\underline{C}H{\equiv}CCH_2CH_2$), 79.94 ($(CH_3)_3\underline{C}$), 82.98 ($CH{\equiv}\underline{C}CH_2CH_2$), 155.78 (CO), 171.53 (CO), 171.87 (CO), 204.51 (CO); [Found (ESI+) 841.4114 $[M+H]^+$, $C_{39}H_{61}N_4O_{16}$ requires 841.4082].

3,3,13,13-Tetraisopropyl-2,14-dimethyl-8-(3-((triisopropylsilyl)oxy) propyl)-4,12-dioxa-3,13-disilapentadecan-8-amine (111)

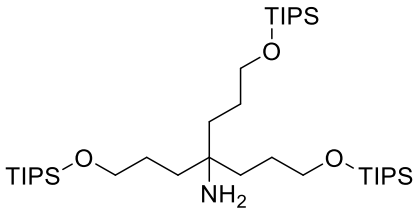

A solution of (**98)** (0.5 g, 2.4 mmol) in DMF (20 mL) was treated with imidazole (0.99 g, 14.6 mmol) and TIPS-Cl (2.87 mL, 14.6 mmol) was added. The reaction mixture was then heated at 50 °C while stirring under N_2 for 48 h. The mixture was cooled down to RT and DMF was removed under reduced pressure and the resulting crude mixture was dissolved in a mixture of EtOAc and H_2O (60 mL, 1:1). The organic phase was washed with 10% aq. $NaHCO_3$ (30 mL), brine (3 x 30 mL) and dried over $MgSO_4$. The organic extract was filtered, and the solvent was evaporated to give **(111)** as a colourless oil (1.54 g, 94%) which was used without further purification. IR 3466 (NH), 2942 (CH), 2866 (CH); ^{1}H NMR ($CDCl_3$, 400 MHz) δ 1.02-1.06 (63H, m, 9 x (OSiC<u>H</u>$(CH_3)_2$, OSiCH(C<u>H</u>$_3)_2$), 1.35-1.39 (6H, m, 3 x C<u>H</u>$_2$$CH_2CH_2O$), 1.48-1.53 (6H, m, 3 x CH_2C<u>H</u>$_2$$CH_2O$), 3.65 (6H, t, J = 6.3, 3 x CH_2CH_2C<u>H</u>$_2$O); ^{13}C NMR ($CDCl_3$, 100 MHz) δ 12.42 (OSi<u>C</u>H$(CH_3)_2$), 18.18 (OSiCH(<u>C</u>H$_3)_2$), 27.33 (C<u>C</u>$H_2CH_2CH_2O$), 36.47 (CCH_2<u>C</u>H_2CH_2O), 52.80 (<u>C</u>$CH_2CH_2CH_2O$), 64.09 (CCH_2CH_2<u>C</u>H_2O); [Found (ESI+) 696.5608 $[M+Na]^+$, $C_{37}H_{83}N_1NaO_3Si_3$ requires 696.5578].

***N*-(3,3,13,13-Tetraisopropyl-2,14-dimethyl-8-(3-((triisopropylsilyl)oxy) propyl)-4,12-dioxa-3,13-disilapentadecan-8-yl) pent-4-ynamide (113)**

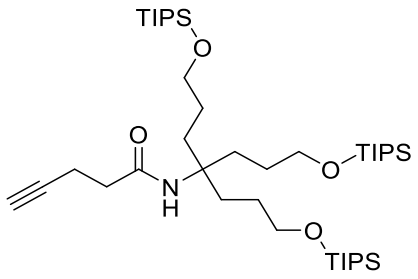

A solution of **(104)** (0.22 g, 2.26 mmol) in DMF (10 mL) was treated with

EDC.HCl (0.52 g, 2.71 mmol) and HOBt. hydrate (0.59 g, 3.85 mmol) and the mixture was cooled to 0 °C for 40 min. DIEA (0.47 mL, 2.71 mmol) was then added to the reaction mixture and the pH checked (basic). The mixture was then treated with **(111)** (1.58 g, 2.26 mmol) and was stirred at RT under N_2 for 25 h. DMF was then removed under reduced pressure and the residue was dissolved in a mixture of EtOAc/H_2O (80 mL, 1:1). The organic layer was washed with 5% aq. citric acid (40 mL), 10% aq. $NaHCO_3$ (40 mL), brine (40 mL) and dried over $MgSO_4$. The organic extract was filtered, and the solvent was evaporated to give the crude product as a colourless oil (1.72 g). Purification by column chromatography on silica gel eluting with 0-5% EtOAc in petroleum ether gave **(113)** as a colourless oil (1.39 g, 81%); R_f = 0.35 (5% EtOAc in petroleum ether); IR (film) 3325 (NH), 2944 (CH), 2866 (CH), 2115 (C≡C), 1660 (CO); ^{1}H NMR ($CDCl_3$, 400 MHz) δ 1.02-1.06 (63H, m, 9 x (OSiC<u>H</u>$(CH_3)_2$, OSiCH(C<u>H</u>$_3)_2$), 1.46-1.51(6H, m, 3 x C<u>H</u>$_2$CH$_2$CH$_2$O), 1.71-1.75 (6H, m, 3 x CH$_2$C<u>H</u>$_2$CH$_2$O), 1.96 (1H, t, J = 2.6, <u>H</u>C≡CCH$_2$CH$_2$CO), 2.28-2.31 (2H, m, HC≡CCH$_2$C<u>H</u>$_2$CO), 2.44-2.48 (2H, m, HC≡CC<u>H</u>$_2$CH$_2$CO), 3.64 (6H, t, J= 6.5, 3 x CH$_2$CH$_2$C<u>H</u>$_2$O), 5.28 (1H, s, NH); ^{13}C NMR ($CDCl_3$, 100 MHz) δ 12.10 (OSi<u>C</u>H$(CH_3)_2$), 15.19 (HC≡C<u>C</u>H$_2$CH$_2$), 18.17 (OSiCH(<u>C</u>H$_3)_2$), 27.04 (CH$_2$<u>C</u>H$_2$CH$_2$O) 31.47 (HC≡CCH$_2$<u>C</u>H$_2$CO), 36.47 (<u>C</u>H$_2$CH$_2$CH$_2$O), 58.75 (<u>C</u>CH$_2$CH$_2$CH$_2$O), 63.66 (CH$_2$CH$_2$<u>C</u>H$_2$OH), 69.41 (H<u>C</u>≡CCH$_2$CH$_2$CO), 83.36 (HC≡<u>C</u>CH$_2$CH$_2$CO), 169.93 (CO); [Found (ESI+) 754.6087 $[M+H]^+$, $C_{42}H_{88}N_1O_4Si_3$ requires 754.6021].

***N*-[1,7-Dihydroxy-4-(3-hydroxypropyl)heptan-4-yl]pent-4-ynamide (114)**

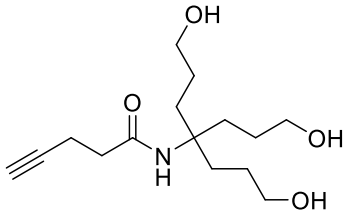

A solution of **(113)** (1.38 g, 1.83 mmol) in THF (35 mL) was treated with TBAF.H_2O (2.59 g, 8.23 mmol) and AcOH (0.36 mL) was added to the reaction mixture (pH- neutral). The reaction mixture was stirred under N_2 for 16 h at RT and the solvent was removed under reduced pressure. The residue was then dissolved in MeOH (25 mL) and Dowex (50WX8, hydrogen form, 200-400

mesh) (5.74 g) and $CaCO_3$ (1.90 g) were added to the above solution. The mixture was stirred for 3 h, and then it was filtered through celite, which was washed with MeOH. The solvents were evaporated to give the crude product (0.71 g). Purification by column chromatography on silica gel eluting with 0-50% EtOAc in petroleum ether and then with 0 to 20% MeOH in EtOAc gave **(114)** as a white solid (0.34 g, 65%); Mp = 118-120 °C; R_f = 0.40 (5% MeOH in EtOAc); IR (KBr disc) 3400-3315 (OH), 2943 (CH), 2869 (CH), 2118 (C≡C), 1683 (CO); ^{1}H NMR (CD_3OD, 400 MHz) δ 1.52-1.59 (6H, m, 3 x $CCH_2CH_2CH_2OH$), 1.78-1.82 (6H, m, 3 x $CCH_2CH_2CH_2OH$), 2.34 (1H, t, J = 2.6, $HC{\equiv}CCH_2CH_2CO$), 2.40-2.44 (2H, m, $HC{\equiv}CCH_2CH_2CO$), 2.48-2.52 (2H, m, $HC{\equiv}CCH_2CH_2CO$), 3.59 (6H, t, J = 6.6, $CCH_2CH_2CH_2O$); ^{13}C NMR (CD_3OD, 100 MHz) δ 15.87 ($HC{\equiv}CCH_2CH_2CO$), 27.41 ($CCH_2CH_2CH_2OH$), 32.13 ($CCH_2CH_2CH_2OH$), 36.68 ($HC{\equiv}CCH_2CH_2CO$), 59.61 ($CCH_2CH_2CH_2OH$), 63.32 ($CCH_2CH_2CH_2OH$), 70.37 ($HC{\equiv}CCH_2CH_2CO$), 83.78 ($HC{\equiv}CCH_2CH_2CO$), 173.25 (CO); [Found (ESI+) 286.2003 $[M+H]^+$, $C_{15}H_{28}N_1O_4$ requires 286.2012].

7-({5-[(*tert*-Butoxycarbonyl) amino]-4-oxopentanoyl} oxy)-4-[3-({5-[(*tert*-butoxy carbonyl) amino]-4-oxopentanoyl} oxy) propyl]-4-(pent-4-ynoylamino)heptyl 5-[(*tert*-butoxycarbonyl)amino]-4-oxopentanoate (107)

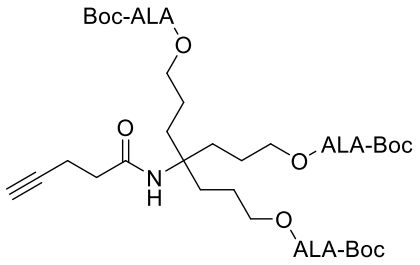

Method A

A solution of **(103)** (0.24 g, 0.27 mmol) in DMF (10 mL) was treated with **(106)** (0.10 g, 0.53mmol). The reaction mixture was treated with DIEA (55 µL, 0.32 mmol) added over 1 h and stirred under N_2 for 48 h. The solvent was evaporated and the residue was dissolved in a mixture of EtOAc/H_2O (20 mL, 1:1) and the organic layer was washed with 5% aq. citric acid (10 mL), 10%

aq. $NaHCO_3$ (10 mL), brine (10 mL) and dried over $MgSO_4$. The organic extract was filtered, and the solvent was evaporated to give the crude product as a yellowish oil (0.18 g). Purification by column chromatography on silica gel eluting with 70-100% acetone in DCM gave **(107)** as a yellowish oil (0.10 g, 40%).

Method B

A solution of **(114)** (0.24 g, 0.84 mmol) in dry DCM (40 mL) was treated with **(99)** (0.73 g, 3.36 mmol) and DMAP (0.04 g, 0.34 mmol). The reaction mixture was cooled in an ice bath for 10 min and EDC.HCl (0.71 g, 3.70 mmol) was added. The reaction mixture was stirred under N_2 for 32 h at 30 °C, then the solvent was evaporated and the residue was dissolved in a mixture of EtOAc/H_2O (40 mL, 1:1) and the organic layer was washed with 5% aq. citric acid (20 mL), 10% aq. $NaHCO_3$ (20 mL), brine (20 mL) and dried over $MgSO_4$. The organic extract was filtered, and solvent was evaporated to give the crude product as a yellowish oil (0.78 g). Purification by column chromatography on silica gel eluting with 70-100% acetone in DCM gave **(107)** as a yellowish oil (0.60 g, 77%); R_f = 0.68 (10% acetone in DCM); IR (film) 3383 (NH), 3005 (CH), 2917 (CH), 2099 (C≡C), 1717 (CO); ^{1}H NMR ($CDCl_3$, 400 MHz) δ 1.33 (27H, s, 3 x $(C\underline{H}_3)_3C$), 1.41-1.48 (6H, m, 3 x $CC\underline{H}_2CH_2CH_2O$), 1.59-1.63 (3 x $CCH_2C\underline{H}_2CH_2O$), 1.95 (1H, t, J = 2.6, $\underline{H}C{\equiv}CCH_2CH_2$), 2.23-2.26 (2H, m, $HC{\equiv}CCH_2C\underline{H}_2$), 2.36-2.40 (2H, m, $HC{\equiv}CC\underline{H}_2CH_2$), 2.49-2.52 (6H, m, 3 x $COCH_2C\underline{H}_2$), 2.62-2.66 (6H, s, 3 x $COC\underline{H}_2CH_2$), 3.91-3.96 (12H, m, 3 x $CCH_2CH_2C\underline{H}_2O$, 3 x $COC\underline{H}_2NH$), 5.39-5.46 (3H, m, $COCH_2N\underline{H}$), 5.60 ($CON\underline{H}C$); ^{13}C NMR ($CDCl_3$, 100 MHz) δ 14.90 ($HC{\equiv}C\underline{C}H_2CH_2CO$), 22.44 ($CCH_2\underline{C}H_2CH_2O$), 27.67 ($CO\underline{C}H_2CH_2$), 28.22 ($(\underline{C}H_3)_3C$), 30.87 ($COCH_2\underline{C}H_2$), 34.15 ($C\underline{C}H_2CH_2CH_2O$), 35.80 ($HC{\equiv}CCH_2\underline{C}H_2CO$), 50.09 ($CO\underline{C}H_2NH$), 57.99 ($\underline{C}CH_2CH_2CH_2O$), 64.55 ($CCH_2CH_2\underline{C}H_2O$), 69.51 ($H\underline{C}{\equiv}CCH_2CH_2CO$), 79.62 ($(CH_3)_3\underline{C}$), 83.11 ($HC{\equiv}\underline{C}CH_2CH_2CO$), 155.71 (CO), 170.39 (CO), 172.29 (CO), 204.82 (CO); [Found (ESI+) 925.5055 $[M+H]^+$, $C_{45}H_{73}N_4O_{16}$ requires 925.5016].

Di-tert-butyl 3,3'-((2-amino-2-((3-(tert-butoxy)-3-oxopropoxy) methyl) propane-1,3-diyl)bis(oxy))dipropanoate (117)[228]

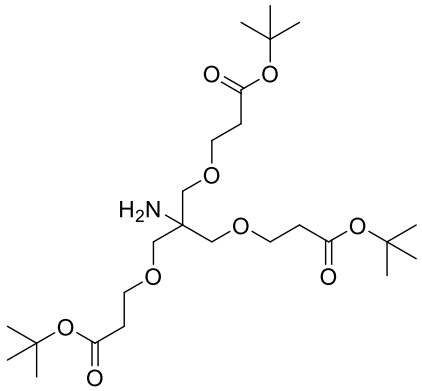

A solution of tris(hydroxylmethyl)methylamine **(97)** (1.21 g, 10.0 mmol) in dry DMSO (2.0 mL) was cooled to 15 °C under N_2. 5.0 M aq. NaOH (0.2 mL) was then added to the reaction mixture while stirring, followed by dropwise addition of *tert* butyl propenoate (5.0 mL, 34 mmol). The reaction mixture was stirred at RT for 24 h, followed by removal of excess reagent and solvent under vacuum at RT. The crude product was purified by column chromatography on silica gel eluting with 67% EtOAc in petroleum ether + 0.01% NH_4OH) to give **(117)** as a colourless oil (1.3 g, 26%); R_f = 0.6, EtOAc in petroleum ether (2:1 + 0.01% NH_4OH); IR (film) 3448 (NH), 3382 (NH), 2978 (CH), 1731 (CO); ^{1}H NMR ($CDCl_3$, 400 MHz) δ 1.40 (27H, s, C(C$\underline{H}_3$)$_3$), 2.40 (6H, t, J = 6.4, 3 x $CH_2C\underline{H}_2COO$), 3.27 (6H, s, CC$\underline{H}_2$O), 3.60 (6H, t, J = 6.4, 3 x C$\underline{H}_2CH_2COO$).

Di-tert-Butyl 3,3'-((2-((3-(tert-butoxy)-3-oxopropoxy)methyl)- 2- (pent-4-ynamido) propane-1,3-diyl)bis(oxy))dipropanoate (118)

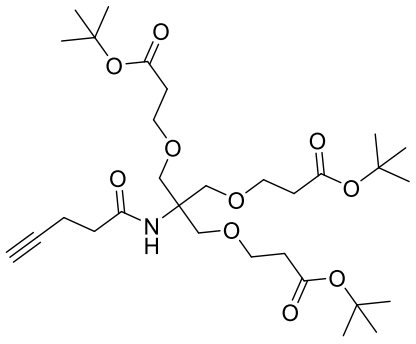

A solution of **(104)** (0.06 g, 0.63 mmol) was treated with EDC.HCl (0.15 g, 0.76 mmol) and HOBt. hydrate (0.16 g, 1.07 mmol) and the mixture was cooled

to 0 °C for 40 min. DIEA (0.13 mL, 0.76 mmol) was then added to the reaction mixture and the pH checked (basic). The mixture was then treated with **(117)** (32 g, 0.63 mmol) and was stirred at RT under N_2 for 36 h. DMF was then removed under reduced pressure and the residue was dissolved in a mixture of EtOAc/H_2O (40 mL, 1:1). The organic layer was washed with 5% aq. citric acid (20 mL), 10% aq. $NaHCO_3$ (20 mL), brine (20 mL) and dried $MgSO_4$. The organic extract was filtered, and the solvent was evaporated to give the crude product as a colourless oil (0.37 g). Purification by column chromatography on silica gel eluting with 10-30% EtOAc in petroleum ether gave **(118)** as a colourless oil (0.23 g, 63%); IR (film) 3335 (NH), 3283 (≡-H), 2943 (CH), 2119 (C≡C), 1709 (CO); ^{1}H NMR ($CDCl_3$, 400 MHz) δ 1.37 [27H, s, 3 x C(C<u>H</u>$_3$)$_3$], 1-88-1.90 (1H, m, C<u>H</u>≡CC<u>H</u>$_2$C<u>H</u>$_2$CO), 2.32-2.41 (10H, m, HC≡CC<u>H</u>$_2$C<u>H</u>$_2$CO, 3 x CH$_2$C<u>H</u>$_2$CO), 3.56 (6H, t, J = 6.4, 3 x CH$_2$C<u>H</u>$_2$COO), 3.62 (6H, s, 3 x CCH$_2$O), 6.16 (1H, CON<u>H</u>); ^{13}C NMR ($CDCl_3$, 100 MHz) δ 14.82 (HC≡C<u>C</u>H$_2$CH$_2$CO), 28.12 [C(<u>C</u>H$_3$)$_3$], 35.83 (HC≡CCH$_2$<u>C</u>H$_2$CO), 36.14 (CH$_2$<u>C</u>H$_2$CO), 59.85 (<u>C</u>CH$_2$O), 67.04 (<u>C</u>H$_2$CH$_2$CO), 68.90 (H<u>C</u>≡CCH$_2$CH$_2$CO), 69.14 (C<u>C</u>H$_2$O), 80.46 [<u>C</u>(CH$_3$)$_3$], 83.15 (HC≡<u>C</u>CH$_2$CH$_2$CO), 170.97 (CO), 171.14 (CO); [Found (ESI+) 586.3603 [M+H]$^+$, $C_{30}H_{52}N_1O_{10}$ requires 586.3591].

3,3'-((2-((2-Carboxyethoxy)methyl)-2-(pent-4-ynamido)propane-1,3-diyl)bis (oxy)) dipropanoic acid (119)

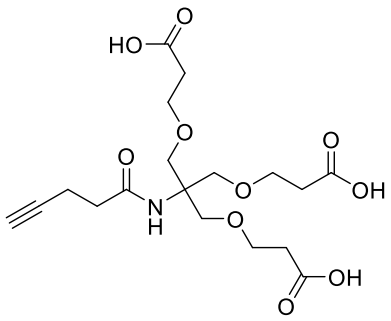

A solution of **(118)** (1.9 g, 3.2 mmol) in DCM (10 mL) was cooled to 0 °C and TFA (5 mL) was added dropwise. The reaction mixture was stirred for 4 h at RT, then the solvent was evaporated under vacuum and the residue was co-evaporated with Et_2O (x 3) to remove excess TFA. The crude product was obtained as a yellowish oil and was dried under vacuum, then used without further purification **(119)** (1.19 g, 88%). R_f = 0.09, 50% EtOAc in petroleum

ether. IR (film) 3285 (≡-H), 3055-2610(OH broad), 2915 (CH), 2115 (C≡C), 1705 (CO); ^{1}H NMR (CD_3OD, 400 MHz) δ 2.22-2.26 (1H, m, HC≡CCH$_2$CH$_2$), 2.37-2.42 (4H, m, HC≡CCH$_2$CH$_2$), 2.50-2.58 (6H, m, 3 x CH$_2$CH$_2$COOH), 3.63-3.71 (12H, m, 3 x CH$_2$CH$_2$COOH, 3 x CCH$_2$O); ^{13}C NMR (CD_3OD, 100 MHz) δ 15.66 (HC≡CCH$_2$CH$_2$), 35.70 (CH$_2$CH$_2$COOH), 36.58 (HC≡CCH$_2$CH$_2$), 61.49 (CCH$_2$O), 68.11 (CH$_2$CH$_2$COOH), 69.94 (CCH$_2$O), 70.20 (HC≡CCH$_2$CH$_2$), 83.71 (HC≡CCH$_2$CH$_2$), 174.01 (CO), 175.45 (CO); [Found (ESI+) 440.1535 $[M+Na]^+$, $C_{18}H_{27}N_1NaO_{10}$ requires 440.1532].

Benzyl (3-oxo-3- ((3,3,9,9-tetraisopropyl-2,10- dimethyl-6- (((triisopropylsilyl)oxy) methyl)-4 ,8-dioxa-3,9-disilaundecan-6-yl)amino)propyl)carbamate (121)

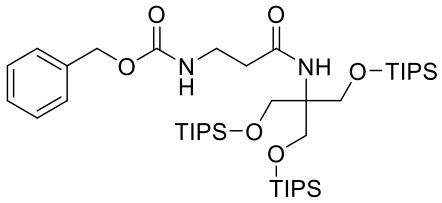

A solution of Z-β-ALA-OH **(120)** (0.87 g, 3.91 mmol) in DMF (15 mL) was treated with EDC.HCl (0.89 g, 4.69 mmol) and HOBt. hydrate (1.06 g, 6.64 mmol) and the mixture was cooled to 0 °C for 40 min. DIEA (0.82 mL, 4.69 mmol) was then added to the reaction mixture and the pH checked (basic). The mixture was then treated with **(110)** (2.31 g, 3.91 mmol) and was stirred at RT under N_2 for 36 h. DMF was then removed under reduced pressure and the residue was dissolved in a mixture of EtOAc/H_2O (80 mL, 1:1). The organic layer was washed with 5% aq. citric acid (40 mL), 10% aq. $NaHCO_3$ (40 mL), brine (40 mL) and dried over $MgSO_4$. The organic extract was filtered, and the solvent was evaporated to give the crude product as a colourless oil (1.89 g). Purification by column chromatography on silica gel eluting with 0-5% EtOAc in petroleum ether gave **(121)** as a colourless oil (1.53 g, 49%); ^{1}H NMR ($CDCl_3$, 400 MHz) δ 0.98-1.09 (63H, m, 9 x (OSiCH(CH$_3$)$_2$, OSiCH(CH$_3$)$_2$), 2.30-2.35 (2H, m, CONHCH$_2$CH$_2$CONH), 2.40-2.46 (2H, m, CONHCH$_2$CH$_2$CONH). 4.01 (6H, s, NHCCH$_2$), 5.06 (2H, s, Ph-CH$_2$), 7.27-7.33 (5H, m, Ph); ^{13}C NMR ($CDCl_3$, 100 MHz) δ 11.53 (OSiCH(CH$_3$)$_2$), 17.89 (OSiCH(CH$_3$)$_2$), 36.28 (CONHCH$_2$CH$_2$CONH), 36.84 (CONHCH$_2$CH$_2$CONH),

61.12 (NHC<u>C</u>H$_2$), 62.27 (NH<u>C</u>CH$_2$), 66.44 (Ph-<u>C</u>H$_2$), 127.88 (Ph), 127.91 (Ph), 128.36 (Ph), 136.62 (Ph), 156.33 (CO), 170.68 (CO); [Found (ESI+) 795.5607 $[M+H]^+$, $C_{42}H_{83}N_2O_6Si_3$ requires 795.5558].

Benzyl (3-((1,3-dihydroxy-2-(hydroxymethyl)propan-2-yl) amino)-3-oxopropyl) carbamate (122)

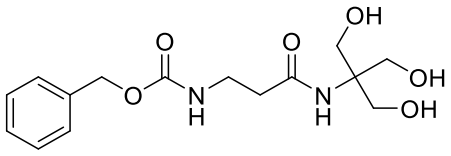

A solution of **(121)** (1.50 g, 1.88 mmol) in THF (30 mL) was treated with TBAF.H_2O (2.67 g, 8.49 mmol) and AcOH (0.37 mL) was added to the reaction mixture (pH-neutral). The reaction mixture was stirred under N_2 for 3 h at RT and the solvent was removed under reduced pressure. The residue was then dissolved in MeOH (35 mL) and Dowex (50WX8, hydrogen form, 200-400 mesh) (5.91 g) and $CaCO_3$ (1.96 g) were added to the above solution. The mixture was stirred for 3 h, and then it was filtered through celite, which was washed with MeOH. The solvents were evaporated to give the crude product (0.61 g). Purification by column chromatography on silica gel eluting with 0-100% EtOAc in petroleum ether and then with 5- 20% MeOH in EtOAc gave **(122)** as a white solid (0.45 g, 74%); Mp = 82.5-83.0 °C (Uncorrected); IR (KBr disc) 3443-3198 (OH), 2942 (CH), 1693 (CO); ^{1}H NMR (CD_3OD, 400 MHz) δ 2.50 (2H, t, J = 6.5, CONHCH$_2$C<u>H</u>$_2$CONH), 3.46 (2H, t, J = 6.5, CONHC<u>H</u>$_2$CH$_2$CONH), 3.78 (6H, s, NHCC<u>H</u>$_2$), 5.13 (2H, s, Ph-C<u>H</u>$_2$), 7.35-7.41 (5H, m, Ph); ^{13}C NMR (CD_3OD, 100 MHz) δ 37.85 (CONHCH$_2$<u>C</u>H$_2$CONH), 38.52 (CONH<u>C</u>H$_2$CH$_2$CONH), 62.37 (NHC<u>C</u>H$_2$), 63.70 (<u>C</u>CH$_2$), 67.46 (Ph-<u>C</u>H$_2$), 128.80 (Ph), 128.96 (Ph), 129.45 (Ph), 138.33 (Ph), 158.88 (CO), 174.89 (CO); [Found (ESI+) 327.1561 $[M+H]^+$, $C_{15}H_{23}N_2O_6$ requires 327.1556].

Z-NH-beta-alanine ALA-dendron (123)

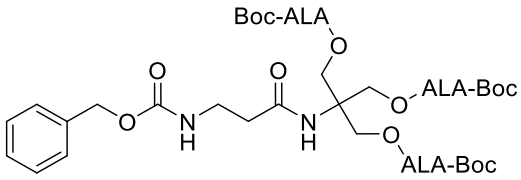

A solution of **(99)** (1.09 g, 5.03 mmol) in dry DCM (30 mL) was treated with **(122)** (0.41 g, 1.26 mmol) and DMAP (0.06 g, 0.05 mmol). The reaction mixture was cooled in an ice bath for 10 min and EDC.HCl (1.06 g, 5.53 mmol) was added. The reaction mixture was stirred under N_2 for 36 h at 32 °C, then the solvent was evaporated and the residue was dissolved in a mixture of EtOAc/H_2O (60 mL, 1:1). The organic layer was washed with 5% aq. citric acid (30 mL), 10% aq. $NaHCO_3$ (30 mL), brine (30 mL) and dried over $MgSO_4$. The organic extract was filtered, and the solvent was evaporated to give the crude product as a yellowish oil (1.18 g). Purification by column chromatography on silica gel eluting with 0-5% MeOH in DCM gave **(123)** as a yellowish oil (0.88 g, 72%); ^{1}H NMR ($CDCl_3$, 400 MHz) δ 1.43 (27H, s, 3 x (C<u>H</u>$_3$)$_3$C), 2.43.244 (2H, m, NHCH$_2$C<u>H</u>$_2$CONH), 2.57-2.60 (6H, m, 3 x COCH$_2$C<u>H</u>$_2$), 2.67-2.68 (6H, m, 3 x COC<u>H</u>$_2$CH$_2$), 3.44-3.48 (2H, m, NHC<u>H</u>$_2$CH$_2$CONH), 3.98-3.99 (6H, m, 3 x COC<u>H</u>$_2$NH), 4.40 (6H, s, 3 x CC<u>H</u>$_2$O), 5.07 (2H, s, C<u>H</u>$_2$), 5.29-5.34 (3H, m, 3 x COCH$_2$N<u>H</u>), 5.62 (1H, s, N<u>H</u>), 6.29 (1H, s, NH), 7.33-7.35 (5H, m, Ph); [Found (ESI+) 966.4564 $[M+H]^+$, $C_{45}H_{68}N_5O_{18}$ requires 966.4559].

Attempted acylation of (119) and (124)

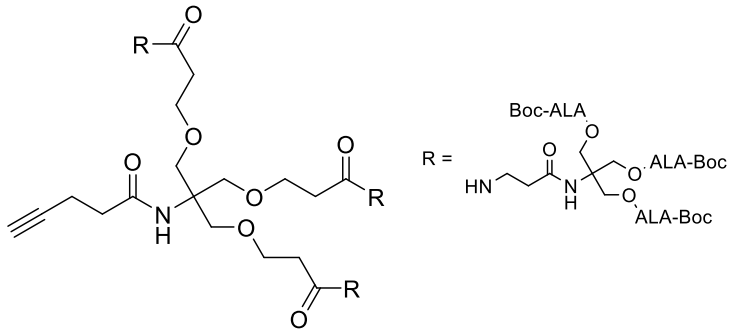

Step 1. Cleavage of Z group from **(123)**

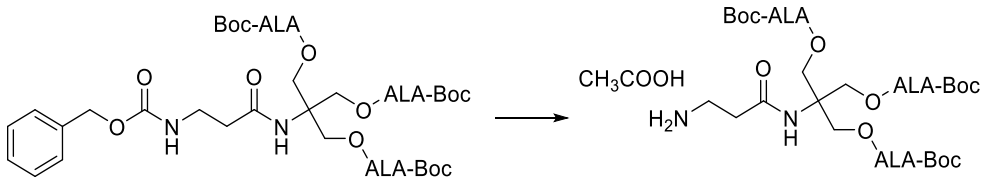

(123) **(124)**

A solution of Z-protected amine **(123)** (0.57 g, 0.59 mmol) in MeOH: AcOH (16 mL, 3:1) was treated with 10% Pd/C (113 mg) and the pH of the solution was checked (acidic, pH 2.0). The mixture was stirred under an atmosphere of H_2 for 20 min at RT. The reaction mixture was filtered through celite, which was washed with MeOH. The solvents were evaporated and the residue was dried under vacuum to give **(124)** as a white solid (0.41, 79%) which was used without further purification. [Found (ESI+) 854.4036 $[M+Na]^+$, $C_{37}H_{61}N_5NaO_{16}$ requires 854.4011].

Step 2. Attachment of **(119)**

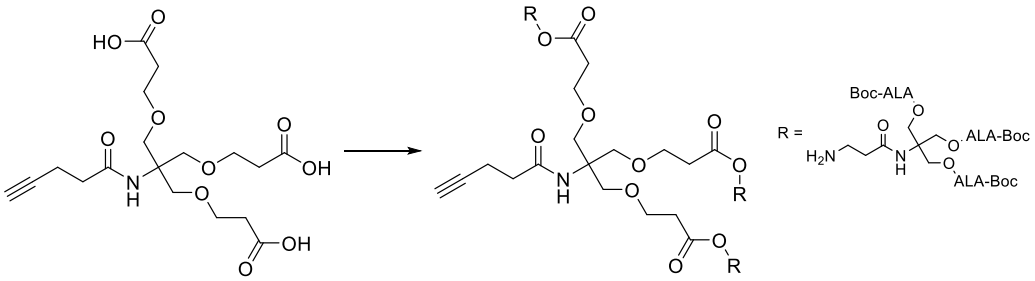

(119) **(115)**

A solution of **(119)** (6.5 mg, 16 µmol) in DMF (2 mL) was pre-activated with

HATU (18 mg, 47 µmol) for 3 min and added to a vial containing **(124)** (56 mg, 62 µmol) in DMF (2 mL). The reaction was stirred at RT for 32 h and monitored by TLC. No disappearance of starting material **(119)** and **(124)** nor appearance of new species was observed.

Diethyl 5-aminobenzene-1,3-dicarboxylate (128)[313]

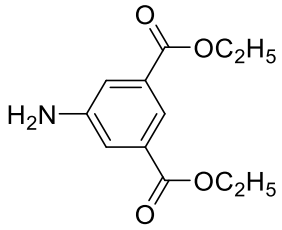

A solution of 5-aminoisophthalic acid **(126)** (3.0 g, 17 mmol) in EtOH (50 mL) was treated with conc. sulfuric acid (1.5 mL) and was heated under reflux for 20 h. The reaction mixture was cooled down and the solvent was evaporated. The residue was diluted with EtOAc (50 mL) and extracted with 10% aq. $NaHCO_3$ (2 x 50 mL) and brine (2 x 50 mL) and dried over $MgSO_4$. The solvent was evaporated under reduced pressure to give the product **(128)** as a white solid (3.06 g, 77%) which was used without further purification. Mp = 118-119 °C (lit. 117-118 °C)[313]; R_f = 0.50 (30% petroleum ether in EtOAc); IR (KBr disc) 3456 (NH), 3362 (NH), 2998 (CH), 1695 (CO); ^{1}H NMR ($CDCl_3$, 400 MHz) δ 1.37 (6H, t, J = 7.2, $COOCH_2C\underline{H}_3$), 3.96 (2H, br, NH_2), 4.35 (4H, q, J = 6.8, $COOC\underline{H}_2CH_3$), 7.51 (2H, d, J = 1.2, 2 x Ar-CH), 8.04 (1H, t, J = 1.6, Ar-CH).

Diethyl 5-(pent-4-ynamido)benzene-1,3-dicarboxylate (129)

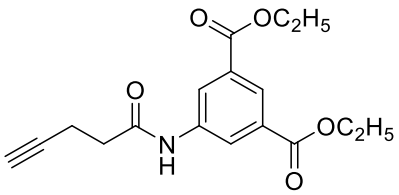

A solution of **(104)** (0.62 g, 6.32 mmol) was treated with EDC.HCl (1.5 g, 7.6 mmol) and HOBt. hydrate (1.64 g, 10.7 mmol) and the mixture was cooled to 0 °C for 40 min. DIEA (4.4 mL, 25.3 mmol) was then added to the reaction mixture and the pH checked (basic). The mixture was then treated with **(128)** (1.5 g, 6.3 mmol) and was stirred at RT under N_2 for 36 h. DMF was then

removed under reduced pressure and the residue was dissolved in a mixture of EtOAc/H_2O (60 mL, 1:1) and the organic layer was washed with 5% aq. citric acid (30 mL), 10% aq. $NaHCO_3$ (30 mL), brine (30 mL), and dried over $MgSO_4$. The organic extract was filtered, and the solvent was evaporated to give the crude product as a colourless solid (2.05 g). Purification by column chromatography on silica gel eluting with 10-30% EtOAc in petroleum ether gave **(129)** as a colourless solid (1.94 g, 97%); Mp = 182-184 °C; R_f = 0.68 (40% EtOAc in petroleum ether); IR (KBr disc) 3364 (NH), 3257 (≡-H), 2991 (CH), 2113 (C≡C), 1706, 1608 (C=C); ^{1}H NMR [$(CD_3)_2CO$, 400 MHz] δ 1.38 (6H, t, J = 7.2, $COOCH_2CH_3$), 2.35-2.36 (1H, m, $HC{\equiv}CCH_2CH_2CO$), 2.55-2.59 (2H, m, $HC{\equiv}CCH_2CH_2CO$), 2.66-2.70 (2H, m, $HC{\equiv}CCH_2CH_2CO$), 4.38 (4H, q, J = 7.2, $COOCH_2CH_3$), 8.28 (1H, t, J = 1.6, Ar-CH), 8.53 (2H, d, J = 1.6, 2 x Ar-CH); ^{13}C NMR [$(CD_3)_2CO$, 100 MHz] δ 14.59 ($COOCH_2CH_3$), 14.88 ($HC{\equiv}CCH_2CH_2CO$), 36.64 ($HC{\equiv}CCH_2CH_2CO$), 61.97 ($COOCH_2CH_3$), 70.36 ($HC{\equiv}CCH_2CH_2CO$), 79.21 ($HC{\equiv}CCH_2CH_2CO$), 124.54 (Ar-CH), 124.63 (Ar-CH), 125.49 (Ar-C), 132.46 (Ar-C), 140.85 (Ar-C), 165.87 (CO), 170.62 (CO); [Found (ESI+) 340.1159 $[M+Na]^+$, $C_{17}H_{19}N_1O_5Na$ requires 340.1160].

5-(pent-4-ynamido)-N^1,N^3-bis(3,3,13,13-tetraisopropyl-2,14-dimethyl-8-(3-((triisopropylsilyl) oxy) propyl)-4,12-dioxa-3,13-disilapentadecan-8-yl) isophthalamide (130)

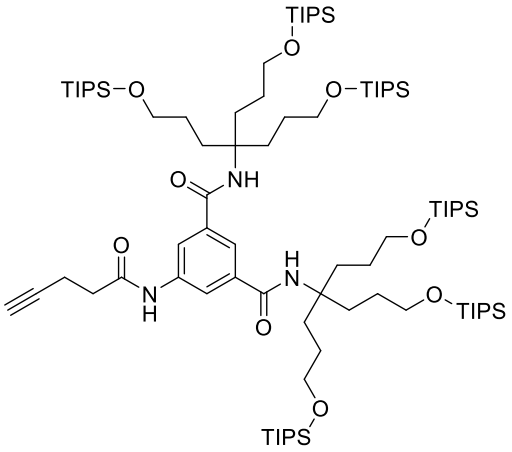

Step 1. Hydrolysis of diethyl 5-(pent-4-ynamido)isophthalate **(129)**

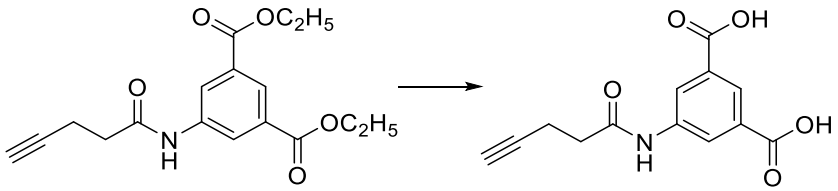

(129) **(127)**

A solution of **(129)** (1.0 g, 3.15 mmol) in MeOH (30 mL) was heated at 55 °C and NaOH (0.38 g, 9.45 mmol) was added. The mixture was stirred for 2 h and the reaction was monitored by TLC which showed disappearance of the starting material and appearance of new species. The reaction mixture was then neutralized with 1M aq. HCl (1.5 mL) and extracted with EtOAc/H_2O (1:1, 30 mL). The combined organic extracts were dried over $MgSO_4$, filtered and the solvent was evaporated to give the crude product as a yellowish solid **(127)** (0.79 g, 96%) which was used in the next step without further purification. IR 3389 (NH), 3257 (≡-H), 3011-2588 (OH broad), 1702 (CO); [Found (ESI+) 260.0564 $[M-H]^+$, $C_{13}H_{10}N_1O_5$ requires 260.0558].

Step 2. Attachment of **(111)**

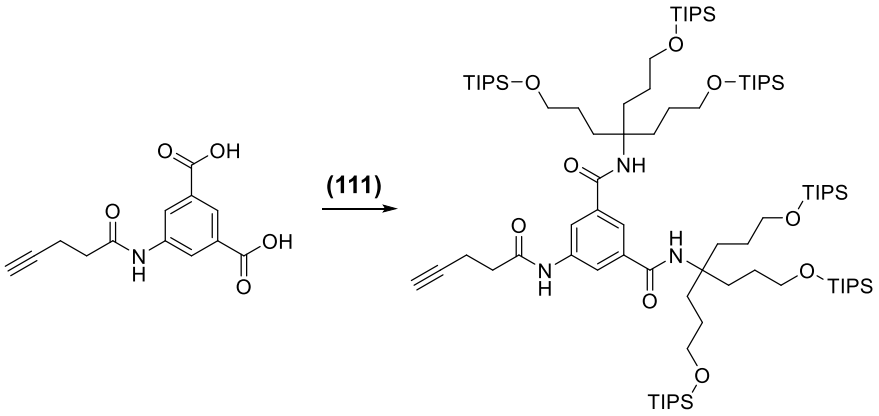

(127) **(130)**

A solution of **(127)** (0.1 g, 0.4 mmol) in DMF (10 mL) was treated with EDC.HCl (0.15 g, 0.76 mmol) and HOBt. hydrate (0.2 g, 1.3 mmol) and the mixture was cooled to 0 °C for 40 min. DIEA (0.26 mL, 1.52 mmol) was then added to the reaction mixture and the pH checked (basic). The mixture was then treated with **(111)** (1.02 g, 1.52 mmol) and was stirred at RT under N_2 for 36 h. DMF was then removed under reduced pressure and the residue was dissolved in a mixture of EtOAc/H_2O (20 mL, 1:1) and the organic layer was washed with 5% aq. citric acid (10 mL), 10% aq. $NaHCO_3$ (10 mL), brine (10 mL) and dried over $MgSO_4$. The organic extract was filtered, and solvent was evaporated to obtain the crude product as a colourless oil (0.62 g). Purification by column chromatography on silica gel eluting with 0-20% EtOAc in petroleum ether gave **(130)** as a colourless oil (0.38 g, 64%); R_f = 0.45 (15% EtOAc in petroleum ether); ^{1}H NMR ($CDCl_3$, 400 MHz) δ 0.97-1.10 (126H, m, 18 x (OSiC<u>H</u>$(CH_3)_2$, 18 x OSiCH(C<u>H</u>$_3)_2$), 1.47-1.54 (12H, m, 6 x CC<u>H</u>$_2$$CH_2CH_2O$), 1.84-1.88 (12H, m, 6 x CCH_2C<u>H</u>$_2$$CH_2O$), 2.051-2.057 (1H, m, C<u>H</u>≡CCH_2CH_2CO), 2.59-2.60 (CH≡CC<u>H</u>$_2$C<u>H</u>$_2$CO), 3.66 (12H, t, J = 6.4, CCH_2CH_2C<u>H</u>$_2$O), 5.88 (2H, s, 2 x N<u>H</u>), 7.79 (1H, s, Ar-C<u>H</u>), 8.06-8.07 (2H, m, 2 x Ar-C<u>H</u>); ^{13}C NMR ($CDCl_3$, 100 MHz) δ 12.05 (OSi<u>C</u>H$(CH_3)_2$), 14.53 (CH≡C<u>C</u>H_2CH_2CO), 18.14 (OSiCH(<u>C</u>H$_3)_2$), 27.01 (CCH_2<u>C</u>H_2CH_2O), 31.53 (C<u>C</u>$H_2CH_2CH_2O$), 36.33 (CH≡CCH_2<u>C</u>H_2CO), 59.47 (<u>C</u>$CH_2CH_2CH_2O$), 63.60 (CCH_2CH_2<u>C</u>H_2O), 70.12 (<u>C</u>H≡CCH_2CH_2CO), 82.60 (CH≡<u>C</u>CH_2CH_2CO), 120.42 (Ar-<u>C</u>H), 120.62 (Ar-<u>C</u>H), 136.88 (Ar-<u>C</u>), 138.69 (Ar-<u>C</u>), 165.46 (CO),

169.90 (CO).

Alkyne-Isophthalic-ALA-Boc (125)

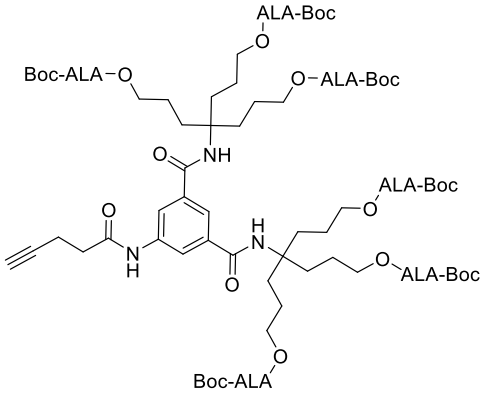

Step 1. Desilylation of **(130)**

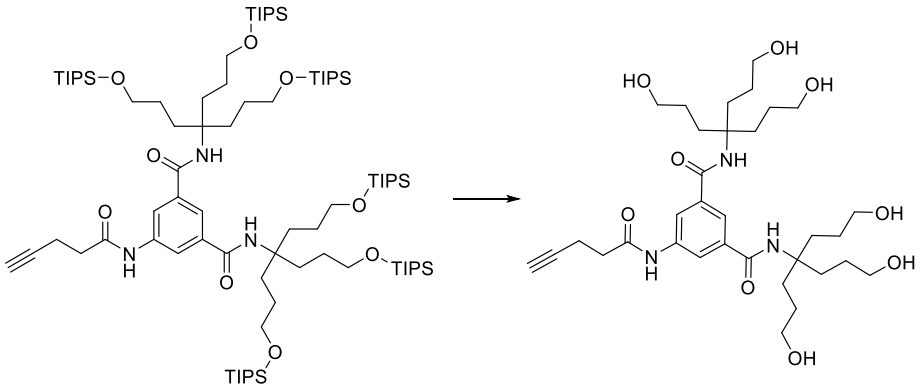

(130) **(131)**

A solution of **(130)** (100 mg, 0.06mmol) in THF (5 mL) was treated with TBAF.H_2O (241 mg, 0.762 mmol) and AcOH (50 µL) was added to the reaction mixture (pH- neutral). The reaction mixture was stirred under N_2 for 4 h at RT and the solvent was removed under reduced pressure. The residue was then dissolved in MeOH (10 mL) and Dowex (50WX8, hydrogen form, 200-400 mesh, 615 mg) and $CaCO_3$ (204 mg) was added to the above solution. The mixture was stirred for 3 h, and then it was filtered through celite, which was washed with MeOH. The solvents were evaporated to give the crude product (75 mg) which was used in the next step without further purification. [Found (ESI+) 636.3853 $[M+H]^+$, $C_{33}H_{54}N_3O_9$ requires 636.3860].

Step 2. Attachment of Boc-ALA **(99)**

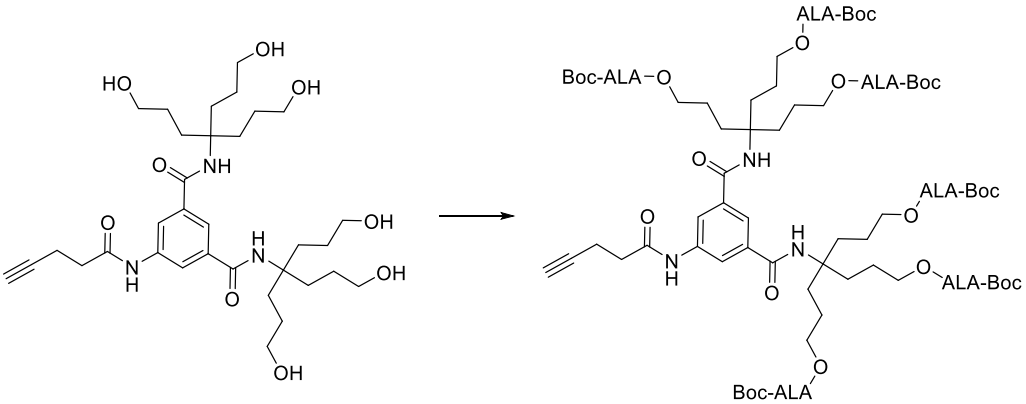

(131) **(125)**

A solution of **(131)** (7.5 mg, 0.01 mmol) in dry DCM (5 mL) was treated with **(99)** (22 mg, 0.10 mmol) and DMAP (1.50 mg, 0.02 mmol). The reaction mixture was cooled in an ice bath for 10 min and EDC.HCl (20 mg, 0.11 mmol) was added. The reaction mixture was stirred under N_2 for 48 h at 30 °C, then the solvent was evaporated and the residue was dissolved in a mixture of EtOAc/H_2O (10 mL, 1:1) and the organic layer was washed with 5% aq. citric acid (5 mL), 10% aq. $NaHCO_3$ (5 mL), brine (5 mL), dried over $MgSO_4$ and concentrated to give the crude product as a yellowish oil (71 mg). Purification by semi-preparative HPLC gave **(125)** as a yellowish oil; R_f = 0.68 (10% acetone in DCM); [Found (ESI+) 979.9798 $[M+2Na]^{2+}$, $C_{93}H_{143}N_9Na_2O_{33}$ requires 979.9786].

2-[2-(2-azidoethoxy) ethoxy] ethanol (134)[230]

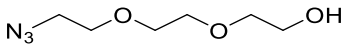

A solution of 2-[2-(2-chloroethoxy) ethoxy] ethanol (1.53 g, 9.07 mmol) in H_2O (5 mL) was treated with sodium azide (1.18 g, 18.1 mmol) and the reaction mixture was heated at 75 °C while stirring for 48 h. The reaction mixture was then cooled down to RT and H_2O was evaporated under reduced pressure. The resulting residue was suspended in diethyl ether (10 mL) and filtered through a sintered funnel. The solvent was evaporated to obtain **(134)** as a colourless liquid (1.58 g, 99%) which was used without further purification. IR (film) 3435 (OH), 2871 (CH), 2101 (N_3); ^{1}H NMR ($CDCl_3$, 400 MHz) δ 3.2-3.4

(2H, m, CH_2N_3), 3.50-3.80 (10H, m, 5 x OCH_2).

1-azido-2-[2-(2-chloroethoxy) ethoxy] ethane (135)[230]

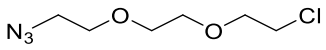

A mixture of **(134)** (1.30 g, 7.37 mmol) and benzyltriethylammonium chloride (BTEAC) (5.00 mg, 0.02 mmol) was heated at 65 °C in a three-necked round bottom flask under Ar. The reaction mixture was treated with $SOCl_2$ (4.30 mL, 59.2 mmol) added dropwise via an addition funnel, and the reaction was stirred for 3 h. After cooling at RT, excess $SOCl_2$ was removed under reduced pressure and the resulting crude product was suspended in phosphate buffer (50 mM, pH 7.0, 20 mL) and extracted with a mixture of EtOAc/petroleum ether (40 mL, 1:1). The organic layer was washed with phosphate buffer (20 mL) and dried over $MgSO_4$. The organic extract was filtered, and solvent was evaporated to give **(135)** as a pale yellow liquid (1.05 g, 74%) which was used without further purification. IR (film) 2892 (CH), 2109 (N_3); ^{1}H NMR ($CDCl_3$, 400 MHz) δ 3.33-3.40 (2H, m, CH_2N_3), 3.58-3.77 (10H, m, 5 x OCH_2).

Methyl- 4-hydroxy benzoate (137)[314]

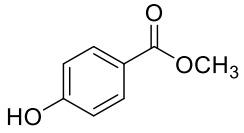

A solution of 4-hydroxybenzoic acid **(136)** (5.00 g, 36.2 mmol) in MeOH (36 mL) was treated with conc. sulfuric acid (0.72 mL) and was heated under reflux for 20 h. The reaction mixture was concentrated down to half the original volume under reduced pressure and was extracted with EtOAc/H_2O (40 mL, 1:1). The organic layer was washed with 1M aq. NaOH (20 mL), H_2O (20 mL), brine (20 mL) and dried over $MgSO_4$. The organic extract was filtered and evaporated to give the crude product as a white solid (2.3 g). Purification by column chromatography on silica gel eluting with 30-70 % EtOAc in petroleum ether gave **(137)** as a white solid (2.21 g, 40.0%); Mp = 125-127 °C (lit. 122-124 °C)[314]; R_f = 0.78 (30% petroleum ether in EtOAc; IR (film) 3299 (OH), 1682 (C=O); ^{1}H NMR (CD_3OD, 500 MHz) δ 3.74 (3H, s, OCH_3), 6.71

(2H, d, J = 9.0, Ar-CH), 7.76 (2H, d, J = 9.0, Ar-CH).

Methyl (4-(2-(2-(2-Azidoethoxy)ethoxy)ethoxy)benzoate (138)[315]

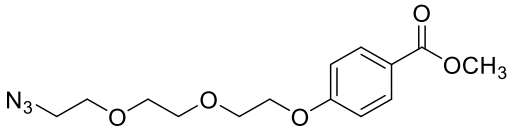

A stirred solution of **(135)** (0.4 g, 2 mmol) in DMF (18 mL) was treated with **(137)** (0.29 g, 1.90 mmol), dry K_2CO_3 (0.88 g, 6.3 mmol) and 18-crown-6 (0.02 g, 0.06 mmol). The mixture was heated at 80 °C for 36 h under N_2, and was partitioned between EtOAc and H_2O (30 mL, 1:1). The aqueous phase was extracted with EtOAc (15 mL) and the combined organic extracts were washed with brine (2 x 30 mL) and dried over $MgSO_4$. The organic extract was filtered and evaporated to give the crude product as a colourless oil. Purification by column chromatography on silica gel eluting with EtOAc/petroleum (2:1) gave **(138)** as a colourless oil (0.41 g, 75%); R_f = 0.35 (EtOAc: petroleum ether, 3:7); IR (film) 2951 (CH), 2879 (CH), 2106 (N_3), 1714 (CO), 1607 (C=C); ^{1}H NMR ($CDCl_3$, 500 MHz) δ 3.30 (2H, t, J = 5.0, CH_2N_3), 3.59-3.62 (4H, m, 2 x OCH_2), 3.65-3.69 (2H, m, OCH_2), 3.80-3.82 (5H, m, OCH_3, OCH_2), 4.11 (2H, t, J = 5.0, OCH_2), 6.85 (2H, d, J = 8.5, Ar-CH) 7.90 (2H, d, J = 8.5, Ar-CH); ^{13}C NMR ($CDCl_3$, 100 MHz) δ 50.72 (CH_2N_3), 51.93 (OCH_3), 67.61 (OCH_2), 67.61 (OCH_2), 69.70 (OCH_2) 70.17 (OCH_2) 70.80 (OCH_2) 70.98 (OCH_2), 114.24 (Ar-CH), 122.77 (Ar-C), 131.61 (Ar-CH), 162.60 (CO), 166.89 (Ar-C); [Found (ESI+) 310.1425 $[M+H]^+$, $C_{14}H_{20}N_3O_5$ requires 310.1402].

4-(2-(2-(2-Azidoethoxy)ethoxy)ethoxy)benzoic acid (142)[315]

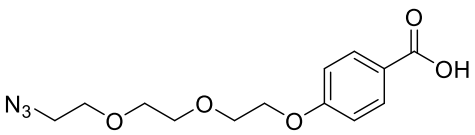

A solution of **(138)** (0.1 g, 0.3 mmol) in THF (3 mL) was treated with KOH (0.02 g, 0.40 mmol) in H_2O (0.5 mL) and the reaction was stirred at 50 °C for 24 h. The reaction mixture was then neutralized with 1M aq. HCl (0.3 mL) and extracted with EtOAc/H_2O (1:1, 20 mL) and combined organics were dried over

$MgSO_4$. The organic extract was filtered and evaporated to give the crude product as white solid (99 mg). Purification by column chromatography on silica gel eluting with 0-40 % EtOAc in petroleum ether gave **(142)** as a white solid (83 mg, 87%); Mp = 75-77 °C (Uncorrected); R_f = 0.2 (EtOAc: Petroleum ether, 2:8); IR (film) 3005-2665 (OH broad), 2908 (CH), 2111 (N_3), 1705 (CO); Analytical HPLC (Gradient 1) R_t = 7.89 min; ^{1}H NMR ($CDCl_3$, 400 MHz) δ 3.38 (2H, t, J = 5.0, CH_2N_3), 3.66-3.70 (4H, m, 2 x OCH_2), 3.73-3.77 (2H, m, OCH_2), 3.88-3.92 (2H, m, OCH_2), 4.18-4.22 (2H, m, OCH_2), 6.95 (2H. d, J = 9.2, Ar-CH), 8.04 (2H, d, J = 8.8, Ar-CH); ^{13}C NMR ($CDCl_3$, 100 MHz) δ 50.77 (CH_2N_3), 67.71 (OCH_2), 69.73 (OCH_2), 70.25 (OCH_2), 70.86 (OCH_2), 71.04 (OCH_2), 114.41 (Ar-CH), 121.89 (Ar-C), 132.43 (Ar-CH), 163.36 (CO), 171.85 (Ar-C); [Found (ESI+) 318.1065 $[M+Na]^+$, $C_{13}H_{17}N_3NaO_5$ requires 318.1065].

Methyl 3,4,5-tris(2-(2-(2-azidoethoxy)ethoxy)ethoxy)benzoate (140)[230]

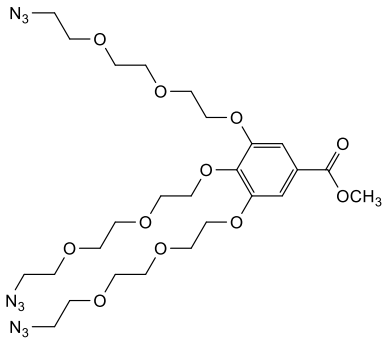

A solution of **(135)** (2.80 g, 14.5 mmol) in DMF (40 mL) was treated with methyl gallate **(139)** (0.84 g, 4.59 mmol), dry K_2CO_3 (6.48 g, 46.8 mmol) and 18-crown-6 (0.10 g, 0.40 mmol) and the resulting suspension was heated at 80 °C under N_2 for 36 h. After cooling down to RT, the solvent was evaporated and the residue was extracted with EtOAc and H_2O (80 mL, 1:1). The aqueous phase was extracted with EtOAc (40 mL) and the combined organic phases were washed with brine (2 x 40 mL) and dried over $MgSO_4$. The organic extract was filtered, and solvent was evaporated to obtain the crude product (2.85 g). Purification by column chromatography on silica gel eluting with EtOAc gave **(140)** as a dark yellow oil (2.16 g, 72%); R_f = 0.42 (EtOAc); IR (film) 2902 (CH), 2112 (N_3), 1718 (CO); ^{1}H NMR ($CDCl_3$, 400 MHz) δ 3.37-3.42 (6H, m, 3 x OCH_2), 3.59-3.86 (27H, m, OCH_3 + 12 x OCH_2), 4.16-4.22 (6H, m, 3 x OCH_2),

7.26 (2H, s, Ar-CH).

3,4,5-Tris(2-(2-(2-azidoethoxy)ethoxy)ethoxy)benzoic acid (147)

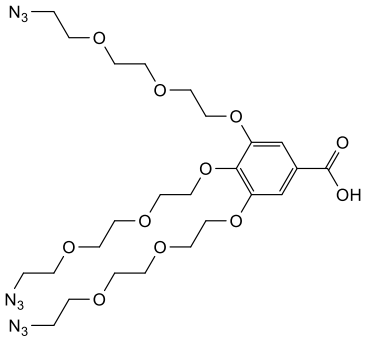

A solution of **(140)** (0.55 g, 0.84 mmol) in THF (6 mL) was treated with KOH (0.06 g, 1.05 mmol) in H_2O (1 mL) and the reaction was stirred at 50 °C for 24 h. The reaction mixture was then neutralized with 1M aq. HCl (0.5 mL) and extracted with EtOAc/H_2O (1:1, 40 mL) and combined organics were dried over $MgSO_4$. The organic extract was filtered and evaporated under reduced pressure to give **(147)** as yellowish oil (0.5 g, 94%) which was used in next step without further purification. R_f = 0.3 (EtOAc: Petroleum ether, 2:8); IR (film) 3025-2776 (OH broad), 2908 (CH), 2111 (N_3), 1705 (CO); ^{1}H NMR ($CDCl_3$, 400 MHz) δ 3.36-3.40 (6H, m, 3 x OCH_2), 3.64-3.90 (24H, m, 12 x OCH_2), 4.20-4.27 (6H, m, 3 x OCH_2), 7.36 (2H, s, Ar-CH).

Dend-(Tris-ALA-Boc) (143)

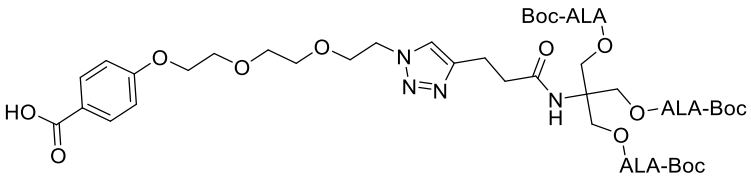

A solution of **(138)** (5.40 mg, 18.3 µmol) and **(105)** (20.0 mg, 23.7 µmol) in DMSO (4.25 mL) was treated with 1M aq. $CuSO_4$ (25.0 µL, 23.7 µmol), a solution of sodium ascorbate (90.5 mg, 0.46 mmol) in H_2O (250 µL) and *t*-BuOH (450 µL). The reaction mixture was left stirring for 12 h and monitored by analytical HPLC (Gradient 1) which showed complete disappearance of **(138)** and formation of new species at 9.43 min. The crude product was purified by semi-preparative HPLC (Gradient 2) to give **(143)** as a white solid (11 mg,

53%); Analytical HPLC (Gradient 1) R_t = 9.43 min; ^{1}H NMR ($CDCl_3$, 400 MHz) δ 1.43 (27H, s, 3 x $C(CH_3)_3$), 2.58-2.61 (6H, m, 3 x $C\underline{H}_2CH_2CO$), 2.67-2.73 (8H, m, 3 x $CH_2C\underline{H}_2CO$ + $CH_2C\underline{H}_2CONH$), 2.99-3.05 (2H, m, $C\underline{H}_2CH_2CONH$), 3.64-3.69 (4H, m, 2 x OCH_2), 3.84-3.88 (4H, m, 2 x OCH_2), 4.02 (6H, s, 3 x $COC\underline{H}_2NH$), 4.20-4.22 (2H, m, OCH_2), 4.31 (6H, s, 3 x CCH_2), 4.54-4.57 (2H, m, OCH_2), 5.48 (3H, s, 3 x $COCH_2N\underline{H}$), 5.96 (1H, s, $CH_2CH_2CON\underline{H}$), 6.93-6.95 (2H, m, Ar-CH), 7.78 (1H, s, triazole CH), 8.00-8.02 (2H, m, Ar-CH); ^{13}C NMR ($CDCl_3$, 100 MHz) 20.32 ($\underline{C}H_2CH_2CONH$), 27.78 ($\underline{C}H_2CH_2CO$), 28.44 ($C(\underline{C}H_3)_3$), 34.39 ($CH_2\underline{C}H_2CO$), 35.19 ($CH_2\underline{C}H_2CONH$), 50.27 ($CO\underline{C}H_2NH$), 51.69 (OCH_2), 58.29 ($\underline{C}CH_2O$), 62.37 ($C\underline{C}H_2O$), 67.77 (OCH_2), 68.89 (OCH_2), 69.73 (OCH_2), 70.70 (OCH_2), 70.83 (OCH_2), 80.21 ($\underline{C}(CH_3)_3$), 114.48 (Ar-CH), 125.26 (triazole-CH), 132.37 (Ar-CH), 156.22 (CO), 163.12 (Ar-C), 169.85 (CO), 172.02 (CO), 172.64 (CO), 204.88 (CO); [Found (ESI+) 1136.5245 $[M+H]^+$, $C_{52}H_{78}N_7O_{21}$ requires 1136.5226].

Dend-(Tris-ALA) .3TFA (145)

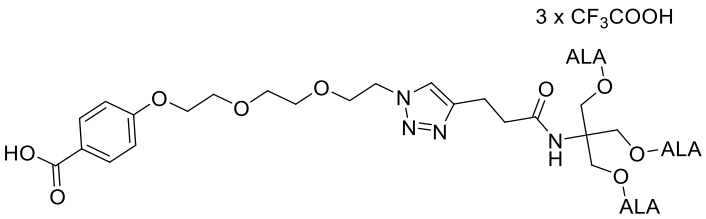

A solution of **(143)** (20.0 mg, 17.6 µmol) in DCM (4 mL) was treated with TFA (4 mL) at 0 °C and the reaction mixture was stirred for 30 min and monitored by HPLC which showed complete disappearance of starting material. The solvent was evaporated under vacuum and the residue was co-evaporated with Et_2O (x 3) to remove excess TFA. This material was freeze-dried from H_2O to give **(145)** as a off-white solid (18 mg, 92%); Analytical HPLC (Gradient 1) R_t = 4.80 min); ^{1}H NMR (CD_3OD, 400 MHz) 2.58 (2H, t, J = 7.6, $CH_2C\underline{H}_2CONH$), 2.64-2.70 (6H, m, 3 x $C\underline{H}_2CH_2CO$), 2.81-2.89 (6H, m, 3 x $CH_2C\underline{H}_2CO$), 2.91-2.94 (2H, m, $C\underline{H}_2CH_2CONH$), 3.61-3.64 (2H, m, OCH_2), 3.66-3.69 (2H, m, $NHCOCH_2C\underline{H}_2$), 3.79-3.85 (2H, m, OCH_2), 3.87 (2H, t, J = 5.0, OCH_2), 4.05 (6H, s, 3 x $NH_2C\underline{H}_2CO$), 4.16-4.21 (2H, m, OCH_2), 4.39 (6H, s, 3 x $CC\underline{H}_2O$), 4.54 (2H, t, J = 5.0, OCH_2), 6.96-7.02 (2H, m, Ar-CH), 7.80 (1H, m, triazole CH), 7.93-7.99 (2H, m, Ar-CH); ^{13}C NMR (CD_3OD, 100 MHz) 22.13

($\underline{C}H_2CH_2CONH$) 28.27 ($\underline{C}H_2CH_2CO$), 35.29 ($CH_2\underline{C}H_2CO$), 36.41 ($CH_2\underline{C}H_2CONH$), 48.14 ($CO\underline{C}H_2NH_2$), 51.44 (OCH_2), 63.29 ($C\underline{C}H_2O$), 68.83 (OCH_2), 70.35(OCH_2), 70.59 (OCH_2), 71.41 (OCH_2), 71.64 (OCH_2), 115.30 (Ar-CH), 124.23 (triazole CH), 132.86 (Ar-CH), 147 (CO), 164.16 (Ar-C), 169.70 (CO), 173.51 (CO), 174.98 (CO), 203.18 (CO); [Found (ESI+) 836.3694 $[M+H]^+$, $C_{37}H_{54}N_7O_{15}$ requires 836.3677].

Dend-(Ext.Tris-ALA-Boc) (144)

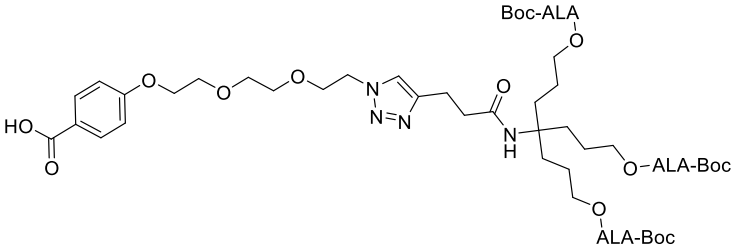

A solution of alkyne **(107)** (85.0 mg, 0.10 mmol) and azide **(138)** (15 mg, 0.05 mmol) in DMSO/ H_2O (9:1, 1.5 mL) was treated with 1M aq $CuSO_4$ (50.0 µL, 0.05 mmol) and sodium ascorbate (149 mg, 0.75 mmol). The reaction was stirred for 12 h and monitored by analytical HPLC (Gradient 1) which showed complete disappearance of **(138)** and formation of a new species at 9.62 min. The reaction mixture was purified by semi-preparative HPLC (Gradient 2) to give **(144)** as white solid (26.7 mg, 44%); Analytical HPLC (Gradient 1) R_t = 9.62 min); ^{1}H NMR ($CDCl_3$, 400 MHz) 1.37-1.46 (33H, m, 3 x $C(C\underline{H}_3)_3$, 3 x $CC\underline{H}_2CH_2CH_2$), 1.62-1.66 (6H, m, 3 x $CCH_2C\underline{H}_2CH_2$), 2.59-2.62 (6H, m, 3 x $C\underline{H}_2CH_2CO$), 2.70-2.73 (8H, m, 3 x $CH_2C\underline{H}_2CO$, $CH_2C\underline{H}_2CONH$), 3.09 (2H, t, J = 7.2, $C\underline{H}_2CH_2CONH$), 3.63-3.68 (4H, m, 2 x OCH_2), 3.82-3.84 (2H, m, OCH_2), 3.87-3.89 (2H, m, OCH_2), 3.98-4.04 (12H, m, 3 x $COC\underline{H}_2NH$, 3 x $CCH_2CH_2C\underline{H}_2$), 4.18-4.20 (2H, m, OCH_2), 4.53-4.56 (2H, m OCH_2), 5.51 (3H, s, 3 x $COCH_2N\underline{H}$), 6.32 (1H, s, $CH_2CH_2CON\underline{H}$), 6.68 (1H, s, $N\underline{H}COCH_2CH_2$), 6.92-6.94 (2H, m, Ar-CH), 7.77 (1H, s, triazole CH), 7.99-8.01 (2H, m, Ar-CH); ^{13}C NMR ($CDCl_3$, 100 MHz) 21.22 ($\underline{C}H_2CH_2CONH$), 22.63 ($C\underline{C}H_2CH_2CH_2$), 27.95 ($\underline{C}H_2CH_2CO$), 28.46 ($C(\underline{C}H_3)_3$), 31.24 ($CCH_2\underline{C}H_2CH_2$), 34.47 ($CH_2\underline{C}H_2CO$), 35.88 ($CH_2\underline{C}H_2CONH$), 50.37 ($CO\underline{C}H_2NH$), 51.33 ($OCH_2$), 58.34 ($\underline{C}CH_2CH_2CH_2O$), 64.81 ($CCH_2CH_2\underline{C}H_2$), 67.77 ($OCH_2$), 69.11 ($OCH_2$), 69.75 ($OCH_2$), 70.71 ($OCH_2$), 70.87 ($OCH_2$), 80.05 ($\underline{C}(CH_3)_3$), 114.46 (Ar-CH),

122.48 (triazole-CH), 132.32 (Ar-CH), 156.04 (CO), 163.03 (Ar-C), 169.46 (CO), 171.86 (CO), 172.54 (CO), 204.87 (CO); [Found (ESI+) 1218.6053 $[M-H]^+$, $C_{58}H_{88}N_7O_{21}$ requires 1218.6039].

Dend-(Ext.Tris-ALA) .3TFA (146)

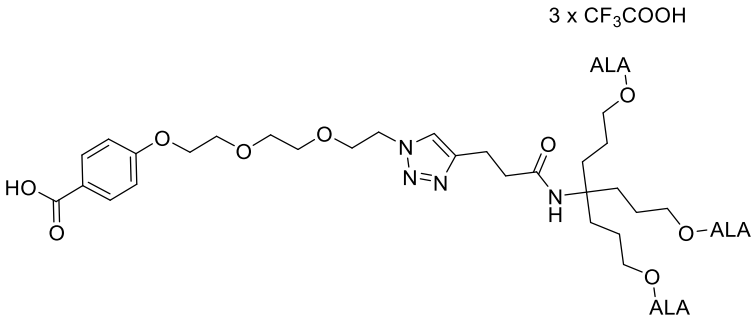

A solution of **(145)** (25 mg, 20 µmol) in DCM (5 mL) was treated with TFA (5 mL) at 0 °C and reaction mixture was stirred for 30 min and monitored by HPLC (Gradient 1) which showed complete disappearance of **(145)** and formation of new species at 4.98 min. The solvent was evaporated under vacuum and residue was co-evaporated with Et_2O (x 3) to remove excess TFA. This material was freeze-dried from H_2O to give **(146)** as a off-white solid (23.8 mg, 94%); Analytical HPLC (Gradient 1) R_t = 4.98 min; ^{1}H NMR (CD_3OD, 400 MHz) δ 1.43-53 (6H, m, 3 x $CCH_2CH_2CH_2$), 1.64-1.72 (6H, m, 3 x $CCH_2CH_2CH_2$), 2.53 (2H, t, J = 7.6, CH_2CH_2CONH), 2.63-2.70 (6H, m, CH_2CH_2CO), 2.79-2.87 (6H, m, CH_2CH_2CO), 2.93 (2H, t, J = 7.2, CH_2CH_2CONH), 3.61-3.65 (2H, m, OCH_2), 3.67-3.71 (2H, m, OCH_2), 3.80-3.84 (2H, m, OCH_2), 3.85-3.91 (2H, m, OCH_2), 4.00-4.07 (12H, m, 3 x $COCH_2NH$, 3 x $CCH_2CH_2CH_2$), 4.17-4.21 (2H, m, OCH_2), 4.51-4.56 (2H, m, OCH_2), 6.97-7.02 (2H, m, Ar-CH), 7.81 (1H, s, triazole CH), 7.94-7.99 (2H, m, Ar-CH); ^{13}C NMR (CD_3OD, 100 MHz) 22.64 (CH_2CH_2CONH), 23.60 (CH_2CH_2CO), 28.52 ($CCH_2CH_2CH_2O$), 31.77 (CH_2CH_2CONH), 35.30 ($CCH_2CH_2CH_2O$), 36.82 (CH_2CH_2CO), 48.15 ($COCH_2NH_2$), 51.41 (OCH_2), 59.10 ($CCH_2CH_2CH_2O$), 66.03 ($CCH_2CH_2CH_2O$), 68.87 (OCH_2), 70.42 (OCH_2), 70.64 (OCH_2), 71.45 (OCH_2), 71.69 (OCH_2), 115.32 (Ar-CH), 124.30 (triazole-CH), 132.89 (Ar-CH), 164.18 (Ar-C), 169.67 (CO), 174.10 (CO), 203.12 (CO); [Found (ESI+) 920.4649 $[M+H]^+$, $C_{43}H_{66}N_7O_{15}$ requires 920.4616].

Dend-(Tris-ALA-Boc)$_3$ (148)

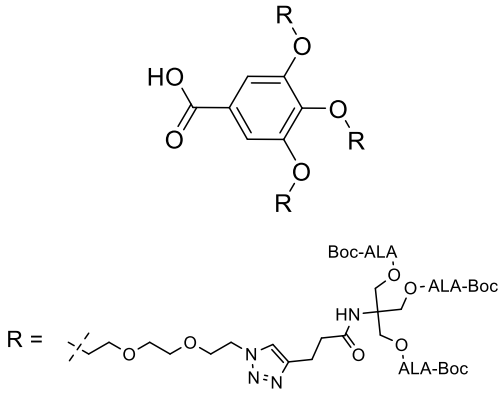

A solution of **(147)** (10.0 mg, 15.5 µmol) and **(105)** (78.6 mg, 93.5 µmol) in DMSO/ H_2O (9:1, 2 mL) was treated with 1M aq. $CuSO_4$ (0.14 mL, 0.14 mmol) and sodium ascorbate (108 mg, 0.55 mmol) were added. The reaction was stirred for 72 h and monitored by analytical HPLC (Gradient 1) which showed complete disappearance of **(147)** and formation of new species at 10.53 min. The reaction mixture was purified by semi-preparative HPLC (Gradient 2) to obtain **(148)** as a white solid (24.5 mg, 50%); Analytical HPLC (Gradient 1) R_t = 10.53 min; ^{1}H NMR (CD_3OD, 500 MHz) δ 1.43-1.49 (81H, s, 9 x C(CH_3)$_3$), 2.57-2.65 (24H, m, 9 x CH_2CH_2CO, 3 x CH_2CH_2CONH), 2.74-2.82 (18H, m, 9 x CH_2CH_2CO), 2.92-2.99 (6H, m, 3 x CH_2CH_2CONH), 3.60-3.72 (12H, m, 6 x OCH_2), 3.75-3.79 (2H, m, OCH_2), 3.83-3.97 (28H, m, 5 x OCH_2, 9 x $COCH_2NH$), 4.20-4.25 (6H, m, 3 x OCH_2), 4.35-4.42 (18 H, s, 9 x CCH_2O), 4.55-4.60 (6H, m, 3 x OCH_2), 7.38 (2H, s, Ar-CH), 7.83-7.88 (3H, m, triazole CH); ^{13}C NMR (CD_3OD, 125 MHz) 24.21 (CH_2CH_2CONH), 28.59 (CH_2CH_2CO), 28.77 (C(CH_3)$_3$), 35.01 (CH_2CH_2CO), 36.30 (CH_2CH_2CONH), 50.75 ($COCH_2NH$), 51.60 (OCH_2), 59.17 (CCH_2O), 63.18 (CCH_2O), 70.11 (OCH_2), 70.39 (OCH_2), 70.81 (OCH_2), 71.53 (OCH_2), 73.68 (OCH_2), 80.61 (C(CH_3)$_3$), 110.10 (Ar-CH), 124.83 (triazole CH), 127.01 (Ar-C), 143.56 (Ar-C), 158.41 (CO), 169.17 (CO), 173.64 (CO), 174.76 (CO), 207.40 (CO); [Found (ESI+) 1604.2249 $[M+2H]^{2+}$, $C_{142}H_{219}N_{21}O_{59}$ requires 1604.2283].

Dend-(Tris-ALA)$_3$ .9TFA (150)

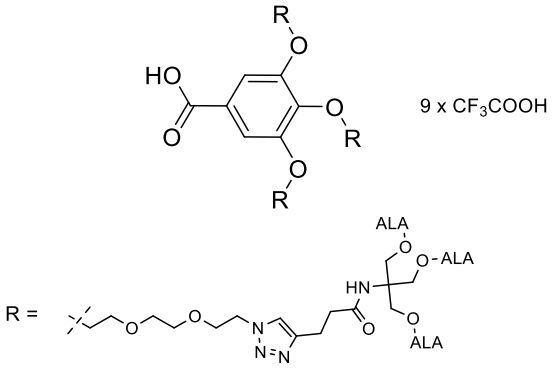

A solution of **(148)** (20 mg, 6.32 µmol) in DCM (5 mL) was treated with TFA (5 mL) at 0 °C and the reaction mixture was stirred for 30 min and monitored by HPLC (Gradient 1) which showed complete disappearance of starting material **(148)**. The solvent was evaporated under vacuum and the residue was co-evaporated with Et_2O (x 3) to remove excess TFA. This material was freeze-dried from H_2O to give **(150)** as a off-white solid (17.5 mg, 88.0%); Analytical HPLC (Gradient 1) R_t = 4.35 min; ^{1}H NMR (CD_3OD, 400 MHz) δ 2.59 (6H, t, J = 7.4, 3 x $CH_2C\underline{H}_2CONH$), 2.65-2.69 (18H, m, 9 x $C\underline{H}_2CH_2CO$), 2.84-2.87 (18H, m, 9 x $CH_2C\underline{H}_2CO$), 2.92 (6H, t, J = 7.4, 3 x $C\underline{H}_2CH_2CONH$), 3.60-3.68 (12H, m, 6 x OCH_2), 3.73-3.76 (2H, m, OCH_2), 3.82-3.89 (10H, m, 5 x OCH_2), 4.05 (18H, s, 9 x $COC\underline{H}_2NH_2$), 4.19-4.22 (6H, m , 3 x OCH_2), 4.39 (18H, s, 9 x $CC\underline{H}_2O$), 4.52-4.54 (6H, m, 3 x OCH_2), 7.37 (2H, s, Ar-CH), 7.78-7.79 (3H, m, triazole CH); ^{13}C NMR (CD_3OD, 125 MHz) 22.22 ($\underline{C}H_2CH_2CONH$), 28.28 ($\underline{C}H_2CH_2CO$), 35.27 ($CH_2\underline{C}H_2CO$), 36.45 ($CH_2\underline{C}H_2CONH$), 48.10 ($COCH_2NH_2$), 51.29 (OCH_2), 51.37 (OCH_2), 59.12 ($\underline{C}CH_2O$), 63.32 ($C\underline{C}H_2O$), 69.98 (OCH_2), 70.44 (OCH_2), 70.76 (OCH_2), 71.29 (OCH_2), 71.47 (OCH_2), 71.59 (OCH_2), 71.70 (OCH_2), 73.64 (OCH_2), 110.04 (Ar-CH), 124.38 (triazole CH), 127.31 (Ar-C), 143.13 (Ar-C), 147.57 (triazole-C), 153.60 (Ar-C), 169.20 (CO), 173.55 (CO), 175.05 (CO), 203.24 (CO); [Found (ESI+) 1132.0125 $[M+2H]^{2+}$, $C_{97}H_{149}N_{21}O_{41}$ requires 1132.0104].

Dend-(Ext.Tris-ALA-Boc)$_3$ (149)

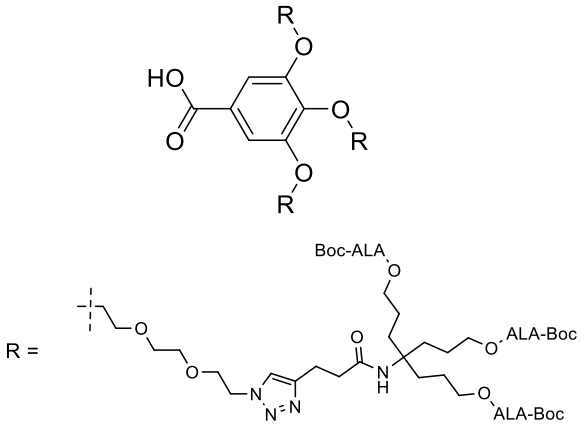

A solution of **(147)** (5.8 mg, 9.0 µmol) and **(107)** (50 mg, 54 µmol) in DMSO/ H_2O (9: 1, 2 mL) was treated with 1M aq. $CuSO_4$ (80 µL, 80 µmol) and sodium ascorbate (44.6 mg, 0.23 mmol). The reaction was stirred for 72 h and monitored by analytical HPLC (Gradient 1) which showed complete disappearance of **(147)** and formation of a new species at 11.03 min. The reaction mixture was purified by semi-preparative HPLC (Gradient 2) to give **(149)** as a white solid (16 mg, 52%); Analytical HPLC (Gradient 1) R_t = 11.03 min; ^{1}H NMR (CD_3OD, 500 MHz) δ 1.40-1.52 (99H, m, 9 x C($C\underline{H}_3$)$_3$, 9 x $C\underline{H}_2CH_2CO$), 1.64-1.73 (18H, m, 9 x $CC\underline{H}_2CH_2CH_2O$), 2.52-2.59 (24H, m, 9 x $C\underline{H}_2CH_2CO$, 3 x $CH_2C\underline{H}_2CONH$), 2.71-2.78 (18H, m, 9 x $CH_2C\underline{H}_2CO$), 2.90-2.98 (6H, m, 3 x $C\underline{H}_2CH_2CONH$), 3.57-3.67 (12H, m, 6 x OCH_2), 3.72-3.76 (2H, m, OCH_2), 3.80-3.94 (28H, m, 9 x $COC\underline{H}_2NH_2$, 5 x OCH_2), 3.98-4.05 (18H, m, 9 x $CCH_2CH_2C\underline{H}_2O$), 4.18-4.22 (6H, m, 3 x OCH_2), 4.51-4.54 (6H, m, 3 x OCH_2), 7.36 (2H, s, Ar-CH), 7.81 (3H, s, triazole CH); ^{13}C NMR (CD_3OD, 125 MHz) 22.57 ($\underline{C}H_2CH_2CONH$), 23.62 ($CCH_2\underline{C}H_2CH_2O$), 28.57 ($\underline{C}H_2CH_2CO$), 28.75 (C($\underline{C}H_3$)$_3$), 31.78 ($C\underline{C}H_2CH_2CH_2O$), 35.03 ($CH_2\underline{C}H_2CO$), 36.79 ($CH_2\underline{C}H_2CONH$), 50.80 ($CO\underline{C}H_2NH$), 51.42 ($OCH_2$) 51.93 ($OCH_2$), 59.12 ($\underline{C}CH_2CH_2CH_2O$), 65.91 ($CCH_2CH_2\underline{C}H_2O$), 70.13 ($OCH_2$), 70.45 ($OCH_2$), 70.82 ($OCH_2$), 73.69 ($OCH_2$), 80.56 ($\underline{C}(CH_3)_3$), 110.15 (Ar-CH), 124.48 (triazole CH), 127.05 (Ar-C), 143.61 (Ar-C), 153.70 (Ar-C), 158.35 (CO), 169.10 (CO), 174.34 (CO), 207.43 (CO); [Found (ESI+) 1708.3880 $[M+2H]^{2+}$, $C_{160}H_{257}N_{21}O_{59}$ requires 1708.3872].

Dend-(Ext.Tris-ALA)$_3$ .9TFA (151)

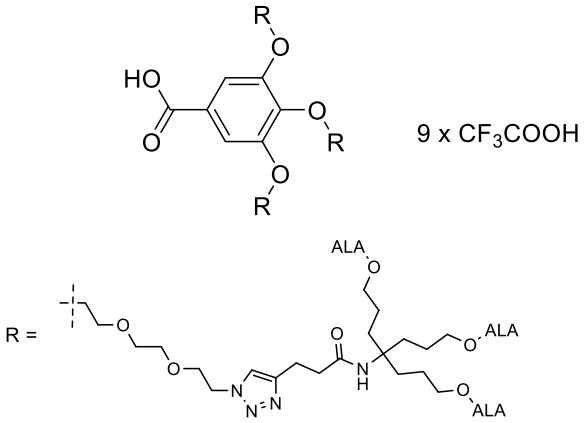

A solution of **(149)** (15.5 mg, 4.53 µmol) in DCM (6 mL) was treated with TFA (6 mL) at 0 °C and the reaction mixture was stirred for 30 min and monitored by HPLC (Gradient 1) which showed complete disappearance of starting material **(149)**. The solvent was evaporated under vacuum and the residue was co-evaporated with Et_2O (x 3) to remove excess TFA. This material was freeze-dried from H_2O to give **(151)** as a off-white solid (13.8 mg, 90%); Analytical HPLC (Gradient 1) R_t = 4.63 min; ^{1}H NMR (CD_3OD, 500 MHz) δ 1.43-53 (18H, m, 9 x CC$\underline{H}_2CH_2CH_2$), 1.64-1.74 (18H, m, 9 x $CCH_2C\underline{H}_2CH_2$), 2.51-2.58 (6H, m, 3 x $CH_2C\underline{H}_2CONH$), 2.63-2.69 (18H, m, 9 x $C\underline{H}_2CH_2CO$), 2.80-2.89 (18H, m, 9 x $CH_2C\underline{H}_2CO$), 2.92-2.97 (6H, m, 3 x $C\underline{H}_2CH_2CONH$), 3.60-3.68 (12H, m, 6 x OCH_2), 3.72-3.75 (2H, m, OCH_2), 3.80-3.85 (4H, m, 2 x OCH_2), 3.86-3.91 (6H, m, 3 x OCH_2), 4.02-4.08 (36H, m, 9 x $COC\underline{H}_2NH_2$, 9 x $CCH_2CH_2C\underline{H}_2$), 4.17-4.21 (6H, m, 3 x OCH_2), 4.52-4.55 (6H, m, 3 x OCH_2), 7.37 (2H, m, Ar-CH), 7.82 (3H, s, triazole-CH); ^{13}C NMR (CD_3OD, 125 MHz) δ 22.66 ($\underline{C}H_2CH_2CONH$), 23.60 ($\underline{C}H_2CH_2CO$), 28.52 ($CCH_2\underline{C}H_2CH_2O$), 31.76 ($CH_2\underline{C}H_2CONH$), 35.33 ($C\underline{C}H_2CH_2CH_2O$), 36.80 ($CH_2\underline{C}H_2CO$), 48.15 ($CO\underline{C}H_2NH_2$), 51.35 ($OCH_2$), 59.11 ($\underline{C}CH_2CH_2CH_2O$), 66.04 ($CCH_2CH_2\underline{C}H_2O$), 70.00 ($OCH_2$), 70.45 ($OCH_2$), 70.77 ($OCH_2$), 71.33 ($OCH_2$), 71.48 ($OCH_2$), 71.61 ($OCH_2$), 71.71 ($OCH_2$), 73.64 ($OCH_2$), 110.05 (Ar-CH), 124.34 (triazole CH), 127.31 (Ar-C), 143.17 (triazole-C), 153.62 (CO), 161.58 (Ar-C), 169.15 (CO), 174.11 (CO), 203.19 (CO); [Found (ESI+) 839.1056 $[M+3H]^{3+}$, $C_{115}H_{186}N_{21}O_{41}$ requires 839.1033].

(R)-2,5,7,8-tetramethyl-2-((4S,8S)-4,8,12-trimethyltridecyl)chroman-6-yl 4-(2-(2-(2-azidoethoxy)ethoxy)ethoxy)benzoate (153)

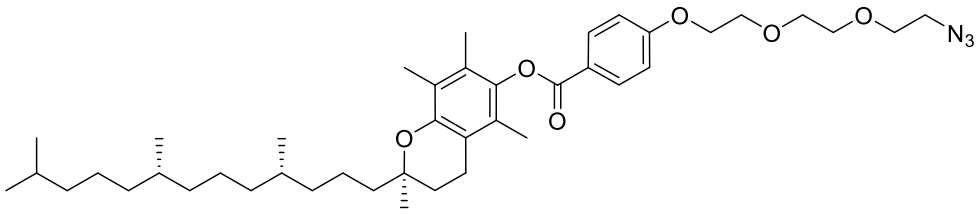

A solution of **(142)** (0.15 g, 0.5 mmol) in dry DCM (15 mL) was treated with **(152)** (0.2 g, 0.46 mmol) and DMAP (5 mg, 46 µmol). The reaction mixture was cooled in an ice bath for 10 min and EDC.HCl (0.11 g, 0.55 mmol) was added. The reaction was stirred at 32 °C for 36 h under N_2, then the solvent was evaporated and the residue was dissolved in a mixture of EtOAc/H_2O (30 mL, 1:1). The organic layer was washed with 5% aq. citric acid (15 mL), 10% aq. $NaHCO_3$ (15 mL), brine (15 mL), dried over $MgSO_4$ and concentrated to give the crude product as a colourless oil (0.34 g). The crude product was purified by semi-preparative HPLC (Gradient 4) to give **(153)** as colourless oil (0.24 g, 75%); Analytical HPLC (Gradient 3) R_t = 10.1 min; ^{1}H NMR ($CDCl_3$, 400 MHz) δ 0.84-0.89 (12H, m, 4 x CH_3), 1.01-1.57 (24H, m, 9 x CH_2, 3 x CH, CH_3), 1.73-1.88 (2H, m, CH_2), 2.00 (3H, s, CH_3), 2.04 (3H, s, CH_3), 2.11 (3H, s, CH_3), 2.61 (2H, t, J = 6.6, CH_2), 3.39 (2H, t, J = 5.2, OCH_2), 3.68-3.71 (4H, m, 2 x OCH_2), 3.75-3.79 (2H, m, OCH_2), 3.90-3.95 (2H, m, OCH_2), 4.21-4.26 (2H, m OCH_2), 7.00-7.04 (2H, m, Ar-CH), 8.17-8.21 (2H, m, Ar-CH); ^{13}C NMR ($CDCl_3$, 100 MHz) 11.98 (CH_3), 12.33 (CH_3), 13.18 (CH_3), 19.73 (CH_3), 19.82 (CH_3), 19.89 (CH_3), 20.76 (CH_2), 21.18 (CH_2), 22.76 (CH_3), 22.85 (CH_3), 23.84 (CH_3), 24.33 (CH_3), 24.58 (CH_2), 24.95 (CH_2), 28.11 (CH), 32.91 (CH_2), 37.42 (CH_2), 37.52 (CH_2), 37.59 (CH_2), 37.67 (CH_2), 39.50 (CH_2), 50.82 (OCH_2), 67.78 (OCH_2), 69.78 (OCH_2), 70.27 (OCH_2), 70.90 (OCH_2), 71.09 (OCH_2), 114.53 (Ar-CH), 117.55 (Ar-C), 122.28 (Ar-C), 123.18 (Ar-C), 125.35 (Ar-C), 127.14 (Ar-C), 132.33 (Ar-CH), 140.77 (Ar-C), 149.50 (Ar-C), 163.09 (Ar-C), 165.01 (CO); [Found (ESI+) 708.4984 $[M+H]^+$, $C_{42}H_{66}N_3O_6$ requires 708.4951].

Dend-(Tris-ALA-Boc)-Vit-E (154)

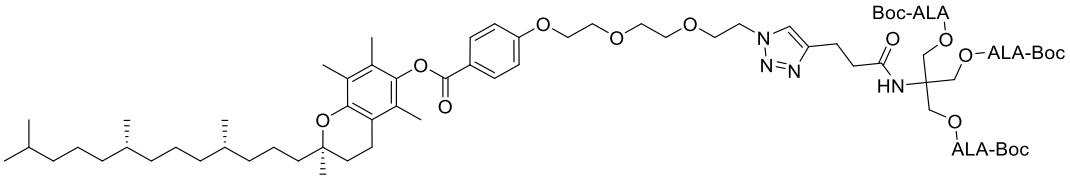

A solution of **(153)** (50 mg, 71 µmol) and **(105)** (118 mg, 141 µmol) in DMSO (2 mL) was treated with copper(I) trifluoromethanesulfonate benzene complex (17.7 mg, 70.6 µmol). The reaction was stirred for 72 h and monitored by analytical HPLC (Gradient 3) which showed complete disappearance of **(153)** and formation of new species at 14.66 min. The reaction mixture was purified by semi-preparative HPLC (Gradient 4) to give **(154)** as a white solid (59 mg, 54%); Analytical HPLC (Gradient 3) R_t = 14.66 min; ^{1}H NMR ($(CD_3)_2SO$, 500 MHz) δ 0.86-0.90 (12H, m, 4 x CH_3), 1.11-1.65 (51H, 9 x CH_2, 3 x CH, CH_3, 3 x $C(CH_3)_3$), 1.77-1.85 (2H, m, CH_2), 1.96 (3H, s, CH_3), 1.98 (3H, s, CH_3), 2.08 (3H, s, CH_3), 2.51-2.55 (8H, m, 3 x C<u>H</u>$_2$CH$_2$CO, CH_2), 2.60-2.64 (2H, m, CH_2C<u>H</u>$_2$CONH), 2.69-2.74 (6H, m, 3 x CH_2C<u>H</u>$_2$CO), 2.81-2.88 (2H, m, C<u>H</u>$_2$CH$_2$CONH), 3.58-3.72 (4H, m, 2 x OCH_2), 3.79-3.83 (8H, m, 3 x COC<u>H</u>$_2$NH, OCH_2), 3.84-3.87 (2H, m, OCH_2), 4.23-4.27 (2H, m, OCH_2), 4.31-4.35 (6H, m, 3 x CCH_2O), 4.45-4.49 (2H, m, OCH_2), 6.49-6.58 (3H, br, 3 x $COCH_2N$<u>H</u>), 7.13 (2H, *d*, J = 8.5, Ar-CH), 7.35-7.38 (1H, m, CH_2CH_2CON<u>H</u>), 7.69-7.72 (1H, m, triazole C<u>H</u>), 8.10 (2H, *d*, J = 8.5, Ar-CH); ^{13}C NMR ($(CD_3)_2SO$, 125 MHz) δ 11.55 (CH_3), 11.86 (CH_3), 12.70 (CH_3), 19.52 (CH_3), 19.58 (CH_3), 19.90 (CH_2), 21.05 (CH_2), 22.42 (CH_3), 22.50 (CH_3), 23.66 (CH_2), 24.10 (CH_2), 26.87 (<u>C</u>H$_2$CH$_2$CO), 27.12 (CH), 27.34 (CH), 27.80 (CH), 28.10 (C(<u>C</u>H$_3$)$_3$), 31.97 (CH), 32.01 (CH), 33.57 (CH$_2$<u>C</u>H$_2$CO), 34.11 (CH_2), 35.06 (CH_2), 36.54 (CH_2), 36.66 (CH_2), 38.72 (CH_2), 46.67 (CH_2), 49.19 (OCH_2), 49.40 ($COCH_2NH$), 56.91 (<u>C</u>CH$_2$O), 61.69 (C<u>C</u>H$_2$O), 67.56 (OCH_2), 68.64 (OCH_2), 68.80 (OCH_2), 69.53 (OCH_2), 69.74 (OCH_2), 114.77 (Ar-CH), 117.38 (Ar-C), 120.91 (Ar-C), 121.82 (Ar-C), 122.20 (triazole-CH), 125.00 (Ar-C), 126.41 (Ar-C), 131.79 (Ar-CH), 140.35 (Ar-C or triazole C), 148.61 (Ar-C or triazole C), 164.01 (CO), 171.68 (CO), 172.07 (CO), 205.92 (CO); [Found (ESI+) 1570.8777 $[M+H]^+$, $C_{81}H_{125}N_7NaO_{22}$ requires 1570.8770].

Dend-(Tris-ALA)$_1$-Vit-E. 3TFA (156)

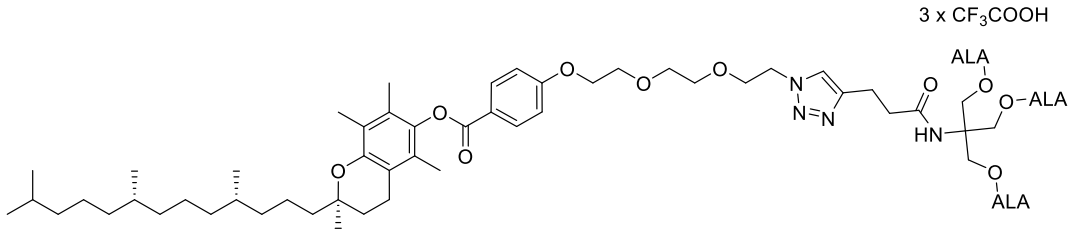

A solution of **(154)** (25 mg, 16 µmol) in DCM (2 mL) was treated with TFA (2 mL) at 0 °C and the reaction mixture was stirred for 30 min and monitored by HPLC (Gradient 3) which complete disappearance of starting material **(154)**. The solvent was evaporated under vacuum and the residue was co-evaporated with Et_2O (x 3) to remove excess TFA. This material was freeze-dried from H_2O to give **(156)** as a off-white solid (19 mg, 97%); Analytical HPLC (Gradient 3) R_t = 4.63 min; ^{1}H NMR (CD_3OD, 500 MHz) δ 0.86-0.91 (12H, m, 4 x CH_3), 1.10-1.63 (24H, m, 9 x CH_2, 3 x CH, CH_3), 1.79-1.84 (2H, m, CH_2), 1.98 (3H, s, CH_3), 2.01 (3H, s, CH_3), 2.11 (3H, s, CH_3), 2.59 (2H, t, J = 7.5, $CH_2C\underline{H}_2CONH$), 2.64-2.69 (8H, m, 3 x $C\underline{H}_2CH_2CO$, CH_2), 2.81-2.87 (6H, m, 3 x $CH_2C\underline{H}_2CO$), 2.93 (2H, t, J = 6, $C\underline{H}_2CH_2CONH$), 3.63-3.67 (2H, m, OCH_2), 3.68-3.72 (2H, m, OCH_2), 3.85-3.91 (4H, m, 2 x OCH_2), 4.03 (6H, s, $COC\underline{H}_2NH_2$), 4.23-4.27 (2H, m, OCH_2), 4.39 (6H, s, 3 x CCH_2O), 4.53-4.57 (2H, m, OCH_2), 7.10 (2H, d, J = 8.5, Ar-C$\underline{H}$), 7.80 (1H, s, triazole-CH), 8.16 (2H, d, J = 9.0, Ar-C$\underline{H}$); ^{13}C NMR (CD_3OD, 125 MHz) δ 12.08 (CH_3), 12.28 (CH_3), 13.16 (CH_3), 20.14 (CH_3), 20.19 (CH_3), 21.56 (CH_2), 22.21 ($\underline{C}H_2CH_2CONH$), 23.00 (CH_3), 23.09 (CH_3), 25.42 (CH_2), 25.90 (CH_2), 28.26 ($\underline{C}H_2CH_2CO$), 29.14 (CH), 33.92 (CH), 35.28 ($CH_2\underline{C}H_2CO$), 36.49 ($CH_2\underline{C}H_2CONH$), 38.38 (CH_2), 40.53 (CH_2), 48.08 ($CO\underline{C}H_2NH_2$), 51.41 (OCH_2), 59.13 ($\underline{C}CH_2O$), 63.29 ($C\underline{C}H_2O$), 68.99 (OCH_2), 70.44 (OCH_2), 70.62 (OCH_2), 71.46 (OCH_2), 71.72 (OCH_2), 115.70 (Ar-CH), 118.94 (Ar-$\underline{C}$), 122.92 (Ar-$\underline{C}$), 124.47 (triazole-CH), 126.44 (Ar-$\underline{C}$), 127.99 (Ar-$\underline{C}$), 133.25 (Ar-C$\underline{H}$), 150.57 (Ar-$\underline{C}$), 164.88 (CO), 166.77 (Ar-$\underline{C}$), 173.53 (CO), 175.03 (CO), 203.17 (CO); [Found (ESI+) 624.8729 $[M+2H]^{2+}$, $C_{66}H_{103}N_7O_{16}$ requires 624.8725].

Dend-(Ext. Tris-ALA-Boc)-Vit-E (155)

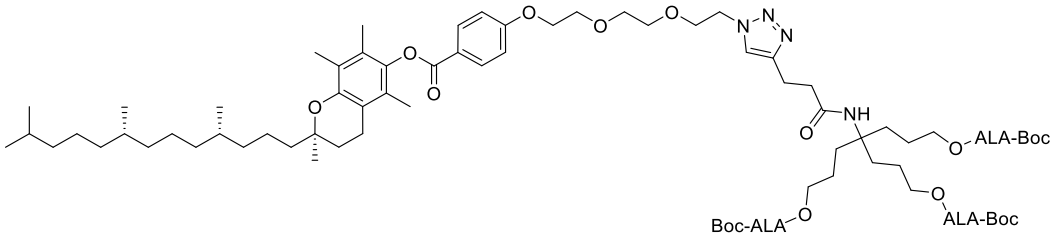

A solution of **(153)** (25 mg, 35 µmol) and **(107)** (65 mg, 70 µmol) in DMSO (2 mL) was treated with copper(I) trifluoromethanesulfonate benzene complex (18 mg, 35 µmol). The reaction was stirred for 72 h and monitored by analytical HPLC (Gradient 3) which showed complete disappearance of starting material **(153)** and formation of new species at 11.80 min. The reaction mixture was purified by semi-preparative HPLC (Gradient 4) to give **(155)** as a colourless oil (34 mg, 59%); Analytical HPLC (Gradient 3) R_t = 11.80 min; ^{1}H NMR ($(CD_3)_2SO$, 500 MHz) δ 0.80-0.86 (12H, m, 4 x CH_3), 1.05-1.68 (63H, m, 9 x CH_2, 3 x CH, CH_3, 3 x CC$\underline{H}_2CH_2CH_2$, 3 x $CCH_2C\underline{H}_2CH_2$, 3 x $C(CH_3)_3$), 1.73-1.80 (2H, m, CH_2), 1.91 (3H, s, CH_3), 1.93 (3H, s, CH_3), 2.03 (3H, s, CH_3), 2.38-2.43 (2, m, $CH_2C\underline{H}_2CONH$), 2.44-2.49 (6H, m, 3 x $C\underline{H}_2CH_2CO$), 2.53-2.60 (2H, m, CH_2), 2.63-2.69 (6H, m, 3 x $CH_2C\underline{H}_2CO$), 2.77-2.82 (2H, m, $C\underline{H}_2CH_2CONH$), 3.55-3.80 (14H, m, 4 x OCH_2, 3 x $COC\underline{H}_2NH$), 3.90-3.97 (6H, m, 3 x $CCH_2CH_2C\underline{H}_2O$), 4.19-4.23 (2H, m, OCH_2), 4.43-4.48 (2H, m, OCH_2), 7.02-7.07 (1H, m, 3 x $COCH_2N\underline{H}$), 7.09-7.18 (2H, m, Ar-CH), 7.74- 7.78 (1H, m, triazole CH), 8.03-8.12 (2H, m, Ar-CH); ^{13}C NMR ($(CD_3)_2SO$, 125 MHz) δ 11.58 (CH_3), 11.89 (CH_3), 12.70 (CH_3), 19.56 (CH_3), 19.62 (CH_3), 19.94 (CH_2), 20.39 ($\underline{C}H_2CH_2CONH$), 21.44 (CH_2), 22.08 (CH_2), 22.45 (CH_3), 22.54 (CH_3), 23.35 (CH_2), 23.70 (CH_2), 23.84 (CH_2), 23.91 (CH_3), 24.15 (CH_2), 27.25 (2 signals, $\underline{C}H_2CH_2CO$), 27.37 (CH_3), 27.68 (CH, 27.82 (CH3.), 28.14 ($C(\underline{C}H_3)_3$), 30.22 (CH_2), 32.01 (CH), 32.06 (CH), 33.64 ($CH_2\underline{C}H_2CO$), 34.21 (CH_2), 35.45 ($CH_2C\underline{H}_2CONH$), 36.60 (CH_2), 36.69 (CH_2), 38.76 (CH_2), 46.71 (CH_2), 49.18 (OCH_2), 49.47 ($CO\underline{C}H_2NH$), 56.91 ($\underline{C}CH_2CH_2CH_2$), 64.26 ($CCH_2CH_2\underline{C}H_2$), 67.60 ($OCH_2$), 68.69 ($OCH_2$), 68.84 ($OCH_2$), 69.58 ($OCH_2$), 69.78 ($OCH_2$), 78.08 ($\underline{C}(CH_3)_3$), 110.88 (Ar-C), 114.81 (Ar-CH), 117.42 (Ar-$\underline{C}$), 120.94 (Ar-$\underline{C}$), 121.86 (triazole CH), 122.18 (Ar-$\underline{C}$), 125.03 (Ar-$\underline{C}$), 126.44 (Ar-$\underline{C}$), 131.82 (Ar-CH), 140.38 (Ar-C), 145.96 (triazole C), 148.64 (Ar-C),

155.74 (CO), 162.93 (Ar-C), 164.04 (CO), 170.76 (CO), 172.11 (CO), 206.13 (CO); [Found (ESI+) 1633.0436 $[M+H]^+$, $C_{87}H_{138}N_7O_{22}$ requires 1632.9889].

Dend-(Ext. Tris-ALA)$_1$-Vit-E. 3TFA (157)

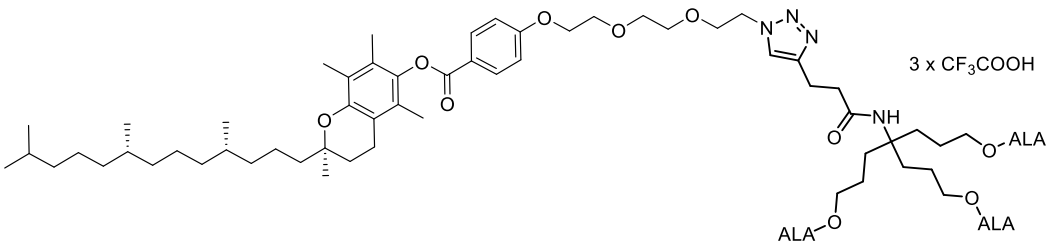

A solution of **(155)** (25 mg, 15 µmol) in DCM (2.5 mL) was treated with TFA (2.5 mL) at 0 °C and reaction mixture was stirred for 30 min and monitored by HPLC (Gradient 3) which showed complete disappearance of starting material. The solvent was evaporated under vacuum and the residue was co-evaporated with Et_2O (x 3) to remove excess TFA. This material **(157)** was freeze-dried from H_2O to give **(157)** as a off-white solid (24 mg, 96%); Analytical HPLC (Gradient 3) R_t = 4.53 min; ^{1}H NMR (CD_3OD, 500 MHz) δ 0.86-0.91 (12H, m, 4 x c), 1.08-1.89 (38H, m, 9 x CH_2, 3 x CH, CH_3, 3 x $CC\underline{H}_2CH_2CH_2$, 3 x $CCH_2C\underline{H}_2CH_2$, CH_2), 1.98 (3H, s, CH_3), 2.01 (3H, s, CH_3), 2.11 (3H,s, CH_3), 2.54 (2H, t, J = 7.25, $CH_2C\underline{H}_2CONH$), 2.63-2.70 (8H, m, 3 x $C\underline{H}_2CH_2CO$, CH_2), 2.80-2.85 (6H, m, 3 x $CH_2C\underline{H}_2CO$), 2.94 (2H, t, J = 7.25, $C\underline{H}_2CH_2CONH$), 3.11-3.16 (2H, m, OCH_2), 3.65-3.70 (4H, m, 2 x OCH_2), 3.83-3.87 (2H, m, OCH_2), 3.88-3.92 (2H, m, OCH_2), 4.02-4.06 (12H, m, 3 x $COC\underline{H}_2NH_2$, 3 x $CCH_2CH_2C\underline{H}_2O$), 4.23-4.28 (2H, m, OCH_2), 4.53-4.58 (2H,m, OCH_2), 7.10 (2H, d, J = 9.0, Ar-CH), 7.81 (1H, s, triazole-CH), 8.16 (2H, d, J = 8.5, Ar-C$\underline{H}$); ^{13}C NMR (CD_3OD, 125 MHz) δ 12.02 (CH_3), 12.29 (CH_3), 13.18 (CH_3), 20.14 (CH_3), 20.19 (CH_3), 21.56 (CH_2), 22.67 ($\underline{C}H_2CH_2CONH$), 23.01 (CH_3), 23.04 (CH_3), 23.09 (CH_2), 23.59 (CH_2), 23.76 (CH_2), 25.42 (CH_2), 25.91 (CH_2), 28.50 ($\underline{C}H_2CH_2CO$), 29.15 (CH), 30.75 (CH), 31.76 (CH_2), 33.89 (CH), 35.29 ($CH_2\underline{C}H_2CO$), 36.84 ($CH_2C\underline{H}_2CONH$), 38.38 (CH_2), 40.53 (CH_2), 45.71 (CH_2), 48.08 ($CO\underline{C}H_2NH_2$), 51.38 (OCH_2), 59.09 ($\underline{C}CH_2CH_2CH_2$), 66.03 ($CCH_2CH_2\underline{C}H_2$), 68.99 ($OCH_2$), 69.00 ($OCH_2$), 70.45 ($OCH_2$), 70.62 ($OCH_2$), 71.46 ($OCH_2$), 71.72 ($OCH_2$), 115.77 (Ar-CH), 118.94 (Ar-C), 122.93 (Ar-C), 123.93 (triazole-CH), 126.43 (Ar-C), 127.98 (Ar-C), 133.26 (Ar-CH), 150.58

(Ar-C), 164.87 (Ar-C), 166.74 (CO), 174.09 (CO), 203.12 (CO); [Found (ESI+) 688.9005 $[M+2Na]^{2+}$, $C_{72}H_{113}N_7O_{22}Na_2$ requires 688.9014].

Attempted synthesis of azido-PEG benzoic acid-Thy (159)

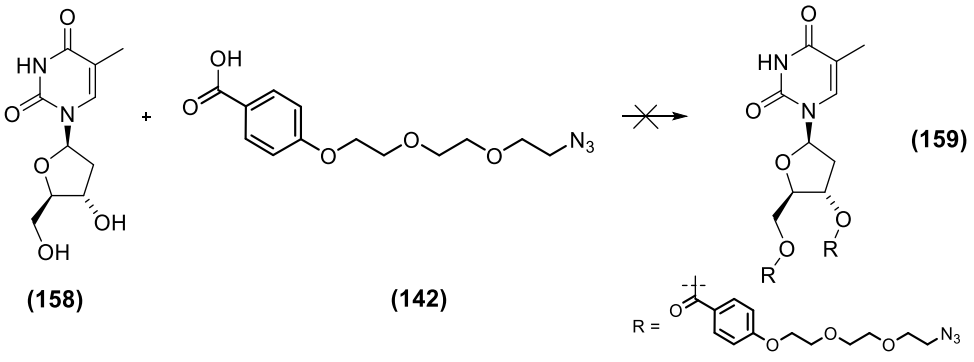

(158) (142) (159)

A suspension of thymidine **(158)** (0.16 g, 0.66 mmols) in dioxane (15 mL) was treated with TEA (0.53 mL, 3.76 mmol) at 0 °C. EDC.HCl (0.63 g, 3.30 mmol), **(142)** (0.97 g, 3.29 mmol) and DMAP (6.44 mg, 0.05 mmol) were added to the reaction mixture which was stirred for 36 h at RT. The reaction was monitored by HPLC (Gradient 1). No change was observed.

11-Azidoundecanoic acid (160)[316]

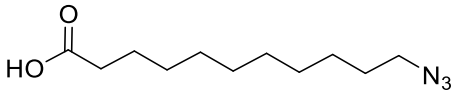

A suspension of 11-bromoundecanoic acid (2 g, 7.5 mmol) and sodium azide (1.96 g, 30.2 mmol) in DMF (25 mL) was heated at 80 °C under N_2 for 16 h. DMF was then removed under reduced pressure and the residue was taken in $CHCl_3$ (30 mL). The organic layer was washed with H_2O (30 mL) acidified with 3 mL of 5% aq. HCl, H_2O (30 mL), and dried over $MgSO_4$. The organic extract was filtered, and the solvent was evaporated to give the crude product as a colourless oil (1.57 g). Purification by column chromatography on silica gel eluting with 5-15% EtOAc in petroleum ether gave **(160)** as a colourless oil (1.29 g, 78%); IR (film) 2885 (CH), 2115 (N_3), 1730 (CO); ^{1}H NMR ($CDCl_3$, 400 MHz) δ 1.26-1.38 (12H, 6 x CH_2), 1.54-1.67 (4H, 2 x CH_2), 2.34 (2H, t, J = 7.5, CH_2), 3.24 (2H, t, J = 7.0, CH_2).

(3-((11-Azidoundecanoyl)oxy)-5-(5-methyl-2,4-dioxo-3,4-dihydropyrimidin-1(*2H*)-yl)tetrahydrofuran-2-yl)methyl-11-azidoundecanoate (161)

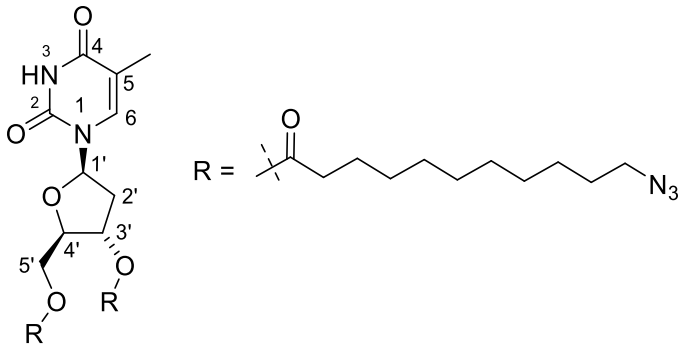

A suspension of thymidine **(158)** (0.16 g, 0.66 mmols) in dioxane (15 mL) was treated with TEA (0.53 mL, 3.76 mmol) at 0 °C. EDC.HCl (0.63 g, 3.30 mmol), azidoundecanoic acid **(160)** (0.75 g, 3.29 mmol) and DMAP (6.44 mg, 0.05 mmol) were added to the reaction mixture which was stirred for 48 h at RT. The reaction was monitored by HPLC (Gradient 1) which showed complete disappearance of thymidine and formation of a new species at 11.30 min. The crude product was purified by semi-preparative HPLC (Gradient 2) to give **(161)** as a yellowish oil (0.32 g, 73%); Analytical HPLC (Gradient 1) R_t = 11.30 min; IR (film) 3315 (NH), 3066 (CH), 2928 (CH), 2856 (CH), 2099 (N_3), 1737 (ester CO), 1694 (amide/imide CO); ^{1}H NMR ($CDCl_3$, 400 MHz) δ 1.20-1.38 (24H, m, 12 x CH_2), 1.53-1.63 (8H, m, 4 x CH_2), 1.89- 1.94 (3H, s, 5-CH_3), 2.07-2.15 (1H, m, CH<u>H</u>, 2'), 2.30-2.35 (4H, m, 2 x CH_2), 2.42-2.47 (1H, m, CH<u>H</u>, 2'), 3.21-3.25 (4H, t, J = 6.94 , 2 x C<u>H</u>$_2$$N_3$), 4.19-4.24 (1H, m, 4'), 4.27-4.31 (1H, m, CH<u>H</u>, 5'), 4.36-4.41 (1H, m, CH<u>H</u>, 5'), 5.17-5.19 (1H, m, 4'), 6.27-6.33 (1H, m, 1'), 7.27-7.31 (1H, m, 6), 9.33 (1H, s, 3); ^{13}C NMR ($CDCl_3$, 100 MHz) 12.74 (5-CH_3), 24.83 (CH_2), 24.89 (CH_2), 26.76 (CH_2), 28.90 (CH_2), 29.12 (CH_2), 29.17 (CH_2), 29.23 (CH_2), 29.26 (CH_2), 29.36 (CH_2), 29.45 (CH_2), 34.00 (CH_2), 34.15 (CH_2), 34.23 (CH_2), 37.75 (2'), 51.55 (CH_2), 63.78 (5'), 74.04 (3'), 82.45 (4'), 84.93 (1'), 111.57 (5), 134.71 (6), 150.42 (2), 163.84 (4), 173.12 (CO), 173.36 (CO); [Found (ESI+) 661.4056 $[M+H]^+$, $C_{32}H_{53}N_8O_7$ requires 661.4037].

Dend-(Tris-ALA-Boc)$_2$-Thy (162)

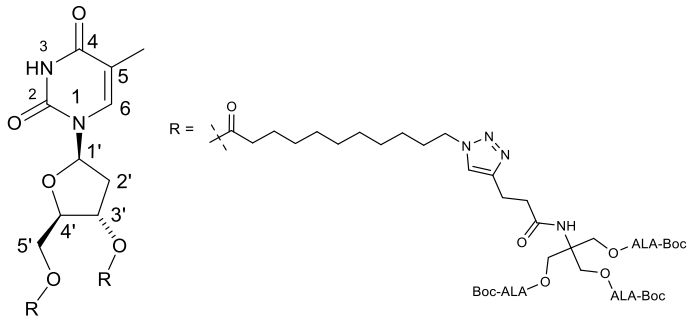

A solution of **(161)** (15 mg, 22 µmol) and **(105)** (76 mg, 91 µmol) in DMSO (2.5 mL) was treated with copper(I) trifluoromethanesulfonate benzene complex (23 mg, 71 µmol). The reaction was stirred for 24 h and monitored by analytical HPLC (Gradient 1) which showed complete disappearance of **(161)** and formation of new species was observed at 12.89 min. The reaction mixture was purified by semi-preparative HPLC (Gradient 2) to give **(162)** as white solid (28 mg, 54%); Analytical HPLC (Gradient 1) R_t = 12.89 min; ^{1}H NMR ($CDCl_3$, 400 MHz) δ 1.19-1.1.47 (78H, m, 12 CH_2, 6 x $C(CH_3)_3$), 1.55-1.65 (4H, m, 2 x CH_2), 1.82-1.93 (7H, m, 2 x CH_2, 5-CH_3), 2.07-2.15 (1H, m, CH<u>H</u>, 2'), 2.30-2.35 (4H, m, 2 x CH_2), 2.42-2.47 (1H, m, 1H, m, CH<u>H</u>, 2'), 2.54-2.76 (28H, m, 6 x C<u>H</u>$_2$$CH_2$CO, 2 x CH_2C<u>H</u>$_2$CONH, 6 x CH_2C<u>H</u>$_2$CO), 3.02-3.05 (4H, m, 2 x C<u>H</u>$_2$$CH_2$CONH), 4.00 (12H, s, 6 x COC<u>H</u>$_2$NH), 4.19-4.24 (1H, m, 4'), 4.27-4.41 (18H, m, 6 x CCH_2O, 5', 2 x CH_2), 5.15-5.20 (1H, m, 3'), 5.37-5.72 (6H, m, 6 x $COCH_2$N<u>H</u>), 6.26-6.29 (1H, m, 1'), 6.68-6.74 (2H, m, 2 x CH_2CH_2CON<u>H</u>), 7.27-7.32 (1H, m, 6), 7.56-7.65 (2H, m, 2 x triazole CH), 9.12 (1H, s, 3); ^{13}C NMR ($CDCl_3$, 125 MHz) 12.61 (5-CH_3), 20.29 (<u>C</u>H_2CH_2CONH), 24.66 (CH_2), 24.72 (CH_2), 26.26 (CH_2), 27.57 (<u>C</u>H_2CH_2CO), 28.26 (C(<u>C</u>H_3)$_3$), 28.78 (CH_2), 28.91 (CH_2), 28.96 (CH_2), 29.02 (CH_2), 29.05 (CH_2), 29.15 (CH_2), 29.83 (CH_2), 33.98 (CH_2), 34.07 (CH_2), 34.18 (CH_2<u>C</u>H_2CO), 35.24 (CH_2<u>C</u>H_2CONH), 37.61 (2'), 50.06 (CO<u>C</u>H_2NH), 51.23 (CH_2), 58.05 (<u>C</u>CH_2O), 62.18 (C<u>C</u>H_2O), 63.63 (5'), 73.95 (3'), 79.90 (<u>C</u>$(CH_3)_3$), 82.31 (4'), 84.84 (1'), 111.25 (5), 123.33 (triazole CH), 123.37 (triazole CH), 134.67 (6), 145.00 (CO), 150.13 (2 or 4), 155.95 (CO), 163.63 (2 or 4), 171.83 (CO), 172.50 (CO), 173.00 (CO), 173.22 (CO), 204.73 (CH_2CH_2<u>C</u>O); [Found (ESI+) 1193.5967 $[M+2Na]^{2+}$, $C_{110}H_{172}N_{16}O_{39}Na_2$ requires 1193.5876].

Dend-(Tris-ALA)$_2$-Thy .6TFA (163)

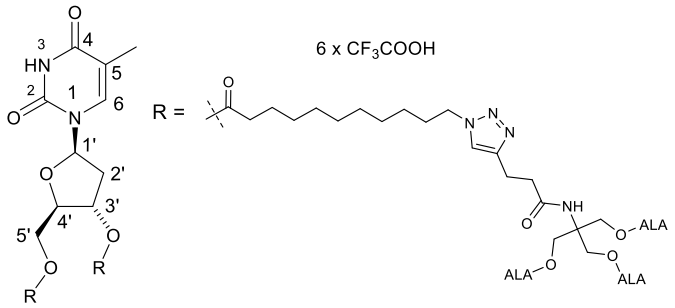

A solution of **(162)** (25 mg, 10.67 µmol) in DCM (5 mL) was treated with TFA (5 mL) at 0 °C and the reaction mixture was stirred for 30 min and monitored by analytical HPLC (Gradient 1) which showed complete disappearance of starting material **(162)**. The solvent was evaporated under vacuum and the residue was co-evaporated with Et_2O (x3) to remove excess TFA. This material was freeze-dried from H_2O to give **(163)** as a off-white solid (23 mg, 93%); Analytical HPLC (Gradient 1) R_t = 5.97 min; ^{1}H NMR (CD_3OD, 400 MHz) δ 1.24-1.37 (24H, m, 12 x CH_2), 1.57-1.66 (4H, m, 2 x CH_2), 1.83-1.93 (7H, m, 2 x CH_2, 5-CH_3), 2.34-2.44 (6H, m, 2 x CH_2, 2'), 2.60 (4H, t, J = 7.6, 2 x $CH_2C\underline{H}_2CONH$), 2.66-2.73 (12H, m, 6 x $C\underline{H}_2CH_2CO$), 2.82-2.90 (12H, m, 6 x $CH_2C\underline{H}_2CO$), 2.95 (4H, t, J = 7.6, 2 x $C\underline{H}_2CH_2CONH$), 4.05 (12H, s, 6 x $COC\underline{H}_2NH_2$), 4.17-4.24 (1H, m, 4'), 4.28-4.45 (18H, m, 6 x CCH_2O, 5', 2 x CH_2), 5.24.5.27 (1H, m, 3'), 6.21-6.25 (1H, m, 1'), 7.48-7.53 (1H, m, 6), 7.73-7.79 (2H, m, 2 x triazole CH); ^{13}C NMR (CD_3OD, 100 MHz) 12.61 (5-CH_3), 22.22 ($\underline{C}H_2CH_2CONH$), 25.84 (CH_2), 25.94 (CH_2), 27.43 (CH_2), 28.28 ($\underline{C}H_2CH_2CO$), 30.00 (CH_2), 30.07 (CH_2), 30.25 (CH_2), 30.37 (CH_2), 30.40 (CH_2), 31.23 (CH_2), 34.86 (CH_2), 34.92 (CH_2), 35.30 ($CH_2\underline{C}H_2CO$), 36.50 ($CH_2\underline{C}H_2CONH$), 37.83 (2'), 48.08 ($CO\underline{C}H_2NH_2$), 51.40 (CH_2), 59.14 ($\underline{C}CH_2O$), 63.29 ($C\underline{C}H_2O$), 64.79 (5'), 75.58 (3'), 83.69 (4'), 86.59 (1'), 111.90 (5), 123.66 (triazole CH), 137.31 (6), 147.55 (triazole C), 152.20 (2 or 4), 166.17 (2 or 4), 173.52 (CO), 174.75 (CO), 174.88 (CO), 175.07 (CO), 203.18 (CO); [Found (ESI+) 1763.8666 $[M+H]^+$, $C_{80}H_{124}N_{16}O_{27}Na$ requires 1763.8714].

(2RS,3R,4R,5R,6R)-3,4,5-tris(benzyloxy)-6-((benzyloxy)methyl) tetrahydro-2H-pyran-2-yl4-(2-(2-(2-azidoethoxy)ethoxy)ethoxy)benzoate (165)

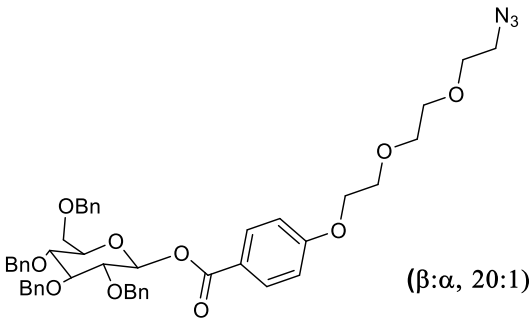

A solution of **(142)** (44 mg, 148 µmol) in DCM (5 mL) was treated with EDC.HCl (28 mg, 148 µmol) and DMAP (3 mg, 28 µmol) and stirred at 0 °C. 2,3,4,6-tetra-O-benzyl-D-gluco-pyranose **(162)** (50 mg, 92 µmol) was added to the reaction mixture and stirred at RT for 36 h. the solvent was evaporated and the crude product was purified by semi-preparative HPLC (Gradient 2) to obtain **(165)** as an oil (83 mg, 70%, major β anomer); Analytical HPLC (Gradient 1) R_t = 10.07 min; ^{1}H NMR ($CDCl_3$, 400 MHz) δ 3.38 (2H, t, J = 5.0, CH_2), 3.64-3.84 (12H, m, 4 x CH_2 + 4 x CH), 3.87-3.92 (2H, m, CH_2), 4.17-4.22 (2H, m, CH_2), 4.46-4.93 (8H, m, 4 x CH_2), 5.86 (0.95H, d, J = 8.0, anomeric CH (β)), 6.58 (0.05H, d, J = 4.0, anomeric CH (α)), 6.92-6.96 (2H, m, Ar-CH), 7.13-7.32 (20H, m, Ar-CH), 7.99-8.03 (2H, m, Ar-CH); [Found (ESI+) 840.3484 $[M+Na]^+$, $C_{47}H_{51}N_3O_{10}Na$ requires 840.3467].

Dend-Tris-ALA-Boc-Glc-OBn (166)

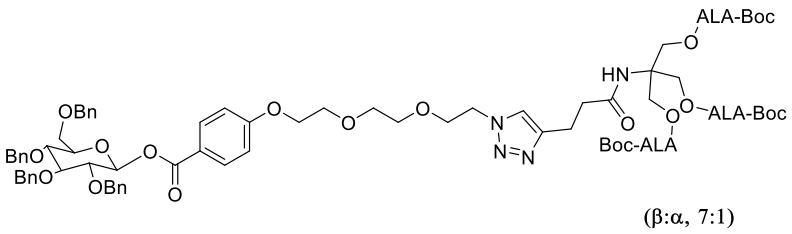

A solution of **(165)** (20 mg, 24 µmol) and **(105)** (41 mg, 49 µmol) in DMSO (1.5 mL) was treated with copper(I) trifluoromethanesulfonate benzene complex (12 mg, 24 µmol). The reaction was stirred for 36 h and monitored by analytical HPLC (Gradient 1) which showed complete disappearance of

starting material **(165)** and formation of new species at 12.53 min. The reaction mixture was purified by semi-preparative HPLC (Gradient 2) to give **(166)** as a white solid (22 mg, 54%, major β anomer); Analytical HPLC (Gradient 3) R_t = 12.53 min; ^{1}H NMR ($CDCl_3$, 500 MHz) δ 1.49 (27H, s, 3 x C(CH_3)$_3$), 2.62-2.69 (6H, m, 3 x C$\underline{H}_2$CH_2CO), 2.73-2.81 (8H, m, 3 x CH_2C$\underline{H}_2$CO, CH_2C$\underline{H}_2$CONH), 3.11-3.17 (2H, m, C$\underline{H}_2$CH_2CONH), 3.69-3.73 (3H, m, CH_2, CH), 3.74-3.78 (2H, m, CH_2), 3.79-3.87 (5H, m, CH_2, 3 x CH), 3.90-3.94 (2H, m, CH_2), 3.95-3.99 (2H, m, CH_2), 4.08 (6H, br, 3 x NHC$\underline{H}_2$CO), 4.24-4.28 (2H, m, OCH_2), 4.36 (6H, s, 3 x C(CH_2)O), 4.51-4.72 (4H, m, 2 x OBnCH_2), 4.79-4.97 (4H, m, 2 x OBnCH_2), 5.54 (3H, br, 3 x N$\underline{H}$CH_2CO), 5.90 (0.88H, d, J = 7.5, anomeric CH (β)), 6.63 (0.12H, d, J = 3.5, anomeric CH (α)), 6.91 (1H, br, CH_2CH_2CON$\underline{H}$), 6.97-7.02 (2H, m, Ar-CH), 7.18-7.22 (2H, m, 2 x Ar-CH), 7.24-7.41 (18H, m, 18 x Ar-CH), 7.92 (1H, br, triazole-CH), 8.04-8.09 (2H, m, Ar-CH); ^{13}C NMR ($CDCl_3$, 125 MHz) δ 20.07 (C$\underline{H}_2$CH_2CONH), 27.70 (C$\underline{H}_2$CH_2CO), 28.42 (C(C$\underline{H}_3$)$_3$), 34.32 (CH_2C$\underline{H}_2$CO), 50.20 (NH_2C$\underline{H}_2$CO), 58.31 (C(CH_2)O), 62.21 (C(C$\underline{H}_2$)O), 67.70 (CH_2), 68.21 (CH_2), 68.70 (CH_2), 69.59 (CH_2), 70.64 (CH_2), 70.80 (CH_2), 73.60 (CH_2), 75.11 (CH_2), 75.14 (CH_2), 75.60 (CH), 75.83 (CH_2), 77.27 (CH), 80.28 (CH), 81.05 (CH), 84.98 (CH), 94.65 (anomeric CH), 114.40 (Ar-CH), 125.79 (triazole-CH), 127.81 (Ar-CH), 127.82 (Ar-CH), 127.89 (Ar-CH), 127.97 (Ar-CH), 128.00 (Ar-CH), 128.11 (Ar-CH), 128.16 (Ar-CH), 128.28 (Ar-CH), 128.47 (Ar-CH), 128.51 (Ar-CH), 128.52 (Ar-CH), 128.59 (Ar-CH), 132.33 (Ar-CH), 137.88 (Ar-C), 137.92 (Ar-C), 138.10 (Ar-C), 138.49 (triazole C or Ar-C), 144.14 (triazole C or Ar-C), 156.23 (Ar-C or CO), 163.09 (Ar-C or CO), 164.64 (Ar-C or CO), 171.98 (CO), 172.63 (CO). 204.80 (CO); [Found (ESI+) 1680.7363 $[M+Na]^+$, $C_{86}H_{111}N_7O_{26}Na$ requires 1680.7471].

Attempted synthesis of Dend-Tris-ALA-Boc-Glc-OH (167)

(166)

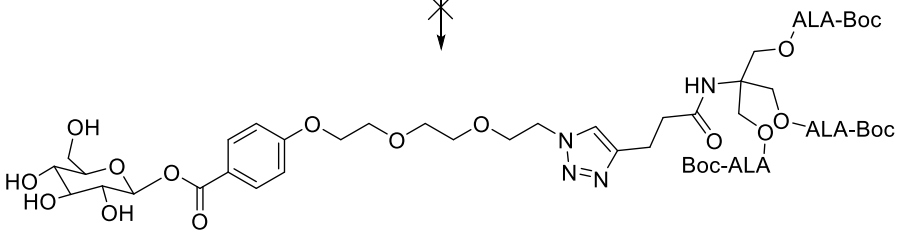

(167)

Method A[249]

A solution of **(166)** (0.06 g, 0.03 mmol) in DCM: EtOH (10 mL, 2:1) was treated with Pd/C (11.6 mg, 20%) and the mixture was stirred under an atmosphere of H_2 for 12 h at RT. The reaction was monitored by analytical HPLC. No change was observed.

Method B

Method A was repeated, but replacing the solvent with MeOH.

Method C

Method B was repeated, but replacing the Pd/C with $Pd(OH)_2$ on carbon.

H-Leu-Ala-Arg(Pmc)-Leu-Leu-Thr(tBu)-2-Chlorotrityl resin (171)

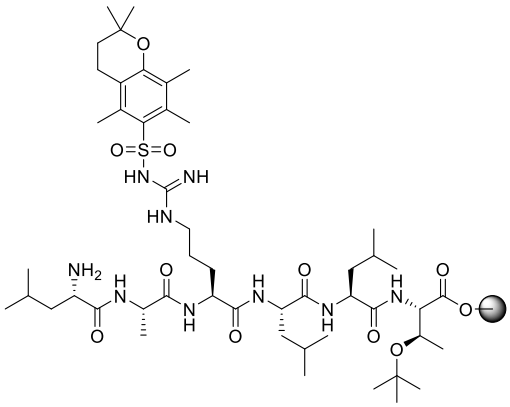

2-Chlorotrityl resin (0.5 g, 1.3 mmol/g) was pre-swollen in a SPPS vessel using DCM (5 mL) for 15 min, and the procedure was repeated twice. Pre-loading of

the first amino acid was accomplished by adding a solution of Fmoc-Thr(tBu)-OH (0.775 g, 1.95 mmol) and DIEA (0.69 mL, 3.9 mmol) in DMF (2 mL). The vessel was agitated for 1 h and the solvent was removed under reduced pressure. The resin was washed with DMF (5 mL), then piperidine/DMF (3 mL, 1:4 v/v) was added to the resin and the vessel was agitated for 5 min. The procedure was repeated and the vessel was shaken for 10 min. The solvent was removed under reduced pressure and the resin was washed with DMF (5 x 5 mL). Successful removal of the Fmoc group was confirmed by the Kaiser test. The remaining amino acids were coupled using an Activotec automated peptide synthesiser using 3 eq. of Fmoc-protected amino acid (Fmoc-Leu-OH, Fmoc-Arg(Pmc)-OH, or Fmoc-Ala-OH), 3 eq of PyBOP as coupling agent, 6 eq of DIEA as base and DMF (6.0 mL) as solvent. The peptide resin was washed thoroughly with DMF (2 x 5.0 mL), DCM (2 x 5.0 mL), MeOH (5.0 mL) and Et_2O (2 x 5.0 mL), and dried in vacuo to give **(171)** (1.3 g) of peptide resin. The final loading of the peptide was found to be 0.745 mmol/g by Fmoc loading test (see section 7.1).

H_2N-Leu-Ala-Arg(Pmc)-Leu-Leu-Thr(tBu)-OH (173)

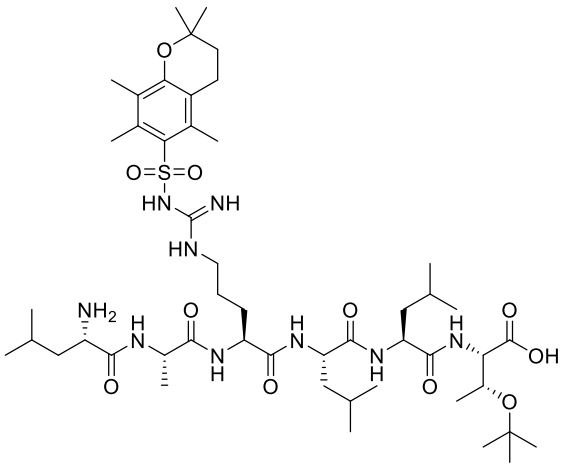

Peptide resin **(171)** (50 mg, 65 µmol) was swollen in a SPPS vessel with DCM (2 mL) for 15 min, and the step was repeated twice. 1% TFA in DCM (0.5 mL) was then added to the SPPS vessel which was agitated for 2 min, then the resin was filtered under reduced pressure and the filtrate was collected in a flask containing 10% pyridine in MeOH (2 mL). The above step was repeated ten times and the resin was washed with DCM (3 x 1.5 mL), MeOH (3 x 1.5

mL), DCM (2 x 1.5 mL) and MeOH (3 x 1.5 mL). The filtrate was evaporated under reduced pressure to 5% of the original volume, then water (8 mL) was added to precipitate the product, which was collected by centrifugation. The final product was washed with fresh water (8 mL) and the process repeated 3 times. **(173)** was obtained as a white solid after drying under vacuum (61 mg, 69%); HPLC (Gradient 1, R_t- 8.55 min); [Found (ESI+) 1008.6231 $[M+H]^+$, $C_{14}H_{20}N_3O_5$ requires 1008.6064].

H-Leu-Ala-Arg-Leu-Leu-Thr-OH. 2TFA (172)

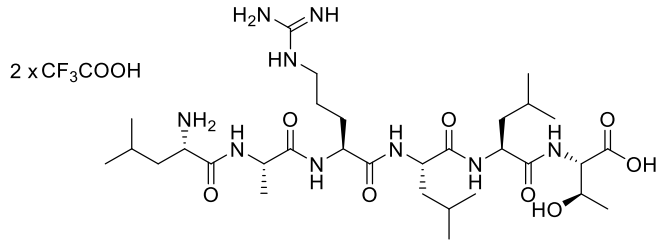

Peptide resin **(171)** (100 mg, 0.75 mmol/g) was placed in a 5 mL vial and was treated with TFA/TIS/H_2O (2 mL, 95:2.5:2.5) for 3 h. The resin beads were filtered off, washed with TFA, and the combined filtrates were collected into a Falcon tube containing Et_2O (5.0 mL) to precipitate the peptide. The resulting precipitate was collected by centrifugation and was washed repeatedly with Et_2O to remove excess TFA. The precipitated material was dissolved in 0.1% aq. TFA, filtered using a 0.2 μm syringe filter and the resulting solution was directly purified by semi-preparative HPLC (Gradient 1). The purified peptide was then freeze-dried from H_2O to give **(172)** as a white solid (55 mg, 85%); Analytical HPLC (Gradient 1) R_t = 5.5 min; ^{1}H NMR (CD_3OD, 500 MHz) δ 0.86-1.04 (18H, m, 6 x CH_3), 1.18 (3H, d, J = 6.0, CH_3), 1.41 (3H, d, J = 7.0, CH_3), 1.61-1.80 (12H, m, 3 x CH, 4 x CH_2, CH<u>H</u>), 1.85-1.92 (1H, m, CH<u>H</u>), 3.21 (2H, t, J = 7.0, CH_2), 3.90-3.92 [1H, m, CH), 4.32-4.50 [6H, m, 6 x CH); ^{13}C NMR (CD_3OD, 125 MHz) δ 17.99 (CH_3), 20.55 (CH_3), 21.86 (CH_3), 21.99 (CH_3), 22.05 (CH_3), 23.15 (CH_3), 23.47 (CH_3), 25.35 (CH_3), 25.81 (CH), 25.88 (CH), 25.96 (CH_2), 30.19 (CH_2), 41.70 (CH_2), 41.72 (CH_2), 41.97 (CH_2), 42.03 (CH_2), 50.53 (CH), 52.83 (CH), 53.18 (CH), 53.40 (CH), 53.95 (CH), 58.97 (CH), 68.44 (CH), 158.65 [NH<u>C</u>(NH)NH_2], 170.57 (CO), 173.36 (CO), 173.47 (CO), 174.33 (CO), 174.89 (CO); [Found (ESI+) 686.4558 $[M+H]^+$, $C_{31}H_{60}N_9O_8$

requires 686.4564].

Azido PEG benzoic acid spacer-H-Leu-Ala-Arg(Pmc)-Leu-Leu-Thr(tBu)-2-Chlorotrityl resin (176)

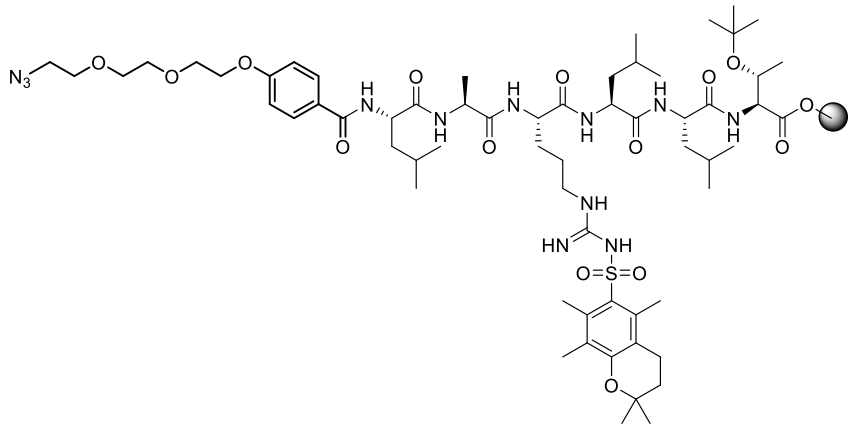

Peptide resin **(171)** (200 mg, 151 µmol) was swollen in DCM (3.0 mL) for 10 min and then in DMF (3 x 3.0 mL) for 5 min each. A solution of **(142)** (89.1 mg, 302 µM) in DMF (400 µL) was treated with HATU (115 mg, 302 µM) followed by DIEA (110 µL, 604 µM). After 3 min of preactivation, the mixture was added to the peptide resin. The resin was shaken for 24 h, then the solvent was removed under reduced pressure. The resin beads were washed with DMF (3 x 2.0 mL), DCM (3 x 2.0 mL), MeOH (2.0 mL) and DCM (2 x 2.0 mL). Successful attachment of **(142)** was confirmed by a negative Kaiser test.

Azido PEG benzoic acid spacer-H-Leu-Ala-Arg-Leu-Leu-Thr-OH. TFA (177)

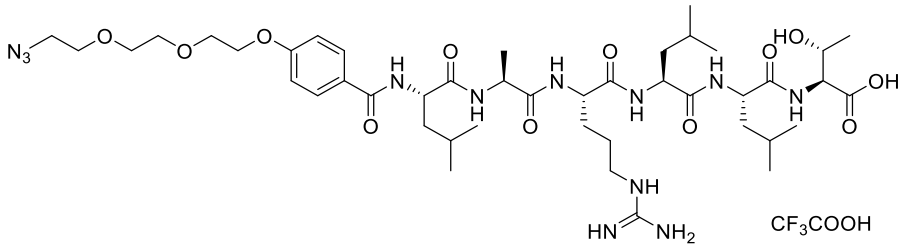

Peptide resin **(176)** (73 mg, 55 µmol) was placed in a 3 mL vial and was treated with TFA/TIS/H_2O (1 mL, 95:2.5:2.5 v/v/v) for 3 h. The resin beads were filtered off, washed with TFA, and the combined filtrates were collected into a Falcon tube containing Et_2O (5.0 mL) to precipitate the peptide. The resulting

precipitate was collected by centrifugation and was washed repeatedly with Et_2O to remove excess TFA. The precipitated material was dissolved in 0.1% aq. TFA, filtered using a 0.2 μm syringe filter and the resulting solution was purified by semi-preparative HPLC (Gradient 2). The purified peptide was freeze-dried from H_2O to give **(177)** as white solid (34 mg, 57%); Analytical HPLC (Gradient 1) R_t = 7.89 min; ^1H NMR (CD_3OD, 500 MHz) δ 0.90-1.02 (18H, m, 6 x CH_3), 1.18 (3H, d, J = 6.5, CH_3), 1.37 (3H, d, J = 7.0, CH_3), 1.61-1.93 (13H, m, 3 x CH, 5 x CH_2), 3.15-3.23 (2H, m, CH_2), 3.35-3.39 (2H, m, CH_2N_3), 3.66-3.70 (4H, m, OCH_2), 3.71-3.75 (2H, m, OCH_2), 3.87-3.90 (2H, m, OCH_2), 4.19-4.28 (3H, m, OCH_2, CH), 4.29-4.45 (6H, m, 6 x CH), 7.03 (2H, d, J = 7.0, Ar-CH), 7.87 (2H, d, J = 7.0, Ar-CH); ^{13}C NMR (CD_3OD, 125 MHz) δ 17.29 (CH_3), 20.45 (CH_3), 21.68 (CH_3), 21.73 (CH_3), 22.20 (CH_3), 23.28 (CH_3), 23.55 (CH_3), 23.60 (CH_3), 25.74 (CH), 25.90 (CH), 26.07 (CH_2), 26.10 (CH), 29.74 (CH_2), 41.37 (CH_2), 41.57 (CH_2), 41.92 (CH_2), 51.51 (CH), 51.75 (OCH_2), 53.29 (CH), 53.61 (CH), 54.57 (CH), 54.98 (CH), 59.10 (CH), 68.63 (CH), 68.82 (OCH_2), 70.74 (OCH_2), 71.16 (OCH_2), 71.55 (OCH_2), 71.84 (OCH_2), 115.37 (Ar-CH), 127.08 (Ar-C), 130.59 (Ar-CH), 158.56 (Ar-C), 163.46 (CO), 170.37 (CO), 173.27 (CO), 174.14 (CO), 174.85 (CO), 174.92 (CO), 175.68 (CO), 175.87 (CO); [Found (ESI+) 963.5664 $[M+H]^+$, $C_{44}H_{75}N_{12}O_{12}$ requires 963.5627].

Azido PEG Gallic acid spacer-H-Leu-Ala-Arg(Pmc)-Leu-Leu-Thr(tBu)-2-Chlorotrityl resin (178)

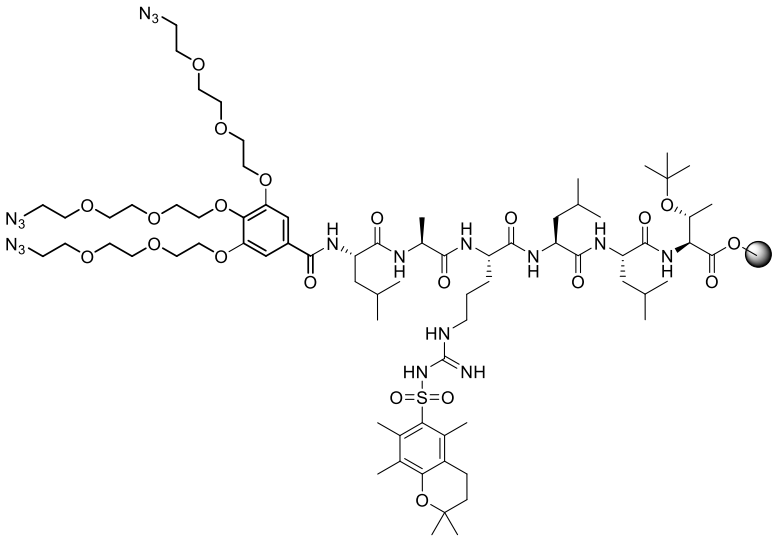

Peptide resin **(171)** (115 mg, 65.5 µmol) was swollen in DCM (3.0 mL) for 10 min and then in DMF (3 x 3.0 mL) for 5 min. A solution of **(147)** (84.0 mg, 131 µM) in DMF (400 µL) was treated with HATU (49.0 mg, 131 µmol) followed by DIEA (45.0 µL, 262 µmol). After 3 min of preactivation, the mixture was added to the peptide resin. The resin was shaken for 24 h, then the solvent was removed and the resin beads were washed with DMF (3 x 2.0 mL), DCM (3 x 2.0 mL), MeOH (2.0 mL) and DCM (2 x 2.0 mL). Successful attachment of **(147)** was confirmed by the negative Kaiser test.

Azido PEG Gallic acid spacer-H-Leu-Ala-Arg-Leu-Leu-Thr-OH. TFA (179)

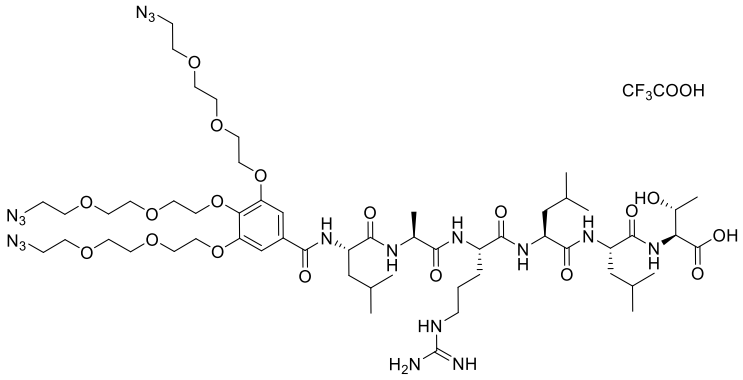

Peptide resin **(178)** (50 mg, 37.7 µmol) was placed in a 3 mL vial and was treated with TFA/TIS/H_2O (1 mL, 95:2.5:2.5 v/v/v) for 3 h. The resin beads were

filtered off, washed with TFA, and the combined filtrates were collected into a Falcon tube containing Et_2O (5.0 mL) to precipitate the peptide. The resulting precipitate was collected by centrifugation and was washed repeatedly with Et_2O. The precipitated material was dissolved in 0.1% aq. TFA, filtered using a 0.2 μm syringe filter and the resulting solution was purified by semi-preparative HPLC (Gradient 2). The purified peptide was then freeze-dried from H_2O to give **(179)** as a off-white solid (29 mg, 54%); Analytical HPLC (Gradient 1) R_t = 8.48 min; ^{1}H NMR (CD_3OD, 500 MHz) δ 0.86-1.06 (18H, m, 6 x CH_3), 1.18 (3H, d, J = 6.5, CH_3), 1.38 (3H, d, J = 7.0, CH_3), 1.60-1.82 (12H, m, 3 x CH, 4 x CH_2, CHH), 1.87-1.94 (1H, m, CHH), 3.16-3.19 (2H, m, CH_2), 3.34-3.38 (6H, m, 3 x CH_2N_3), 3.63-3.69 (12H, m, OCH_2), 3.71-3.75 (6H, m, 3 x OCH_2), 3.81-3.85 (2H, m, OCH_2), 3.87-3.92 (4H, m, OCH_2), 4.21-4.36 (9H, m, 3 x OCH_2, 3 x CH), 4.38-4.42 (2H, m, 2 x CH), 4.45-4.51 (2H, m, 2 x CH), 7.25 (2H, s, Ar-CH); ^{13}C NMR (CD_3OD, 125 MHz) δ 17.44 (CH_3), 20.49 (CH_3), 21.76 (CH_3), 21.82 (CH_3), 22.21 (CH_3), 23.34 (CH_3), 23.54 (CH_3), 23.57 (CH_3), 25.77 (CH), 25.92 (CH), 26.00 (CH_2), 26.11 (CH), 29.89 (CH_2), 41.38 (CH_2), 41.63 (CH_2), 41.70 (CH_2), 41.94 (CH_2), 51.26 (CH), 51.79 (OCH_2), 53.32 (CH), 53.48 (CH), 54.27 (CH), 54.82 (CH), 59.04 (CH), 68.58 (CH), 70.25 (OCH_2), 70.94 (OCH_2), 71.15 (OCH_2), 71.62 (OCH_2), 71.65 (OCH_2), 71.89 (OCH_2), 73.65 (OCH_2), 108.37 (Ar-CH), 153.84 (Ar-C), 173.29 (CO), 173.90 (CO), 174.85 (CO); [Found (ESI+) 1307.7079 $[M+H]^+$, $C_{56}H_{95}N_{18}O_{18}$ requires 1307.7077].

Dend-(Tris-ALA)$_1$-LARLLT. 4TFA (175)

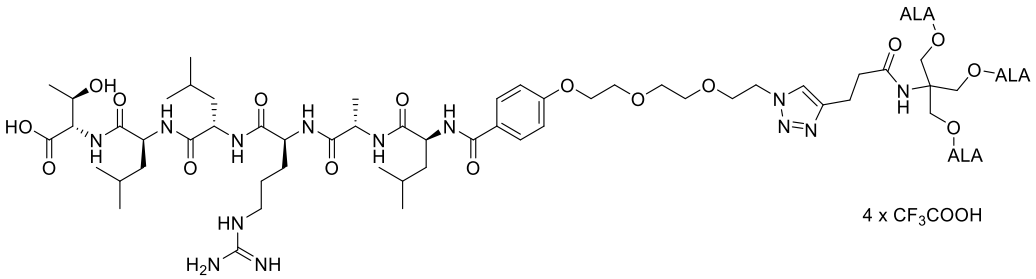

Peptide resin **(176)** (20 mg, 15 μmol) was swollen in DCM (2.0 mL) for 10 min (x 3), then DMSO (2.0 mL) for 10 min (x 3). A solution of **(105)** (25 mg, 30 μmol) in DMSO (200 μL) was treated with copper(I)

trifluoromethanesulfonate benzene complex (15 mg, 30 µmol) and the mixture was added to the reaction vessel containing the resin which was agitated for 5 days. The solvent was removed and the resin washed with DMSO (5 x 1.0 mL), DCM (3 x 2.0 mL), MeOH (2.0 mL) and DCM (2 x 2.0 mL). The resin was placed in a 3 mL vial and was treated with TFA/TIS/H_2O (1 mL, 95:2.5:2.5 v/v/v) for 3 h. The resin beads were filtered off, washed with TFA, and the combined filtrates were collected into a Falcon tube containing Et_2O (3.0 mL) to precipitate the peptide-dendrimer. The resulting precipitate was collected by centrifugation and was washed repeatedly with Et_2O. The precipitated material was dissolved in 0.1 % aq. TFA, filtered using a 0.2 µm syringe filter and the resulting solution was purified by semi-preparative HPLC (Gradient 2). The product was freeze-dried from H_2O to give **(175)** as a white solid (16 mg, 53%); Analytical HPLC (Gradient 1) R_t = 6.09 min; ^{1}H NMR (CD_3OD, 500 MHz) δ 0.90-1.02 (18H, m, 6 x CH_3), 1.18 (3H, d, J = 6.5, CH_3), 1.38 (3H, t, J = 7.0, CH_3), 1.63-1.78 (13H, m, 3 x CH, 5 x CH_2), 2.59 (2H, t, J = 7.5, NHCOC$\underline{H}_2CH_2$), 2.67-2.70 (6H, m, 3 x C$\underline{H}_2CH_2CO$), 2.84-2.87 (6H, m, 3 x $CH_2C\underline{H}_2CO$), 2.92 (2H, t, J = 7.5, $NHCOCH_2C\underline{H}_2$), 3.19 (2H, t, J = 7.25, CH_2), 3.63-3.69 (4H, m, CH_2N + OCH_2), 3.81-3.85 (2H, m, OCH_2), 3.88 (2H, t, J = 5.0, OCH_2), 4.04 (6H, m, 3 x COC$\underline{H}_2NH_2$), 4.16-4.21 (2H, m, OCH_2), 4.23-4.35 (3H, m, 3 x CH), 4.37-4.43 (8H, m, CCH_2O, 2 x CH), 4.44-4.55 (4H, m, 2 x CH, OCH_2), 7.01 (2H, d, J = 9.0, Ar-CH), 7.79 (1H, s, triazole CH), 7.86 (2H, d, J = 9.0, Ar-CH); ^{13}C NMR (CD_3OD, 125 MHz) δ 17.45 (CH_3), 20.49 (CH_3), 21.71 (CH_3), 21.77 (CH_3), 22.15 (CH_3), 22.23 ($NHCOCH_2\underline{C}H_2$), 23.36 (CH_3), 24.21 (CH_3), 25.75 (CH), 25.90 (CH), 26.02 (CH), 28.23 ($\underline{C}H_2CH_2CO$), 29.85 (CH_2), 35.27 ($CH_2\underline{C}H_2CO$), 36.50 ($NHCO\underline{C}H_2CH_2$), 41.45 (CH_2), 41.60 (CH_2), 41.95 (CH_2), 51.32 (CH), 51.37 (CH_2-N), 53.32 (CH), 53.52 (CH), 54.43 (CH), 59.11 (CH), 63.27 ($CO\underline{C}H_2NH_2$), 68.57 (CH), 68.82 (OCH_2), 70.45 (OCH_2), 70.66 (OCH_2), 71.41 (OCH_2), 71.69 (OCH_2), 115.34 (Ar-CH), 124.40 (triazole CH), 130.62 (Ar-CH), 173.55 (CO), 175.71 (CO), 203.19 (CO); [Found (ESI+) 752.4095 $[M+2H]^{2+}$, $C_{68}H_{112}N_{16}O_{22}$ requires 752.4063].

Dend-(Ext. Tris-ALA)$_1$-LARLLT. 4TFA (180)

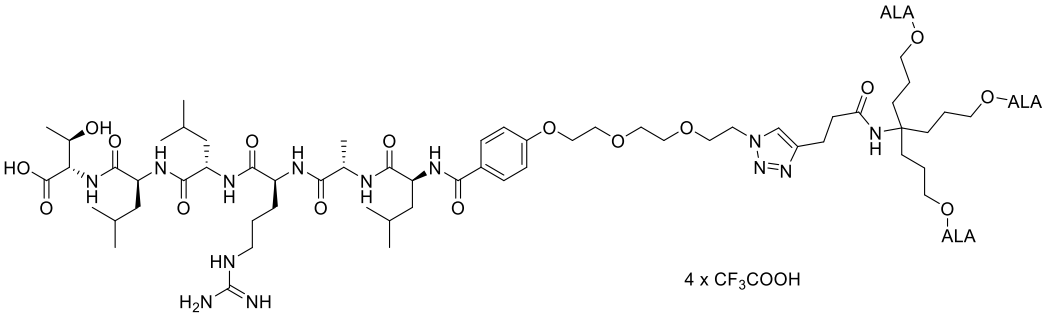

Peptide resin **(176)** (40 mg, 30 µmol) was swollen in DCM (3.0 mL) for 10 min (x 3), then DMSO (3.0 mL) for 10 min (x 3). A solution of **(107)** (55 mg, 60 µmol) in DMSO (200 µL) was treated with copper(I) trifluoromethanesulfonate benzene complex (30 mg, 60 µmol) and the mixture was added to the reaction vessel containing the resin and agitated for 5 days. Solvent was removed and the resin was washed with DMSO (5 x 1.0 mL), DCM (3 x 2.0 mL), MeOH (2.0 mL) and DCM (2 x 2.0 mL). The resin was placed in a 3 mL vial and was treated with TFA/TIS/H_2O (1 mL, 95:2.5:2.5 v/v/v) for 3 h. The resin beads were filtered off, washed with TFA, and the combined filtrates were collected into a Falcon tube containing Et_2O (5.0 mL) to precipitate the peptide-dendrimer. The resulting precipitate was collected by centrifugation and was washed repeatedly with Et_2O. The precipitated material was dissolved in 0.1 % aq. TFA, filtered using a 0.2 µm syringe filter and the resulting solution was purified by semi-preparative HPLC (Gradient 2). The product was freeze-dried to obtain **(180)** as a off-white solid (23 mg, 38%); Analytical HPLC (Gradient 1) R_t = 6.16 min; ^{1}H NMR (CD_3OD, 500 MHz) δ 0.86-0.91 (6H, m, 2 x CH_3), 0.95-1.05 (12H, m, 4 x CH_3), 1.15-1.22 (3H, m, CH_3), 1.35-1.41 (3H, m, CH_3), 1.44-1.55 (6H, m, 3 x C$\underline{H}_2$CH_2CH_2O), 1.61-1.85 (18H, m, 3 x CH, 4 x CH_2, C$\underline{H}$H, 3 x CH_2C$\underline{H}_2$CH_2O), 1.89-1.96 (1H, m, C$\underline{H}$H), 2.54 (6H, t, J = 7.5, NHCOC$\underline{H}_2$CH_2), 2.63-2.70 (6H, m, 3 x C$\underline{H}_2$CH_2CO), 2.79-2.87 (6H, m, 3 x CH_2C$\underline{H}_2$CO), 2.93 (6H, t, J = 7.3, NHCOCH_2C$\underline{H}_2$), 3.21 (2H, t, J = 7.3, CH_2), 3.62-3.71 (4H, m, 2 x OCH_2), 3.80-3.85 (2H, m, OCH_2), 3.89 (2H, t, J = 5.3, OCH_2), 3.99-4.07 (12H, m, 3 x COC$\underline{H}_2$NH_2, 3 x CH_2CH_2C$\underline{H}_2$O), 4.17-4.20 (2H, m, OCH_2), 4.23-4.28 (1H, m, CH), 4.30-4.34 (2H, m, 2 x CH), 4.37-4.41 (2H, m, 2 x CH), 4.45-4.49 (2H, m, 2 x CH), 4.54 (2H, t, J = 5.0,

OCH_2), 6.97-7.05 (2H, m, Ar-CH), 7.80 (1H, s, triazole CH), 7.83-7.89 (2H, m, Ar-CH); ^{13}C NMR (CD_3OD, 125 MHz) δ 17.37 (CH_3), 20.47 (CH_3), 21.75 (CH_3), 22.18 (CH_3), 22.66 ($NHCOCH_2\underline{C}H_2$), 23.33 (CH_3), 23.55 (CH_3), 23.59 ($\underline{C}H_2CH_2CH_2O$), 25.75 (CH), 25.91 (CH), 26.07 (CH_2), 26.11 (CH), 28.50 ($\underline{C}H_2CH_2CO$), 29.77 (CH_2), 31.77 ($\underline{C}H_2CH_2CH_2O$), 35.30 ($CH_2\underline{C}H_2CO$), 36.82 ($NHCO\underline{C}H_2CH_2$), 41.41 ($CH_2$), 41.59 ($CH_2$), 41.94 ($CH_2$), 48.15 ($NH\underline{C}H_2CO$), 51.37 ($OCH_2$), 51.47 (CH), 53.33 (CH), 53.62 (CH), 54.57 (CH), 54.83 (CH), 57.48 ($\underline{C}CH_2CH_2CH_2O$), 59.11 (CH), 66.03 ($CH_2CH_2\underline{C}H_2O$), 68.61 (CH), 68.84 ($OCH_2$), 70.45 ($OCH_2$), 70.66 ($OCH_2$), 71.42 ($OCH_2$), 71.69 ($OCH_2$), 115.37 (Ar-CH), 124.28 (triazole-CH), 127.21 (Ar-C), 130.63 (Ar-CH), 158.60 (Ar-C), 163.37 (CO), 170.25 (CO), 173.32 (CO), 173.86 (CO), 174.11 (CO), 174.89 (CO), 174.95 (CO), 175.67 (CO), 175.81 (CO), 203.15 (CO); [Found (ESI+) 794.4517 $[M+2H]^{2+}$, $C_{74}H_{124}N_{16}O_{22}$ requires 794.4533].

Dend-(Tris-ALA)$_3$-LARLLT. 10TFA (181)

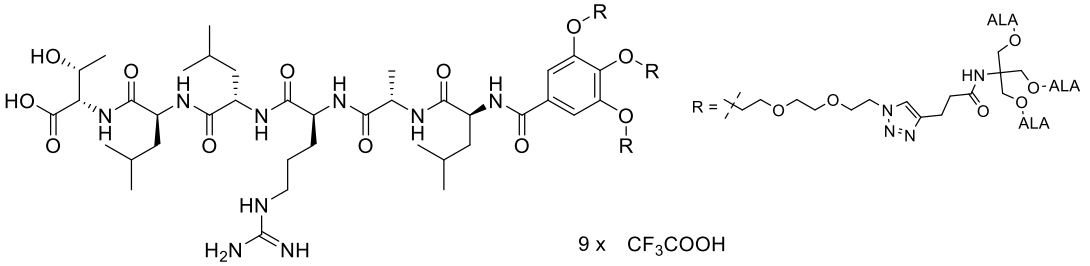

Method A

A solution of **(148)** (10 mg, 3.2 µmol) in DMF (2.0 mL) was treated with EDC.HCl (0.72 mg, 3.8 µmol) and HOBt.hydrate (0.8 mg, 5.4 µM) at 0 °C, then DIEA (0.66 µL) was added to the mixture. The reaction was stirred for 30 min, then peptide **(173)** (3.18 mg, 3.2 µmol) was added. The reaction was stirred at RT for 16 h and was monitored by HPLC (Gradient 1). No consumption of **(148)** was observed nor the appearance of any new peaks.

Method B

Method A was repeated but by replacing EDC.HCl and HOBt.hydrate with HATU. The reaction was monitored by HPLC (Gradient 1), however similar results were obtained as in *Method A*.

Method C

Peptide resin **(171)** (5.0 mg, 7.6 µmol) was swollen in DCM (2.0 mL) for 10 min (x 3), then in DMF (2.0 mL) for 10 min (x 3). A solution of **(148)** (36.0 mg, 11.4 µmol) in DMF (500 µL) was preactivated with HATU (4.33 mg, 11.4 µmol) and DIEA (2 mL, 22.4 µmol) for 3 min before adding to the reaction vessel containing the peptide resin **(171)**. The vessel for agitated for 16 h and the solvent was removed under reduced pressure. The resin was washed with DMF (5 x 1.0 mL), DCM (3 x 2.0 mL), MeOH (2.0 mL) and DCM (2 x 2.0 mL). The resin was placed in a 3 mL vial and was treated with TFA/TIS/H_2O (1 mL, 95:2.5:2.5 v/v/v) for 3 h. The resin beads were filtered off, washed with TFA, and the combined filtrates were collected into a Falcon tube containing Et_2O (3.0 mL) to precipitate the peptide-dendrimer. The resulting precipitate was collected by centrifugation and was washed repeatedly with Et_2O. The precipitated material was dissolved in 0.1 % aq. TFA, filtered using a 0.2 µm syringe filter and the resulting solution was purified by semi-preparative HPLC (Gradient 2). The product was freeze-dried from H_2O to give **(181)** as a white solid (1 mg, 5%); Analytical HPLC (Gradient 1) R_t = 5.18 min.

Method D

Peptide resin **(178)** (50 mg, 37.8 µmol) was swollen in DCM (2.0 mL) for 10 min (x 3), then in DMSO (2.0 mL) for 10 min (x 3). A solution of **(105)** (190 mg, 226 µmol) in DMSO (600 µL) was treated with copper(I) trifluoromethanesulfonate benzene complex (114 mg, 226 µmol) and the mixture was added to the reaction vessel containing the resin and agitated for 5 days. The solvent was removed and the resin was washed with DMSO (5 x 1.0 mL), DCM (3 x 2.0 mL), MeOH (2.0 mL) and DCM (2 x 2.0 mL). The resin was placed in a 3 mL vial and was treated with TFA/TIS/H_2O (1 mL, 95:2.5:2.5 v/v/v) for 3 h. The resin beads were filtered off, washed with TFA, and the combined filtrates were collected into a Falcon tube containing Et_2O (5.0 mL) to precipitate the peptide-dendrimer. The resulting precipitate was collected by centrifugation and was washed repeatedly with Et_2O. The precipitated material was dissolved in 0.1 % aq. TFA, filtered using a 0.2 µm syringe filter and the resulting solution was purified by semi-preparative HPLC

(Gradient 2). The product was freeze-dried from H_2O to give **(181)** as a white solid (44 mg, 30%). Analytical HPLC (Gradient 1) R_t = 5.18 min.

Method E

A solution of peptide targeted core **(179)** (5 mg, 3.55 µmol) in DMSO (100 µL) was treated with **(105)** (18 mg, 21 µmol) and copper(I) trifluoromethanesulfonate benzene complex (11 mg, 21 µmol), and the reaction mixture was stirred for 36 h and monitored by analytical HPLC (Gradient 1) which showed the disappearance of the starting material and appearance of new species at 9.94 min. The reaction mixture was diluted with 0.1% aq. TFA and the product was isolated by semi-preparative HPLC (Gradient 2) and freeze-dried from H_2O to give Boc-protected peptide-targeted dendrimer **(183)** (9.5 mg, 69%). Analytical HPLC (Gradient 1) R_t = 9.94 min. The resulting product was dissolved in dry DCM (3 mL) and the reaction mixture was cooled to 0 °C. TFA (3 mL) was added dropwise and the reaction mixture was stirred for 30 min at RT and monitored by analytical HPLC (Gradient 1), which showed complete disappearance of **(183)**. The solvent was evaporated under vacuum and the residue was co-evaporated with Et_2O (x 3) to remove excess TFA. This material was freeze-dried from H_2O to give **(181)** as a white solid (9 mg, 94%); Analytical HPLC (Gradient 1) R_t = 5.18 min; [Found (ESI+) 1915.9682 $[M+2H]^{2+}$, $C_{173}H_{278}N_{30}O_{66}$ requires 1915.9654].

Method F

The reaction carried was out in a microwave (MW) reaction vial (Biotage Initiator Microwave reactor) which was irradiated for 10 min (at constant power, 10-15 W; temp = 70˚C). The reaction was allowed to reach RT and the vial was removed from the MW cavity. The reaction mixture was analysed by HPLC (Gradient 1) which showed complete disappearance of the starting material **(179)** and formation of a new species at 9.79 min. The product was isolated by semi-preparative HPLC and freeze-dried from H_2O to give Boc protected peptide targeted dendrimer **(183)** (10.3 mg, 75%). Analytical HPLC (Gradient 1) R_t = 9.79 min. The resulting product was dissolved in dry DCM (3 mL) and the reaction mixture cooled to 0 °C. TFA (3 mL) was added dropwise

and the reaction mixture stirred for 30 min at RT and monitored by analytical HPLC (Gradient 1) which showed complete disappearance of **(183)** and appearance of new species at 5.18 min. The solvent was evaporated under reduced pressure and the residue was co-evaporated with Et_2O (x 3) to remove excess TFA. This material was freeze dried from H_2O to give final product **(181)** as a white solid (9.1 mg, 95%); Analytical HPLC (Gradient 1) R_t = 5.18 min; ^{1}H NMR (CD_3OD, 500 MHz) δ 0.92-1.03 (18H, m, 6 x CH_3), 1.19-1.23 (3H, m, CH_3), 1.38-1.43 (3H, m, CH_3), 1.66-1.85 (12H, m, 3 x CH + 4 x CH_2 + CH<u>H</u>), 1.92-1.95 (1H, m, CH<u>H</u>), 2.61 (6H, t, J = 7.5, NHCOC<u>H</u>$_2$$CH_2$), 2.68-2.73 (18H, m, 9 x C<u>H</u>$_2$$CH_2$CO), 2.87-2.91 (18H, m, 9 x CH_2C<u>H</u>$_2$CO), 2.94 (6H, t, J = 7.0, NHCOCH$_2$C<u>H</u>$_2$), 3.21 (2H, t, J = 7.0, CH_2), 3.64-3.70 (12H, m, 3 x CH_2N + 3 x OCH_2), 3.74-3.79 (2H, m, OCH_2), 3.85-3.91 (10H, m, 5 x OCH_2), 4.08 (18H, s, 9 x COC<u>H</u>$_2$$NH_2$), 4.18-4.23 (6H, m, 3 x OCH_2), 4.26-4.31 (1H, m, CH), 4.33-4.37 (2H, m, 2 x CH), 4.38-4.45 (20H, m, CC<u>H</u>$_2$O + 2 x CH), 4.46-4.52 (1H, m, CH), 4.54-4.59 (7H, m, 3 x OCH_2 + CH), 7.29-7.33 (2H, m, Ar-CH), 7.79-7.83 (3H, m, triazole CH); ^{13}C NMR (CD_3OD, 125 MHz) δ 17.50 (CH_3), 20.50 (CH_3), 21.78 (CH_3), 22.23 (NHCOCH$_2$<u>C</u>H$_2$), 23.38 (CH_3), 23.56 (CH_3), 23.60 (CH_3), 25.75 (CH), 25.91 (CH), 26.09 (CH), 28.27 (<u>C</u>H$_2$$CH_2$CO), 35.31 ($CH_2$<u>C</u>H$_2$CO), 36.46 (NHCO<u>C</u>H$_2$$CH_2$), 41.34 ($CH_2$), 41.61 ($CH_2$), 41.94 ($CH_2$), 48.14 (CO<u>C</u>H$_2$$NH_2$), 51.25 ($OCH_2$), 51.32 ($OCH_2$), 53.36 (CH), 53.61 (CH), 54.50 (CH), 54.85 (CH), 59.10 (αCH), 63.29 (C<u>C</u>H$_2$O), 68.57 (CH), 69.97 (OCH_2), 70.44 (OCH_2), 70.73 (OCH_2), 71.28 (OCH_2), 71.43 (OCH_2), 71.57 (OCH_2), 71.65 (OCH_2), 73.63 (OCH_2), 108.08 (Ar-CH), 124.32 (triazole-CH), 147.59 (triazole C or Ar-C), 153.66 (triazole C or Ar-C), 158.58 (Ar-C), 173.47 (CO), 173.55 (CO), 174.94 (CO), 175.08 (CO), 203.26 (CO); [Found (ESI+) 977.4865 $[M+3H]^{3+}$, $C_{128}H_{204}N_{30}O_{48}$ requires 977.4888].

Dend-(Ext. Tris-ALA)$_3$-LARLLT. 10TFA (182)

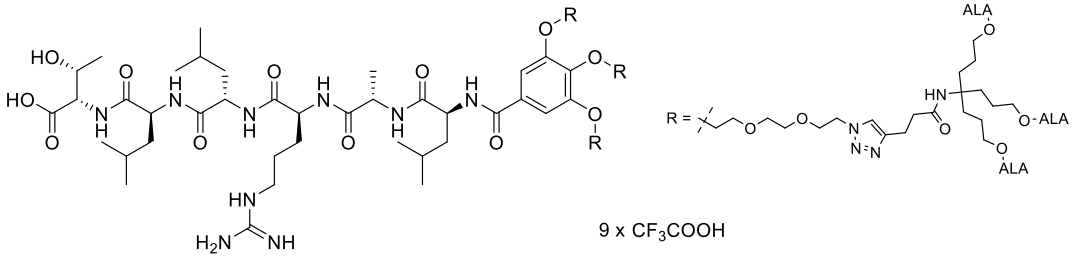

Peptide resin **(178)** (50 mg, 37.8 µmol) was swollen in DCM (2.0 mL) for 10 min (x 3), then DMSO (2.0 mL) for 10 min (x 3). A solution of **(105)** (209 mg, 226 µmol) in DMSO (600 µL) was treated with copper(I) trifluoromethanesulfonate benzene complex (114 mg, 226 µmol) and the mixture was added to the reaction vessel containing the resin and which was agitated for 5 days. The solvent was removed and the resin was washed with DMSO (5 x 1.0 mL), DCM (3 x 2.0 mL), MeOH (2.0 mL) and DCM (2 x 2.0 mL). The resin was placed in a 3 mL vial and was treated with TFA/TIS/H_2O (1 mL, 95:2.5:2.5 v/v/v) for 3 h. The resin beads were filtered off, washed with TFA, and the combined filtrates were collected into a Falcon tube containing Et_2O to precipitate the peptide-dendrimer. The resulting precipitate was collected by centrifugation and was washed repeatedly with Et_2O. The precipitated material was dissolved in 0.1 % aq. TFA, filtered using a 0.2 µm syringe filter and the resulting solution was analysed by HPLC (Gradient 1) and purified by semi-preparative HPLC (Gradient 2). The product was freeze-dried from H_2O to give **(182)** as a white solid (40 mg, 25%); Analytical HPLC (Gradient 1) R_t = 5.34 min; ^{1}H NMR (CD_3OD, 500 MHz) δ 0.86-1.03 (18H, m, 6 x CH_3), 1.18 (3H, d, J = 6.5, CH_3), 1.38-1.43 (3H, m, CH_3), 1.45-1.53 (18H, m, 6 x CC$\underline{H}_2$CH$_2$CH$_2$O), 1.55-1.85 (31H, m, 3 x CH, 3 x CH_2, 9 x CCH$_2$C$\underline{H}_2$CH$_2$O), 2.55 (6H, t, J = 7.0, NHCOC$\underline{H}_2$CH$_2$), 2.61-2.71 (18H, m, 9 x C$\underline{H}_2$CH$_2$CO), 2.77-2.87 (18H, m, 9 x CH$_2$C$\underline{H}_2$CO), 2.93 (6H, t, J = 7.0, NHCOCH$_2$C$\underline{H}_2$), 3.19 (2H, t, J = 7.0, CH_2), 3.58-3.70 (12H, m, 6 x OCH_2), 3.72-3.77 (2H, m, OCH_2), 3.80-3.84 (4H, m, 2 x OCH_2), 3.87-3.92 (6H, m, 3 x OCH_2), 3.98-4.09 (36H, m, 9 x COC$\underline{H}_2$NH$_2$, 9 x CH$_2$CH$_2$C$\underline{H}_2$O), 4.14-4.21 (6H, m, 3 x OCH_2), 4.24-4.34 (4H, m, 4 x CH), 4.36-4.42 (2H, m, 2 x CH), 4.43-4.49 (1H, m, CH), 4.51-4.57 (7H, m, 3 x OCH_2, CH), 7.78-7.86 (3H, m, triazole CH); ^{13}C NMR (CD_3OD, 125 MHz) δ 17.54

(CH_3), 20.50 (CH_3), 21.81 (CH_3), 22.21 (CH_3), 22.68 ($NHCOCH_2\underline{C}H_2$), 23.60 ($C\underline{C}H_2CH_2CH_2O$), 25.76 (CH), 25.92 (CH), 26.07 (CH), 28.52 ($\underline{C}H_2CH_2CO$), 30.88 (CH), 31.77 ($CCH_2\underline{C}H_2CH_2O$), 35.33 ($CH_2\underline{C}H_2CO$), 36.82 ($NHCO\underline{C}H_2CH_2$), 41.62 ($CH_2$), 48.16 ($CO\underline{C}H_2NH_2$), 51.27 ($OCH_2$), 51.32 (CH), 53.38 (CH), 54.48 (CH), 54.81 (CH), 59.12 (CH), 66.05 ($CCH_2CH_2\underline{C}H_2O$), 68.58 (CH), 70.01 ($OCH_2$), 70.47 ($OCH_2$), 70.77 ($OCH_2$), 71.33 ($OCH_2$), 71.46 ($OCH_2$), 71.60 ($OCH_2$), 108.23 (Ar-CH), 124.30 (triazole CH), 153.70 (Ar-C), 158.64 (Ar-C), 173.38 (CO), 173.89 (CO), 174.11 (CO), 175.63 (CO), 203.20 (CO); [Found (ESI+) 796.4429 $[M+4H]^{4+}$, $C_{146}H_{244}N_{30}O_{48}$ requires 796.4388].

5-(4-Aminophenyl)-10,15,20-triphenylporphyrin (190)[289]

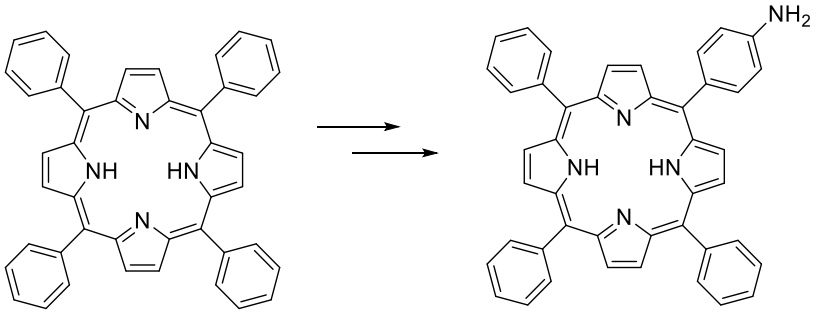

(6) **(190)**

Step 1

The conjugate **(190)** was synthesized according to the procedure of Luguya *et al*.[289] modified as follows: A solution of **(6)** (0.5 g, 0.81 mmol) in TFA (30 mL) in an air-open round-bottom flask was treated with $NaNO_2$ (0.1 g, 1.44 mmol) in a single portion. The reaction mixture was stirred at 18 °C for 3 min and then quenched with H_2O (40 mL). The mixture was transferred to a separatory funnel and further diluted with H_2O (40 mL) and DCM (80 mL). After separation, the aqueous phase was extracted with DCM (2 x 100 mL). The organic phases were combined, washed with sat. aq. $NaHCO_3$ (2 x 100 mL), brine (100 mL), dried over $MgSO_4$, filtered and the solvent was evaporated to give a residue (0.59 g), which was a mixture of unchanged **(6)**, mono- and dinitrated materials. This was used in the next step with further purification.

Step 2

A solution of the crude mixture from step 1 (0.59 g) in DCM (250 mL) and MeOH (60 mL) was treated with Pd/C 5% (0.09 g). $NaBH_4$ (0.75 g, 19.8 mmol) was then added in small portions over 10 min, while stirring and keeping the flask open to the atmosphere. After 15 min of additional stirring, the reaction was quenched with the addition of H_2O (75 mL), then transferred to a separatory funnel. The organic phase was separated, washed with brine (75 mL), dried over $MgSO_4$, filtered and the solvent was evaporated. Purification by column chromatography on silica gel using toluene to elute unreacted **(6)**, then 0-10% EtOAc in DCM gave **(190)** as a purple solid (0.16 g, 31%); ^{1}H NMR (400 MHz, $CDCl_3$ δ -2.75 (2H, br, internal 2 x N-H of the porphyrin), 6.97-7.02 (2H, m, Ar), 7.65-7.78 (9H, m, Ar), 7.94-8.01 (2H, m, Ar), 8.13-8.26 (6H, m, Ar), 8.74-8.82 (6H, m, Ar), 8.86-8.91 (2H, m, Ar).

5-[4-(6-dibenzoazacyclooctynecaproateamido)ethylamidophenyl]-10,15,20-triphenylporphyrin (192)

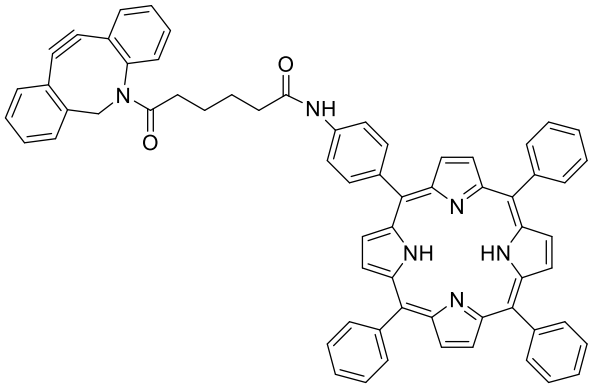

A solution of **(190)** (22.6 mg, 0.04 mmol) in anhydrous DCM (1.5 mL) was treated with HOBt (7.54 mg, 0.05 mmol), dibenzocyclooctyne-acid (10.0 mg, 0.03 mmol), EDC.HCl (6.88 mg, 0.04 mmol) and DIEA (10 µL, 0.04 mmol). The reaction mixture was stirred at RT overnight, then it was purified directly by column chromatography on silica gel eluting with 1-10% acetone in DCM to give **(192)** as a red solid (21 mg, 76%); R_f (DCM/acetone 9:1) = 0.75; MP > 250 °C; HPLC: Analytical HPLC (Gradient 1) R_t = 11.91 min; UV-Vis ($CHCl_3$), nm (%): 420 (100), 516 (8.4), 543 (4.88), 595 (3.51), 643 (2.98); ^{1}H NMR (500 MHz, $(CD_3)_2SO$, 60 °C) δ 1.33-1.47 (4H, m, $CH_2CH_2CH_2CH_2CONH$),

1.89-1.95 (1H, m, CH<u>H</u>$CH_2CH_2CH_2$CONH), 2.23-2.28 (3H, m, CH<u>H</u>CH_2CH_2C<u>H</u>$_2$CONH), 3.56-3.62 (1H, m, CH<u>H</u>), 5.00-5.08 (1H, m, CH<u>H</u>), 7.25-7.68 (9H, m, 9 x Ar-CH), 7.79-7.83 (9H, m, 9 x Ar-CH), 7.99 (2H, d, J = 8.0, 2 x Ar-CH), 8.11 (2H, d, J = 8.0, 2 x Ar-CH), 8.20 (6H, d, J = 7.5, 6 x Ar-CH), 8.79-8.84 (6H, m, 6 x Ar-CH); ^{13}C NMR (125 MHz, $(CD_3)_2SO$, 60 °C), δ 24.33, 24.38, 30.27, 33.76, 36.07, 54.58, 117.30, 117.87, 119.56, 119.66, 119.79, 121.35, 124.83, 126.48, 126.64, 127.33, 127.45, 127.65, 127.73, 128.05, 128.30, 128.58, 129.12, 130.87, 132.06, 132.19, 133.89, 134.26, 135.43, 137.38, 139.03, 141.01, 141.03, 148.19, 151.64, 171.04, 171.43. [Found (ESI+) 945.3966 $[M+H]^+$, $C_{65}H_{49}N_6O_2$ requires 945.3912].

13'-(2-aminoethylamido)-15',17'-dimethyl-chlorin e_6 (191)

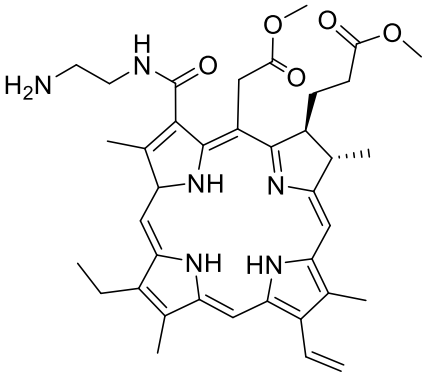

Pheophorbide-a was prepared by extraction and purification of pheophytin-a from spirulina spp. followed by methanolysis of the phytol group.[290] A solution of pheophorbide-a **(30)** (100 mg, 0.17 mmol) in anhydrous THF (25 mL) was treated with 1,2-diaminoethane (397 µL, 5.94 mmol). The resulting solution was stirred at RT overnight. The mixture was then diluted with DCM (100 mL) and washed with H_2O (3 x 50 mL) and brine (3 x 50 mL). The organic phase was dried (Na_2SO_4) and the solvent was evaporated. The crude product **(191)** (107 mg, quant.) was used in the subsequent steps without further purifications.

13’-[(6-dibenzoazacyclooctynecaproateamido)ethylamido-15’,17’-dimethylchlorin e_6 (193)

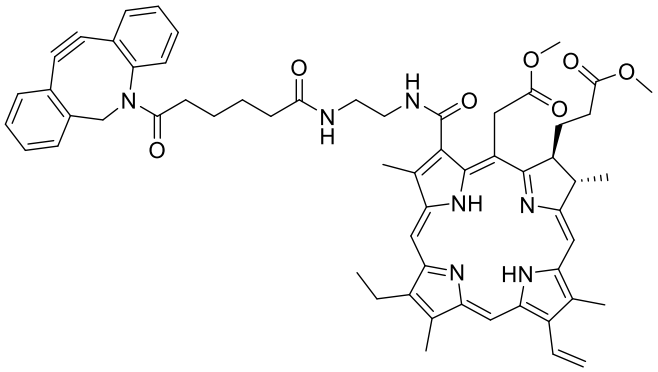

A solution of **(191)** (22.0 mg, 0.03 mmol) was treated with HOBt (5.0 mg, 0.04 mmol), dibenzocyclooctyne-acid (10.0 mg, 0.03 mmol), EDC.HCl (7.0 mg, 0.04 mmol) and DIEA (16.0 µL, 0.09 mmol) in anhydrous DCM (1.5 mL) and stirred at RT overnight. The crude product was purified directly by column chromatography on silica gel eluting with EtOAc to give **(193)** as a green solid (17 mg, 57%); R_f (EtOAc) = 0.23; Analytical HPLC (Gradient 1) R_t = 10.36 min; UV-Vis ($CHCl_3$), nm (%): 404 (100), 489 (9.95), 609 (4.15), 665 (32.86); ^{1}H-NMR (500 MHz, $(CD_3)_2SO$, 60 °C) δ -2.15 - -1.70 (2 H, m internal N-H chlorin), 1.21 - 1.42 (4H, m, 2 x CH_2), 1.58 - 1.75 (7H, m, 2 x CH_3 + CHH), 1.82 (1H, m, CHH), 1.93-2.04 (2H, m, CH_2), 2.18 (2 H, dd, J = 13.6, 5.5, CHH + CHH), 2.24 - 2.37 (1H, m, CHH), 3.27-3.74 (20H, m, CHH + 2 x CH_2 + 5 x CH_3), 2.61-2.70 (1H, m, CHH), 3.86 (2H, q, J = 7.2, CH_2), 4.45 (1H, d, J = 10.4, CH), 4.63 (1H, d, J = 7.1, CH), 5.01-5.10 (1H, m, CHH), 5.31 (1 H, d, J = 18.8, CHH), 5.53 (1H, d, J = 18.8, CHH), 6.21 (1H, d, J = 11.6, CHH), 6.46 (1H, d, J = 17.8, CHH), 7.25-7.66 (8H, m, DBCO aromatic protons), 7.73 (1H, br, N_2-H), 8.29 (1H, dd, J = 17.8, 11.6, CH), 8.94 (1H, br, N_1-H), 9.13 (1H, br, CH), 9.78 (1H, br, CH), 9.83 (1H, br, CH); ^{13}C-NMR (125 MHz, $(CD_3)_2SO$, 60 °C), 11.4, 12.1, 12.4, 18.0, 19.4, 23.4, 24.3, 24.8, 25.0, 25.1, 30.0, 31.1, 33.8, 34.2, 34.4, 35.7, 37.5, 38.8, 48.7, 51.7, 52.2, 53.3, 55.3, 79.2, 79.4, 79.7, 94.9, 98.9, 101.2, 103.6, 108.6, 114.9, 122.0, 122.6, 123.0, 125.5, 127.2, 128.0, 128.4, 128.5, 129.2, 129.8, 130.2, 130.5, 130.8, 132.8, 134.4, 136.3, 138.9, 144.6, 148.9, 152.4, 168.4, 168.6, 172.1, 172.6, 173.1, 173.5, 174.3; [Found (ESI+) 982.4862 $[M+H]^+$, $C_{59}H_{63}N_7O_7$ requires 982.4995].

LARLLT TPP-DBCO (195)

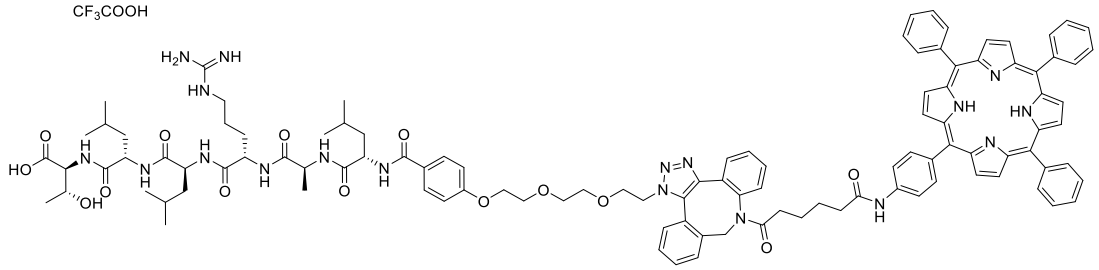

A solution of azido-peptide **(177)** (15 mg, 13.9 µmol) and **(192)** (26 mg, 28 µmol) in DMSO (500 µL) was stirred at room temperature for 8 h, shielded from light. Reaction was monitored by analytical HPLC (Gradient 1) which showed disappearance of starting material **(177)** and appearance of new species at 10.08 min. The crude product was purified by semi-preparative HPLC (Gradient 2) and was freeze-dried to give **(195)** as a dark green solid (19 mg, 68%); Analytical HPLC (Gradient 1) R_t = 10.08 min; UV-Vis (0.1% aq TFA), nm (%): 412 (100), 521 (13.5), 539 (9.75), 584 (8.35), 642 (7.69); fluorescence $\lambda_{max.}$ (0.1% aq TFA, $\lambda_{exc.}$ = 420 nm) 690 nm; [Found (ESI+) 1907.9407 $[M+2H]^{2+}$, $C_{109}H_{123}N_{18}O_{14}$ requires 1907.9461];

LARLLT Ce6-DBCO (196)

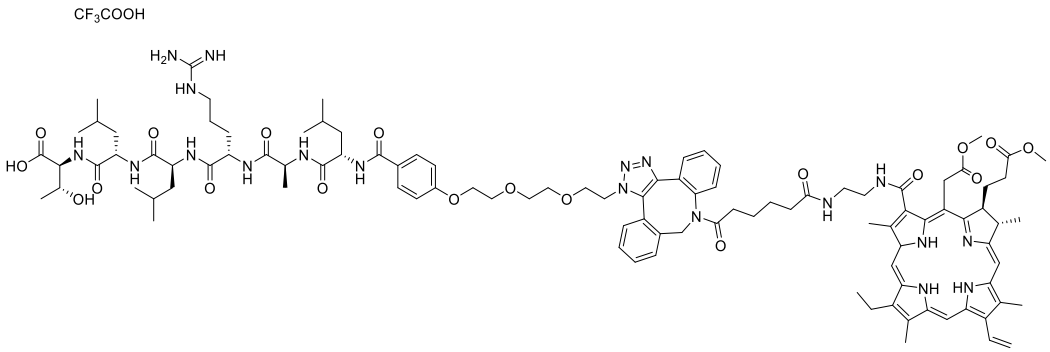

A solution of azido-peptide **(177)** (10 mg, 0.01 mmol) and **(193)** (19.68 mg, 0.02 mmol) in DMSO (1.0 mL) was stirred at RT for 8 h. Reaction was monitored by analytical HPLC (Gradient 1) which showed disappearance of starting material **(177)** and appearance of new species at 8.83 min. The crude product was purified by semi-preparative HPLC (Gradient 2) and was freeze-dried to give **(196)** as a dark blue solid (12.7 mg, 66%); Analytical HPLC (Gradient 1) R_t = 8.83 min; UV-Vis (0.1% aq TFA), nm (%): 400 (100), 498

(10.73), 606 (3.81), 662 (31.47); fluorescence $\lambda_{max.}$ (0.1% aq TFA, $\lambda_{exc.}$ = 420 nm) 667 nm; [Found (ESI+) 995.0128 $[M+2Na]^{2+}$, $C_{103}H_{137}N_{19}O_{19}Na$ requires 995.0061].

LARLLT Verteporfin-DBCO (197)

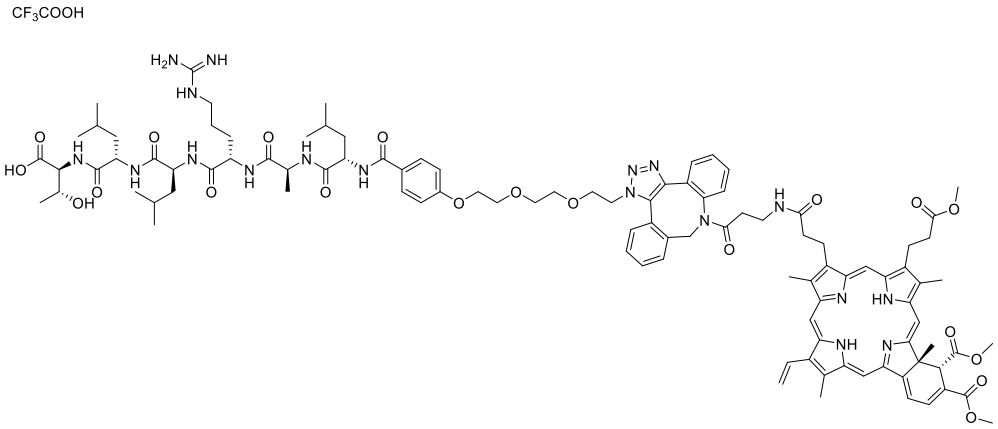

A solution of azido-peptide **(177)** (10 mg, 0.01 mmol) and **(194)** (27.6 mg, 0.02 mmol) in DMSO (1.0 mL) was stirred at RT for 8 h. Reaction was monitored by analytical HPLC (Gradient 1) which showed disappearance of starting material **(177)** and appearance of new species at 9.33 min. The crude product was purified by semi-preparative HPLC (Gradient 2) and was freeze-dried to give **(197)** as a dark blue solid (14.5 mg, 73%); Analytical HPLC (Gradient 1) R_t = 9.33 min; UV-Vis (0.1% aq TFA), nm: 421 (100), 575 (17.21), 628 (8.09), 687 (39.98); fluorescence $\lambda_{max.}$ (0.1% aq TFA, $\lambda_{exc.}$ = 420 nm) 693 nm; [Found (ESI+) 992.4846 $[M+2Na]^{2+}$, $C_{103}H_{130}N_{18}O_{20}Na$ requires 992.4747].

Imidazole-1-sulfonyl azide. HCl (204a)[308, 317]

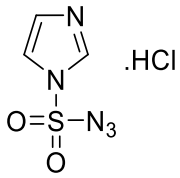

An ice-cooled suspension of NaN_3 (4.8 g, 73 mmol) in MeCN (100 mL) was treated with sulfuryl chloride (5.9 mL, 73 mmol) added dropwise. The reaction mixture was stirred at RT overnight. Imidazole (10 g, 146 mmol) was added in small portions to the ice-cooled mixture and the resulting slurry was stirred at

RT for 3 h. The mixture was diluted with EtOAc (200 mL), washed with H_2O (2 x 200 mL), sat. aq. $NaHCO_3$ (2 x 200 mL), dried over $MgSO_4$ and filtered. A solution of HCl in EtOH [obtained by drop-wise addition of AcCl (7.8 mL, 109 mmol) to ice-cooled dry EtOH (40 mL) was added dropwise to the filtrate with stirring. The mixture was chilled in an ice-bath, filtered and the residue washed with EtOAc (3 x 50 mL) to give **(204a)** as colourless needles (9.3 g, 61%); Mp = 94-96 °C (lit. 96-98 °C)[317]; ^{1}H NMR (D_2O, 400 MHz) δ 7.57 (1H, s, H-4), 7.97 (1H, s, H-5), 9.45 (1H, s, H-2).

Fmoc-azido Lysine (205)[308]

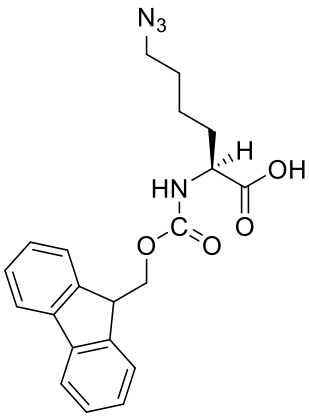

A solution of Fmoc-L-Lysine-OH (5.50 g, 14.93 mmol) in water was treated with aq. HCl (1.2 mL, 14.9 mmol), and the reaction mixture was diluted with H_2O/ MeOH (1:2, 65 mL). A solution of imidazole-1-sulfonyl azide hydrochloride **(204a)** (3.75 g, 17.9 mmol), $NaHCO_3$ (8.11 g, 96.54 mmol) and $CuSO_4.5H_2O$ (37.3 mg, 0.149 mmol) in water (1 mL) was added and the mixture was stirred for 16 h at RT. The reaction mixture was concentrated to 50 mL, then it was diluted with more H_2O (150 mL), and acidified to pH 2.0 by dropwise addition of 5 M aq. HCl. The aqueous layer was extracted with EtOAc (3 x 50 mL) and dried over $MgSO_4$. The organic layer was filtered and the solvent was evaporated to give the crude product. Purification by column chromatography on silica gel eluting with (Toluene / EtOAc / AcOH 85:10:5 v/v/v) gave **(205)** as a yellowish gum (3.61 g, 68%); ^{1}H NMR ($CDCl_3$, 400 MHz) δ 1.26-1.77 (5H, m, $CHC\underline{H}HC\underline{H}_2C\underline{H}_2CH_2N_3$), 1.93-2.04 (1H, m, $CHCH\underline{H}CH_2CH_2CH_2N_3$), 3.17-3.34 (2H, m, $CHCH_2CH_2CH_2C\underline{H}_2N_3$), 4.22 (1H, t, J = 6.8, Fmoc CH), 4.37-4.62 (3H, m, α-H, Fmoc-OCH_2), 5.25-5.35 (1H, m,

NH), 7.29-7.34 (2H, m, Fmoc CH), 7.38-7.44 (2H, m, Fmoc CH), 7.53-7.63 (2H, m, Fmoc CH), 7.76 (2H, d, J = 7.2, Fmoc CH); ^{13}C-NMR ($CDCl_3$, 100 MHz) δ 22.58 ($CH\underline{C}H_2CH_2CH_2CH_2N_3$/$CHCH_2\underline{C}H_2CH_2CH_2N_3$/ $CHCH_2CH_2\underline{C}H_2CH_2N_3$), 28.48 ($CH\underline{C}H_2CH_2CH_2CH_2N_3$ / $CHCH_2\underline{C}H_2CH_2CH_2N_3$/ $CHCH_2CH_2\underline{C}H_2CH_2N_3$), 31.96 ($CH\underline{C}H_2CH_2CH_2CH_2N_3$ / $CHCH_2\underline{C}H_2CH_2CH_2N_3$/ $CHCH_2CH_2\underline{C}H_2CH_2N_3$), 47.31 (Fmoc CH), 51.20 ($CHCH_2CH_2CH_2\underline{C}H_2N_3$), 53.61 ($\underline{C}HCH_2CH_2CH_2CH_2N_3$), 67.34 (Fmoc-O$\underline{C}H_2$), 120.18 (Ar-CH), 125.15 (Ar-CH), 127.24 (Ar-CH), 127.93 (Ar-CH), 141.51 (Ar-C), 143.76 (Ar-C), 143.92 (Ar-C), 156.26 (CO), 176.35 (CO); [Found (ESI+) 395.1697 $[M+H]^+$, $C_{21}H_{23}N_4O_4$ requires 395.1719].

H-Arg-Arg-Met-Lys-Trp-Lys-Lys(N_3)-Gly-NH_2 (Penetratin (9-15) (200)

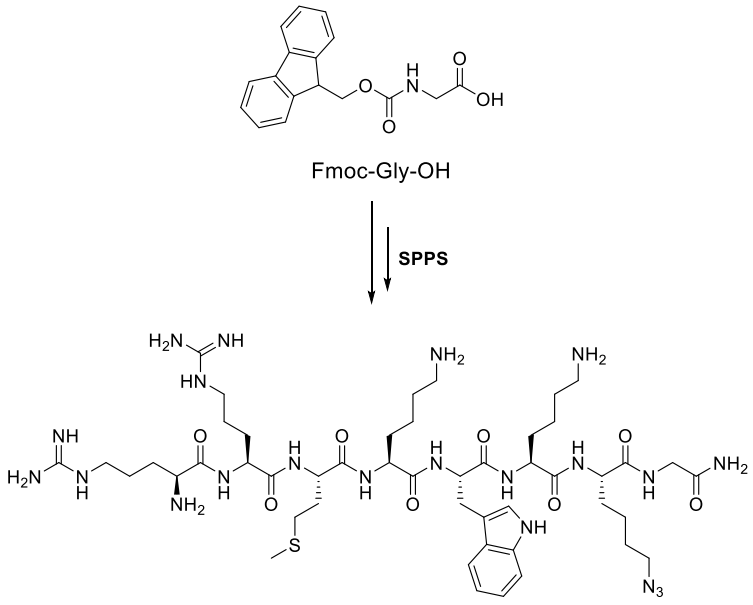

H_2N-RRMKWKK(N_3)G-NH_2, **(200)**

Rink Amide MBHA Resin (250 mg, 0.59 mmol/g) was pre-swollen in a SPPS vessel using DCM (5 mL) for 15 min, and the procedure was repeated twice. The Fmoc group from the resin was removed by adding piperidine/DMF (3.0 mL, 1:4 v/v) to the resin and the vessel was agitated for 5 min. The procedure was repeated and the vessel was agitated for 10 min. Successful removal of Fmoc group was confirmed by Kaiser test. Preloading of the first amino acid was accomplished by adding a solution of of Fmoc-Gly (178 mg, 0.60 mmol), DIC (93.9 µL, 0.60 mmol) and DIEA (160 µL, 0.90 mmol) in DMF (3.0 mL) and the vessel was agitated for 1 h and the solvent removed under

reduced pressure. The resin was washed with DMF (5 x 5 mL) and was followed by an acetylation step (Ac_2O/DIEA/DMF = 2.5 mL, 1/1/8 v/v/v, 1 x 10 min), then the Fmoc group was removed using the similar procedure as above. The remaining amino acids were coupled using a Activotec automated peptide synthesiser using 3 eq. of Fmoc-protected amino acid (Fmoc-Lys(N_3)-OH, Fmoc-Arg(Pmc)-OH, Fmoc-Met-OH, Fmoc-Trp(Boc)-OH, Fmoc-Lys(Boc)-OH, or Fmoc-Gly-OH), 3 eq. of PyBOP as coupling agent, 6 eq. of DIEA as base and DMF (4.3 mL) as solvent. The last step of the synthesis was Fmoc de-protection using the procedure same as above. The peptide resin **(206)** was washed thoroughly with DMF (2 x 5.0 mL), DCM (2 x 5.0 mL), MeOH (5.0 mL) and Et_2O (2 x 5.0 mL), and dried in vacuo. to have 1.1 g of peptide-resin **(206)**. Resin (50 mg, 0.03 mmol) was placed in a 10 mL vial and was treated with TFA/TIS/H_2O (1 mL, 95:2.5:2.5 v/v/v) for 4 h. The resin beads were filtered off, washed with TFA, and the combined filtrates were collected into a Falcon tube containing Et_2O (5mL) to precipitate the peptide. The resulting precipitate was collected by centrifugation and was washed repeatedly with Et_2O to remove excess TFA. The precipitated material was dissolved in 0.1% aq. TFA, filtered using 0.2 µm syringe filter and the resulting solution was directly purified by semi-preparative HPLC (Gradient 2). The purified peptide was then freeze-dried to give **(200)** as a white solid (33 mg, 65%); Analytical HPLC (Gradient 1, R_t = 5.06 min); [Found (ESI+) 557.8337 $[M+2H]^{2+}$, $C_{48}H_{85}N_{21}O_8S$ requires 557.8330].

H-Gly-Arg-Lys-Lys-Arg-Arg-Gln-Arg-Arg-Arg-Gly-Tyr-Lys(N_3)-Gly-NH_2 (Tat (48-57)-GYKG (201)

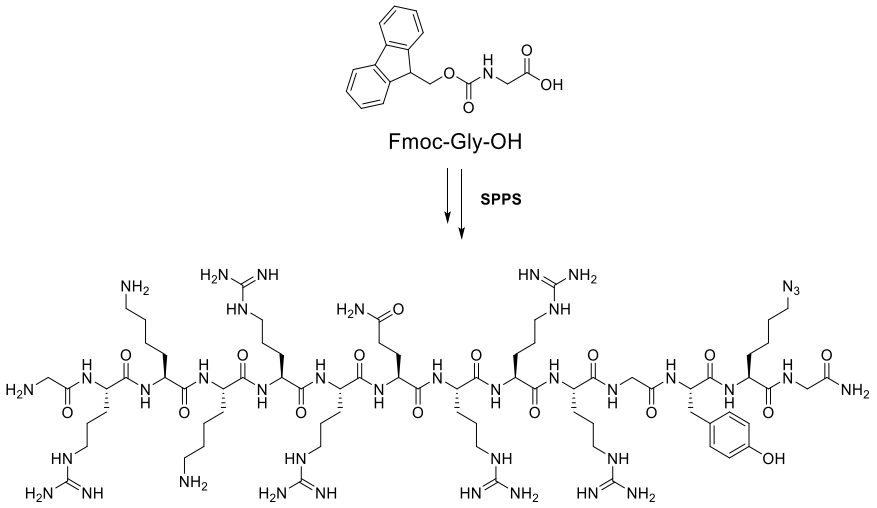

H_2N-GRKKRRQRRRGYK(N_3)G-NH_2, **(201)**

The protected peptide resin **(207)** was synthesized as for **(200)** on a 0.15 mmol scale. Cleavage of a sample of resin (50 mg, 0.03 mmol) as previously gave peptide **(201)** as a white solid (54 mg, 67%); Analytical HPLC (Gradient 1) R_t- 4.52 min; [Found (ESI+) 609.7098 $[M+3H]^{3+}$, $C_{74}H_{138}N_{39}O_{16}$ requires 609.7056].

H-Leu-Gly-Ala-Ser-Trp-His-Arg-Pro-Asp-Lys-Gly-Gly-Arg-Lys-Lys-Arg-Arg-Gln-Arg-Arg-Arg-Gly-Tyr-Lys(N_3)-Gly-NH_2 (vMIP-II- Tat (48-57)-GYKG chimera (202)

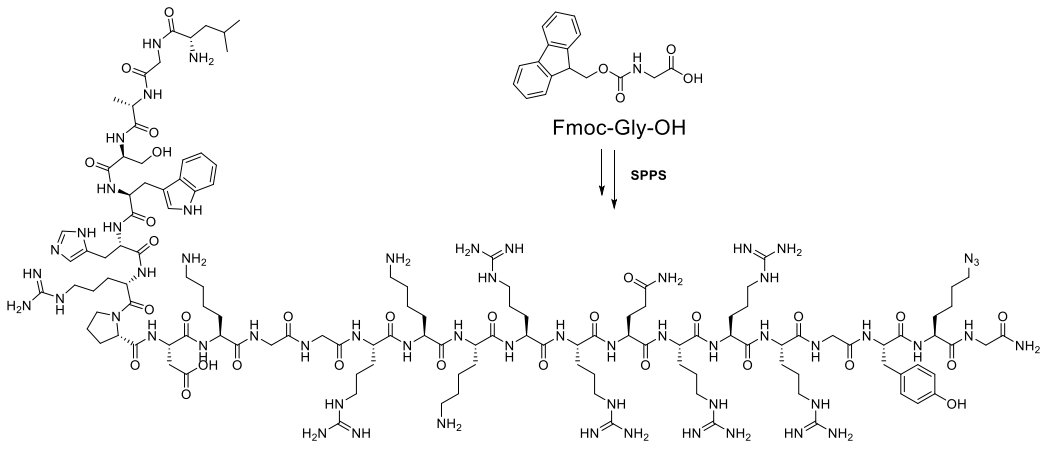

H_2N-LGASWHRPDKGGRKKRRQRRRGYK(N_3)G-NH_2, **(202)**

The protected peptide resin **(208)** was synthesized as for **(206)** on a 0.15 mmol

scale. Cleavage of a sample of resin (50 mg, 0.03 mmol) as previously gave peptide **(202)** as a white solid (61 mg, 47%); Analytical HPLC (Gradient 1) R_t- 5.41 min; [Found (ESI+) 758.6892 $[M+4H]^{4+}$, $C_{128}H_{219}N_{57}O_{30}$ requires 758.6835].

H-Leu-Leu-Ile-Ile-Leu-Arg-Arg-Arg-Ile-Arg-Lys-Gln-Ala-His-Ala-His-Ser-Lys(N_3)-NH_2 (PVec) (203)

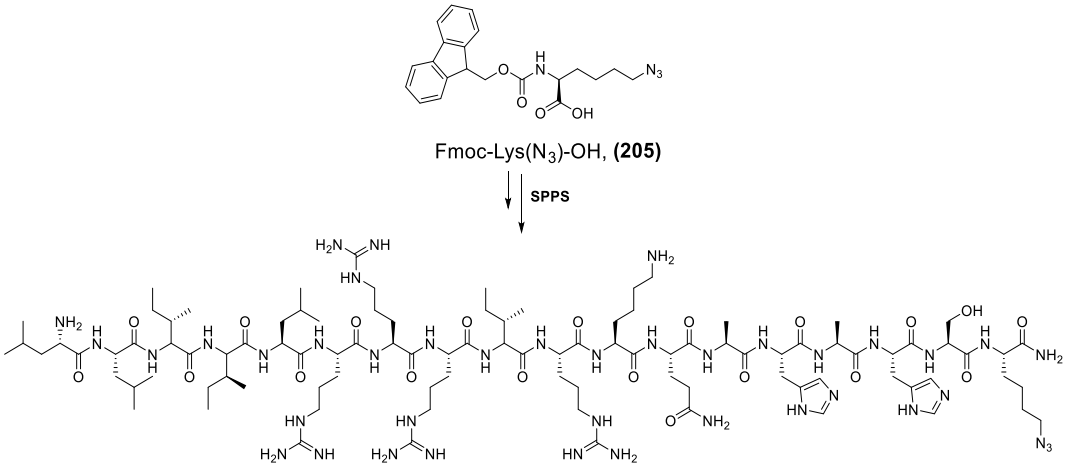

H_2N-LLIILRRRIRKQAHAHSK(N_3)-NH_2, **(203)**

The protected peptide resin **(209)** was synthesized as for **(206)** on a 0.15 mmol scale. Cleavage of a sample of resin (50 mg, 0.03 mmol) as previously gave peptide **(203)** as a white solid (39.5 mg, 59%); Analytical HPLC (Gradient 1) R_t- 4.58 min; [Found (ESI+) 745.8039 $[M+3H]^{3+}$, $C_{98}H_{179}N_{40}O_{20}$ requires 745.8076].

H-Arg-Arg-Met-Lys-Trp-Lys-Lys(Tris-ALA)-Gly-NH_2 (Penetratin (9-15)-Tris-ALA (210)

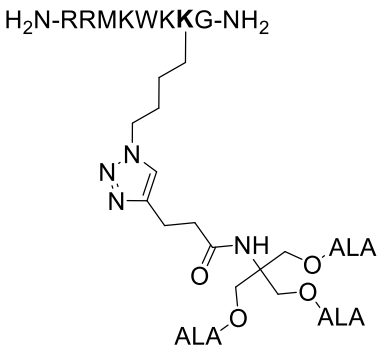

Peptide resin **(206)** (20 mg, 12 µmol) was swollen in DCM (2 mL) for 10 min

and then in DMSO for 3 min (3 x 2 mL). A solution of **(105)** (20 mg, 24 µmol) in DMSO (500 µL) was treated with copper(I) trifluoromethanesulfonate benzene complex (12 mg, 24 µmol) and the mixture was added to the reaction vessel containing the resin which was agitated for 5 days. The solvent was removed and the resin was washed with DMSO (5 x 2 mL), DCM (3 x 2 mL), MeOH (3 x 2 mL) and DCM (3 x 2 mL). The resin was placed in a 3 mL vial and was treated with TFA/TIS/H_2O (1 mL, 95:2.5:2.5 v/v/v) for 4 h. The resin beads were filtered off, washed with TFA, and the combined filtrates were collected into a Falcon tube containing Et_2O (3 mL) to precipitate the peptide conjugate. The resulting product was collected by centrifugation and was washed repeatedly with Et_2O to remove excess TFA. The peptide conjugate was dissolved in 0.1% aq. TFA, filtered using 0.2 µm syringe filter and the resulting solution was purified by semi-preparative HPLC (Gradient 2). The purified peptide was then freeze-dried to give **(210)** as a white solid (13 mg, 43%); Analytical HPLC (Gradient 1) R_t = 4.33 min; [Found (ESI+) 552.3047 $[M+3H]^{3+}$, $C_{72}H_{122}N_{25}O_{18}S$ requires 552.3035].

H-Gly-Arg-Lys-Lys-Arg-Arg-Gln-Arg-Arg-Arg-Gly-Tyr-Lys(Tris-ALA)-Gly-NH_2 (Tat (48-57)-GYKG-Tris-ALA) (211)

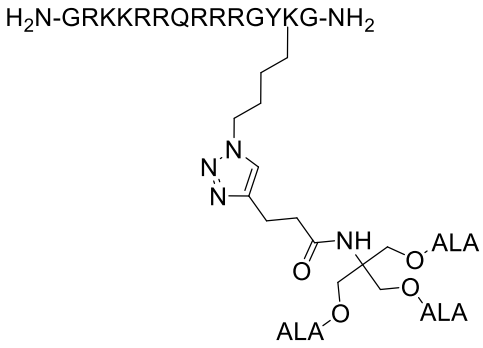

The peptide-ALA conjugate **(211)** was synthesized as for **(210)** using peptide resin **(206)** (20 mg, 12 µmol). The purified peptide obtained was freeze-dried to give **(211)** as a white solid (18 mg, 41%); Analytical HPLC (Gradient 1) R_t = 4.03 min; [Found (ESI+) 1184.1784 $[M+2H]^{2+}$, $C_{98}H_{173}N_{43}O_{26}$ requires 1184.1763].

H-Leu-Gly-Ala-Ser-Trp-His-Arg-Pro-Asp-Lys-Gly-Gly-Arg-Lys-Lys-Arg-Arg-Gln-Arg-Arg-Arg-Gly-Tyr-Lys(Tris-ALA)-Gly-NH_2 (vMIP-II- Tat (48-57)-GYKG chimera-Tris-ALA) (212)

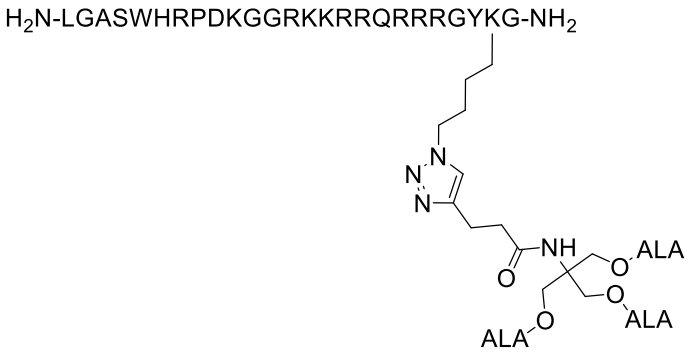

The peptide-ALA conjugate **(212)** was synthesized as for **(210)** on a 12 µmol scale. The purified peptide obtained was freeze-dried to give **(212)** as a white solid (29 mg, 46%); Analytical HPLC (Gradient 1) R_t = 4.31 min; [Found (ESI+) 893.7541 $[M+4H]^{4+}$, $C_{152}H_{255}N_{61}O_{40}$ requires 893.7443].

H-Leu-Leu-Ile-Ile-Leu-Arg-Arg-Arg-Ile-Arg-Lys-Gln-Ala-His-Ala-His-Ser-Lys(Tris-ALA)-NH_2 (pVEC-Tris-ALA) (213)

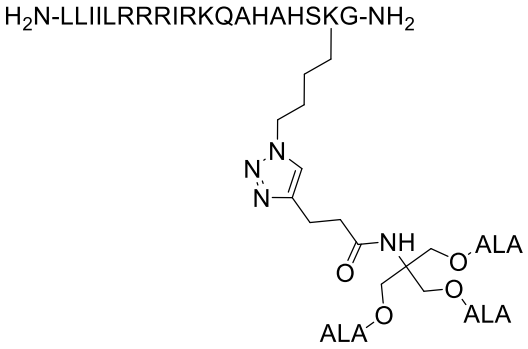

Peptide resin (**209)** (50 mg, 30 µmol) was swollen in DCM (2 mL) for 10 min and then in DMSO for 3 min (3 x 2 mL). A solution of **(105)** (50 mg, 60 µmol) in DMSO (500 µL) was treated with copper(I) trifluoromethanesulfonate benzene complex (30 mg, 60 µmol) and the mixture was added to the reaction vessel containing the resin which was agitated for 5 days. Solvent was removed and the resin was washed with DMSO (5 x 2 mL), DCM (3 x 2 mL), MeOH (3 x 2 mL) and DCM (3 x 2 mL). The resin was transferred to a 5 mL vial and was treated with TFA/TIS/H_2O (1 mL, 95:2.5:2.5 v/v/v) for 4 h. The resin beads were filtered off, washed with TFA, and the combined filtrates were

collected into a Falcon tube containing Et_2O (3 mL) to precipitate the peptide conjugate. The resulting product was collected by centrifugation and was washed repeatedly with Et_2O to remove excess TFA. The peptide conjugate was dissolved in 0.1% aq. TFA, filtered using 0.2 µm syringe filter and the resulting solution was purified by semi-preparative HPLC (Gradient 2). The purified peptide was then freeze-dried to give **(213)** as a white solid (37 mg, 31%); Analytical HPLC (Gradient 1) R_t = 5.23 min; [Found (ESI+) 925.5547 $[M+3H]^{3+}$, $C_{122}H_{215}N_{44}O_{30}$ requires 925.5545].

H-Leu-Leu-Ile-Ile-Leu-Arg-Arg-Arg-Ile-Arg-Lys-Gln-Ala-His-Ala-His-Ser-Lys(Ex.TRIS-ALA)-NH_2 (pVEC-Ex.Tris-ALA) (214)

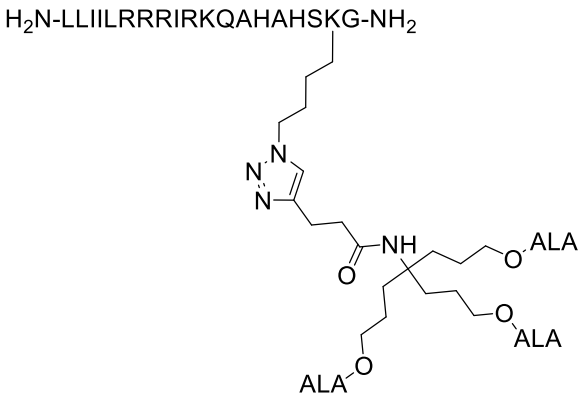

Peptide resin **(209)** (35 mg, 21 µmol) was swollen in DCM (2 mL) for 10 min and then in DMSO for 3 min (3 x 2 mL). A solution of **(105)** (39 mg, 42 µmol) in DMSO (500 µL) was treated with copper(I) trifluoromethanesulfonate benzene complex (30 mg, 42 µmol) and the mixture was added to the reaction vessel containing the resin which was agitated for 5 days. The solvent was removed and the resin was washed with DMSO (5 x 2 mL), DCM (3 x 2 mL), MeOH (3 x 2 mL) and DCM (3 x 2 mL). The resin was transferred to a 5 mL vial and was treated with TFA/TIS/H_2O (1 mL, 95:2.5:2.5 v/v/v) for 4 h. The resin beads were filtered off, washed with TFA, and the combined filtrates were collected into a Falcon tube containing Et_2O (3 mL) to precipitate the peptide conjugate. The resulting product was collected by centrifugation and was washed repeatedly with Et_2O to remove excess TFA. The peptide conjugate was dissolved in 0.1% aq. TFA, filtered using 0.2 µm syringe filter and the resulting solution was purified by semi-preparative HPLC (Gradient 2). The purified peptide was then freeze-dried to give **(214)** as a white solid (32 mg,

39%); Analytical HPLC (Gradient 1) R_t = 5.22 min; [Found (ESI+) 1429.8704 $[M+2H]^{2+}$, $C_{128}H_{226}N_{44}O_{30}$ requires 1429.8750].

pVEC TPP-DBCO (215)

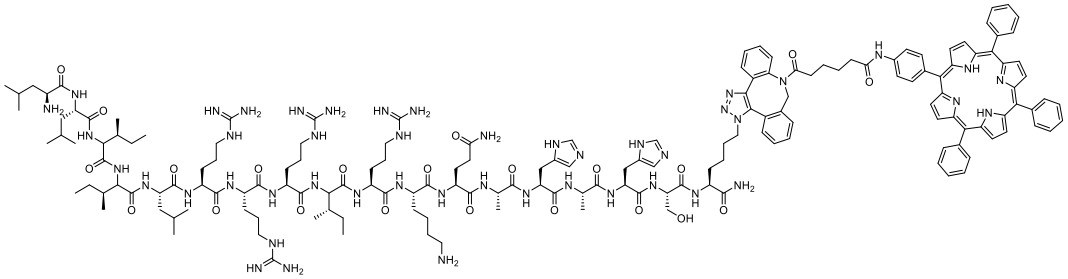

A solution of peptide **(203)** (10 mg, 3.31 µmol) and **(192)** (6.26 mg, 6.62 µmol) in DMSO (500 µL) was stirred at room temperature overnight, shielded from light. The reaction was monitored by analytical HPLC (Gradient 1) which showed disappearance of starting material **(203)** and appearance of a new species at 7.62 min. The crude product was purified by semi-preparative HPLC (Gradient 2) and was freeze-dried to give **(215)** as a dark green solid (9.1 mg, 69%); Analytical HPLC (Gradient 1) R_t = 7.63 min; UV-vis (MeOH), nm (%): 415 (100), 513 (12.96), 547 (9.50), 590 (8.23), 646 (7.81); fluorescence $\lambda_{max.}$ (MeOH, $\lambda_{exc.}$ = 420 nm) nm (%) 653 (100), 716 (35.31); [Found (ESI+) 1589.9035 $[M+2H]^{2+}$, $C_{163}H_{226}N_{46}O_{22}$ requires 1589.8984].

7.3 Biological assays

7.3.1 Materials and Methods

All the reagents were purchased from Sigma-Aldrich. Cell culture materials were obtained from Life Sciences Technologies (Paisley, UK). Phenol red and phenol red-free Dulbeco's Minimum Essential Medium (DMEM) was purchased from Gibco BRL Invitrogen Corporation (Life Technologies, UK). MilliQ water (Millipore, MA, USA) was used to prepare phosphate-buffered saline (PBS) to minimise transition metal levels. ALA was purchased from Carbosynth.

Light source

PDT studies carried out at Bath were conducted using a broad spectrum 4kW lamp (Sellas, Germany) which emits primarily UVA irradiation and has a significant emission in the range of 350-400 nm and some near visible radiation at wavelengths longer than 400 nm. The above lamp was suitable for ALA-PDT studies, as the absorption maximum of PpIX (405 nm) overlaps with the emission of the lamp near the visible region (Figure 103). It also overlaps with the Soret band absorptions of **(196)** and **(197)**.

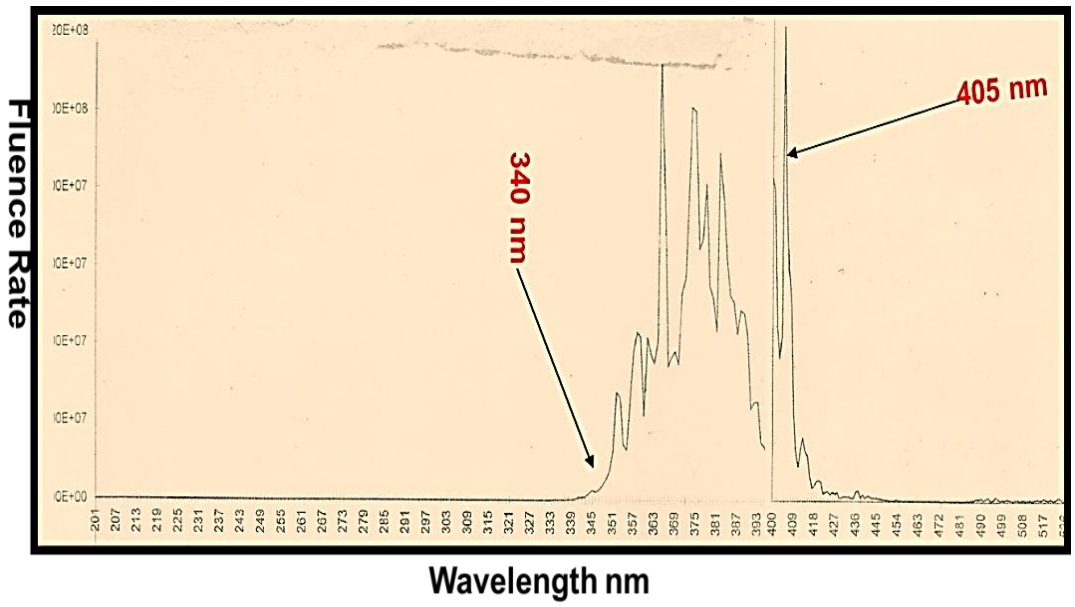

Figure 103. Spectrum of the Sellas 4kW UVA lamp as measured by spectroradiometer

For PDT experiments carried out at University College London (Prof. A. J. MacRobert) 96 well plates (TPP® cell culture plates, Sigma Aldrich) were illuminated from below with a LumiSource lamp (PCI Biotech). The lamp delivered, through four fluorescent tubes, blue light in the spectrum range of 375-450 nm.

7.3.2 Stock solutions

Stock solutions of all prodrugs under investigation, including ALA were prepared in DMSO at a concentration of 100 mM. Aliquots were kept at -20˚C until required.

MTT stock solution was prepared at a final concentration of 5 mg/mL in PBS and was filtered through a 0.22 µm filter for sterilization. The stock solutions were stored in small aliquots at -20 °C.

7.3.3 Cell lines

Studies carried out at Bath:

Fluorescence time-course studies and cytotoxicity studies were carried out in the MDA-MB-231 cell line. Cell culturing was carried out in 10% FCS DMEM (high glucose Dulbecco's modified Eagle's medium) with 30 mM $NaHCO_3$, 2 mM L-glutamine, and 50 IU/mL of each of penicillin/ streptomycin (P/S). The FCS stock was heat-inactivated at 56 °C for 45 min before use. Cells were passaged once every 5 days and seeded at a density of 8 x 10^3 cells per well in media (200 µL), and grown for 24 h prior to the treatment with compounds for 4 or 24 h, depending on the experimental requirement.

Studies carried out at UCL:

Cytotoxicity studies and fluorescence microscopy were undertaken in MDA-MB-231 and MCF-7 cell lines. Both the cell lines were grown in 10% FCS DMEM containing 1% of penicillin streptomycin. Cells were seeded into 96 well plates at a density of 6 x 10^3 cells per well and grown for 24 h prior to treatment with compounds for 24 or 48 h depending on the experimental requirement.

7.3.4 Trypsination

Stock cells were passaged by trypsinisation once or twice a week. As a general rule, stock cell flasks were maintained in culture until they reached a confluency of 70-80%, after which they were trypsinised as detailed below:

The medium was removed from the flask and the cells were then washed with PBS (2 x 10 mL). Trypsin (0.25% w/v, 2 mL) was then added to the flask and the cells were incubated at 37 °C for 3 min, or until detached. 10 % w/v DMEM (4 mL) was added to the flask in order to inactivate the trypsin. The cells were then centrifuged for 5 min at 1200 rpm (Jouan B3.11 centrifuge). The supernatant was then removed and the cell pellet was resuspended in fresh medium (10% w/v DMEM). A small aliquot of the cell suspension (0.1 mL) was mixed with trypan blue dye (0.1 mL) and then counted under a microscope using a Neubauer-improved haemocytometer purchased from Marienfeld (Germany). Cells were then diluted with fresh medium at the required density and incubated at 37 °C.

7.3.5 Statistical Analysis

Results were expressed as mean +/- standard deviation (SD). Data were analysed using paired and unpaired t-tests. The p value of <0.05 was considered as a significant difference between groups of data. GraphPad Prism 7.01 and Microsoft Excel 2013 software was used to carry out statistical analysis.

The ranges given to the number of experiments for each graph presented in the Results section (i.e. n = 3, 4 or 6), indicates the number of independent experiments carried out with different compounds/treatments.

7.3.6 Time-course fluorescence studies

Cells were seeded into clear 96-well cell culture micro-plates (CELLSTAR®, Greiner Bio-one, United Kingdom) at a density of 8 x 10^3 cells per well for 24 h. The culture medium was removed and each well was washed with PBS (2 x 100 µL). Varying concentrations of ALA and ALA-containing prodrugs in phenol red (100 µL) and serum-free medium (100 µL) were then added to designated series of wells in triplicates under subdued lighting. Each plate contained control wells with cells but without added drug to determine the background reading. Each plate was covered with aluminium foil and placed in the incubator at 37 °C CO_2 for 4-24 h. The fluorescence signal from each well was measured at 4, 8 and 24 h interval with a CLARIOstar high performance microplate reader (CLARIOstar® BMG LABTECH, United Kingdom) using 410 nm excitation and 635 nm emission wavelengths with slit widths set to 10 nm.

7.3.7 Photodynamic treatment

Studies carried out at Bath:

Cells were seeded into 96-well black cell culture micro-plates (CELLSTAR®, Greiner Bio-one, United Kingdom) at a density of 8 x 10^3 cells per well for 24 h. The culture medium was removed and each well was washed with PBS (2 x100 µL). Varying concentrations of ALA and ALA-containing prodrugs in phenol red and serum-free medium (100 µL) were then added to designated series of wells in triplicates under subdued lighting. Each plate contained control wells with cells but without added drug to determine the background reading. Each plate was covered with aluminium foil and placed in the incubator for 4 h at 37 °C under an atmosphere of 5% CO_2. After 4 h, drug samples were removed and PBS (100 µL) was added to each well. The plates were irradiated from above using the broad spectrum 4kW lamp for 30, 60 and 90 sec (6, 12 and 18 J/cm^2) by moving a box covered with foil across the plate to expose the appropriate wells (Figure 104). After the irradiation, the PBS was replaced with serum-free medium and plates were incubated for further 48 h and the cell viability was assessed using MTT assay.

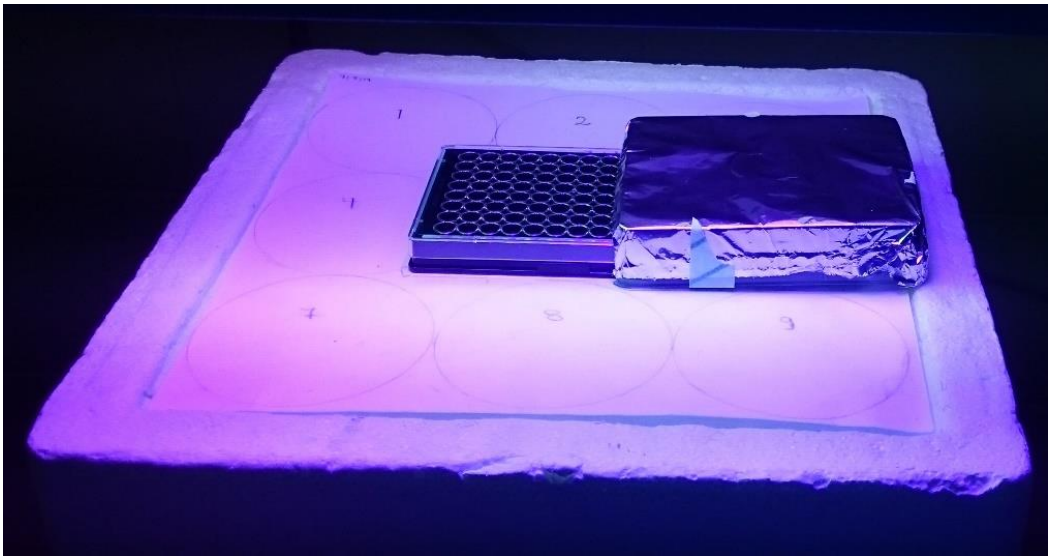

Figure 104. PDT activity on a protected 96-well plate been carried under UVA lamp.

Studies carried out at UCL:

Cells were seeded in 96 well plates for 24 h, after which medium was removed and cells were washed with PBS. Freshly prepared solutions of compounds at varying concentrations were then added to designated wells and the plates were covered with foil to protect them from light and incubated for further a 24 h. The plates were then irradiated from below with the by LumiSource lamp by keeping them on top of the light source area for specified times (7 and 10 min). An opaque box was used to shelter throughout the duration of light exposure. The plates were further incubated for 48 h and cell viability was assessed by MTT assay. In each well plate, some wells were incubated with only culture medium (without any compound) and were used as controls.

7.3.8 MTT assay

Studies carried out at Bath:

Prior to the experiment, a solution of MTT in serum free medium (SFM) was prepared at a final concentration of 0.5 mg/mL from the stock solution. 96 well plates were removed from the incubator and SFM from each well was replaced with MTT/SFM solution (100 µL). The plates were then incubated for a further 3 h. The MTT/SFM solution was removed and DMSO (100 µL) was added to each well. The plates were then kept swirling for few minutes on a 3D rocking

platform (Stuart Scientific UK) under dim lighting. The DMSO solutions were then transferred to a new 96 well plate (transparent) and read with a Dynatech plate reader MR-5000 (Dynatech, Guernsey, Channel Islands) at 570 nm using DMSO as a blank control. The mean values obtained from the raw data for each condition were expressed as percentage enzymatic activity.

Studies carried out at UCL:

A stock solution of MTT at a concentration of 1 mg/mL was prepared and 100 µL was added to each well. The plates were covered with foil and incubated for 2 h. The solution was removed and formazan crystals were dissolved in DMSO. The absorbance was read with a plate reader (MR 700 Dynatech) with a 570 nm band pass filter. The results obtained from the analysis above were averaged out for each concentration from each plate and then normalised. These were then plotted as % cell viability against normalised controls. Normalised standard deviations were also calculated and displayed as error bars on the graphs generated.

7.3.9 Fluorescence Microscopy

Fluorescence microscopy was carried out at UCL in Prof. A. J. MacRobert's laboratory.

In order to investigate the cellular uptake of the EGFR-targeted porphyrin **(195)**, fluorescence microscopy was performed using an upright epifluorescence microscope (Olympus IMT-2) equipped with a 16 bit cooled 512 x 512 CCD camera. Fluorescence excitation was delivered by a 405 nm laser diode module and the emission filter was centred at 660 ± 15 nm. Cells were seeded seeding in a Fluorodish and incubated with a final concentration of 10 µM of **(195)**. The images were obatined at 10 X magnification and phase contrast images were also recorded.

Overall summary and Future work

The current project focussed on the synthesis and application of targeted-dendrimeric ALA prodrugs for photodynamic therapy.

Chapter 2 focussed on developing and optimising a synthetic route to first and second generation ALA dendrons with three or six ALA units suitable for further ligation by CuAAC. An initial attempt using Z-protection of Tris-derived building blocks led to problems of O- to N- acyl group migration, and subsequent acylation with 4-pentynoic acid gave the final Tris-conjugate **(105)** in low yield (7%). The main highlight of this chapter was the development of an alternative synthetic route involving a silyl protection strategy (using TIPS-Cl) of the Tris and ext. Tris building blocks **(97)** and **(98).** This not only avoided the O- to N-acyl group migration, but also in subsequent steps gave the first generation alkynyl-ALA dendrons **(105)** and **(107)** in good yields (89% and 77% respectively). The synthesis of a second generation ALA dendron with six ALA units **(125)** was carried out on a trial scale using 5-aminoisophthalic acid as the dendron core. This was successful, however further optimisation of the route to larger ALA dendrons is required.

In Chapter 3, the core prodrug units with one (based on 4-hydroxybenzoic acid) or three azido arms (based on gallic acid) were synthesised. These azido units were then conjugated with the first generation ALA dendrons **(105)** and **(107)** via CuAAC. Optimised reaction conditions were obtained when the stoichiometry of the alkyne to azide in the reaction was (2:1) and with $CuSO_4$ as the copper source in DMSO/H_2O/t-BuOH. These reaction conditions were used to synthesise non-targeted ALA dendrimers with three or nine ALA units in excellent yields. The synthetic procedure was also adapted successfully to synthesise simple biomolecule-targeted ALA prodrugs which involved attachment of vitamin E and thymidine to ALA dendrons via CuAAC, using Cu(I) trifluoromethanesulfonate benzene complex. Biological evaluation to monitor the PpIX release from these conjugates and PDT activity may now be carried out in relevant cancer cell lines. An attempt to conjugate a benzyl-protected glucose derivative with an ALA dendron was also successful, but further optimisation is needed to facilitate the final deprotection. This may

involve exchanging the hydroxyl protecting groups with ones which would be stable towards click reaction conditions, but at the same time are removable under mild conditions that are compatible with the ALA esters, avoiding hydrogenolysis.

Chapter 4 focussed on investigating different synthetic strategies for attachment of an EGFR-targeting peptide (LARLLT) to the clicked ALA dendrons developed in Chapter 3. An attempt to initially couple a partially protected peptide to a dendrimer in solution under different amide coupling conditions (EDC.HCl/HOBt.hydrate or HATU) did not show the formation of any new species on HPLC. An alternative strategy of attaching the clicked ALA dendron to the peptide on resin was successful, however HPLC purification gave the final product in low yield (5%). Subsequent attempts focussed on modifying the synthetic strategy and included the attachment of the azido core to the targeting peptide, followed by click coupling on-resin or in solution. On-resin click coupling with the previously developed click coupling conditions of $CuSO_4$ and sodium ascorbate in DMSO/H_2O were not successful, probably due to shrinking of the polystyrene resin under aqueous conditions. Alternative copper(I) sources were therefore investigated including copper(I) iodide and copper(I) trifluoromethanesulfonate benzene complex, and the click coupling of azido-peptides on resin with ALA dendrons was then found to proceed effectively in DMSO for 5 days. The best results were obtained when the reaction was carried out with copper(I) trifluoromethanesulfonate benzene complex which on full deprotection and cleavage from the resin showed the presence of a single major species and no unconjugated peptide. The identities of the final targeted conjugates with three or nine ALA units were confirmed by ^{1}H, ^{13}C NMR and mass spectrometry. The reaction time of five days could be significantly decreased to 36 h for the targeted nine ALA derivative **(181)** when the CuAAC reaction was performed with a fully deprotected azido peptide and alkynyl dendron. The final conjugate was obtained in 69% yield. A final attempt to further reduce the reaction time was carried out, and the coupling reaction to produce **(183)** in solution was carried out under microwave conditions. The final conjugate was then obtained in 75% yield, with a reaction time of only 10 min,

Biological data obtained from time-course fluorescence studies and PDT experiments in an EGFR-overexpressing cell line (MDA-MB-231) showed enhanced ALA-induced PpIX fluorescence at different time intervals and higher phototoxicity for the peptide-targeted 9-ALA dendrimer **(181)** in comparison to equimolar doses of ALA and ALA dendrimers (with 3 or 9 copies of ALA). Further studies involving evaluation of these targeted dendrimers in other EGFR-overexpressing cell lines and exploring attachment of other targeting peptides to the ALA dendrimer are now required to further validate the application of this model for ALA delivery.

In Chapter 5, EGFR targeting-peptide **(177)** was successfully attached to different classical photosensitiser derivatives **(190)**, **(191)** and **(13)** via SPAAC which avoided the use of any copper catalyst. The resulting peptide-photosensitiser conjugates **(195)**-**(197)** were obtained in good yield. PDT studies for porphyrin derivative **(190)** were carried out in MDA-MB-231 (EGFR overexpressing) and MCF-7 (non-EGFR overexpressing) cells which showed an enhanced PDT effect in MDA-MB-231 cells, whereas no such effect was observed in the MCF-7 cell line. Biological evaluation involving Ce6 conjugate **(196)** and verteporfin conjugate **(197)** also showed enhanced PDT effects across different concentrations and time intervals in MDA-MB-231 cells.

Chapter 6 focussed on the synthesis of a group of novel CPP-ALA conjugates **(210)**-**(214)** via CuAAC. Four CPPs were selected for the current work, with each of them containing a functionalised amino acid with a reactive azido group which could take part in CuAAC with the ALA dendrons **(105)** and **(107)**. The CPP-ALA conjugates were obtained in good yields and will now be tested in relevant cell lines. Conjugation of pVEC derivative **(203)** with DBCO-porphyrin derivative **(192)** was also attempted using SPAAC, and here biological evaluation in both MDA-MB-231 and MCF-7 cells showed significant PDT effects across a range of concentrations and light doses.

References

1. R. Ackroyd, C. Kelty, N. Brown and M. Reed, *Photochem. Photobiol.*, 2001, **74**, 656-669.

2. R. Bonnett, *Chemical aspects of photodynamic therapy*, CRC Press, Singapore, 2000.

3. N. Finsen, *Phototherapy*, Edward Arnold, 1901.

4. T. B. Fitzpatrick and M. A. Pathak, *J. Invest. Dermatol.*, 1959, **32**, 229-231.

5. O. Raab, *Z. Biol*, 1900, **39**, 524-526.

6. H. von Tappeiner, *Raab. Muench. Med. Wochenschr*, 1900, **47**, 5.

7. A. Jesionek and H. von Tappeiner, *Dtsch. Arch. Klin. Med.*, 1905, **82**, 223-227.

8. H. von Tappeiner and A. Jodlbauer, *Dtsch. Arch. Klin. Med.*, 1904, **80**, 427-487.

9. M. D. Daniell and J. S. Hill, *Aust. N. Z. J. Surg.*, 1991, **61**, 340-348.

10. M. H. Abdel-Kader, *Photodynamic therapy: from theory to application*, Springer Science & Business Media, Heidelberg, 2014.

11. H. Scherer, *Ann. D. Chem. Pharm*, 1841, **40**, 1-64.

12. J. Thudichum, HM Stationary Office, London, 1867, pp. 152-233.

13. F. Hoppe-Seyler, *Medicinisch-chemische Untersuchungen*, 1871, **4**, 124-528.

14. W. Hausmann, *Wien. Klin. Wochenschr*, 1908, **21**, 1527-1528.

15. H. Pfeiffer, *Berlin, Urban Schwarzinber*, 1911, **1**, 563-571.

16. F. Meyer-Betz, *Dtsch. Arch. Klin. Med.*, 1913, **112**, 476-503.

17. A. Policard, *C.R. Soc .Biol.*, 1924, **91**, 1423-1424.

18. H. Auler and G. Banzer, *Z. Krebsforsch.*, 1942, **53**, 65-68.

19. W. M. Sharman, C. M. Allen and J. E. van Lier, *Drug Discovery Today*, 1999, **4**, 507-517.

20. S. S. Lucky, K. C. Soo and Y. Zhang, *Chem. Rev.*, 2015, **115**, 1990-2042.

21. R. Bonnett, *Rev. Contemp. Pharmaco.*, 1999, **10**, 1-17.

22. S. Schwartz, K. Absolon and H. Vermund, *Univ. Minn. Med. Bull.*, 1955, **27**, 7-8.

23. R. L. Lipson and E. J. Baldes, *Arch. Dermatol.*, 1960, **82**, 508-516.

24. R. L. Lipson, E. J. Baldes and A. M. Olsen, *J. Natl. Cancer Inst.*, 1961, **26**, 1-11.

25. R. Lipson, E. Baldes and A. Olsen, *J. Thorac. Cardiovasc. Surg.*, 1961, **42**, 623.

26. R. L. Lipson, E. J. Baldes and A. M. Olsen, *Chest*, 1964, **46**, 676-679.

27. R. L. Lipson, E. J. Baldes and M. J. Gray, *Cancer*, 1967, **20**, 2255-2257.

28. I. Diamond, A. F. Mcdonagh, C. B. Wilson, S. G. Granelli, A. Mcdonagh, S. Nielsen and R. Jaenicke, *Lancet*, 1972, **300**, 1175-1177.

29. J. F. Kelly, M. E. Snell and M. C. Berenbaum, *Br. J. Cancer*, 1975, **31**, 237-244.

30. T. J. Dougherty, J. E. Kaufman, A. Goldfarb, K. R. Weishaupt, D. Boyle and A. Mittleman, *Cancer Res.*, 1978, **38**, 2628-2635.

31. E. S. Nyman and P. H. Hynninen, *J. Photochem. Photobiol., B*, 2004, **73**, 1-28.

32. B. C. Wilson, W. P. Jeeves, D. M. Lowe and G. Adam, *Prog. Clin. Biol. Res.*, 1984, **170**, 115-132.

33. D. E. J. G. J. Dolmans, D. Fukumura and R. K. Jain, *Nature Reviews: Cancer*, 2003, **3**, 380-387.

34. K. Berg, P. K. Selbo, A. Weyergang, A. Dietze, L. Prasmickaite, A. Bonsted, B. Ø. Engesaeter, E. Angell-Petersen, T. Warloe, N. Frandsen and A. Høgset, *J. Microsc.*, 2005, **218**, 133-147.

35. A. B. Ormond and H. S. Freeman, *Materials*, 2013, **6**, 817-840.

36. R. Bonnett, *Chem. Soc. Rev.*, 1995, **24**, 19-33.

37. B. Krammer and K. Plaetzer, *Photochem. Photobiol. Sci.*, 2008, **7**, 283-289.

38. Photocure. A Double Blinded, Prospective, Randomized, Vehicle Controlled Multi-center Study of Photodynamic Therapy With Visonac® Cream in Patients With Acne Vulgaris, https://clinicaltrials.gov/ct2/show/NCT01347879, (accessed 02/03/2016, 2016).

39. V. H. Fingar, P. K. Kik, P. S. Haydon, P. B. Cerrito, M. Tseng, E. Abang and T. J. Wieman, *Br. J. Cancer*, 1999, **79**, 1702.

40. N. Rousset, L. Bourré and S. Thibaud, *Sensitizers in Photodynamic Therapy*, Royal Society of Chemistry, Cambridge, UK, 2003.

41. M. Ethirajan, Y. H. Chen, P. Joshi and R. K. Pandey, *Chem. Soc. Rev.*, 2011, **40**, 340-362.

42. M. Triesscheijn, M. Ruevekamp, M. Aalders, P. Baas and F. A. Stewart, *Photochem. Photobiol.*, 2005, **81**, 1161-1167.

43. D. E. Dolmans, D. Fukumura and R. K. Jain, *Nat. Rev. Cancer*, 2003, **3**, 380-387.

44. R. R. Allison, G. H. Downie, R. Cuenca, X. H. Hu, C. J. H. Childs and C. H. Sibata, *Photodiagnosis Photodyn. Ther.*, 2004, **1**, 27-42.

45. J. Berlanda, T. Kiesslich, V. Engelhardt, B. Krammer and K. Plaetzer, *J. Photochem. Photobiol., B*, 2010, **100**, 173-180.

46. Photodynamic Therapy Clinical Trial For Cutaneous AIDS-Related Kaposi's Sarcoma Study Summary, https://clinicaltrials.gov/ct2/show/NCT00002167?term=SnET2&rank=1, (accessed 3rd February 2016).

47. A. E. O'Connor, W. M. Gallagher and A. T. Byrne, *Photochem. Photobiol.*, 2009, **85**, 1053-1074.

48. J. Usuda, H. Kato, T. Okunaka, K. Furukawa, H. Tsutsui, K. Yamada, Y. Suga, H. Honda, Y. Nagatsuka, T. Ohira, M. Tsuboi and T. Hirano, *J. Thorac. Oncol.*, 2006, **1**, 489-493.

49. W. Kobayashi, Q. Liu, H. Nakagawa, H. Sakaki, B. Teh, T. Matsumiya, H. Yoshida, T. Imaizumi, K. Satoh and H. Kimura, *Oral Oncology*, 2006, **42**, 45-49.

50. S. Gross, A. Gilead, A. Scherz, M. Neeman and Y. Salomon, *Nat. Med.*, 2003, **9**, 1327-1331.

51. A.-R. Azzouzi, S. Lebdai, F. Benzaghou and C. Stief, *World J. Urol.*, 2015, **33**, 937-944.

52. Photodynamic Therapy With LUZ11 in Advanced Head and Neck Cancer, https://clinicaltrials.gov/ct2/show/NCT02070432?term=Luz11&rank=1, (accessed 7th March 2016).

53. H. Abrahamse and M. R. Hamblin, *Biochem. J.*, 2016, **473**, 347-364.

54. P. Zimcik and M. Miletin, in *Dyes & Pigments: New Research*, ed. A. R. Lang, Nova Science Publishers, 2008, ch. Photodynamic Therapy, pp. 1-62.

55. Photodynamic Therapy using Silicon Phthalocyanine 4 in treating patients with Actinic Keratosis, Bowen's Disease, Skin Cancer, or Stage I or Stage II Mycosis Fungoides, http://clinicaltrials.gov/show/NCT00103246 NLM Identifier: NCT00103246, (accessed 21st May 2016).

56. R. Sanovic, B. Krammer, S. Grumboeck and T. Verwanger, *Int. J. Oncol.*, 2009, **35**, 921-939.

57. T. A. Theodossiou, J. S. Hothersall, P. A. De Witte, A. Pantos and P. Agostinis, *Mol. Pharm.*, 2009, **6**, 1775-1789.

58. J. P. Tardivo, F. Adami, J. A. Correa, M. A. S. Pinhal and M. S. Baptista, *Photodiagnosis Photodyn. Ther.*, 2014, **11**, 342-350.

59. T. B. Graciano, T. S. Coutinho, C. B. Cressoni, C. de Paula Freitas, M. B. Pierre, S. A. de Lima Pereira, M. M. Shimano, R. C. da Cunha Frange and M. T. Garcia, *Photodiagnosis Photodyn. Ther.*, 2015, **12**, 98-107.

60. Y. Lu, R. Q. Jiao, X. P. Chen, J. Y. Zhong, A. G. Ji and P. P. Shen, *J. Cell. Biochem.*, 2008, **105**, 1451-1460.

61. Photodynamic Therapy Associated With Full-mouth Ultrasonic Debridement in the Treatment of Severe Chronic Periodontitis, https://clinicaltrials.gov/ct2/show/NCT01535690?term=NCT01535690&rank=1, (accessed 27th Jan 2016).

62. Adjunctive Photodynamic Therapy in the Treatment of Chronic Periodontitis, https://clinicaltrials.gov/ct2/show/NCT01330082?term=NCT01330082&rank=1, (accessed 15th January 2016).

63. R. Broady, J. Yu and M. K. Levings, *J. Clin. Apher.*, 2008, **23**, 82-91.

64. D. P. V. Leite, F. R. Paolillo, T. N. Parmesano, C. R. Fontana and V. S. Bagnato, *Photomed. Laser Surg.*, 2014, **32**, 627-632.

65. K. O. Wikene, A. B. Hegge, E. Bruzell and H. H. Tønnesen, *Drug Dev. Ind. Pharm.*, 2015, **41**, 969-977.

66. S. Yano, S. Hirohara, M. Obata, Y. Hagiya, S.-i. Ogura, A. Ikeda, H. Kataoka, M. Tanaka and T. Joh, *J. Photochem. Photobiol., C*, 2011, **12**, 46-67.

67. H. You, H.-E. Yoon, P.-H. Jeong, H. Ko, J.-H. Yoon and Y.-C. Kim, *Bioorg. Med. Chem.*, 2015, **23**, 1453-1462.

68. T. Stuchinskaya, M. Moreno, M. J. Cook, D. R. Edwards and D. A. Russell, *Photochem. Photobiol. Sci.*, 2011, **10**, 822-831.

69. Z. Hu, B. Rao, S. Chen and J. Duanmu, *BMC Cancer*, 2010, **10**, 235.

70. S. Kaščáková, L. J. Hofland, H. S. De Bruijn, Y. Ye, S. Achilefu, K. van der Wansem, A. van der Ploeg-van den Heuvel, P. M. van Koetsveld, M. P. Brugts, A.-J. van der Lelij, H. J. C. M. Sterenborg, T. L. M. ten Hagen, D. J. Robinson and M. P. van Hagen, *PLoS One*, 2014, **9**, e104448.

71. M. E. Davis, Z. Chen and D. M. Shin, *Nat. Rev. Drug Discovery*, 2008, **7**, 771-782.

72. H. Maeda, J. Wu, T. Sawa, Y. Matsumura and K. Hori, *J. Controlled Release*, 2000, **65**, 271-284.

73. A. Master, M. Livingston and A. Sen Gupta, *J. Controlled Release*, 2013, **168**, 88-102.

74. R. R. Allison, V. S. Bagnato and C. H. Sibata, *Future Oncology*, 2010, **6**, 929-940.

75. E. Reddi, *J. Photochem. Photobiol., B*, 1997, **37**, 189-195.

76. W.-T. Li, in *Handbook of Biophotonics*, ed. J. Popp, Wiley-VCH Verlag GmbH & Co. KGaA, Germany, 1 edn., 2013, vol. 2, pp. 321-336.

77. A. Khdair, B. Gerard, H. Handa, G. Mao, M. P. V. Shekhar and J. Panyam, *Mol. Pharm.*, 2008, **5**, 795-807.

78. S. Brown, *Nature Photonics*, 2008, **2**, 394-395.

79. H. A. Collins, M. Khurana, E. H. Moriyama, A. Mariampillai, E. Dahlstedt, M. Balaz, M. K. Kuimova, M. Drobizhev, V. X. D. Yang, D. Phillips, A. Rebane, B. C. Wilson and H. L. Anderson, *Nature Photonics*, 2008, **2**, 420-424.

80. D. Hanahan, G. Bergers and E. Bergsland, *J. Clin. Invest.*, 2000, **105**, 1045-1047.

81. R. S. Kerbel, G. Klement, K. I. Pritchard and B. Kamen, *Ann. Oncol.*, 2002, **13**, 12-15.

82. S. K. Bisland, L. Lilge, A. Lin, R. Rusnov and B. C. Wilson, *Photochem. Photobiol.*, 2004, **80**, 22-30.

83. N. Davies and B. C. Wilson, *Photodiagnosis Photodyn. Ther.*, 2007, **4**, 202-212.

84. J. Funkhouser, *Curr. Drug Discovery*, 2002, 17-19.

85. S. S. Kelkar and T. M. Reineke, *Bioconjugate Chem.*, 2011, **22**, 1879-1903.

86. R. Kopelman, Y.-E. L. Koo, M. Philbert, B. A. Moffat, G. R. Reddy, P. McConville, D. E. Hall, T. L. Chenevert, M. S. Bhojani, S. M. Buck, A. Rehemtulla and B. D. Ross, *J. Magn. Magn. Mater.*, 2005, **293**, 404-410.

87. L. B. Josefsen and R. W. Boyle, *Theranostics*, 2012, **2**, 916-966.

88. Z. M. Barbara Krammer, Roy Pottier, Herbert Stepp, *Photodynamic Therapy with ALA*, Royal Society of Chemistry, Cambridge, 2006.

89. L. Brancaleon and H. Moseley, *Lasers Med. Sci.*, 2002, **17**, 173-186.

90. T. S. Mang, *Photodiagnosis Photodyn. Ther.*, 2004, **1**, 43-48.

91. B. A. Gilchrest, *Supplement to Skin & Aging*, 2010, 10-12.

92. L. B. Josefsen and R. W. Boyle, *Met.-Based Drugs*, 2008, **2008**, 1-24.

93. F. Wilkinson, W. P. Helman and A. B. Ross, *J. Phys. Chem. Ref. Data*, 1993, **22**, 113-262.

94. G. E. Ronsein, M. C. B. Oliveira, S. Miyamoto, M. H. G. Medeiros and P. Di Mascio, *Chem. Res. Toxicol.*, 2008, **21**, 1271-1283.

95. G. A. Hamilton, *Adv. Enzymol. Relat. Areas Mol. Biol.*, 1969, **32**, 55-96.

96. C. Rochester, *Organic Chemistry, A Series of Monographs*, Academic Press: New York, NY, USA, 1970.

97. I. Saito, T. Matsuura, M. Nakagawa and T. Hino, *Acc. Chem. Res.*, 1977, **10**, 346-352.

98. M. Nakagawa, S. Kato, S. Kataoka and T. Hino, *J. Am. Chem. Soc.*, 1979, **101**, 3136-3137.

99. M. Nakagawa, Y. Yokoyama, S. Kato and T. Hino, *Tetrahedron*, 1985, **41**, 2125-2132.

100. T. J. Dougherty, C. J. Gomer, B. W. Henderson, G. Jori, D. Kessel, M. Korbelik, J. Moan and Q. Peng, *J. Natl. Cancer Inst.*, 1998, **90**, 889-905.

101. N. L. Oleinick, R. L. Morris and T. Belichenko, *Photochem. Photobiol. Sci.*, 2002, **1**, 1-21.

102. M. Gracanin, C. L. Hawkins, D. I. Pattison and M. J. Davies, *Free Radical Biol. Med.*, 2009, **47**, 92-102.

103. A. P. Castano, T. N. Demidova and M. R. Hamblin, *Photodiagnosis Photodyn. Ther.*, 2004, **1**, 279-293.

104. B. B. Noodt, K. Berg, T. Stokke, Q. Peng and J. M. Nesland, *Br. J. Cancer*, 1996, **74**, 22.

105. P. Baluk, H. Hashizume and D. M. McDonald, *Curr. Opin. Genet. Dev.*, 2005, **15**, 102-111.

106. C. Abels, *Photochem. Photobiol. Sci.*, 2004, **3**, 765-771.

107. K. Pizova, K. Tomankova, A. Daskova, S. Binder, R. Bajgar and H. Kolarova, *Biomedical Papers*, 2012, **156**, 93-102.

108. R. R. Allison and K. Moghissi, *Clin Endosc*, 2013, **46**, 24-29.

109. L. R. Braathen, R.-M. Szeimies, N. Basset-Seguin, R. Bissonnette, P. Foley, D. Pariser, R. Roelandts, A.-M. Wennberg and C. A. Morton, *J. Am. Acad. Dermatol.*, 2007, **56**, 125-143.

110. M. S. Nestor, M. H. Gold, A. N. Kauvar, A. F. Taub, R. G. Geronemus, E. C. Ritvo, M. P. Goldman, D. J. Gilbert, D. F. Richey, T. S. Alster, R. R. Anderson, D. E. Bank, A. Carruthers, J. Carruthers, D. J. Goldberg, C. W. Hanke, N. J. Lowe, D. M. Pariser, D. S. Rigel, P. Robins, J. M. Spencer and B. D. Zelickson, *J. Drugs Dermatol.*, 2006, **5**, 140-154.

111. P. J. F. Quaedvlieg, E. Tirsi, M. R. T. M. Thissen and G. A. Krekels, *Eur. J. Dermatol.*, 2006, **16**, 335-339.

112. P. Agostinis, K. Berg, K. A. Cengel, T. H. Foster, A. W. Girotti, S. O. Gollnick, S. M. Hahn, M. R. Hamblin, A. Juzeniene, D. Kessel, M. Korbelik, J. Moan, P. Mroz, D. Nowis, J. Piette, B. C. Wilson and J. Golab, *CA Cancer J. Clin.*, 2011, **61**, 250-281.

113. M. A. Biel, *The Laryngoscope*, 1998, **108**, 1259-1268.

114. A. K. D'Cruz, M. H. Robinson and M. A. Biel, *Head Neck*, 2004, **26**, 232-240.

115. M. O. Senge and J. C. Brandt, *Photochem. Photobiol.*, 2011, **87**, 1240-1296.

116. L. Corti, J. Skarlatos, C. Boso, F. Cardin, L. Kosma, M. I. Koukourakis, A. Giatromanolaki, L. Norberto, M. Shaffer and K. Beroukas, *Int. J. Radiat. Oncol., Biol., Phys.*, 2000, **47**, 419-424.

117. B. F. Overholt, K. K. Wang, J. S. Burdick, C. J. Lightdale, M. Kimmey, H. R. Nava, M. V. Sivak, Jr., N. Nishioka, H. Barr, N. Marcon, M. Pedrosa, M. P. Bronner, M. Grace, M. Depot and D. Int Photodynamic Grp High-Grade, *Gastrointest. Endosc.*, 2007, **66**, 460-468.

118. H. C. Wolfsen, *J. Clin. Gastroenterol.*, 2005, **39**, 653-664.

119. S. G. Bown, A. Z. Rogowska, D. E. Whitelaw, W. R. Lees, L. B. Lovat, P. Ripley, L. Jones, P. Wyld, A. Gillams and A. W. R. Hatfield, *Gut*, 2002, **50**, 549-557.

120. S. Wang, E. Bromley, L. Xu, J. C. Chen and L. Keltner, *Expert Opin. Pharmacother.*, 2010, **11**, 133-140.

121. G. R. Prout Jr, C.-W. Lin, R. Benson Jr, U. O. Nseyo, J. J. Daly, P. P. Griffin, J. Kinsey, M. Tian, Y.-H. Lao, Y.-Z. Mian, X. Chen, F. Ren and S. Qiao, *N. Engl. J. Med.*, 1987, **317**, 1251-1255.

122. T. Uchibayashi, K. Koshida, K. Kunimi and H. Hisazumi, *Br. J. Cancer*, 1995, **71**, 625-628.

123. M. A. Dhallewin and L. Baert, *Urology*, 1995, **45**, 763-767.

124. U. O. Nseyo, B. Shumaker, E. A. Klein, K. Sutherland and G. Bladder Photofrin Study, *J. Urol.*, 1998, **160**, 39-44.

125. A. P. Berger, H. Steiner, A. Stenzl, T. Akkad, G. Bartsch and L. Holtl, *Urology*, 2003, **61**, 338-341.

126. R. Pottier, B. Krammer, H. Stepp and Z. Malik, in *Photodynamic Therapy with Ala: A Clinical Handbook*, eds. R. Baumgartner, R. Pottier, B. Krammer and H. Stepp, The Royal Society of Chemistry, Cambridge, 1 edn., 2006, vol. 6, pp. 42-43.

127. Y. Hayata, C. Konaka, N. Takizawa and H. Kato, *Chest*, 1982, **81**, 269-277.

128. K. Furuse, M. Fukuoka, H. Kato, T. Horai, K. Kubota, N. Kodama, Y. Kusunoki, N. Takifuji, T. Okunaka, C. Konaka, H. Wada and Y. Hayata, *J. Clin. Oncol.*, 1993, **11**, 1852-1857.

129. S. Lam, N. L. Muller, R. R. Miller, E. C. Kostashuk, E. Laukkanen, K. Evans, I. J. Szasz, J. C. Leriche and P. Champion, *Lasers Surg. Med.*, 1987, **7**, 29-35.

130. S. S. Stylli, A. H. Kaye, L. MacGregor, M. Howes and P. Rajendra, *J. Clin. Neurosci.*, 2005, **12**, 389-398.

131. P. J. Muller and B. C. Wilson, *Lasers Surg. Med.*, 2006, **38**, 384-389.

132. W. Stummer, U. Pichlmeier, T. Meinel, O. D. Wiestler, F. Zanella, H.-J. Reulen and A.-G. S. Group, *Lancet Oncol.*, 2006, **7**, 392-401.

133. G. B. Kharkwal, S. K. Sharma, Y. Y. Huang, T. Dai and M. R. Hamblin, *Lasers Surg. Med.*, 2011, **43**, 755-767.

134. M. J. Shikowitz, A. L. Abramson, K. Freeman, B. M. Steinberg and M. Nouri, *Laryngoscope*, 1998, **108**, 962-967.

135. A. L. Abramson, M. J. Shikowitz, V. M. Mullooly, B. M. Steinberg, C. A. Amella and H. R. Rothstein, *Arch. Otolaryngol. Head Neck Surg.*, 1992, **118**, 25-29.

136. C. A. Schroeter, J. Pleunis, C. v. N. t. Pannerden, T. Reineke and H. A. M. Neumann, *Dermatol. Surg.*, 2005, **31**, 71-75.

137. W. Hongcharu, C. R. Taylor, Y. C. Chang, D. Aghassi, K. Suthamjariya and R. R. Anderson, *J. Invest. Dermatol.*, 2000, **115**, 183-192.

138. Y. Itoh, Y. Ninomiya, S. Tajima and A. Ishibashi, *Br. J. Dermatol.*, 2001, **144**, 575-579.

139. M. Goldman, *Cosmet. Dermatol.*, 2003, **16**, 57-60.

140. R. R. de Oliveira, H. O. Schwartz-Filho, A. B. Novaes, Jr. and M. Taba, Jr., *J. Periodontol.*, 2007, **78**, 965-973.

141. L. Ge, R. Shu, Y. Li, C. Li, L. Luo, Z. Song, Y. Xie and D. Liu, *Photomed. Laser Surg.*, 2011, **29**, 33-37.

142. A. Asilian and M. Davami, *Clin. Exp. Dermatol.*, 2006, **31**, 634-637.

143. C. H. Wilder-Smith, P. Wilder-Smith, P. Grosjean, H. van den Bergh, A. Woodtli, P. Monnier, G. Dorta, F. Meister and G. Wagnieres, *Lasers Surg. Med.*, 2002, **31**, 18-22.

144. Q. Peng, T. Warloe, K. Berg, J. Moan, M. Kongshaug, K. E. Giercksky and J. M. Nesland, *Cancer*, 1997, **79**, 2282-2308.

145. Q. A. Peng, T. Warloe, J. Moan, H. Heyerdahl, H. B. Steen, J. M. Nesland and K. E. Giercksky, *Photochem. Photobiol.*, 1995, **62**, 906-913.

146. D. I. J. Morrow, P. A. McCarron, A. D. Woolfson, P. Juzenas, A. Juzeniene, V. Iani, J. Moan and R. F. Donnelly, *J. Pharm. Pharmacol.*, 2010, **62**, 685-695.

147. A. Casas, H. Fukuda, G. Di Venosa and A. M. D. Batlle, *Br. J. Dermatol.*, 2000, **143**, 564-572.

148. Z. Malik, G. Kostenich, L. Roitman, B. Ehrenberg and A. Orenstein, *J. Photochem. Photobiol., B*, 1995, **28**, 213-218.

149. J. T. H. v. d. M. Akker, V. Iani, W. M. Star, H. J. C. M. Sterenborg and J. Moan, *Photochem. Photobiol.*, 2000, **72**, 681-689.

150. R. Steluti, F. S. De Rosa, J. Collett, A. C. Tedesco and M. V. L. B. Bentley, *Eur. J. Pharm. Biopharm.*, 2005, **60**, 439-444.

151. B. G. Auner, E. Petzenhauser and C. Valenta, *J. Pharm. Sci.*, 2004, **93**, 2780-2787.

152. M. B. R. Pierre, E. Ricci Jr, A. C. Tedesco and M. V. L. B. Bentley, *Pharm. Res.*, 2006, **23**, 360-366.

153. Ø. B. Gadmar, J. Moan, E. Scheie, L.-W. Ma and Q. Peng, *J. Photochem. Photobiol., B*, 2002, **67**, 187-193.

154. M. Novo, G. Huttmann and H. Diddens, *J. Photochem. Photobiol., B*, 1996, **34**, 143-148.

155. A. Bunke, O. Zerbe, H. Schmid, G. Burmeister, H. P. Merkle and B. Gander, *J. Pharm. Sci.*, 2000, **89**, 1335-1341.

156. B. Franck and H. Stratmann, *Heterocycles*, 1981, **15**, 919-923.

157. J. J. Scott, *Biochem. J*, 1956, **62**, P6-P6.

158. A. Casas, A. M. D. Batlle, A. R. Butler, D. Robertson, E. H. Brown, A. MacRobert and P. A. Riley, *Br. J. Cancer*, 1999, **80**, 1525-1532.

159. M. Kaliszewski, A. Juzeniene, P. Juzenas, M. Kwasny, J. Kaminski, Z. Dabrowski, J. Golinski and J. Moan, *Photodiagnosis Photodyn. Ther.*, 2005, **2**, 129-134.

160. R. F. Donnelly, P. A. McCarron and A. D. Woolfson, *Photochem. Photobiol.*, 2005, **81**, 750-767.

161. N. Fotinos, M. A. Campo, F. Popowycz, R. Gurny and N. Lange, *Photochem. Photobiol.*, 2006, **82**, 994-1015.

162. R. F. V. Lopez, N. Lange, R. Guy and M. V. L. B. Bentley, *Adv. Drug Delivery Rev.*, 2004, **56**, 77-94.

163. J. M. Gaullier, K. Berg, Q. Peng, H. Anholt, P. K. Selbo, L. W. Ma and J. Moan, *Cancer Res.*, 1997, **57**, 1481-1486.

164. J. Kloek and G. M. J. B. vanHenegouwen, *Photochem. Photobiol.*, 1996, **64**, 994-1000.

165. Q. Peng, J. Moan, T. Warloe, V. Iani, H. B. Steen, A. Bjørseth and J. M. Nesland, *J. Photochem. Photobiol., B*, 1996, **34**, 95-96.

166. P. Uehlinger, M. Zellweger, G. Wagnières, L. Juillerat-Jeanneret, H. van den Bergh and N. Lange, *J. Photochem. Photobiol., B*, 2000, **54**, 72-80.

167. M. Kaliszewski, M. Kwasny, A. Juzeniene, P. Juzenas, A. Graczyk, L.-W. Ma, V. Iani, P. Mikolajewska and J. Moan, *J. Photochem. Photobiol., B*, 2007, **87**, 67-72.

168. J. Kloek, W. Akkermans and G. M. J. B. Henegouwen, *Photochem. Photobiol.*, 1998, **67**, 150-154.

169. C. J. Whitaker, S. H. Battah, M. J. Forsyth, C. Edwards, R. W. Boyle and E. K. Matthews, *Anti-Cancer Drug Des.*, 2000, **15**, 161-170.

170. T. Satoh and M. Hosokawa, *Annu. Rev. Pharmacol. Toxicol.*, 1998, **38**, 257-288.

171. A. Godal, N. O. Nilsen, J. Klaveness, J. E. Branden, J. M. Nesland and Q. Peng, *J. Environ. Pathol. Toxicol. Oncol.*, 2006, **25**, 109-126.

172. Y. Berger, A. Greppi, O. Siri, R. Neier and L. Juillerat-Jeanneret, *J. Med. Chem.*, 2000, **43**, 4738-4746.

173. H. Brunner, F. Hausmann, R. Krieg, E. Endlicher, J. Schölmerich, R. Knuechel and H. Messmann, *Photochem. Photobiol.*, 2001, **74**, 721-725.

174. A. Curnow, A. J. MacRobert and S. G. Bown, *Lasers Surg. Med.*, 2006, **38**, 325-331.

175. K. Berg, H. Anholt, O. Bech and J. Moan, *Br. J. Cancer*, 1996, **74**, 688-697.

176. J. L. Buss, F. M. Torti and S. V. Torti, *Curr. Med. Chem.*, 2003, **10**, 1021-1034.

177. M. J. Miller, *Chem. Rev.*, 1989, **89**, 1563-1579.

178. P. T. Doulias, S. Christoforidis, U. T. Brunk and D. Galaris, *Free Radical Biol. Med.*, 2003, **35**, 719-728.

179. R. C. Hider, J. B. Porter and S. Singh, *The Development of Iron Chelators for Clinical Use*, CRC, Boca Raton, USA, 1994.

180. E. Blake and A. Curnow, *Photochem. Photobiol.*, 2010, **86**, 1154-1160.

181. A. Mrozek-Wilczkiewicz, M. Serda, R. Musiol, G. Malecki, A. Szurko, A. Muchowicz, J. Golab, A. Ratuszna and J. Polanski, *ACS Med. Chem. Lett.*, 2014, **5**, 336-339.

182. R. Schneider, L. Tirand, C. Frochot, R. Vanderesse, N. Thomas, J. Gravier, F. Guillemin and M. Barberi-Heyob, *Anticancer Agents Med. Chem.*, 2006, **6**, 469-488.

183. Y. Berger, L. Ingrassia, R. Neier and L. Juillerat-Jeanneret, *Bioorg. Med. Chem.*, 2003, **11**, 1343-1351.

184. L. M.-A. Rogers, P. G. McGivern, A. R. Butler, A. J. MacRobert and I. M. Eggleston, *Tetrahedron*, 2005, **61**, 6951-6958.

185. L. Bourré, F. Giuntini, I. M. Eggleston, M. Wilson and A. J. MacRobert, *Br. J. Cancer*, 2009, **100**, 723-731.

186. L. Bourré, F. Giuntini, I. M. Eggleston, M. Wilson and A. J. MacRobert, *Mol. Cancer Ther.*, 2008, **7**, 1720-1729.

187. F. Giuntini, L. Bourré, A. J. MacRobert, M. Wilson and I. M. Eggleston, *J. Med. Chem.*, 2009, **52**, 4026-4037.

188. G. Di Venosa, P. Vallecorsa, F. Giuntini, L. Mamone, A. Batlle, S. Vanzuli, A. Juarranz, A. J. MacRobert, I. M. Eggleston and A. Casas, *Mol. Cancer Ther.*, 2015, **14**, 440-451.

189. M. J. Dixon, L. Bourré, A. J. MacRobert and I. M. Eggleston, *Bioorg. Med. Chem. Lett.*, 2007, **17**, 4518-4522.

190. R. P. Johnson, C.-W. Chung, Y.-I. Jeong, D. H. Kang, H. Suh and I. Kim, *Int. J. Nanomed.*, 2012, **7**, 2497-2512.

191. W. R. Abd-Elgaliel, Z. Cruz-Monserrate, H. Wang, C. D. Logsdon and C.-H. Tung, *J. Controlled Release*, 2013, **167**, 221-227.

192. A. Guaragna, G. N. Roviello, S. D'Errico, C. Paolella, G. Palumbo and D. D'Alonzo, *Tetrahedron Lett.*, 2015, **56**, 775-778.

193. R. Vallinayagam, J. Weber and R. Neier, *Org. Lett.*, 2008, **10**, 4453-4455.

194. G. Sigounas, A. Anagnostou and M. Steiner, *Nutr. Cancer*, 1997, **28**, 30-35.

195. D. A. Gewirtz, M. S. Gupta and S. Sundaram, *Curr. Med. Chem. Anticancer Agents*, 2002, **2**, 683-690.

196. L. P. Jordheim, D. Durantel, F. Zoulim and C. Dumontet, *Nat. Rev. Drug Discovery*, 2013, **12**, 447-464.

197. P. Gurba, R. Vallinayagam, F. Schmitt, J. Furrer, L. Juillerat-Jeanneret and R. Neier, *Synthesis*, 2008, 3957-3962.

198. I. Laville, T. Figueiredo, B. Loock, S. Pigaglio, P. Maillard, D. S. Grierson, D. Carrez, A. Croisy and J. Blais, *Bioorg. Med. Chem.*, 2003, **11**, 1643-1652.

199. B. Di Stasio, C. Frochot, D. Dumas, P. Even, J. Zwier, A. Müller, J. Didelon, F. Guillemin, M.-L. Viriot and M. Barberi-Heyob, *Eur. J. Med. Chem.*, 2005, **40**, 1111-1122.

200. Y. Mikata, Y. Onchi, M. Shibata, T. Kakuchi, H. Ono, S.-i. Ogura, I. Okura and S. Yano, *Bioorg. Med. Chem. Lett.*, 1998, **8**, 3543-3548.

201. H. Tong, Y. Wang, H. Li, Q. Jin and J. Ji, *Chem. Commun.*, 2016, **52**, 3966-3969.

202. B. Klajnert, M. Rozanek and M. Bryszewska, *Curr. Med. Chem.*, 2012, **19**, 4903-4912.

203. S. H. Battah, C.-E. Chee, H. Nakanishi, S. Gerscher, A. J. MacRobert and C. Edwards, *Bioconjugate Chem.*, 2001, **12**, 980-988.

204. S. Battah, S. O'Neill, C. Edwards, S. Balaratnam, P. Dobbin and A. J. MacRobert, *Int. J. Biochem. Cell Biol.*, 2006, **38**, 1382-1392.

205. G. M. Di Venosa, A. G. Casas, S. Battah, P. Dobbin, H. Fukuda, A. J. MacRobert and A. Batlle, *Int. J. Biochem. Cell Biol.*, 2006, **38**, 82-91.

206. S. Battah, S. Balaratnam, A. Casas, S. O'Neill, C. Edwards, A. Batlle, P. Dobbin and A. J. MacRobert, *Mol. Cancer Ther.*, 2007, **6**, 876-885.

207. A. Casas, S. Battah, G. Di Venosa, P. Dobbin, L. Rodriguez, H. Fukuda, A. Batlle and A. J. MacRobert, *J. Controlled Release*, 2009, **135**, 136-143.

208. A. François, S. Battah, A. J. MacRobert, L. Bezdetnaya, F. Guillemin and M.-A. D'Hallewin, *BJU International*, 2012, **110**, E1155-E1162.

209. L. Rodriguez, P. Vallecorsa, S. Battah, G. Di Venosa, G. Calvo, L. Mamone, D. Sáenz, M. C. Gonzalez, A. Batlle, A. J. MacRobert and A. Casas, *Photochem. Photobiol. Sci.*, 2015, **14**, 1617-1627.

210. U. Boas and P. M. H. Heegaard, *Chem. Soc. Rev.*, 2004, **33**, 43-63.

211. E. R. Gillies and J. M. J. Frèchet, *Drug Discovery Today*, 2005, **10**, 35-43.

212. B. Klajnert and M. Bryszewska, *Acta Biochim. Pol.*, 2001, **48**, 199-208.

213. A. W. Bosman, H. M. Janssen and E. W. Meijer, *Chem. Rev.*, 1999, **99**, 1665-1688.

214. C. J. Hawker and J. M. J. Frèchet, *J. Am. Chem. Soc.*, 1990, **112**, 7638-7647.

215. C. J. Hawker and J. M. J. Frèchet, *J. Chem. Soc., Chem. Commun.*, 1990, 1010-1013.

216. M. Meldal and C. W. Tornøe, *Chem. Rev.*, 2008, **108**, 2952-3015.

217. G. Franc and A. K. Kakkar, *Chem. Soc. Rev.*, 2010, **39**, 1536-1544.

218. P. A. Ledin, F. Friscourt, J. Guo and G.-J. Boons, *Chem. Eur. J.*, 2011, **17**, 839-846.

219. H. Maeda, H. Nakamura and J. Fang, *Adv. Drug Delivery Rev.*, 2013, **65**, 71-79.

220. S. Kumar, S. Valarmathi, P. Bhima, P. Devabaktuni, A. Raja and S. D. Vallabhaneni, *J. Pharm. Sci. Technol.*, 2012, **4**, 972-984.

221. N. Nishiyama, H. R. Stapert, G. D. Zhang, D. Takasu, D. L. Jiang, T. Nagano, T. Aida and K. Kataoka, *Bioconjugate Chem.*, 2003, **14**, 58-66.

222. G. R. Newkome and C. Shreiner, *Chem. Rev.*, 2010, **110**, 6338-6442.

223. F. Giuntini and I. M. Eggleston, unpublished work.

224. C. Baldoli, C. Rigamonti, S. Maiorana, E. Licandro, L. Falciola and P. R. Mussini, *Chem. Eur. J.*, 2006, **12**, 4091-4100.

225. R. F. Cunico and L. Bedell, *J. Org. Chem.*, 1980, **45**, 4797-4798.

226. Y. Kaburagi and Y. Kishi, *Org. Lett.*, 2007, **9**, 723-726.

227. G. C. Feast, T. Lepitre, X. Mulet, C. E. Conn, O. E. Hutt, G. P. Savage and C. J. Drummond, *Beilstein J. Org. Chem.*, 2014, **10**, 1578-1588.

228. C. M. Cardona and R. E. Gawley, *J. Org. Chem.*, 2002, **67**, 1411-1413.

229. J. B. Schwarz, S. D. Kuduk, X. T. Chen, D. Sames, P. W. Glunz and S. J. Danishefsky, *J. Am. Chem. Soc.*, 1999, **121**, 2662-2673.

230. S. P. Amaral, M. Fernandez-Villamarin, J. Correa, R. Riguera and E. Fernandez-Megia, *Org. Lett.*, 2011, **13**, 4522-4525.

231. S. J. Meunier, Q. Q. Wu, S. N. Wang and R. Roy, *Can. J. Chem.*, 1997, **75**, 1472-1482.

232. R. Roy, W. K. C. Park, Q. Q. Wu and S. N. Wang, *Tetrahedron Lett.*, 1995, **36**, 4377-4380.

233. H. Sashiwa, Y. Shigemasa and R. Roy, *Macromolecules*, 2001, **34**, 3905-3909.

234. J. Li and P. R. Chen, *Nat. Chem. Biol.*, 2016, **12**, 129-137.

235. H. C. Hang, C. Yu, D. L. Kato and C. R. Bertozzi, *Proc. Natl. Acad. Sci. U. S. A.*, 2003, **100**, 14846-14851.

236. E. M. Sletten and C. R. Bertozzi, *Acc. Chem. Res.*, 2011, **44**, 666-676.

237. E. M. Sletten and C. R. Bertozzi, *Angew. Chem. Int. Ed.*, 2009, **48**, 6974-6998.

238. R. K. Lim and Q. Lin, *Chem. Commun.*, 2010, **46**, 1589-1600.

239. V. V. Rostovtsev, L. G. Green, V. V. Fokin and K. B. Sharpless, *Angew. Chem., Int. Ed.*, 2002, **41**, 2596-2599.

240. R. Huisgen, G. Szeimies and L. Möebius, *Chem. Ber.*, 1967, **100**, 2494-2507.

241. R. Huisgen, *Pure Appl. Chem.*, 1989, **61**, 613-628.

242. N. V. Sokolova, T. Schotten, H. J. Berthold, J. Thiem and V. G. Nenajdenko, *Synthesis*, 2013, **45**, 556-561.

243. N. Zabarska, A. Stumper and S. Rau, *Dalton Transactions*, 2016, **45**, 2338-2351.

244. G. M. Entract, F. Bryden, J. Domarkas, H. Savoie, L. Allott, S. J. Archibald, C. Cawthorne and R. W. Boyle, *Mol. Pharm.*, 2015, **12**, 4414-4423.

245. E. Fernandez-Megia, J. Correa, I. Rodriguez-Meizoso and R. Riguera, *Macromolecules*, 2006, **39**, 2113-2120.

246. R. Dondi and I. Eggleston, unpublished work.

247. L. Wyld, M. W. R. Reed and N. J. Brown, *Br. J. Cancer*, 1998, **77**, 1621.

248. Z. S. Zhang and E. Fan, *Tetrahedron Lett.*, 2006, **47**, 665-669.

249. R. Vallinayagam, F. Schmitt, J. Barge, G. Wagnieres, V. Wenger, R. Neier and L. Juillerat-Jeanneret, *Bioconjugate Chem.*, 2008, **19**, 821-839.

250. H. M. Kouchesfehani, M. Nabiuni, M. H. Majlesara, E. Amini and S. Irian, *Journal of Paramedical Sciences*, 2011, **2**, 16-23.

251. E.-S. A. Al-Sherbini, A. H. El Noury, M. N. El Rouby and T. Ibrahim, *Medical Laser Application*, 2009, **24**, 65-73.

252. S. Ballut, A. Makky, B. Chauvin, J.-P. Michel, A. Kasselouri, P. Maillard and V. Rosilio, *Org. Biomol. Chem.*, 2012, **10**, 4485-4495.

253. S. Castro, E. C. Cherney, N. L. Snyder and M. W. Peczuh, *Carbohydr. Res.*, 2007, **342**, 1366-1372.

254. A. Nanashima, T. Abo, T. Nonaka, Y. Nonaka, T. Morisaki, R. Uehara, K. Ohnita, D. Fukuda, G. Murakami, K. Tou, M. Kunizaki, S. Hidaka, T. Tsuchiya, H. Takeshita, K. Nakao and T. Nagayasu, *Anticancer Res.*, 2012, **32**, 4931-4938.

255. H. Shibaguchi, H. Tsuru, M. Kuroki and M. Kuroki, *Anticancer Res.*, 2011, **31**, 2425-2429.

256. N. Shirasu, S. O. Nam and M. Kuroki, *Anticancer Res.*, 2013, **33**, 2823-2831.

257. A. I. Minchinton and I. F. Tannock, *Nat. Rev. Cancer*, 2006, **6**, 583-592.

258. M. B. R. Pierre, A. C. Tedesco, J. M. Marchetti and M. V. L. B. Bentley, *BMC Dermatol.*, 2001, **1**, 5-5.

259. W. Tang, H. Xu, E. J. Park, M. A. Philbert and R. Kopelman, *Biochem. Biophys. Res. Commun.*, 2008, **369**, 579-583.

260. A. Zaczek, B. Brandt and K. P. Bielawski, *Histol. Histopathol.*, 2005, **20**, 1005-1015.

261. C. Yewale, D. Baradia, I. Vhora, S. Patil and A. Misra, *Biomaterials*, 2013, **34**, 8690-8707.

262. K. M. Kadish, K. M. Smith and R. Guilard, *Handbook of porphyrin science*, World Scientific Pub. Co., Singapore, 1st edn., 2010.

263. A. M. Master, Y. Qi, N. L. Oleinick and A. S. Gupta, *Nanomedicine: Nanotechnology, Biology and Medicine*, 2012, **8**, 655-664.

264. B. G. Ongarora, K. R. Fontenot, X. Hu, I. Sehgal, S. D. Satyanarayana-Jois and M. G. H. Vicente, *J. Med. Chem.*, 2012, **55**, 3725-3738.

265. S. Song, D. Liu, J. Peng, H. Deng, Y. Guo, L. X. Xu, A. D. Miller and Y. Xu, *The FASEB Journal*, 2009, **23**, 1396-1404.

266. F. García-Martín, N. Bayó-Puxan, L. J. Cruz, J. C. Bohling and F. Albericio, *QSAR & Combinatorial Science*, 2007, **26**, 1027-1035.

267. M. van Dijk, K. Mustafa, A. C. Dechesne, C. F. van Nostrum, W. E. Hennink, D. T. S. Rijkers and R. M. J. Liskamp, *Biomacromolecules*, 2007, **8**, 327-330.

268. M. v. Dijk, M. L. Nollet, P. Weijers, A. C. Dechesne, C. F. v. Nostrum, W. E. Hennink, D. T. S. Rijkers and R. M. J. Liskamp, *Biomacromolecules*, 2008, **9**, 2834-2843.

269. J. E. Hein and V. V. Fokin, *Chem. Soc. Rev.*, 2010, **39**, 1302-1315.

270. T. Mosmann, *J. Immunol. Methods*, 1983, **65**, 55-63.

271. M. Olivo, R. Bhuvaneswari, S. S. Lucky, N. Dendukuri and P. Soo-Ping Thong, *Pharmaceuticals*, 2010, **3**, 1507-1529.

272. N. J. Agard, J. A. Prescher and C. R. Bertozzi, *J. Am. Chem. Soc.*, 2004, **126**, 15046-15047.

273. A. J. Link and D. A. Tirrell, *J. Am. Chem. Soc.*, 2003, **125**, 11164-11165.

274. M. King and A. Wagner, *Bioconjugate Chem.*, 2014, **25**, 825-839.

275. D. H. Ess, G. O. Jones and K. N. Houk, *Org. Lett.*, 2008, **10**, 1633-1636.

276. X. Ning, J. Guo, M. A. Wolfert and G. J. Boons, *Angew. Chem. Int. Ed.*, 2008, **47**, 2253-2255.

277. S. S. ávan Berkel, P. Floris, J. C. ávan Hest and F. L. ávan Delft, *Chem. Commun.*, 2010, **46**, 97-99.

278. J. Dommerholt, S. Schmidt, R. Temming, L. J. Hendriks, F. P. Rutjes, J. van Hest, D. J. Lefeber, P. Friedl and F. L. van Delft, *Angew. Chem. Int. Ed.*, 2010, **49**, 9422-9425.

279. R. W. Jinadasa, Z. Zhou, M. G. H. Vicente and K. M. Smith, *Org. Biomol. Chem.*, 2016, **14**, 1049-1064.

280. X. Zheng, J. Morgan, S. K. Pandey, Y. Chen, E. Tracy, H. Baumann, J. R. Missert, C. Batt, J. Jackson and D. A. Bellnier, *J. Med. Chem.*, 2009, **52**, 4306-4318.

281. F. Giuntini, C. M. Alonso and R. W. Boyle, *Photochem. Photobiol. Sci.*, 2011, **10**, 759-791.

282. T. V. Akhlynina, D. A. Jans, A. A. Rosenkranz, N. V. Statsyuk, I. Y. Balashova, G. Toth, I. Pavo, A. B. Rubin and A. S. Sobolev, *J. Biol. Chem.*, 1997, **272**, 20328-20331.

283. N. S. Soukos, M. R. Hamblin and T. Hasan, *Photochem. Photobiol.*, 1997, **65**, 723-729.

284. U. Schmidt-Erfurth, H. Diddens, R. Birngruber and T. Hasan, *Br. J. Cancer*, 1997, **75**, 54-61.

285. S. K. Bisland, D. Singh and J. Gariépy, *Bioconjugate Chem.*, 1999, **10**, 982-992.

286. S. Kimani, G. Ghosh, A. Ghogare, B. Rudshteyn, D. Bartusik, T. Hasan and A. Greer, *J. Org. Chem.*, 2012, **77**, 10638-10647.

287. B. Čunderlíková, L. Gangeskar and J. Moan, *J. Photochem. Photobiol., B*, 1999, **53**, 81-90.

288. A. Chopdar, U. Chakravarthy and D. Verma, *Br. Med. J.*, 2003, **326**, 485-488.

289. R. Luguya, L. Jaquinod, F. R. Fronczek, M. G. H. Vicente and K. M. Smith, *Tetrahedron*, 2004, **60**, 2757-2763.

290. K. M. Smith, D. A. Goff and D. J. Simpson, *J. Am. Chem. Soc.*, 1985, **107**, 4946-4954.

291. A. O. Abu-Yousif, A. C. E. Moor, X. Zheng, M. D. Savellano, W. Yu, P. K. Selbo and T. Hasan, *Cancer Lett.*, 2012, **321**, 120-127.

292. I. Rizvi, T. A. Dinh, W. Yu, Y. Chang, M. E. Sherwood and T. Hasan, *Isr. J. Chem.*, 2012, **52**, 776-787.

293. C. Bechara and S. Sagan, *FEBS Lett.*, 2013, **587**, 1693-1702.

294. D. M. Copolovici, K. Langel, E. Eriste and Ü. Langel, *ACS Nano*, 2014, **8**, 1972-1994.

295. F. Heitz, M. C. Morris and G. Divita, *Br. J. Pharmacol.*, 2009, **157**, 195-206.

296. K. M. Stewart, K. L. Horton and S. O. Kelley, *Org. Biomol. Chem.*, 2008, **6**, 2242-2255.

297. M. Zahid and P. D. Robbins, *Molecules*, 2015, **20**, 13055-13070.

298. M. Sibrian-Vazquez, T. J. Jensen, R. P. Hammer and M. G. H. Vicente, *J. Med. Chem.*, 2006, **49**, 1364-1372.

299. M. Sibrian-Vazquez, T. J. Jensen and M. G. H. Vicente, *J. Med. Chem.*, 2008, **51**, 2915-2923.

300. M. Sibrian-Vazquez, X. Hu, T. J. Jensen and M. G. H. Vicente, *J. Porphyrins Phthalocyanines*, 2012, **16**, 603-615.

301. F. Moret, M. Gobbo and E. Reddi, *Photochem. Photobiol. Sci.*, 2015, **14**, 1238-1250.

302. L. Bourré, F. Giuntini, I. M. Eggleston, C. A. Mosse, A. J. MacRobert and M. Wilson, *Photochem. Photobiol. Sci.*, 2010, **9**, 1613-1620.

303. G. A. Johnson, E. A. Ellis, H. Kim, N. Muthukrishnan, T. Snavely and J.-P. Pellois, *PLoS One*, 2014, **9**, e91220.

304. J. T.-W. Wang, F. Giuntini, I. M. Eggleston, S. G. Bown and A. J. MacRobert, *J. Controlled Release*, 2012, **157**, 305-313.

305. D. Derossi, A. H. Joliot, G. Chassaing and A. Prochiantz, *J. Biol. Chem.*, 1994, **269**, 10444-10450.

306. Z. Luo, X. Fan, N. Zhou, M. Hiraoka, J. Luo, H. Kaji and Z. Huang, *Biochemistry*, 2000, **39**, 13545-13550.

307. A. Elmquist, M. Lindgren, T. Bartfai and Ü. Langel, *Exp. Cell Res.*, 2001, **269**, 237-244.

308. R. Chapman, K. A. Jolliffe and S. Perrier, *Aust. J. Chem.*, 2010, **63**, 1169-1172.

309. E. Kaiser, R. L. Colescot, C. D. Bossinge and P. I. Cook, *Anal. Biochem.*, 1970, **34**, 595-598.

310. M. Gude, J. Ryf and P. D. White, *Lett. Pept. Sci.*, 2002, **9**, 203-206.

311. M. Galibert, P. Dumy and D. Boturyn, *Angew. Chem. Int. Ed.*, 2009, **48**, 2576-2579.

312. E. D. Funder, A. B. Jensen, T. Tørring, A. L. B. Kodal, A. R. Azcargorta and K. V. Gothelf, *J. Org. Chem.*, 2012, **77**, 3134-3142.

313. L. Liao, Y. Pang, L. Ding and F. E. Karasz, *Macromolecules*, 2004, **37**, 3970-3972.

314. S. G. Ramkumar, K. A. A. Rose and S. Ramakrishnan, *J. Polym. Sci., Part A: Polym. Chem.*, 2010, **48**, 3200-3208.

315. R. K. Goswami, Y. Liu, C. Liu, R. A. Lerner and S. C. Sinha, *Mol. Pharm.*, 2012, **10**, 538-543.

316. V. Neto, R. Granet and P. Krausz, *Tetrahedron*, 2010, **66**, 4633-4646.

317. C. Meyer, B. Hoeger, J. Chatterjee and M. Köhn, *Bioorg. Med. Chem.*, 2015, **23**, 2848-2853.